

Proceedings to the 21st Workshop
**What Comes Beyond the
Standard Models**

Bled, June 23– July 1, 2018

Edited by

Norma Susana Mankoč Borštnik

Holger Bech Nielsen

Dragan Lukman

**The 21st Workshop *What Comes Beyond the Standard Models*,
23.– 29. June 2018, Bled**

was organized by

Society of Mathematicians, Physicists and Astronomers of Slovenia

and sponsored by

Department of Physics, Faculty of Mathematics and Physics, University of Ljubljana

Society of Mathematicians, Physicists and Astronomers of Slovenia

Beyond Semiconductor (Matjaž Breškvar)

Scientific Committee

John Ellis, King's College London / CERN

Roman Jackiw, MIT

Masao Ninomiya, Yukawa Institute for Theoretical Physics, Kyoto University and

Mathematical Institute, Osaka-city University

Organizing Committee

Norma Susana Mankoč Borštnik

Holger Bech Nielsen

Maxim Yu. Khlopov

The Members of the Organizing Committee of the International Workshop “What Comes Beyond the Standard Models”, Bled, Slovenia, state that the articles published in the Proceedings to the 21st Workshop “What Comes Beyond the Standard Models”, Bled, Slovenia are refereed at the Workshop in intense in-depth discussions.

Workshops organized at Bled

- ▷ *What Comes Beyond the Standard Models*
(June 29–July 9, 1998), Vol. **0** (1999) No. 1
(July 22–31, 1999)
(July 17–31, 2000)
(July 16–28, 2001), Vol. **2** (2001) No. 2
(July 14–25, 2002), Vol. **3** (2002) No. 4
(July 18–28, 2003) Vol. **4** (2003) Nos. 2-3
(July 19–31, 2004), Vol. **5** (2004) No. 2
(July 19–29, 2005), Vol. **6** (2005) No. 2
(September 16–26, 2006), Vol. **7** (2006) No. 2
(July 17–27, 2007), Vol. **8** (2007) No. 2
(July 15–25, 2008), Vol. **9** (2008) No. 2
(July 14–24, 2009), Vol. **10** (2009) No. 2
(July 12–22, 2010), Vol. **11** (2010) No. 2
(July 11–21, 2011), Vol. **12** (2011) No. 2
(July 9–19, 2012), Vol. **13** (2012) No. 2
(July 14–21, 2013), Vol. **14** (2013) No. 2
(July 20–28, 2014), Vol. **15** (2014) No. 2
(July 11–19, 2015), Vol. **16** (2015) No. 2
(July 11–19, 2016), Vol. **17** (2016) No. 2
(July 9–17, 2017), Vol. **18** (2017) No. 2
(June 23–July 1, 2018), Vol. **19** (2018) No. 2
- ▷ *Hadrons as Solitons* (July 6–17, 1999)
- ▷ *Few-Quark Problems* (July 8–15, 2000), Vol. **1** (2000) No. 1
- ▷ *Selected Few-Body Problems in Hadronic and Atomic Physics* (July 7–14, 2001),
Vol. **2** (2001) No. 1
- ▷ *Quarks and Hadrons* (July 6–13, 2002), Vol. **3** (2002) No. 3
- ▷ *Effective Quark-Quark Interaction* (July 7–14, 2003), Vol. **4** (2003) No. 1
- ▷ *Quark Dynamics* (July 12–19, 2004), Vol. **5** (2004) No. 1
- ▷ *Exciting Hadrons* (July 11–18, 2005), Vol. **6** (2005) No. 1
- ▷ *Progress in Quark Models* (July 10–17, 2006), Vol. **7** (2006) No. 1
- ▷ *Hadron Structure and Lattice QCD* (July 9–16, 2007), Vol. **8** (2007) No. 1
- ▷ *Few-Quark States and the Continuum* (September 15–22, 2008),
Vol. **9** (2008) No. 1
- ▷ *Problems in Multi-Quark States* (June 29–July 6, 2009), Vol. **10** (2009) No. 1
- ▷ *Dressing Hadrons* (July 4–11, 2010), Vol. **11** (2010) No. 1
- ▷ *Understanding hadronic spectra* (July 3–10, 2011), Vol. **12** (2011) No. 1
- ▷ *Hadronic Resonances* (July 1–8, 2012), Vol. **13** (2012) No. 1
- ▷ *Looking into Hadrons* (July 7–14, 2013), Vol. **14** (2013) No. 1
- ▷ *Quark Masses and Hadron Spectra* (July 6–13, 2014), Vol. **15** (2014) No. 1
- ▷ *Exploring Hadron Resonances* (July 5–11, 2015), Vol. **16** (2015) No. 1
- ▷ *Quarks, Hadrons, Matter* (July 3–10, 2016), Vol. **17** (2016) No. 1
- ▷ *Advances in Hadronic Resonances* (July 2–9, 2017), Vol. **18** (2017) No. 1
- ▷ *Double-charm Baryons and Dimesons* (June 17–23, 2018), Vol. **18** (2018) No. 1
- ▷
 - *Statistical Mechanics of Complex Systems* (August 27–September 2, 2000)
 - *Studies of Elementary Steps of Radical Reactions in Atmospheric Chemistry*
(August 25–28, 2001)

Contents

Preface in English and Slovenian Language	VII
Talk Section	1
1 Inflation From Supersymmetry Breaking	
<i>I. Antoniadis</i>	1
2 New Model independent Results From the First Six Full Annual Cycles of DAMA/LIBRA–Phase2	
<i>R. Bernabei et al.</i>	27
3 HS YM and CS Theories in Flat Spacetime	
<i>L. Bonora</i>	58
4 Emergent Photons and Gravitons	
<i>J.L. Chkareuli, J. Jejelava and Z. Kepuladze</i>	74
5 A Deeper Probe of New Physics Scenarii at the LHC	
<i>A. Djouadi</i>	90
6 The Symmetry of 4×4 Mass Matrices Predicted by the <i>Spin-charge-family</i> Theory — $SU(2) \times SU(2) \times U(1)$ — Remains in All Loop Corrections	
<i>A. Hernandez-Galeana and N.S. Mankoč Borštnik</i>	102
7 Extending Starobinsky Inflationary Model in Gravity and Supergravity	
<i>S.V. Ketov and M. Yu. Khlopov</i>	148
8 Phenomenological Mass Matrices With a Democratic Origin	
<i>A. Kleppe</i>	164
9 Why Nature Made a Choice of Clifford and not Grassmann Coordinates?	
<i>N.S. Mankoč Borštnik and H.B.F. Nielsen</i>	175
10 Do We Find High Energy Physics Inside (Almost) Every Solid or Fluid at Low Temperature?	
<i>H.B. Nielsen and M. Ninomiya</i>	216

11 Electric Dipole Moment and Dark Matter in a CP Violating Minimal Supersymmetric SM	
<i>T. Shindou</i>	247
Discussion Section	257
12 On Triple-periodic Electrical Charge Distribution as a Model of Physical Vacuum and Fundamental Particles	
<i>E.G. Dmitrieff</i>	261
13 The Correspondence Between Fermion Family Members in Spin-charge-family Theory and Structure Defects in Electrically-charged Tessellations	
<i>E.G. Dmitrieff</i>	285
14 $K^0 - \bar{K}^0$, $D^0 - \bar{D}^0$ in a Local $SU(3)$ Family Symmetry	
<i>A. Hernandez-Galeana</i>	299
15 Beyond the Standard Models of Particle Physics and Cosmology	
<i>M.Yu. Khlopov</i>	314
16 The γ^a Matrices, $\tilde{\gamma}^a$ Matrices and Generators of Lorentz Rotations in Clifford Space — Determining in the <i>Spin-charge-family</i> Theory Spins, Charges and Families of Fermions — in $(3 + 1)$-dimensional Space	
<i>D. Lukman and N.S. Mankoč Borštnik</i>	327
17 Properties of Fermions With Integer Spin Described in Grassmann Space	
<i>D. Lukman and N.S. Mankoč Borštnik</i>	335
18 Could Experimental Anomalies Reflect Non-perturbative Effects?	
<i>H.B. Nielsen and C.D. Froggatt</i>	359
Virtual Institute of Astroparticle Physics Presentation	381
19 The Platform of Virtual Institute of Astroparticle Physics in Studies of Physics Beyond the Standard Model	
<i>M.Yu. Khlopov</i>	383
Poem by Astri Kleppe	395
20 June	
<i>Astri Kleppe</i>	397

Preface

The series of annual workshops on "What Comes Beyond the Standard Models?" started in 1998 with the idea of Norma and Holger for organizing a real workshop, in which participants would spend most of the time in discussions, confronting different approaches and ideas. Workshops take place in the picturesque town of Bled by the lake of the same name, surrounded by beautiful mountains and offering pleasant walks and mountaineering. Since the 20th workshop we offer every year during or at the end of the workshop a talk to the general audience of Bled. This year the talk with the title "How far do we understand the Universe in this moment?", was given by Norma Susana Mankoč Borštnik in the lecture hall of the Bled School of Management. The lecture hall was kindly offered by the founder of the school Danica Purg. The talk was, due to the schedule constraint at the school, delivered after the workshop already finished.

In our very open minded, friendly, cooperative, long, tough and demanding discussions several physicists and even some mathematicians have contributed. Most of topics presented and discussed in our Bled workshops concern the proposals how to explain physics beyond the so far accepted and experimentally confirmed both standard models – in elementary particle physics and cosmology – in order to understand the origin of assumptions of both standard models and be consequently able to make predictions for future experiments. Although most of participants are theoretical physicists, many of them with their own suggestions how to make the next step beyond the accepted models and theories, experts from experimental laboratories were very appreciated, helping a lot to understand what do measurements really tell and which kinds of predictions can best be tested.

The (long) presentations (with breaks and continuations over several days), followed by very detailed discussions, have been extremely useful, at least for the organizers. We hope and believe, however, that this is the case also for most of participants, including students. Many a time, namely, talks turned into very pedagogical presentations in order to clarify the assumptions and the detailed steps, analyzing the ideas, statements, proofs of statements and possible predictions, confronting participants' proposals with the proposals in the literature or with proposals of the other participants, so that all possible weak points of the proposals, those from the literature as well as our own, showed up very clearly. The ideas therefore seem to develop in these years considerably faster than they would without our workshops.

This year neither the cosmological nor the particle physics experiments offered much new, which would offer new insight into the elementary particles and fields, although a lot of work and effort have been put in, but the news will hopefully come when analyses of the data gathered with energies up to 13 TeV on the LHC will be finished.

We also expect that new cosmological experiments will help to resolve the origin of the dark matter. Since the results of the DAMA/LIBRA experiments, presented in this year proceedings, can hardly be explained in some other way than with the signal of the dark matter, it is expected that sooner or latter other laboratories will confirm the DAMA/LIBRA results. Several contributions in this proceedings discuss proposals for the dark matter, suggesting that they might be supersymmetric partners, dark atoms made of dark barions and ordinary barions, the stable neutrons of the second group of four families.

Understanding the universe through the cosmological theories and theories of the elementary fermion and boson fields, have, namely, so far never been so dependent on common knowledge and experiments in both fields.

The experiments on the LHC and other laboratories around the world might offer the accurately enough mixing matrices for quark and leptons, so that it will become clear whether there is the new family to the observed three as well as several scalar fields, which determine the higgs and the Yukawa couplings, predicted by the spin-charge-family theory. The symmetry in all orders of corrections of the 4×4 mass matrices, determined by the scalars of this theory, studied in this proceedings, limits the number of free parameters of mass matrices, and would for accurately enough measured matrix elements of the 3×3 sub-matrices of the 4×4 mixing matrices predict properties of the fourth family of quarks and leptons. The accurate $(n - 1) \times (n - 1)$ submatrix of any $n \times n$ matrix, namely, determines the $n \times n$ matrix uniquely.

The properties of mass matrices of the observed 3 families of quarks are presented, following while taking into account the measured masses of quarks and the standard parametrization of the mixing matrix. It is not surprising that the mass matrices are close to the democratic matrix, since the top quark has much higher mass and is much weaker coupled to the rest of quarks. Also the spin-charge family theory predicts that the 4×4 mass matrices of quarks and leptons are close to the democratic ones. This is even less surprising, since the fourth family with the masses close to 1 TeV for leptons and above 1 TeV for quarks is even weaker coupled with the rest three families than it is the third u-quark coupled to the rest of quarks.

The new data might answer the question, whether laws of nature are elegant (as predicted by the spin-charge-family theory and also — up to the families — other Kaluza-Klein-like theories and the string theories) or “she is just using gauge groups when needed” (what many models assume, also some presented in this proceedings). Can the higgs scalars be guessed by smaller steps from the standard model case, or they must be recognized in more general theories as it is in the spin-charge-family theory?

The evidences obviously tell that fermion fields have half integer spin and the charges in the fundamental representations of the so far observed groups.

Shall the study of Grassmann space in confrontation with Clifford space for the description of the internal degrees of freedom for fermions, discussed in this proceedings in the first and second quantization of fields, help to better understand the “elegance of the laws of nature”? While the Clifford space offers the explanation for all the properties of quarks and leptons, carrying the half integer spin and all

the charges in the fundamental representations of the groups (which are subgroups of the large enough Lorentz group), with the families included (the properties of which are also explainable by the half integer "family spins and charges"), in the Grassmann space there are the second quantizable fermions, which carry the integer spin and charges, both in adjoint representations of the subgroup of the Lorentz group and no families. And yet there exists the "Dirac-Grassmann" sea. While in the Clifford case one Weyl representation includes in $SO(13, 1)$ all the quarks and leptons and anti-quarks and anti-leptons observed so far (as well as the right handed neutrino), in Grassmann space particles and anti-particles are in different representations.

Is the working hypotheses that "all the mathematics is a part of nature" acceptable and must be taken seriously? If "nature would make a choice" of the Grassmann instead of the Clifford algebra, all the atoms, molecules and correspondingly all the world would look completely different, but yet possible. Why "she make a choice" of the Clifford algebra? All these is discussed in this proceedings, in order to understand better why the spin-charge-family theory is offering so many answers to the open questions in both standard models.

In one of the contributions the higher integer spin Yang-Mills-like gauge fields are studied, allowing infinite number of higher spin states. Such theories might, namely, help to avoid ultraviolet divergences in gauge fields.

Also the supersymmetry offers avoiding some of divergences. The analyze is done for the possibility that the LHC would confirm the existence of the supersymmetric partners with masses close or above 1 TeV, as well as of several higgs and of a new family of quarks and leptons. The spin-charge family theory, offering the explanation for all the assumptions of the standard model(s), predicting the fourth family of quarks and leptons around 1 TeV or above, as well as three singlets and two triplets of scalar fields (all with the properties of the higgs with respect to the weak and hyper charges) and four additional families, the lowest of which explains the appearance of the dark matter, does not "see" the supersymmetric particles.

Even if the supersymmetry might not be confirmed in the low energy regime, yet the supergravity models, inspired by the string models, can help to better understand the inflation in our universe and the observations at its present stage. The supersymmetry might also help to understand the presence of the (very small) amount of dark energy, of the dark matter, even for primordial formation of black holes. All these is studied in three contributions of this proceedings.

It is an interesting observation in this proceedings discussing properties of any material with only the translational symmetry that there must be regions in quasi momentum space where an approximate Weyl equation (relativistic equation for massless particles) determines properties of material, observed, let say, in graphene. The same effect can be observed also in the universe with a strong Hubble expansion. Authors explain this effect with the "homolumo-gap".

As we know from several fields of physics, there are many different models, seeming to have very little in common, which explain well the same phenomena. The challenge is to find out what they have in common. There is the contribution in this proceedings treating electrodynamics and linearized gravity in common,

causing the spontaneous break of Lorentz invariance by constraints on the electromagnetic and tensor fields. The model is at low energies still in agreement with the observations.

Two contributions in the discussion section try to extract properties of quarks and leptons, that is their masses and the forces among them, from the geometrical picture of quarks and leptons carrying the charges of the spin-charge-family theory. How far can such an attempt help to understand our nature?

What is the most efficient way to understand our universe? Is it now the time that we should make a new step, as it was the standard model step 50 years ago, with the theory which explains all the assumptions of the standard models? Is the spin-charge-family the right first step beyond the standard models? Will experiments confirm the predictions of this theory? Or should we insist with small steps stimulated by experiments? Is the space-time $(3 + 1)$ -dimensional? Or d is much larger, infinite? Is the interaction among fermions only gravitational one, manifesting at $(3 + 1)$ the gravity and the observed gauge fields, with scalar fields included? Only the theory and the experiment together can answer this question. Since, as every year also this year there has been not enough time to mature the very discerning and innovative discussions, for which we have spent a lot of time, into the written contributions, only two months, authors can not really polish their contributions. Organizers hope that this is well compensated with fresh contents. Questions and answers as well as lectures enabled by M.Yu. Khlopov via Virtual Institute of Astroparticle Physics (viavca.in2p3.fr/site.html) of APC have in ample discussions helped to resolve many dilemmas.

The reader can find the records of all the talks delivered by cosmopia since Bled 2009 on viavca.in2p3.fr/site.html in Previous - Conferences. The three talks delivered by: Norma Mankoč Borštnik (Understanding nature with the spin-charge-family theory, making several predictions), Sergey V. Ketov (Starobinsky inflation in gravity and supergravity) and H.B Nielsen(Theory for initial State Conditions), can be accessed directly at

http://viavca.in2p3.fr/what_comes_beyond_the_standard_model_2018.html

Most of the talks can be found on the workshop homepage

<http://bsm.fmf.uni-lj.si/>.

Bled Workshops owe their success to participants who have at Bled in the heart of Slovene Julian Alps enabled friendly and active sharing of information and ideas, yet their success was boosted by videoconferences.

Let us conclude this preface by thanking cordially and warmly to all the participants, present personally or through the teleconferences at the Bled workshop, for their excellent presentations and in particular for really fruitful discussions and the good and friendly working atmosphere.

*Norma Mankoč Borštnik, Holger Bech Nielsen, Maxim Y. Khlopov,
(the Organizing committee)*

*Norma Mankoč Borštnik, Holger Bech Nielsen, Dragan Lukman,
(the Editors)*

Ljubljana, December 2018

1 Predgovor (Preface in Slovenian Language)

Vsakoletne delavnice z naslovom „Kako preseči oba standardna modela, kozmološkega in elektrošibkega“ (“What Comes Beyond the Standard Models?”) sta postavila leta 1998 Norma in Holger z namenom, da bi udeleženci v izčrpnih diskusijah kritično soočali različne ideje in teorije. Delavnice domujejo v Plemljevi hiši na Bledu ob slikovitem jezeru, kjer prijetni sprehodi in pohodi na čudovite gore, ki kipijo nad mestom, ponujajo priložnosti in vzpodbudo za diskusije. Od lanske, 20. delavnice, dalje ponudimo vsako leto med ali ob koncu delavnice predavanje za splošno občinstvo na Bledu. Letošnje je imelo naslov “Kako dobro razumemo naše Vesolje v tem trenutku?”, ki ga je imela Norma Susana Mankovč Borštnik v predavalnici IEDC (Blejska šola za management). Predavalnico nam je prijazno ponudila ustanoviteljica te šole, gospa Danica Purg. Žal je bilo predavanje, zaradi urnika na šoli, šele po končani delavnici.

K našim zelo odprtim, prijateljskim, dolgim in zahtevnim diskusijam, polnim iskrivega sodelovanja, je prispevalo veliko fizikov in celo nekaj matematikov. Večina predlogov teorij in modelov, predstavljenih in diskutiranih na naših Blejskih delavnicah, išče odgovore na vprašanja, ki jih v fizikalni skupnosti sprejeta in s številnimi poskusi potrjena standardni model osnovnih fermionskih in bozonskih polj ter kozmološki standardni model puščata odprta. Čeprav je večina udeležencev teoretičnih fizikov, mnogi z lastnimi idejami kako narediti naslednji korak onkraj sprejetih modelov in teorij, so še posebej dobrodošli predstavniki eksperimentalnih laboratorijev, ki nam pomagajo v odprtih diskusijah razjasniti resnično sporočilo meritev in nam pomagajo razumeti kakšne napovedi so potrebne, da jih lahko s poskusi dovolj zanesljivo preverijo.

Organizatorji moramo priznati, da smo se na blejskih delavnicah v (dolgih) predstavitev (z odmori in nadaljevanji preko več dni), ki so jim sledile zelo podrobne diskusije, naučili veliko, morda več kot večina udeležencev. Upamo in verjamemo, da so veliko odnesli tudi študentje in večina udeležencev. Velikokrat so se predavanja spremenila v zelo pedagoške predstavitve, ki so pojasnile predpostavke in podrobne korake, soočile predstavljene predloge s predlogi v literaturi ali s predlogi ostalih udeležencev ter jasno pokazale, kje utegnejo tičati šibke točke predlogov. Zdi se, da so se ideje v teh letih razvijale bistveno hitreje, zahvaljujoč prav tem delavnicam.

To leto eksperimenti v kozmologiji in fiziki osnovnih fermionskih in bozonskih polj niso ponudili veliko novih rezultatov, ki bi omogočili nov vpogled v fiziko osnovnih delcev in polj, čeprav je bilo vanje vložene veliko truda. Upamo, da bodo podrobne analize podatkov, zbranih na LHC do energij 13 TeV, prinesle odločujoče rezultate.

Pričakujemo tudi, da bodo nove kozmološke meritve uspele razrešiti izvor temne snovi. Ker je dolgoletne rezultate poskusa DAMA/LIBRA, ki so predstavljeni v tem zborniku, le težko pojasniti drugače kot s signali temne snovi, je pričakovati,

da bodo tudi ostali poskusi sčasoma potrdili njihove rezultate. Več prispevkov v tem zborniku obravnava različne predloge, ki naj pojasnijo izvor temne snovi: supersimetrični partnerji, temni atomi iz temnih barionov in iz barionov običajne snovi, neutroni iz stabilne pete družine kvarkov in leptonov, ki pripadajo grupi štirih družin z družinskimi kvantnimi števili in so (skoraj) nesklepljeni s spodnjimi štirimi družinami, med katerimi tri že poznamo.

Kozmološka spoznanja in spoznanja v teoriji osnovnih fermionskih in bozonskih polj delcev še nikoli doslej niso bila tako zelo povezana in soodvisna.

Ko bodo z eksperimenti na LHC in v ostalih laboratorijih po svetu uspeli ponuditi dovolj natančne vrednosti za elemente mešalnih matrik za kvarke in leptone, bo znan odgovor na vprašanje ali obstaja poleg opaženih treh tudi četrta družina in več novih skalarnih polj, ki določajo higgsove in Yukawine sklopitve — kar napoveduje teorija spinov-nabojev-družin. Simetrija popravkov masnih matrik 4×4 v vseh redih, ki jo določajo skalarji v tej teoriji in jo obravnava prispevek v zborniku, omeji število prostih parametrov masnih matrik tako, da dovolj natančno izmerjeni matrični elementi podmatrik 3×3 v mešalnih matrikah 4×4 omogočijo napoved lastnosti četrte družine kvarkov in leptonov, saj podmatrika $(n - 1) \times (n - 1)$ matrike $n \times n$ to enolično določa.

Eden od prispevkov v zborniku predstavi študijo, ki določi masne matrike opaženih 3 družin kvarkov iz standardne parametrizacije mešalne matrike in izmerjenih mass kvarkov. Ne preseneča ugotovitev, da so masne matrike blizu demokratični matriki, saj ima top kvark veliko večjo maso od odtalih kvarkov in je šibko sklopjen z ostalimi člani družin. Tudi teorija spinov-nabojev-družin pričakovano napove, da so masne matrike 4×4 blizu demokratičnim, saj je četrta družina, ki ima maso nad 1 TeV, šibko sklopljena s člani ostalih treh družin.

Novi podatki bodo morda dali odgovor tudi na vprašanje, ali so zakoni narave preprosti (kot napove teorija spinov-nabojev-družin in tudi ostale teorije Kaluza-Kleinovega tipa, ki pa pojava družin ne pojasnijo, pa tudi teorije strun) ali pa narava preprosto "uporabi umeritvene grupe, kadar jih potrebuje" (kar predpostavi veliko modelov, tudi nekateri v tem zborniku). In tudi ali lahko ugibamo pojav higgsovih skalarjev z majhnimi odmiki od standardnega modela fermionskih in bozonskih polj, ali pa morajo obstoj skalarnih polj pojasniti splošnejše teorije (kot je teorija spinov-nabojev-družin)?

Vse meritve doslej potrdijo, da imajo fermioni polštevilčne spine ter naboje v fundamentalnih upodobitvah dosedaj opaženih grup. Eden od prispevkov obravnava prvo in drugo kvantizacijo fermionskih polj v Grassmannovem prostoru. Fermioni nosijo v Grassmannovem prostoru celoštevilčne spine in naboje v adjungirani upodobitvi grup. Bo primerjava lastnosti fermionskih polj, ki "živijo" v Grassmannovem prostoru, s tistimi, ki živijo v Cliffordovem prostoru, pripomogla k boljšemu razumevanju "elegance naravnih zakonov" kot avtorji upajo? Cliffordov prostor ponudi razlago za vse lastnosti kvarkov in leptonov, ki imajo polštevilski spin in vse naboje v fundamentalni upodobitvi grupe (ki so podgrupe v dovolj veliki Lorentzovi grupi), vključno z družinami (katerih lastnosti lahko prav tako pojasnimo s polštevilskimi "spini in naboji družin"). V Grassmannovem prostoru pa druga kvantizacija ponudi fermione, ki imajo celoštevilške spine in naboje, oboje v adjungirani upodobitvi podgrupe Lorentzove grupe in nobenih družin.

“Dirac-Grassmannovo morje” igra vlogo Diracovega morja. Medtem, ko v Cliffordovem primeru ena Weylova upodobitev vključuje v $SO(13, 1)$ vse kvarke in leptone ter antikvarke in antileptone, ki so jih dosedaj opazili (pa tudi desnoročni nevtrino), so v Grassmannovem prostoru delci in antidelci v različnih upodobitvah. Je delovna hipoteza, da je “vsa matematika del narave”, sprejemljiva in jo moramo upoštevati? Če bi “narava izbrala” Grassmannovo namesto Cliffordove algebre, bi atomi, molekule in vse vesolje izgledali drugače. Zakaj je ni?

Eden od prispevkov pokaže, kako v ravnem prostoru definirati umeritvena polja Yang-Millsovega tipa z višjimi spini, ki ponudijo neskončno število stanj umeritvenih polj in omogočijo, da se izognemo divergencam pri visokih energijah.

Tudi supersimetrija ponuja možnost obvladovanja nekaterih neskončnosti. Analiza v prispevku obravnava možnosti, da bi meritve na LHC potrdile obstoj supersimetričnih partnerjev, ki imajo maso nekaj TeV, pa tudi obstoj večjega števila skalarnih polj in nove družine kvarkov in leptonov. Teorija spinov-nabojev-družin, ki napove tri singlete and dva tripleta skalarnih polj, pa tudi četrto družino, ne “vidi” supersimetričnih delcev.

Tudi če poskusi ne potrdijo obstoja supersimetričnih delcev pri nizkih energijah, lahko modeli supergravitacije, ki jih porodi teorija strun, pomagajo razumeti pojav inflacije, ki jo je moralo doživeti v naše vesolje, ker lahko le tako pojasnimo izmerjene lastnosti vesolja. Supersimetrija bi morda lahko pojasnila, zakaj je gostota temne energije tako zelo majhna, pojasnila pa bi tudi prisotnost temne snovi, ter celo tvorbo prvotnih črnih lukenj. Te možnosti obravnavajo trije prispevki.

Zanimivo je, da iz lastnosti poljubne snovi, ki ima samo translacijsko simetrijo, sledi, kot obravnavana en prispevek, da v prostoru kvazi gibalne količine obstajajo majhna področja, v katerih približna Weylova enačba (relativistična enačba za brezmasne delce) določa lastnosti materila, kot je, denimo, grafen. Enak pojav bi lahko opazili v vesolju pri močni Hubblovi ekspanziji. Avtorja to pojasnjujeta z vrzeljo “homo-lumo”.

Na različnih področjih fizike obstajajo različni modeli, ki na videz nimajo veliko skupnega, pa vendar opisujejo iste pojave enako dobro. Prispevek v zborniku obravnava skupaj elektrodinamiko in linearizirano gravitacijo v modelu elektrogravitacije, v katerem pogoj na vsako od polj povzroči spontano zlomitev Lorentzove invariance. Model je pri nizkih energijah skladen z opažanji.

Dva prispevka v sekciji diskusij poskušata iz geometrijske slike v celice porazdeljenih fermionov, ki nosijo različne naboje, določiti silo med fermioni. Do kolikšne mere nam lahko tak pristop pomaga razumeti naravo?

Kakšna je učinkovita pot pri razumevanju našega vesolja? Je dozorel čas, ko lahko napravimo odločen korak v razumevanju vesolja samo s predlogom teorije, ki pojasni vse privzetke obeh standardnih modelov? Je teorija spinov, nabojev in družin pravi predlog? Bodo poskusi potrdili njene napovedi? Ali pa so majhni koraki proč od obeh standardnih modelov bolj varna pot pri načrtovanju poskusov? Je prostor-čas štiri razsežen? Ali pa je njegova razsežnost mnogo večja, neskončna? Je interakcija med fermioni v mnogo razsežnem prostoru ena sama, tedaj gravitacijska, ki se kaže v opazljivem delu vesolja kot vse poznane sile? Samo teorija in eksperiment skupaj lahko odgovorita na ta vprašanja.

Ker je vsako leto le malo časa od delavnice do zaključka redakcije, manj kot dva meseca, avtorji ne morejo izpiliti prispevkov, vendar upamo, da to nadomesti svežina prispevkov.

Četudi so k uspehu „Blejskih delavnic“ največ prispevali udeleženci, ki so na Bledu omogočili prijateljsko in aktivno izmenjavo mnenj v osrčju slovenskih Julijcev, so k uspehu prispevale tudi videokonference, ki so povezale delavnice z laboratoriji po svetu. Vprašanja in odgovori ter tudi predavanja, ki jih je v zadnjih letih omogočil M.Yu. Khlopov preko Virtual Institute of Astroparticle Physics (viavca.in2p3.fr/site.html, APC, Pariz), so v izčrpnih diskusijah pomagali razčistiti marsikatero vprašanje.

Bralec najde zapise vseh predavanj, objavljenih preko "cosmovia" od leta 2009, na viavca.in2p3.fr/site.html v povezavi Previous - Conferences. Troje letošnjih predavanj,

Norma Mankoč Borštnik (Understanding nature with the spin-charge-family theory, making several predictions), Sergey V. Ketov (Starobinsky inflation in gravity and supergravity) in H.B Nielsen (Theory for initial State Conditions), je dostopnih na

http://viavca.in2p3.fr/what_comes_beyond_the_standard_model_2018.html

Večino predavanj najde bralec na spletni strani delavnice na

<http://bsm.fmf.uni-lj.si/>.

Naj zaključimo ta predgovor s prisrčno in toplo zahvalo vsem udeležencem, prisotnim na Bledu osebno ali preko videokonferenc, za njihova predavanja in še posebno za zelo plodne diskusije in odlično vzdušje.

Norma Mankoč Borštnik, Holger Bech Nielsen, Maxim Y. Khlopov,
(Organizacijski odbor)

Norma Mankoč Borštnik, Holger Bech Nielsen, Dragan Lukman,
(uredniki)

Ljubljana, grudna (decembra) 2018

Talk Section

All talk contributions are arranged alphabetically with respect to the authors' names.



1 Inflation From Supersymmetry Breaking

I. Antoniadis

Laboratoire de Physique Théorique et Hautes Énergies - LPTHE
Sorbonne Université, CNRS, 4 Place Jussieu, 75005 Paris, France
and

Albert Einstein Center, Institute for Theoretical Physics
University of Bern, Sidlerstrasse 5, 3012 Bern, Switzerland

Abstract. I discuss a general class of models where the inflation is driven by supersymmetry breaking with the superpartner of the goldstino (sgoldstino) playing the role of the inflaton. Imposing an R-symmetry allows to satisfy easily the slow-roll conditions, avoiding the so-called η -problem, and leads to two different classes of small field inflation models; they are characterised by an inflationary plateau around the maximum of the scalar potential, where R-symmetry is either restored or spontaneously broken, with the inflaton rolling down to a minimum describing the present phase of our Universe. Inflation can be driven by either an F- or a D-term, while the minimum has a positive tuneable vacuum energy. The models agree with cosmological observations and in the simplest case predict a tensor-to-scalar ratio of primordial perturbations $10^{-9} \lesssim r \lesssim 10^{-4}$ and an inflation scale $10^{10} \text{ GeV} \lesssim H_* \lesssim 10^{12} \text{ GeV}$.

Povzetek. Avtor obravnava razred modelov, v katerih zlomitev supersimetrije povzroči inflacijo, vlogo inflatona pa igra superpartner goldstina (sgoldstino). Avtorjev privzetek, da imajo modeli simetrijo R, omogoči, da je izpolnjen pogoj za 'slow-roll', s čimer se izogne problemu η . Tem pogojem zadostita dve vrsti modelov inflacije z majhnim poljem. Zanje je značilen inflacijski plato okrog maksimuma skalarnega potenciala, kjer se simetrija R bodisi ohrani ali pa spontano zlomi, inflaton pa se zapelje po potencialu do minimuma, ki opisuje sedanjo fazo našega vesolja. Inflacijo lahko poganja ali člen F ali člen D, minimum ima pozitivno vakuumsko energijo, ki jo z izbiro parametrov lahko spreminjamo tako, da se ujemajo s kozmološkimi meritvami. V najpreprostejšem primeru modeli napovedo, da je bilo, ko je bila v začetku vesolja energijska skala inflacije $10^{10} \text{ GeV} \lesssim H_* \lesssim 10^{12} \text{ GeV}$, razmerje tenzorskih in skalarnih nehomogenosti $10^{-9} \lesssim r \lesssim 10^{-4}$.

Keywords: supersymmetry breaking, R-symmetry, supergravity, cosmology, inflation

1.1 Introduction

If String Theory is a fundamental theory of Nature and not just a tool for studying systems with strongly coupled dynamics, it should be able to describe at the same time particle physics and cosmology, which are phenomena that involve very different scales from the microscopic four-dimensional (4d) quantum gravity

length of 10^{-33} cm to large macroscopic distances of the size of the observable Universe $\sim 10^{28}$ cm spanned a region of about 60 orders of magnitude. In particular, besides the 4d Planck mass, there are three very different scales with very different physics corresponding to the electroweak, dark energy and inflation. These scales might be related via the scale of the underlying fundamental theory, such as string theory, or they might be independent in the sense that their origin could be based on different and independent dynamics. An example of the former constraint and more predictive possibility is provided by TeV strings with a fundamental scale at low energies due for instance to large extra dimensions transverse to a four-dimensional braneworld forming our Universe [1]. In this case, the 4d Planck mass is emergent from the fundamental string scale and inflation should also happen around the same scale [2].

Here, we will adopt a more conservative approach, trying to relate the scales of supersymmetry breaking and inflation, assuming that supersymmetry breaking is realised in a metastable de Sitter vacuum with an infinitesimally small (tuneable) cosmological constant independent of the breaking scale that may be in the TeV region or higher.

In a recent work [3], we studied a simple $N = 1$ supergravity model having this property and motivated by string theory. Besides the gravity multiplet, the minimal field content consists of a chiral multiplet with a shift symmetry promoted to a gauged R-symmetry using a vector multiplet. In the string theory context, the chiral multiplet can be identified with the string dilaton (or an appropriate compactification modulus) and the shift symmetry associated to the gauge invariance of a two-index antisymmetric tensor that can be dualized to a (pseudo)scalar. The shift symmetry fixes the form of the superpotential and the gauging allows for the presence of a Fayet-Iliopoulos (FI) term [4], leading to a supergravity action with two independent parameters that can be tuned so that the scalar potential possesses a metastable de Sitter minimum with a tiny vacuum energy (essentially the relative strength between the F- and D-term contributions). A third parameter fixes the Vacuum Expectation Value (VEV) of the string dilaton at the desired (phenomenologically) weak coupling regime. An important consistency constraint of the model is anomaly cancellation which has been studied in [5] and implies the existence of additional charged fields under the gauged R-symmetry.

In a subsequent work [6], we analysed a small variation of this model which is manifestly anomaly free without additional charged fields and allows to couple in a straight forward way a visible sector containing the minimal supersymmetric extension of the Standard Model (MSSM) and studied the mediation of supersymmetry breaking and its phenomenological consequences. It turns out that an additional ‘hidden sector’ field z is needed to be added for the matter soft scalar masses to be non-tachyonic; although this field participates in the supersymmetry breaking and is similar to the so-called Polonyi field, it does not modify the main properties of the metastable de Sitter (dS) vacuum. All soft scalar masses, as well as trilinear A-terms, are generated at the tree level and are universal under the assumption that matter kinetic terms are independent of the ‘Polonyi’ field, since matter fields are neutral under the shift symmetry and supersymmetry breaking is driven by a combination of the $U(1)$ D-term and the dilaton and z -field F-term.

Alternatively, a way to avoid the tachyonic scalar masses without adding the extra field z is to modify the matter kinetic terms by a dilaton dependent factor.

A main difference of the second analysis from the first work is that we use a field representation in which the gauged shift symmetry corresponds to an ordinary $U(1)$ and not an R -symmetry. The two representations differ by a Kähler transformation that leaves the classical supergravity action invariant. However, at the quantum level, there is a Green-Schwarz term generated that amounts an extra dilaton dependent contribution to the gauge kinetic terms needed to cancel the anomalies of the R -symmetry. This creates an apparent puzzle with the gaugino masses that vanish in the first representation but not in the latter. The resolution to the puzzle is based on the so called anomaly mediation contributions [7,8] that explain precisely the above apparent discrepancy. It turns out that gaugino masses are generated at the quantum level and are thus suppressed compared to the scalar masses (and A -terms).

This model has the necessary ingredients to be obtained as a remnant of moduli stabilisation within the framework of internal magnetic fluxes in type I string theory, turned on along the compact directions for several abelian factors of the gauge group. All geometric moduli can in principle be fixed in a supersymmetric way, while the shift symmetry is associated to the 4d axion and its gauging is a consequence of anomaly cancellation [9,10].

We then made an attempt to connect the scale of inflation with the electroweak and supersymmetry breaking scales within the same effective field theory, that at the same time allows the existence of an infinitesimally small (tuneable) positive cosmological constant describing the present dark energy of the universe. We thus addressed the question whether the same scalar potential can provide inflation with the dilaton playing also the role of the inflaton at an earlier stage of the universe evolution [11]. We showed that this is possible if one modifies the Kähler potential by a correction that plays no role around the minimum, but creates an appropriate plateau around the maximum. In general, the Kähler potential receives perturbative and non-perturbative corrections that vanish in the weak coupling limit. After analysing all such corrections, we find that only those that have the form of (Neveu-Schwarz) NS5-brane instantons can lead to an inflationary period compatible with cosmological observations. The scale of inflation turns out then to be of the order of low energy supersymmetry breaking, in the TeV region. On the other hand, the predicted tensor-to-scalar ratio is too small to be observed.

Inflationary models [12] in supergravity¹ suffer in general from several problems, such as fine-tuning to satisfy the slow-roll conditions, large field initial conditions that break the validity of the effective field theory, and stabilisation of the (pseudo) scalar companion of the inflaton arising from the fact that bosonic components of superfields are always even. The simplest argument to see the fine tuning of the potential is that a canonically normalised kinetic term of a complex scalar field X corresponds to a quadratic Kähler potential $K = X\bar{X}$ that brings one unit contribution to the slow-roll parameter $\eta = V''/V$, arising from the e^K proportionality factor in the expression of the scalar potential V . This problem can be avoided in models with no-scale structure where cancellations arise naturally

¹ For reviews on supersymmetric models of inflation, see for example [13].

due to non-canonical kinetic terms leading to potentials with flat directions (at the classical level). However, such models require often trans-Planckian initial conditions that invalidate the effective supergravity description during inflation. A concrete example where all these problems appear is the Starobinsky model of inflation [14], despite its phenomenological success.

All three problems above are solved when the inflaton is identified with the scalar component of the goldstino superfield², in the presence of a gauged R-symmetry [16]. Indeed, the superpotential is in that case linear and the big contribution to η described above cancels exactly. Since inflation arises at a plateau around the maximum of the scalar potential (hill-top) no large field initial conditions are needed, while the pseudo-scalar companion of the inflaton is absorbed into the R-gauge field that becomes massive, leading the inflaton as a single scalar field present in the low-energy spectrum. This model provides therefore a minimal realisation of natural small-field inflation in supergravity, compatible with present observations, as we show below. Moreover, it allows the presence of a realistic minimum describing our present Universe with an infinitesimal positive vacuum energy arising due to a cancellation between an F- and D-term contributions to the scalar potential, without affecting the properties of the inflationary plateau, along the lines of Refs. [3,11,17].

In the above models the D-term has a constant FI contribution but plays no role during inflation and can be neglected, while the pseudoscalar partner of the inflaton is absorbed by the $U(1)_R$ gauge field that becomes massive away from the origin. Recently, a new FI term was proposed [19] that has three important properties: (1) it is manifestly gauge invariant already at the Lagrangian level; (2) it is associated to a $U(1)$ that should not gauge an R-symmetry and (3) supersymmetry is broken by (at least) a D-auxiliary expectation value and the extra bosonic part of the action is reduced in the unitary gauge to a constant FI contribution leading to a positive shift of the scalar potential, in the absence of matter fields. In the presence of matter fields, the FI contribution to the D-term acquires a special field dependence $e^{2K/3}$ that violates invariance under Kähler transformations.

In a recent work [18], we studied the properties of the new FI term and explored its consequences to the class of inflation models we introduced in [16].³ We first showed that matter fields charged under the $U(1)$ gauge symmetry can consistently be added in the presence of the new FI term, as well as a non-trivial gauge kinetic function. We then observed that the new FI term is not invariant under Kähler transformations. On the other hand, a gauged R-symmetry in ordinary Kähler invariant supergravity can always be reduced to an ordinary (non-R) $U(1)$ by a Kähler transformation. By then going to such a frame, we find that the two FI contributions to the $U(1)$ D-term can coexist, leading to a novel contribution to the scalar potential.

The resulting D-term scalar potential provides an alternative realisation of inflation from supersymmetry breaking, driven by a D- instead of an F-term. The inflaton is still a superpartner of the goldstino which is now a gaugino within

² See [15] for earlier work relating supersymmetry and inflation.

³ This new FI term was also studied in [20] to remove an instability from inflation in Polonyi-Starobinsky supergravity.

a massive vector multiplet, where again the pseudoscalar partner is absorbed by the gauge field away from the origin. For a particular choice of the inflaton charge, the scalar potential has a maximum at the origin where inflation occurs and a supersymmetric minimum at zero energy, in the limit of negligible F-term contribution (such as in the absence of superpotential). The slow roll conditions are automatically satisfied near the point where the new FI term cancels the charge of the inflaton, leading to higher than quadratic contributions due to its non trivial field dependence.

The Kähler potential can be canonical, modulo the Kähler transformation that takes it to the non R-symmetry frame. In the presence of a small superpotential, the inflation is practically unchanged and driven by the D-term, as before. However, the maximum is now slightly shifted away from the origin and the minimum has a small non-vanishing positive vacuum energy, where supersymmetry is broken by both F- and D-auxiliary expectation values of similar magnitude. The model predicts in general small primordial gravitational waves with a tensor-to-scalar ratio r well below the observability limit. However, when higher order terms are included in the Kähler potential, one finds that r can increase to large values $r \simeq 0.015$.

On general grounds, there are two classes of such models depending on whether the maximum corresponds to a point of unbroken (case 1) or broken (case 2) R-symmetry. The latter corresponds actually to a generalisation of the model we discussed above [11], inspired by string theory [3]. It has the same field content but in a different field basis with a chiral multiplet $S \propto \ln X$ playing the role of the string dilaton. Thus, S has a shift symmetry which is actually an R-symmetry gauged by a vector multiplet and the superpotential is a single exponential. The scalar potential has a minimum with a tuneable vacuum energy and a maximum that can produce inflation when appropriate corrections are included in the Kähler potential. In these coordinates R-symmetry is restored at infinity, corresponding to the weak coupling limit. Small field inflation is again guaranteed consistently with the validity of the effective field theory.

In the following, we will present the main features of models of case 1, where inflation occurs near the maximum of the scalar potential where R-symmetry is restored and supersymmetry breaking is driven predominantly either by an F-term or by a D-term.

1.2 Conventions

Throughout this paper we use the conventions of [21]. A supergravity theory is specified (up to Chern-Simons terms) by a Kähler potential \mathcal{K} , a superpotential W , and the gauge kinetic functions $f_{AB}(z)$. The chiral multiplets z^α, χ^α are enumerated by the index α and the indices A, B indicate the different gauge groups. Classically, a supergravity theory is invariant under Kähler transformations, viz.

$$\begin{aligned}\mathcal{K}(z, \bar{z}) &\longrightarrow \mathcal{K}(z, \bar{z}) + J(z) + \bar{J}(\bar{z}), \\ W(z) &\longrightarrow e^{-\kappa^2 J(z)} W(z),\end{aligned}\tag{1.1}$$

where κ is the inverse of the reduced Planck mass, $M_{\text{Pl}} = \kappa^{-1} = 2.4 \times 10^{15}$ TeV. The gauge transformations of chiral multiplet scalars are given by holomorphic Killing vectors, i.e. $\delta z^\alpha = \theta^A k_A^\alpha(z)$, where θ^A is the gauge parameter of the gauge group A . The Kähler potential and superpotential need not be invariant under this gauge transformation, but can change by a Kähler transformation

$$\delta \mathcal{K} = \theta^A [r_A(z) + \bar{r}_A(\bar{z})], \quad (1.2)$$

provided that the gauge transformation of the superpotential satisfies $\delta W = -\theta^A \kappa^2 r_A(z) W$. One then has from $\delta W = W_\alpha \delta z^\alpha$

$$W_\alpha k_A^\alpha = -\kappa^2 r_A W, \quad (1.3)$$

where $W_\alpha = \partial_\alpha W$ and α labels the chiral multiplets. The supergravity theory can then be described by a gauge invariant function

$$\mathcal{G} = \kappa^2 \mathcal{K} + \log(\kappa^6 W \bar{W}). \quad (1.4)$$

The scalar potential is given by

$$\begin{aligned} V &= V_F + V_D \\ V_F &= e^{\kappa^2 \mathcal{K}} \left(-3\kappa^2 W \bar{W} + \nabla_\alpha W g^{\alpha\beta} \bar{\nabla}_{\bar{\beta}} \bar{W} \right) \\ V_D &= \frac{1}{2} (\text{Ref})^{-1 A B} \mathcal{P}_A \mathcal{P}_B, \end{aligned} \quad (1.5)$$

where W appears with its Kähler covariant derivative

$$\nabla_\alpha W = \partial_\alpha W(z) + \kappa^2 (\partial_\alpha \mathcal{K}) W(z). \quad (1.6)$$

The moment maps \mathcal{P}_A are given by

$$\mathcal{P}_A = i(k_A^\alpha \partial_\alpha \mathcal{K} - r_A). \quad (1.7)$$

In this paper we will be concerned with theories having a gauged R-symmetry, for which $r_A(z)$ is given by an imaginary constant $r_A(z) = i\kappa^{-2}\xi$. In this case, $\kappa^{-2}\xi$ is a Fayet-Iliopoulos [4] constant parameter.

1.3 Symmetric versus non-symmetric point

Here, we present a class of inflation models in supergravity theories containing a single chiral multiplet transforming under a gauged R-symmetry with a corresponding abelian vector multiplet [16]. We assume that the chiral multiplet \mathcal{X} (with scalar component X) transforms as:

$$X \longrightarrow X e^{-iq\omega}. \quad (1.8)$$

where q is its charge, and ω is the gauge parameter.

The Kähler potential is therefore a function of $X\bar{X}$, while the superpotential is constrained to be of the form X^b :

$$\begin{aligned}\mathcal{K} &= \mathcal{K}(X\bar{X}), \\ W &= \kappa^{-3} f X^b,\end{aligned}\tag{1.9}$$

where X is a dimensionless field. For $b \neq 0$, the gauge symmetry eq. (1.8) becomes a gauged R-symmetry. The gauge kinetic function can have a constant contribution as well as a contribution proportional to $\ln X$

$$f(X) = \gamma + \beta \ln X.\tag{1.10}$$

The latter contribution proportional to β is not gauge invariant and can be used as a Green-Schwarz counter term to cancel possible anomalies. One can show however that the constant β is fixed to be very small by anomaly cancellation conditions and does not change our results [16]. We will therefore omit this term in our analysis below.

We are interested in the general properties of supergravity theories of inflation that are of the above form. Before performing our analysis, a distinction should be made concerning the initial point where slow-roll inflation starts. The inflaton field (which will turn out to be ρ , where $X = \rho e^{i\theta}$) can either have its initial value close to the symmetric point where $X = 0$, or at a generic point $X \neq 0$. The minimum of the potential, however, is always at a nonzero point $X \neq 0$. This is because at $X = 0$ the negative contribution to the scalar potential vanishes and no cancellation between F-term and D-term is possible. The supersymmetry breaking scale is therefore related to the cosmological constant as $\kappa^{-2} m_{3/2}^2 \approx \Lambda$. One could in principle assume that the value of the potential at its minimum is of the order of the supersymmetry breaking scale. However, in this case additional corrections are needed to bring down the minimum of the potential to the present value of the cosmological constant, and we therefore do not discuss this possibility.

In the first case, inflation starts near $X = 0$, and the inflaton field will roll towards a minimum of the potential at $X \neq 0$. On the other hand, in the second case inflation will start at a generic point $X \neq 0$. It is then convenient to work with another chiral superfield S , which is invariant under a shift symmetry

$$S \longrightarrow S - i c \alpha\tag{1.11}$$

by performing a field redefinition

$$X = e^S.\tag{1.12}$$

In this case the most general Kähler potential and superpotential are of the form

$$\begin{aligned}\mathcal{K} &= \mathcal{K}(S + \bar{S}), \\ W &= \kappa^{-3} a e^{bS}.\end{aligned}\tag{1.13}$$

Note that this field redefinition is not valid at the symmetric point $X = 0$ for the first case.

1.4 Case 1: Inflation near the symmetric point

1.4.1 Slow roll parameters

In this section we derive the conditions that lead to slow-roll inflation scenarios, where the start of inflation is near a local maximum of the potential at $X = 0$. Since the superpotential has charge 2 under R-symmetry, one has $\langle W \rangle = 0$ as long as R-symmetry is preserved. Therefore, $\langle W \rangle$ can be regarded as the order parameter of R-symmetry breaking. On the other hand, the minimum of the potential requires $\langle W \rangle \neq 0$ and broken R-symmetry. It is therefore attractive to assume that at earlier times R-symmetry was a good symmetry, switching off dangerous corrections to the potential. As similar approach was followed in [22], where a discrete R-symmetry is assumed. Instead, we assume a gauged R-symmetry which is spontaneously broken at the minimum of the potential.

While the superpotential is uniquely fixed in eq. (1.9), the Kähler potential is only fixed to be of the form $\mathcal{K}(X\bar{X})$. We expand the Kähler potential as follows

$$\begin{aligned}\mathcal{K}(X, \bar{X}) &= \kappa^{-2} X\bar{X} + \kappa^{-2} A(X\bar{X})^2, \\ W(X) &= \kappa^{-3} f X^b, \\ f(X) &= 1,\end{aligned}\tag{1.14}$$

where A and f are constants. The gauge kinetic function is taken to be constant since it was shown that the coefficient β in front of the logarithmic term in eq. (1.10) is fixed to be very small by anomaly cancellation conditions [16]. As far as the scalar potential is concerned, the coefficient γ can be absorbed in other parameters of the theory. We therefore take $\gamma = 1$.

The scalar potential is given by

$$\mathcal{V} = \mathcal{V}_F + \mathcal{V}_D,\tag{1.15}$$

where

$$\mathcal{V}_F = \kappa^{-4} f^2 (X\bar{X})^{b-1} e^{X\bar{X}(1+AX\bar{X})} \left[-3X\bar{X} + \frac{(b + X\bar{X}(1 + 2AX\bar{X}))^2}{1 + 4AX\bar{X}} \right]\tag{1.16}$$

and

$$\mathcal{V}_D = \kappa^{-4} \frac{q^2}{2} [b + X\bar{X}(1 + 2AX\bar{X})]^2.\tag{1.17}$$

The superpotential is not gauge invariant under the $U(1)$ gauge symmetry. Instead it transforms as

$$W \rightarrow W e^{-iq b w}.\tag{1.18}$$

Therefore, the $U(1)$ is a gauged R-symmetry which we will further denote as $U(1)_R$. From $W_X k_R^X = -r_R \kappa^2 W$, where $k_R^X = -iqX$ is the Killing vector for the field X under the R-symmetry, $r_R = i\kappa^{-2} \xi_R$ with $\kappa^{-2} \xi_R$ the Fayet-Iliopoulos contribution to the scalar potential, and W_X is short-hand for $\partial W / \partial X$, we find

$$r_R = i\kappa^{-2} q b.\tag{1.19}$$

A consequence of the gauged R-symmetry is that the superpotential coupling b enters the D-term contribution of the scalar potential as a constant Fayet-Iliopoulos contribution.⁴

Note that the scalar potential is only a function of the modulus of X and that the potential contains a Fayet-Iliopoulos contribution for $b \neq 0$. Moreover, its phase will be ‘eaten’ by the $U(1)$ gauge boson upon a field redefinition of the gauge potential similarly to the standard Higgs mechanism. After performing a change of field variables

$$X = \rho e^{i\theta}, \quad \bar{X} = \rho e^{-i\theta}, \quad (\rho \geq 0) \quad (1.20)$$

the scalar potential is a function of ρ ,

$$\kappa^4 \mathcal{V} = f^2 \rho^{2(b-1)} e^{\rho^2 + A\rho^4} \left(-3\rho^2 + \frac{(b + \rho^2 + 2A\rho^4)^2}{1 + 4A\rho^2} \right) + \frac{q^2}{2} (b + \rho^2 + 2A\rho^4)^2. \quad (1.21)$$

Since we assume that inflation starts near $\rho = 0$, we require that the potential eq. (1.21) has a local maximum at this point. It turns out that the potential only allows for a local maximum at $\rho = 0$ when $b = 1$. For $b < 1$ the potential diverges when ρ goes to zero. For $1 < b < 1.5$ the first derivative of the potential diverges, while for $b = 1.5$, one has $V'(0) = \frac{2}{4}f^2 + \frac{3}{2}q^2 > 0$, and for $b > 1.5$, one has $V''(0) > 0$. We thus take $b = 1$ and the scalar potential reduces to

$$\kappa^4 \mathcal{V} = f^2 e^{\rho^2 + A\rho^4} \left(-3\rho^2 + \frac{(1 + \rho^2 + 2A\rho^4)^2}{1 + 4A\rho^2} \right) + \frac{q^2}{2} (1 + \rho^2 + 2A\rho^4)^2. \quad (1.22)$$

A plot of the potential for $A = 1/2$, $q = 1$ and f tuned so that the minimum has zero energy is given in Figure 1.1.

Note that in this case the the superpotential is linear $W = fX$, describing the sgoldstino (up to an additional low-energy constraint) [26]. Indeed, modulo a D-term contribution, the inflaton in this model is the superpartner of the goldstino. In fact, for $q = 0$ the inflaton reduces to the partner of the goldstino as in Minimal Inflation models [27]. The important difference however is that this is a microscopic realisation of the identification of the inflaton with the sgoldstino, and that the so-called η -problem is avoided (see discussion below).

The kinetic terms for the scalars can be written as⁵

$$\begin{aligned} \mathcal{L}_{\text{kin}} &= -g_{X\bar{X}} \hat{\partial}_\mu X \hat{\partial}^\mu \bar{X} \\ &= -g_{X\bar{X}} \left[\partial_\mu \rho \partial^\mu \rho + \rho^2 (\partial_\mu \theta + qA_\mu) (\partial^\mu \theta + qA^\mu) \right]. \end{aligned} \quad (1.23)$$

It was already anticipated above that the phase θ plays the role of the longitudinal component of the gauge field A_μ , which acquires a mass by a Brout-Englert-Higgs mechanism.

⁴ For other studies of inflation involving Fayet-Iliopoulos terms see for example [24], or [25] for more recent work. Moreover, our motivations have some overlap with [22], where inflation is also assumed to start near an R-symmetric point at $X = 0$. However, this work uses a discrete R-symmetry which does not lead to Fayet-Iliopoulos terms.

⁵ The covariant derivative is defined as $\hat{\partial}_\mu X = \partial_\mu X - A_\mu k_R^X$, where $k_R^X = -iqX$ is the Killing vector for the $U(1)$ transformation eq. (1.8).

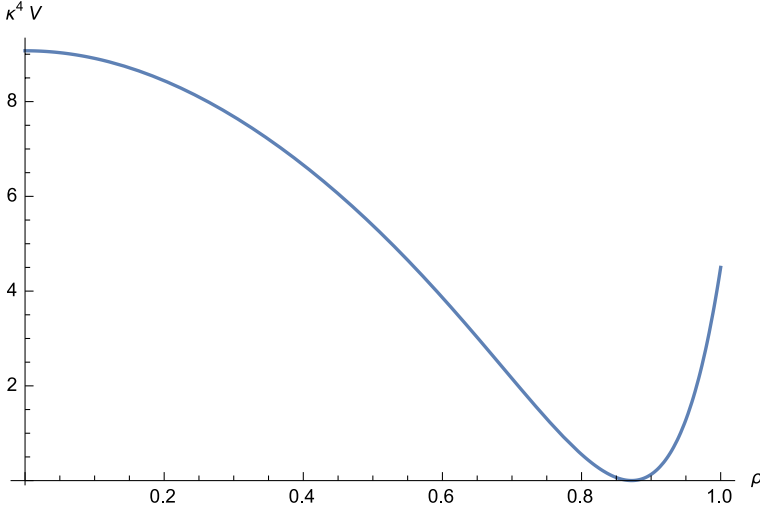


Fig.1.1.

We now interpret the field ρ as the inflaton. It is important to emphasise that, in contrast with usual supersymmetric theories of inflation where one necessarily has two scalar degrees of freedom resulting in multifield inflation [28], our class of models contains only one scalar field ρ as the inflaton. In order to calculate the slow-roll parameters, one needs to work with the canonically normalised field χ satisfying

$$\frac{d\chi}{d\rho} = \sqrt{2g_{\chi\chi}}. \quad (1.24)$$

The slow-roll parameters are given in terms of the canonical field χ by

$$\epsilon = \frac{1}{2\kappa^2} \left(\frac{dV/d\chi}{V} \right)^2, \quad \eta = \frac{1}{\kappa^2} \frac{d^2V/d\chi^2}{V}. \quad (1.25)$$

Since we assume inflation to start near $\rho = 0$, we expand

$$\begin{aligned} \epsilon &= 4 \left(\frac{-4A+x^2}{2+x^2} \right)^2 \rho^2 + \mathcal{O}(\rho^4), \\ \eta &= 2 \left(\frac{-4A+x^2}{2+x^2} \right) + \mathcal{O}(\rho^2), \end{aligned} \quad (1.26)$$

where we defined $q = fx$. Notice that for $\rho \ll 1$ the ϵ parameter is very small, while the η parameter can be made small by carefully tuning the parameter A . Any higher order corrections to the Kähler potential do not contribute to the leading contributions in the expansion near $\rho = 0$ for η and ϵ . Such corrections can therefore be used to alter the potential near its minimum, at some point $X \neq 0$ without influencing the slow-roll parameters.

A comment on the η -problem in Supergravity A few words are now in order concerning the η -problem [29]. The η problem in $\mathcal{N} = 1$ supergravity is often

stated as follows (see for example [30]): If, for instance, a theory with a single chiral multiplet with scalar component φ is taken, then the Kähler potential can be expanded around a reference location $\varphi = 0$ as $\mathcal{K} = \mathcal{K}(0) + \mathcal{K}_{\varphi\bar{\varphi}}(0)\varphi\bar{\varphi} + \dots$. The Lagrangian becomes

$$\mathcal{L} = -\partial_\mu\phi\partial^\mu\bar{\phi} - \mathcal{V}(0) (1 + \kappa^2\phi\bar{\phi} + \dots), \quad (1.27)$$

where ϕ is the canonically normalised field $\phi\bar{\phi} = \mathcal{K}_{\varphi\bar{\varphi}}(0)\varphi\bar{\varphi}$, and the ellipses stand for extra terms in the expansion coming from \mathcal{K} and W . Following this argument, the mass m_ϕ turns out to be proportional to the Hubble scale

$$m_\phi^2 = \kappa^2\mathcal{V}(0) + \dots = 3H^2 + \dots, \quad (1.28)$$

and therefore

$$\eta = \frac{m_\phi^2}{3H^2} = 1 + \dots \quad (1.29)$$

Or otherwise stated, this leading contribution of order 1 to the η -parameter has its origin from the fact that the F-term contribution to the scalar potential contains an exponential factor $e^{\mathcal{K}}$: $\mathcal{V} = e^{\mathcal{K}} [\dots]$ resulting in its second derivative $\mathcal{V}_{\chi\bar{\chi}} = \mathcal{V}[1 + \dots]$.

However, in our model the factor '1' drops out for the particular choice $b = 1$ in the superpotential⁶, resulting in an inflaton mass m_ρ^2 which is determined by the next term $A(X\bar{X})^2$ in the expansion of the Kähler potential,

$$\begin{aligned} m_\chi^2 &= (-4A + x^2) \kappa^{-2}f^2 + \mathcal{O}(\rho^2), \\ H^2 &= \frac{\kappa^{-2}f^2}{6}(2 + x^2) + \mathcal{O}(\rho^2). \end{aligned} \quad (1.30)$$

As a result, there are two ways to evade the η -problem:

- First, one can obtain a small η by having a small $q \ll f$, while A should be of order $\mathcal{O}(10^{-1})$. In this case, the rôle of the gauge symmetry is merely to constrain the form of the Kähler potential and the superpotential, and to provide a Higgs mechanism that eliminates the extra scalar (phase) degree of freedom.
- Alternatively there could be a cancellation between q^2 and $4Af^2$.

Since A is the second term in the expansion of the Kähler potential eq. (1.14), it is natural to be of order $\mathcal{O}(10^{-1})$ and therefore providing a solution to the η -problem.

Note that the mass of the inflaton given in eqs. (1.30) is only valid during inflation at small ρ . The mass of the inflaton at its VEV will be affected by additional corrections that are needed to obtain in particular a vanishing value for the scalar potential at its minimum [16].

⁶ Note that in hybrid inflation models the η -problem is also evaded by a somewhat similar way, but these models generally include several scalar fields (and superfields) besides the inflaton (see e.g. [31]).

The upper bound on the tensor-to-scalar ratio Before moving on to the next section, let us focus on the approximation at $\rho \ll 1$ where the perturbative expansion of the slow-roll parameters in eqs. (1.26) is valid, and assume that the horizon exit occurs at the field value ρ_* very close to the maximum $\rho = 0$. In this approximation, eqs. (1.26) become

$$\epsilon(\rho) \approx \epsilon^{\text{pert}}(\rho) = |\eta_*|^2 \rho^2, \quad \eta(\rho) \approx \eta_*, \quad (1.31)$$

where the asterisk refers to the value of parameters evaluated at the horizon exit.

To discuss the upper bound on the tensor-to-scalar ratio, it is convenient to divide the region $[\rho = 0, \rho_{\text{end}}]$ into two regions: one is $[0, \rho_p]$, where the approximation 1.31 is valid, and the other is the rest $[\rho_p, \rho_{\text{end}}]$. Here ρ_{end} means the inflation end. Note that $\rho_p < \rho_{\text{end}}$ because the approximation 1.31 breaks down before the end of inflation where $\epsilon(\rho_{\text{end}}) = 1$ or $|\eta(\rho_{\text{end}})| = 1$. In terms of this division, the number of e-folds from the horizon exit to the end of inflation can be approximated by

$$N_{\text{CMB}} \simeq N^{\text{pert}}(\rho_*, \rho_p) + \kappa \int_{\chi_p}^{\chi_{\text{end}}} \frac{d\chi}{\sqrt{2\epsilon(\chi)}}, \quad (1.32)$$

where we introduced

$$N^{\text{pert}}(\rho_1, \rho_2) = \kappa \int_{\chi_1}^{\chi_2} \frac{d\chi}{\sqrt{2\epsilon^{\text{pert}}(\chi)}} = \frac{1}{|\eta_*|} \ln \left(\frac{\rho_2}{\rho_1} \right). \quad (1.33)$$

Here χ is the canonically normalised field defined by eq. (1.24). Let us next focus on the region $[\rho_p, \rho_{\text{end}}]$. It is natural to expect the following inequality

$$\kappa \int_{\chi_p}^{\chi_{\text{end}}} \frac{d\chi}{\sqrt{2\epsilon(\chi)}} \lesssim \kappa \int_{\chi_p}^{\chi_{\text{end}}} \frac{d\chi}{\sqrt{2\epsilon^{\text{pert}}(\chi)}}. \quad (1.34)$$

This is based on the following observation. The right hand side describes a hypothetical situation, as if the slow-roll condition were valid throughout the inflation until its end. But since in the actual inflation the slow-roll condition breaks down in the region $[\rho_p, \rho_{\text{end}}]$, the actual number of e-folds in this region will be smaller than that in the hypothetical situation. Adding $N^{\text{pert}}(\rho_*, \rho_p)$ to the both hand sides of 1.34 and using 1.32, we find

$$N_{\text{CMB}} \lesssim \frac{1}{|\eta_*|} \ln \left(\frac{\rho_{\text{end}}}{\rho_*} \right). \quad (1.35)$$

Using 1.31 and the definition of the tensor-to-scalar ratio $r = 16\epsilon_*$, we obtain the upper bound:

$$r \lesssim 16 \left(|\eta_*| \rho_{\text{end}} e^{-|\eta_*| N_{\text{CMB}}} \right)^2. \quad (1.36)$$

To satisfy CMB data, let us choose $\eta = -0.02$ and $N_{\text{CMB}} \approx 50$. Assuming $\rho_{\text{end}} \lesssim 1/2$, we obtain the upper bound $r \lesssim 10^{-4}$. Note that this is a little bit lower than the Lyth bound [32] for small field inflation, $r \lesssim 10^{-3}$. From the upper bound on r , we can also find the upper bound on the Hubble parameter as follows. In general, the

power spectrum amplitude A_s is related to the Hubble parameter at horizon exit H_* by

$$A_s = \frac{2\kappa^2 H_*^2}{\pi^2 r}. \quad (1.37)$$

Combining this with the upper bound $r \lesssim 10^{-4}$ and the value $A_s = 2.2 \times 10^{-9}$ by CMB data, we find the upper bound on the Hubble parameter $H_* \lesssim 10^9$ TeV.

In Ref. [16], we will also find the lower bound $r \gtrsim 10^{-9}$ (equivalently $H_* \gtrsim 10^7$ TeV), based on an model-independent argument. This bound can be lowered at the cost of naturalness between parameters in the potential.

1.5 On the new FI term

1.5.1 Review

In [19], the authors propose a new contribution to the supergravity Lagrangian of the form⁷

$$\mathcal{L}_{\text{FI}} = \xi_2 \left[S_0 \bar{S}_0 \frac{w^2 \bar{w}^2}{T(w^2) \bar{T}(\bar{w}^2)} (V)_D \right]_D. \quad (1.38)$$

The chiral compensator field S_0 , with Weyl and chiral weights (Weyl, Chiral) = (1, 1), has components $S_0 = (s_0, P_L \Omega_0, F_0)$. The vector multiplet has vanishing Weyl and chiral weights, and its components are given by $V = (v, \zeta, \mathcal{H}, v_\mu, \lambda, D)$. In the Wess-Zumino gauge, the first components are put to zero $v = \zeta = \mathcal{H} = 0$. The multiplet w^2 is of weights (1, 1), and given by

$$w^2 = \frac{\bar{\lambda} P_L \lambda}{S_0^2}, \quad \bar{w}^2 = \frac{\lambda P_R \bar{\lambda}}{\bar{S}_0^2}. \quad (1.39)$$

The components of $\bar{\lambda} P_L \lambda$ are given by

$$\bar{\lambda} P_L \lambda = \left(\bar{\lambda} P_L \lambda ; \sqrt{2} P_L \left(-\frac{1}{2} \gamma \cdot \hat{F} + iD \right) \lambda ; 2 \bar{\lambda} P_L \not{D} \lambda + \hat{F}^- \cdot \hat{F}^- - D^2 \right). \quad (1.40)$$

The kinetic terms for the gauge multiplet are given by

$$\mathcal{L}_{\text{kin}} = -\frac{1}{4} [\bar{\lambda} P_L \lambda]_F + \text{h.c.} . \quad (1.41)$$

The operator T (\bar{T}) is defined in [34,35], and leads to a chiral (antichiral) multiplet. For example, the chiral multiplet $T(\bar{w}^2)$ has weights (2, 2). In global supersymmetry the operator T corresponds to the usual chiral projection operator \bar{D}^2 .⁸

From now on, we will drop the notation of h.c. and implicitly assume its presence for every $[\]_F$ term in the Lagrangian. Finally, the multiplet $(V)_D$ is a linear multiplet with weights (2, 0), given by

$$(V)_D = (D, \not{D} \lambda, 0, \mathcal{D}^b \hat{F}_{ab}, -\not{D} \not{D} \lambda, -\square^C D). \quad (1.42)$$

⁷ A similar, but not identical term was studied in [33].

⁸ The operator T indeed has the property that $T(Z) = 0$ for a chiral multiplet Z . Moreover, for a vector multiplet V we have $T(ZC) = ZT(C)$, and $[C]_D = \frac{1}{2} [T(C)]_F$.

The definitions of $\mathcal{D}\lambda$ and the covariant field strength \hat{F}_{ab} can be found in eq. (17.1) of [23], which reduce for an abelian gauge field to

$$\begin{aligned}\hat{F}_{ab} &= e_a^\mu e_b^\nu (2\partial_{[\mu} A_{\nu]} + \bar{\Psi}_{[\mu} \gamma_{\nu]} \lambda) \\ \mathcal{D}_\mu \lambda &= \left(\partial_\mu - \frac{3}{2} b_\mu + \frac{1}{4} w_\mu^{ab} \gamma_{ab} - \frac{3}{2} i \gamma_* \mathcal{A}_\mu \right) \lambda - \left(\frac{1}{4} \gamma^{ab} \hat{F}_{ab} + \frac{1}{2} i \gamma_* D \right) \psi_\mu.\end{aligned}\tag{1.43}$$

Here, e_a^μ is the vierbein, with frame indices a, b and coordinate indices μ, ν . The fields w_μ^{ab} , b_μ , and \mathcal{A}_μ are the gauge fields corresponding to Lorentz transformations, dilatations, and T_R symmetry of the conformal algebra respectively, while ψ_μ is the gravitino. The conformal d'Alembertian is given by $\square^C = \eta^{ab} \mathcal{D}_a \mathcal{D}_b$.

It is important to note that the FI term given by eq. (1.38) does not require the gauging of an R-symmetry, but breaks invariance under Kähler transformations. In fact, a gauged R-symmetry would forbid such a term \mathcal{L}_{FI} [19].⁹

The resulting Lagrangian after integrating out the auxiliary field D contains a term

$$\mathcal{L}_{FI, \text{new}} = -\frac{\xi_2^2}{2} (s_0 \bar{s}_0)^2.\tag{1.44}$$

In the absence of additional matter fields, one can use the Poincaré gauge $s_0 = \bar{s}_0 = 1$, resulting in a constant D-term contribution to the scalar potential. This prefactor however is relevant when matter couplings are included in the next section.

1.5.2 Adding (charged) matter fields

In this section we couple the term \mathcal{L}_{FI} given by eq. (1.38) to additional matter fields charged under the $U(1)$. For simplicity, we focus on a single chiral multiplet X . The extension to more chiral multiplets is trivial. The Lagrangian is given by

$$\mathcal{L} = -3 \left[S_0 \bar{S}_0 e^{-\frac{1}{3} K(X, \bar{X})} \right]_D + [S_0^3 W(X)]_F - \frac{1}{4} [f(X) \bar{\lambda} P_L \lambda]_F + \mathcal{L}_{FI},\tag{1.45}$$

with a Kähler potential $K(X, \bar{X})$, a superpotential $W(X)$ and a gauge kinetic function $f(X)$. The first three terms in eq. (1.45) give the usual supergravity Lagrangian [23]. We assume that the multiplet X transforms under the $U(1)$,

$$\begin{aligned}V &\rightarrow V + \Lambda + \bar{\Lambda}, \\ X &\rightarrow X e^{-q\Lambda},\end{aligned}\tag{1.46}$$

with gauge multiplet parameter Λ . We assume that the $U(1)$ is not an R-symmetry. In other words, we assume that the superpotential does not transform under the gauge symmetry. For a model with a single chiral multiplet this implies that the superpotential is constant

$$W(X) = F.\tag{1.47}$$

⁹ We kept the notation of [19]. Note that in this notation the field strength superfield \mathcal{W}_α is given by $\mathcal{W}^2 = \bar{\lambda} P_L \lambda$, and $(V)_D$ corresponds to $\mathcal{D}^\alpha \mathcal{W}_\alpha$.

Gauge invariance fixes the Kähler potential to be a function of $Xe^{qV}\bar{X}$ (for notational simplicity, in the following we omit the e^{qV} factors).

Indeed, in this case the term \mathcal{L}_{FI} can be consistently added to the theory, similar to [19], and the resulting D-term contribution to the scalar potential acquires an extra term proportional to ξ_2

$$\mathcal{V}_D = \frac{1}{2} \text{Re}(f(X))^{-1} \left(i k_X \partial_X K + \xi_2 e^{\frac{2}{3}K} \right)^2, \quad (1.48)$$

where the Killing vector is $k_X = -iqX$ and $f(X)$ is the gauge kinetic function. The F-term contribution to the scalar potential remains the usual

$$\mathcal{V}_F = e^{K(X, \bar{X})} \left(-3W\bar{W} + g^{X\bar{X}} \nabla_X W \bar{\nabla}_{\bar{X}} \bar{W} \right). \quad (1.49)$$

For a constant superpotential (1.47) this reduces to

$$\mathcal{V}_F = |F|^2 e^{K(X, \bar{X})} \left(-3 + g^{X\bar{X}} \partial_X K \partial_{\bar{X}} \bar{K} \right). \quad (1.50)$$

From eq. (1.48) it can be seen that if the Kähler potential includes a term proportional to $\xi_1 \log(X\bar{X})$, the D-term contribution to the scalar potential acquires another constant contribution. For example, if

$$K(X, \bar{X}) = X\bar{X} + \xi_1 \ln(X\bar{X}), \quad (1.51)$$

the D-term contribution to the scalar potential becomes

$$\mathcal{V}_D = \frac{1}{2} \text{Re}(f(X))^{-1} \left(qX\bar{X} + q\xi_1 + \xi_2 e^{\frac{2}{3}K} \right)^2. \quad (1.52)$$

In fact the contribution proportional to ξ_1 is the usual FI term in a non R-symmetric Kähler frame, which can be consistently added to the model including the new FI term proportional to ξ_2 .

In the absence of the extra term, a Kähler transformation

$$\begin{aligned} K(X, \bar{X}) &\rightarrow K(X, \bar{X}) + J(X) + \bar{J}(\bar{X}), \\ W(X) &\rightarrow W(X) e^{-J(X)}, \end{aligned} \quad (1.53)$$

with $J(X) = -\xi_1 \ln X$ allows one to recast the model in the form

$$\begin{aligned} K(X, \bar{X}) &= X\bar{X}, \\ W(X) &= m_{3/2} X. \end{aligned} \quad (1.54)$$

The two models result in the same Lagrangian, at least classically¹⁰. However, in the Kähler frame of eqs. (1.54) the superpotential transforms nontrivially under the gauge symmetry. As a consequence, the gauge symmetry becomes an R-symmetry. Note that [18]:

1. The extra term (1.38) violates the Kähler invariance of the theory, and the two models related by a Kähler transformation are no longer equivalent.
2. The model written in the Kähler frame where the gauge symmetry becomes an R-symmetry in eqs. (1.54) can not be consistently coupled to \mathcal{L}_{FI} .

¹⁰ At the quantum level, a Kähler transformation also introduces a change in the gauge kinetic function f , see for example [36].

1.6 The scalar potential in a Non R-symmetry frame

In this section, we work in the Kähler frame where the superpotential does not transform, and take into account the two types of FI terms which were discussed in the last section. For convenience, we repeat here the Kähler potential in eq. (1.51) and restore the inverse reduced Planck mass $\kappa = M_{\text{Pl}}^{-1} = (2.4 \times 10^{18} \text{ GeV})^{-1}$:

$$K = \kappa^{-2} (X\bar{X} + \xi_1 \ln X\bar{X}). \quad (1.55)$$

The superpotential and the gauge kinetic function are set to be constant¹¹:

$$W = \kappa^{-3} F, \quad f(X) = 1. \quad (1.56)$$

After performing a change of the field variable $X = \rho e^{i\theta}$ where $\rho \geq 0$ and setting $\xi_1 = b$, the full scalar potential $\mathcal{V} = \mathcal{V}_F + \mathcal{V}_D$ is a function of ρ . The F-term contribution to the scalar potential is given by

$$\mathcal{V}_F = \frac{1}{\kappa^4} F^2 e^{\rho^2} \rho^{2b} \left[\frac{(b + \rho^2)^2}{\rho^2} - 3 \right], \quad (1.57)$$

and the D-term contribution is

$$\mathcal{V}_D = \frac{q^2}{2\kappa^4} \left(b + \rho^2 + \xi \rho^{\frac{4b}{3}} e^{\frac{2}{3}\rho^2} \right)^2. \quad (1.58)$$

Note that we rescaled the second FI parameter by $\xi = \xi_2/q$. We consider the case with $\xi \neq 0$ because we are interested in the role of the new FI-term in inflationary models driven by supersymmetry breaking. Moreover, the limit $\xi \rightarrow 0$ is ill-defined [19].

The first FI parameter b was introduced as a free parameter. We now proceed to narrowing the value of b by the following physical requirements. We first consider the behaviour of the potential around $\rho = 0$,

$$\mathcal{V}_D = \frac{q^2}{2\kappa^4} \left[(b^2 + 2b\rho^2 + O(\rho^4)) + 2b\xi\rho^{\frac{4b}{3}} (1 + O(\rho^2)) + \xi^2\rho^{\frac{8b}{3}} (1 + O(\rho^2)) \right], \quad (1.59)$$

$$\mathcal{V}_F = \frac{F^2}{\kappa^4} \rho^{2b} \left[b^2 \rho^{-2} + (2b - 3) + O(\rho^2) \right]. \quad (1.60)$$

Here we are interested in small-field inflation models in which the inflation starts in the neighbourhood of a local maximum at $\rho = 0$. In [16], we considered models of this type with $\xi = 0$ (which were called Case 1 models), and found that the choice $b = 1$ is forced by the requirement that the potential takes a finite value at the local maximum $\rho = 0$. Now, we will investigate the effect of the new FI parameter ξ on the choice of b under the same requirement.

¹¹ Strictly speaking, the gauge kinetic function gets a field-dependent correction proportional to $q^2 \ln \rho$, in order to cancel the chiral anomalies [11]. However, the correction turns out to be very small and can be neglected below, since the charge q is chosen to be of order of 10^{-5} or smaller.

First, in order for $\mathcal{V}(0)$ to be finite, we need $b \geq 0$. We first consider the case $b > 0$. We next investigate the condition that the potential at $\rho = 0$ has a local maximum. For clarity we discuss below the cases of $F = 0$ and $F \neq 0$ separately. The $b = 0$ case will be treated at the end of this section.

1.6.1 Case $F = 0$

In this case $\mathcal{V}_F = 0$ and the scalar potential is given by only the D-term contribution $\mathcal{V} = \mathcal{V}_D$. Let us first discuss the first derivative of the potential:

$$\mathcal{V}'_D = \frac{q^2}{2\kappa^4} \left[4b\rho(1 + O(\rho^2)) + \frac{8b^2}{3}\xi\rho^{\frac{4b}{3}-1}(1 + O(\rho^2)) + \frac{8b}{3}\xi^2\rho^{\frac{8b}{3}-1}(1 + O(\rho^2)) \right]. \quad (1.61)$$

For $\mathcal{V}'_D(0)$ to be convergent, we need $b \geq 3/4$ (note that $\xi \neq 0$). When $b = 3/4$, we have $\mathcal{V}'_D(0) = 8b^2\xi/3$, which does not give an extremum because we chose $\xi \neq 0$. On the other hand, when $b > 3/4$, we have $\mathcal{V}'_D(0) = 0$. To narrow the allowed value of b further, let us turn to the second derivative,

$$\begin{aligned} \mathcal{V}''_D = \frac{q^2}{2\kappa^4} & \left[4b(1 + O(\rho^2)) + \frac{8b^2}{3} \left(\frac{4b}{3} - 1 \right) \xi \rho^{\frac{4b}{3}-2}(1 + O(\rho^2)) \right. \\ & \left. + \frac{8b}{3} \left(\frac{8b}{3} - 1 \right) \xi^2 \rho^{\frac{8b}{3}-2}(1 + O(\rho^2)) \right]. \end{aligned} \quad (1.62)$$

When $3/4 < b < 3/2$, the second derivative $\mathcal{V}''_D(0)$ diverges. When $b > 3/2$, the second derivative becomes $\mathcal{V}''_D(0) = 2\kappa^{-4}q^2b > 0$, which gives a minimum.

We therefore conclude that to have a local maximum at $\rho = 0$, we need to choose $b = 3/2$, for which we have

$$\mathcal{V}''_D(0) = 3\kappa^{-4}q^2(\xi + 1). \quad (1.63)$$

The condition that $\rho = 0$ is a local maximum requires $\xi < -1$.

Let us next discuss the global minimum of the potential with $b = 3/2$ and $\xi < -1$. The first derivative of the potential without approximation reads

$$\mathcal{V}'_D \propto \rho(3 + 3\xi e^{\frac{2}{3}\rho^2} + 2\xi\rho^2 e^{\frac{2}{3}\rho^2})(3 + 2\rho^2 + 2\xi\rho^2 e^{\frac{2}{3}\rho^2}). \quad (1.64)$$

Since $3 + 3\xi e^{\frac{2}{3}\rho^2} + 2\xi\rho^2 e^{\frac{2}{3}\rho^2} < 0$ for $\rho \geq 0$ and $\xi < -1$, the extremum away from $\rho = 0$ is located at ρ_v satisfying the condition

$$3 + 2\rho_v^2 + 2\xi\rho_v^2 e^{\frac{2}{3}\rho_v^2} = 0. \quad (1.65)$$

Substituting this condition into the potential \mathcal{V}_D gives $\mathcal{V}_D(\rho_v) = 0$.

We conclude that for $\xi < -1$ and $b = 3/2$ the potential has a maximum at $\rho = 0$, and a supersymmetric minimum at ρ_v . We postpone the analysis of inflation near the maximum of the potential in section 1.7, and the discussion of the uplifting of the minimum in order to obtain a small but positive cosmological constant below. In the next subsection we investigate the case $F \neq 0$.

We finally comment on supersymmetry (SUSY) breaking in the scalar potential. Since the superpotential is zero, the SUSY breaking is measured by the D-term order parameter, namely the Killing potential associated with the gauged $U(1)$, which is defined by

$$\mathcal{D} = i\kappa^{-2} \frac{-iqX}{W} \left(\frac{\partial W}{\partial X} + \kappa^2 \frac{\partial \mathcal{K}}{\partial X} W \right). \quad (1.66)$$

This enters the scalar potential as $\mathcal{V}_D = \mathcal{D}^2/2$. So, at the local maximum and during inflation \mathcal{D} is of order q and supersymmetry is broken. On the other hand, at the global minimum, supersymmetry is preserved and the potential vanishes.

1.6.2 Case $F \neq 0$

In this section we take into account the effect of \mathcal{V}_F ; its first derivative reads:

$$\mathcal{V}'_F = \kappa^{-4} F^2 \left[b^2(2b-2)\rho^{2b-3} + 2b(2b-3)\rho^{2b-1}(1 + O(\rho^2)) \right]. \quad (1.67)$$

For $\mathcal{V}'(0)$ to be convergent, we need $b \geq 3/2$, for which $\mathcal{V}'_D(0) = 0$ holds. For $b = 3/2$, we have $\mathcal{V}'_F(0) = (9/4)\kappa^{-4}F^2 > 0$, that does not give an extremum. For $b > 3/2$, we have $\mathcal{V}'_F(0) = 0$. To narrow the allowed values of b further, let us turn to the second derivative,

$$\mathcal{V}''_F = \kappa^{-4} F^2 \left[b^2(2b-2)(2b-3)\rho^{2b-4} + 2b(2b-3)(2b-1)\rho^{2b-2}(1 + O(\rho^2)) \right]. \quad (1.68)$$

For $3/2 < b < 2$, the second derivative $\mathcal{V}''_F(0)$ diverges. For $b \geq 2$, the second derivative is positive $\mathcal{V}''(0) > 0$, that gives a minimum (note that $\mathcal{V}''_D(0) > 0$ as well in this range).

We conclude that the potential cannot have a local maximum at $\rho = 0$ for any choice of b . Nevertheless, as we will show below, the potential can have a local maximum in the neighbourhood of $\rho = 0$ if we choose $b = 3/2$ and $\xi < -1$. For this choice, the derivatives of the potential have the following properties,

$$\mathcal{V}'(0) < 0, \quad \mathcal{V}''(0) = 3\kappa^{-4} q^2 (\xi + 1). \quad (1.69)$$

The extremisation condition around $\rho = 0$ becomes

$$3\kappa^{-4} q^2 (\xi + 1) \rho + \frac{9}{4} \kappa^{-4} F^2 \simeq 0. \quad (1.70)$$

So the extremum is at

$$\rho \simeq -\frac{3F^2}{4q^2(\xi + 1)}. \quad (1.71)$$

Note that the extremum is in the neighbourhood of $\rho = 0$ as long as we keep the F-contribution to the scalar potential small by taking $F^2 \ll q^2|\xi + 1|$, which guarantees the approximation ignoring higher order terms in ρ . We now choose

$\xi < -1$ so that ρ for this extremum is positive. The second derivative at the extremum reads

$$\mathcal{V}'' \simeq 3\kappa^{-4} q^2 (\xi + 1), \quad (1.72)$$

as long as we ignore higher order terms in $F^2/(q^2|\xi + 1|)$. By our choice $\xi < -1$, the extremum is a local maximum, as desired.

Let us comment on the global minimum after turning on the F-term contribution. As long as we choose the parameters so that $F^2/q^2 \ll 1$, the change in the global minimum ρ_v is very small, of order $\mathcal{O}(F^2/q^2)$, because the extremisation condition depends only on the ratio F^2/q^2 . So the change in the value of the global minimum is of order $\mathcal{O}(F^2)$. The plot of this change is given in Fig. 1.2.

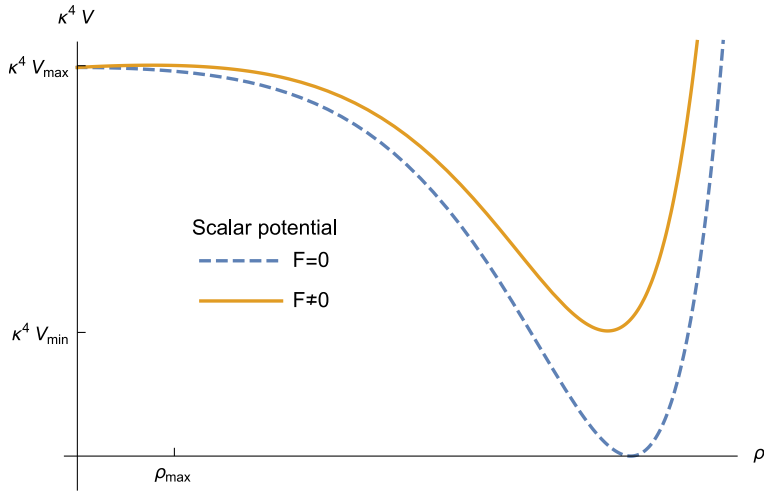


Fig. 1.2. This plot shows the scalar potentials in $F = 0$ and $F \neq 0$ cases. When $F = 0$, we have a local maximum at $\rho_{\max} = 0$ and a global minimum with zero cosmological constant. For $F \neq 0$, the local maximum is shifted by a small positive value to $\rho_{\max} \neq 0$. The global minimum now has a positive cosmological constant.

In the present case $F \neq 0$, the order parameters of SUSY breaking are both the Killing potential \mathcal{D} and the F-term contribution \mathcal{F}_X , which read

$$\mathcal{D} \propto q(\tfrac{3}{2} + \rho^2), \quad \mathcal{F}_X \propto F\rho^{1/2}e^{\rho^2/2}, \quad (1.73)$$

where the F-term order parameter \mathcal{F}_X is defined by

$$\mathcal{F}_X = -\frac{1}{\sqrt{2}} e^{\kappa^2 \mathcal{K}/2} \left(\frac{\partial^2 \mathcal{K}}{\partial X \partial \bar{X}} \right)^{-1} \left(\frac{\partial \bar{W}}{\partial \bar{X}} + \kappa^2 \frac{\partial \mathcal{K}}{\partial \bar{X}} \bar{W} \right). \quad (1.74)$$

Therefore, at the local maximum, $\mathcal{F}_X/\mathcal{D}$ is of order $\mathcal{O}((\xi + 1)^{-1/2} F^2/q^2)$ because ρ there is of order $\mathcal{O}((\xi + 1)^{-1} F^2/q^2)$. On the other hand, at the global minimum, both \mathcal{D} and \mathcal{F}_X are of order $\mathcal{O}(F)$, assuming that ρ at the minimum is of order

$\mathcal{O}(1)$, which is true in our models below. This makes tuning of the vacuum energy between the F- and D-contribution in principle possible, along the lines of [16,11].

A comment must be made here on the action in the presence of non-vanishing F and ξ . As mentioned above, the supersymmetry is broken both by the gauge sector and by the matter sector. The associated goldstino therefore consists of a linear combination of the $U(1)$ gaugino and the fermion in the matter chiral multiplet X . In the unitary gauge the goldstino is set to zero, so the gaugino is not vanishing anymore, and the action does not simplify as in Ref. [19]. This, however, only affects the part of the action with fermions, while the scalar potential does not change. This is why we nevertheless used the scalar potential (1.57) and (1.58).

Let us consider now the case $b = 0$ where only the new FI parameter ξ contributes to the potential. In this case, the condition for the local maximum of the scalar potential at $\rho = 0$ can be satisfied for $-\frac{3}{2} < \xi < 0$. When F is set to zero, the scalar potential (1.58) has a minimum at $\rho_{\min}^2 = \frac{3}{2} \ln \left(-\frac{3}{2\xi} \right)$. In order to have $\mathcal{V}_{\min} = 0$, we can choose $\xi = -\frac{3}{2e}$. However, we find that this choice of parameter ξ does not allow slow-roll inflation near the maximum of the scalar potential. Similar to the previous model of section 1.4, it may be possible to achieve both the scalar potential satisfying slow-roll conditions and a small cosmological constant at the minimum by adding correction terms to the Kähler potential and turning on a parameter F . However, here, we will focus on $b = 3/2$ case where, as we will see shortly, less parameters are required to satisfy the observational constraints.

1.7 Application in Inflation

We recall that the the models we described in section 1.4, the inflaton is identified with the sgoldstino, carrying a $U(1)$ charge under a gauged R-symmetry and inflation occurs around the maximum of the scalar potential, where the $U(1)$ symmetry is restored, with the inflaton rolling down towards the electroweak minimum. These models avoid the so-called η -problem in supergravity by taking a linear superpotential, $W \propto X$. In contrast, here we will consider models with two FI parameters b, ξ in the Kähler frame where the $U(1)$ gauge symmetry is not an R-symmetry. If the new FI term ξ is zero, these models are Kähler equivalent to those with a linear superpotential (Case 1 models with $b = 1$). The presence of non-vanishing ξ , however, breaks the Kähler invariance as we discussed before. Moreover, the FI parameter b cannot be 1 but is forced to be $b = 3/2$, according to the argument in Section 1.6. So the new models do not seem to avoid the η -problem. Nevertheless, we will show below that this is not the case and the new models with $b = 3/2$ avoid the η -problem thanks to the other FI parameter ξ which is chosen near the value at which the effective charge of X vanishes between the two FI-terms. Inflation is again driven from supersymmetry breaking but from a D-term rather than an F-term as we had before.

1.7.1 Example for slow-roll D-term inflation

In this section we focus on the case where $b = 3/2$ and derive the condition that leads to slow-roll inflation scenarios, where the start of inflation (or, horizon

crossing) is near the maximum of the potential at $\rho = 0$. We also assume that the scalar potential is D-term dominated by choosing $F = 0$, for which the model has only two parameters, namely q and ξ . The parameter q controls the overall scale of the potential and it will be fixed by the amplitude A_s of the CMB data. The only free-parameter left over is ξ , which can be tuned to satisfy the slow-roll condition.

In order to calculate the slow-roll parameters, we need to work with the canonically normalised field χ defined by eqs. (1.24), (1.25). Since we assume inflation to start near $\rho = 0$, the slow-roll parameters for small ρ can be expanded as

$$\begin{aligned}\epsilon &= \frac{F^4}{q^4} + \frac{4F^2 (2(\xi + 1)q^4 - 3F^4)}{3q^6} \rho \\ &+ \left(\frac{16}{9}(\xi + 1)^2 + \frac{2F^4 (18F^4 - q^4(20\xi + 11))}{3q^8} \right) \rho^2 + \mathcal{O}(\rho^3), \\ \eta &= \frac{4(1 + \xi)}{3} + \mathcal{O}(\rho).\end{aligned}\tag{1.75}$$

Note also that η is negative when $\xi < -1$. We can therefore tune the parameter ξ to avoid the η -problem. The observation is that at $\xi = -1$, the effective charge of X vanishes and thus the ρ -dependence in the D-term contribution (1.58) becomes of quartic order.

For our present choice $F = 0$, the potential and the slow-roll parameters become functions of ρ^2 and the slow-roll parameters for small ρ^2 read

$$\begin{aligned}\eta &= \frac{4(1 + \xi)}{3} + \mathcal{O}(\rho^2), \\ \epsilon &= \frac{16}{9}(\xi + 1)^2 \rho^2 + \mathcal{O}(\rho^4) \simeq \eta(0)^2 \rho^2.\end{aligned}\tag{1.76}$$

Note that we obtain the same relation between ϵ and η as in the model of inflation from supersymmetry breaking driven by an F-term from a linear superpotential and $b = 1$ (see eq. (1.26)). Thus, there is a possibility to have flat plateau near the maximum that satisfies the slow-roll condition and at the same time a small cosmological constant at the minimum nearby.

The number of e-folds N during inflation is determined by

$$N = \kappa^2 \int_{\chi_*}^{\chi_{\text{end}}} \frac{\mathcal{V}}{\partial_\chi \mathcal{V}} d\chi = \kappa^2 \int_{\rho_*}^{\rho_{\text{end}}} \frac{\mathcal{V}}{\partial_\rho \mathcal{V}} \left(\frac{d\chi}{d\rho} \right)^2 d\rho,\tag{1.77}$$

where we choose $|\epsilon(\chi_{\text{end}})| = 1$. Notice that the slow-roll parameters for small ρ^2 satisfy the simple relation $\epsilon = \eta(0)^2 \rho^2 + \mathcal{O}(\rho^4)$ by eq. (1.76). Therefore, the number of e-folds between $\rho = \rho_1$ and ρ_2 ($\rho_1 < \rho_2$) takes the following simple approximate form as in (1.32):

$$N \simeq \frac{1}{|\eta(0)|} \ln \left(\frac{\rho_2}{\rho_1} \right) = \frac{3}{4|\xi + 1|} \ln \left(\frac{\rho_2}{\rho_1} \right).\tag{1.78}$$

as long as the expansions in (1.76) are valid in the region $\rho_1 \leq \rho \leq \rho_2$. Here we also used the approximation $\eta(0) \simeq \eta_*$, which holds in this approximation.

We can compare the theoretical predictions of our model to the observational data via the power spectrum of scalar perturbations of the CMB, namely the amplitude A_s , tilt n_s and the tensor-to-scalar ratio of primordial fluctuations r . These are written in terms of the slow-roll parameters:

$$\begin{aligned} A_s &= \frac{\kappa^4 \mathcal{V}_*}{24\pi^2 \epsilon_*}, \\ n_s &= 1 + 2\eta_* - 6\epsilon_* \simeq 1 + 2\eta_*, \\ r &= 16\epsilon_*, \end{aligned} \tag{1.79}$$

where all parameters are evaluated at the field value at horizon crossing χ_* . From the relation of the spectral index above, one should have $\eta_* \simeq -0.02$, and thus eq. (1.78) gives approximately the desired number of e-folds when the logarithm is of order one. Actually, using this formula, we can estimate the upper bound of the tensor-to-scalar ratio r and the Hubble scale H_* following the same argument given in section 1.4; that is, the upper bounds are given by computing the parameters r, H_* assuming that the expansions (1.76) hold until the end of inflation. We then get the bound

$$r \lesssim 16(|\eta_*| \rho_{\text{end}} e^{-|\eta_*|N})^2 \simeq 10^{-4}, \quad H_* \lesssim 10^{12} \text{ GeV}, \tag{1.80}$$

where we used $|\eta_*| = 0.02$, $N \simeq 50 - 60$ and $\rho_{\text{end}} \lesssim 0.5$, which are consistent with our models. In the next subsection, we will present a model which gives a tensor-to-scalar ratio bigger than the upper bound above, by adding some perturbative corrections to the Kähler potential.

As an example, let us consider the case where

$$q = 4.544 \times 10^{-7}, \quad \xi = -1.005. \tag{1.81}$$

By choosing the initial condition $\rho_* = 0.055$ and $\rho_{\text{end}} = 0.403$, we obtain the results $N = 58$, $n_s = 0.9542$, $r = 7.06 \times 10^{-6}$ and $A_s = 2.2 \times 10^{-9}$, which are within the 2σ -region of Planck'15 data [18].

As was shown in Section 1.6.1, this model has a supersymmetric minimum with zero cosmological constant because F is chosen to be zero. One possible way to generate a non-zero cosmological constant at the minimum is to turn on the superpotential $W = \kappa^{-3}F \neq 0$, as mentioned in Section 1.6.2. In this case, the scale of the cosmological constant is of order $\mathcal{O}(F^2)$. It would be interesting to find an inflationary model which has a minimum at a tiny tuneable vacuum energy with a supersymmetry breaking scale consistent with the low energy particle physics.

1.7.2 A small field inflation model from supergravity with observable tensor-to-scalar ratio

While the results in the previous example agree with the current limits on r set by Planck, supergravity models with higher r are of particular interest. In this section we show that our model can get large r at the price of introducing some additional

terms in the Kähler potential. Let us consider the previous model with additional quadratic and cubic terms in $X\bar{X}$:

$$K = \kappa^{-2} (X\bar{X} + A(X\bar{X})^2 + B(X\bar{X})^3 + b \ln X\bar{X}), \quad (1.82)$$

while the superpotential and the gauge kinetic function remain as in eq. (1.56). We now assume that inflation is driven by the D-term, setting the parameter $F = 0$. In terms of the field variable ρ , we obtain the scalar potential:

$$\mathcal{V} = q^2 \left(b + \rho^2 + 2A\rho^4 + 3B\rho^6 + \xi\rho^{\frac{4b}{3}} e^{\frac{2}{3}(\Lambda\rho^4 + B\rho^6 + \rho^2)} \right)^2. \quad (1.83)$$

We thus have two more parameters A and B . This does not affect the arguments of the choices of b in the previous sections because these parameters appear in higher orders in ρ in the scalar potential. So, we consider the case $b = 3/2$. The simple formula (1.78) for the number of e-folds for small ρ^2 also holds even when A, B are turned on because the new parameters appear at order ρ^4 and higher. To obtain $r \approx 0.01$, we can choose for example

$$q = 2.121 \times 10^{-5}, \quad \xi = -1.140, \quad A = 0.545, \quad B = 0.230. \quad (1.84)$$

By choosing the initial condition $\rho_* = 0.240$ and $\rho_{\text{end}} = 0.720$, we obtain the results $N = 57$, $n_s = 0.9603$, $r = 0.015$ and $A_s = 2.2 \times 10^{-9}$, which agree with Planck'15 data as shown in Fig. 1.3.

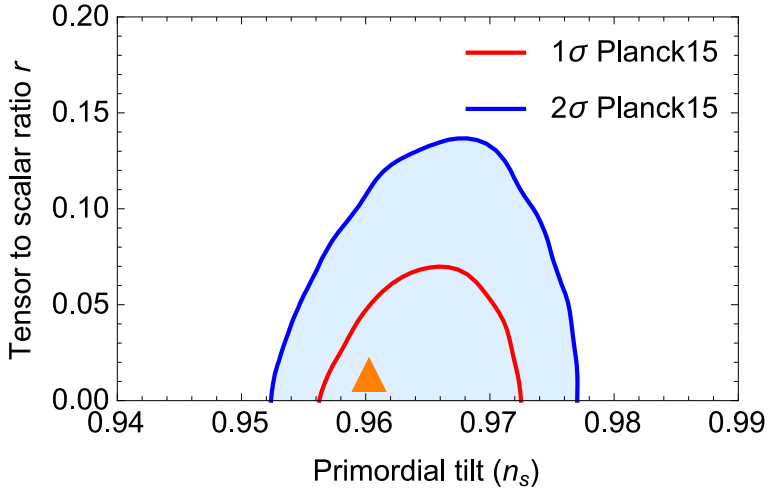


Fig. 1.3. A plot of the predictions for the scalar potential with $F = 0$, $b = 3/2$, $A = 0.545$, $B = 0.230$, $\xi = -1.140$ and $q = 2.121 \times 10^{-5}$ in the $n_s - r$ plane, versus Planck'15 results.

In summary, in contrast to the model in section 1.4, where the F-term contribution is dominant during inflation, here inflation is driven purely by a D-term. Moreover, a canonical Kähler potential (1.55) together with two FI-parameters (q and ξ) is enough to satisfy Planck'15 constraints, and no higher order correction to

the Kähler potential is needed. However, to obtain a larger tensor-to-scalar ratio, we have to introduce perturbative corrections to the Kähler potential up to cubic order in $X\bar{X}$ (i.e. up to order ρ^6). This model provides a supersymmetric extension of the model [37], which realises large r at small field inflation without referring to supersymmetry.

Acknowledgements

This work was supported in part by the Swiss National Science Foundation and in part by a CNRS PICS grant.

References

1. I. Antoniadis, N. Arkani-Hamed, S. Dimopoulos and G. R. Dvali, “New dimensions at a millimeter to a Fermi and superstrings at a TeV,” *Phys. Lett. B* **436** (1998) 257 [arXiv:hep-ph/9804398].
2. I. Antoniadis and S. P. Patil, *Eur. Phys. J. C* **75** (2015) 182 [arXiv:1410.8845 [hep-th]].
3. I. Antoniadis and R. Knoops, *Nucl. Phys. B* **886** (2014) 43 [arXiv:1403.1534 [hep-th]]; G. Villadoro and F. Zwirner, *Phys. Rev. Lett.* **95** (2005) 231602 [hep-th/0508167].
4. P. Fayet and J. Iliopoulos, “Spontaneously Broken Supergauge Symmetries and Goldstone Spinors,” *Phys. Lett.* **51B** (1974) 461; P. Fayet, *Phys. Lett. B* **69** (1977) 489.
5. I. Antoniadis, D. M. Ghilencea and R. Knoops, *JHEP* **1502** (2015) 166 [arXiv:1412.4807 [hep-th]].
6. I. Antoniadis and R. Knoops, *Nucl. Phys. B* **902** (2016) 69 [arXiv:1507.06924 [hep-ph]].
7. L. Randall and R. Sundrum, *Nucl. Phys. B* **557** (1999) 79 [hep-th/9810155]; G. F. Giudice, M. A. Luty, H. Murayama and R. Rattazzi, *JHEP* **9812** (1998) 027 [hep-ph/9810442].
8. J. A. Bagger, T. Moroi and E. Poppitz, *JHEP* **0004** (2000) 009 [hep-th/9911029].
9. I. Antoniadis and T. Maillard, “Moduli stabilization from magnetic fluxes in type I string theory,” *Nucl. Phys. B* **716** (2005) 3 [hep-th/0412008]; I. Antoniadis, A. Kumar and T. Maillard, “Magnetic fluxes and moduli stabilization,” *Nucl. Phys. B* **767** (2007) 139 [hep-th/0610246].
10. I. Antoniadis, J.-P. Derendinger and T. Maillard, “Nonlinear $N=2$ Supersymmetry, Effective Actions and Moduli Stabilization,” *Nucl. Phys. B* **808** (2009) 53 [arXiv:0804.1738 [hep-th]].
11. I. Antoniadis, A. Chatrabhuti, H. Isono and R. Knoops, “Inflation from Supergravity with Gauged R-symmetry in de Sitter Vacuum,” *Eur. Phys. J. C* **76** (2016) no.12, 680 [arXiv:1608.02121 [hep-ph]].
12. A. H. Guth, “The Inflationary Universe: A Possible Solution to the Horizon and Flatness Problems,” *Phys. Rev. D* **23** (1981) 347; A. D. Linde, “A New Inflationary Universe Scenario: A Possible Solution of the Horizon, Flatness, Homogeneity, Isotropy and Primordial Monopole Problems,” *Phys. Lett.* **108B** (1982) 389; A. Albrecht and P. J. Steinhardt, “Cosmology for Grand Unified Theories with Radiatively Induced Symmetry Breaking,” *Phys. Rev. Lett.* **48** (1982) 1220.
13. D. H. Lyth and A. Riotto, “Particle physics models of inflation and the cosmological density perturbation,” *Phys. Rept.* **314** (1999) 1 [hep-ph/9807278]; A. D. Linde, “Particle physics and inflationary cosmology,” *Contemp. Concepts Phys.* **5** (1990) 1 [hep-th/0503203].
14. A. A. Starobinsky, “A New Type of Isotropic Cosmological Models Without Singularity,” *Phys. Lett.* **91B** (1980) 99.

15. L. Randall and S. D. Thomas, "Solving the cosmological moduli problem with weak scale inflation," Nucl. Phys. B **449** (1995) 229 [hep-ph/9407248]; A. Riotto, "Inflation and the nature of supersymmetry breaking," Nucl. Phys. B **515** (1998) 413 [hep-ph/9707330]; K. I. Izawa, "Supersymmetry - breaking models of inflation," Prog. Theor. Phys. **99** (1998) 157 [hep-ph/9708315]; W. Buchmuller, L. Covi and D. Delepine, "Inflation and supersymmetry breaking," Phys. Lett. B **491** (2000) 183 [hep-ph/0006168].
16. I. Antoniadis, A. Chatrabhuti, H. Isono and R. Kneops, "Inflation from Supersymmetry Breaking," Eur. Phys. J. C **77** (2017) no.11, 724 [arXiv:1706.04133 [hep-th]].
17. F. Catino, G. Villadoro and F. Zwirner, JHEP **1201** (2012) 002 [arXiv:1110.2174 [hep-th]].
18. I. Antoniadis, A. Chatrabhuti, H. Isono and R. Kneops, "Fayet-Iliopoulos terms in supergravity and D-term inflation," Eur. Phys. J. C **78** (2018) no.5, 366 [arXiv:1803.03817 [hep-th]].
19. N. Cribiori, F. Farakos, M. Tournoy and A. Van Proeyen, "Fayet-Iliopoulos terms in supergravity without gauged R-symmetry," arXiv:1712.08601 [hep-th].
20. Y. Aldabergenov and S. V. Ketov, "Removing instability of inflation in Polonyi-Starobinsky supergravity by adding FI term," Mod. Phys. Lett. A **91** (2018) no.05, 1850032 [arXiv:1711.06789 [hep-th]].
21. D. Z. Freedman and A. Van Proeyen, Cambridge, UK: Cambridge Univ. Pr. (2012) 607 p.
22. K. Schmitz and T. T. Yanagida, "Dynamical supersymmetry breaking and late-time R symmetry breaking as the origin of cosmic inflation," Phys. Rev. D **94** (2016) no.7, 074021 [arXiv:1604.04911 [hep-ph]].
23. D. Z. Freedman and A. Van Proeyen, "Supergravity," Cambridge, UK: Cambridge Univ. Press (2012).
24. P. Binetruy and G. R. Dvali, "D term inflation," Phys. Lett. B **388** (1996) 241 [hep-ph/9606342].
25. C. Wieck and M. W. Winkler, "Inflation with Fayet-Iliopoulos Terms," Phys. Rev. D **90** (2014) no.10, 103507 [arXiv:1408.2826 [hep-th]]; V. Domcke and K. Schmitz, "Unified model of D-term inflation," Phys. Rev. D **95** (2017) no.7, 075020 [arXiv:1702.02173 [hep-ph]].
26. D. V. Volkov and V. P. Akulov, Is the neutrino a Goldstone particle?; Phys. Lett. B **46** (1973) 109; M. Roček, Linearizing the Volkov-Akulov model, Phys. Rev. Lett. **41** (1978) 451; U. Lindström, M. Roček, Constrained local superfields, Phys. Rev. D **19** (1979) 2300; R. Casalbuoni, S. De Curtis, D. Dominici, F. Feruglio and R. Gatto, Nonlinear realization of supersymmetry algebra from supersymmetric constraint, Phys. Lett. B **220** (1989) 569; Z. Komargodski and N. Seiberg, From linear SUSY to constrained superfields, JHEP **0909** (2009) 066; [arXiv:0907.2441 [hep-th]]; S. M. Kuzenko and S. J. Tyler, On the Goldstino actions and their symmetries, JHEP **1105**, (2011) 055: [arXiv:1102.3043 [hep-th]].
27. L. Alvarez-Gaume, C. Gomez and R. Jimenez, "Minimal Inflation," Phys. Lett. B **690** (2010) 68 [arXiv:1001.0010 [hep-th]]; L. Alvarez-Gaume, C. Gomez and R. Jimenez, "A Minimal Inflation Scenario," JCAP **1103** (2011) 027 [arXiv:1101.4948 [hep-th]]; S. Ferrara and D. Roest, "General sGoldstino Inflation," JCAP **1610** (2016) no.10, 038 [arXiv:1608.03709 [hep-th]].
28. D. Baumann and D. Green, "Signatures of Supersymmetry from the Early Universe," Phys. Rev. D **85** (2012) 103520 [arXiv:1109.0292 [hep-th]].
29. E. J. Copeland, A. R. Liddle, D. H. Lyth, E. D. Stewart and D. Wands, "False vacuum inflation with Einstein gravity," Phys. Rev. D **49** (1994) 6410 [astro-ph/9401011].
30. D. Baumann and L. McAllister, "Inflation and String Theory," arXiv:1404.2601 [hep-th]; M. Cicoli and F. Quevedo, "String moduli inflation: An overview," Class. Quant. Grav. **28** (2011) 204001 [arXiv:1108.2659 [hep-th]].

31. G. R. Dvali, Q. Shafi and R. K. Schaefer, "Large scale structure and supersymmetric inflation without fine tuning," *Phys. Rev. Lett.* **73** (1994) 1886 [hep-ph/9406319].
32. L. Boubekeur and D. H. Lyth, "Hilltop inflation," *JCAP* **0507** (2005) 010 [hep-ph/0502047].
33. S. M. Kuzenko, "Taking a vector supermultiplet apart: Alternative Fayet-Iliopoulos-type terms," arXiv:1801.04794 [hep-th].
34. T. Kugo and S. Uehara, "N = 1 Superconformal Tensor Calculus: Multiplets With External Lorentz Indices and Spinor Derivative Operators," *Prog. Theor. Phys.* **73** (1985) 235.
35. S. Ferrara, R. Kallosh, A. Van Proeyen and T. Wrase, "Linear Versus Non-linear Supersymmetry, in General," *JHEP* **1604** (2016) 065 [arXiv:1603.02653 [hep-th]].
36. V. Kaplunovsky and J. Louis, "Field dependent gauge couplings in locally supersymmetric effective quantum field theories," *Nucl. Phys. B* **422** (1994) 57 [hep-th/9402005].
37. I. Wolfson and R. Brustein, "Most probable small field inflationary potentials," arXiv:1801.07057 [astro-ph].



2 New Model independent Results From the First Six Full Annual Cycles of DAMA/LIBRA–Phase2

R. Bernabei¹, P. Belli¹, A. Bussolotti¹, R. Cerulli¹,
A. Di Marco¹, V. Merlo¹, F. Montecchia^{1***},
F. Cappella², A. d’Angelo², A. Incicchitti², A. Mattei²,
V. Caracciolo³,
C.J. Dai⁴, H.L. He⁴, X.H. Ma⁴,
X.D. Sheng⁴, Z.P. Ye^{4†}

¹Dip. di Fisica, Università di Roma “Tor Vergata” and
INFN, sez. Roma “Tor Vergata”, Rome, Italy

²Dip. di Fisica, Università di Roma “La Sapienza” and
INFN, sez. Roma, Rome, Italy

³Laboratori Nazionali del Gran Sasso
I.N.F.N., Assergi, Italy

⁴Key Laboratory of Particle Astrophysics
IHEP, Chinese Academy of Sciences, Beijing, China

Abstract. New model-independent results from the first six full annual cycles of DAMA/LIBRA–phase2 (total exposure of $1.13 \text{ ton} \times \text{yr}$) are presented. The new improved DAMA/LIBRA–phase2 experimental configuration ($\simeq 250 \text{ kg}$ highly radio-pure NaI(Tl) with new HAMAMATSU high quantum efficiency photomultipliers and new electronics) allowed lower software energy threshold down to 1 keV . The DAMA/LIBRA–phase2 data confirm the evidence of a signal that meets all the requirements of the model independent Dark Matter (DM) annual modulation signature, at 9.5σ C.L. in the $(1\text{--}6) \text{ keV}$ energy range. In the $(2\text{--}6) \text{ keV}$ energy range, considering all together the data of DAMA/NaI, DAMA/LIBRA–phase1 and DAMA/LIBRA–phase2 (total exposure $2.46 \text{ ton} \times \text{yr}$, collected over 20 annual cycles with three different set-ups), the achieved C.L. is 12.9σ . No systematics or side reaction able to mimic the exploited DM signature (i.e. to account for the whole measured modulation amplitude and to simultaneously satisfy all the requirements of the signature), has been found or suggested by anyone throughout some decades thus far.

Povzetek. Avtorji predstavijo nove rezultate meritev iz obdobja prvih šest let na experientu DAMA/LIBRA - faza 2 (z ekspozicijo $1.13 \text{ ton} \times \text{šest let}$). Poskrbijo, da so rezultati meritev neodvisni od izbire modela za opis dogodkov.

Izboljšana izvedba poskusa — z $\simeq 250 \text{ kg}$ visoko čistega NaI(Tl), z novimi fotopomnoževalkami Hamamatsu z višjim kvantnim izkoristkom ter izboljšano elektroniko — je omogočila, da so energijski prag znižali na 1 keV . Tudi te meritve potrjuje obstoj signala z letno modulacijo z zanesljivostjo 9.5σ v območju energij $(1\text{--}6) \text{ keV}$. Ko združijo

*** also Dip. di Ingegneria Civile e Ingegneria Informatica, Università di Roma “Tor Vergata”, Rome, Italy

† also University of Jiangangshan, Jiangxi, China

v območju energij (2–6) keV meritve vseh dosedanjih poskusov v več kot 20 letih, to je poskusov DAMA/NaI, DAMA/LIBRA-faza1 in DAMA/LIBRA-faza2, ki doseže kupaj ekspozicijo $2.46 \text{ ton} \times \text{let}$, dosežejo zanesljivost 12.9σ . Nikomur dosedaj, bodisi v skupini DAMA/LIBRA bodisi v katerikoli drugi skupini, ni uspelo najti drugega pojasnila za ta izmerjeni signal, kot da ga povzroča temne snovi.

Keywords: dark matter detection, experiment, annual modulation signature, galactic dark halo, DAMA/LIBRA

2.1 Introduction

The DAMA/LIBRA [1–12] experiment, as the former DAMA/NaI [10,13–17], investigates the presence of DM particles in the galactic halo by exploiting the DM annual modulation signature (originally suggested in Ref. [18,19]). The developed highly radio-pure NaI(Tl) target-detectors [1,6,9,20] offer sensitivity to a wide range of DM candidates, interaction types and astrophysical scenarios (see e.g. in [10] and in literature).

The DM annual modulation signature and its peculiar features are linked to the Earth motion with respect to the DM particles constituting the Galactic Dark Halo; thus, it is not related to terrestrial seasons. In fact as a consequence of the Earth’s revolution around the Sun, which is moving in the Galaxy with respect to the Local Standard of Rest toward the star Vega near the constellation of Hercules, the Earth should be crossed by a larger flux of DM particles around $\simeq 2$ June (when the Earth orbital velocity is summed to that of the solar system with respect to the Galaxy) and by a smaller one around $\simeq 2$ December (when the two velocities are subtracted). In particular, the effect induced by DM particles must simultaneously satisfy all the following requirements: the rate must contain a component modulated according to a cosine function (1) with one year period (2) and a phase that peaks roughly $\simeq 2$ June (3); this modulation must only be found in a well-defined low energy range, where DM particle induced events can be present (4); it must apply only to those events in which just one detector of many actually “fires” (*single-hit* events), since the DM particle multi-interaction probability is negligible (5); the modulation amplitude in the region of maximal sensitivity must be $\lesssim 7\%$ for usually adopted halo distributions (6), but it can be larger in case of some proposed scenarios such as e.g. those in Ref. [21–25] (even up to $\simeq 30\%$). Thus, this signature is very distinctive, has many peculiarities and allows to test a wide range of parameters in many possible astrophysical, nuclear and particle physics scenarios.

This DM signature might be mimicked only by systematic effects or side reactions able to account for the whole observed modulation amplitude and to simultaneously satisfy all the requirements given above; none able to do that has been found or suggested by anyone throughout some decades thus far [1–5,7,8,10,15–17].

The data of the former DAMA/NaI setup and, later, those of the DAMA/LIBRA-phase1 have already given positive evidence with high confidence level for the

presence of a signal that satisfies all the requirements of the exploited DM signature [2–5,10,16,17]. Here the model independent result of six full annual cycles of DAMA/LIBRA–phase2 is presented [12]. The total exposure of DAMA/LIBRA–phase2 is: $1.13 \text{ ton} \times \text{yr}$ with an energy threshold at 1 keV. When including also that of the first generation DAMA/NaI experiment and of DAMA/LIBRA–phase1 the cumulative exposure is $2.46 \text{ ton} \times \text{yr}$. Details on the annual cycles of DAMA/LIBRA–phase2 are reported in Ref. [12]; in particular, the total number of events collected for the energy calibrations during DAMA/LIBRA–phase2 is about 1.3×10^8 , while about 3.4×10^6 events/keV have been collected for the evaluation of the acceptance window efficiency for noise rejection near the software energy threshold [1,6].

The investigation of the DM annual modulation at lower software energy threshold with respect to DAMA/LIBRA–phase1 is deeply supported by the interest in studying the nature of the DM candidate particles, the features of related astrophysical, nuclear and particle physics aspects and by the potentiality of an improved future sensitivity to investigate both DM annual and diurnal signatures.

2.2 The set-up

The full description of the DAMA/LIBRA set-up and the adopted procedures during the phase1 and other related arguments (such as e.g. detector’s radiopurity) have been discussed in details e.g. in Ref. [1–5,20] and references therein.

At the end of 2010 the upgrade DAMA/LIBRA–phase2 started. All the photomultipliers (PMTs) were replaced by a second generation PMTs Hamamatsu R6233MOD, with higher quantum efficiency (Q.E.) and with lower background with respect to those used in phase1; they were produced after a dedicated R&D in the company, and tests and selections [6,20]. The new PMTs have Q.E. in the range 33–39% at 420 nm, wavelength of NaI(Tl) emission, and in the range 36–44% at peak. The commissioning of the experiment was successfully performed in 2011, allowing the achievement of the software energy threshold at 1 keV, and the improvement of some detector’s features such as energy resolution and acceptance efficiency near software energy threshold[6]; the overall efficiency for *single-hit* events as a function of the energy is also given in Ref. [6]. The procedure adopted in the data analysis has been the same along all the data taking, throughout the months and the annual cycles.

At the end of 2012 new preamplifiers and specially developed trigger modules were installed and the apparatus was equipped with more compact electronic modules [26]. Here we just remind that the sensitive part of DAMA/LIBRA–phase2 set-up is made of 25 highly radio-pure NaI(Tl) crystal scintillators (5-rows by 5-columns matrix) having 9.70 kg mass each one. Quantitative estimates of residual contaminants in the detectors were given in Ref. [1]; the detectors are maintained underground since many years. In each detector two 10 cm long UV light guides (made of Suprasil B quartz) act also as optical windows on the two end faces of the crystal, and are coupled to the two low background high Q.E. PMTs working in coincidence at single photoelectron level. The detectors are housed

in a sealed low-radioactive copper box installed in the center of a multi-ton low-radioactive Cu/Pb/Cd-foils/polyethylene/paraffin shield; moreover, about 1 m concrete (made from the Gran Sasso rock material) almost fully surrounds (mostly outside the barrack) this passive shield, acting as a further neutron moderator. The shield is decoupled from the ground by a metallic structure mounted above a concrete basement; a neoprene layer separates the concrete basement and the floor of the laboratory. The space between this basement and the basis of the metallic structure is filled by paraffin for several tens cm in height.

A threefold-level sealing system prevents the detectors from contact with the environmental air of the underground laboratory and continuously maintains them in HP (high-purity) Nitrogen atmosphere. The whole installation is under air conditioning to ensure a suitable and stable working temperature. The huge heat capacity of the multi-tons passive shield ($\approx 10^6$ cal/°C) guarantees further relevant stability of the detectors' (whose metallic housings are in direct contact with the metallic shield) operating temperature. In particular, two independent systems of air conditioning are available for redundancy: one cooled by water refrigerated by a dedicated chiller and the other operating with cooling gas. A hardware/software monitoring system provides data on the operating conditions. In particular, several probes are read out and the results are stored with the production data. Moreover, self-controlled computer based processes automatically monitor several parameters, including those from DAQ, and manage the alarms system. All these procedures, already experienced during DAMA/LIBRA-phase1 [1–5], allow us to control and to maintain the running conditions stable at a level better than 1% also in DAMA/LIBRA-phase2 (see below).

The light response of the detectors during phase2 typically ranges from 6 to 10 photoelectrons/keV, depending on the detector. Energy calibration with X-rays/ γ sources are regularly carried out in the same running condition down to few keV (for details see e.g. Ref. [1]; in particular, double coincidences due to internal X-rays from ^{40}K in trace provide (when summing the data over long periods) an intrinsic calibration point at 3.2 keV, close to the software energy threshold. It is worth noting that, while DAMA/LIBRA-phase1 showed a very good linearity between the calibration with the 59.5 keV line of ^{241}Am and the tagged 3.2 keV line of ^{40}K [1], in DAMA/LIBRA-phase2 a slight non-linearity is observed (it gives a shift of about 0.2 keV at the software energy threshold, as estimated from the tagged 3.2 keV line of ^{40}K , and vanishes above 15 keV which is the position of a bump ascribed to Iodine K-escape peak from small 45 keV structure). This has been taken into account here¹. It is worth noting that the rates are always already corrected for efficiency and that keV means keV electron equivalent.

The DAQ system records both *single-hit* events (where just one of the detectors fires) and *multiple-hit* events (where more than one detector fires). Data are collected up to the MeV region despite the optimization is performed for the lowest energy range. The duty cycle of the experiment is high, ranging between

¹ Similar non-linear effects cannot be highlighted in experiments where the energy scale is extrapolated from calibrations at much higher energies or estimated through MonteCarlo modeling.

76% and 85%. The routine calibrations and, in particular, the data collection for the acceptance windows efficiency mainly affect it.

The adopted procedures provide sensitivity to large and low mass DM candidates inducing nuclear recoils and/or electromagnetic signals.

2.3 The annual modulation of the residual rate

The analysis of DAMA/LIBRA-phase2 exploits the same procedures already adopted for the DAMA/LIBRA-phase1 [1–5].

In particular, the time behaviour of the experimental residual rates of the *single-hit* scintillation events in the (1–3), and (1–6) keV energy intervals for the DAMA/LIBRA-phase2 is shown in Fig. 2.1. The residual rates are calculated from the measured rate of the *single-hit* events after subtracting the unmodulated part [2–5,16,17]. The null modulation hypothesis is rejected at very high C.L. by χ^2 test: $\chi^2/\text{d.o.f.} = 127.3/52$ and $150.3/52$ (P-values: 3.0×10^{-8} and 1.7×10^{-11}), respectively. We remind that the residuals of the DAMA/NaI data ($0.29 \text{ ton} \times \text{yr}$) are given in Ref. [2,5,16,17], while those of DAMA/LIBRA-phase1 ($1.04 \text{ ton} \times \text{yr}$) in Ref. [2–5].

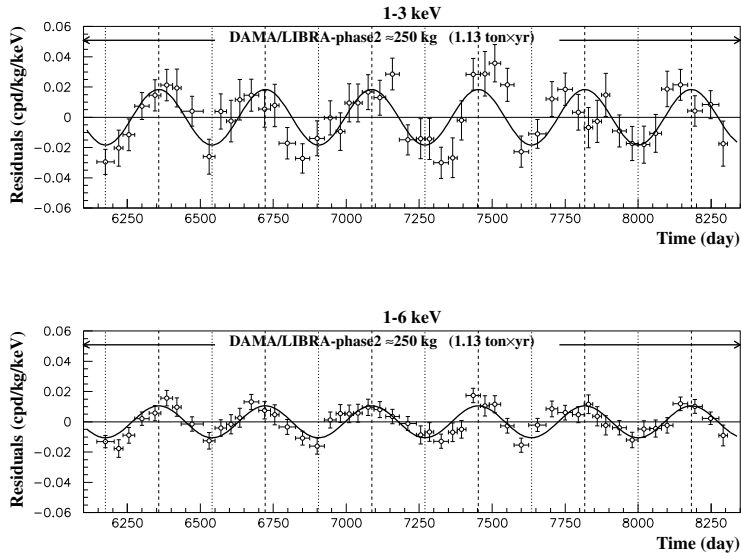


Fig. 2.1. Experimental residual rate of the *single-hit* scintillation events measured by DAMA/LIBRA-phase2 in the (1–3), (1–6) keV energy intervals, respectively, as a function of the time. The time scale is the same as in the previous DAMA data releases for consistency. The data points present the experimental errors as vertical bars, and the widths of the associated time bins as horizontal bars. The superimposed curves are the cosinusoidal functional forms $A \cos \omega(t - t_0)$ with a period $T = \frac{2\pi}{\omega} = 1 \text{ yr}$, a phase $t_0 = 152.5 \text{ day}$ (June 2nd) and modulation amplitudes, A , equal to the central values obtained by best fit on the data points of the entire DAMA/LIBRA-phase2. The dashed vertical lines correspond to the maximum expected for the DM signal (June 2nd), while the dotted vertical lines correspond to the minimum.

Fig. 2.2 shows the residual rates of the *single-hit* scintillation events of the former DAMA/LIBRA-phase1 and of the new DAMA/LIBRA-phase2; the energy interval is from the software energy threshold of DAMA/LIBRA-phase1 (2keV) up to 6 keV. Again the null modulation hypothesis is rejected at very high C.L. by χ^2 test ($\chi^2/\text{d.o.f.} = 199.3/102$, corresponding to P-value = 2.9×10^{-8}).

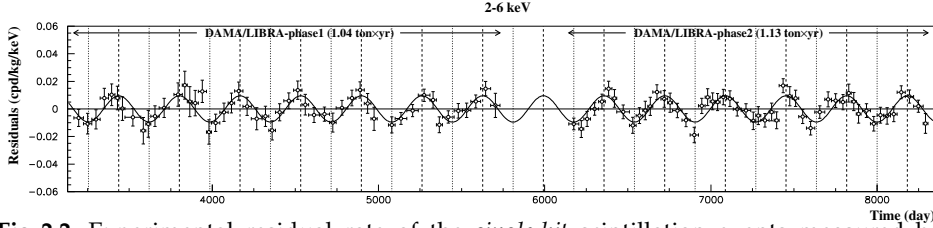


Fig. 2.2. Experimental residual rate of the *single-hit* scintillation events measured by DAMA/LIBRA-phase1 and DAMA/LIBRA-phase2 in the (2–6) keV energy intervals as a function of the time. The superimposed curve is the cosinusoidal functional forms $A \cos \omega(t - t_0)$ with a period $T = \frac{2\pi}{\omega} = 1$ yr, a phase $t_0 = 152.5$ day (June 2nd) and modulation amplitude, A , equal to the central value obtained by best fit on the data points.

The *single-hit* residual rates of the DAMA/LIBRA-phase2 (Fig. 2.1) have been fitted with the function: $A \cos \omega(t - t_0)$, considering a period $T = \frac{2\pi}{\omega} = 1$ yr and a phase $t_0 = 152.5$ day (June 2nd) as expected by the DM annual modulation signature; this can be repeated for the case of (2–6) keV energy interval including also the former DAMA/NaI and DAMA/LIBRA-phase1 data. The goodness of the fits is well supported by the χ^2 test [12]. The results of the fit obtained for DAMA/LIBRA-phase2 either including or not DAMA/NaI and DAMA/LIBRA-phase1 with period and phase kept free in the fitting procedure are reported in Ref. [12]; the obtained period and phase are well compatible with the expectations for a DM annual modulation signal. In particular, the phase is consistent with about June 2nd and is fully consistent with the value independently determined by Maximum Likelihood analysis (see later). For completeness, we recall that a slight energy dependence of the phase could be expected (see e.g. Ref. [24,25,27–30]), providing intriguing information on the nature of the Dark Matter candidate(s) and related aspects.

2.3.1 Absence of background modulation in DAMA/LIBRA-phase2

As done in previous data releases (see e.g. Ref. [5], and references therein), absence of any significant background modulation in the energy spectrum has also been verified in the present data taking for energy regions not of interest for DM. In fact, the background in the lowest energy region is essentially due to “Compton” electrons, X-rays and/or Auger electrons, muon induced events, etc., which are strictly correlated with the events in the higher energy region of the spectrum. Thus, if a modulation detected in the lowest energy region were due to a modulation of the background (rather than to a signal), an equal or larger modulation in the higher energy regions should be present.

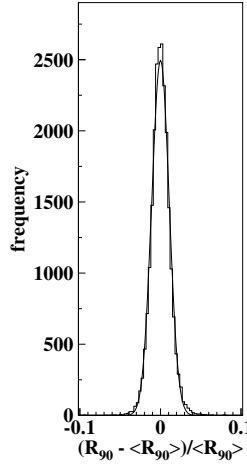


Fig. 2.3. Distribution of the percentage variations of R_{90} with respect to the mean values for all the detectors in DAMA/LIBRA-phase2 (histogram); the superimposed curve is a gaussian fit. See text.

For example, the measured rate integrated above 90 keV, R_{90} , as a function of the time has been analysed. Fig. 2.3 shows the distribution of the percentage variations of R_{90} with respect to the mean values for all the detectors in DAMA/LIBRA-phase2; this has a cumulative gaussian behaviour with $\sigma \simeq 1\%$, well accounted by the statistical spread expected from the used sampling time. Moreover, fitting the time behaviour of R_{90} including also a term with phase and period as for DM particles, a modulation amplitude $A_{R_{90}}$ compatible with zero has been found for all the annual cycles (see Ref. [12]). This also excludes the presence of any background modulation in the whole energy spectrum at a level much lower than the effect found in the lowest energy range for the *single-hit* scintillation events. In fact, otherwise – considering the R_{90} mean values – a modulation amplitude of order of tens cpd/kg would be present for each annual cycle, that is $\simeq 100 \sigma$ far away from the measured values. Similar results are obtained when comparing the *single-hit* residuals in the (1–6) keV with those in other energy intervals [12].

A further relevant investigation on DAMA/LIBRA-phase2 data has been performed by applying the same hardware and software procedures, used to acquire and to analyse the *single-hit* residual rate, to the *multiple-hit* one. Since the probability that a DM particle interacts in more than one detector is negligible, a DM signal can be present just in the *single-hit* residual rate. Thus, the comparison of *single-hit* events with *multiple-hit* events corresponds to compare the cases of DM particles beam-on and beam-off. This procedure also allows an additional test of the background behaviour in the same energy interval where the positive effect is observed. We note that an event is considered *multiple-hit* when there is a deposition of energy in coincidence in more than one detector of the set-up. The multiplicity can, in principle, range from 2 to 25. A *multiple-hit* event in a given energy interval, say (1–6) keV, is given by an energy deposition between 1 and 6

keV in one detector and other deposition(s) in other detector(s). The residual rate of events with multiplicity equal or greater than 2 with an energy deposition in the range 1-6 keV is shown in Fig. 2.4; the only procedure applied to *multiple-hit* events is that used to reject noise events near software energy threshold and is the same used for *single-hit* events. In particular, in Fig. 2.4 the residual rates of the

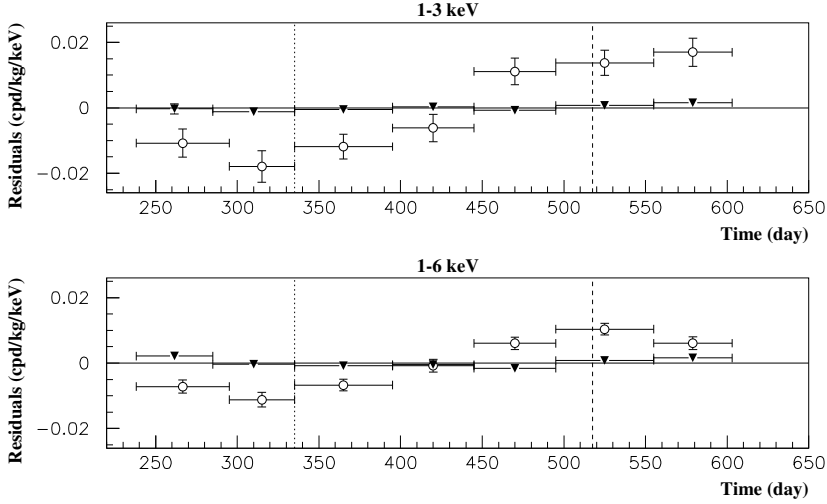


Fig. 2.4. Experimental residual rates of DAMA/LIBRA-phase2 *single-hit* events (open circles), class of events to which DM events belong, and for *multiple-hit* events (filled triangles), class of events to which DM events do not belong. They have been obtained by considering for each class of events the data as collected in a single annual cycle and by using in both cases the same identical hardware and the same identical software procedures. The initial time of the figure is taken on August 7th. The experimental points present the errors as vertical bars and the associated time bin width as horizontal bars. Analogous results were obtained for DAMA/NaI (two last annual cycles) and DAMA/LIBRA-phase1 [2–5,17,10].

single-hit scintillation events collected during DAMA/LIBRA-phase2 are reported, as collected in a single cycle, together with the residual rates of the *multiple-hit* events, in the considered energy intervals². While, as already observed, a clear modulation, satisfying all the peculiarities of the DM annual modulation signature, is present in the *single-hit* events, the fitted modulation amplitudes for the *multiple-hit* residual rate are well compatible with zero: (0.0007 ± 0.0006) cpd/kg/keV, and (0.0004 ± 0.0004) cpd/kg/keV, in the energy regions (1–3) keV, and (1–6) keV, respectively. Thus, again evidence of annual modulation with proper features as required by the DM annual modulation signature is present in the *single-hit* residuals (events class to which the DM particle induced events belong), while it is absent in the *multiple-hit* residual rate (event class to which only background events belong). Similar results were also obtained for the two last annual cycles of DAMA/NaI [17] and for DAMA/LIBRA-phase1 [2–5]. Since the same identical

² Just for completeness, it is worth noting that the rate of the *multiple-hit* events is $\lesssim 0.1$ cpd/kg/keV and is dominated by double hit events from residual ^{40}K in the crystals.

hardware and the same identical software procedures have been used to analyse the two classes of events, the obtained result offers an additional support for the presence of a DM particle component in the galactic halo.

In conclusion, no background process able to mimic the DM annual modulation signature (that is, able to simultaneously satisfy all the peculiarities of the signature and to account for the measured modulation amplitude) has been found or suggested by anyone throughout some decades thus far (see also discussions e.g. in Ref. [1–5,7,8,10]).

2.3.2 The analysis in frequency

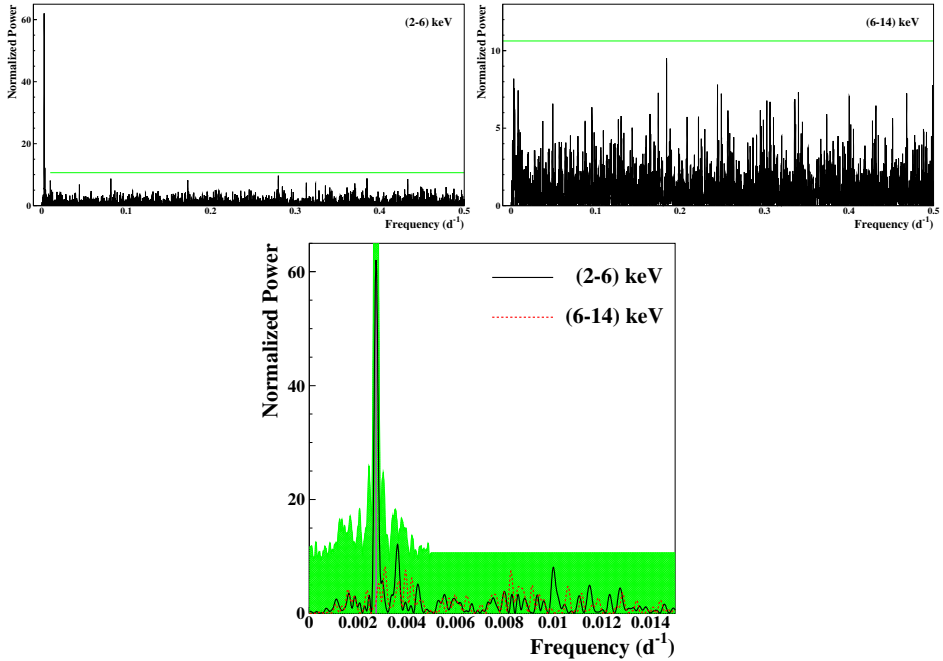


Fig.2.5. Power spectra of the time sequence of the measured *single-hit* events for DAMA/LIBRA–phase1 and DAMA/LIBRA–phase2 grouped in 1 day bins. From top to bottom: spectra up to the Nyquist frequency for (2–6) keV and (6–14) keV energy intervals and their zoom around the 1 y^{-1} peak, for (2–6) keV (solid line) and (6–14) keV (dotted line) energy intervals. The main mode present at the lowest energy interval corresponds to a frequency of $2.74 \times 10^{-3} \text{ d}^{-1}$ (vertical line, purple on-line). It corresponds to a period of $\simeq 1$ year. A similar peak is not present in the (6–14) keV energy interval. The shaded (green on-line) area in the bottom figure – calculated by Monte Carlo procedure – represents the 90% C.L. region where all the peaks are expected to fall for the (2–6) keV energy interval. In the frequency range far from the signal for the (2–6) keV energy region and for the whole (6–14) keV spectrum, the upper limit of the shaded region (90% C.L.) can be calculated to be 10.6 (continuous lines, green on-line).

To perform the Fourier analysis of the DAMA/LIBRA–phase1 and –phase2 data in a wider region of considered frequency, the *single-hit* events have been

grouped in 1 day bins. Because of the low statistics in each time bin, a procedure described in Ref. [31] has been followed. The whole power spectra up to the Nyquist frequency and the zoomed ones are reported in Fig. 2.5. For the lowest energy interval a clear peak corresponding to a period of 1 year is evident, while in the (6–14) keV energy region the same analysis gives only aliasing peaks. Neither other structure at different frequencies has been observed.

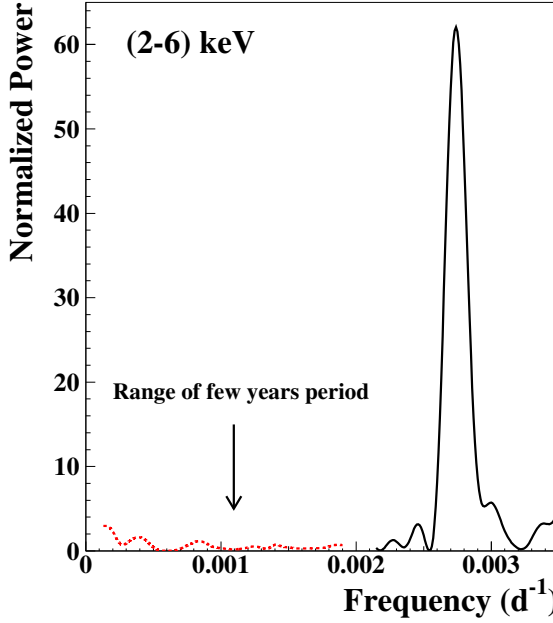


Fig. 2.6. Power spectrum of the annual baseline counting rates for the *single-hit* events of DAMA/LIBRA–phase1 and DAMA/LIBRA–phase2 in the (2–6) keV energy interval (dotted line, red on-line). Also shown for comparison is the power spectrum reported in Fig. 2.5 (solid line). The calculation has been performed according to Ref. [5]. As can be seen, a principal mode is present at a frequency of $2.74 \times 10^{-3} \text{ d}^{-1}$, that corresponds to a period of $\simeq 1$ year. No statistically-significant peak is present at lower frequencies. This implies that no evidence for a long term modulation is present in the *single-hit* scintillation event in the low energy range.

As regards the significance of the peaks present in the periodogram, we remind that the periodogram ordinate, z , at each frequency follows a simple exponential distribution e^{-z} in the case of the null hypothesis or white noise [32]. Thus, if M independent frequencies are scanned, the probability to obtain values larger than z is: $P(> z) = 1 - (1 - e^{-z})^M$; in general M depends on the number of sampled frequencies, the number of data points N , and their detailed spacing. It turns out that M is very nearly equal to N when the data points are approximately equally spaced, and when the sampled frequencies cover the frequency range from 0 to the Nyquist frequency [33,34].

The number of data points used to obtain the spectra in Fig. 2.5 is $N = 4341$ (days measured over the 4748 days of the 13 DAMA/LIBRA–phase1 and

–phase2 annual cycles) and the full frequencies region up to Nyquist frequency has been scanned. Therefore, assuming $M = N$, the significance levels $P = 0.10$, 0.05 and 0.01 , correspond to peaks with heights larger than $z = 10.6$, 11.3 and 13.0 , respectively, in the spectra of Fig 2.5.

In the case below 6 keV, a signal is present; thus, the signal must be included to properly evaluate the C.L.. This has been done by a dedicated Monte Carlo procedure where a large number of similar experiments has been simulated. The 90% C.L. region (shaded, green on-line) where all the peaks are expected to fall for the (2–6) keV energy interval is shown in Fig 2.5; several peaks, satellite of the one year period frequency, are present.

The case of the (1–6) keV energy interval can be studied only for DAMA/LIBRA–phase2 and is shown in Ref. [12]; as previously, the only significant peak is that corresponding to one year period. No other peak is statistically significant being below the area obtained by Monte Carlo procedure.

In conclusion, apart from the peak corresponding to a 1 year period, no other peak is statistically significant either in the low and in the high energy regions.

In addition, for each annual cycle of DAMA/LIBRA–phase1 and –phase2, the annual baseline counting rates have been calculated for the (2–6) keV energy interval. Their power spectrum in the frequency range $0.0002 - 0.0018 \text{ d}^{-1}$ (corresponding to a period range 13.7–1.5 year) is reported in Fig. 2.6; for comparison the power spectrum (solid black line) above 0.0022 d^{-1} of Fig. 2.5 is shown. The calculation has been performed according to Ref. [5]. No statistically-significant peak is present at frequencies lower than 1 y^{-1} . This implies that no evidence for a long term modulation in the counting rate is present.

2.4 The modulation amplitudes by maximum likelihood approach

The annual modulation present at low energy can also be pointed out by depicting the energy dependence of the modulation amplitude, $S_m(E)$, obtained by maximum likelihood method considering fixed period and phase: $T = 1 \text{ yr}$ and $t_0 = 152.5 \text{ day}$. For such purpose the likelihood function of the *single-hit* experimental data in the k –th energy bin is defined as:

$$\mathbf{L}_k = \prod_{ij} e^{-\mu_{ijk}} \frac{\mu_{ijk}^{N_{ijk}}}{N_{ijk}!}, \quad (2.1)$$

where N_{ijk} is the number of events collected in the i -th time interval (hereafter 1 day), by the j -th detector and in the k -th energy bin. N_{ijk} follows a Poisson's distribution with expectation value:

$$\mu_{ijk} = [b_{jk} + S_i(E_k)] M_j \Delta t_i \Delta E \epsilon_{jk}. \quad (2.2)$$

The b_{jk} are the time-independent background contributions that depend on the energy and on the detector, M_j is the mass of the j –th detector, Δt_i is the detector running time during the i -th time interval, ΔE is the chosen energy bin, ϵ_{jk} is the overall efficiency.

The signal can be written as:

$$S_i(E) = S_0(E) + S_m(E) \cdot \cos \omega(t_i - t_0), \quad (2.3)$$

where $S_0(E)$ is the constant part of the signal and $S_m(E)$ is the modulation amplitude. The usual procedure is to minimize the function $y_k = -2\ln(L_k) - \text{const}$ for each energy bin; the free parameters of the fit are the twenty-five (one for each detector) $f_{jk} = (b_{jk} + S_0)$ contributions and the S_m parameter.

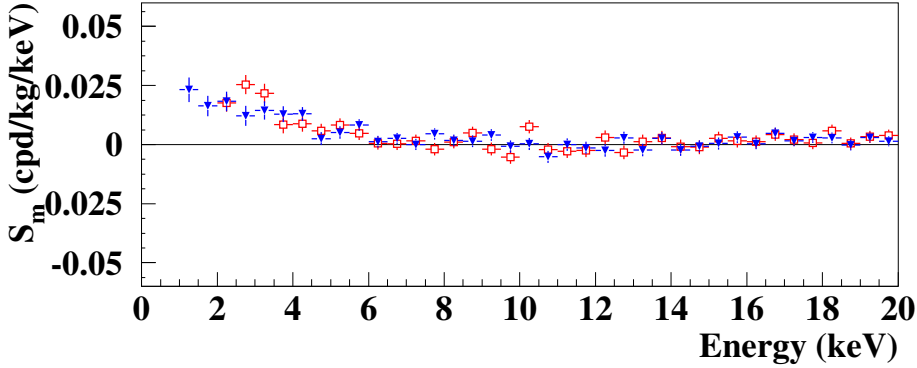


Fig. 2.7. Modulation amplitudes, S_m , for DAMA/LIBRA-phase2 (exposure 1.13 ton \times yr) from the energy threshold of 1 keV up to 20 keV (full triangles, blue data points on-line) – and for DAMA/NaI and DAMA/LIBRA-phase1 (exposure 1.33 ton \times yr) [4] (open squares, red data points on-line). The energy bin ΔE is 0.5 keV. The modulation amplitudes obtained in the two data sets are consistent in the (2–20) keV: the χ^2 is 32.7 for 36 d.o.f., and the corresponding P-value is 63%. In the (2–6) keV energy region, where the signal is present, the $\chi^2/\text{d.o.f.}$ is 10.7/8 (P-value = 22%).

The modulation amplitudes obtained considering the DAMA/LIBRA-phase2 data are reported in Fig. 2.7 as full triangles (blue points on-line) from the energy threshold of 1 keV up to 20 keV; superimposed to the picture as open squared (red on-line) data points are the modulation amplitudes of the former DAMA/NaI and DAMA/LIBRA-phase1 [4]. The modulation amplitudes obtained in the two data sets are consistent in the (2–20) keV, since the χ^2 is 32.7 for 36 d.o.f. corresponding to P-value = 63%. In the (2–6) keV energy region, where the signal is present, the $\chi^2/\text{d.o.f.}$ is 10.7/8 (P-value = 22%).

As shown in Fig. 2.7 positive signal is present below 6 keV also in the case of DAMA/LIBRA-phase2. Above 6 keV the S_m values are compatible with zero; actually, they have random fluctuations around zero, since the χ^2 in the (6–20) keV energy interval for the DAMA/LIBRA-phase2 data is equal to 29.8 for 28 d.o.f. (upper tail probability of 37%). Similar considerations have been done for DAMA/NaI and DAMA/LIBRA-phase1 where the χ^2 in the (6–20) keV energy interval is 35.8 for 28 d.o.f. (upper tail probability of 15%) [4].

The modulation amplitudes for the whole data sets: DAMA/NaI, DAMA/LIBRA-phase1 and DAMA/LIBRA-phase2 are plotted in Fig. 2.8; the data below 2 keV refer only to DAMA/LIBRA-phase2. It can be inferred that positive signal

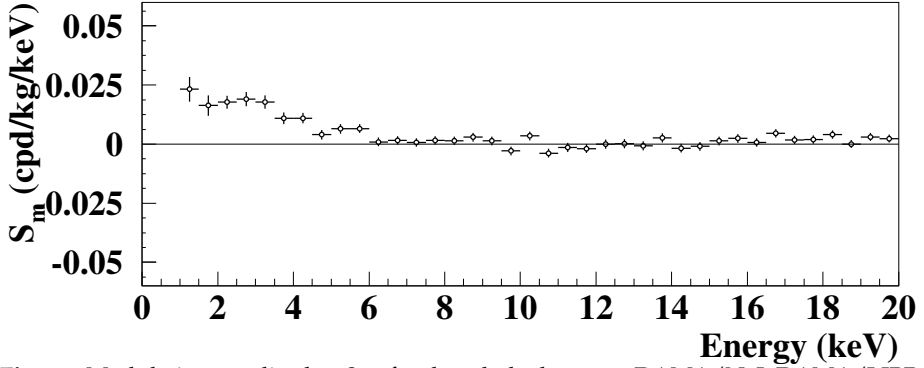


Fig. 2.8. Modulation amplitudes, S_m , for the whole data sets: DAMA/NaI, DAMA/LIBRA-phase1 and DAMA/LIBRA-phase2 (total exposure $2.46 \text{ ton} \times \text{yr}$) above 2 keV; below 2 keV only the DAMA/LIBRA-phase2 exposure ($1.13 \text{ ton} \times \text{yr}$) is available and used. The energy bin ΔE is 0.5 keV. A clear modulation is present in the lowest energy region, while S_m values compatible with zero are present just above. In fact, the S_m values in the (6–20) keV energy interval have random fluctuations around zero with χ^2 equal to 42.6 for 28 d.o.f. (upper tail probability of 4%); see text for comments.

is present in the (1–6) keV energy interval, while S_m values compatible with zero are present just above. All this confirms the previous analyses. The test of the hypothesis that the S_m values in the (6–14) keV energy interval have random fluctuations around zero yields χ^2 equal to 19.0 for 16 d.o.f. (upper tail probability of 27%).

For the case of (6–20) keV energy interval $\chi^2/\text{d.o.f.} = 42.6/28$ (upper tail probability of 4%). The obtained χ^2 value is rather large due mainly to two data points, whose centroids are at 16.75 and 18.25 keV, far away from the (1–6) keV energy interval. The P-values obtained by excluding only the first and either the points are 11% and 25%.

2.4.1 The S_m distributions

The S_m values for each detector in the energy intervals of interest can be obtained by the maximum likelihood approach. In particular, Fig. 2.9 shows the modulation amplitudes S_m in the range (2–6) keV for each one of the 25 detectors in the DAMA/LIBRA-phase1 and DAMA/LIBRA-phase2 periods. The hypothesis that the signal is well distributed over all the 25 detectors is supported by the χ^2 analysis; in fact, the S_m values show a random behaviour around the weighted averaged value (shaded band), and the $\chi^2/\text{d.o.f.}$ is 23.9/24.

The S_m values for each detector for each annual cycle and for the energy bin of interest are expected to follow a normal distribution in absence of systematic effects. One can consider the variable $x = \frac{S_m - \langle S_m \rangle}{\sigma}$ in each detector, in 16 energy bins ($\Delta E = 0.25 \text{ keV}$) in the (2–6) keV energy interval, for the seven DAMA/LIBRA-phase1 annual cycles and in the 20 energy bins in the (1–6) keV energy interval for the six DAMA/LIBRA-phase2 annual cycles. The errors associated to S_m are σ and $\langle S_m \rangle$ are the mean values of the S_m averaged over the detectors and the

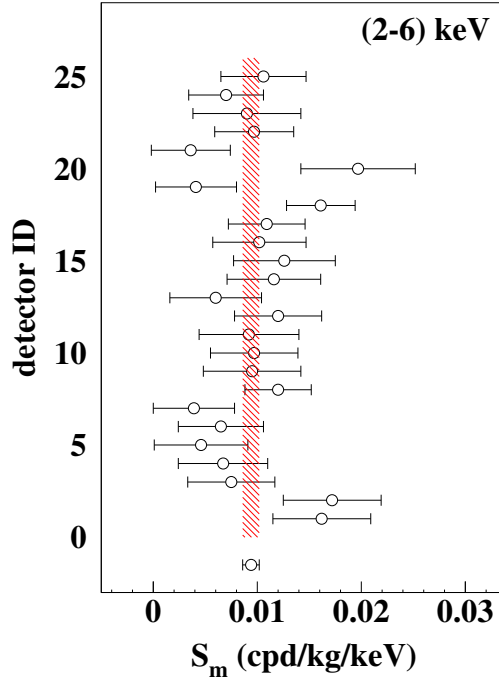


Fig. 2.9. Modulation amplitudes S_m integrated in the range (2–6) keV for each of the 25 detectors for the DAMA/LIBRA–phase1 and DAMA/LIBRA–phase2 periods. The errors are at 1σ confidence level. The weighted averaged point and 1σ band (shaded area) are also reported. The χ^2 is 23.9 over 24 d.o.f., supporting the hypothesis that the signal is well distributed over all the 25 detectors.

annual cycles for each considered energy bin. Fig. 2.10 shows the x distributions and the gaussian fits.

Defining $\chi^2 = \Sigma x^2$, where the sum is extended over all the 232 (152 for the 16th detector [4]), $\chi^2/\text{d.o.f.}$ values ranging from 0.69 to 1.95 are obtained for the 25 detectors. The mean value of $\chi^2/\text{d.o.f.}$ is 1.07, value slightly larger than 1; this can be still ascribed to statistical fluctuations, anyhow in case one would assume it as ascribed to systematics an additional error to the modulation amplitude measured below 6 keV would be derived as: $\leq 2.1 \times 10^{-4}$ cpd/kg/keV, if combining quadratically the errors, or $\leq 3.0 \times 10^{-5}$ cpd/kg/keV, if linearly combining them. This possible additional error: $\leq 2\%$ or $\leq 0.3\%$, respectively, on the DAMA/LIBRA–phase1 and DAMA/LIBRA–phase2 modulation amplitudes is an upper limit of possible systematic effects.

The analysis of the energy behaviour of the modulation amplitudes obtained considering the nine inner detectors and the remaining external ones has also been carried out for DAMA/LIBRA–phase2 as already done for the other data sets. The hypothesis that the two sets of modulation amplitudes as a function of the energy belong to same distribution has been verified by χ^2 test, obtaining e.g.: $\chi^2/\text{d.o.f.}$ = 2.5/6 and 40.8/38 for the energy intervals (1–4) and (1–20) keV, respectively (ΔE

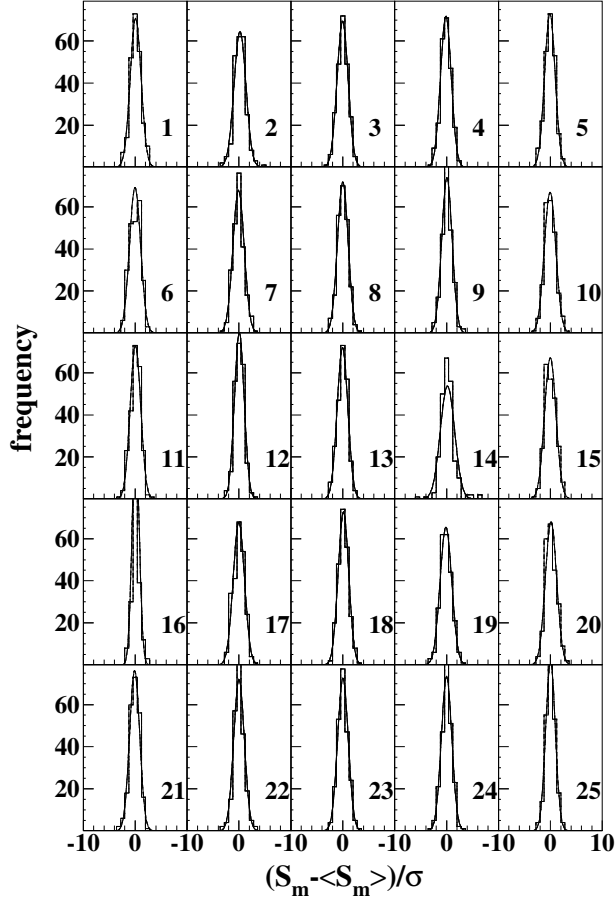


Fig. 2.10. Histograms of the variable $\frac{S_m - \langle S_m \rangle}{\sigma}$, where σ are the errors associated to the S_m values and $\langle S_m \rangle$ are the mean values of the modulation amplitudes averaged over the detectors and the annual cycles for each considered energy bin (here $\Delta E = 0.25$ keV). Each panel refers to a single DAMA/LIBRA detector. The entries of each histogram are 232 (the 16 energy bins in the (2–6) keV energy interval of the seven DAMA/LIBRA–phase1 annual cycles and the 20 energy bins in the (1–6) keV energy interval of the six DAMA/LIBRA–phase2 annual cycles), but 152 for the 16th detector (see Ref. [4]). The superimposed curves are gaussian fits.

= 0.5 keV). Thus it is possible to conclude that the effect is well shared between internal and external detectors.

To evaluate the hypothesis that the modulation amplitudes obtained for each annual cycle are compatible and normally fluctuating around their mean values a χ^2 test can be applied. The distribution of these modulation amplitudes are reported in Fig. 2.11, where the $\chi^2/\text{d.o.f.}$ are also given; they corresponds to upper tail probability of 5.2%, 97%, 25%, 67% and 72%, respectively. In addition to the χ^2 test, also the *run test* has been applied (see e.g. Ref. [35]); it verifies the hypothesis

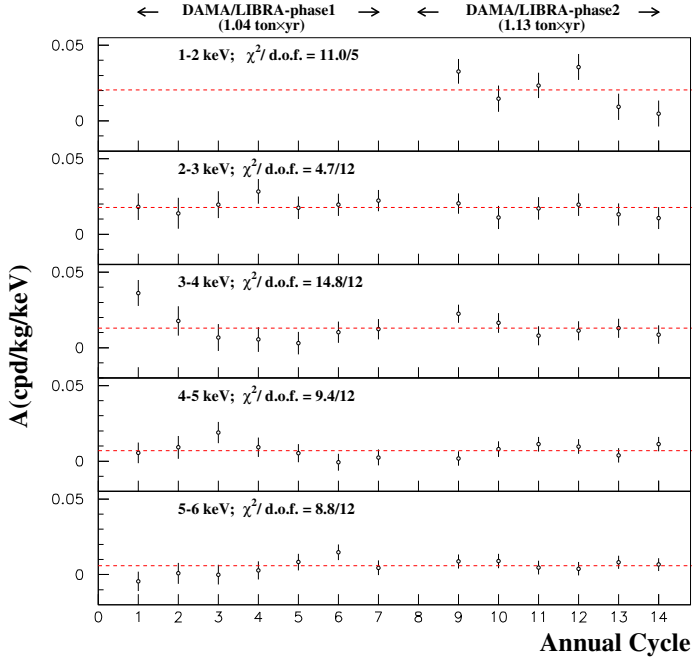


Fig. 2.11. Modulation amplitudes of each single annual cycle of DAMA/LIBRA-phase1 and DAMA/LIBRA-phase2. The error bars are the 1σ errors. The dashed horizontal lines show the central values obtained by best fit over the whole data set. The χ^2 test and the *run test* accept the hypothesis at 95% C.L. that the modulation amplitudes are normally fluctuating around the best fit values.

that the positive (above the mean value) and negative (under the mean value) data points are randomly distributed. The lower (upper) tail probabilities obtained by the *run test* are: 70(70)%, 50(73)%, 85(35)%, 88(30)% and 88(30)%, respectively; this confirms that the data collected in all the annual cycles with DAMA/LIBRA-phase1 and phase2 are statistically compatible and can be considered together.

2.5 The phase of the measured modulation effect

In order to investigate the phase of the annual modulation effect, it is useful to write the the signal as:

$$\begin{aligned} S_i(E) &= S_0(E) + S_m(E) \cos \omega(t_i - t_0) + Z_m(E) \sin \omega(t_i - t_0) \\ &= S_0(E) + Y_m(E) \cos \omega(t_i - t^*) \end{aligned} \quad (2.4)$$

releasing the assumption of a fixed phase at $t_0 = 152.5$ day. For DM induced signals: i) $Z_m \sim 0$ (because of the orthogonality between the cosine and the sine functions); ii) $S_m \simeq Y_m$; iii) $t^* \simeq t_0 = 152.5$ day. In fact, these conditions hold for most of the dark halo models with some exceptions (see e.g. Ref. [24,25,27–30]).

In Fig. 2.12–*left* the obtained 2σ contours in the plane (S_m, Z_m) are shown for the (2–6) keV and (6–14) keV energy intervals considering cumulatively the data

of DAMA/NaI, DAMA/LIBRA-phase1 and DAMA/LIBRA-phase2. In Fig. 2.12–*right* instead the obtained 2σ contours in the plane (Y_m, t^*) are depicted. Fig. 2.12 also shows – obviously only for DAMA/LIBRA-phase2 – the 2σ contours in the (1–6) keV energy interval.

The best fit values in the considered cases (1σ errors) for S_m versus Z_m and Y_m versus t^* are reported in Table 2.1.

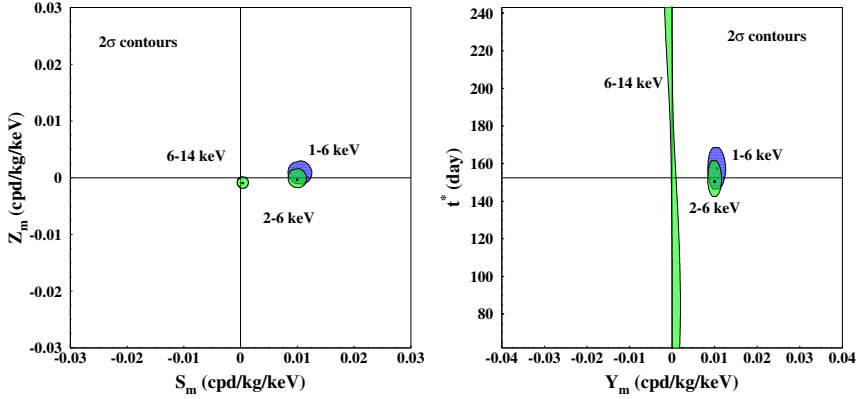


Fig. 2.12. 2σ contours in the plane (S_m, Z_m) (*left*) and in the plane (Y_m, t^*) (*right*) for: i) DAMA/NaI, DAMA/LIBRA-phase1 and DAMA/LIBRA-phase2 in the (2–6) keV and (6–14) keV energy intervals (light areas, green on-line); ii) only DAMA/LIBRA-phase2 in the (1–6) keV energy interval (dark areas, blue on-line). The contours have been obtained by the maximum likelihood method. A modulation amplitude is present in the lower energy intervals and the phase agrees with that expected for DM induced signals.

E (keV)	S_m (cpd/kg/keV)	Z_m (cpd/kg/keV)	Y_m (cpd/kg/keV)	t^* (day)
DAMA/NaI+DAMA/LIBRA-phase1+DAMA/LIBRA-phase2:				
2–6	(0.0100 ± 0.0008)	$-(0.0003 \pm 0.0008)$	(0.0100 ± 0.0008)	(150.5 ± 5.0)
6–14	(0.0003 ± 0.0005)	$-(0.0009 \pm 0.0006)$	(0.0010 ± 0.0013)	undefined
DAMA/LIBRA-phase2:				
1–6	(0.0105 ± 0.0011)	(0.0009 ± 0.0010)	(0.0105 ± 0.0011)	(157.5 ± 5.0)

Table 2.1. Best fit values (1σ errors) for S_m versus Z_m and Y_m versus t^* , considering: i) DAMA/NaI, DAMA/LIBRA-phase1 and DAMA/LIBRA-phase2 in the (2–6) keV and (6–14) keV energy intervals; ii) only DAMA/LIBRA-phase2 in the (1–6) keV energy interval. See also Fig. 2.12.

The Z_m values, obtained in the hypothesis of S_m set to zero in eq. (2.4), are reported in Fig. 2.13 for DAMA/NaI, DAMA/LIBRA-phase1, and DAMA/LIBRA-phase2; they are expected to be zero. The χ^2 test of the data supports the hypothesis

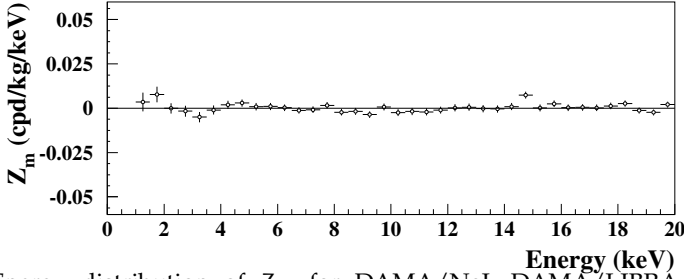


Fig. 2.13. Energy distribution of Z_m for DAMA/NaI, DAMA/LIBRA-phase1, and DAMA/LIBRA-phase2 once setting S_m in eq. (2.4) to zero. The energy bin ΔE is 0.5 keV. The χ^2 test applied to the data supports the hypothesis that the Z_m values are simply fluctuating around zero, as expected. See text.

that the Z_m values are simply fluctuating around zero; in fact, in the (1–20) keV energy region the $\chi^2/\text{d.o.f.}$ is equal to 44.5/38 corresponding to a P-value = 22%.

Fig. 2.14 shows Y_m and t^* as a function of the energy for DAMA/NaI, DAMA/LIBRA-phase1, and DAMA/LIBRA-phase2. The Y_m are superimposed with the S_m values with 1 keV energy bin. As in the previous analyses, an annual modulation effect is present in the lower energy intervals and the phase agrees with that expected for DM induced signals. No modulation is present above 6 keV and the phase is undetermined.

2.6 Further investigation on possible systematic effects and side reactions in DAMA/LIBRA-phase2

The DAMA/LIBRA-phase2 results – as those of DAMA/LIBRA-phase1 and DAMA/NaI – fulfill the requirements of the DM annual modulation signature and investigations on absence of any significant systematics or side reaction effect are already present in the previous sections; however, here the topic is further addressed.

Sometimes naive statements are put forwards as the fact that in nature several phenomena may show annual periodicity. However, the point is whether they might mimic the annual modulation signature, i.e. whether they might be not only able to quantitatively account for the observed modulation amplitude but also to contemporaneously satisfy all the requirements of the DM annual modulation signature. This was deeply investigated in the former DAMA/NaI and DAMA/LIBRA-phase1 experiments (see e.g. Ref. [16,17,2] and references therein; no one able to mimic the signature has been found or suggested by anyone so far) and will be further addressed in the following for the present DAMA/LIBRA-phase2 data.

Firstly, in order to continuously monitor the running conditions, several pieces of information are acquired with the production data and quantitatively analysed; information on technical aspects of DAMA/LIBRA has been given in Ref. [1], where the sources of possible residual radioactivity have also been analysed.

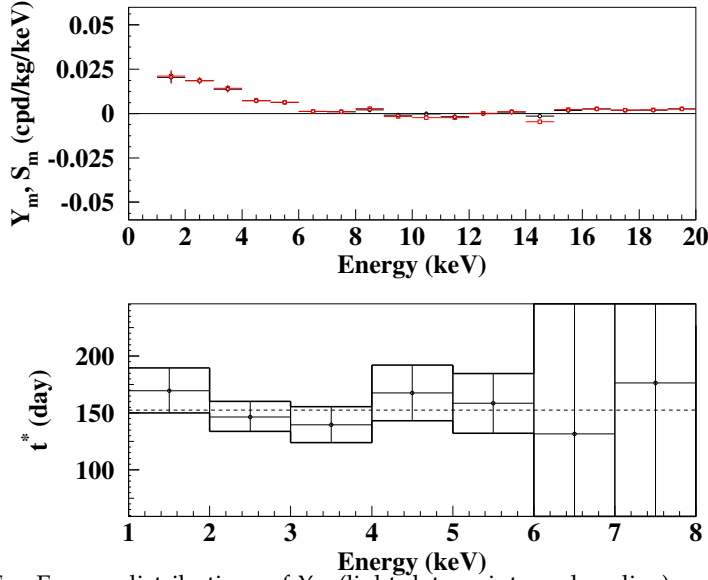


Fig. 2.14. *Top:* Energy distributions of Y_m (light data points; red on-line) and of the S_m variable (solid data points; black on-line) for DAMA/NaI, DAMA/LIBRA-phase1, and DAMA/LIBRA-phase2. Here, unlike the data of Fig. 2.8, the energy bin is 1 keV. *Bottom:* Energy distribution of the phase t^* for DAMA/NaI, DAMA/LIBRA-phase1, and DAMA/LIBRA-phase2; here the errors are at 2σ . The vertical scale spans over \pm a quarter of period around 2 June; other intervals are replica of it. The phase agrees with that expected for DM induced signals at low energy. No modulation is present above 6 keV and thus the phase is undetermined.

	LIBRA-phase2-2	LIBRA-phase2-3	LIBRA-phase2-4	LIBRA-phase2-5	LIBRA-phase2-6	LIBRA-phase2-7
Temperature ($^{\circ}\text{C}$)	(0.0012 ± 0.0051)	$-(0.0002 \pm 0.0049)$	$-(0.0003 \pm 0.0031)$	(0.0009 ± 0.0050)	(0.0018 ± 0.0036)	$-(0.0006 \pm 0.0035)$
Flux (l/h)	$-(0.15 \pm 0.18)$	$-(0.02 \pm 0.22)$	$-(0.02 \pm 0.12)$	$-(0.02 \pm 0.14)$	$-(0.01 \pm 0.10)$	$-(0.01 \pm 0.16)$
Pressure (mbar)	$(1.1 \pm 0.9)10^{-3}$	$(0.2 \pm 1.1)10^{-3}$	$(2.4 \pm 5.4)10^{-3}$	$(0.6 \pm 6.2)10^{-3}$	$(1.5 \pm 6.3)10^{-3}$	$(7.2 \pm 8.6)10^{-3}$
Radon (Bq/m^3)	(0.015 ± 0.034)	$-(0.002 \pm 0.050)$	$-(0.009 \pm 0.028)$	$-(0.044 \pm 0.050)$	(0.082 ± 0.086)	(0.06 ± 0.11)
Hardware rate (Hz)	$-(0.12 \pm 0.16)10^{-2}$	$(0.00 \pm 0.12)10^{-2}$	$-(0.14 \pm 0.22)10^{-2}$	$-(0.05 \pm 0.22)10^{-2}$	$-(0.06 \pm 0.16)10^{-2}$	$-(0.08 \pm 0.17)10^{-2}$

Table 2.2. Modulation amplitudes (1σ error) obtained – for each annual cycle – by fitting the time behaviours of main running parameters including a possible annual modulation with phase and period as for DM particles. These running parameters, acquired with the production data, are: i) the operating temperature of the detectors; ii) the HP Nitrogen flux in the inner Cu box housing the detectors; iii) the pressure of the HP Nitrogen atmosphere of that inner Cu box; iv) the environmental Radon in the inner part of the barrack from which the detectors are however excluded by other two sealing systems (see text and Ref. [1] for details); v) the hardware rate above single photoelectron threshold. All the measured amplitudes are compatible with zero.

In particular, all the time behaviours of the running parameters, acquired with the production data, have been investigated. Table 2.2 shows the modulation

amplitudes obtained for each annual cycle when fitting the time behaviours of the values of the main parameters including a cosine modulation with the same phase and period as for DM particles. As can be seen, all the measured amplitudes are well compatible with zero.

Let us now enter in some more details.

2.6.1 The temperature

The full experiment is placed underground and works in an air-conditioned environment; moreover, the detectors have Cu housing in direct contact with the multi-tons metallic passive shield whose huge heat capacity definitively assures a relevant stability of the detectors' operating temperature [1]. Nevertheless the operating temperature is read out by a probe and stored with the production data, in order to offer the possibility of further investigations.

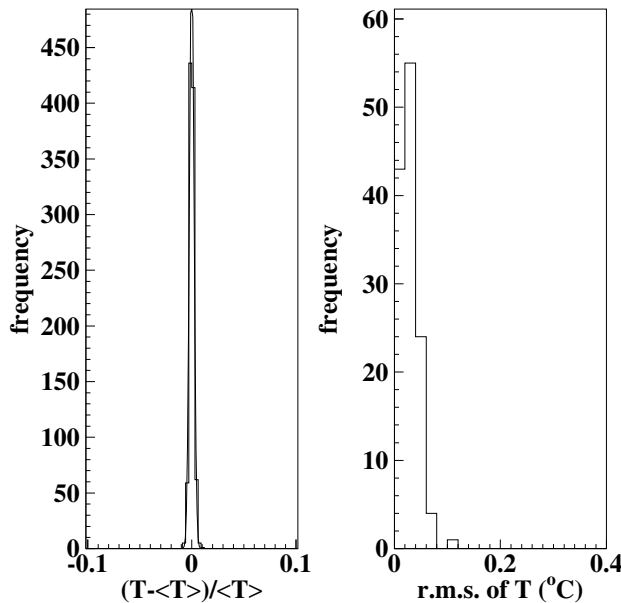


Fig. 2.15. *left* - Distribution of the relative variations of the operating temperature measured during the DAMA/LIBRA-phase2 six annual cycles (histogram); the superimposed curve is a gaussian fit. The standard deviation is 0.2%. *Right* - Distribution of the root mean square (r.m.s.) detectors' operating temperature variations within periods with the same calibration factors (typically $\simeq 10$ days) during the DAMA/LIBRA-phase2 six annual cycles. The mean value is 0.03 °C.

Specific information on the DAMA/LIBRA-phase2 six annual cycles can be derived from Fig. 2.15-*left*; no evidence for any operating temperature modulation has been observed, as also quantitatively reported in Table 2.2. However, to properly evaluate the real effect of possible variations of the detectors' operating temperature on the light output, we consider the distribution of the root mean square temperature variations within periods with the same calibration factors (typically $\simeq 10$ days); this is given in Fig. 2.15-*right* cumulatively for the

DAMA/LIBRA-phase2 data. The mean value of the root mean square of the variation of the detectors' operating temperature is $\simeq 0.03^\circ\text{C}$ and, considering the known value of the slope of the light output $\lesssim -0.2\%/^\circ\text{C}$, the relative light output variation is $\lesssim 10^{-4}$, that would correspond to a modulation amplitude $\lesssim 10^{-4}$ cpd/kg/keV (that is $\lesssim 0.5\%$ of the observed modulation amplitude).

Moreover, for temperature variations the specific requirements of the DM annual modulation signature (such as e.g. the 4th and the 5th) would fail, while they are instead satisfied by the DAMA/LIBRA-phase2 production data.

In conclusion, all the arguments given above quantitatively exclude any role of possible effects on the observed rate modulation directly correlated with temperature.

For the sake of completeness, we comment that sizeable temperature variations in principle might also induce variations in the electronic noise, in the Radon release from the rocks and in some environmental background; these specific topics will be further addressed in the following.

2.6.2 The noise

Despite the good noise identification near energy threshold and the stringent noise rejection procedure which is used [1,6], the role of a possible noise tail in the data after the noise rejection procedure has been quantitatively investigated.

The hardware rate of each detector above a single photoelectron, R_{Hj} (j identifies the detector), has been considered. Indeed, this hardware rate is significantly determined by the noise.

For the proposed purpose the variable: $R_H = \Sigma_j (R_{Hj} - \langle R_{Hj} \rangle)$, can be built; in the present case $\langle R_{Hj} \rangle \lesssim 0.2$ Hz. The time behaviour of R_H during each DAMA/LIBRA-phase2 annual cycle is shown in Fig. 2.16. As can be seen in Fig. 2.17, the cumulative distribution of R_H for the DAMA/LIBRA-phase2 annual cycles shows a gaussian behaviour with $\sigma = 0.3\%$, that is well in agreement with that expected on the basis of simple statistical arguments.

Moreover, by fitting the time behaviour of R_H in the six data taking periods – including a modulation term as that for DM particles – a modulation amplitude compatible with zero is obtained: $-(0.061 \pm 0.067) \times 10^{-2}$ Hz, corresponding to the upper limit: $< 0.6 \times 10^{-3}$ Hz at 90% C.L.. Since the typical noise contribution to the hardware rate of each detector is $\simeq 0.10$ Hz, the upper limit on the noise relative modulation amplitude is given by: $\frac{0.6 \times 10^{-3} \text{ Hz}}{2.5 \text{ Hz}} \simeq 2.4 \times 10^{-4}$ (90% C.L.). Therefore, even in the worst hypothetical case of a 10% contamination of the residual noise – after rejection – in the counting rate, the noise contribution to the modulation amplitude in the lowest energy bins would be $< 2.4 \times 10^{-5}$ of the total counting rate. This means that a hypothetical noise modulation could account at maximum for absolute amplitudes less than 10^{-4} cpd/kg/keV.

In conclusion, there is no role of any hypothetical tail of residual noise after rejection.

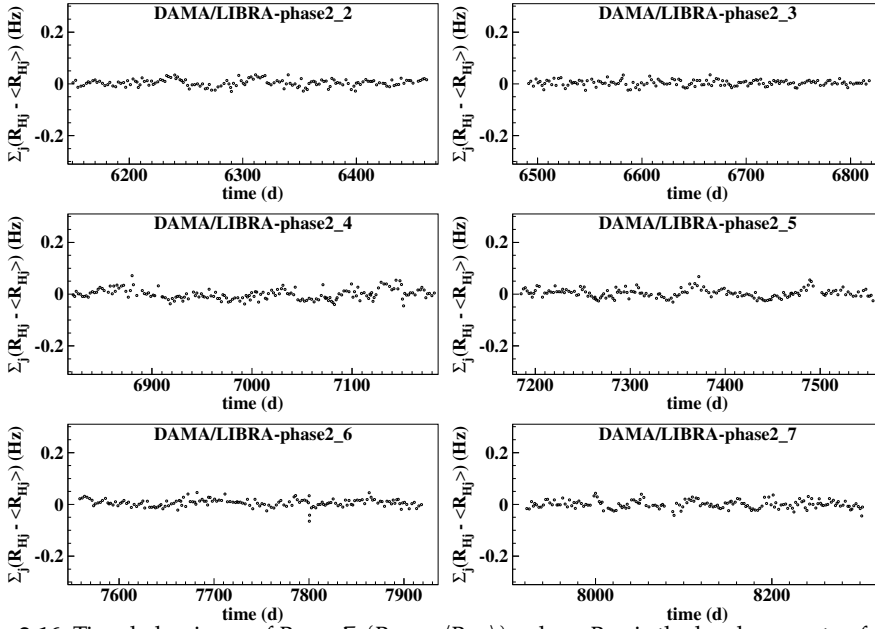


Fig. 2.16. Time behaviours of $R_H = \Sigma_j(R_{Hj} - \langle R_{Hj} \rangle)$, where R_{Hj} is the hardware rate of each detector above single photoelectron threshold (that is including the noise), j identifies the detector and $\langle R_{Hj} \rangle$ is the mean value of R_{Hj} in the corresponding annual cycle.

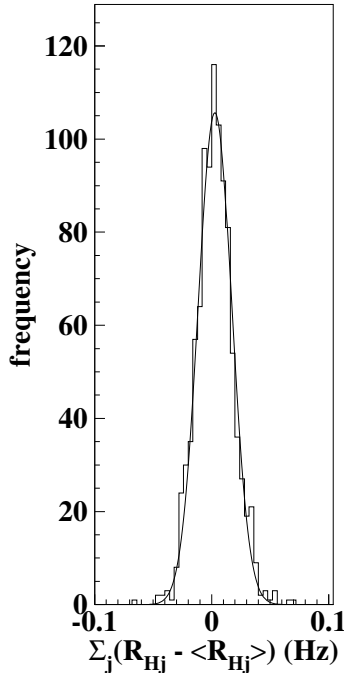


Fig. 2.17. Distribution of R_H during the DAMA/LIBRA-phase2 annual cycles (histogram); the superimposed curve is a gaussian fit.

2.6.3 The calibration factor

In long term running conditions the periodical calibrations are performed every $\simeq 10$ days with ^{241}Am source [1]. Although it is highly unlikely that a variation of the calibration factor (proportionality factor between the area of the recorded pulse and the energy), tdcal , could play any role, a quantitative investigation on that point has been carried out.

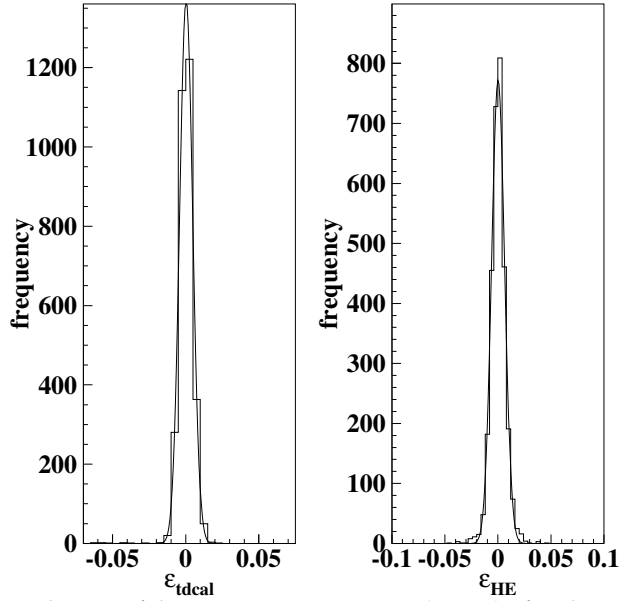


Fig. 2.18. *Left:* Distribution of the percentage variations (ϵ_{tdcal}) of each energy scale factor (tdcal) with respect to the value measured in the previous calibration (histogram); the standard deviation is 0.5%. *Right:* Distribution of the percentage variations (ϵ_{HE}) of the high energy scale factor with respect to the mean values (histogram); the standard deviation is 0.6%. The panels refer to the DAMA/LIBRA-phase2 annual cycles and the superimposed curves are gaussian fits.

For this purpose, we define the percentage variation of each energy scale factor (tdcal) with respect to the value measured in the previous calibration: $\epsilon_{\text{tdcal}} = \frac{\text{tdcal}_k - \text{tdcal}_{k-1}}{\text{tdcal}_{k-1}}$ (here tdcal_k is the value of the calibration factor in the k -th calibration). The distribution of ϵ_{tdcal} for all the detectors during the DAMA/LIBRA-phase2 annual cycles is given in Fig. 2.18-*Left*. This distribution shows a gaussian behaviour with $\sigma \simeq 0.5\%$. Since the results of the routine calibrations are properly taken into account in the data analysis, such a result allows us to conclude that the energy calibration factor for each detector is known with an uncertainty $\ll 1\%$ during the data taking periods.

Moreover, the distribution of the percentage variations (ϵ_{HE}) of the high energy scale factor with respect to the mean values for all the detectors and for the DAMA/LIBRA-phase2 annual cycles is reported in Fig. 2.18-*right*. Also this distribution shows a gaussian behaviour with $\sigma \simeq 0.6\%$.

As also discussed in Ref. [2,15,16], the possible variation of the calibration factor for each detector during the data taking would give rise to an additional energy spread (σ_{cal}) besides the detector energy resolution (σ_{res}). The total energy spread can be, therefore, written as: $\sigma = \sqrt{\sigma_{\text{res}}^2 + \sigma_{\text{cal}}^2} \simeq \sigma_{\text{res}} \cdot [1 + \frac{1}{2} \cdot (\frac{\sigma_{\text{cal}}}{\sigma_{\text{res}}})^2]$; clearly the contribution due to the calibration factor variation is negligible since $\frac{1}{2} \cdot (\frac{\sigma_{\text{cal}}/\text{E}}{\sigma_{\text{res}}/\text{E}})^2 \lesssim 7.5 \times 10^{-4} \frac{\text{E}}{20\text{keV}}$ (where the adimensional ratio $\frac{\text{E}}{20\text{keV}}$ accounts for the energy dependence of this limit value). This order of magnitude is confirmed by a MonteCarlo calculation, which credits – as already reported in Ref. [2,15,16] – a maximum value of the effect of similar variations of tdcal on the modulation amplitude equal to $1 - 2 \times 10^{-4}$ cpd/kg/keV. Thus, also the unlikely idea that the calibration factor could play a role can be safely ruled out.

2.6.4 The efficiencies

The behaviour of the overall efficiencies during the whole data taking periods has been investigated. Their possible time variation depends essentially on the stability of the efficiencies related to the adopted acceptance windows; they are regularly measured by dedicated calibrations [1].

In particular, Fig. 2.19 shows the percentage variations of the efficiency values in the (1-8) keV energy interval for DAMA/LIBRA-phase2. They show a gaussian distribution with $\sigma = 0.3\%$. Moreover, we have verified that the time behaviour of these percentage variations does not show any modulation with period and phase expected for a possible DM signal. In Table 2.3 the modulation amplitudes of the efficiencies in each energy bin between 1 and 10 keV are reported, showing that they are all consistent with zero. In particular, modulation amplitudes – considering the six DAMA/LIBRA-phase2 annual cycles all together – equal to $-(0.10 \pm 0.32) \times 10^{-3}$ and $(0.00 \pm 0.41) \times 10^{-3}$ are found for the (1-4) keV and (4-6) keV energy bins, respectively; both consistent with zero. Thus, also the unlikely idea of a possible role played by the efficiency is ruled out.

Energy (keV)	Modulation amplitudes ($\times 10^{-3}$)					
	LIBRA-ph2-2	LIBRA-ph2-3	LIBRA-ph2-4	LIBRA-ph2-5	LIBRA-ph2-6	LIBRA-ph2-7
1-4	$-(0.8 \pm 0.7)$	(0.7 ± 0.8)	(0.9 ± 0.8)	$-(1.3 \pm 0.8)$	$-(0.1 \pm 0.8)$	(0.2 ± 0.8)
4-6	(0.9 ± 1.0)	(0.9 ± 1.0)	$-(1.3 \pm 1.0)$	(0.5 ± 1.0)	$-(1.0 \pm 1.1)$	$-(0.2 \pm 1.0)$
6-8	(0.8 ± 0.8)	$-(0.7 \pm 0.7)$	(0.6 ± 0.8)	$-(0.1 \pm 0.8)$	$-(1.1 \pm 0.8)$	(0.5 ± 0.8)
8-10	$-(0.3 \pm 0.6)$	$-(0.5 \pm 0.5)$	$-(0.5 \pm 0.5)$	$-(0.3 \pm 0.5)$	(0.4 ± 0.6)	(0.3 ± 0.6)

Table 2.3. Modulation amplitudes obtained by fitting the time behaviour of the efficiencies including a cosine modulation with phase and period as for DM particles for the DAMA/LIBRA-phase2 annual cycles.

2.6.5 The background

In order to verify the absence of any significant background modulation, the energy distribution measured during the data taking periods in energy regions not

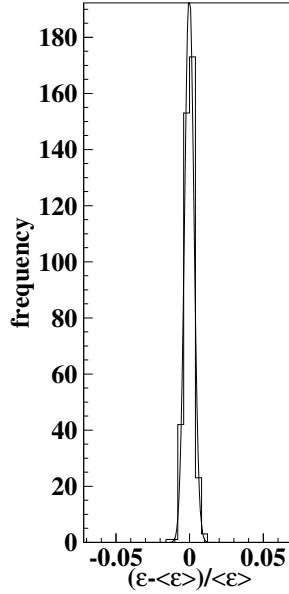


Fig. 2.19. Percentage variations of the overall efficiency values with the respect to their mean values for DAMA/LIBRA-phase2 (histogram); the superimposed curve is a gaussian fit.

of interest for DM detection has been investigated. The presence of background (of whatever nature) modulation is already excluded by the results on the measured rate integrated above 90 keV, R_{90} , as a function of the time; the latter one not only does not show any modulation, but allows one to exclude the presence of a background modulation in the whole energy spectrum at a level some orders of magnitude lower than the annual modulation observed in the *single-hit* events in the (1–6) keV energy region.

A further relevant support is given by the result of the analysis of the *multiple-hit* events which independently proves that there is no modulation at all in the background event in the same energy region where the *single-hit* events present an annual modulation satisfying all the requirements of the DM annual modulation signature.

These results obviously already account for whatever kind of background including that possibly induced by neutrons, by Radon and by side reactions.

... more on Radon The DAMA/LIBRA detectors are excluded from the air of the underground laboratory by a 3-level sealing system [1]; in fact, this air contains traces of the radioactive Radon gas (^{222}Rn – $T_{1/2} = 3.82$ days – and of ^{220}Rn – $T_{1/2} = 55$ s – isotopes, which belong to the ^{238}U and ^{232}Th chains, respectively), whose daughters attach themselves to surfaces by various processes. In particular: i) the walls, the floor and the top of the inner part of the installation are insulated by Supronyl (permeability: 2×10^{-11} cm²/s [36]) and a large flux of HP Nitrogen is released in the closed space of this inner part of the barrack housing the set-up. An Oxygen level alarm informs the operator before entering it, when necessary; ii)

the whole passive shield is sealed in a Plexiglas box and maintained continuously in HP Nitrogen atmosphere in slight overpressure with respect to the environment as well as the upper glove box for calibrating the detectors; iii) the detectors are housed in an inner sealed Cu box also maintained continuously in HP Nitrogen atmosphere in slight overpressure with respect to the environment; the Cu box can enter in contact only with the upper glove box – during calibrations – which is also continuously maintained in HP Nitrogen atmosphere in slightly overpressure with respect to the external environment.

Notwithstanding the above considerations, the Radon in the installation outside the Plexiglas box, containing the passive shield, is continuously monitored; it is at level of sensitivity of the used Radon-meter as reported in Fig. 2.20. Table 2.2 has already shown that no modulation of Radon is present in the environment of the set-up; moreover, the detectors are further isolated by the other two levels of sealing [1].

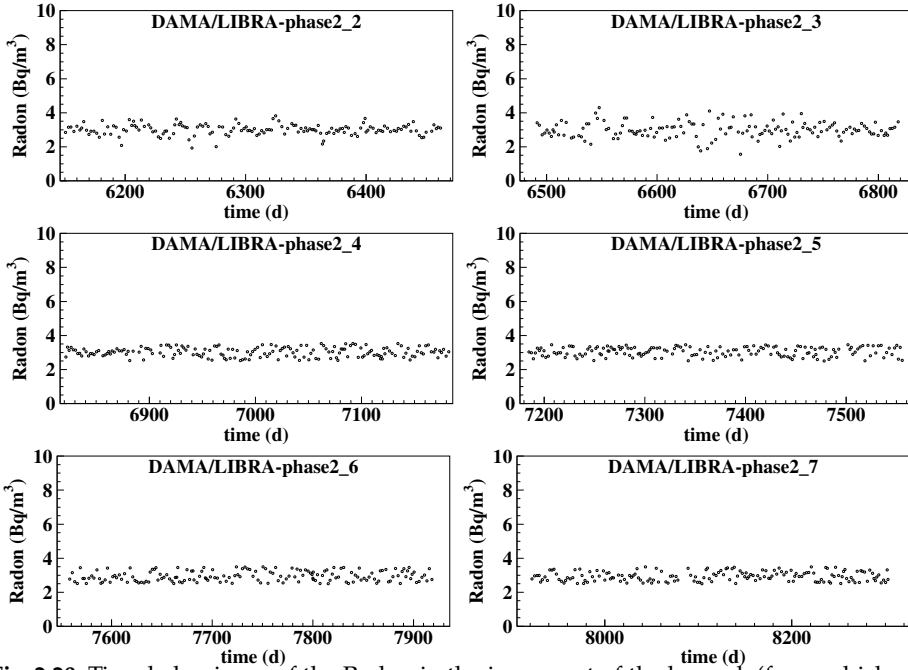


Fig. 2.20. Time behaviours of the Radon in the inner part of the barrack (from which – in addition - the detectors are further isolated by other two levels of sealing [1]) during the DAMA/LIBRA-phase2 annual cycles. The measured values are at the level of sensitivity of the used Radon-meter.

In Fig. 2.21 the distributions of the relative variations of the HP Nitrogen flux in the inner Cu box housing the detectors and of the pressure of it are shown as measured during the DAMA/LIBRA-phase2 annual cycles (the typical flux mean value for each annual cycle is of order of $\simeq 320$ l/h and the typical overpressure mean value is of order of 3.1 mbar).

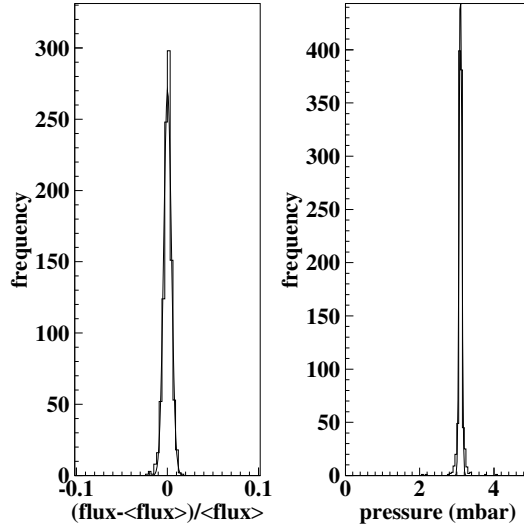


Fig. 2.21. Distributions of the HP Nitrogen flux in the inner Cu box housing the detectors and of the pressure of it as measured during the DAMA/LIBRA-phase2 annual cycles (histograms); the superimposed curves are gaussian fits. For clarity the HP Nitrogen flux has been given in terms of relative variations.

Possible Radon trace in the HP Nitrogen atmosphere inside the Cu box, housing the detectors, has been searched through the double coincidences of the gamma-rays (609 and 1120 keV) from ^{214}Bi Radon daughter, obtaining an upper limit on the possible Radon concentration in the Cu box HP Nitrogen atmosphere: $< 5.8 \times 10^{-2} \text{ Bq/m}^3$ (90% C.L.) [2]. Thus, a rate roughly $< 2.5 \times 10^{-5} \text{ cpd/kg/keV}$ can be expected from this source at low energy. This shows that even an hypothetical, e.g. 10%, modulation of possible Radon in the HP Nitrogen atmosphere of the Cu box, housing the detectors, would correspond to a modulation amplitude $< 2.5 \times 10^{-6} \text{ cpd/kg/keV}$ ($< 0.01\%$ of the observed modulation amplitude).

Moreover, it is worth noting that, while the possible presence of a sizeable quantity of Radon nearby a detector would forbid the investigation of the annual modulation signature (since every Radon variation would induce both the variation in the whole energy distribution and the continuous pollution of the exposed surfaces by the non-volatile daughters), it cannot mimic the DM annual modulation signature in experiments such as the former DAMA/NaI and DAMA/LIBRA-phase1 and the present DAMA/LIBRA-phase2 which record the whole energy distribution; in fact, possible presence of Radon variation can easily be identified in this case and some of the six requirements of the DM annual modulation signature would fail.

In conclusion, no significant role is possible from the Radon.

... more on side processes As mentioned, possible side reactions have also been carefully investigated and none able to mimic the exploited signature is available;

previous results on the topics hold (see e.g. Ref. [5], and references therein). In particular, the case of neutrons, muons and solar neutrinos has been discussed in details in Ref. [7,8], where it has been demonstrated that they cannot give any significant contribution to the DAMA annual modulation result. Table 2.6.5 summarizes the safety upper limits on the contributions to the observed modulation amplitude due to the total neutron flux at LNGS, either from (α, n) reactions, from fissions and from muons and solar-neutrinos interactions in the rocks and in the lead around the experimental set-up; the direct contributions of muons and solar neutrinos are reported there too. Not only the limits are quantitatively marginal, but none of such contributions is able to simultaneously satisfy all the requirements of the exploited signature. Other arguments can be found in Ref. [1-4,7,5,11,8,16,17,15].

Source	$\Phi_{0,k}^{(n)}$ (neutrons $\text{cm}^{-2} \text{s}^{-1}$)	η_k	t_k	$R_{0,k}$ (cpd/kg/keV)	$A_k = R_{0,k}\eta_k$ (cpd/kg/keV)	A_k/S_m^{exp}
SLOW neutrons	thermal n ($10^{-2} - 10^{-1}$ eV)	1.08×10^{-6} $\simeq 0$ however $\ll 0.1$	—	$< 8 \times 10^{-6}$	$\ll 8 \times 10^{-7}$	$\ll 7 \times 10^{-5}$
	epithermal n (eV-keV)	2×10^{-6} $\simeq 0$ however $\ll 0.1$	—	$< 3 \times 10^{-3}$	$\ll 3 \times 10^{-4}$	$\ll 0.03$
FAST neutrons	fission, $(\alpha, n) \rightarrow n$ (1-10 MeV)	$\simeq 0.9 \times 10^{-7}$ $\simeq 0$ however $\ll 0.1$	—	$< 6 \times 10^{-4}$	$\ll 6 \times 10^{-5}$	$\ll 5 \times 10^{-3}$
	$\mu \rightarrow n$ from rock (> 10 MeV)	$\simeq 3 \times 10^{-9}$	0.0129 end of June	$\ll 5 \times 10^{-4}$	$\ll 7 \times 10^{-6}$	$\ll 6 \times 10^{-4}$
	$\mu \rightarrow n$ from Pb shield (> 10 MeV)	$\simeq 6 \times 10^{-9}$	0.0129 end of June	$\ll 1.1 \times 10^{-3}$	$\ll 1.4 \times 10^{-5}$	$\ll 1.3 \times 10^{-3}$
	$\nu \rightarrow n$ (few MeV)	$\simeq 3 \times 10^{-10}$	0.03342* Jan. 4th*	$\ll 5 \times 10^{-5}$	$\ll 1.8 \times 10^{-6}$	$\ll 1.6 \times 10^{-4}$
direct μ	$\Phi_0^{(\mu)} \simeq 20 \text{ m}^{-2}\text{d}^{-1}$	0.0129	end of June	$\simeq 10^{-7}$	$\simeq 10^{-9}$	$\simeq 10^{-7}$
direct ν	$\Phi_0^{(\nu)} \simeq 6 \times 10^{10} \text{ } \nu \text{ cm}^{-2}\text{s}^{-1}$	0.03342*	Jan. 4th*	$\simeq 10^{-5}$	3×10^{-7}	3×10^{-5}

Table 2.4. Summary of the contributions to the total neutron flux at LNGS; the value, $\Phi_{0,k}^{(n)}$, the relative modulation amplitude, η_k , and the phase, t_k , of each component is reported. It is also reported the counting rate, $R_{0,k}$, in DAMA/LIBRA-phase2 for *single-hit* events, in the (1 – 6) keV energy region induced by neutrons, muons and solar neutrinos, detailed for each component. The modulation amplitudes, A_k , are reported as well, while the last column shows the relative contribution to the annual modulation amplitude observed by DAMA/LIBRA-phase2, $S_m^{\text{exp}} \simeq 0.011$ cpd/kg/keV. For details see Ref. [8] and references therein.

* The annual modulation of solar neutrino is due to the different Sun-Earth distance along the year; so the relative modulation amplitude is twice the eccentricity of the Earth orbit and the phase is given by the perihelion.

2.6.6 Conclusions on possible systematics effects and side reactions

No modulation has been found in any possible source of systematics or side reactions; thus, upper limits (90% C.L.) on the possible contributions to the DAMA/LIBRA-phase2 measured modulation amplitude are summarized in Table

2.5. In particular, they cannot account for the measured modulation both because quantitatively not relevant and unable to mimic the observed effect.

Source	Main comment (see also Ref. [1])	Cautious upper limit (90%C.L.)
Radon	Sealed Cu Box in HP Nitrogen atmosphere, 3-level of sealing	$< 2.5 \times 10^{-6}$ cpd/kg/keV
Temperature	Air conditioning + huge heat capacity	$< 10^{-4}$ cpd/kg/keV
Noise	Efficient rejection	$< 10^{-4}$ cpd/kg/keV
Energy scale	Routine + intrinsic calibrations	$< 1 - 2 \times 10^{-4}$ cpd/kg/keV
Efficiencies	Regularly measured	$< 10^{-4}$ cpd/kg/keV
Background	No modulation above 6 keV; no modulation in the (1 – 6) keV <i>multiple-hit</i> events; this limit includes all possible sources of background	$< 10^{-4}$ cpd/kg/keV
Side reactions	From muon flux variation measured by MACRO	$< 3 \times 10^{-5}$ cpd/kg/keV
In addition: no effect can mimic the signature		

Table 2.5. Summary of the results obtained by investigating possible sources of systematics or of side reactions in the data of the DAMA/LIBRA-phase2 annual cycles. None able to give a modulation amplitude different from zero has been found; thus cautious upper limits (90% C.L.) on the possible contributions to the measured modulation amplitude have been calculated and are shown here.

2.7 Conclusions

The data of the new DAMA/LIBRA-phase2 confirm a peculiar annual modulation of the *single-hit* scintillation events in the (1–6) keV energy region satisfying all the many requirements of the DM annual modulation signature; the cumulative exposure by the former DAMA/NaI, DAMA/LIBRA-phase1 and DAMA/LIBRA-phase2 is $2.46 \text{ ton} \times \text{yr}$.

As required by the exploited DM annual modulation signature: 1) the *single-hit* events show a clear cosine-like modulation as expected for the DM signal; 2) the measured period is equal to $(0.999 \pm 0.001) \text{ yr}$ well compatible with the 1 yr period as expected for the DM signal; 3) the measured phase $(145 \pm 5) \text{ days}$ is compatible with the roughly $\simeq 152.5 \text{ days}$ expected for the DM signal; 4) the modulation is present only in the low energy (1–6) keV interval and not in other

higher energy regions, consistently with expectation for the DM signal; 5) the modulation is present only in the *single-hit* events, while it is absent in the *multiple-hit* ones as expected for the DM signal; 6) the measured modulation amplitude in NaI(Tl) target of the *single-hit* scintillation events in the (2–6) keV energy interval, for which data are also available by DAMA/NaI and DAMA/LIBRA-phase1, is: (0.0103 ± 0.0008) cpd/kg/keV (12.9σ C.L.). No systematic or side processes able to mimic the signature, i.e. able to simultaneously satisfy all the many peculiarities of the signature and to account for the whole measured modulation amplitude, has been found or suggested by anyone throughout some decades thus far. In particular, arguments related to any possible role of some natural periodical phenomena have been discussed and quantitatively demonstrated to be unable to mimic the signature (see e.g. Ref. [7,8]). Thus, on the basis of the exploited signature, the model independent DAMA results give evidence at 12.9σ C.L. (over 20 independent annual cycles and in various experimental configurations) for the presence of DM particles in the galactic halo.

In order to perform corollary investigation on the nature of the DM particles in given scenarios, model-dependent analyses are necessary³; thus, many theoretical and experimental parameters and models are possible and many hypotheses must also be exploited. In particular, the DAMA model independent evidence is compatible with a wide set of astrophysical, nuclear and particle physics scenarios for high and low mass candidates inducing nuclear recoil and/or electromagnetic radiation, as also shown in a wide literature. Moreover, both the negative results and all the possible positive hints, achieved so-far in the field, can be compatible with the DAMA model independent DM annual modulation results in many scenarios considering also the existing experimental and theoretical uncertainties; the same holds for indirect approaches. For a discussion see e.g. Ref. [5] and references therein. Model dependent analyses, to update the allowed regions in various scenarios and to enlarge the investigations to other ones, will be presented elsewhere.

Finally, we stress that to efficiently disentangle among the many possible candidates and scenarios an increase of exposure in the new lowest energy bin is important. The experiment is collecting data and related R&D is under way.

References

1. R. Bernabei et al., Nucl. Instr. and Meth. A **592**, 297 (2008).
2. R. Bernabei et al., Eur. Phys. J. C **56**, 333 (2008).
3. R. Bernabei et al., Eur. Phys. J. C **67**, 39 (2010).
4. R. Bernabei et al., Eur. Phys. J. C **73**, 2648 (2013).
5. R. Bernabei et al., Int. J. of Mod. Phys. A **28**, 1330022 (2013).
6. R. Bernabei et al., J. of Instr. **7**, P03009 (2012).
7. R. Bernabei et al., Eur. Phys. J. C **72**, 2064 (2012).
8. R. Bernabei et al., Eur. Phys. J. C **74**, 3196 (2014).

³ It is worth noting that it does not exist in direct and indirect DM detection experiments approaches which can offer such information independently on assumed models.

9. DAMA coll., issue dedicated to DAMA, Int. J. of Mod. Phys. A **31** (2016) and references therein.
10. for complete references: <http://people.roma2.infn.it/dama/web/publ.html>
11. R. Bernabei et al., Eur. Phys. J. C **74**, 2827 (2014).
12. R. Bernabei et al., *arXiv:1805.10486*.
13. P. Belli, R. Bernabei, C. Bacci, A. Incicchitti, R. Marcovaldi, D. Prosperi, DAMA proposal to INFN Scientific Committee II, April 24th 1990.
14. R. Bernabei et al., Il Nuovo Cim. A **112**, 545 (1999).
15. R. Bernabei et al., Eur. Phys. J. C **18**, 283 (2000).
16. R. Bernabei et al., La Rivista del Nuovo Cimento **26** n.1, 1-73 (2003), and references therein.
17. R. Bernabei et al., Int. J. Mod. Phys. D **13**, 2127 (2004) and references therein.
18. K.A. Drukier et al., Phys. Rev. D **33**, 3495 (1986).
19. K. Freese et al., Phys. Rev. D **37**, 3388 (1988).
20. R. Bernabei and A. Incicchitti, Int. J. Mod. Phys. A **32**, 1743007 (2017).
21. D. Smith and N. Weiner, Phys. Rev. D **64**, 043502 (2001).
22. D. Tucker-Smith and N. Weiner, Phys. Rev. D **72**, 063509 (2005).
23. D. P. Finkbeiner et al, Phys. Rev. D **80**, 115008 (2009).
24. K. Freese et al., Phys. Rev. D **71**, 043516 (2005).
25. K. Freese et al., Phys. Rev. Lett. **92**, 111301 (2004).
26. P. Belli et al., Int. J. of Mod. Phys. A **31**, 1642005 (2016).
27. R. Bernabei et al., Eur. Phys. J. C **47**, 263 (2006).
28. P. Gondolo et al., New Astron. Rev. **49**, 193 (2005).
29. G. Gelmini and P. Gondolo, Phys. Rev. D **64**, 023504 (2001).
30. F.S. Ling, P. Sikivie and S. Wick, Phys. Rev. D **70**, 123503 (2004).
31. G. Ranucci and M. Rovere, Phys. Rev. D **75**, 013010 (2007).
32. J.D. Scargle, Astrophys. J. **263**, 835 (1982).
33. W.H. Press et al., "Numerical recipes in Fortran 77: the art of scientific computing", Cambridge University Press, Cambridge, England 1992, section 13.8.
34. J.H. Horne and S.L. Baliunas, Astrophys. J. **302**, 757 (1986).
35. W.T. Eadie et al., "Statistical methods in experimental physics", ed. American Elsevier Pub. (1971).
36. M. Wojcik, Nucl. Instrum. and Meth. B **61**, 8 (1991).



3 HS YM and CS Theories in Flat Spacetime

L. Bonora

International School for Advanced Studies (SISSA),
Via Bonomea 265, 34136 Trieste, Italy, and INFN, Sezione di Trieste

Abstract. It is shown that in a flat background one can define higher spin (HS) gauge theories with an infinite number of fields. In particular here HS YM-like in any dimension and HS CS-like theories in any odd dimension are introduced and analyzed. They are invariant under HS gauge transformations which include ordinary $U(1)$ gauge transformations and diffeomorphisms. It is also shown how to recover local Lorentz invariance. The action, equations of motion and conserved currents in the HS YM-like theories are explicitly exhibited.

Povzetek. Avtor v prispevku pokaže, da lahko definira na ravnem ozadju umeritvene teorije višjih spinov z neskončnim številom polj. Kot poseben primer uvede in analizira teorije Yang-Millsovega tipa z višjim spinom v poljubni dimenziji in teorije Cherna-Simmonsna z višjim spinom v poljubni lihi dimenziji. Te teorije so invariantne na umeritvene transformacije za višje spine, ki vključujejo običajne transformacije $U(1)$ in difeomorfizme. Pokaže še, kako znova vpeljati lokalno Lorentzovo invarianco. V teorijah Yang-Millsovega tipa z višjim spinom zapiše akcijo ter enačbe gibanja in ohranitvene tokove.

Keywords: Higher spin theories, Yang-Mills like theories, Chern-Simmons theories, flat spacetime

3.1 Introduction...

There are compelling motivations for research to study spin (HS) theories, that is theories with an infinite number of fields with increasing spin. In a theory that unifies all the forces of nature such a feature seems to be inevitable. First (super)string theories have this characteristic. It is well known that the infinite number of fields with increasing spins is related to their good UV behavior. Also the AdS/CFT correspondence indicates that if we wish to resolve the singularities of the theory on the boundary we have to turn to the dual theory, which is a (super)string theory. Other arguments suggest that, when gravity is involved, infinite many local fields of increasing spins are needed in order to avoid possible conflicts with causality [1].

Starting from on these general motivations, in this contribution I will focus on a specific problem, for which for a long time there have been no answers, or only negative ones, in the literature: can one formulate a sensible local massless

HS theory in a flat space-time? The standard lore in the literature may be summarized by two objections: first, there are the so-called no-go theorems, which prevent the existence of such theories under rather general conditions; second, the construction of massless HS theories has been so far only successful in AdS spaces. However here I will exhibit examples of HS theories defined in flat spacetime in any dimension, which are massless, gauge invariant and, at least classically, consistent.

In [3] and, later on, in [4,7] a method has been proposed to produce HS effective actions by integrating out matter fields coupled to external potentials and quantized according to the worldline quantization. The method consists in computing current correlators, see [5,6], and explicitly determine the effective action. Barring anomalies, we are guaranteed that the result is HS gauge invariant. Unfortunately the method is very cumbersome and the resulting effective action is not guaranteed to be local.

In this paper I would like to show that there exists a shortcut. Exploiting the analogy of the HS gauge transformations with the gauge transformations in ordinary non-Abelian gauge theories, one can construct analogous local HS invariants and covariant objects, and in particular actions. In this way one can define (perturbatively) local HS Yang-Mills theories in any dimension and HS Chern-Simons theories in any odd dimension. I will focus in particular on the former. They are characterized by a coupling constant, like the ordinary YM theories. I will show how to define the action, their equations of motion and their conserved quantities. The HS gauge transformations contains in particular the ordinary $U(1)$ gauge transformations and the diffeomorphisms. They do not include the local Lorentz transformations. Since the HS YM-like theories are formulated in a frame-like formalism, local Lorentz transformations are relevant in order to permit their gravitational interpretation. Below I will show how to local Lorentz invariance is hidden in the formalism and how to recover it.

3.2 Higher spin effective action

This section is devoted to a concise presentation of the effective action method. The effective action here is defined via the worldline quantization method. This method consists, roughly speaking, in considering the coordinates on which the field depends, as the position of a quantum particle, while the latter is quantized according to the Weyl-Wigner quantization.

Let us consider a free fermion theory

$$S_0 = \int d^d x \bar{\psi}(i\gamma \cdot \partial - m)\psi, \quad (3.1)$$

coupled to external sources. According to the Weyl quantization method for a particle worldline, the full action is expressed as an expectation value of operators

$$S = \langle \bar{\psi} | -\gamma^a (\hat{P}_a - \hat{H}_a) - m | \psi \rangle \quad (3.2)$$

We recall that a quantum operator \hat{O} can be represented with a symbol $O(x, u)$ through the Weyl map

$$\hat{O} = \int d^d x d^d y \frac{d^d k}{(2\pi)^d} \frac{d^d u}{(2\pi)^d} O(x, u) e^{ik \cdot (x - \hat{X}) - iy \cdot (u - \hat{P})} \quad (3.3)$$

where \hat{X} is the position operator. The symbol of the product of two operators is the $*$ product (or Moyal product) of the corresponding symbols.

In (3.2) \hat{P}_a is the momentum operator whose symbol is the classical momentum u_a ¹. \hat{H}_a is an operator whose symbol is $h_a(x, u)$, where

$$h_a(x, u) = \sum_{n=0}^{\infty} \frac{1}{n!} h_a^{\mu_1 \dots \mu_n}(x) u_{\mu_1} \dots u_{\mu_n} \quad (3.4)$$

$s = n + 1$ is the spin and the tensors are assumed to be symmetric in μ_1, \dots, μ_n . Any field like $h_a(x, u)$, which depends also from the momentum u , will be referred to as *master field*.

One should notice that there are two kind of labels a and μ_i . They will be interpreted later as flat and curved indices, respectively, but in a flat background they play the same role. Their true nature will be illustrated later on.

Now one makes the above formalism explicit in (3.2), where we also insert two completenesses $\int d^d x |x\rangle \langle x|$, and make the identification $\psi(x) = \langle x | \psi \rangle$. Expressing S in terms of symbols one finds

$$\begin{aligned} S &= S_0 + \int \frac{d^d u}{(2\pi)^d} d^d x d^d z e^{iu \cdot z} \bar{\psi} \left(x + \frac{z}{2} \right) \gamma \cdot h(x, u) \psi \left(x - \frac{z}{2} \right) \\ &= S_0 + \sum_{s=1}^{\infty} \int d^d x J_{\mu_1 \dots \mu_s}^{(s)}(x) h_{(s)}^{\mu_1 \dots \mu_s}(x) \end{aligned} \quad (3.5)$$

The tensor field $h_a^{\mu_1 \dots \mu_n}$ is linearly coupled to the HS current

$$J_{\mu_1 \dots \mu_n}^a(x) = \frac{i^n}{n!} \frac{\partial}{\partial z^{(\mu_1}} \dots \frac{\partial}{\partial z^{\mu_n)}} \bar{\psi} \left(x + \frac{z}{2} \right) \gamma_a \psi \left(x - \frac{z}{2} \right) \Big|_{z=0}. \quad (3.6)$$

For instance, for $s = 1$ and $s = 2$ one obtains

$$J_a^{(1)} = \bar{\psi} \gamma_a \psi \quad (3.7)$$

$$J_{a\mu_1}^{(2)} = \frac{i}{2} (\partial_{(\mu_1} \bar{\psi} \gamma_a) \psi - \bar{\psi} \gamma_a \partial_{\mu_1}) \psi \quad (3.8)$$

The HS currents are on-shell conserved in the free theory (3.1)

$$\partial_a J_{(s)}^{a\mu_1 \dots \mu_{s-1}} = 0 \quad (3.9)$$

¹ Throughout the paper the position in the phase space are denoted by couples of letters (x, u) , (y, v) , (z, t) , (w, r) , the first letter refers to the space-time coordinate and the second the momentum of the worldline particle. The letters k, p, q will be reserved to the momenta of the (Fourier-transformed) physical amplitudes.

3.2.1 HS gauge symmetries

The action (3.2) is trivially invariant under the operation

$$S = \langle \bar{\psi} | \hat{O} \hat{O}^{-1} \hat{G} \hat{O} \hat{O}^{-1} | \psi \rangle \quad (3.10)$$

where $\hat{G} = -\gamma \cdot (\hat{P} - \hat{H}) - m$. So it is invariant under

$$\hat{G} \longrightarrow \hat{O}^{-1} \hat{G} \hat{O}, \quad |\psi\rangle \longrightarrow \hat{O}^{-1} |\psi\rangle \quad (3.11)$$

Writing $\hat{O} = e^{-i\hat{E}}$ we easily find the infinitesimal version.

$$\delta|\psi\rangle = i\hat{E}|\psi\rangle, \quad \delta\langle\bar{\psi}| = -i\langle\bar{\psi}|\hat{E}, \quad (3.12)$$

and

$$\delta\hat{G} = i[\hat{E}, \hat{G}] = i[\gamma \cdot (\hat{P} - \hat{H}), \hat{E}] = \gamma \cdot \delta\hat{H} \quad (3.13)$$

Let the symbol of \hat{E} be $\varepsilon(x, u)$, then the symbol of $[i\gamma \cdot \hat{P}, \hat{E}]$ is

$$\int d^d y \langle x - \frac{y}{2} | [i\gamma \cdot \hat{P}, \hat{E}] | x + \frac{y}{2} \rangle e^{iy \cdot u} = -i\gamma \cdot \partial_x \varepsilon(x, u) \quad (3.14)$$

Similarly

$$\text{Symb}([\hat{H}_a, \hat{E}]) = [h_a(x, u) * \varepsilon(x, u)] \quad (3.15)$$

where $[a * b] \equiv a * b - b * a$ is the $*$ -commutator. Therefore, in terms of symbols,

$$\delta_\varepsilon h_a(x, u) = \partial_a^x \varepsilon(x, u) - i[h_a(x, u) * \varepsilon(x, u)] \equiv \mathcal{D}_a^{*x} \varepsilon(x, u) \quad (3.16)$$

where the covariant derivative defined by

$$\mathcal{D}_a^{*x} = \partial_a^x - i[h_a(x, u) * \quad] \quad (3.17)$$

has been introduced.

The variation in eq.(3.16) will be referred to hereafter as HS gauge transformation, and the corresponding symmetry *HS gauge symmetry*. For the transformations of ψ , see [4] .

It is easy to see that the conservation law in the classical interacting theory

$$\mathcal{D}_x^{*a} J_a(x, u) = 0 \quad (\text{on-shell}) \quad (3.18)$$

follows from the above.

Using the $*$ -Jacobi identity (which holds also for the Moyal product, because the latter is associative) one can easily get

$$\begin{aligned} (\delta_{\varepsilon_2} \delta_{\varepsilon_1} - \delta_{\varepsilon_1} \delta_{\varepsilon_2}) h^\mu(x, u) &= i(\partial_a^x [\varepsilon_1 * \varepsilon_2](x, u) - i[h_a(x, u) * [\varepsilon_1 * \varepsilon_2](x, u)]) \\ &= i\mathcal{D}_a^{*x} [\varepsilon_1 * \varepsilon_2](x, u) \end{aligned} \quad (3.19)$$

i.e. the HS ε -transform is of Lie algebra type.

3.2.2 The HS effective action

The general formula for the effective action is

$$W[h] = W[0] + \sum_{n=1}^{\infty} \frac{1}{n!} \int \prod_{i=1}^n d^d x_i \frac{d^d u_i}{(2\pi)^d} \mathcal{W}_{a_1, \dots, a_n}^{(n)}(x_1, u_1, \dots, x_n, u_n, \epsilon) \times h^{a_1}(x_1, u_1) \dots h^{a_n}(x_n, u_n) \quad (3.20)$$

where $\mathcal{W}_{a_1, \dots, a_n}^{(n)}(x_1, u_1, \dots, x_n, u_n, \epsilon)$ are the n -point functions of the currents $J_{a_1}(x_1, u_1), \dots, J_{a_n}(x_n, u_n)$. $W[0]$ is the constant 0-point contribution, which will be disregarded in the sequel. There are various ways to compute these amplitudes. The most popular is by means of Feynman diagrams. For instance, the 3-point function can be calculated via the Feynman diagram integral

$$\begin{aligned} & \langle J_{a_1}(x_1, u_1) J_{a_2}(x_2, u_2) J_{a_3}(x_3, u_3) \rangle \\ &= -i \int \frac{d^d q_1}{(2\pi)^d} \frac{d^d q_2}{(2\pi)^d} e^{i(q_1 + q_2) \cdot x_1} e^{-i q_1 \cdot x_2} e^{-i q_2 \cdot x_3} \\ & \times \delta\left(u_1 - \frac{2p - q_1 - q_2}{2}\right) \delta\left(u_2 - \frac{2p - q_1}{2}\right) \delta\left(u_3 - \frac{2p - 2q_1 - q_2}{2}\right) \\ & \times \int \frac{d^d p}{(2\pi)^d} \text{tr} \left(\gamma_{a_1} \frac{1}{\not{p} + m} \gamma_{a_2} \frac{1}{\not{p} - \not{q}_1 + m} \gamma_{a_3} \frac{1}{\not{p} - \not{q}_1 - \not{q}_2 + m} \right), \end{aligned} \quad (3.21)$$

to which one must add the cross term. q_1, q_2 are the momenta of two external outgoing legs. The third one has incoming momentum $q_1 + q_2$.

These amplitudes have cyclic symmetry. The invariance of the effective action under (3.16) is expressed by

$$\begin{aligned} 0 &= \delta_\epsilon W[h] = \sum_{n=1}^{\infty} \frac{1}{(n-1)!} \int \prod_{i=1}^n d^d x_i \frac{d^d u_i}{(2\pi)^d} \\ & \times \mathcal{W}_{a_1, \dots, a_n}^{(n)}(x_1, u_1, \dots, x_n, u_n) \mathcal{D}_x^{*\mu_1} \epsilon(x_1, u_1) h^{a_2}(x_2, u_2) \dots h^{a_n}(x_n, u_n) \end{aligned} \quad (3.22)$$

The generalized equations of motion are obtained by varying $W[h]$ with respect to the master field $h_a(x, u)$. Let us write them in the compact form

$$\mathcal{F}_a(x, u) = 0 \quad (3.23)$$

where

$$\begin{aligned} \mathcal{F}_a(x, u) &\equiv \sum_{n=0}^{\infty} \frac{1}{n!} \int \prod_{i=1}^n d^d x_i \frac{d^d u_i}{(2\pi)^d} \mathcal{W}_{a a_1 \dots a_n}^{(n+1)}(x, u, x_1, u_1, \dots, x_n, u_n, \epsilon) \\ & \times h^{a_1}(x_1, u_1) \dots h^{a_n}(x_n, u_n) \end{aligned}$$

The EoM's (3.23) are covariant under HS gauge transformation

$$\delta_\epsilon \mathcal{F}_a(x, u) = i[\epsilon(x, u) * \mathcal{F}_a(x, u)] \quad (3.24)$$

3.3 Yang-Mills-like theories

3.3.1 The gauge transformation in the fermion model

Let us return to the gauge transformation (3.16)

$$\delta_\varepsilon h_a(x, u) = \partial_a^\chi \varepsilon(x, u) - i[h_a(x, u) \star \varepsilon(x, u)] \equiv \mathcal{D}_a^{\chi*} \varepsilon(x, u) \quad (3.25)$$

and write it down in components. To avoid a proliferation of numerical indices, let us write the expansion of $h_a(x, u)$ as

$$h_a(x, u) = A_a(x) + \chi_a^\mu(x) u_\mu + \frac{1}{2} b_a^{\mu\nu} u_\mu u_\nu + \frac{1}{6} c_a^{\mu\nu\lambda} u_\mu u_\nu u_\lambda + \dots \quad (3.26)$$

As noted above we use two different types of indices. In the expansion (3.4) the indices μ_1, \dots, μ_n are upper (contravariant), as it should be, because in the Weyl quantization procedure the momentum has lower index, since it must satisfy $[\chi^\mu, p_\nu] = i\delta_\nu^\mu$. The index a instead is traditionally reserved for a flat index. Of course when the background metric is flat the indices a and μ_i are on the same footing, but it is useful to keep them distinct. Let us see why.

For the HS gauge parameter we write

$$\varepsilon(x, u) = \epsilon(x) + \xi^\mu u_\mu + \frac{1}{2} \Lambda^{\mu\nu} u_\mu u_\nu + \frac{1}{3!} \Sigma^{\mu\nu\lambda} u_\mu u_\nu u_\lambda + \dots \quad (3.27)$$

The transformation (3.25) to the lowest order reads,

$$\begin{aligned} \delta A_a &= \partial_a \epsilon + \xi \cdot \partial A_a - \partial_\rho \epsilon \chi_a^\rho + \dots \\ \delta \chi_a^\nu &= \partial_a \xi^\nu + \xi \cdot \partial \chi_a^\nu - \partial_\rho \xi^\nu \chi_a^\rho + \partial^\rho A_a \Lambda_{\rho}{}^\nu - \partial_\lambda \epsilon b_a^{\lambda\nu} + \dots \\ \delta b_a^{\nu\lambda} &= \partial_a \Lambda^{\nu\lambda} + \xi \cdot \partial b_a^{\nu\lambda} - \partial_\rho \xi^\nu b_a^{\rho\lambda} - \partial_\rho \xi^\lambda b_a^{\rho\nu} + \partial_\rho \chi_a^\nu \Lambda_{\rho}{}^\lambda + \partial_\rho \chi_a^\lambda \Lambda_{\rho}{}^\nu \\ &\quad - \chi_a^\rho \partial_\rho \Lambda_{\nu\lambda} + \dots \end{aligned} \quad (3.28)$$

The next nontrivial order contains terms with three derivatives, and so on.

It is natural to compare the previous HS gauge variations with the ordinary gauge, diff, ... transformations. To this end let us denote by \tilde{A}_a the standard U(1) gauge field and by $\tilde{e}_a^\mu = \delta_a^\mu - \tilde{\chi}_a^\mu$ the standard inverse vielbein, and let us restrict the previous general transformation to gauge and diff transformations alone. We have

$$\begin{aligned} \delta \tilde{A}_a &\equiv \delta(\tilde{e}_a^\mu \tilde{A}_\mu) \equiv \delta((\delta_a^\mu - \tilde{\chi}_a^\mu) \tilde{A}_\mu) \\ &= (-\xi \cdot \partial \tilde{\chi}_a^\mu + \partial_\lambda \xi^\mu \tilde{\chi}_a^\lambda) \tilde{A}_\mu + (\delta_a^\mu - \tilde{\chi}_a^\mu) (\partial_\mu \epsilon + \xi \cdot \tilde{A}_\mu) \\ &\approx \partial_a \epsilon + \xi \cdot \tilde{A}_a - \tilde{\chi}_a^\mu \partial_\mu \epsilon \end{aligned} \quad (3.29)$$

and

$$\delta \tilde{e}_a^\mu \equiv \delta(\delta_a^\mu - \tilde{\chi}_a^\mu) = \xi \cdot \partial \tilde{e}_a^\mu - \partial_\lambda \xi^\mu \tilde{e}_a^\lambda = -\xi \cdot \tilde{\chi}_a^\mu - \partial_a \xi^\mu + \partial_\lambda \xi^\mu \tilde{\chi}_a^\lambda \quad (3.30)$$

so that

$$\delta \tilde{\chi}_a^\mu = \xi \cdot \partial \tilde{\chi}_a^\mu + \partial_a \xi^\mu - \partial_\lambda \xi^\mu \tilde{\chi}_a^\lambda \quad (3.31)$$

where we have retained only the terms at most linear in the fields. From the above we see that the natural identifications are

$$A_a = \tilde{A}_a, \quad \chi_a^\mu = \tilde{\chi}_a^\mu \quad (3.32)$$

The transformations (3.28) are consistent with the ordinary gauge and diffeomorphism transformations. Therefore the master field h_a can describe in particular the geometry of the gauge theories and the geometry of gravity. The above does not explain the nature of the index a . It is natural to interpret it as a flat index, but this calls for local Lorentz symmetry. This issue will be resumed later on.

3.3.2 Analogy with gauge transformations in gauge theories

It should be remarked that in eq.(3.25) and (3.28) the derivative ∂_a means $\partial_a = \delta_a^\mu \partial_\mu$, not $\partial_a = e_a^\mu \partial_\mu = (e_a^\mu - \chi_a^\mu + \dots) \partial_\mu$. In fact the linear correction $-\chi_a^\mu \partial_\mu$ is contained in the term $-i[h_a(x, u) * \varepsilon(x, u)]$, see for instance the second term in the RHS of the first equation (3.28). The obvious remark is that the transformation (3.25) looks similar to the ordinary gauge transformation of a non-Abelian gauge field

$$\delta_\lambda A_a = \partial_a \lambda + [A_a, \lambda] \quad (3.33)$$

where $A_a = A_a^\alpha T^\alpha$, $\lambda = \lambda^\alpha T^\alpha$, T^α being the Lie algebra generators.

In gauge theories it is useful to represent the gauge potential as a connection one form $\mathbf{A} = A_a dx^a$, so that (3.33) becomes

$$\delta_\lambda \mathbf{A} = d\lambda + [\mathbf{A}, \lambda] \quad (3.34)$$

We can do the same for (3.25)

$$\delta_\varepsilon \mathbf{h}(x, u) = d\varepsilon(x, u) - i[\mathbf{h}(x, u) * \varepsilon(x, u)] \equiv \mathbf{D}\varepsilon(x, u) \quad (3.35)$$

where $d = \partial_a dx^a$, $\mathbf{h} = h_a dx^a$ and x^a are coordinates in the tangent spacetime, and it is understood that

$$[\mathbf{h}(x, u) * \varepsilon(x, u)] = [h_a(x, u) * \varepsilon(x, u)] dx^a$$

We will apply this formalism to the construction of HS CS or YM-like actions.

3.3.3 HS Yang-Mills action

In analogy with the ordinary Yang-Mills theory one can introduce the curvature 2-form

$$\mathbf{G} = d\mathbf{h} - \frac{i}{2}[\mathbf{h} * \mathbf{h}], \quad (3.36)$$

whose components are

$$G_{ab} = \partial_a h_b - \partial_b h_a - i[h_a * h_b] \quad (3.37)$$

Their transformation rule is

$$\delta_\varepsilon G_{ab} = -i[G_{ab} * \varepsilon] \quad (3.38)$$

Next we will consider functionals which are integrated polynomials of \mathbf{G} or of its components G_{ab} . In order to exploit the transformation property (3.16) in the construction we need the ‘trace property’, analogous to the trace of polynomials in ordinary non-Abelian gauge theories. The only object with trace properties we can define in the HS context is

$$\begin{aligned} \langle\langle f * g \rangle\rangle &\equiv \int d^d x \int \frac{d^d u}{(2\pi)^d} f(x, u) * g(x, u) \\ &= \int d^d x \int \frac{d^d u}{(2\pi)^d} f(x, u) g(x, u) = \langle\langle g * f \rangle\rangle \end{aligned} \quad (3.39)$$

From this, plus associativity, it follows that

$$\langle\langle f_1 * f_2 * \dots * f_n \rangle\rangle = (-1)^{\varepsilon_1(\varepsilon_2 + \dots + \varepsilon_n)} \langle\langle f_2 * \dots * f_n * f_1 \rangle\rangle \quad (3.40)$$

where ε_i is the Grassmann degree of f_i . In particular

$$\langle\langle [f_1 * f_2 * \dots * f_n] \rangle\rangle = 0 \quad (3.41)$$

where $[*]$ is the $*$ -commutator or anti-commutator, as appropriate.

This property holds also when the f_i are valued in a Lie algebra, provided the symbol $\langle\langle \rangle\rangle$ includes also the trace over the Lie algebra generators.

Let us return to G_{ab} . From the property (3.41) it follows that

$$\delta_\varepsilon \langle\langle G^{ab} * G_{ab} \rangle\rangle = -i \langle\langle G^{ab} * G_{ab} * \varepsilon - \varepsilon * G^{ab} * G_{ab} \rangle\rangle = 0 \quad (3.42)$$

Therefore

$$\mathcal{YM}(\mathbf{h}) = -\frac{1}{4g^2} \langle\langle G^{ab} * G_{ab} \rangle\rangle \quad (3.43)$$

is invariant under the HS gauge transformation and it is a well defined functional in any dimension.

This construction can be easily generalized to the non-Abelian case, that is when the master field \mathbf{h}_a is valued in a Lie algebra with generators T^α : $\mathbf{h}_a = h_a^\alpha T^\alpha$. See [8].

3.3.4 HS CS action

Using the above properties it is not hard to prove, [7] that

$$\mathcal{CS}(\mathbf{h}) = n \int_0^1 dt \langle\langle \mathbf{h} * \mathbf{G}_t * \dots * \mathbf{G}_t \rangle\rangle \quad (3.44)$$

where

$$\mathbf{G}_t = d\mathbf{h}_t - \frac{i}{2} [\mathbf{h}_t * \mathbf{h}_t], \quad \mathbf{h}_t = t\mathbf{h}, \quad (3.45)$$

is HS gauge invariant in a space of odd dimension $d = 2n - 1$. It defines the HS CS action in any odd-dimensional spacetime.

3.3.5 Covariant YM-type eom's

From(3.43) we get the following eom:

$$\partial_b G^{ab} - i[h_b, *, G^{ab}] \equiv \mathcal{D}_b^* G^{ab} = 0 \quad (3.46)$$

which is covariant under the HS gauge transformation

$$\delta_\varepsilon (\mathcal{D}_b^* G^{ab}) = -i[\mathcal{D}_b^* G^{ab}, \varepsilon] \quad (3.47)$$

In components this equation splits into an infinite set according to the powers of u . Let us expand G_{ab} in the notation of sec.3.3.1. We have

$$G_{ab} = F_{ab} + X_{ab}^\mu u_\mu + \frac{1}{2} B_{ab}^{\mu\nu} u_\mu u_\nu + \frac{1}{6} C_{ab}^{\mu\nu\lambda} u_\mu u_\nu u_\lambda + \dots \quad (3.48)$$

and express them in terms of the component fields of $h_a(x, u)$.

For instance, the first eom ($\mathcal{O}(u^0)$) is

$$\begin{aligned} 0 = & \square A_b - \partial_b \partial \cdot A + \frac{1}{2} (\partial_\sigma \partial \cdot A \chi_b^\sigma + \partial_\sigma A^a \partial_a \chi_b^\sigma - \partial_\sigma \partial^a A_b \chi_a^\sigma - \partial_\sigma A_b \partial \cdot \chi^\sigma) \\ & + \frac{1}{2} \partial_\sigma A^a \left(\partial_a \chi_b^\sigma - \partial_b \chi_a^\sigma + \frac{1}{2} (\partial_\lambda A_a b_b^{\lambda\sigma} - \partial_\lambda A_b b_a^{\lambda\sigma} + \partial_\lambda \chi_a^\sigma \chi_b^\lambda - \partial_\lambda \chi_b^\sigma \chi_a^\lambda) \right) \\ & - \frac{1}{2} \chi_a^\sigma \left(\partial_\sigma \partial^a A_b - \partial_\sigma \partial_b A^a \right. \\ & \left. + \frac{1}{2} (\partial_\sigma \partial_\lambda A^a \chi_b^\lambda + \partial_\lambda A^a \partial_\sigma \chi_b^\lambda - \partial_\sigma \partial_\lambda A_b \chi^{a\lambda} - \partial_\lambda A_b \partial_\sigma \chi^{a\lambda}) \right) \\ & + \dots \end{aligned} \quad (3.49)$$

The second ($\mathcal{O}(u^1)$)

$$\begin{aligned} \square \chi_a^\mu - \partial_a \partial^b \chi_b^\mu = & \frac{1}{2} \left(\partial^b (\partial_\sigma A_a b_b^{\sigma\mu} - \partial_\sigma A_b b_a^{\sigma\mu} + \partial_\sigma \chi_a^\mu \chi_b^\sigma - \partial_\sigma \chi_b^\mu \chi_a^\sigma) \right. \\ & + \partial_\tau A^b \partial_a b_b^{\mu\tau} - \partial_\tau A^b \partial_b b_a^{\mu\tau} + \partial_\tau \chi^{b\mu} \partial_a \chi_b^\tau - \partial_\tau \chi^{b\mu} \partial_b \chi_a^\tau \\ & \left. - \partial_\tau \partial_a A_b b^{b\tau\mu} + \partial_\tau \partial_b A_a b^{b\tau\mu} - \partial_\tau \partial_a \chi_b^\mu \chi^{b\tau} + \partial_\tau \partial_b \chi_a^\mu \chi^{b\tau} \right) + \dots \end{aligned} \quad (3.50)$$

Ellipses denote terms with a larger number of spacetime derivatives.

Let us see a few elementary examples. Consider the case of a pure $U(1)$ gauge field A alone. The equation of motion is

$$\partial_a F^{ab} = \square A^b - \partial_b \partial \cdot A = 0 \quad (3.51)$$

In the 'Feynman gauge' $\partial \cdot A = 0$ this reduces to $\square A^b = 0$.

Let us suppose next that only gravity is present. Eq.(3.50) becomes

$$\partial_a \chi^{ab\mu} = \square \chi_b^\mu - \partial_b \partial \cdot \chi^\mu = 0 \quad (3.52)$$

In the 'Feynman gauge' $\partial \cdot \chi^\mu = 0$, (3.52) reduces to $\square \chi_b^\mu = 0^2$.

² In ordinary gravity ($R_{\mu\nu} = 0$) we have to impose the DeDonder gauge in order to obtain the same result.

Finally, keeping only the spin 3 field the eom becomes

$$\partial_a B^{ab\mu\nu} = \square b_b^{\mu\nu} - \partial_b \partial^a b_a^{\mu\nu} = 0 \quad (3.53)$$

Again in the 'Feynman gauge' $\partial^a b_a^{\mu\nu} = 0$ we get $\square b_b^{\mu\nu} = 0$.

In general we can impose for all the fields the Feynman gauge

$$\partial^a h_a(x, u) = 0 \quad (3.54)$$

As is clear from (3.49), for instance, the above eom's are characterized by the fact that at each order, defined by the number of derivatives, there is a finite number of terms. This defines a *perturbatively local* theory.

3.3.6 Conserved currents

The conservation laws of the HS models can be found following the analogy of a current in an ordinary gauge theory or the energy momentum tensor in gravity theories. For instance, if in HS YM we express the invariance of the action under the HS gauge transformation we can write

$$\begin{aligned} 0 &= -\frac{1}{4} \delta_\varepsilon \langle\langle G_{ab} * G^{ab} \rangle\rangle = \langle\langle \delta_\varepsilon h_a * \mathcal{D}_b^* G^{ab} \rangle\rangle \\ &= \langle\langle \mathcal{D}_a^* \varepsilon * \mathcal{D}_b^* G^{ab} \rangle\rangle = -\langle\langle \varepsilon * \mathcal{D}_a^* \mathcal{D}_b^* G^{ab} \rangle\rangle, \end{aligned} \quad (3.55)$$

This implies the off-shell relation or conservation law

$$\mathcal{D}_a^* \mathcal{D}_b^* G^{ab} = 0 \quad (3.56)$$

from which we can identify the conserved master current

$$\mathcal{J}_a = \mathcal{D}_b^* G^{ab} \quad (3.57)$$

These conserved currents vanish on shell and are conserved off-shell. Expanding in u

$$\mathcal{J}_a = \sum_{n=0}^{\infty} \frac{1}{n!} \mathcal{J}_a^{\mu_1 \dots \mu_n}(x) u_{\mu_1} \dots u_{\mu_n} \quad (3.58)$$

we find the conserved components.

Remark. The approach to covariance implicit in the HS YM theory (but also in the effective action method) is entirely new. Unlike most HS approaches we do not start from the EH action for gravity, and we do not replace ordinary derivatives with Riemannian covariant derivatives. We obtain nevertheless an action invariant under HS gauge transformations. The gauge transformation (3.16) reproduces both ordinary U(1) gauge transformations and diffeomorphisms, but the action functional is defined in the phase space. It gives nevertheless rise to local (HS gauge covariant) equations of motion that reproduce the ordinary YM eoms, and, although not completely, the metric equations of motion of EH gravity: the linear eom coincide with the ordinary one after gauge fixing. Although the equations (3.50) is very reminiscent of ordinary gravity, this is not yet enough to identify the type of gravity described by it. In fact this problem requires further investigation and will be discussed in a forthcoming paper.

3.4 Local Lorentz symmetry

As pointed out before the HS YM action is fully invariant in particular under diffeomorphisms. This prompted us to interpret the second component of $h_a(s, u)$ in the u expansion, χ_a^μ , as a vielbein fluctuation, and $\delta_a^\mu - \chi_a^\mu$ as a vielbein or local frame. However this implies that $_a$ is a flat index and must transform appropriately under local Lorentz transformations. But, at least at first sight, local Lorentz invariance is absent. Consider simply the case in which only the field A_a is non-vanishing, the form of the Lagrangian is

$$L_A \sim F_{ab} F^{ab}, \quad F_{ab} = \partial_a A_b - \partial_b A_a \quad (3.59)$$

This is not invariant under a Lorentz transformation, because when $A_a \rightarrow A_a + \Lambda_a{}^b A_b$ we generate terms $((\partial_a \Lambda_b{}^c) A_c - (\partial_b \Lambda_a{}^c) A_c) F^{ab}$, that do not vanish. This is a simple example of a general problem in HS YM. It is crucial to clarify it.

3.4.1 Inertial frames and connections

Let us start from the definition of trivial frame. A trivial (inverse) frame $e_a^\mu(x)$ is a frame that can be reduced to a Kronecker delta by means of a local Lorentz transformation (LLT), i.e. there exists a (pseudo)orthogonal transformation $O_a{}^b(x)$ such that

$$O_a{}^b(x) e_b{}^\mu(x) = \delta_a^\mu \quad (3.60)$$

As a consequence $e_b{}^\mu(x)$ contains only inertial (non-dynamical) information. A full gravitational (dynamical) frame is the sum of a trivial frame and a nontrivial piece

$$\tilde{E}_a{}^\mu(x) = e_a{}^\mu(x) - \tilde{\chi}_a^\mu(x) \quad (3.61)$$

By means of a suitable LLT it can be cast in the form

$$E_a{}^\mu(x) = \delta_a^\mu - \chi_a^\mu(x) \quad (3.62)$$

This is the form we have encountered above in HS theories. But it should not be forgotten that the Kronecker delta is a trivial frame. If we want to recover local Lorentz covariance instead of $\partial_a = \delta_a^\mu \partial_\mu$ we must understand

$$\partial_a = e_a{}^\mu(x) \partial_\mu \quad (3.63)$$

where $e_a{}^\mu(x)$ is a trivial (or purely inertial) vielbein. In particular, under an infinitesimal LLT, it transforms according to

$$\delta_\Lambda e_a{}^\mu(x) = \Lambda_a{}^b(x) e_b{}^\mu(x) \quad (3.64)$$

A trivial connection (or inertial spin connection) is defined by

$$\mathcal{A}^a{}_{b\mu} = (O(x) \partial_\mu O^{-1}(x))^a{}_b \quad (3.65)$$

where $O(x)$ is a generic local (pseudo)orthogonal transformation (finite local Lorentz transformation). As a consequence its curvature vanishes

$$\mathcal{R}^a{}_{b\mu\nu} = \partial_\mu \mathcal{A}^a{}_{b\nu} - \partial_\nu \mathcal{A}^a{}_{b\mu} + \mathcal{A}^a{}_{c\mu} \mathcal{A}^c{}_{b\nu} - \mathcal{A}^a{}_{c\nu} \mathcal{A}^c{}_{b\mu} = 0 \quad (3.66)$$

Let us recall that the space of connections is affine. We can obtain any connection from a fixed one by adding to it adjoint-covariant tensors. When the spacetime is topologically trivial we can choose as origin of the affine space the 0 connection. The latter is a particular member in the class of the trivial connections. To see this let us suppose we start with the spin connection (3.65). A Lorentz transformation of a spin connection $\mathcal{A}_\mu = \mathcal{A}_\mu{}^{ab} \Sigma_{ab}$ is

$$\mathcal{A}_\mu(x) \rightarrow L(x) D_\mu L^{-1}(x) = L(x) (\partial_\mu + \mathcal{A}_\mu) L^{-1}(x) \quad (3.67)$$

where $L(x)$ is a (finite) LLT. If we choose $L = O^{-1}$ we get

$$\mathcal{A}_\mu(x) \rightarrow 0 \quad (3.68)$$

But at this point the LL symmetry is completely fixed. Thus choosing the zero spin connection amounts to fixing the local Lorentz gauge.

The connection \mathcal{A}_μ contains inertial and no gravitational information. It will be referred to as the *inertial connection*. It is a *non-dynamical* object (its content is pure gauge). The dynamical degrees of freedom will be contained in the adjoint tensor to be added to \mathcal{A}_μ in order to form a fully dynamical spin connection³. \mathcal{A}_μ is nevertheless a connection and it makes sense to introduce the inertial derivative

$$D_\mu = \partial_\mu - \frac{i}{2} \mathcal{A}_\mu \quad (3.69)$$

which is Lorentz covariant.

It is clear that the results ensuing from the effective action method, as well as the HS YM and HS CS theories, are all formulated in a trivial frame setting, eq.(3.62), with a trivial spin connection. In other words the local Lorentz gauge is completely fixed. However from this formalism it is not difficult to recover explicit local Lorentz covariance.

3.4.2 How to recover local Lorentz symmetry

Let us restart from the definition of $J_a(x, u)$

$$\begin{aligned} J_a(x, u) &= \sum_{n,m=0}^{\infty} \frac{(-i)^n i^m}{2^{n+m} n! m!} \partial_{\mu_1} \dots \partial_{\mu_m} \bar{\psi}(x) \gamma_a \partial_{\nu_1} \dots \partial_{\nu_n} \psi(x) \\ &\quad \times \frac{\partial^{n+m}}{\partial u_{\mu_1} \dots \partial u_{\mu_m} \partial u_{\nu_1} \dots \partial u_{\nu_n}} \delta(u) \\ &= \sum_{s=1}^{\infty} (-1)^{s-1} J_{a\mu_1 \dots \mu_{s-1}}^{(s)}(x) \frac{\partial^{s-1}}{\partial u_{\mu_1} \dots \partial u_{\mu_{s-1}}} \delta(u) \end{aligned} \quad (3.70)$$

³ The splitting of vierbein and spin connection into an inertial and a dynamical part is characteristic of teleparallelism, [9]

from which we derive

$$J_{a\mu_1 \dots \mu_{s-1}}^{(s)}(x) = \sum_{n=0}^{s-1} \frac{(-1)^n}{s^{s-1}(s-1)!} \partial_{(\mu_1} \dots \partial_{\mu_n} \bar{\psi}(x) \gamma_a \partial_{\mu_{n+1}} \dots \partial_{\mu_{s-1}}) \psi(x) \quad (3.71)$$

Assume now the following LLT

$$\begin{aligned} \delta_\Lambda \psi &= -\frac{i}{2} \Lambda \psi, & \Lambda &= \Lambda^{ab} \Sigma_{ab}, & \Sigma_{ab} &= \frac{i}{4} [\gamma_a, \gamma_b] \\ \delta_\Lambda \bar{\psi} &= \frac{i}{2} \bar{\psi} \Lambda \end{aligned} \quad (3.72)$$

and replace in (3.71) the ordinary derivative on ψ with the inertial covariant derivative

$$\partial_\mu \psi \rightarrow D_\mu \psi = \left(\partial_\mu - \frac{i}{2} \mathcal{A}_\mu \right) \psi \quad (3.73)$$

and on $\bar{\psi}$ with

$$\partial_\mu \bar{\psi} \rightarrow D_\mu^\dagger \bar{\psi} = \partial_\mu \bar{\psi} + \frac{i}{2} \bar{\psi} \mathcal{A}_\mu \quad (3.74)$$

Eq.(3.71) becomes

$$\begin{aligned} J'_{a\mu_1 \dots \mu_{s-1}}^{(s)}(x) \\ = \sum_{n=0}^{s-1} \frac{(-1)^n}{s^{s-1}(s-1)!} D_{(\mu_1}^\dagger \dots D_{\mu_n}^\dagger \bar{\psi}(x) \gamma_a D_{\mu_{n+1}} \dots D_{\mu_{s-1}}) \psi(x) \end{aligned} \quad (3.75)$$

Now, given

$$\delta_\Lambda \mathcal{A}_\mu = -\partial_\mu \Lambda + \frac{i}{2} [\mathcal{A}_\mu, \Lambda] \quad (3.76)$$

and (3.12), it is easy to prove that

$$\delta_\Lambda (D_\mu \psi) = -\frac{i}{2} \Lambda (D_\mu \psi), \quad \delta (D_\mu^\dagger \psi) = \frac{i}{2} (D_\mu^\dagger \psi) \Lambda \quad (3.77)$$

The same holds for multiple covariant derivatives

$$\delta_\Lambda (D_{\mu_1} \dots D_{\mu_n} \psi) = \frac{i}{2} \Lambda (D_{\mu_1} \dots D_{\mu_n} \psi), \quad \text{etc.}$$

It follows that

$$\begin{aligned} \delta_\Lambda J'_{a\mu_1 \dots \mu_{s-1}}^{(s)}(x) \\ = - \sum_{n=0}^{s-1} \frac{(-1)^n}{s^{s-1}(s-1)!} D_{(\mu_1}^\dagger \dots D_{\mu_n}^\dagger \bar{\psi}(x) [\gamma_a, \Lambda] D_{\mu_{n+1}} \dots D_{\mu_{s-1}}) \psi(x) \\ = \Lambda_a{}^b(x) J'_{b\mu_1 \dots \mu_{s-1}}^{(s)}(x) \end{aligned} \quad (3.78)$$

Therefore the interaction term

$$S'_{\text{int}} = \sum_{s=1}^{\infty} \int d^d x J'^{(s)}_{a^{\mu_1} \dots \mu_{s-1}}(x) h^{a^{\mu_1} \dots \mu_{s-1}} \quad (3.79)$$

is invariant under (3.12) and (3.76) provided

$$\delta_{\Lambda} h^{a^{\mu_1} \dots \mu_n}(x) = \Lambda^a{}_b(x) h^{b^{\mu_1} \dots \mu_n}(x) \quad (3.80)$$

On the other hand, writing

$$S'_0 = \int d^d x \bar{\psi} \left(i\gamma^a \left(\partial_a - \frac{i}{2} \mathcal{A}_a \right) - m \right) \psi \quad (3.81)$$

instead of S_0 , also S'_0 turns out to be invariant under LLT. So, provided we define LLT via (3.12) and (3.76), $S' = S'_0 + S'_{\text{int}}$ is invariant.

Replacing simple spacetime derivatives ∂_{μ} with the inertial ones D_{μ} everywhere is not enough. As pointed out above instead of $\partial_a = \delta_a^{\mu} \partial_{\mu}$ we should write $\partial_a = e_a^{\mu}(x) \partial_{\mu}$, where $e_a^{\mu}(x)$ is a purely inertial frame. Moreover, whenever it appears, we should rewrite $\mathcal{A}_a(x) = e_a^{\mu}(x) \mathcal{A}_{\mu}(x)$.

With this new recipes all inconsistencies disappear. For instance

$$\delta_{\Lambda}(D_a J_b) = \Lambda_a{}^c (D_c J_b) + \Lambda_b{}^c (D_a J_c)$$

Therefore $\delta_{\Lambda}(\eta^{ab} D_a J_b) = 0$. Likewise

$$\delta_{\Lambda} G_{ab} = \Lambda_a{}^c G_{cb} + \Lambda_b{}^c G_{ac} \quad (3.82)$$

which implies the local Lorentz invariance of $G_{ab} G^{ab}$.

Summary. *The HS effective action approach fixes completely the local Lorentz gauge. This is due the fact that in its formalism (and in the general in the HS YM and CS formalism) the choice $e_a^{\mu} = \delta_a^{\mu}$ and $\mathcal{A}_a = 0$ for the inertial frame and connection, is implicit. However the same formalism offers the possibility to recover the LL invariance by means of a simple recipe:*

1. *replace any spacetime derivative, even in the $*$ product, with the inertial covariant derivative,*
2. *interpret any flat index a attached to any object O_a as $e_a^{\mu}(x) O_{\mu}$.*

Anticipating future developments we add that in the process of quantization $e_a^{\mu}(x)$ and $\mathcal{A}_a(x)$ will be treated as classical backgrounds.

3.5 Conclusions

The main message of this paper is that it is possible to construct field theory models of Yang-Mills type with infinite many HS fields in flat spacetime in any dimension. It is also possible to construct similar models of Chern-Simons type in any odd

dimensional flat spacetime. We have seen that of such models we can define the actions, invariant under HS gauge transformations, which encompass the ordinary gauge transformations and the diffeomorphisms. It was also shown that although the local Lorentz gauge is fixed in this formalism, local Lorentz invariance can be easily implemented. We can derive sensible eom's. A more detailed account and further developments are contained in related papers[7,8] : for instance one can introduce matter master scalar and fermion fields, and realize the analog of Higgs mechanism; one can also introduce ghosts, and carry out the BRST quantization and develop the practical machinery for perturbative calculations via Feynman diagrams.

All these results may be at first surprising, because, as noted in the introduction, there exist no-go (Weiberg-Witten) theorems forbidding the existence of interacting massless HS theories in flat spacetime (for a review see [10]). A full discussion of this problem will be given in [8] . Here let us simply notice that such theorems are based on a set of hypotheses, which are very plausible in ordinary field theories, but can be circumvented in theories like the ones introduced here. For instance two basic requirements are the minimal coupling of the matter fields to gravity and the polynomial structure of the energy-momentum tensor. It turns out that none of these requirements is realized in HS YM-like theories: gravity is non-minimally coupled to HS fields and the energy-momentum tensor is not a polynomial of the fields, but a series.

Acknowledgments

I would like to thank my collaborators Maro Cvitan, Predrag Dominis Prester, Stefano Giaccari and Tamara T. Štemberga. I would like to thank Norma Susana Mankoč Borštnik and Holger Nielsen for inviting me to give this talk at the Workshop.

References

1. X. O. Camanho, J. D. Edelstein, J. Maldacena and A. Zhiboedov, *Causality Constraints on Corrections to the Graviton Three-Point Coupling*, JHEP **1602**, 020 (2016) [arXiv:1407.5597 [hep-th]].
2. M. A. Vasiliev, *Consistent equation for interacting gauge fields of all spins in (3+1)-dimensions*, Phys. Lett. B **243**, 378 (1990); *Properties of equations of motion of interacting gauge fields of all spins in (3+1)-dimensions*, Class. Quant. Grav. **8** 1387 (1991) ; *Algebraic aspects of the higher spin problem*, Phys. Lett. B **257**, 111 (1991); *More on equations of motion for interacting massless fields of all spins in (3+1)-dimensions*, Phys. Lett. B **285**, 225 (1992).
3. X. Bekaert, E. Joung and J. Mourad, "Effective action in a higher-spin background," JHEP **1102** (2011) 048
4. L. Bonora, M. Cvitan, P. Dominis Prester, S. Giaccari, M. Paulisic and T. Štemberga, *Worldline quantization of field theory, effective actions and L_∞ structure*, JHEP **1804**, 095 (2018)
5. L. Bonora, M. Cvitan, P. Dominis Prester, S. Giaccari, B. Lima de Souza and T. Štemberga, *One-loop effective actions and higher spins*, JHEP **1612** (2016) 084.

6. L. Bonora, M. Cvetan, P. Dominis Prester, S. Giaccari, and T. Štemberga, *One-loop effective actions and higher spins. II* JHEP **1801** (2018) 080.
7. L. Bonora, M. Cvetan, P. Dominis Prester, S. Giaccari and T. Štemberga, *HS in flat spacetime. The effective action method*, [ArXiv:1811.04847]
8. L. Bonora, M. Cvetan, P. Dominis Prester, S. Giaccari and T. Štemberga, *HS in flat spacetime. YM-like theories*, to appear.
9. R. Aldrovandi and J. G. Pereira *Teleparallel gravity. An introduction*, Springer, Dordrecht Heidelberg New York London 2013, and references therein.
10. X. Bekaert, N. Boulanger and P. Sundell, *How higher-spin gravity surpasses the spin two barrier: no-go theorems versus yes-go examples*, Rev. Mod. Phys. **84** (2012) 987 doi:10.1103/RevModPhys.84.987 [arXiv:1007.0435 [hep-th]].



4 Emergent Photons and Gravitons

J.L. Chkareuli, J. Jejelava and Z. Kepuladze

Center for Elementary Particle Physics, Ilia State University, 0162 Tbilisi, Georgia
E. Andronikashvili Institute of Physics, 0177 Tbilisi, Georgia

Abstract. Now, it is already not a big surprise that due to the spontaneous Lorentz invariance violation (SLIV) there may emerge massless vector and tensor Goldstone modes identified particularly with photon and graviton. Point is, however, that this mechanism is usually considered separately for photon and graviton, though in reality they appear in fact together. In this connection, we recently develop the common emergent electrogravity model which would like to present here. This model incorporates the ordinary QED and tensor field gravity mimicking linearized general relativity. The SLIV is induced by length-fixing constraints put on the vector and tensor fields, $A_\mu^2 = \pm M_A^2$ and $H_{\mu\nu}^2 = \pm M_H^2$ (M_A and M_H are the proposed symmetry breaking scales) which possess the much higher symmetry than the model Lagrangian itself. As a result, the twelve Goldstone modes are produced in total and they are collected into the vector and tensor field multiplets. While photon is always the true vector Goldstone boson, graviton contain pseudo-Goldstone modes as well. In terms of the appearing zero modes, theory becomes essentially nonlinear and contains many Lorentz and CPT violating interaction. However, as argued, they do not contribute in processes which might lead to the physical Lorentz violation. Nonetheless, how the emergent electrogravity theory could be observationally differed from conventional QED and GR theories is also briefly discussed.

Povzetek. Avtorji so razvili model za elektrogravitacijo, ki vsebuje običajno kvantno elektrodinamiko in tenzorsko polje gravitacije. Slednje predstavlja linearizirano splošno teorijo relativnosti. Spontano kršitev Lorentzove invariance sprožijo s predpisom za vektorska in tenzorska polja: $A_\mu^2 = \pm M_A^2$ in $H_{\mu\nu}^2 = \pm M_H^2$ (M_A in M_H sta predlagani skali zlomitve simetrije). Predpis prinese mnogo višjo simetrijo kot jo ima Lagrangeva gostota modela. Dvanajst Goldstonovih delcev tvori multiplete vektorskih in tenzorskih polj. Foton je vedno pravi vektorski Goldstonov bozon, graviton pa vsebuje tudi psevdo Goldstonove načine. Model postane tako nelinearen in vsebuje vrsto interakcij, ki zlomijo Lorentzovo in CPT simetrijo, ki pa ne vodijo do fizikalne zlomitve Lorentzove simetrije. Avtorji komentirajo, v čem se elektrogravitacija razlikuje od elektrodinamike in gravitacije.

Keywords: Spontaneous symmetry violation, Lorentz invariance violation, emergent field theory.

4.1 Introduction

While Lorentz symmetry looks physically as an absolutely exact spacetime symmetry, the spontaneous Lorentz invariance violation (SLIV) suggests a beautiful

scenario where massless vectors and/or tensor fields emerge as the corresponding zero modes which may be identified with photons, gravitons and other gauge fields [1–3]. Though they appear through condensation of the pure gauge degrees of freedom in the starting theory their masslessness are provided by their Nambu-Goldstone nature [4–12] rather than a conventional gauge invariance.

4.1.1 Emergent vector fields theory

In order to violate Lorentz invariance one necessarily needs field(s) being sensitive to the spacetime transformations, as vector or tensor fields are. They can evolve vacuum expectation value which fixes direction of the violation in the spacetime and create the corresponding condensate. Therefore, if there is an interaction with this condensate one could expect Lorentz violation to be manifested physically. If we want to arrange spontaneous Lorentz violation by the vector field, we could start, as usual, with the potential terms in the Lagrangian

$$L = -\frac{1}{4}F_{\mu\nu}^2 - V; \quad V = \lambda (A_\mu^2 - n_\mu^2 M_A^2)^2 \quad (4.1)$$

$$F_{\mu\nu}^2 = F_{\mu\nu}F^{\mu\nu}; \quad A_\mu^2 = A_\mu A^\mu; \quad n_\mu^2 = n_\mu n^\mu$$

where n_μ is an unit constant vector specifying character of Lorentz violation. If n_μ is time-like vector, we have time-like violation breaking $SO(1,3)$ to $SO(3)$. If n_μ is space-like vector, we have space-like violation breaking $SO(1,3)$ to $SO(1,2)$.

We started with gauge invariant kinetic term, but since potential violates gauge invariance anyway, we could have started with general kinetic terms

$$L_k = a (\partial_\alpha A_\beta)^2 + b (\partial_\alpha A^\alpha)^2 \quad (4.2)$$

but problem arising here is a propagating ghost mode, which we get ride off with the gauge invariant form of kinetic terms.

Such a system of vector field with potential, generally appears not stable, its energy is not bound from below unless phase space is restricted with condition

$$A_\mu^2 - n_\mu^2 M_A^2 = 0 \quad (4.3)$$

While this condition may appear out of the blue, it is actually motivated by the conserved current of (4.1)

$$J_\mu = A_\mu (A_\alpha^2 - n_\alpha^2 M_A^2) \quad (4.4)$$

and if in the initial condition the conserved charge of this current is set to zero, which means (4.3) is always zero, no propagating ghosts, Hamiltonian is positively defined and Coulomb law stays the same [13]. So, basically we arrived to the point where we accept to take λ in (4.1) to infinity as a Lagrange multiplier and get conventional vector field kinetics with the addition of (4.3) condition. This condition still is a cause for spontaneous Lorentz invariance violation, but in contrast now Higgs mode is set to zero. This was Nambu's original idea [14]. It is

easy to see, if we write expansion of the vector field A into Goldstone and Higgs modes in the exponential manner, which is

$$A_\mu = (M_A + h)n_\nu \exp J_\mu^\nu \quad (4.5)$$

where h is Higgs mode and Goldstone modes a_μ are sitting in J_μ^ν (generators for Lorentz transformation) and $a_\mu = M_A n_\nu J_\mu^\nu$, $a_\mu n^\mu = M_A n^\mu n_\nu J_\mu^\nu = 0$. So,

$$A_\mu^2 = (M_A + h)^2 n_\nu^2 = n_\alpha^2 M_A^2 \implies h = 0 \quad (4.6)$$

Expansion (4.5) is nonlinear with respect to vector Goldstone modes, but $\frac{a_\mu}{M_A}$ is a small parameter and we can expand exponent in the power series and in the second approximation get

$$A_\mu = \left(M_A - \frac{n_\alpha^2 a_\alpha^2}{2M_A} \right) n_\mu + a_\mu \quad (4.7)$$

It is clear now that we get nonlinear Lagrangian for vector Goldstone modes, which in the first approximation is

$$L(A) \rightarrow L(a) = -\frac{1}{4} f_{\mu\nu} f^{\mu\nu} - \frac{1}{2} \delta (n_\alpha a^\alpha)^2 - \frac{1}{2} \frac{n^2}{M_A} f_{\mu\nu} n^\mu \partial^\nu a^2 \quad (4.8)$$

δ is Lagrange multiplier setting orthogonality condition for the vector Goldstone field, thus treating it as gauge fixing one. In general, we have here plethora Lorentz and CPT violating couplings like $\frac{n^2}{M_A} f_{\mu\nu} n^\mu \partial^\nu a^2$ in the higher orders, especially if charged currents are introduced as well, but it appears in all physical processes (photon-photon, matter-photon, matter-matter interactions) at least in the tree and one loop level, there is no sign of physical Lorentz invariance violation. Looks like Lorentz invariance is realized in nonlinear fashion and Lorentz breaking condition (4.3) is treated like a nonlinear gauge choice for vector field [16,17].

Consideration of the spontaneous Lorentz violation scenarios for non-Abelian vector fields meet same challenges, though consequently lead to the same conclusions as in the Abelian vector field case, despite the fact that there are some significant differences as well. The length fixing constraint adapted for non-Abelian vector fields in fact violates not only Lorentz symmetry, but an accidental symmetry $SO(N, 3N)$ of the constraint itself (here N defines unitary symmetry group of vector fields) which is much higher than symmetry of the theory Lagrangian. This gives extra massless modes which together with the true Lorentzian Goldstone complete the whole gauge multiplet of the non-Abelian theory taken [18].

4.1.2 Emergent tensor field gravity

Actually, for the tensor field gravity we can use the similar nonlinear constraint for a symmetric two-index tensor field

$$H_{\mu\nu}^2 = n^2 M_H^2, \quad H_{\mu\nu}^2 \equiv H_{\mu\nu} H^{\mu\nu}, \quad n^2 \equiv n_{\mu\nu} n^{\mu\nu} = \pm 1 \quad (4.9)$$

(where $n_{\mu\nu}$ is now a properly oriented unit Lorentz tensor, which supposedly specifies vacuum expectation values, while M_H is the proposed scale for Lorentz

violation in the gravity sector) which fixes its length in the same manner as it appears for the vector field (4.3). Again, the nonlinear constraint (4.9) may in principle appear from the standard potential terms added to the tensor field Lagrangian

$$U(H) = \lambda_H (H_{\mu\nu}^2 - n^2 M_H^2)^2 \quad (4.10)$$

in the nonlinear σ -model type limit when the coupling constant λ_H goes to infinity. Just in this limit the tensor field theory appears stable, but doing so, we are effectively excluding corresponding Higgs mode from the theory and it does not lead to physical Lorentz violation [19].

This constraint (4.9), like the non-Abelian vector field, has higher symmetry than the kinetic term, particularly $SO(7, 3)$. So, spontaneous symmetry violation breaks not only Lorentz symmetry, but also this $SO(7, 3)$ and therefore produces also PGM-s, but in contrast to vector field, when we had only two channels of Lorentz symmetry violation to $SO(3)$ or $SO(1, 2)$ and three true Goldstone modes always, for tensor field we have more possibilities. If we write down constraint in more details

$$H_{\mu\nu}^2 = H_{00}^2 + H_{i=j}^2 + (\sqrt{2}H_{i\neq j})^2 - (\sqrt{2}H_{0i})^2 = n^2 M_H^2 = \pm M_H^2 \quad (4.11)$$

we see that if only one component of the tensor field should acquire vacuum expectation value (assuming minimal vacuum configuration) we have following alternatives:

$$\begin{aligned} (a) \quad & n_{00} \neq 0, \quad SO(1, 3) \rightarrow SO(3) \\ (b) \quad & n_{i=j} \neq 0, \quad SO(1, 3) \rightarrow SO(1, 2) \\ (c) \quad & n_{i\neq j} \neq 0, \quad SO(1, 3) \rightarrow SO(1, 1) \end{aligned} \quad (4.12)$$

for $n^2 = 1$ and

$$(d) \quad n_{0i} \neq 0, \quad SO(1, 3) \rightarrow SO(2) \quad (4.13)$$

for $n^2 = -1$. For a, b cases we have three true Goldstone modes and for c, d we have five, since only one generator of Lorentz transformations remains unbroken. While in b, c, d cases physical graviton consists, at least partially, from true Goldstone modes, in case a only true goldstones are H_{0i} components, thus physical graviton will be constructed from PGM-s. One should notice that pseudo-Goldstone nature of some components of tensor multiplet poses no threats and generally in contrast to the scalar pseudo-Goldstone modes they do not acquire mass duo to the quantum effects, if diffeomorphism (diff) invariance is present.

So, we are putting (4.9) on the tensor field mimicking linearized general relativity

$$L = L(H) + L_S - \frac{1}{M_P} H_{\mu\nu} T_S^{\mu\nu} \quad (4.14)$$

where

$$L(H) = \frac{1}{2} \partial_\lambda H^{\mu\nu} \partial^\lambda H_{\mu\nu} - \frac{1}{2} \partial_\lambda H_{tr} \partial^\lambda H_{tr} - \partial_\lambda H^{\lambda\nu} \partial^\mu H_{\mu\nu} + \partial^\nu H_{tr} \partial^\mu H_{\mu\nu} \quad (4.15)$$

Here H_{tr} stands for the trace of $H_{\mu\nu}$ ($H_{tr} = \eta^{\mu\nu} H_{\mu\nu}$) and $L(H)$ is invariant under the diff transformations

$$\delta H_{\mu\nu} = \partial_\mu \xi_\nu + \partial_\nu \xi_\mu, \quad \delta x^\mu = \xi^\mu(x), \quad (4.16)$$

while L_S and $T_S^{\mu\nu}$ are the Lagrangian and corresponding energy momentum tensor of whatever is gravitating, (vector fields, matter). In case, vector field is considered

$$L(A) = -\frac{1}{4} F_{\mu\nu} F^{\mu\nu}, \quad T^{\mu\nu}(A) = -F^{\mu\rho} F_\rho^\nu + \frac{1}{4} \eta^{\mu\nu} F_{\alpha\beta} F^{\alpha\beta} \quad (4.17)$$

where $L(H)$ is fully diff invariant, but that is not the case for other parts of Lagrangian and diff invariance is satisfied only proximately, but they become more and more invariant when the tensor field gravity Lagrangian (4.14) is properly extended to GR with higher terms in H-fields included¹.

Once tensor field acquires vacuum expectation value, we can expand it into Goldstone mode

$$H_{\mu\nu} = h_{\mu\nu} + n_{\mu\nu} M_H - \frac{n^2 h^2}{2M_H} + O(1/M_H^2), \quad n \cdot h = 0 \quad (4.18)$$

Here $h_{\mu\nu}$ corresponds to the pure emergent modes satisfying the orthogonality condition and $h^2 \equiv h_{\mu\nu} h^{\mu\nu}$, $n \cdot h \equiv n_{\mu\nu} h^{\mu\nu}$.

Lets specify once again that $h_{\mu\nu}$ consists of Goldstone and PGM-s. Only case, when physical graviton will consists of only Goldstone mode is when Lorentz invariance is fully broken, we have six emergent goldstone modes and other pseudo Goldstone components is gauged away by fixing remaining gauge freedom (more about supplementary conditions below). Such a scenario can not be achieved by minimal vacuum configuration. Nevertheless, whether tensor field will be defined only by Goldstone modes or by a mixture with PGM-s, hole tensor multiplet always stays strictly massless. A particular case of interest is that of the traceless VEV tensor $n_{\mu\nu}$

$$n_{\mu\nu} \eta^{\mu\nu} = 0 \quad (4.19)$$

in terms of which the emergent gravity Lagrangian acquires an especially simple form (see below). It is clear that the VEV in this case can be developed on several $H_{\mu\nu}$ components simultaneously, which in general may lead to total Lorentz violation with all six Goldstone modes generated. For simplicity, we will use sometimes this form of vacuum configuration in what follows, while our arguments can be applied to any type of VEV tensor $n_{\mu\nu}$.

Alongside to basic emergent orthogonality condition in (4.18) one must also specify other supplementary conditions for the tensor field $h^{\mu\nu}$ (appearing eventually as possible gauge fixing terms in the emergent tensor field gravity). We have

¹ Such an extension means that in all terms included in the GR action, particularly in the QED Lagrangian term, $(-g)^{1/2} g_{\mu\nu} g_{\lambda\rho} F^{\mu\lambda} F^{\nu\rho}$, one expands the metric tensors

$$g_{\mu\nu} = \eta_{\mu\nu} + H_{\mu\nu}/M_P, \quad g^{\mu\nu} = \eta^{\mu\nu} - H^{\mu\nu}/M_P + H^{\mu\lambda} H_\lambda^\nu / M_P^2 + \dots$$

taking into account the higher terms in H-fields.

remaining three degrees of gauge freedom. Usually, spin 1 states in tensor field is gauged away by the conventional Hilbert-Lorentz condition

$$\partial^\mu h_{\mu\nu} + q \partial_\nu h_{t\tau} = 0 \quad (4.20)$$

(q is an arbitrary constant, giving for $q = -1/2$ the standard harmonic gauge condition), because spin-1 component always has negative contribution in energy and therefore it is desirable action. However, as we have already imposed the emergent constraint (4.18), we can not use the full Hilbert-Lorentz condition (4.20) eliminating four more degrees of freedom in $h_{\mu\nu}$. Otherwise, we would have an "over-gauged" theory with a non-propagating graviton. In fact, the simplest set of conditions which conform with the emergent condition $n \cdot h = 0$ in (4.18) turns out to be

$$\partial^\rho (\partial_\mu h_{\nu\rho} - \partial_\nu h_{\mu\rho}) = 0 \quad (4.21)$$

This set excludes only three degrees of freedom² in $h_{\mu\nu}$ and, besides, it automatically satisfies the Hilbert-Lorentz spin condition as well.

Putting parameterization (4.18) into the total Lagrangian given in (4.14), one comes to the truly emergent tensor field gravity Lagrangian containing an infinite series in powers of the $h_{\mu\nu}$ modes. For the traceless VEV tensor $n_{\mu\nu}$, without loss of generality, we get the especially simple form

$$\begin{aligned} L = & \frac{1}{2} \partial_\lambda h^{\mu\nu} \partial^\lambda h_{\mu\nu} - \frac{1}{2} \partial_\lambda h_{t\tau} \partial^\lambda h_{t\tau} - \partial_\lambda h^{\lambda\nu} \partial^\mu h_{\mu\nu} + \partial^\nu h_{t\tau} \partial^\mu h_{\mu\nu} + \\ & - \frac{n^2}{M_H} h^2 n^{\mu\lambda} \left[\partial_\lambda \partial^\nu h_{\mu\nu} - \frac{1}{2} \partial_\mu \partial_\lambda h_{t\tau} \right] + \frac{n^2}{8M_H^2} \left(\eta^{\mu\nu} - \frac{n^{\mu\lambda} n^{\nu\lambda}}{n^2} \right) \partial_\mu h^2 \partial_\nu h^2 \\ & + L_S - \left(M_H n_{\mu\nu} + h_{\mu\nu} - \frac{h^2 n_{\mu\nu}}{2M_H} \right) \frac{T_S^{\mu\nu}}{M_P} + O(1/M_H^2) \end{aligned} \quad (4.22)$$

The bilinear field term

$$\frac{M_H}{M_P} n_{\mu\nu} T_S^{\mu\nu} \quad (4.23)$$

in the third line in the Lagrangian (4.22) merits special notice. This term arises from the interaction term with tensor field. It could significantly affect the dispersion relation for the all the fields included in $T_S^{\mu\nu}$, thus leading to an unacceptably large Lorentz violation if the SLIV scale M_H were comparable with the Planck mass M_P . However, this term can be gauged away [19] by an appropriate redefinition of the fields involved by going to the new coordinates

$$x^\mu \rightarrow x^\mu + \xi^\mu. \quad (4.24)$$

In fact, with a simple choice of the parameter function $\xi^\mu(x)$ being linear in 4-coordinate

² The solution for a gauge function $\xi_\mu(x)$ satisfying the condition (4.21) can generally be chosen as $\xi_\mu = \square^{-1} (\partial^\rho h_{\mu\rho}) + \partial_\mu \theta$, where $\theta(x)$ is an arbitrary scalar function, so that only three degrees of freedom in $h_{\mu\nu}$ are actually eliminated.

$$\xi^\mu(x) = \frac{M_H}{M_P} n^{\mu\nu} x_\nu, \quad (4.25)$$

the term (4.23) is cancelled by an analogous term stemming from the kinetic term in L_S . On the other hand, since the diff invariance is an approximate symmetry of the Lagrangian L we started with (4.14), this cancellation will only be accurate up to the linear order corresponding to the tensor field theory. Indeed, a proper extension of this theory to GR^1 with its exact diff invariance will ultimately restore the usual dispersion relation for the vector field and other matter fields involved. We will consider all that in significant detail in the next section.

So, with the Lagrangian (4.22) and the supplementary conditions (4.18) and (4.21) lumped together, one eventually comes to a working model for the emergent tensor field gravity [19]. Generally, from ten components of the symmetric two-index tensor $h_{\mu\nu}$ four components are excluded by the supplementary conditions (4.18) and (4.21). For a plane gravitational wave propagating in, say, the z direction another four components are also eliminated, due to the fact that the above supplementary conditions still leave freedom in the choice of a coordinate system, $x^\mu \rightarrow x^\mu + \xi^\mu(t - z/c)$, much as it takes place in standard GR. Depending on the form of the VEV tensor $n_{\mu\nu}$, caused by SLIV, the two remaining transverse modes of the physical graviton may consist solely of Lorentzian Goldstone modes or of pseudo-Goldstone modes, or include both of them. This theory, similar to the nonlinear QED [14], while suggesting an emergent description for graviton, does not lead to physical Lorentz violation [19].

4.1.3 Length Fixing Constraints and Nonlinear Gauge

We have overviewed above the SLIV scenarios for vector and tensor fields and could see that, though the well motivated length fixing constraint for a given field causes spontaneous Lorentz violation, somewhat counterintuitively, in physical processes, Lorentz symmetry appears intact. Therefore we rightfully suspect that the Lorentz breaking constraint condition acts effectively as a gauge fixing condition. To prove or disprove whether this suspicion is reasonable one either should check the SLIV effects in the corresponding physical processes in all orders, that looks unrealistic, or has to find some generic argument, particularly find a solution for gauge function or, at least, prove that such a solution exists.

In case of vector field A_α and Lorentz breaking condition $A_\alpha^2 = n_\beta^2 M_A^2$, the corresponding equation for gauge function S is

$$(A_\alpha + \partial_\alpha S)^2 = n_\beta^2 M_A^2 \quad (4.26)$$

This equation is nonlinear and its exact solution for arbitrary A_α is not yet found. However, to our fortune, it is well known that this equation taken for time-like violation case ($n_\beta^2 = 1$) is in fact the Hamilton-Jacobi equation for the relativistic particle, which moves in the external electromagnetic field. An action for such a

system is given by

$$\begin{aligned} S &= \int M \sqrt{dx_\alpha dx^\alpha} - A_\alpha dx^\alpha \\ &= \int (M \sqrt{u_\alpha u^\alpha} - A_\alpha u^\alpha) d\tau \end{aligned} \quad (4.27)$$

where τ is evolution parameter and $u_\alpha = \frac{dx_\alpha}{d\tau}$. In this case, even though we do not have exact solution for that, we know that an action S describes a physical system and therefore it has a solution for an arbitrary electromagnetic field A_α .

Analogously, for the space-like n_β ($n_\beta^2 = -1$) our basic equation (4.26) might be considered as the Hamilton-Jacobi equation for a hypothetical tachyon moving in the external electromagnetic field

$$S = \int M \sqrt{-dx_\alpha dx^\alpha} - A_\alpha dx^\alpha = \int (M \sqrt{-u_\alpha u^\alpha} - A_\alpha u^\alpha) d\tau \quad (4.28)$$

So, though this action can only correspond to a hypothetical particle, which is not discovered so far, theoretically it might exist at least as a free particle state. At this point we are unable to solve (4.26) exactly nor for time-like, neither for space-like cases, but we can check that ultra-relativistic particle and tachyon (in the limit of very large momenta, when particle velocity $v_p \rightarrow c$ from below and tachyon velocity $v_t \rightarrow c$ from above) have somewhat similar equations of motions

$$\begin{aligned} \frac{d}{dt} p_i &= F_{0i} - \frac{p_i}{\sqrt{p_k^2}} F_{li} \\ \frac{d}{dt} p_i &= -F_{0i} + \frac{p_i}{\sqrt{p_k^2}} F_{li} \end{aligned} \quad (4.29)$$

with the electromagnetic field flipped for tachyon (p_i stands for the corresponding three-momenta). No dependent, one believes or not in an existence of charged tachyon one might at least can take this similarity as a hint that in space-like case, similar to a time-like violation, we are dealing with effectively nonlinear gauge fixing condition.

For the tensor field, diff gauge invariance also could only fully be approved, when corresponding gauge function $\xi_\alpha(x_\mu)$ is found, which satisfies the following equation

$$(H_{\alpha\beta} + \partial_\alpha \xi_\beta + \partial_\beta \xi_\alpha)^2 = \pm M_H^2 \quad (4.30)$$

While we do not have a heuristic argument like that we had above for the vector field time-like SLIV case, we can provide some arguments very similar to its space-like violation case leading again to the mainly intuitive suggestion.

So, to conclude, though the above discussion looks highly suggestive towards the vector and tensor field constraints, (4.3) and (4.9), to consider them as the be nonlinear gauge choices, they are not yet, sure, the rigorous proofes. Therefore, presently the only way to check whether these constraints are just gauge choices or not is actually related to seeking of the SLIV effects by a direct analysis of the corresponding physical processes.

4.2 Electrogravity model

Usually, an emergent gauge field framework is considered either regarding emergent photons or regarding emergent gravitons, but in nature they do not exist in separate framework, they are different parts of one picture and therefore the most natural thing is to discuss them as such. For the first time, we consider it regarding them both in the so-called electrogravity theory where together with the Nambu QED model [14] with its gauge invariant Lagrangian we propose the linearized Einstein-Hilbert kinetic term for the tensor field preserving a diff invariance (more details can be found in our recent paper [20]). We show that such a combined SLIV pattern, conditioned by the constraints (4.3) and (4.9), induces the massless Goldstone modes which appear shared among photon and graviton. One needs in common nine zero modes both for photon (three modes) and graviton (six modes) to provide all necessary (physical and auxiliary) degrees of freedom. They actually appear in our electrogravity theory due to spontaneous breaking of high symmetries of our constraints. While for a vector field case the symmetry of the constraint coincides with Lorentz symmetry $SO(1, 3)$, the tensor field constraint itself possesses much higher global symmetry $SO(7, 3)$, whose spontaneous violation provides a sufficient number of zero modes collected in a graviton. As we understand already these modes are largely pseudo-Goldstone modes since $SO(7, 3)$ is symmetry of the constraint (4.9) rather than the electrogravity Lagrangian whose symmetry is only given by Lorentz invariance.

4.2.1 Constraints and zero mode spectrum

Before going any further, let us make some necessary comments. Note first of all that, apart from dynamics that will be described by the total Lagrangian, the vector and tensor field constraints (4.3, 4.9) are also proposed to be satisfied. In principle, these constraints, like in previous cases, could be formally obtained from the conventional potential introduced in the total Lagrangian. The most general potential, where the vector and tensor field couplings possess the Lorentz and $SO(7, 3)$ symmetry, respectively, must be solely a function of $A_\mu^2 \equiv A_\mu A^\mu$ and $H_{\mu\nu}^2 \equiv H_{\mu\nu} H^{\mu\nu}$. Indeed, it cannot include any contracted and intersecting terms like as H_{tr} , $H^{\mu\nu} A_\mu A_\nu$ and others which would immediately reduce the above symmetries to the common Lorentz one. So, one may only write

$$U(A, H) = \lambda_A (A_\mu^2 - n^2 M_A^2)^2 + \lambda_H (H_{\mu\nu}^2 - n^2 M_H^2)^2 + \lambda_{AH} A_\mu^2 H_{\rho\nu}^2 \quad (4.31)$$

where $\lambda_{A,H,AH}$ stand for the coupling constants of the vector and tensor fields, while values of $n^2 = \pm 1$ and $n^2 = \pm 1$ determine their possible vacuum configurations. As a consequence, an absolute minimum of the potential (4.31) might appear for the couplings satisfying the conditions

$$\lambda_{A,H} > 0, \quad \lambda_A \lambda_H > \lambda_{AH}/4 \quad (4.32)$$

However, as in the pure vector field case discussed in section 1, this theory is generally unstable with the Hamiltonian being unbounded from below unless

the phase space is constrained just by the above nonlinear conditions (4.3, 4.9). They in turn follow from the potential (4.31) when going to the nonlinear σ -model type limit $\lambda_{A,H} \rightarrow \infty$. In this limit, the massive Higgs mode disappears from the theory, the Hamiltonian becomes positive, and one comes to the pure emergent electrogravity theory considered here.

We note again that the Goldstone modes appearing in the theory are caused by breaking of global symmetries related to the constraints (4.3, 4.9) rather than directly to Lorentz violation. Meanwhile, for the vector field case symmetry of the constraint (4.3) coincides in fact with Lorentz symmetry whose breaking causes the Goldstone modes depending on the vacuum orientation vector n_μ , as can be clearly seen from an appropriate exponential parametrization for the starting vector field (4.5). However, in the tensor field case, due to the higher symmetry $SO(7, 3)$ of the constraint (4.9), there are much more tensor zero modes than would appear from SLIV itself. In fact, they complete the whole tensor multiplet $h_{\mu\nu}$ in the parametrization (4.18). However, as was discussed in the previous section, only a part of them are true Goldstone modes, others are pseudo-Goldstone ones. In the minimal VEV configuration case, when these VEVs are developed only on the single A_μ and $H_{\mu\nu}$ components, one has several possibilities determined by the vacuum orientations n_μ and $n_{\mu\nu}$. There appear the twelve zero modes in total, three from Lorentz violation itself and nine from a violation of the $SO(7, 3)$ symmetry that is more than enough to have the necessary three photon modes (two physical and one auxiliary ones) and six graviton modes (two physical and four auxiliary ones). We could list below all possible cases corresponding $n - n$ values, the timelike-spacelike SLIV, when $n_0 \neq 0$ and $n_{i=j} \neq 0$, the spacelike-timelike (nonzero n_i and n_{00}), spacelike-spacelike diagonal (nonzero n_i and $n_{i=j}$) and spacelike-spacelike nondiagonal (nonzero n_i and $n_{i \neq j}$) cases, but for brevity, instead we only list the most interesting cases corresponding to minimal and maximal Lorentz symmetry breaking.

(1) When both $n_\mu \neq 0$ and $n_{\mu\mu} \neq 0$, whether μ is time or space component we have minimally broken Lorentz invariance and only three broken generators and therefore three Goldstone modes and all of them is collected into the photon, while components of $h_{\alpha\beta}$ needed for physical graviton and its auxiliary components can be only provided by the pseudo-Goldstone modes following from the symmetry breaking $SO(7, 3) \rightarrow SO(6, 3)$ related to the tensor-field constraint (4.9).

(2) For the case, when $n_i \neq 0$ and $n_{\beta\gamma} \neq 0$ (one of the nondiagonal space components of the unit tensor $n_{\mu\nu}$ is nonzero), when $i \neq \beta \neq \gamma$ Lorentz symmetry appears fully broken so that the photon a_μ has three Goldstone components, while the graviton is collected by the rest of true Goldstone and PGM-s.

(3) Only case when both physical photon and graviton h_{ij} consists of true Goldstone modes is when $n_0 \neq 0$ and $n_{i \neq j} \neq 0$, but some gauge degrees of freedom for a graviton are given by the PGM states stemming from the symmetry breaking of the tensor-field constraint (4.9).

In any case, while photon may only contain true Goldstone modes, some PGM-s appear necessary to be collected in graviton together with some true Goldstone modes to form full tensor multiplet.

4.2.2 The Model

In the previous section and Generally in emergent tensor field gravity theories we considered the vector field A_μ as an unconstrained material field which the emergent gravitons interacted with, but now in electrogravity model we propose that the vector field also develops the VEV through the SLIV constraint (4.3), thus generating the massless vector Goldstone modes associated with a photon. We also include the complex scalar field φ (taken to be massless, for simplicity) as an actual matter in the theory

$$\mathcal{L}(\varphi) = D_\mu \varphi (D_\mu \varphi)^*, \quad D_\mu = \partial_\mu + ieA_\mu. \quad (4.33)$$

So, the proposed total starting electrogravity Lagrangian is

$$\mathcal{L}_{\text{tot}} = L(A) + L(H) + L(\varphi) + L_{\text{int}}(H, A, \varphi) \quad (4.34)$$

where $L(A)$ and $L(H)$ are $U(1)$ gauge invariant and diff invariant vector and tensor field Lagrangians, while the gravity interaction part

$$L_{\text{int}}(H, A, \varphi) = -\frac{1}{M_P} H_{\mu\nu} [T^{\mu\nu}(A) + T^{\mu\nu}(\varphi)] \quad (4.35)$$

contains the tensor field couplings with canonical energy-momentum tensors of vector and scalar fields.

In the symmetry broken phase one goes to the pure Goldstone vector and tensor modes, a_μ and $h_{\mu\nu}$, respectively, Which is thoroughly discussed in the previous sections (4.8), (4.22). At the same time, the scalar field Lagrangian $\mathcal{L}(\varphi)$ in (4.34) is going now to

$$\mathcal{L}(\varphi) = \left| \left(\partial_\mu + ie a_\mu + ie M_A n_\mu - ie \frac{n^2}{2M_A} a^2 n_\mu \right) \varphi \right|^2 \quad (4.36)$$

while tensor field interacting terms (4.35) in $\mathcal{L}_{\text{int}}(H, A, \varphi)$ convert to

$$\mathcal{L}_{\text{int}} = -\frac{1}{M_P} \left(h_{\mu\nu} + M_H n_{\mu\nu} - \frac{n^2}{2M_H} h^2 n_{\mu\nu} \right) \left[T^{\mu\nu} \left(a_\mu - \frac{n^2}{2M_A} a^2 n_\mu \right) + T^{\mu\nu}(\varphi) \right] \quad (4.37)$$

where the vector field energy-momentum tensor is now solely a function of the Goldstone a_μ modes.

4.2.3 Emergent electrogravity interactions

To proceed further, one should eliminate, first of all, the large terms of the false Lorentz violation being proportional to the SLIV scales M_A and M_H in the interaction Lagrangians (4.36) and (4.37). Arranging the phase transformation for the scalar field in the following way

$$\varphi \rightarrow \varphi \exp[-ie M_A n_\mu x^\mu] \quad (4.38)$$

one can simply cancel that large term in the scalar field Lagrangian (4.36), thus coming to

$$\mathcal{L}(\varphi) = \left| \left(D_\mu - ie \frac{n^2}{2M_A} a^2 n_\mu \right) \varphi \right|^2 \quad (4.39)$$

where the covariant derivative D_μ is read from now on as $D_\mu = \partial_\mu + ie a_\mu$. Another unphysical set of terms (4.23) appear from the gravity interaction Lagrangian L_{int} (4.37) where the large SLIV entity $M_H n_{\mu\nu}$ couples to the energy-momentum tensor. They also can be eliminated by going to the new coordinates (4.24), as was mentioned in the previous section.

For infinitesimal translations $\xi_\mu(x)$ the tensor field transforms according to (4.16), while scalar and vector fields transform as

$$\delta\varphi = \xi_\mu \partial^\mu \varphi, \quad \delta a_\mu = \xi_\lambda \partial^\lambda a_\mu + \partial_\mu \xi_\nu a^\nu, \quad (4.40)$$

respectively. One can see, therefore, that the scalar field transformation has only the translation part, while the vector one has an extra term related to its nontrivial Lorentz structure. For the constant unit vector n_μ this transformation looks as

$$\delta n_\mu = \partial_\mu \xi_\nu n^\nu, \quad (4.41)$$

having no the translation part. Using all that and also expecting that the phase parameter ξ_λ is in fact linear in coordinate x_μ (that allows to drop out its high-derivative terms), we can easily calculate all scalar and vector field variations, such as

$$\delta(D_\mu \varphi) = \xi_\lambda \partial^\lambda (D_\mu \varphi) + \partial_\mu \xi_\lambda D^\lambda \varphi, \quad \delta f_{\mu\nu} = \xi_\lambda \partial^\lambda f_{\mu\nu} + \partial_\mu \xi^\lambda f_{\lambda\nu} + \partial_\nu \xi^\lambda f_{\mu\lambda} \quad (4.42)$$

and others. This finally leads to the total variations of the above Lagrangians. Whereas the pure tensor field Lagrangian $L(H)$ (4.15) is invariant under diff transformations, $\delta L(H) = 0$, the interaction Lagrangian L_{int} in (4.34) is only approximately invariant being compensated (in the lowest order in the transformation parameter ξ_μ) by kinetic terms of all the fields involved. However, this Lagrangian becomes increasingly invariant once our theory is extending to GR¹.

In contrast, the vector and scalar field Lagrangians acquire some nontrivial additions

$$\begin{aligned} \delta L(A) &= \xi_\lambda \partial_\lambda L(A) \\ &\quad - \frac{1}{2} (\partial_\mu \xi_\lambda + \partial_\lambda \xi_\mu) \left[f^{\mu\nu} f_\nu^\lambda + \frac{n^2}{M_A} \left(f_\nu^\lambda \partial^{\mu\nu} a^2 + \frac{1}{2} f_{\rho\nu} \partial^{\rho\nu} (a^\mu a^\lambda) \right) \right] \\ \delta L(\varphi) &= \xi_\lambda \partial_\lambda L(\varphi) + (\partial_\mu \xi_\nu + \partial_\nu \xi_\mu) \left[(\mathfrak{D}^\mu \varphi)^* \mathfrak{D}^\nu \varphi + \frac{a^\mu a^\nu n^2}{2M_A} n_\lambda J_\lambda \right] \end{aligned} \quad (4.43)$$

where J_μ stands for the conventional vector field source current

$$J_\mu = ie[\varphi^* D_\mu \varphi - \varphi (D_\mu \varphi)^*] \quad (4.44)$$

while $\mathfrak{D}_\nu \varphi$ is the SLIV extended covariant derivative for the scalar field

$$\mathfrak{D}_\nu \varphi = D_\nu \varphi - ie \frac{n^2}{2M_A} a^2 n_\nu \varphi \quad (4.45)$$

The first terms in the variations (4.43) are unessential since they simply show that these Lagrangians transform, as usual, like as scalar densities under diff transformations.

Combining these variations with L_{int} (4.37) in the total Lagrangian (4.34) one finds after simple, though long, calculations that the largest Lorentz violating terms in it

$$- \left(\frac{M_H}{M_P} n_{\mu\nu} - \frac{\partial_\mu \xi_\lambda + \partial_\lambda \xi_\mu}{2} \right) \left[-f^{\mu\nu} f_\nu^\lambda - \frac{n^2}{M_A} f_\lambda^\nu \partial^{\mu\lambda} a^2 + 2\mathfrak{D}^\nu \varphi (\mathfrak{D}^\mu \varphi)^* \right] \quad (4.46)$$

will immediately cancel if the transformation parameter is chosen exactly as is given in (4.25) in the previous section. So, with this choice we finally have for the modified interaction Lagrangian

$$\mathcal{L}'_{\text{int}}(h, a, \varphi) = -\frac{1}{M_P} h_{\mu\nu} T^{\mu\nu}(a, \varphi) + \frac{1}{M_P M_A} \mathcal{L}_1 + \frac{1}{M_P M_H} \mathcal{L}_2 + \frac{M_H}{M_P M_A} \mathcal{L}_3 \quad (4.47)$$

where

$$\begin{aligned} \mathcal{L}_1 &= n^2 h_{\mu\nu} \left[f_\lambda^\nu \partial^{\mu\lambda} a^2 - n^\mu J^\nu + \eta^{\mu\nu} \left(-\frac{1}{4} f_{\lambda\rho} \partial^{\lambda\rho} a^2 + n^\lambda J_\lambda \right) \right] \\ \mathcal{L}_2 &= \frac{1}{2} n^2 h^2 n_{\mu\nu} \left[-f^{\mu\lambda} f_\lambda^\nu + 2D^\nu \varphi (D^\mu \varphi)^* \right] \\ \mathcal{L}_3 &= n^2 n_{\mu\lambda} \left[\frac{1}{2} f_{\rho\nu} \partial^{\rho\nu} (a^\mu a^\lambda) - (a^\mu a^\lambda) n^\nu J_\nu \right] \end{aligned} \quad (4.48)$$

Thereby, apart from a conventional gravity interaction part given by the first term in (4.47), there are Lorentz violating couplings in $\mathcal{L}_{1,2,3}$ being properly suppressed by corresponding mass scales. Note that the coupling presented in \mathcal{L}_3 between the vector and scalar fields is solely induced by the tensor field SLIV. Remarkably, this coupling may be in principle of the order of a normal gravity coupling or even stronger, if $M_H > M_A$. However, appropriately simplifying this coupling (and using also a full derivative identity) one comes to

$$\mathcal{L}_3 \sim n^2 (n_{\mu\lambda} a^\mu a^\lambda) n^\rho [\partial^\nu f_{\nu\rho} - J_\rho] \quad (4.49)$$

that after applying of the vector field equation of motion turns it into zero. We consider it in more detail in the next section where we calculate some tree level processes.

4.3 The lowest order SLIV processes

The emergent vector field Lagrangian (4.8) and emergent gravity Lagrangian in (4.22) taken separately present in fact highly nonlinear theory which contains lots of Lorentz and CPT violating couplings. Nevertheless, as it was shown in [19,16,17] in the lowest order calculations, they all are cancelled and do not manifest themselves in physical processes. As we talked about earlier, this may mean that the length-fixing constraints (4.3,4.9) put on the vector and tensor fields appear as the

gauge fixing conditions rather than a source of an actual Lorentz violation. In the context of electrogravity model, which contains both photon and graviton as the emergent gauge fields, this means that only source of new physics can be (4.47). Even if suspicion that length fixing constraints are nonlinear gauge choices is true, for Lorentz invariance to be realized anyway, $U(1)$ and diff gauge transformations should commute in the symmetry broken phase and then we could claim that \mathcal{L}_1 and \mathcal{L}_2 in (4.47) will have no physical effects, but there is also (4.48), which is proportional to diff transformation parameter and strictly speaking it is not zero Lagrangian. So, in this picture to be logically sound and consistent we should check all interactions in the (4.47) anyway.

For that one properly derive all necessary Feynman rules and then calculate the basic lowest order processes, such as photon-graviton scattering and their conversion, photon scattering on the matter scalar field and other, that has been thoroughly carried out in our paper mentioned above [20] where can be found all necessary details. These calculations explicitly demonstrate that all the SLIV effects in these processes are strictly cancelled. This appears due to an interrelation between the longitudinal graviton and photon exchange diagrams and the corresponding contact interaction diagrams. So, physical Lorentz invariance in all processes is left intact. Apart, many other tree level Lorentz violating processes related to gravitons and vector fields (interacting with each other and the matter scalar field in the theory) may also appear in higher orders in the basic SLIV parameters $1/M_H$ and $1/M_A$, by iteration of couplings presented in our basic Lagrangians (4.22, (4.47)) or from a further expansions of the effective vector and tensor field Higgs modes (4.7, 4.18) inserted into the starting total Lagrangian (4.34). Again, their amplitudes appear to cancel each other, thus eliminating physical Lorentz violation in the theory.

Most likely, the same conclusion could be expected for SLIV loop contributions as well. Actually, as in the massless QED case considered earlier [16], the corresponding one-loop matrix elements in our emergent electrogravity theory could either vanish by themselves or amount to the differences between pairs of similar integrals whose integration variables are shifted relative to each other by some constants (being in general arbitrary functions of the external four-momenta of the particles involved) which, in the framework of dimensional regularization, could lead to their total cancellation.

So, after all, it should not come as too much of a surprise that emergent electrogravity theory considered here is likely to eventually possess physical Lorentz invariance provided that the underlying gauge and diff invariance in the theory remains unbroken.

4.4 Conclusion

We have combined emergent photon and graviton into one framework of electrogravity. While photon emerges as true vector Goldstone mode from SLIV, graviton at least partially consists of PGM-s as well, because alongside of Lorentz symmetry much bigger global symmetry of (4.9) $SO(7, 3)$ is broken as well. Configuration of true Goldstone and PGM-s inside graviton solely depends on VEV-s of vector and

tensor fields. So, in total 12 massless Goldstone modes are born to complete photon and graviton multiplets with an orthogonality conditions $n^\mu a_\mu = 0$, $n^{\mu\nu} h_{\mu\nu} = 0$ in place. Emergent electrogravity theory is nonlinear and in principal contains many Lorentz and CPT violating interactions, when expressed in terms of Goldstone modes. Nonetheless, all non-invariant effects disappear in all possible lowest order physical processes, which means that Lorentz invariance is intact and hence Lorentz invariance breaking conditions (4.3, 4.9) act as a gauge fixing for photon and graviton, instead of being actual source of physical Lorentz violation in the theory. If this cancellation occurs in all orders (i.e. (4.3, 4.9) are truly nonlinear gauge fixing conditions), then emergent electrogravity is physically indistinguishable from conventional gauge theories and spontaneous Lorentz violation caused by the vector and tensor field constraints (4.3, 4.9) appear hidden in gauge degrees of freedom, and only results in a noncovariant gauge choice in an otherwise gauge invariant emergent electrogravity theory.

From this standpoint, the only way for physical Lorentz violation to take place would be if the above gauge invariance were slightly broken by near Planck scale physics, presumably by quantum gravity or some other high dimensional theory. This is in fact a place where the emergent vector and tensor field theories may drastically differ from conventional QED, Yang-Mills and GR theories where gauge symmetry breaking could hardly induce physical Lorentz violation. In contrast, in emergent electrogravity such breaking could readily lead to many violation effects including deformed dispersion relations for all matter fields involved. Another basic distinction of emergent theories with non-exact gauge invariance is a possible origin of a mass for graviton and other gauge fields (namely, for the non-Abelian ones, see [18]), if they, in contrast to photon, are partially composed from pseudo-Goldstone modes rather than from pure Goldstone ones. Indeed, these PGM-s are no longer protected by gauge invariance and may properly acquire tiny masses, which still do not contradict experiment. This may lead to a massive gravity theory where the graviton mass emerges dynamically, thus avoiding the notorious discontinuity problem [21].

So, while emergent theories with an exact local invariance are physically indistinguishable from conventional gauge theories, there are some principal distinctions when this local symmetry is slightly broken which could eventually allow us to differentiate between the two types of theory in an observational way.

Acknowledgements

We would like to thank Colin Froggatt, Archil Kobakhidze and Holger Nielsen for useful discussions and comments. Z.K. wants to thank participants of the 21st Workshop "What Comes Beyond the Standard Models?" (23-30 June, Bled, Slovenia) for interesting and useful discussions, as well as the organizers for such a productive and working environment. This work is partially supported by Georgian National Science Foundation (grant No. YS-2016-81).

References

1. J.D. Bjorken, Ann. Phys. (N.Y.) **24** (1963) 174.
2. P.R. Phillips, Phys. Rev. **146** (1966) 966.
3. T. Eguchi, Phys.Rev. D **14** (1976) 2755;
4. Y. Nambu and G. Jona-Lasinio, Phys. Rev. **122** (1961) 345;
J. Goldstone, Nuovo Cimento **19** (1961) 154.
5. J.L. Chkareuli, C.D. Froggatt and H.B. Nielsen, Phys. Rev. Lett. **87** (2001) 091601;
Nucl. Phys. B **609** (2001) 46.
6. J.D. Bjorken, hep-th/0111196.
7. Per Kraus and E.T. Tomboulis, Phys. Rev. D **66** (2002) 045015.
8. A. Jenkins, Phys. Rev. D **69** (2004) 105007.
9. V.A. Kostelecky, Phys. Rev. D **69** (2004) 105009.
10. Z. Berezhiani and O.V. Kancheli, arXiv:0808.3181.
11. V.A. Kostelecky and R. Potting, Phys. Rev. D **79** (2009) 065018.
12. S.M. Carroll, H.Tam and I.K. Wehus, Phys. Rev. D **80** (2009) 025020.
13. R. Bluhm, N.L. Cage, R. Potting and A. Vrublevskis, Phys. Rev. D **77** (2008) 125007.
14. Y. Nambu, Progr. Theor. Phys. Suppl. Extra 190 (1968).
15. S. Weinberg, *The Quantum Theory of Fields*, v.2, Cambridge University Press, 2000.
16. A.T. Azatov and J.L. Chkareuli, Phys. Rev. D **73** (2006) 065026 .
17. J.L. Chkareuli and Z.R. Kepuladze, Phys. Lett. B **644** (2007) 212 .
18. J.L. Chkareuli and J.G. Jejelava, Phys. Lett. B **659** (2008) 754.
19. J.L. Chkareuli, J.G. Jejelava, G. Tatishvili, Phys. Lett. B 696 (2011) 126;
J.L. Chkareuli, C.D. Froggatt and H.B. Nielsen, Nucl. Phys. B 848 (2011) 498.
20. J.L. Chkareuli, J. Jejelava, Z. Kepuladze, Eur. Phys. J. C **78** (2018) 156; e-Print:
arXiv:1709.02736 [hep-th].
21. H. van Dam and M. J. G. Veltman, Nucl. Phys. B **22** (1970) 397.



5 A Deeper Probe of New Physics Scenarii at the LHC [★]

A. Djouadi ^{★★}

Laboratoire de Physique Théorique, Université Paris–Sud and CNRS,
F–91405 Orsay, France

Abstract. The implications of the discovery of a Higgs boson at the LHC with a mass of 125 GeV are summarised in the context of the Standard Model of particle physics and in new physics scenarios beyond it, taking the example of the minimal supersymmetric Standard Model extension, the MSSM. The perspectives for Higgs and new physics searches at the next LHC upgrades as well as at future hadron and lepton colliders are then briefly summarized.

Povzetek. Avtor povzame implikacijo odkritja higgsovega bozona z maso 125 GeV na pospeševalniku LHC na standardni model osnovnih delcev ter na nekatere modele, ki poskušajo narediti nov korak v fiziki osnovnih delcev. Kot primer omeni minimalno supersimetrično razširitev standardnega modela znano kot MSSM. Pregleda obete za iskanje znakov nove fizike v naslednji nadgradnji LHC in na bodočih leptonskih in hadronskih pospeševalnikih.

Keywords: Higgs boson, new physics scenarios, supersymmetry, MSSM

5.1 Introduction

The ATLAS and CMS historical discovery of a particle with a mass of 125 GeV [1] and properties that are compatible with those of a scalar Higgs boson [2,3] has far reaching consequences not only for the Standard Model (SM) but also for new physics models beyond it. In the SM, electroweak symmetry breaking is achieved spontaneously via the Brout–Englert–Higgs mechanism [2], wherein the neutral component of an isodoublet scalar field acquires a non-zero vacuum expectation value v . This gives rise to nonzero masses for the fermions and the electroweak gauge bosons while preserving the $SU(2) \times U(1)$ gauge symmetry. One of the four degrees of freedom of the original isodoublet field, corresponds to a physical particle [3]: a scalar boson with $J^{PC} = 0^{++}$ quantum numbers under parity and charge conjugation. The couplings of the Higgs boson to the fermions and gauge bosons are related to the masses of these particles and are thus decided by the

[★] Presented at 20th Bled Workshop in 2017. Contribution received too late for inclusion in 2017 Proceedings.

^{★★} E-mail: abdelhak.djouadi@th.u-psud.fr

symmetry breaking mechanism. In contrast, the Higgs mass itself M_H , although expected to be in the vicinity of the weak scale $v \approx 250$ GeV, is undetermined. Let us summarise the known information on this parameter before the start of the LHC.

A direct information was the lower limit $M_H \gtrsim 114$ GeV at 95% confidence level (CL) established at LEP2 [4]. Furthermore, a global fit of the electroweak precision data to which the Higgs boson contributes, yields the value $M_H = 92^{+34}_{-26}$ GeV, corresponding to a 95% CL upper limit of $M_H \lesssim 160$ GeV [4]. From the theoretical side, the presence of this new weakly coupled degree of freedom is a crucial ingredient for a unitary electroweak theory. Indeed, the SM without the Higgs particle leads to scattering amplitudes of the W/Z bosons that grow with the square of the center of mass energy and perturbative unitarity would be lost at energies above the TeV scale. In fact, even in the presence of a Higgs boson, the W/Z bosons could interact very strongly with each other and, imposing the unitarity requirement leads to the important mass bound $M_H \lesssim 700$ GeV [5], implying that the particle is kinematically accessible at the LHC.

Another theoretical constraint emerges from the fact that the Higgs self-coupling, $\lambda \propto M_H^2$, evolves with energy and at some stage, becomes very large and even infinite and the theory completely loses its predictability. If the energy scale up to which the couplings remains finite is of the order of M_H itself, one should have $M_H \lesssim 650$ GeV [6]. On the other hand, for small values of λ and hence M_H , the quantum corrections tend to drive the self-coupling to negative values and completely destabilize the scalar Higgs potential to the point where the minimum is not stable anymore [6]. Requiring $\lambda \geq 0$, up to the TeV scale implies that $M_H \gtrsim 70$ GeV. If the SM is to be extended to the Planck scale $M_P \sim 10^{18}$ GeV, the requirements on λ from finiteness and positivity constrain the Higgs mass to lie in the range $130 \text{ GeV} \lesssim M_H \lesssim 180 \text{ GeV}$ [6]. This narrow margin is close to the one obtained from the direct and indirect experimental constraints.

The discovery of the Higgs particle with a mass of 125 GeV, a value that makes the SM perturbative, unitary and extrapolable to the highest possible scales, is therefore a consecration of the model and crowns its past success in describing all experimental data available. In particular, the average mass value measured by the ATLAS and CMS teams, $M_H = 125.1 \pm 0.24$ GeV [7], is remarkably close to the best-fit of the precision data which should be considered as a great achievement and a triumph for the SM. In addition, a recent analysis that includes the state-of-the-art quantum corrections [8] gives for the condition of absolute stability of the electroweak vacuum, $\lambda(M_P) \geq 0$, the bound $M_H \gtrsim 129$ GeV for the present value of the top quark mass and the strong coupling constant, $m_t^{\text{exp}} = 173.2 \pm 0.9$ GeV and $\alpha_s(M_Z) = 0.1184 \pm 0.0007$ [4]. Allowing for a 2σ variation of m_t^{exp} , one obtains $M_H \geq 125.6$ GeV that is close to the measured M_H value [7]. In fact, for an unambiguous and well-defined determination of the top mass, one should rather use the total cross section for top pair production at hadron colliders which can unambiguously be defined theoretically; this mass has a larger error, $\Delta m_t \approx 3$ GeV, which allows more easily absolute stability of the SM vacuum up to M_P [9].

Nevertheless, the SM is far from being perfect in many respects. It does not explain the proliferation of fermions and the large hierarchy in their mass spectra

and does not say much about the small neutrino masses. The SM does not unify in a satisfactory way the electromagnetic, weak and strong forces, as one has three different symmetry groups with three coupling constants which shortly fail to meet at a common value during their evolution with the energy scale; it also ignores the fourth force, gravitation. Furthermore, it does not contain a particle that could account for the cosmological dark matter and fails to explain the baryon asymmetry in the Universe.

However, the main problem that calls for beyond the SM is related to the special status of the Higgs boson which, contrary to fermions and gauge bosons has a mass that cannot be protected against quantum corrections. Indeed, these are quadratic in the new physics scale which serves as a cut-off and hence, tend to drive M_H to very large values, ultimately to M_P , while we need $M_H = \mathcal{O}(100 \text{ GeV})$. Thus, the SM cannot be extrapolated beyond $\mathcal{O}(1 \text{ TeV})$ where some new physics should emerge. This is the reason why we expect something new to manifest itself at the LHC.

There are three avenues for the many new physics scenarios beyond the SM. There are first theories with extra space-time dimensions that emerge at the TeV scale (the cut-off is then not so high) and, second, composite models inspired from strong interactions also at the TeV scale (and thus the Higgs is not a fundamental spin-zero particle). Some versions of these scenarios do not incorporate any Higgs particle in their spectrum and are thus ruled out by the Higgs discovery. However, the option that emerges in the most natural way is Supersymmetry (SUSY) [10] as it solves most of the SM problems discussed above. In particular, SUSY protects M_H as the quadratically divergent radiative corrections from standard particles are exactly compensated by the contributions of their supersymmetric partners. These new particles should not be much heavier than 1 TeV not to spoil this compensation [11] and, thus, they should be produced at the LHC.

The Higgs discovery is very important for SUSY and, in particular, for its simplest low energy manifestation, the minimal supersymmetric SM (MSSM) that indeed predicts a light Higgs state. In the MSSM, two Higgs doublet fields H_u and H_d are required, leading to an extended Higgs consisting of five Higgs bosons, two CP-even h and H , a CP-odd A and two charged H^\pm states [12]. Nevertheless, only two parameters are needed to describe the Higgs sector at tree-level: one Higgs mass, which is generally taken to be that of the pseudoscalar boson M_A , and the ratio of vacuum expectation values of the two Higgs fields, $\tan \beta = v_d/v_u$, expected to lie in the range $1 \lesssim \tan \beta \lesssim 60$. The masses of the CP-even h , H and the charged H^\pm states, as well as the mixing angle α in the CP-even sector are uniquely defined in terms of these two inputs at tree-level, but this nice property is spoiled at higher orders [13]. For $M_A \gg M_Z$, one is in the so-called decoupling regime in which the h state is light and has almost exactly the SM-Higgs couplings, while the other CP-even H and the charged H^\pm bosons become heavy, $M_H \approx M_{H^\pm} \approx M_A$, and decouple from the massive gauge bosons. In this regime, the MSSM Higgs sector thus looks almost exactly as the one of the SM with its unique Higgs boson.

Nevertheless, contrary to the SM Higgs boson, the lightest MSSM CP-even h mass is bounded from above and, depending on the SUSY parameters that enter the important quantum corrections, is restricted to $M_h^{\max} \lesssim 130 \text{ GeV}$ [13] if one

assumes a SUSY breaking scale that is not too high, $M_S \lesssim \mathcal{O}(1 \text{ TeV})$, in order to avoid too much fine-tuning in the model. Hence, the requirement that the MSSM h boson coincides with the one observed at the LHC, i.e. with $M_h \approx 125 \text{ GeV}$ and almost SM-like couplings as the LHC data seem to indicate, would place very strong constraints on the MSSM parameters, in particular the SUSY-breaking scale M_S . This comes in addition to the LHC limits obtained from the search of the heavier Higgs states and the superparticles.

In this talk, the implications of the discovery of the Higgs boson at the LHC and the measurement of its properties will be summarised and the prospects for the searches of new physics, in particular in the SUSY context, in the future will be discussed.

5.2 Implications: Standard Model and beyond

In many respects, the Higgs particle was born under a very lucky star as the mass value of $\approx 125 \text{ GeV}$ allows to produce it at the LHC in many redundant channels and to detect it in a variety of decay modes. This allows detailed studies of the Higgs properties.

5.2.1 Higgs production and decay

We start by summarizing the production and decay at the LHC of a light SM-like Higgs particle, which should correspond to the lightest MSSM h boson in the decoupling regime. First, for $M_h \approx 125 \text{ GeV}$, the Higgs mainly decays [14] into $b\bar{b}$ pairs but the decays into WW^* and ZZ^* final states, before allowing the gauge bosons to decay leptonically $W \rightarrow \ell\nu$ and $Z \rightarrow \ell\ell$ ($\ell = e, \mu$), are also significant. The $H \rightarrow \tau^+\tau^-$ channel (as well as the gg and $c\bar{c}$ decays that are not detectable at the LHC) is also of significance, while the clean loop induced $H \rightarrow \gamma\gamma$ mode can be easily detected albeit its small rates. The very rare $H \rightarrow Z\gamma$ and even $H \rightarrow \mu^+\mu^-$ channels should be accessible at the LHC but only with a much larger data sample.

On the other hand, many Higgs production processes have significant cross sections [15–17]. While the by far dominant gluon fusion mechanism $gg \rightarrow H$ (ggF) has extremely large rates ($\approx 20 \text{ pb}$ at $\sqrt{s} = 7\text{--}8 \text{ TeV}$), the subleading channels, i.e. the vector boson fusion (VBF) $q\bar{q} \rightarrow Hq\bar{q}$ and the Higgs-strahlung (HV) $q\bar{q} \rightarrow HV$ with $V = W, Z$ mechanisms, have cross sections which should allow for Higgs studies of the already at $\sqrt{s} \gtrsim 7 \text{ TeV}$ with the $\approx 25 \text{ fb}^{-1}$ data collected by each experiment. The associated process $pp \rightarrow t\bar{t}H$ (ttH) would require higher energy and luminosity.

This pattern already allows the ATLAS and CMS experiments to observe the Higgs boson in several channels and to measure some of its couplings in a reasonably accurate way. The channels that have been searched are $H \rightarrow ZZ^* \rightarrow 4\ell^\pm$, $H \rightarrow WW^* \rightarrow 2\ell 2\nu$, $H \rightarrow \gamma\gamma$ where the Higgs is mainly produced in ggF with subleading contributions from Hjj in the VBF process, $H \rightarrow \tau\tau$ where the Higgs is produced in association with one (in ggF) and two (in VBF) jets, and finally $H \rightarrow b\bar{b}$ with the Higgs produced in the HV process. One can ignore for the moment the low sensitivity $H \rightarrow \mu\mu$ and $H \rightarrow Z\gamma$ channels.

A convenient way to scrutinize the couplings of the produced H boson is to look at their deviation from the SM expectation. One then considers for a given search channel the signal strength modifier μ which for the $H \rightarrow XX$ decay mode measures the deviation compared to the SM expectation of the Higgs production cross section times decay branching fraction μ_{XX} . ATLAS and CMS have provided the signal strengths for the various final states with a luminosity of $\approx 5 \text{ fb}^{-1}$ for the 2011 run at $\sqrt{s} = 7 \text{ TeV}$ and $\approx 20 \text{ fb}^{-1}$ for the 2012 run at $\sqrt{s} = 8 \text{ TeV}$. The constraints given by the two collaborations, when combined, lead to a global signal strength $\mu_{\text{tot}}^{\text{ATLAS}} = 1.18 \pm 0.15$ and $\mu_{\text{tot}}^{\text{CMS}} = 1.00 \pm 0.14$ [7]. The global value being very close to unity implies that the observed Higgs is SM-like.

Hence, already with the rather limited statistics at hand, the accuracy of the ATLAS and CMS measurements is reaching the 15% level. This is at the same time impressive and worrisome. Indeed, the main Higgs production channel is the top and bottom quark loop mediated gluon fusion mechanism and, at $\sqrt{s} = 7$ or 8 TeV, the three other mechanisms contribute at a total level below 15%. The majority of the signal events observed at LHC, in particular in the search channels $H \rightarrow \gamma\gamma$, $H \rightarrow ZZ^* \rightarrow 4\ell$, $H \rightarrow WW^* \rightarrow 2\ell 2\nu$ and to some extent $H \rightarrow \tau\tau$, thus come from the ggF mechanism which is known to be affected by large theoretical uncertainties.

Indeed, although $\sigma(gg \rightarrow H)$ is known up next-to-next-to-leading order (NNLO) in perturbative QCD (and at least at NLO for the electroweak interaction) [15,16], there is a significant residual scale dependence which points to the possibility that still higher order contributions cannot be totally excluded. In addition, as the process is of $\mathcal{O}(\alpha_s^2)$ at LO and is initiated by gluons, there are sizable uncertainties due to the gluon parton distribution function (PDF) and the value of the coupling α_s . A third source of theoretical uncertainties, the use of an effective field theory (EFT) approach to calculate the radiative corrections beyond NLO should also be considered [15]. In addition, large uncertainties arise when $\sigma(gg \rightarrow H)$ is broken into the jet categories $H+0j$, $H+1j$ and $H+2j$ [18]. In total, the combined theoretical uncertainty is estimated to be $\Delta^{\text{th}} \approx \pm 15\%$ [16] and would increase to $\Delta^{\text{th}} \approx \pm 20\%$ if the EFT uncertainty is also included. The a priori cleaner VBF process will be contaminated by the $gg \rightarrow H+2j$ mode making the total error in the $H+jj$ “VBF” sample also rather large [18].

Hence, the theoretical uncertainty is already at the level of the accuracy of the cross section measured by the ATLAS and CMS collaborations. Another drawback of the analyses is that they involve strong theoretical assumptions on the total Higgs width since some contributing decay channels not accessible at the LHC are assumed to be SM-like and possible invisible Higgs decays in scenarios beyond the SM do not to occur.

In Ref. [17], following earlier work [19] it has been suggested to consider the ratio $D_{XX}^p = \sigma^p(pp \rightarrow H \rightarrow XX)/\sigma^p(pp \rightarrow H \rightarrow VV)$ for a specific production process p and for a given decay channel $H \rightarrow XX$ when the reference channel $H \rightarrow VV$ is used. In these ratios, the cross sections and hence, their significant theoretical uncertainties will cancel out, leaving out only the ratio of partial decay widths which are better known. The total decay width which includes contributions from channels not under control such as possible invisible Higgs decays, do not appear

in the ratios D_{XX}^p . Some common experimental systematical uncertainties such as the one from the luminosity measurement and the small uncertainties in the Higgs decay branching ratios also cancel out. We are thus left with only with the statistical and some (non common) systematical errors [17].

The ratios D_{XX} involve, up to kinematical factors and known radiative corrections, only the ratios $|c_X|^2/|c_V|^2$ of the Higgs reduced couplings to the particles X and V compared to the SM expectation, $c_X \equiv g_{HXX}/g_{HXX}^{\text{SM}}$. For the time being, three independent ratios can be considered: $D_{\gamma\gamma}$, $D_{\tau\tau}$ and D_{bb} . In order to determine these ratios, the theoretical uncertainties have to be treated as a bias (and not as if they were associated with a statistical distribution) and the fit has to be performed for the two μ extremal values: $\mu_i|_{\text{exp}} \pm \delta\mu_i/|\mu_i|_{\text{th}}$ with $\delta\mu_i/|\mu_i|_{\text{th}} \approx \pm 20\%$ [20].

A large number of analyses of the Higgs couplings from the LHC data have been performed and in most cases, it is assumed that the couplings of the Higgs boson to the massive W, Z gauge bosons are equal to $g_{HZZ} = g_{HWW} = c_V$ and the couplings to all fermions are also the same $g_{Hff} = c_f$. However, as for instance advocated in Ref. [21] to characterize the Higgs particle at the LHC, at least three independent H couplings should be considered, namely c_t , c_b and c_V . While the couplings to W, Z, b, τ particles are derived by considering the decays of the Higgs boson to these particles, the $Ht\bar{t}$ coupling is derived indirectly from $\sigma(gg \rightarrow H)$ and $\text{BR}(H \rightarrow \gamma\gamma)$, two processes that are generated by triangular loops involving the top quarks in the SM. One can assume, in a first approximation, that $c_c = c_t$ and $c_\tau = c_b$ and possible invisible Higgs decays are absent. In Ref. [21], a three-dimensional fit of the H couplings was performed in the space $[c_t, c_b, c_V]$, when the theory uncertainty is taken as a bias and not as a nuisance. The best-fit value for the couplings, with the $\sqrt{s} = 7+8$ TeV ATLAS and CMS data turns out to be $c_t = 0.89$, $c_b = 1.01$ and $c_V = 1.02$, ie very close to the SM values.

5.2.2 Implications of the Higgs couplings measurement

The precise measurements of Higgs couplings allow to draw several important conclusions.

i) A fourth generation fermions is excluded. Indeed, in addition to the direct LHC searches that exclude heavier quarks $m_{b'}, m_{t'} \lesssim 600$ GeV [23], strong constraints can be also obtained from the loop induced Higgs–gluon and Higgs–photon vertices in which any heavy particle coupling to the Higgs proportionally to its mass will contribute. For instance the additional 4th generation t' and b' contributions increase $\sigma(gg \rightarrow H)$ by a factor of ≈ 9 at LO but large $\mathcal{O}(G_F m_{t'}^2)$ electroweak corrections should be considered. It has been shown [23] that with a fourth family, the Higgs signal would have not been observable and the obtained Higgs results unambiguously rule out this possibility.

ii) The invisible Higgs decay width should be small. Invisible decays would affect the properties of the observed Higgs boson and could be constrained if the total decay width is determined. But for a 125 GeV Higgs, $\Gamma_H^{\text{tot}} = 4$ MeV, is too small to be resolved experimentally. Nevertheless, in $pp \rightarrow VV \rightarrow 4f$, a large fraction of the Higgs cross section lies in the high-mass tail [24] allowing to put loose

constrains $\Gamma_H^{\text{tot}}/\Gamma_H^{\text{SM}} \approx 5\text{--}10$ [25]. The invisible Higgs decay width Γ_H^{inv} can be better constrained indirectly by a fit of the Higgs couplings and in particular with the signal strength in the $H \rightarrow ZZ$ process: $\mu_{ZZ} \propto \Gamma(H \rightarrow ZZ)/\Gamma_H^{\text{tot}}$ with $\Gamma_H^{\text{tot}} = \Gamma_H^{\text{inv}} + \Gamma_H^{\text{SM}}$; one obtains $\Gamma_H^{\text{inv}}/\Gamma_H^{\text{SM}} \lesssim 50\%$ at 95% CL with the assumption $c_f = c_V = 1$ [20].

A more model independent approach would be to perform direct searches for missing transverse energy. These have been conducted in $pp \rightarrow HV$ with $V \rightarrow jj, \ell\ell$ and in VBF, $qq \rightarrow qqE_\tau$ leading to $\text{BR}_{\text{inv}} \lesssim 50\%$ at 95%CL for SM-like Higgs couplings [7]. A more promising search for invisible decays is the monojet channel $gg \rightarrow Hj$ which has large rates [26]. While the most recent monojet ATLAS and CMS searches are only sensitive to $\text{BR}_{\text{inv}} \sim 1$, more restrictive results can be obtained in the future.

The Higgs invisible rate and the dark matter detection rate in direct astrophysical searches are correlated in Higgs portal models and it turns out that LHC constraints are competitive [27] with those derived from direct dark matter search experiments [28].

iii) The spin-parity quantum numbers are those of a standard Higgs. One also needs to establish that the observed Higgs state is indeed a CP even scalar and hence with $J^{\text{PC}} = 0^{++}$ quantum numbers. For the spin, the observation of the $H \rightarrow \gamma\gamma$ decay rules out the spin-1 case [29]. The Higgs parity can be probed by studying kinematical distributions in the $H \rightarrow ZZ^* \rightarrow 4\ell$ decay channel and in the VH and VBF production modes [30] and with the 25 fb^{-1} data collected so far, ATLAS and CMS found that the observed Higgs is more compatible with a 0^+ state and the 0^- possibility is excluded at the 98%CL [7]. Other useful diagnostics of the Higgs CP nature that also rely on the tensorial structure of the HVV coupling can be made in the VBF process [31]. Nevertheless, there is a caveat in the analyses relying on the HVV couplings: a CP-odd state has no tree-level VV couplings [32]. In fact, a better way to measure the Higgs parity is to study the signal strength in the $H \rightarrow VV$ channels and in Ref. [20] it was demonstrated that the observed Higgs has indeed a large CP component, $\gtrsim 50\%$ at the 95%CL. In fact, the less unambiguous way to probe the Higgs CP nature would be to look at final states in which the particle decays hadronically, e.g. $pp \rightarrow HZ \rightarrow b\bar{b}\ell\ell$ [32]. These processes are nevertheless extremely challenging even at the upgraded LHC.

5.2.3 Implications for Supersymmetry

We turn now to the implications of the LHC Higgs results for the MSSM Higgs sector and first make a remark on the Higgs masses and couplings, which at tree-level depend only on M_A and $\tan\beta$, when the important radiative corrections are included. In this case many parameters such as the masses of the third generation squarks $m_{\tilde{t}_i}, m_{\tilde{b}_i}$ and their trilinear couplings A_t, A_b enter M_h and M_H through quantum corrections. These are introduced by a general 2×2 matrix $\Delta\mathcal{M}_{ij}^2$ but the leading one is controlled by the top Yukawa coupling and is proportional to $m_t^4, \log M_S$ with $M_S = \sqrt{m_{\tilde{t}_1} m_{\tilde{t}_2}}$ the SUSY-breaking scale and the stop mixing parameter X_t [13]. The maximal value M_h^{max} is then obtained for a decoupling regime $M_A \sim \mathcal{O}(\text{TeV})$, large $\tan\beta$, large M_S that implies heavy stops and maximal mixing $X_t = \sqrt{6}M_S$ [33]. If the parameters are optimized as above, the maximal M_h value reaches the level of 130 GeV.

It was pointed out in Refs. [34,35,21] that when the measured value $M_h = 125$ GeV is taken into account, the MSSM Higgs sector with only the largely dominant correction discussed above, can be again described with only the two parameters $\tan \beta$ and M_A ; in other words, the loop corrections are fixed by the value of M_h . This observation leads to a rather simple but accurate parametrisation of the MSSM Higgs sector, called hMSSM.

The reduced couplings of the CP-even h state (as is the case for the heavier H) depend in principle only on the angles β and α (and hence $\tan \beta$ and M_A), $c_V^0 = \sin(\beta - \alpha)$, $c_t^0 = \cos \alpha / \sin \beta$, $c_b^0 = -\sin \alpha / \cos \beta$, while the couplings of A and H^\pm (as well as H in the decoupling regime) to gauge boson are zero and those to fermions depend only on β : for $\tan \beta > 1$, they are enhanced ($\propto \tan \beta$) for b, τ and suppressed ($\propto 1 / \tan \beta$) for tops.

i) Implications from the Higgs mass value: In the so-called “phenomenological MSSM” (pMSSM) [37] in which the model involves only 22 free parameters, a large scan has been performed [36] using the RGE program *Suspect* [38] that calculates the maximal M_h value and the result confronted to the measured mass $M_h \sim 125$ GeV. For $M_S \lesssim 1$ TeV, only scenarios with X_t/M_S values close to maximal mixing $X_t/M_S \approx \sqrt{6}$ survive. The no-mixing scenario $X_t \approx 0$ is ruled out for $M_S \lesssim 3$ TeV, while the typical mixing scenario, $X_t \approx M_S$, needs large M_S and moderate to large $\tan \beta$ values. In constrained MSSM scenarios (cMSSM) such the minimal supergravity (mSUGRA) model and the gauge and anomaly mediated SUSY-breaking scenarios, GMSB and AMSB, only a few basic inputs are needed and the mixing parameter cannot take arbitrary values. A scan in these models with $M_S \lesssim 3$ TeV not to allow for too much fine-tuning [11] leads $M_h^{\max} \lesssim 122$ GeV in AMSB and GMSB thus disfavoring these scenarios while one has $M_h^{\max} = 128$ GeV in mSUGRA. In high-scale SUSY scenarios, $M_S \gg 1$ TeV, the radiative corrections are very large and need to be resummed [39]. For low $\tan \beta$ values, large scales, at least $M_S \gtrsim 10^4$ GeV, are required to obtain $M_h = 125$ GeV and even higher in most cases

ii) Implications from the production rates of the observed state. Besides the corrections to the Higgs masses and couplings discussed above, there are also direct corrections to the Higgs couplings and the most ones are those affecting the $hb\bar{b}$ vertex [40] and the stop loop contributions to the $gg \rightarrow h$ production and $h \rightarrow \gamma\gamma$ decay rates [41]. A fit of the c_t, c_b and c_V couplings shows that the latter are small [20]. In turn, ignoring the direct corrections and using the input $M_h \approx 125$ GeV, one can make a fit in the plane $[\tan \beta, M_A]$. The best-fit point is $\tan \beta = 1$ and $M_A = 550$ GeV which implies a large SUSY scale, $M_S = \mathcal{O}(100)$ TeV. In all, cases one also has $M_A \gtrsim 200\text{--}350$ GeV.

iii) Implications from heavy Higgs boson searches. At high $\tan \beta$ values, the strong enhancement of the b, τ couplings makes that the $\Phi = H/A$ states decay dominantly into $\tau^+\tau^-$ and $b\bar{b}$ pairs and are mainly produced in $gg \rightarrow \Phi$ fusion with the b -loop included and associated production with b -quarks, $gg/q\bar{q} \rightarrow b\bar{b} + \Phi$ [42]. The most powerful LHC search channel is thus $pp \rightarrow gg + b\bar{b} \rightarrow \Phi \rightarrow \tau^+\tau^-$. For the charged Higgs, the dominant mode is $H^\pm \rightarrow \tau\nu$ with the H^\pm light enough to be produced in top decays $t \rightarrow H^+b \rightarrow \tau\nu b$. In the low $\tan \beta$ regime, $\tan \beta \lesssim 3$, the phenomenology of the A, H, H^\pm states is richer [34]. For the production, only

$gg \rightarrow \Phi$ process with the dominant t and sub-dominant b contributions provides large rates. The $H/A/H^\pm$ decay pattern is in turn rather involved. Above the $t\bar{t}$ (tb) threshold $H/A \rightarrow t\bar{t}$ and $H^\pm \rightarrow t\bar{b}$ are by far dominant. Below threshold, the $H \rightarrow WW, ZZ$ decays are significant. For $2M_h \lesssim M_H \lesssim 2m_t$ ($M_A \gtrsim M_h + M_Z$), $H \rightarrow hh$ ($A \rightarrow hZ$) is the dominant $H(A)$ decay mode. But the $A \rightarrow \tau\tau$ channel is still important with rates $\gtrsim 5\%$. In the case of H^\pm , the channel $H^\pm \rightarrow Wh$ is important for $M_{H^\pm} \lesssim 250$ GeV, similarly to the $A \rightarrow hZ$ case.

In Ref. [34] an analysis of these channels has been performed using current information given by ATLAS and CMS in the context of the SM, MSSM [43] or other scenarios. The outcome is impressive. The ATLAS and CMS $H/A \rightarrow \tau^+\tau^-$ constraint is extremely restrictive and $M_A \lesssim 250$ GeV, it excludes almost the entire intermediate and high $\tan\beta$ regimes. The constraint is less effective for a heavier A but even for $M_A \approx 400$ GeV the high $\tan\beta \gtrsim 10$ region is excluded and one is even sensitive to $M_A \approx 800$ GeV for $\tan\beta \gtrsim 50$. For H^\pm , almost the entire $M_{H^\pm} \lesssim 160$ GeV region is excluded by the process $t \rightarrow H^\pm b$ with the decay $H^\pm \rightarrow \tau\nu$. The other channels, in particular $H \rightarrow VV$ and $H/A \rightarrow t\bar{t}$, are very constraining as they cover the entire low $\tan\beta$ area that was previously excluded by the LEP2 bound up to $M_A \approx 500$ GeV. Even $A \rightarrow hZ$ and $H \rightarrow hh$ would be visible at the current LHC in small portions of the parameter space.

5.3 Perspectives for Higgs and New Physics

The last few years were extremely rich and exciting for particle physics. With the historical discovery of a Higgs boson by the LHC collaborations ATLAS and CMS, crowned by a Nobel prize in fall 2013, and the first probe of its basic properties, they witnessed a giant step in the unraveling of the mechanism that breaks the electroweak symmetry and generates the fundamental particle masses. They promoted the SM as the appropriate theory, up to at least the Fermi energy scale, to describe three of Nature's interactions, the electromagnetic, weak and strong forces. However, it is clear that these few years have also led to some frustration as no signal of physics beyond the SM has emerged from the LHC data. The hope of observing some signs of the new physics models that were put forward to address the hierarchy problem, that is deeply rooted in the Higgs mechanism, with Supersymmetric theories being the most attractive ones, did not materialize.

The Higgs discovery and the non-observation of new particles has nevertheless far reaching consequences for supersymmetric theories and, in particular, for their simplest low energy formulation, the MSSM. The mass of approximately 125 GeV of the observed Higgs boson implies that the scale of SUSY-breaking is rather high, at least $\mathcal{O}(\text{TeV})$. This is backed up by the limits on the masses of strongly interacting SUSY particles set by the ATLAS and CMS searches, which in most cases exceed the TeV range. This implies that if SUSY is indeed behind the stabilization of the Higgs mass against very high scales that enter via quantum corrections, it is either fine-tuned at the permille level at least or its low energy manifestation is more complicated than expected.

The production and decay rates of the observed Higgs particles, as well as its spin and parity quantum numbers, as measured by ATLAS and CMS with the $\approx 25 \text{ fb}^{-1}$ data collected at $\sqrt{s}=7+8 \text{ TeV}$, indicate that its couplings to fermions and gauge bosons are almost SM-like. In the context of the MSSM, this implies that we are close to the decoupling regime and this particle is the lightest h boson, while the other $H/A/H^\pm$ states must be heavier than approximately the Fermi scale. This last feature is also backed up by LHC direct searches of these heavier Higgs states.

This drives up to the question that is now very often asked: what to do next? The answer is, for me, obvious: we are only in the beginning of a new era. Indeed, it was expected since a long time that the probing of the electroweak symmetry breaking mechanism will be at least a two chapters story. The first one is the search and the observation of a Higgs-like particle that will confirm the scenario of the SM and most of its extensions, that is, a spontaneous symmetry breaking by a scalar field that develops a non-zero vev. This long chapter has just been closed by the ATLAS and CMS collaborations with the spectacular observation of a Higgs boson. This observation opens a second and equally important chapter: the precise determination of the Higgs profile and the unraveling of the electroweak symmetry breaking mechanism itself.

A more accurate measurement of the Higgs couplings to fermions and gauge bosons will be mandatory to establish the exact nature of the mechanism and, eventually, to pin down effects of new physics if additional ingredients beyond those of the SM are involved. This is particularly true in weakly interacting theories such as SUSY in which the quantum effects are expected to be small. These measurements could be performed at the upgraded LHC with an energy close to $\sqrt{s}=14 \text{ TeV}$, in particular if a very high luminosity, a few ab^{-1} , is achieved [43,44].

At this upgrade, besides improving the measurements performed so far, rare but important channels such as associated Higgs production with top quarks, $pp \rightarrow t\bar{t}H$, and Higgs decays into $\mu^+\mu^-$ and $Z\gamma$ states could be probed. Above all, a determination of the self-Higgs coupling could be made by searching for double Higgs production e.g. in the gluon fusion channel $gg \rightarrow HH$ [45]; this would be a first step towards the reconstruction of the scalar potential that is responsible of electroweak symmetry breaking. This measurement would be difficult at the LHC even with high-luminosity but a proton collider with $\sqrt{s}=30$ to 100 TeV could do the job [44].

In a less near future, a high-energy lepton collider, which is nowadays discussed in various options (ILC, TLEP, CLIC, μ -collider) would lead to a more accurate probing of the Higgs properties [46], promoting the scalar sector to the very high-precision level of the gauge and fermion sectors achieved by the LEP and SLC colliders in the 1990s [4]. At electron-positron colliders, the process $e^+e^- \rightarrow HZ$, just looking at the recoiling Z boson allows to measure the Higgs mass, the CP parity and the absolute HZZ coupling, allowing to derive the total decay width Γ_H^{tot} . One can then measure precisely, already at $\sqrt{s} \approx 250 \text{ GeV}$ where $\sigma(e^+e^- \rightarrow HZ)$ is maximal, the absolute Higgs couplings to gauge bosons and light fermions from the decay branching ratios. The important couplings to top quarks and the Higgs self-couplings can be measured at the 10% level in the higher-

order processes $e^+e^- \rightarrow t\bar{t}H$ and $e^+e^- \rightarrow HHZ$ at energies of at least 500 GeV with a high-luminosity.

Besides the high precision study of the already observed Higgs, one should also continue to search for the heavy states that are predicted by SUSY, not only the superparticles but also the heavier Higgs bosons. The energy upgrade to ≈ 14 TeV (and eventually beyond) and the planed order of magnitude (or more) increase in luminosity will allow to probe much higher mass scales than presently. In fact, more generally, one should continue to search for any sign of new physics or new particles, new gauge bosons and fermions, as predicted in most of the SM extensions.

In conclusion, it is not yet time to give up on SUSY and more generally on New Physics but, rather, to work harder to be fully prepared for the more precise and larger data set that will be delivered by the upgraded LHC. It will be soon enough to “philosophize” then as the physics landscape will become more clear.

Acknowledgements:

I thank the organisers for their invitation to give a talk at the conference. This work is supported by the ERC Advanced Grant Higgs@LHC.

References

1. ATLAS collaboration, Phys. Lett. B716 (2012) 1; CMS collaboration, Phys. Lett. B716 (2012) 30.
2. F. Englert and R. Brout, Phys. Rev. Lett. 13 (1964) 321; P. Higgs, Phys. Rev. Lett. 13 (1964) 508; P. Higgs, Phys. Lett. 12 (1964) 132; G. Guralnik, C. Hagen, T. Kibble, Phys. Rev. Lett. 13 (1964) 585.
3. For a review of SM Higgs, see: A. Djouadi, Phys. Rept. 457 (2008) 1.
4. K. Olive et al., Particle Data Group, Chin. Phys. C38 (2014) 090001.
5. B.W. Lee, C. Quigg and H.B. Thacker, Phys. Rev. D16 (1977) 1519.
6. N. Cabibbo et al., Nucl. Phys. B158 (1979) 295; M. Sher, Phys. Rept. 179 (1989) 273; G. Altarelli and G. Isidori, Phys. Lett. B337 (1994) 141.
7. See the talks given at the summer conferences.
8. G. Degrandi et al., JHEP 1208 (2012) 098; F. Bezrukov et al., JHEP 1210 (2012) 140.
9. S. Alekhin, A. Djouadi and S. Moch, Phys. Lett. B716 (2012) 214.
10. M. Drees, R. Godbole, P. Roy, *Theory and phenomenology of sparticles*, World Sci., 2005.
11. E. Witten, Nucl. Phys. B188 (1981) 513; R. Barbieri and G. Giudice, Nucl. Phys. B306 (1988) 63; M. Papucci, J. Ruderman and A. Weiler, JHEP 1209 (2012) 035.
12. A. Djouadi, Phys. Rept. 459 (2008) 1; Eur. Phys. J. C74 (2014) 2704.
13. S. Heinemeyer, W. Hollik and G. Weiglein, Phys. Rept. 425 (2006) 265; M. Carena and H. Haber, Prog. Part. Nucl. Phys. 50 (2003) 63; B. Allanach et al., JHEP 0409 (2004) 044.
14. A. Djouadi, J. Kalinowski and M. Spira, Comput. Phys. Commun. 108 (1998) 56; A. Djouadi, M. Muhlleitner and M. Spira, Acta. Phys. Polon. B38 (2007) 635.
15. J. Baglio and A. Djouadi, JHEP 1103 (2011) 055; JHEP 1010 (2010) 064; J. Baglio et al., Phys. Lett. B716 (2012) 203.
16. S. Dittmaier et al., the LHC Higgs xsWG, arXiv:1101.0593 [hep-ph].
17. A. Djouadi, Eur. Phys. J. C73 (2013) 2498; A. Djouadi, J. Quevillon and R. Vega-Morales, arXiv:1509.03913 [hep-ph].
18. S. Dittmaier et al., the LHC Higgs xsWG, arXiv:1201.3084 [hep-ph].

19. D. Zeppenfeld et al. Phys. Rev. D62 (2000) 013009; A. Djouadi et al., hep-ph/0002258; M. Dührssen et al., Phys. Rev. D70 (2004) 113009.
20. A. Djouadi and G. Moreau, Eur. Phys. J. C73 (2013) 2512.
21. A. Djouadi, L. Maiani, G. Moreau, A. Polosa, J. Quevillon, V. Riquer, Eur. Phys. J. C73 (2013) 2650; JHEP 1506 (2015) 168.
22. A. Djouadi and A. Lenz, Phys. Lett. B715 (2012) 310; E. Kuflik, Y. Nir and T. Volansky, Phys. Rev.Lett. 110 (2013) 091801; A. Denner et al., Eur.Phys.J. C72 (2012) 1992; A. Djouadi, P. Gambino, B. Kniehl, Nucl. Phys. B523 (1998) 17; A. Djouadi and P. Gambino, Phys. Rev. Lett. 73 (1994) 2528.
23. CMS collaboration, Phys. Rev. D86 (2012) 112003; ATLAS collaboration, Phys. Rev. Lett. 109 (2012) 032001.
24. See e.g., N. Kauer and G. Passarino, JHEP 1208 (2012) 116.
25. ATLAS collaboration, ATLAS-CONF-2014-042; CMS collaboration, Phys. Lett. B736 (2014) 64.
26. A. Djouadi, A. Falkowski, Y. Mambrini and J. Quevillon, Eur. Phys. J. C73 (2013) 2455.
27. A. Djouadi, O. Lebedev, Y. Mambrini and J. Quevillon, Phys. Lett. B709 (2012) 65.
28. M. Goodman and E. Witten, Phys. Rev. D31 (1985) 3059; M. Drees and M. Nojiri, Phys. Rev. D48 (1993) 3483; A. Djouadi and M. Drees, Phys. Lett. B484 (2000) 183.
29. L. Landau, Dokl. Akad. Nauk Ser. Fiz. 60 (1948) 207; C. Yang, Phys. Rev. 77 (1950) 242.
30. For a review, see e.g. S. Kraml (ed.) et al., hep-ph/0608079.
31. T. Plehn, D. Rainwater and D. Zeppenfeld, Phys. Rev. Lett. 88 (2002) 051801; A. Djouadi, R. Godbole, B. Mellado, K. Mohan, Phys. Lett. B723 (2013) 307.
32. V. Barger et al., Phys. Rev. D49 (1994) 79; B. Grzadkowski, J. Gunion and X. He, Phys. Rev. Lett. 77 (1996) 5172; J. Gunion and J. Pliszka, Phys. Lett. B444 (1998) 136; P. Bhupal Dev et al., Phys. Rev. Lett. 100 (2008) 051801; J. Ellis, V. Sanz, T. You, Phys. Lett. B726 (2013) 244.
33. M. Carena et al., Eur. J. Phys. C26 (2003) 601; Eur. Phys. J. C73 (2013) 2552.
34. A. Djouadi and J. Quevillon, JHEP 1310 (2013) 028.
35. L. Maiani, A. Polosa, V. Riquer, Phys. Lett. B718 (2012) 465; *ibid.* B724 (2013) 274.
36. A. Arbey et al., Phys. Lett. B708 (2012) 162; JHEP 1209 (2012) 107; Phys. Lett. B720 (2013) 153.
37. A. Djouadi et al. (MSSM working group), hep-ph/9901246.
38. A. Djouadi, J.L. Kneur and G. Moultaka, Comput. Phys. Commun. 176 (2007) 426; M. Muhlleitner et al., Comput. Phys. Commun. 168 (2005) 46.
39. L. Hall and Y. Nomura, JHEP 03 (2010) 076; G. Giudice and A. Strumia, Nucl. Phys. B858 (2012) 63; N. Bernal, A. Djouadi, P. Slavich, JHEP 0707 (2007) 016.
40. See e.g., M. Carena et al., Nucl. Phys. B577 (2000) 88.
41. A. Djouadi et al., Phys. Lett. B435 (1998) 101; Eur. Phys. J. C1 (1998) 149; Eur. Phys. J. C1 (1998) 163; A. Arvanitaki, G. Villadoro, JHEP 02 (2012) 144; A. Delgado et al., Eur.Phys.J.C73 (2013) 2370.
42. M. Spira et al., Phys. Lett. B264 (1991) 440; Phys. Lett. B318 (1993) 347; Nucl. Phys. B453 (1995) 17; R. Harlander and W. Kilgore, Phys. Rev. D68 (2003) 013001; R. Harlander, S. Liebler and H. Mantler, Comp. Phys. Comm. 184 (2013) 1605.
43. ATLAS coll., arXiv:1307.7292; CMS coll., arXiv:1307.7135.
44. SN. Arkani-Hamed et al. arXiv:1511.06495 [hep-ph]; J. Baglio, A. Djouadi and J. Quevillon, arXiv:1511.07853 [hep-ph].
45. See e.g., J. Baglio et al., JHEP 1304 (2013) 151.
46. M. Bicer et al., arXiv:1308.6176; H. Baer et al., arXiv:1306.6352; G. Arons et al., arXiv:0709.1893; G. Weiglein et al. Phys. Rept. 426 (2006) 47; J. Aguilar-Saavedra, hep-ph/0106315; E. Accomando et al., Phys. Rept. 299 (1998) 1; A. Djouadi, Int. J. Mod. Phys. A10 (1995) 1.



6 The Symmetry of 4×4 Mass Matrices Predicted by the *Spin-charge-family* Theory — $SU(2) \times SU(2) \times U(1)$ — Remains in All Loop Corrections ^{*}

A. Hernandez-Galeana² and N.S. Mankoč Borštnik¹

¹Department of Physics, University of Ljubljana,
Jadranska 19, SI-1000 Ljubljana, Slovenia

²Departamento de Física, ESFM - Instituto Politécnico Nacional.
U. P. "Adolfo López Mateos". C. P. 07738, Ciudad de México, México

Abstract. The *spin-charge-family* theory [1–7,9–12,15–17,19–24] predicts the existence of the fourth family to the observed three. The 4×4 mass matrices — determined by the nonzero vacuum expectation values and the dynamical parts of the two scalar triplets, the gauge fields of the two groups of $\widetilde{SU}(2)$ determining family quantum numbers, as well as of the three scalar singlets with the family members quantum numbers $(\tau^\alpha = (Q, Q', Y'))$, — manifest the symmetry $\widetilde{SU}(2) \times \widetilde{SU}(2) \times U(1)$. All scalars carry the weak and the hyper charge of the *standard model* higgs field $(\pm\frac{1}{2}, \mp\frac{1}{2})$, respectively). It is demonstrated, using the massless spinor basis, that the symmetry of the 4×4 mass matrices remains $SU(2) \times SU(2) \times U(1)$ in all loop corrections, and it is discussed under which conditions this symmetry is kept under all corrections, that is with the corrections induced by the repetition of the nonzero vacuum expectation values included.

Povzetek. Teorija *spinov-nabojev-družin* [1–7,9–12,15–17,19–24] napove četrto družino k doslej opaženim trem. Masne matrike 4×4 — določajo jih dva skalarna tripleta, ki sta umeritveni polji dveh grup $\widetilde{SU}(2)$ (tripleti določajo družinska kvantna števila), ter trije skalarni singleti s kvantnimi števili družinskih članov $\tau^\alpha = (Q, Q', Y')$ vsak s svojimi neničelnimi vakuumskimi pričakovanimi vrednostmi ter kot dinamična polja — imajo simetrijo $\widetilde{SU}(2) \times \widetilde{SU}(2) \times U(1)$. Vsi skalarji — oba tripleta in vsi trije singleti — imajo enake šibke in hipernaboje kot higgsova polja v *standardnem modelu* $(\pm\frac{1}{2}, \mp\frac{1}{2})$. Avtorja pokažeta, da ostane simetrija masnih matrik 4×4 enaka $SU(2) \times SU(2) \times U(1)$ v vseh redih popravkov, ki jih določajo dinamična polja. Obravnavata pa tudi vključitev ponovitve neničelnih vakuumskih pričakovanih vrednosti v vseh redih in spremembo simetrije, ki jo te ponovitve povzročijo.

Keywords: Unifying theories, Beyond the standard model, Origin of families, Origin of mass matrices of leptons and quarks, Properties of scalar fields, The fourth

^{*} This is the part of the talk presented by N.S. Mankoč Borštnik at the 21st Workshop "What Comes Beyond the Standard Models", Bled, 23 of June to 1 of July, 2018.

family, Origin and properties of gauge bosons, Flavour symmetry, Kaluza-Klein-like theories

PACS:12.15.Ff 12.60.-i 12.90.+b 11.10.Kk 11.30.Hv 12.15.-y 12.10.-g 11.30.-j 14.80.-j

6.1 Introduction

The *spin-charge-family* theory [1–12,15–17,19–24] predicts before the electroweak break four - rather than the observed three — coupled massless families of quarks and leptons.

The 4×4 mass matrices of all the family members demonstrate in this theory the same symmetry [1,5,4,21,22], determined by the scalar fields originating in $d > (3 + 1)$: the two triplets — the gauge fields of the two $\widehat{SU}(2)$ family groups with the generators $\vec{N}_L, \vec{\tau}^1$, operating among families — and the three singlets — the gauge fields of the three charges ($\tau^\alpha = (Q, Q', Y')$) — distinguishing among family members. All these scalar fields carry the weak and the hyper charge as does the scalar higgs of the *standard model*: ($\pm \frac{1}{2}$ and $\mp \frac{1}{2}$, respectively) [1,4,24]. The loop corrections alone, as well as corrections including the repetition of the nonzero vacuum expectation values in all orders, make each matrix element of mass matrices dependent on the quantum numbers of each of the family members.

Since there is no direct observations of the fourth family quarks with masses below 1 TeV, while the fourth family quarks with masses above 1 TeV would contribute according to the *standard model* (the *standard model* Yukawa couplings of the quarks with the scalar higgs is proportional to $\frac{m_4^\alpha}{v}$, where m_4^α is the fourth family member ($\alpha = u, d$) mass and v the vacuum expectation value of the scalar higgs) to either the quark-gluon fusion production of the scalar field (the higgs) or to the scalar field decay too much in comparison with the observations, the high energy physicists do not expect the existence of the fourth family members at all [25,26].

One of the authors (N.S.M.B) discusses in Refs. ([1], Sect. 4.2.) that the *standard model* estimation with one higgs scalar might not be the right way to evaluate whether the fourth family, coupled to the observed three, does exist or not. The u_i -quarks and d_i -quarks of an i^{th} family, namely, if they couple with the opposite sign to the scalar fields carrying the family (\tilde{A}, i) quantum numbers and have the same masses, do not contribute to either the quark-gluon fusion production of the scalar fields with the family quantum numbers or to the decay of these scalars into two photons. The strong influence of the scalar fields carrying the family members quantum numbers to the masses of the lower (observed) three families manifests in the huge differences in the masses of the family members, let say u_i and d_i , $i = (1, 2, 3)$, and families (i). For the fourth family quarks, which are more and more decoupled from the observed three families the higher are their masses [22,21], the influence of the scalar fields carrying the family members quantum numbers on their masses is in the *spin-charge-family* theory expected to be much weaker. Correspondingly the u_4 and d_4 masses become closer to each other the higher are their masses and the weaker are their couplings (the mixing matrix elements) to the lower three families. For u_4 -quarks and d_4 -quarks with

the similar masses the observations might consequently not be in contradiction with the *spin-charge-family* theory prediction that there exists the fourth family coupled to the observed three ([28], which is in preparation).

But three singlet and two triplet scalar fields offer also other explanations.

We demonstrate in the main Sect. 6.2 that the symmetry $\widetilde{\text{SU}}(2) \times \widetilde{\text{SU}}(2) \times \text{U}(1)$, which the mass matrices demonstrate on the tree level, after the gauge scalar fields of the two $\widetilde{\text{SU}}(2)$ family groups triplets gain nonzero vacuum expectation values, keeps the same in all loop corrections. We discuss also the symmetry of mass matrices if all the scalar fields, contributing to mass matrices, have nonzero vacuum expectation values. We use the massless basis.

In Sect. 6.4 we present shortly the *spin-charge-family* theory and its achievements so far. All the mathematical support appears in appendices.

Let be in this introduction stressed what supports the *spin-charge-family* theory to be the right next step beyond the *standard model*. This theory can not only explain — while starting from a very simple action in $d \geq (13 + 1)$, Eqs. (6.35) in App. 6.4, with massless fermions (with the spin of the two kinds, γ^a and $\tilde{\gamma}^a$, one kind taking care of the spin and of all the charges of the family members (Eq. (6.4)), the second kind taking care of families (Eqs. (6.34, 6.50))) coupled only to the gravity (through the vielbeins and the two kinds of the spin connections fields $\omega_{ab\alpha} f^\alpha_c$ and $\tilde{\omega}_{ab\alpha} f^\alpha_c$, the gauge fields of S^{ab} and \tilde{S}^{ab} (Eqs. (6.35)), respectively — all the assumptions of the *standard model*, but also answers several open questions beyond the *standard model*. It offers the explanation for [4–6,1,7,9–12,15–17,19–24]:

- a. The appearance of all the charges of the left and right handed family members and for their families and their properties.
- b. The appearance of all the corresponding vector and scalar gauge fields and their properties (explaining the appearance of higgs and the Yukawa couplings).
- c. The appearance and properties of the dark matter.
- d. The appearance of the matter/antimatter asymmetry in the universe.

This theory predicts for the low energy regime:

- i. The existence of the fourth family to the observed three.
- ii. The existence of twice two triplets and three singlets of scalars, all with the properties of the higgs with respect to the weak and hyper charges, what explains the origin of the Yukawa couplings.
- iii. There are several other predictions, not directly connected with the topic of this paper.

The fact that the fourth family quarks have not yet been observed — directly or indirectly — pushes the fourth family quarks masses to values higher than 1 TeV.

Since the experimental accuracy of the 3×3 submatrix of the 4×4 mixing matrices is not yet high enough [32], it is not yet possible to calculate the mixing matrix elements among the fourth family and the observed three¹. Correspondingly it is not possible yet to estimate masses of the fourth family members by

¹ The 3×3 submatrix, if accurate, determines the 4×4 unitary matrix uniquely.

fitting the experimental data to the free parameters of mass matrices, the number of which is limited by the symmetry $\widetilde{\text{SU}}(2) \times \widetilde{\text{SU}}(2) \times \text{U}(1)$, predicted by the *spin-charge-family* [22,21].

If we assume the masses of the fourth family members, the matrix elements can be estimated from the measured 3×3 submatrix elements of the 4×4 matrix [22,21]².

The more effort and work is put into the *spin-charge-family* theory, the more explanations of the observed phenomena and the more predictions for the future observations follow out of it. Offering the explanation for so many observed phenomena — keeping in mind that all the explanations for the observed phenomena originate in a simple starting action — qualifies the *spin-charge-family* theory as the candidate for the next step beyond the *standard model*.

The reader is kindly asked to learn more about the *spin-charge-family* theory in Refs. [2–4,1,5,6] and the references therein. We shall point out sections in these references, which might be of particular help, when needed.

6.2 The symmetry of the family members mass matrices

The mass term $\sum_{s=7,8} \bar{\psi} \gamma^s p_{0s} \psi$, Eq. (6.3), of the starting action, Eq. (6.35), manifests in the *spin-charge-family* theory [4,1,5,6] the $\widetilde{\text{SU}}(2) \times \widetilde{\text{SU}}(2) \times \text{U}(1)$ symmetry. The infinitesimal generators of the two family groups namely commute among themselves, $\{\vec{N}_L, \vec{\tau}^i\}_- = 0$, Eq. (6.8), and with all the infinitesimal generators of the family members groups, $\{\tilde{\tau}^{Ai}, \tau^\alpha\}_- = 0$, ($\tau^\alpha = (Q, Q', Y')$), Eq. (6.9). After the scalar gauge fields, carrying the space index (7, 8), of the generators \vec{N}_L and $\vec{\tau}^i$ of the two $\widetilde{\text{SU}}(2)$ groups gain nonzero vacuum expectation values, spinors (quarks and leptons), which interact with these scalar gauge fields, become massive. There are the scalar gauge fields, carrying the space index (7, 8), of the group $\text{U}(1)$ with the infinitesimal generators $\tau^\alpha = (Q, Q', Y')$, which are responsible for the differences in mass matrices among the family members ($u^i, v^i, d^i, e^i, i(1, 2, 3, 4)$, i determines four families). Their couplings to the family members depends strongly on the quantum numbers (Q, Q', Y') .

It is shown in this main section that the mass matrix elements of any family member keep the $\widetilde{\text{SU}}(2) \times \widetilde{\text{SU}}(2) \times \text{U}(1)$ symmetry of the tree level in all corrections (the loops one and the repetition of the nonzero vacuum expectation values), provided that the scalar gauge fields of the $\text{U}(1)$ group have no nonzero vacuum expectation values. In the case that the scalar gauge fields of the $\text{U}(1)$ group have nonzero vacuum expectation values, the symmetry is changed, unless some of the scalar fields with the family quantum numbers have nonzero vacuum expectation values. We comment on all these cases in what follows.

Let us first present the symmetry of the mass term in the starting action, Eq. (6.35).

² While the fitting procedure is not influenced considerably by the accuracy of the measured masses of the lower three families, the accuracy of the measured values of the mixing matrices do influence, as expected, the fitting results very much.

We point out that the symmetry $\widetilde{\text{SU}}(2) \times \widetilde{\text{SU}}(2)$ belongs to the two $\widetilde{\text{SO}}(4)$ groups — to $\widetilde{\text{SO}}(4)_{\widetilde{\text{SO}}(3,1)}$ and to $\widetilde{\text{SO}}(4)_{\widetilde{\text{SO}}(4)}$. The infinitesimal operators of the first and the second $\widetilde{\text{SO}}(4)$ groups are, Eqs. (6.40, 6.41),

$$\begin{aligned}\vec{N}_+ (= \vec{N}_L) &:= \frac{1}{2}(\tilde{S}^{23} + i\tilde{S}^{01}, \tilde{S}^{31} + i\tilde{S}^{02}, \tilde{S}^{12} + i\tilde{S}^{03}), \\ \vec{\tau}^1 &:= \frac{1}{2}(\tilde{S}^{58} - \tilde{S}^{67}, \tilde{S}^{57} + \tilde{S}^{68}, \tilde{S}^{56} - \tilde{S}^{78}),\end{aligned}\quad (6.1)$$

respectively. $\text{U}(1)$ contains the subgroup of the subgroup $\text{SO}(6)$ as well as the subgroup of $\text{SO}(4)$ ($\text{SO}(6)$ and $\text{SO}(4)$ are together with $\text{SO}(3, 1)$ the subgroups of the group $\text{SO}(13, 1)$) with the infinitesimal operators equal to, Eq. (6.42),

$$\begin{aligned}\tau^4 &= -\frac{1}{3}(S^{9\ 10} + S^{11\ 12} + S^{13\ 14}), \\ \vec{\tau}^1 &= \frac{1}{2}(S^{58} - S^{67}, S^{57} + S^{68}, S^{56} - S^{78}), \\ \vec{\tau}^2 &= \frac{1}{2}(S^{58} + S^{67}, S^{57} - S^{68}, S^{56} + S^{78}).\end{aligned}\quad (6.2)$$

There are additional subgroups $\widetilde{\text{SU}}(2) \times \widetilde{\text{SU}}(2)$, which belong to $\widetilde{\text{SO}}(4)_{\widetilde{\text{SO}}(3,1)}$ and $\widetilde{\text{SO}}(4)_{\widetilde{\text{SO}}(4)}$, Eqs. (6.40, 6.41), the scalar gauge fields of which do not influence the masses of the four families to which the three observed families belong according to the predictions of the *spin-charge-family* theory³.

All the degrees of freedom and properties of spinors (of quarks and leptons) and of gauge fields, demonstrated below, follow from the simple starting action, Eq. (6.35), after breaking the starting symmetry.

Let us rewrite formally the fermion part of the starting action, Eq. (6.35), in the way that it manifests, Eq. (6.3), the kinetic and the interaction term in $d = (3 + 1)$ (the first line, $m = (0, 1, 2, 3)$), the mass term (the second line, $s = (7, 8)$) and the rest (the third line, $t = (5, 6, 9, 10, \dots, 14)$).

$$\begin{aligned}\mathcal{L}_f &= \bar{\Psi}\gamma^m(p_m - \sum_{A,i} g^{Ai}\tau^{Ai}A_m^{Ai})\Psi + \\ &\quad \{ \sum_{s=7,8} \bar{\Psi}\gamma^s p_{0s} \Psi \} + \\ &\quad \{ \sum_{t=5,6,9,\dots,14} \bar{\Psi}\gamma^t p_{0t} \Psi \},\end{aligned}\quad (6.3)$$

where $p_{0s} = p_s - \frac{1}{2}S^{s's''}\omega_{s's''s} - \frac{1}{2}\tilde{S}^{ab}\tilde{\omega}_{abs}$, $p_{0t} = p_t - \frac{1}{2}S^{t't''}\omega_{t't''t} - \frac{1}{2}\tilde{S}^{ab}\tilde{\omega}_{abt}$ ⁴, with $m \in (0, 1, 2, 3)$, $s \in (7, 8)$, $(s', s'') \in (5, 6, 7, 8)$, (a, b) (appearing in \tilde{S}^{ab})

³ The gauge scalar fields of these additional subgroups $\widetilde{\text{SU}}(2) \times \widetilde{\text{SU}}(2)$ influence the masses of the upper four families, the stable one of which contribute to the dark matter.

⁴ If there are no fermions present, then either ω_{abc} or $\tilde{\omega}_{abc}$ are expressible by vielbeins f^α_a [[2,5], and the references therein]. We assume that there are spinor fields which determine spin connection fields — ω_{abc} and $\tilde{\omega}_{abc}$. In general one would have [6]: $p_{0a} = f^\alpha_a p_{0\alpha} + \frac{1}{2E}\{p_\alpha, E f^\alpha_a\}_-$, $p_{0\alpha} = p_\alpha - \frac{1}{2}S^{s's''}\omega_{s's''\alpha} - \frac{1}{2}\tilde{S}^{ab}\tilde{\omega}_{ab\alpha}$. Since the term $\frac{1}{2E}\{p_\alpha, E f^\alpha_a\}_-$ does not influence the symmetry of mass matrices, we do not treat it in this paper.

run within either $(0, 1, 2, 3)$ or $(5, 6, 7, 8)$, t runs $\in (5, \dots, 14)$, (t', t'') run either $\in (5, 6, 7, 8)$ or $\in (9, 10, \dots, 14)$ ⁵. The spinor function ψ represents all family members, presented on Table 6.3, of all the $2^{\frac{7+1}{2}-1} = 8$ families, presented on Table 6.4. In this paper we pay attention on the lower four families.

The first line of Eq. (6.3) determines in $d = (3+1)$ the kinematics and dynamics of spinor (fermion) fields, coupled to the vector gauge fields. The generators $\tau^{\Lambda i}$ of the charge groups are expressible in terms of S^{ab} through the complex coefficients $c^{\Lambda i}_{ab}$ (the coefficients $c^{\Lambda i}_{ab}$ of $\tau^{\Lambda i}$ can be found in Eqs. (6.38, 6.2)⁶,

$$\tau^{\Lambda i} = \sum_{a,b} c^{\Lambda i}_{ab} S^{ab}, \quad (6.4)$$

fulfilling the commutation relations

$$\{\tau^{\Lambda i}, \tau^{Bj}\}_{-} = i\delta^{\Lambda B} f^{\Lambda ijk} \tau^{\Lambda k}. \quad (6.5)$$

They represent the colour (τ^{3i}), the weak (τ^{1i}) and the hyper (Y) charges⁷. The corresponding vector gauge fields $A_m^{\Lambda i}$ are expressible with the spin connection fields ω_{stm} , Eq. (6.44)⁸

$$A_m^{\Lambda i} = \sum_{s,t} c^{\Lambda i}_{st} \omega^{st}_m. \quad (6.6)$$

The second line of Eq. (6.3) determines masses of each family member (u^i, d^i, v^i, e^i). The scalar gauge fields of the charges — those of the family members, determined by S^{ab} and those of the families, determined by \tilde{S}^{ab} — carry space index s (7, 8). Correspondingly the operators $\gamma^0 \gamma^s$, appearing in the mass term, transform the left handed members of any family into the right handed members of the same family, what can easily be seen in Table 6.3. Operators S^{ab} transform one family member of a particular family into the same family member of another family.

Each scalar gauge fields (they are the gauge fields with space index $s \geq 5$) are as well expressible with the spin connections and vielbeins, Eq. (6.45) [2].

The groups $SO(3, 1)$, $SU(3)$, $SU(2)_I$, $SU(2)_{II}$ and $U(1)_{II}$ (all embedded into $SO(13 + 1)$) determine spin and charges of spinors, the groups $\widetilde{SU}(2)_{\widetilde{SO}(3,1)'}$,

⁵ We use units $\hbar = 1 = c$

⁶ Before the electroweak break there are the conserved (weak) charges $\vec{\tau}^1$ (Eq. (6.38)), $\vec{\tau}^3$ (Eq. (6.2) and $Y := \tau^4 + \tau^{23}$ (Eqs. (6.38, 6.2) and the non conserved charge $Y' := -\tau^4 \tan^2 \vartheta_2 + \tau^{23}$, where ϑ_2 is the angle of the break of $SU(2)_{II}$ from $SU(2)_I \times SU(2)_{II} \times U(1)_{II}$ to $SU(2)_I \times U(1)_I$. After the electroweak break the conserved charges are $\vec{\tau}^3$ and $Q := Y + \tau^{13}$, the non conserved charge is $Q' := -Y \tan^2 \vartheta_1 + \tau^{13}$, where ϑ_1 is the electroweak angle.

⁷ There are as well the $SU(2)_{II}$ (τ^{2i} , Eq. (6.38)) and $U(1)_{II}$ (τ^4 , Eq. (6.2)) charges, the vector gauge fields of these last two groups gain masses when interacting with the condensate, Table 6.5 ([1,4,5] and the references therein). The condensate leaves massless, besides the colour and gravity gauge fields in $d = (3 + 1)$, the weak and the hyper charge vector gauge fields.

⁸ Both fields, $A_m^{\Lambda i}$ and $\tilde{A}_m^{\Lambda i}$, are expressible with only the vielbeins, if there are no spinor fields present [2].

Eqs (6.1), $\widetilde{SU}(2)_{\widetilde{SO}(4)}$, Eqs. (6.1), (embedded into $\widetilde{SO}(13+1)$) determine family quantum numbers⁹.

The generators of these latter groups are expressible by \tilde{S}^{ab}

$$\tilde{\tau}^{Ai} = \sum_{a,b} c^{Ai}_{ab} \tilde{S}^{ab}, \quad (6.7)$$

fulfilling again the commutation relations

$$\{\tilde{\tau}^{Ai}, \tilde{\tau}^{Bj}\}_{-} = i\delta^{AB} f^{Aijk} \tilde{\tau}^{Ak}, \quad (6.8)$$

while

$$\{\tau^{Ai}, \tilde{\tau}^{Bj}\}_{-} = 0. \quad (6.9)$$

The scalar gauge fields of the groups $\widetilde{SU}(2)_I (= \widetilde{SU}(2)_{\widetilde{SO}(3,1)}$ with generators \vec{N}_L , Eq. (6.40)), $\widetilde{SU}(2)_I (= \widetilde{SU}(2)_{\widetilde{SO}(4)}$, with generators $\vec{\tau}^I$, Eq. (6.41)) and $U(1)$ (with generators (Q, Q', Y') , Eq. (6.43)) are presented in Eq. (6.45)¹⁰. The application of the generators $\vec{\tau}^I$, Eq. (6.41), \vec{N}_L , Eq. (6.40), which distinguish among families and are the same for all the family members, is presented in Eqs. (6.49, 6.51, 6.13).

The application of the family members generators (Q, Q', Y') on the family members of any family is presented on Table 6.1. The contribution of the scalar gauge fields to masses of different family members strongly depends on the quantum numbers Q, Q' and Y' as one can read from Table 6.1. In loop corrections the contribution of the scalar gauge fields of (Q, Q', Y') is proportional to the even power of these quantum numbers, while the nonzero vacuum expectation values of these scalar fields contribute in odd powers.

R	$Q_{L,R}$	Y	$\tau^4_{L,R}$	τ^{23}	Y'	Q'	L	Y	τ^{13}	Y'	Q'
$u^i_{L,R}$	$\frac{2}{3}$	$\frac{2}{3}$	$\frac{1}{6}$	$\frac{1}{2}$	$\frac{1}{2}(1 - \frac{1}{3}\tan^2\vartheta_2)$	$-\frac{2}{3}\tan^2\vartheta_1$	$u^i_{L,R}$	$\frac{1}{6}$	$\frac{1}{2}$	$-\frac{1}{6}\tan^2\vartheta_2$	$\frac{1}{2}(1 - \frac{1}{3}\tan^2\vartheta_1)$
$d^i_{L,R}$	$-\frac{1}{3}$	$-\frac{1}{3}$	$-\frac{1}{6}$	$-\frac{1}{2}$	$-\frac{1}{2}(1 + \frac{1}{3}\tan^2\vartheta_2)$	$\frac{1}{3}\tan^2\vartheta_1$	$d^i_{L,R}$	$-\frac{1}{6}$	$-\frac{1}{2}$	$-\frac{1}{6}\tan^2\vartheta_2$	$-\frac{1}{2}(1 + \frac{1}{3}\tan^2\vartheta_1)$
$\nu^i_{L,R}$	0	0	$\frac{1}{6}$	$\frac{1}{2}$	$\frac{1}{2}(1 + \tan^2\vartheta_2)$	0	$\nu^i_{L,R}$	$\frac{1}{6}$	$\frac{1}{2}$	$\frac{1}{6}\tan^2\vartheta_2$	$\frac{1}{2}(1 + \tan^2\vartheta_1)$
$e^i_{L,R}$	-1	-1	$-\frac{1}{6}$	$-\frac{1}{2}$	$\frac{1}{2}(-1 + \tan^2\vartheta_2)$	$\tan^2\vartheta_1$	$e^i_{L,R}$	$-\frac{1}{6}$	$-\frac{1}{2}$	$\frac{1}{6}\tan^2\vartheta_2$	$-\frac{1}{2}(1 - \tan^2\vartheta_1)$

Table 6.1. The quantum numbers $Q, Y, \tau^4, Y', Q', \tau^{23}, \tau^{13}$, Eq. (6.43), of the family members $u^i_{L,R}, \nu^i_{L,R}$ of one family (any one) [6] are presented. The left and right handed members of any family have the same Q and τ^4 , the right handed members have $\tau^{13} = 0$, and $\tau^{23} = \frac{1}{2}$ for (u^i_R, ν^i_R) and $-\frac{1}{2}$ for (d^i_R, e^i_R) , while the left handed members have $\tau^{23} = 0$ and $\tau^{13} = \frac{1}{2}$ for (u^i_L, ν^i_L) and $-\frac{1}{2}$ for (d^i_L, e^i_L) . ν^i_R couples only to $A_s^{Y'}$ as seen from the table.

⁹ $\widetilde{SU}(3)$ do not contribute to the families at low energies. We studied such possibilities in a toy model, Ref. [18].

¹⁰ All the scalar gauge fields, presented in Eq. (6.45), are expressible with the vielbeins and spin connections with the space index $a \geq 5$, Ref. [2].

There are in the *spin-charge-family* theory $2^{\frac{(1+7)}{2}-1} = 8$ families¹¹, which split in two groups of four families, due to the break of the symmetry from $\widetilde{SO}(7, 1)$ into $\widetilde{SO}(3, 1) \times \widetilde{SO}(4)$. Each of these two groups manifests $\widetilde{SU}(2)_{\widetilde{SO}(3,1)} \times \widetilde{SU}(2)_{\widetilde{SO}(4)}$ symmetry [6]. These decoupled twice four families are presented in Table 6.4.

The lowest of the upper four families, forming neutral clusters with respect to the electromagnetic and colour charges, is the candidate to form the dark matter [20].

We discuss in this paper symmetry properties of the lower four families, presented in Table 6.4 in the first four lines. We present in Table 6.2 the representation and the family quantum numbers of the left and right handed members of the lower four families. Since any of the family members ($u_{L,R}^i, d_{L,R}^i, \nu_{L,R}^i, e_{L,R}^i$) behave equivalently with respect to all the operators concerning the family groups $\widetilde{SU}(2)_{\widetilde{SO}(1,3)} \times \widetilde{SU}(2)_{\widetilde{SO}(4)}$, the last five columns are the same for all the family members.

We rewrite the interaction, which is in the *spin-charge-family* theory responsible for the appearance of masses of fermions, presented in Eq. (6.3) in the second line, in a slightly different way, expressing $\gamma^7 = (\overset{78}{+}) + (\overset{78}{-})$ and correspondingly $\gamma^8 = -i((\overset{78}{+}) - (\overset{78}{-}))$.

$$\begin{aligned} \mathcal{L}_{\text{mass}} &= \frac{1}{2} \sum_{+,-} \{ \psi_L^\dagger \gamma^0 (\pm) \left(- \sum_A \tau^\alpha A_\pm^\alpha - \sum_{\tilde{A}i} \tilde{\tau}^{\tilde{A}i} \tilde{A}_\pm^{\tilde{A}i} \right) \psi_R \} + \text{h.c.}, \\ \tau^\alpha &= (Q, Q', Y'), \quad \tilde{\tau}^{\tilde{A}i} = (\vec{N}_L, \vec{\tau}^i), \\ \gamma^0 (\pm) &= \gamma^0 \frac{1}{2} (\gamma^7 \pm i \gamma^8), \\ A_\pm^\alpha &= \sum_{st} c_{st}^\alpha \omega^{st}_\pm, \quad \omega^{st}_\pm = \omega^{st}_7 \mp i \omega^{st}_8, \\ \tilde{A}_\pm^{\tilde{A}i} &= \sum_{ab} c_{ab}^{\tilde{A}i} \tilde{\omega}^{ab}_\pm, \quad \tilde{\omega}^{ab}_\pm = \tilde{\omega}^{ab}_7 \mp i \tilde{\omega}^{ab}_8. \end{aligned} \quad (6.10)$$

In Eq. (6.10) the term p_s is left out since at low energies its contribution is negligible, A determines operators, which distinguish among family members — (Q, Q', Y') ¹², their eigenvalues on basic states are presented on Table 6.1 — (\tilde{A}, i) represent the family operators, determined in Eqs. (6.40, 6.41, 6.42). The detailed explanation can be found in Refs. [4,5,1].

Operators $\tau^{\tilde{A}i}$ are Hermitian $((\tau^{\tilde{A}i})^\dagger = \tau^{\tilde{A}i})$, while $(\gamma^0 (\pm))^\dagger = \gamma^0 (\mp)$. If the scalar fields $A_s^{\tilde{A}i}$ are real it follows that $(A_\pm^{\tilde{A}i})^\dagger = A_\mp^{\tilde{A}i}$.

¹¹ In the break from $SO(13, 1)$ to $SO(7, 1) \times SO(6)$ only eight families remain massless, those for which the symmetry $\widetilde{SO}(7, 1)$ remains. In Ref. [18] such kinds of breaks are discussed for a toy model.

¹² (Q, Q', Y') are expressible in terms of $(\tau^{13}, \tau^{23}, \tau^4)$ as explained in Eq. (6.43). The corresponding superposition of $\omega^{ss'}_\pm$ fields can be found by taking into account Eqs. (6.38, 6.2).

While the family operators $\tilde{\tau}^{1i}$ and \tilde{N}_L^i commute with $\gamma^0 (\pm)$, $\{S^{ab}, \tilde{S}^{cd}\}_- = 0$ for all (a, b, c, d) , the family members operators (τ^{13}, τ^{23}) do not, since S^{78} does not ($S^{78}\gamma^0 (\mp) = -\gamma^0 (\mp) S^{78}$). However $[\psi_L^{k\dagger}\gamma^0 (\mp)]^{78} (Q, Q', Y') A_{\mp}^{(Q, Q', Y')} \psi_R^l]^\dagger = \psi_R^{l\dagger} (Q, Q', Y') A_{\pm}^{(Q, Q', Y')\dagger} \gamma^0 (\pm) \psi_L^k \delta_{k,l} = \psi_R^{l\dagger} (Q_R^k, Q_R^{k'}, Y_R^{k'}) A_{\pm}^{(Q, Q', Y')} \psi_R^k \delta_{k,l}$, where $(Q_R^k, Q_R^{k'}, Y_R^{k'})$ denote the eigenvalues of the corresponding operators on the spinor state ψ_R^k . This means that we evaluate in both cases quantum numbers of the right handed partners.

But, let us evaluate $\frac{1}{\sqrt{2}} < u_L^i + u_R^i | \hat{O}^\alpha | u_L^i + u_R^i > \frac{1}{\sqrt{2}}$, with $\hat{O}^\alpha = \sum_{+,-} \gamma^0 (\pm)$ ($\tau^4 A_{\mp}^{78} + \tau^{23} A_{\mp}^{23} + \tau^{13} A_{\mp}^{13}$). One obtains $\frac{1}{\sqrt{2}} \{ \frac{1}{6} (A_-^4 + A_+^4) + A_-^{23} + A_+^{13} \}$. Equivalent evaluations for $|d_L^i + d_R^i >$ would give $\frac{1}{\sqrt{2}} \{ \frac{1}{6} (A_-^4 + A_+^4) - A_-^{23} - A_+^{13} \}$, while for neutrinos we would obtain $\frac{1}{\sqrt{2}} \{ -\frac{1}{2} (A_-^4 + A_+^4) + A_-^{23} + A_+^{13} \}$ and for e^i we would obtain $\frac{1}{\sqrt{2}} \{ -\frac{1}{2} (A_-^4 + A_+^4) - A_-^{23} - A_+^{13} \}$. Let us point out that the fields include also coupling constants, which change when the symmetry is broken. This means that we must carefully evaluate expectation values of all the operators on each state of broken symmetries. We have here much easier work: To see how does the starting symmetry of the mass matrices behave under all possible corrections up to ∞ we only have to compare how do matrix elements, which are equal on the tree level, change in any order of corrections.

In Table 6.2 four families of spinors, belonging to the group with the nonzero values of \tilde{N}_L and $\tilde{\tau}^1$, are presented. These are the lower four families, presented also in Table 6.4 together with the upper four families¹³. There are indeed the four families of $\psi_{u_R}^i$ and $\psi_{u_L}^i$ presented in this table. All the $2^{\frac{13+1}{2}-1}$ members of the first family are represented in Table 6.3.

The three singlet scalar fields $(A_{\mp}^Q, A_{\mp}^{Q'}, A_{\mp}^{Y'})$ of Eq. (6.10) contribute on the tree level the "diagonal" values to the mass term $-\gamma^0 (\mp) Q A_{\mp}^Q + \gamma^0 (\mp) Q' A_{\mp}^{Q'} + \gamma^0 (\mp) Y' A_{\mp}^{Y'}$ — transforming a right handed member of one family into the left handed member of the same family, or a left handed member of one family into the right handed member of the same family. *These terms are different for different family members but the same for all the families.*

Since $Q = (\tau^{13} + \tau^{23} + \tau^4) = (S^{56} + \tau^4)$, $Y' = (-\tau^4 \tan^2 \vartheta_2 + \tau^{23})$ and $Q' = (-\tau^4 + \tau^{23}) \tan^2 \vartheta_1 + \tau^{13}$ — ϑ_1 is the *standard model* angle and ϑ_2 is the corresponding angle when the second SU(2) symmetry breaks — we could use instead of the operators $(\gamma^0 (\mp) Q A_{\mp}^Q + \gamma^0 (\mp) Q' A_{\mp}^{Q'} + \gamma^0 (\mp) Y' A_{\mp}^{Y'})$ as well the operators $(\gamma^0 (\pm) \tau^4 A_{\pm}^4, \gamma^0 (\pm) \tau^{23} A_{\pm}^{23}, \gamma^0 (\pm) \tau^{13} A_{\pm}^{13})$, if the fact that the coupling constants of all the fields, also of ω_{abs} and $\tilde{\omega}_{abs}$, change with the break of symmetry is taken into account.

¹³ The upper four families have the nonzero values of \tilde{N}_R and $\tilde{\tau}^2$. The stable members of the upper four families offer the explanation for the existence the dark matter [20].

Let us denote by $-a^\alpha$ the nonzero vacuum expectation values of the three singlets for a family member $\alpha = (u^i, v^i, d^i, e^i)$, divided by the energy scale (let say TeV), when (if) these scalars have nonzero vacuum expectation values and we use the basis $\frac{1}{2}|\psi_L^{i\alpha} + \psi_R^{i\alpha}\rangle$:

$$a^\alpha = -\left\{\frac{1}{2} \langle \psi_L^{i\alpha} + \psi_R^{i\alpha} | \right. \\ \left. \sum_{+, -} \gamma^0 (\pm) [Q \langle A_{\pm}^Q \rangle + Q' \langle A_{\pm}^{Q'} \rangle + Y' \langle A_{\pm}^{Y'} \rangle] |\psi_L^{i\alpha} + \psi_R^{i\alpha} \rangle \frac{1}{2}\right\} \delta^{ij} + \text{h.c.}, \quad (6.11)$$

Each family member has a different value for a^α . All the scalar gauge fields $A_{78}^Q, A_{78}^{Q'}, A_{78}^{Y'}$ have the weak and the hypercharge as higgs scalars: $(\pm\frac{1}{2}, \mp\frac{1}{2}, (\pm), (\pm), (\pm))$ respectively).

				$\tilde{\tau}^{13}$	$\tilde{\tau}^{23}$	\tilde{N}_L^3	\tilde{N}_R^3	$\tilde{\tau}^4$
$\psi_{u_R^i}^1$	$\begin{smallmatrix} 03 & 12 & 56 & 78 \\ (+i) & (+) & (+) & (+) \end{smallmatrix} \parallel \dots$	$\psi_{u_L^i}^1$	$\begin{smallmatrix} 03 & 12 & 56 & 78 \\ [-i] & (+) & (+) & (-) \end{smallmatrix} \parallel \dots$	$-\frac{1}{2}$	0	$-\frac{1}{2}$	0	$-\frac{1}{2}$
$\psi_{u_R^i}^2$	$\begin{smallmatrix} 03 & 12 & 56 & 78 \\ [+i] & (+) & (+) & (+) \end{smallmatrix} \parallel \dots$	$\psi_{u_L^i}^2$	$\begin{smallmatrix} 03 & 12 & 56 & 78 \\ (-i) & (+) & (+) & (-) \end{smallmatrix} \parallel \dots$	$-\frac{1}{2}$	0	$\frac{1}{2}$	0	$-\frac{1}{2}$
$\psi_{u_R^i}^3$	$\begin{smallmatrix} 03 & 12 & 56 & 78 \\ (+i) & (+) & (+) & (+) \end{smallmatrix} \parallel \dots$	$\psi_{u_L^i}^3$	$\begin{smallmatrix} 03 & 12 & 56 & 78 \\ [-i] & (+) & (+) & (-) \end{smallmatrix} \parallel \dots$	$\frac{1}{2}$	0	$-\frac{1}{2}$	0	$-\frac{1}{2}$
$\psi_{u_R^i}^4$	$\begin{smallmatrix} 03 & 12 & 56 & 78 \\ [+i] & (+) & (+) & (+) \end{smallmatrix} \parallel \dots$	$\psi_{u_L^i}^4$	$\begin{smallmatrix} 03 & 12 & 56 & 78 \\ (-i) & (+) & (+) & (-) \end{smallmatrix} \parallel \dots$	$\frac{1}{2}$	0	$\frac{1}{2}$	0	$-\frac{1}{2}$

Table 6.2. Four families of the right handed u_R^{c1} with the weak and the hyper charge ($\tau^{13} = 0, Y = \frac{2}{3}$) and of the left handed u_L^{c1} quarks with ($\tau^{13} = \frac{1}{2}, Y = \frac{1}{6}$), both with spin $\frac{1}{2}$ and colour $(\tau^{33}, \tau^{38}) = [(1/2, 1/(2\sqrt{3})), (-1/2, 1/(2\sqrt{3})), (0, -1/(\sqrt{3}))]$ charges are presented. They represent two of the family members from Table 6.3 — u_R^{c1} and u_L^{c1} — appearing on 1st and 7th line of Table 6.3. Spins and charges commute with $\tilde{N}_L^i, \tilde{\tau}^{1i}$ and $\tilde{\tau}^4$, and are correspondingly the same for all the families.

Transitions among families for any family member are caused by $(\tilde{N}_L^i \tilde{A}^{\tilde{N}_L^i})$ and $\tilde{\tau}^{1i} \tilde{A}^{\tilde{\tau}^{1i}}$, what manifests the symmetry $\widetilde{SU}_{N_L}(2) \times \widetilde{SU}_{\tau^1}(2)$. There are corrections in all orders, which make all the matrix elements of the mass matrix for any of the family members α dependent on the three singlets $(\tau^4 A_{\pm}^4, \tau^{23} A_{\pm}^{23}, \tau^{13} A_{\pm}^{13})$, Eq. (6.11).

[illegible]

Continued on next page

i	$ \alpha \psi_i\rangle$ (Anti)octet, $\Gamma(7,1) = (-1)1, \Gamma(6) = (1) - 1$ of (anti)quarks and (anti)leptons	$\Gamma(3,1)$	S^{12}	τ^{13}	τ^{23}	τ^{33}	τ^{38}	τ^4	Y	Q
40	\bar{u}_R^1 $\begin{smallmatrix} 03 & 12 & 56 & 78 \\ [-i] & (-) & (+) & (+) \end{smallmatrix} \parallel \begin{smallmatrix} 9 & 10 & 11 & 12 \\ (-) & (+) & (+) & (+) \end{smallmatrix}$	1	$-\frac{1}{2}$	$-\frac{1}{2}$	0	$-\frac{1}{2}$	$-\frac{1}{2\sqrt{3}}$	$-\frac{1}{6}$	$-\frac{1}{6}$	$-\frac{2}{3}$
41	\bar{d}_L^2 $\begin{smallmatrix} 03 & 12 & 56 & 78 \\ [-i] & (+) & (+) & (+) \end{smallmatrix} \parallel \begin{smallmatrix} 9 & 10 & 11 & 12 \\ (-) & (+) & (+) & (+) \end{smallmatrix}$	-1	$\frac{1}{2}$	0	$\frac{1}{2}$	$\frac{1}{2}$	$-\frac{1}{2\sqrt{3}}$	$-\frac{1}{6}$	$\frac{1}{3}$	$\frac{1}{3}$
42	\bar{d}_L^2 $\begin{smallmatrix} 03 & 12 & 56 & 78 \\ (+i) & (-) & (+) & (+) \end{smallmatrix} \parallel \begin{smallmatrix} 9 & 10 & 11 & 12 \\ (-) & (+) & (+) & (+) \end{smallmatrix}$	-1	$-\frac{1}{2}$	0	$\frac{1}{2}$	$\frac{1}{2}$	$-\frac{1}{2\sqrt{3}}$	$-\frac{1}{6}$	$\frac{1}{3}$	$\frac{1}{3}$
43	\bar{u}_L^2 $\begin{smallmatrix} 03 & 12 & 56 & 78 \\ [-i] & (+) & (-) & (-) \end{smallmatrix} \parallel \begin{smallmatrix} 9 & 10 & 11 & 12 \\ (+) & (-) & (-) & (-) \end{smallmatrix}$	-1	$\frac{1}{2}$	0	$-\frac{1}{2}$	$\frac{1}{2}$	$-\frac{1}{2\sqrt{3}}$	$-\frac{1}{6}$	$-\frac{2}{3}$	$-\frac{2}{3}$
44	\bar{u}_L^2 $\begin{smallmatrix} 03 & 12 & 56 & 78 \\ (+i) & (-) & (-) & (-) \end{smallmatrix} \parallel \begin{smallmatrix} 9 & 10 & 11 & 12 \\ (+) & (-) & (-) & (-) \end{smallmatrix}$	-1	$-\frac{1}{2}$	0	$-\frac{1}{2}$	$\frac{1}{2}$	$-\frac{1}{2\sqrt{3}}$	$-\frac{1}{6}$	$-\frac{2}{3}$	$-\frac{2}{3}$
45	\bar{d}_R^2 $\begin{smallmatrix} 03 & 12 & 56 & 78 \\ (+i) & (+) & (+) & (-) \end{smallmatrix} \parallel \begin{smallmatrix} 9 & 10 & 11 & 12 \\ (+) & (-) & (-) & (+) \end{smallmatrix}$	1	$\frac{1}{2}$	$\frac{1}{2}$	0	$\frac{1}{2}$	$-\frac{1}{2\sqrt{3}}$	$-\frac{1}{6}$	$-\frac{1}{6}$	$\frac{1}{3}$
46	\bar{d}_R^2 $\begin{smallmatrix} 03 & 12 & 56 & 78 \\ (-i) & (-) & (+) & (-) \end{smallmatrix} \parallel \begin{smallmatrix} 9 & 10 & 11 & 12 \\ (-) & (+) & (-) & (+) \end{smallmatrix}$	1	$-\frac{1}{2}$	$\frac{1}{2}$	0	$\frac{1}{2}$	$-\frac{1}{2\sqrt{3}}$	$-\frac{1}{6}$	$-\frac{1}{6}$	$\frac{1}{3}$
47	\bar{u}_R^2 $\begin{smallmatrix} 03 & 12 & 56 & 78 \\ (+i) & (+) & (-) & (+) \end{smallmatrix} \parallel \begin{smallmatrix} 9 & 10 & 11 & 12 \\ (+) & (-) & (+) & (-) \end{smallmatrix}$	1	$\frac{1}{2}$	$-\frac{1}{2}$	0	$\frac{1}{2}$	$-\frac{1}{2\sqrt{3}}$	$-\frac{1}{6}$	$-\frac{1}{6}$	$-\frac{2}{3}$
48	\bar{u}_R^2 $\begin{smallmatrix} 03 & 12 & 56 & 78 \\ (-i) & (-) & (+) & (+) \end{smallmatrix} \parallel \begin{smallmatrix} 9 & 10 & 11 & 12 \\ (-) & (+) & (+) & (-) \end{smallmatrix}$	1	$-\frac{1}{2}$	$-\frac{1}{2}$	0	$\frac{1}{2}$	$-\frac{1}{2\sqrt{3}}$	$-\frac{1}{6}$	$-\frac{1}{6}$	$-\frac{2}{3}$
49	\bar{d}_L^3 $\begin{smallmatrix} 03 & 12 & 56 & 78 \\ [-i] & (+) & (+) & (+) \end{smallmatrix} \parallel \begin{smallmatrix} 9 & 10 & 11 & 12 \\ (+) & (+) & (-) & (-) \end{smallmatrix}$	-1	$\frac{1}{2}$	0	$\frac{1}{2}$	0	$\frac{1}{\sqrt{3}}$	$-\frac{1}{6}$	$\frac{1}{3}$	$\frac{1}{3}$
50	\bar{d}_L^3 $\begin{smallmatrix} 03 & 12 & 56 & 78 \\ (+i) & (-) & (+) & (+) \end{smallmatrix} \parallel \begin{smallmatrix} 9 & 10 & 11 & 12 \\ (+) & (+) & (-) & (-) \end{smallmatrix}$	-1	$-\frac{1}{2}$	0	$\frac{1}{2}$	0	$\frac{1}{\sqrt{3}}$	$-\frac{1}{6}$	$\frac{1}{3}$	$\frac{1}{3}$
51	\bar{u}_L^3 $\begin{smallmatrix} 03 & 12 & 56 & 78 \\ [-i] & (+) & (-) & (-) \end{smallmatrix} \parallel \begin{smallmatrix} 9 & 10 & 11 & 12 \\ (+) & (+) & (-) & (-) \end{smallmatrix}$	-1	$\frac{1}{2}$	0	$-\frac{1}{2}$	0	$\frac{1}{\sqrt{3}}$	$-\frac{1}{6}$	$-\frac{2}{3}$	$-\frac{2}{3}$
52	\bar{u}_L^3 $\begin{smallmatrix} 03 & 12 & 56 & 78 \\ (+i) & (-) & (-) & (-) \end{smallmatrix} \parallel \begin{smallmatrix} 9 & 10 & 11 & 12 \\ (+) & (-) & (-) & (-) \end{smallmatrix}$	-1	$-\frac{1}{2}$	0	$-\frac{1}{2}$	0	$\frac{1}{\sqrt{3}}$	$-\frac{1}{6}$	$-\frac{2}{3}$	$-\frac{2}{3}$
53	\bar{d}_R^3 $\begin{smallmatrix} 03 & 12 & 56 & 78 \\ (+i) & (+) & (+) & (-) \end{smallmatrix} \parallel \begin{smallmatrix} 9 & 10 & 11 & 12 \\ (+) & (-) & (-) & (+) \end{smallmatrix}$	1	$\frac{1}{2}$	$\frac{1}{2}$	0	0	$\frac{1}{\sqrt{3}}$	$-\frac{1}{6}$	$-\frac{1}{6}$	$\frac{1}{3}$
54	\bar{d}_R^3 $\begin{smallmatrix} 03 & 12 & 56 & 78 \\ (-i) & (-) & (+) & (-) \end{smallmatrix} \parallel \begin{smallmatrix} 9 & 10 & 11 & 12 \\ (-) & (+) & (-) & (+) \end{smallmatrix}$	1	$-\frac{1}{2}$	$\frac{1}{2}$	0	0	$\frac{1}{\sqrt{3}}$	$-\frac{1}{6}$	$-\frac{1}{6}$	$\frac{1}{3}$
55	\bar{u}_R^3 $\begin{smallmatrix} 03 & 12 & 56 & 78 \\ (+i) & (+) & (-) & (+) \end{smallmatrix} \parallel \begin{smallmatrix} 9 & 10 & 11 & 12 \\ (+) & (-) & (+) & (-) \end{smallmatrix}$	1	$\frac{1}{2}$	$-\frac{1}{2}$	0	0	$\frac{1}{\sqrt{3}}$	$-\frac{1}{6}$	$-\frac{1}{6}$	$-\frac{2}{3}$
56	\bar{u}_R^3 $\begin{smallmatrix} 03 & 12 & 56 & 78 \\ (-i) & (-) & (+) & (+) \end{smallmatrix} \parallel \begin{smallmatrix} 9 & 10 & 11 & 12 \\ (-) & (+) & (+) & (-) \end{smallmatrix}$	1	$-\frac{1}{2}$	$-\frac{1}{2}$	0	0	$\frac{1}{\sqrt{3}}$	$-\frac{1}{6}$	$-\frac{1}{6}$	$-\frac{2}{3}$
57	\bar{e}_L $\begin{smallmatrix} 03 & 12 & 56 & 78 \\ [-i] & (+) & (+) & (+) \end{smallmatrix} \parallel \begin{smallmatrix} 9 & 10 & 11 & 12 \\ (-) & (-) & (-) & (-) \end{smallmatrix}$	-1	$\frac{1}{2}$	0	$\frac{1}{2}$	0	0	$\frac{1}{2}$	1	1
58	\bar{e}_L $\begin{smallmatrix} 03 & 12 & 56 & 78 \\ (+i) & (-) & (+) & (+) \end{smallmatrix} \parallel \begin{smallmatrix} 9 & 10 & 11 & 12 \\ (-) & (-) & (-) & (-) \end{smallmatrix}$	-1	$-\frac{1}{2}$	0	$\frac{1}{2}$	0	0	$\frac{1}{2}$	1	1
59	$\bar{\nu}_L$ $\begin{smallmatrix} 03 & 12 & 56 & 78 \\ [-i] & (+) & (-) & (-) \end{smallmatrix} \parallel \begin{smallmatrix} 9 & 10 & 11 & 12 \\ (+) & (-) & (-) & (-) \end{smallmatrix}$	-1	$\frac{1}{2}$	0	$-\frac{1}{2}$	0	0	$\frac{1}{2}$	0	0
60	$\bar{\nu}_L$ $\begin{smallmatrix} 03 & 12 & 56 & 78 \\ (+i) & (-) & (-) & (-) \end{smallmatrix} \parallel \begin{smallmatrix} 9 & 10 & 11 & 12 \\ (+) & (-) & (-) & (-) \end{smallmatrix}$	-1	$-\frac{1}{2}$	0	$-\frac{1}{2}$	0	0	$\frac{1}{2}$	0	0
61	$\bar{\nu}_R$ $\begin{smallmatrix} 03 & 12 & 56 & 78 \\ (+i) & (+) & (-) & (-) \end{smallmatrix} \parallel \begin{smallmatrix} 9 & 10 & 11 & 12 \\ (+) & (-) & (-) & (-) \end{smallmatrix}$	1	$\frac{1}{2}$	$-\frac{1}{2}$	0	0	0	$\frac{1}{2}$	$\frac{1}{2}$	0
62	$\bar{\nu}_R$ $\begin{smallmatrix} 03 & 12 & 56 & 78 \\ (-i) & (-) & (+) & (-) \end{smallmatrix} \parallel \begin{smallmatrix} 9 & 10 & 11 & 12 \\ (-) & (+) & (-) & (+) \end{smallmatrix}$	1	$-\frac{1}{2}$	$-\frac{1}{2}$	0	0	0	$\frac{1}{2}$	$\frac{1}{2}$	0
63	\bar{e}_R $\begin{smallmatrix} 03 & 12 & 56 & 78 \\ (+i) & (+) & (+) & (-) \end{smallmatrix} \parallel \begin{smallmatrix} 9 & 10 & 11 & 12 \\ (+) & (-) & (-) & (+) \end{smallmatrix}$	1	$\frac{1}{2}$	$\frac{1}{2}$	0	0	0	$\frac{1}{2}$	$\frac{1}{2}$	1
64	\bar{e}_R $\begin{smallmatrix} 03 & 12 & 56 & 78 \\ (-i) & (-) & (+) & (-) \end{smallmatrix} \parallel \begin{smallmatrix} 9 & 10 & 11 & 12 \\ (-) & (+) & (-) & (+) \end{smallmatrix}$	1	$-\frac{1}{2}$	$\frac{1}{2}$	0	0	0	$\frac{1}{2}$	$\frac{1}{2}$	1

Table 6.3. The left handed ($\Gamma(13,1) = -1$, Eq. (6.53)) multiplet of spinors — the members of the fundamental representation of the $S O(13,1)$ group, manifesting the subgroup $S O(7,1)$ of the colour charged quarks and anti-quarks and the colourless leptons and anti-leptons — is presented in the massless basis using the technique presented in App. 6.5. It contains the left handed ($\Gamma(3,1) = -1$, App. 6.5) weak ($S U(2)_I$) charged ($\tau^{13} = \pm \frac{1}{2}$, Eq. (6.38)), and $S U(2)_{II}$ chargeless ($\tau^{23} = 0$, Eq. (6.38)) quarks and leptons and the right handed ($\Gamma(3,1) = 1$, weak ($S U(2)_I$) chargeless and $S U(2)_{II}$ charged ($\tau^{23} = \pm \frac{1}{2}$) quarks and leptons, both with the spin S^{12} up and down ($\pm \frac{1}{2}$, respectively). Quarks distinguish from leptons only in the $S U(3) \times U(1)$ part: Quarks are triplets of three colours ($c^i = (\tau^{33}, \tau^{38}) = [(\frac{1}{2}, \frac{1}{2\sqrt{3}}), (-\frac{1}{2}, \frac{1}{2\sqrt{3}}), (0, -\frac{1}{\sqrt{3}})]$, Eq. (6.2)) carrying the “fermion charge” ($\tau^4 = \frac{1}{6}$, Eq. (6.2)). The colourless leptons carry the “fermion charge” ($\tau^4 = -\frac{1}{2}$). The same multiplet contains also the left handed weak ($S U(2)_I$) chargeless and $S U(2)_{II}$ charged anti-quarks and anti-leptons and the right handed weak ($S U(2)_I$) charged and $S U(2)_{II}$ chargeless anti-quarks and anti-leptons. Anti-quarks distinguish from anti-leptons again only in the $S U(3) \times U(1)$ part: Anti-quarks are anti-triplets, carrying the “fermion charge” ($\tau^4 = -\frac{1}{6}$). The anti-colourless anti-leptons carry the “fermion charge” ($\tau^4 = \frac{1}{2}$). $Y = (\tau^{23} + \tau^4)$ is the hyper charge, the electromagnetic charge is $Q = (\tau^{13} + Y)$. The states of opposite charges (anti-particle states) are reachable from the particle states besides by $S^{\alpha\beta}$ also by the application of the discrete symmetry operator $C_N \mathcal{P}_N$, presented in Refs. [43,44]. The vacuum state, on which the nilpotents and projectors operate, is not shown. The reader can find this Weyl representation also in Refs. [5,15,16,4] and in the references therein.

Taking into account Table 6.3 and Eqs. (6.49, 6.58) one easily finds what do operators γ^0 (\pm) do on the left handed and the right handed members of any

family $i = (1, 2, 3, 4)$.

$$\begin{aligned}
 \gamma^0 \begin{smallmatrix} 78 \\ (-) \end{smallmatrix} |\psi_{u_R, v_R}^i\rangle &= |\psi_{u_L, v_L}^i\rangle, \\
 \gamma^0 \begin{smallmatrix} 78 \\ (+) \end{smallmatrix} |\psi_{u_L, v_L}^i\rangle &= |\psi_{u_R, v_R}^i\rangle, \\
 \gamma^0 \begin{smallmatrix} 78 \\ (+) \end{smallmatrix} |\psi_{d_R, e_R}^i\rangle &= |\psi_{d_L, e_L}^i\rangle, \\
 \gamma^0 \begin{smallmatrix} 78 \\ (-) \end{smallmatrix} |\psi_{d_L, e_L}^i\rangle &= |\psi_{d_R, e_R}^i\rangle.
 \end{aligned} \tag{6.12}$$

We need to know also what do operators ($\tilde{\tau}^{1\pm} = \tilde{\tau}^{11} \pm i \tilde{\tau}^{12}, \tilde{\tau}^{13}$) and ($\tilde{N}_L^\pm = \tilde{N}_L^1 \pm i \tilde{N}_L^2, \tilde{N}_L^3$) do when operating on any member ($u_{L,R}, v_{L,R}, d_{L,R}, e_{L,R}$) of a particular family $\psi^i, i = (1, 2, 3, 4)$.

Taking into account, Eqs. (6.47, 6.48, 6.58, 6.60, 6.51, 6.40, 6.41),

$$\begin{aligned}
 \tilde{N}_L^\pm &= -\frac{03}{(\mp i)} \frac{12}{(\pm)}, & \tilde{\tau}^{1\pm} &= (\mp) \frac{56}{(\pm)} \frac{78}{(\mp)}, \\
 \tilde{N}_L^3 &= \frac{1}{2} (\tilde{S}^{12} + i \tilde{S}^{03}), & \tilde{\tau}^{13} &= \frac{1}{2} (\tilde{S}^{56} - \tilde{S}^{78}), \\
 \widetilde{(-k)}^{ab} \begin{smallmatrix} ab \\ (k) \end{smallmatrix} &= -i \eta^{aa} \begin{smallmatrix} ab \\ [k] \end{smallmatrix}, & \widetilde{(k)}^{ab} \begin{smallmatrix} ab \\ (k) \end{smallmatrix} &= 0, \\
 \begin{smallmatrix} ab \\ (k) \end{smallmatrix} \begin{smallmatrix} ab \\ [k] \end{smallmatrix} &= i \begin{smallmatrix} ab \\ (k) \end{smallmatrix}, & \begin{smallmatrix} ab \\ (k) \end{smallmatrix} \begin{smallmatrix} ab \\ [-k] \end{smallmatrix} &= 0, \\
 \begin{smallmatrix} ab \\ (k) \end{smallmatrix} &= \frac{1}{2} (\tilde{\gamma}^a + \frac{\eta^{aa}}{ik} \tilde{\gamma}^b), & \widetilde{[k]}^{ab} &= \frac{1}{2} (1 + \frac{i}{k} \tilde{\gamma}^a \tilde{\gamma}^b),
 \end{aligned} \tag{6.13}$$

one finds

$$\begin{aligned}
 \tilde{N}_L^+ |\psi^1\rangle &= |\psi^2\rangle, & \tilde{N}_L^+ |\psi^2\rangle &= 0, \\
 \tilde{N}_L^- |\psi^2\rangle &= |\psi^1\rangle, & \tilde{N}_L^- |\psi^1\rangle &= 0, \\
 \tilde{N}_L^+ |\psi^3\rangle &= |\psi^4\rangle, & \tilde{N}_L^+ |\psi^4\rangle &= 0, \\
 \tilde{N}_L^- |\psi^4\rangle &= |\psi^3\rangle, & \tilde{N}_L^- |\psi^3\rangle &= 0, \\
 \tilde{\tau}^{1+} |\psi^1\rangle &= |\psi^3\rangle, & \tilde{\tau}^{1+} |\psi^3\rangle &= 0, \\
 \tilde{\tau}^{1-} |\psi^3\rangle &= |\psi^1\rangle, & \tilde{\tau}^{1-} |\psi^1\rangle &= 0, \\
 \tilde{\tau}^{1-} |\psi^4\rangle &= |\psi^2\rangle, & \tilde{\tau}^{1-} |\psi^2\rangle &= 0, \\
 \tilde{\tau}^{1+} |\psi^2\rangle &= |\psi^4\rangle, & \tilde{\tau}^{1+} |\psi^4\rangle &= 0, \\
 \tilde{N}_L^3 |\psi^1\rangle &= -\frac{1}{2} |\psi^1\rangle, & \tilde{N}_L^3 |\psi^2\rangle &= +\frac{1}{2} |\psi^2\rangle, \\
 \tilde{N}_L^3 |\psi^3\rangle &= -\frac{1}{2} |\psi^3\rangle, & \tilde{N}_L^3 |\psi^4\rangle &= +\frac{1}{2} |\psi^4\rangle, \\
 \tilde{\tau}^{13} |\psi^1\rangle &= -\frac{1}{2} |\psi^1\rangle, & \tilde{\tau}^{13} |\psi^2\rangle &= -\frac{1}{2} |\psi^2\rangle, \\
 \tilde{\tau}^{13} |\psi^3\rangle &= +\frac{1}{2} |\psi^3\rangle, & \tilde{\tau}^{13} |\psi^4\rangle &= +\frac{1}{2} |\psi^4\rangle,
 \end{aligned} \tag{6.14}$$

independent of the family member $\alpha = (u, d, v, e)$.

The dependence of the mass matrix on the family quantum numbers can easily be understood through Table 6.2, where we notice that the operator \tilde{N}_L^{\Box} transforms the first family into the second (or the second family into the first) and the third family to the fourth (or the fourth family into the third), while the operator $\tilde{\tau}^{\Box}$ transforms the first family into the third (or the third family into the first) and the second family into the fourth (or the fourth family into the second). The application of these two operators, \tilde{N}_L^{\Box} and $\tilde{\tau}^{\Box}$, is presented in Eq. (6.14) and demonstrated in the diagram

$$\begin{array}{c} \tilde{N}_L^{\Box} \\ \updownarrow \\ \begin{pmatrix} \psi^1 & \psi^2 \\ \psi^3 & \psi^4 \end{pmatrix} \end{array} \updownarrow \tilde{\tau}^{\Box}. \quad (6.15)$$

The operators \tilde{N}_L^3 and $\tilde{\tau}^{13}$ are diagonal, with the eigenvalues presented in Eq. (6.14): \tilde{N}_L^3 has the eigenvalue $-\frac{1}{2}$ on $|\psi^1\rangle$ and $|\psi^3\rangle$ and $+\frac{1}{2}$ on $|\psi^2\rangle$ and $|\psi^4\rangle$, while $\tilde{\tau}^{13}$ has the eigenvalue $-\frac{1}{2}$ on $|\psi^1\rangle$ and $|\psi^2\rangle$ and $+\frac{1}{2}$ on $|\psi^3\rangle$ and $|\psi^4\rangle$. If we count $\frac{1}{2}$ as a part of these diagonal fields, then the eigenvalues of both operators on families differ only in the sign.

The sign and the values of Q, Q' and Y' depend on the family members properties and are the same for all the families.

Let the scalars $(\tilde{A}_{78}^{N_L^{\Box}}, \tilde{A}_{78}^{N_L^3}, \tilde{A}_{78}^{1^{\Box}}, \tilde{A}_{78}^{13})$ be scalar gauge fields of the operators $(\tilde{N}_L^{\pm}, \tilde{N}_L^3, \tilde{\tau}^{1\pm}, \tilde{\tau}^{13})$, respectively. Here $\tilde{A}_{78}^{\pm} = \tilde{A}_7 \mp i \tilde{A}_8$ for all the scalar gauge fields, while $\tilde{A}_{78}^{N_L^{\Box}} = \frac{1}{2} (\tilde{A}_{78}^{N_L^1} \mp i \tilde{A}_{78}^{N_L^2})$, respectively, and $\tilde{A}_{78}^{1^{\Box}} = \frac{1}{2} (\tilde{A}_{78}^{11} \mp i \tilde{A}_{78}^{12})$, respectively. All these fields can be expressed by $\tilde{\omega}_{abc}$, as presented in Eq. (6.45), provided that the coupling constants are the same for all the spin connection fields of both kinds, that is if no spontaneous symmetry breaking happens up to the weak scale.

We shall from now on use the notation $A_{\pm}^{\Lambda^i}$ instead of $A_{78}^{\Lambda^i}$ for all the operators with the space index (7, 8).

In what follows we prove that the symmetry of the mass matrix of any family member α remains the same in all orders of loop corrections, while the symmetry in all orders of corrections (which includes besides the loop corrections also the repetition of nonzero vacuum expectation values of the scalar fields) remains unchanged only under certain conditions. In general case the break of symmetry can still be evaluated for small absolute values of α^α , Eq. (6.11). We shall work in the massless basis.

Let us introduce the notation \hat{O} for the operator, which in Eq. (6.10) determines the mass matrices of quarks and leptons. The operator \hat{O} is equal to, Eq. (6.10),

$$\begin{aligned}\hat{O} &= \sum_{+,-} \gamma^0 \binom{78}{\pm} \left(- \sum_{\alpha} \tau^{\alpha} A_{\pm}^{\alpha} - \sum_{\tilde{A}i} \tilde{\tau}^{\tilde{A}i} \tilde{A}_{\pm}^{\tilde{A}i} \right), \\ \tau^{\alpha} A_{\pm}^{\alpha} &= (Q A_{\pm}^Q, Q' A_{\pm}^{Q'}, Y' A_{\pm}^{Y'}), \\ \tilde{\tau}^{\tilde{A}i} \tilde{A}_{\pm}^{\tilde{A}i} &= (\tilde{\tau}^{\tilde{I}i} \tilde{A}_{\pm}^{\tilde{I}i}, \tilde{N}_L^i \tilde{A}_{\pm}^{\tilde{N}_L^i}), \\ \{\tau^{\alpha}, \tau^{\beta}\}_{-} &= 0, \quad \{\tilde{\tau}^{\tilde{A}i}, \tilde{\tau}^{\tilde{B}j}\}_{-} = i \delta^{\tilde{A}\tilde{B}} f^{ijk} \tilde{\tau}^{\tilde{A}k}, \quad \{\tau^{\alpha}, \tilde{\tau}^{\tilde{B}j}\}_{-} = 0. \quad (6.16)\end{aligned}$$

Each of the fields in Eq. (6.16) consists in general of the nonzero vacuum expectation value and the dynamical part: $\tilde{A}_{\pm}^{\tilde{A}i} = (\langle \tilde{A}_{\pm}^{\tilde{I}i} \rangle + \tilde{A}_{\pm}^{\tilde{I}i}(x), \langle \tilde{A}_{\pm}^{\tilde{N}_L^i} \rangle + \tilde{A}_{\pm}^{\tilde{N}_L^i}(x), \langle A_{\pm}^{\alpha} \rangle + A_{\pm}^{\alpha}(x))$, where a common notation for all three singlets is used, since their eigenvalues depend only on the family members ($\alpha = (u, d, \nu, e)$) quantum numbers and are the same for all the families.

We further find that

$$\begin{aligned}\{\gamma^0 \binom{78}{\pm}, \tau^4\}_{-} &= 0, \quad \{\gamma^0 \binom{78}{\pm}, \tilde{\tau}^{\tilde{I}}\}_{-} = 0, \quad \{\gamma^0 \binom{78}{\pm}, \vec{N}_L\}_{-} = 0, \\ \{\gamma^0 \binom{78}{\pm}, \tau^{13}\}_{-} &= -2 \gamma^0 \binom{78}{\pm} S^{78}, \quad \{\gamma^0 \binom{78}{\pm}, \tau^{23}\}_{-} = +2 \gamma^0 \binom{78}{\pm} S^{78}. \quad (6.17)\end{aligned}$$

To calculate the mass matrices of family members $\alpha = (u, d, \nu, e)$ the operator \hat{O} must be taken into account in all orders. Since for our proof the dependence of the operator \hat{O} on the time and space does not play any role (it is the same for all the operators), we introduce the dimensionless operator $\hat{\mathbf{O}}$, in which all the degrees of freedom, except the internal ones determined by the family and family members quantum numbers, are integrated away¹⁴.

Then the change of the massless state of the i^{th} family of the family member α of the left or right handedness (L, R), $|\psi_{L,R}^{\alpha i}\rangle$, changes in all orders of corrections as follows

$$\hat{U} |\psi_{L,R}^{\alpha i}\rangle = i \sum_{n=0}^{\infty} \frac{(-1)^n \hat{\mathbf{O}}^{2n+1}}{(2n+1)!} |\psi_{L,R}^{\alpha i}\rangle. \quad (6.18)$$

In Eq. (6.18) $|\psi_{(L,R)}^{\alpha i}\rangle$ represents the internal degrees of freedom of the i^{th} , $i = (1, 2, 3, 4)$, family state for a particular family member α in the massless basis. The mass matrix element in all orders of corrections between the left handed α^{th} family member of the i^{th} family $\langle \psi_L^{\alpha i} |$ and the right handed α^{th} family member of the j^{th} family $|\psi_R^{\alpha j}\rangle$, both in the massless basis, is then equal to $\langle \psi_L^{\alpha i} | \hat{U} |\psi_R^{\alpha j}\rangle$. Only an odd number of operators $\hat{\mathbf{O}}^{2n+1}$ contribute to the mass matrix elements, transforming $|\psi_R^{\alpha i}\rangle$ into $|\psi_L^{\alpha j}\rangle$ or opposite. The product of an even number of operators $\hat{\mathbf{O}}^{2n}$ does not change the handedness and consequently

¹⁴ \hat{O} is measured in TeV units (as all the scalar and vector gauge fields). If the time evolution is concerned then $\hat{\mathbf{O}} = \hat{O} \cdot (t - t_0)/\text{TeV}$ is in units $\hbar = 1 = c$ dimensionless quantity. We assume that also the integration over space coordinates is in $\langle \psi_R^{\alpha i} | \hat{O} | \psi_R^{\alpha i} \rangle$ already taken into account, only the integration over the family and family members is left to be evaluated.

contributes nothing. Correspondingly without the nonzero vacuum expectation values of scalar fields all the matrix elements would remain zero, since only nonzero vacuum expectation values may appear in an odd orders, while the contribution of the loop corrections always contribute to the mass matrix elements an even contribution (see Fig. (6.1)).

Our purpose is to show how do the matrix elements behave in all orders of corrections

$$\begin{aligned} \langle \psi_L^{\alpha j} | \hat{U} | \psi_R^{\alpha i} \rangle &= i \sum_{n=0}^{\infty} \frac{(-1)^n}{(2n+1)!} \langle \psi_L^{\alpha i} | \sum_{k_1=1}^4 \hat{O} | \psi_R^{\alpha k_1} \rangle \langle \psi_R^{\alpha k_1} | \sum_{k_2=1}^4 \hat{O} | \psi_L^{\alpha k_2} \rangle \dots \\ &\quad \langle \psi_L^{\alpha k_n} | \sum_{k_i=1}^4 \hat{O} | \psi_R^{\alpha k_i} \rangle . \end{aligned} \quad (6.19)$$

Let be repeated again that all the matrix elements

$$\langle \psi_R^{\alpha k_1} | \hat{O} | \psi_L^{\alpha k_2} \rangle$$

or

$$\langle \psi_L^{\alpha k_1} | \sum_{k_2=1}^4 \hat{O} | \psi_R^{\alpha k_2} \rangle$$

only evaluate the internal degrees of freedom, that is the family and family members ones, while all the rest are assumed to be already evaluated. Since the mass matrix is in this notation the dimensionless object, also all the scalar fields are already divided by the energy unit (let say 1 TeV). We correspondingly introduce the dimensionless scalars $(\mathbf{A}_{\pm}^Q, \mathbf{A}_{\pm}^{Q'}, \mathbf{A}_{\pm}^{Y'})$, $\vec{\mathbf{A}}_{\pm}^{\tilde{I}}, \vec{\mathbf{A}}_{\pm}^{\tilde{N}_L}$.

The only operators τ^{α} , distinguishing among family members, are $(\tau^4, \tau^{13}, \tau^{23})$, included in $Q = (\tau^{13} + Y)$, $Y = (\tau^{23} + \tau^4)$, $Q' = (\tau^{13} - Y \tan^2 \vartheta_1)$ and in $Y' = (\tau^{23} - \tau^4 \tan^2 \vartheta_2)$. All the operators contributing to the mass matrices of each family member α have a factor γ^0 ⁷⁸ (\pm) , which transforms the right handed family member to the corresponding left handed family member and opposite.

When taking into account \hat{O}^{2n+1} in all orders, the operators $\tau^{\alpha} \mathbf{A}_{\pm}^{\alpha}$, $\tau^{\alpha} = (Q, Q', Y')$, contribute to all the matrix elements, the diagonal and the off diagonal ones.

To simplify the discussions let us introduce a bit more detailed notation

$$\begin{aligned}
 \hat{\mathbf{O}} &= \sum_i \hat{\mathbf{O}}^i = \hat{\mathbf{O}}^\alpha + \hat{\mathbf{O}}^{\tilde{1}3} + \hat{\mathbf{O}}^{\tilde{N}_L 3} + \hat{\mathbf{O}}^{\tilde{1}\Box} + \hat{\mathbf{O}}^{\tilde{N}_L \Box} \\
 \hat{\mathbf{O}}^\alpha &= - \sum_{+,-} \gamma^0(\pm) (Q \mathbf{A}_\pm^Q, Q' \mathbf{A}_\pm^{Q'}, Y' \mathbf{A}_\pm^{Y'}), \\
 \hat{\mathbf{O}}^{\tilde{1}3} &= - \sum_{+,-} \gamma^0(\pm) \tilde{\tau}^{\tilde{1}3} \tilde{\mathbf{A}}_\pm^{\tilde{1}3}, \\
 \hat{\mathbf{O}}^{\tilde{N}_L 3} &= - \sum_{+,-} \gamma^0(\pm) \tilde{N}_L^3 \tilde{\mathbf{A}}_\pm^{\tilde{N}_L 3}, \\
 \hat{\mathbf{O}}^{\tilde{1}\Box} &= - \sum_{+,-} \gamma^0(\pm) \tilde{\tau}^{\tilde{1}\Box} \tilde{\mathbf{A}}_\pm^{\tilde{1}\Box}, \\
 \hat{\mathbf{O}}^{\tilde{N}_L \Box} &= - \sum_{+,-} \gamma^0(\pm) \tilde{N}_L^{\Box} \tilde{\mathbf{A}}_\pm^{\tilde{N}_L \Box}.
 \end{aligned} \tag{6.20}$$

We shall use the notation for the expectation values among the states $\langle \psi_L^i | = \langle i |, |\psi_R^j \rangle = |j \rangle$ for the zero vacuum expectation values and the dynamical parts as follows:

$$\begin{aligned}
 \text{i. } &\langle i | \hat{\mathbf{O}}^\alpha | j \rangle = \langle i | \sum_{+,-} \gamma^0(\pm) \tau^\alpha (\langle \mathbf{A}_\pm^\alpha \rangle + \mathbf{A}_\pm^\alpha(x)) | j \rangle. \\
 \text{ii. } &\langle i | \hat{\mathbf{O}}^{\tilde{1}3} | j \rangle = \langle i | - \sum_{+,-} \gamma^0(\pm) \tilde{\tau}^{\tilde{1}3} (\langle \tilde{\mathbf{A}}_\pm^{\tilde{1}3} \rangle + \tilde{\mathbf{A}}_\pm^{\tilde{1}3}(x)) | j \rangle. \\
 \text{iii. } &\langle i | \hat{\mathbf{O}}^{\tilde{N}_L 3} | j \rangle = \langle i | - \sum_{+,-} \gamma^0(\pm) \tilde{N}_L^3 (\langle \tilde{\mathbf{A}}_\pm^{\tilde{N}_L 3} \rangle + \tilde{\mathbf{A}}_\pm^{\tilde{N}_L 3}(x)) | j \rangle. \\
 \text{iv. } &\langle i | \hat{\mathbf{O}}^{\tilde{1}\Box} | j \rangle = \langle i | - \sum_{+,-} \gamma^0(\pm) \tilde{\tau}^{\tilde{1}\Box} (\langle \tilde{\mathbf{A}}_\pm^{\tilde{1}\Box} \rangle + \tilde{\mathbf{A}}_\pm^{\tilde{1}\Box}(x)) | j \rangle. \\
 \text{v. } &\langle i | \hat{\mathbf{O}}^{\tilde{N}_L \Box} | j \rangle = \langle i | - \sum_{+,-} \gamma^0(\pm) \tilde{N}_L^{\Box} (\langle \tilde{\mathbf{A}}_\pm^{\tilde{N}_L \Box} \rangle + \tilde{\mathbf{A}}_\pm^{\tilde{N}_L \Box}(x)) | j \rangle. \\
 \text{vi. } &\langle i | \hat{\mathbf{O}}_{\text{dia}}^\alpha | i \rangle = \langle i | \sum_{+,-} \gamma^0(\pm) \{ \tau^\alpha (\langle \mathbf{A}_\pm^\alpha \rangle + \mathbf{A}_\pm^\alpha(x)) - \tilde{\tau}^{\tilde{1}3} (\langle \tilde{\mathbf{A}}_\pm^{\tilde{1}3} \rangle + \tilde{\mathbf{A}}_\pm^{\tilde{1}3}(x)) - \tilde{N}_L^3 (\langle \tilde{\mathbf{A}}_\pm^{\tilde{N}_L 3} \rangle + \tilde{\mathbf{A}}_\pm^{\tilde{N}_L 3}(x)) \} | i \rangle.
 \end{aligned}$$

($\langle \mathbf{A}_\pm^\alpha \rangle, \langle \tilde{\mathbf{A}}_\pm^{\tilde{1}3} \rangle, \langle \tilde{\mathbf{A}}_\pm^{\tilde{N}_L 3} \rangle, \langle \tilde{\mathbf{A}}_\pm^{\tilde{1}\Box} \rangle, \langle \tilde{\mathbf{A}}_\pm^{\tilde{N}_L \Box} \rangle$) represent nonzero vacuum expectation values and ($\mathbf{A}_\pm^\alpha(x), \tilde{\mathbf{A}}_\pm^{\tilde{1}3}(x), \tilde{\mathbf{A}}_\pm^{\tilde{N}_L 3}(x), \tilde{\mathbf{A}}_\pm^{\tilde{1}\Box}(x), \tilde{\mathbf{A}}_\pm^{\tilde{N}_L \Box}(x)$) the corresponding dynamical fields.

In the case **i.** $\langle \mathbf{A}_\pm^\alpha \rangle$ represent the sum of the vacuum expectation values of ($Q^\alpha \mathbf{A}_{(\pm)}^Q, Q'^\alpha \mathbf{A}_{(\pm)}^{Q'}, Y'^\alpha \mathbf{A}_{(\pm)}^{Y'}$) of a particular family member α , where ($Q^\alpha, Q'^\alpha, Y'^\alpha$) are the corresponding quantum numbers of a family member α . $\mathbf{A}_\pm^\alpha(x)$ represent the corresponding dynamical fields.

In the case **vi.** we correspondingly have for the four diagonal terms on the tree level, that is for $n = 0$ in Eq. (6.19) (after taking into account Eq. (6.14): $\langle 1 | \tilde{\mathbf{O}}_{\text{dia}}^\alpha | 1 \rangle = \mathbf{a}^\alpha - (\tilde{\mathbf{a}}_1 + \tilde{\mathbf{a}}_2), \langle 2 | \tilde{\mathbf{O}}_{\text{dia}}^\alpha | 1 \rangle | 2 \rangle = \mathbf{a}^\alpha - (\tilde{\mathbf{a}}_1 - \tilde{\mathbf{a}}_2), \langle 3 | \tilde{\mathbf{O}}_{\text{dia}}^\alpha | 3 \rangle = \mathbf{a}^\alpha + (\tilde{\mathbf{a}}_1 - \tilde{\mathbf{a}}_2)$ and $\langle 4 | \tilde{\mathbf{O}}_{\text{dia}}^\alpha | 4 \rangle = \mathbf{a}^\alpha + (\tilde{\mathbf{a}}_1 + \tilde{\mathbf{a}}_2)$, where ($\tilde{\mathbf{a}}_1, \tilde{\mathbf{a}}_2, \mathbf{a}^\alpha$) represent the nonzero vacuum expectation values of $\frac{1}{2} \frac{1}{\sqrt{2}} (\langle \tilde{\mathbf{A}}_{(+)}^{\tilde{1}3} \rangle + \langle \tilde{\mathbf{A}}_{(-)}^{\tilde{1}3} \rangle), \frac{1}{2} \frac{1}{\sqrt{2}} (\langle \tilde{\mathbf{A}}_{(+)}^{\tilde{N}_L 3} \rangle + \langle \tilde{\mathbf{A}}_{(-)}^{\tilde{N}_L 3} \rangle), \frac{1}{2} \frac{1}{\sqrt{2}} (\langle \mathbf{A}_{(+)}^\alpha \rangle + \langle \mathbf{A}_{(-)}^\alpha \rangle)$, all in dimensionless units.

We are now prepared to show under which conditions the mass matrix elements for any of the family members keep the symmetry $\widetilde{SU}(2) \times \widetilde{SU}(2) \times U(1)$ at each step of corrections, what means that the values of the matrix elements obtained in each correction respect the symmetry of mass matrices on the tree level.

We use the massless basis $|\psi_{L,R}^i\rangle$, making for the basis the choice $\frac{1}{\sqrt{2}}(|\psi_L^i\rangle + |\psi_R^i\rangle)$.

The diagrams for the tree level, one loop and three loop contributions of the operator \hat{O} , determining the masses of quarks and leptons, Eqs. (6.16, 6.20), are presented in Fig. (6.1).

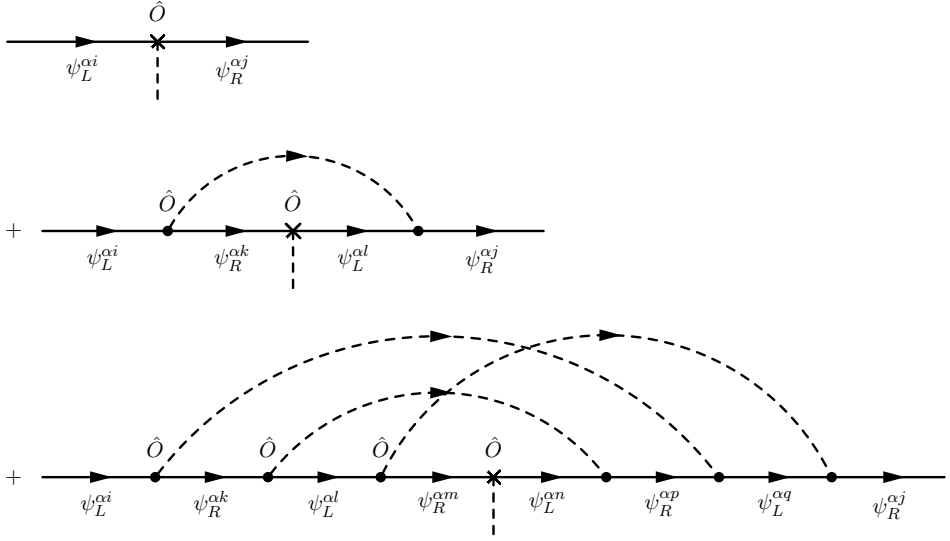


Fig. 6.1. The tree level contributions, one loop contributions (not all possibilities are drawn, the tree level contributions occurs namely also to the left or to the right of the loop, while to \hat{O} three singlets and two triplets, presented in Eq. (6.16), contribute) and two loop contributions are drawn (again not all the possibilities are shown up). Each (i, j, k, l, m, \dots) determines a family quantum number (running within the four families — $(1, 2, 3, 4)$), α denotes one of the family members ($\alpha = (u, v, d, e)$) quantum numbers, all in the massless basis $\psi_{(R,L)}^{\alpha i}$. Dynamical fields start and end with dots \bullet , while \times with the vertical slashed line represents the interaction of the fermion fields with the nonzero vacuum expectation values of the scalar fields.

6.2.1 Mass matrices on the tree level

Let us first present the mass matrix on the tree level for an α^{th} family member, that is for $n = 0$ in Eq. (6.19).

Taking into account Eq. (6.14) one obtains for the diagonal matrix elements on the tree level (for $n = 0$ in Eq. (6.19)) $[a^\alpha - (\tilde{a}_1 + \tilde{a}_2), a^\alpha - (\tilde{a}_1 - \tilde{a}_2), a^\alpha + (\tilde{a}_1 - \tilde{a}_2), a^\alpha + (\tilde{a}_1 + \tilde{a}_2)]$, respectively. The corresponding diagrams are presented in Fig. (6.2).

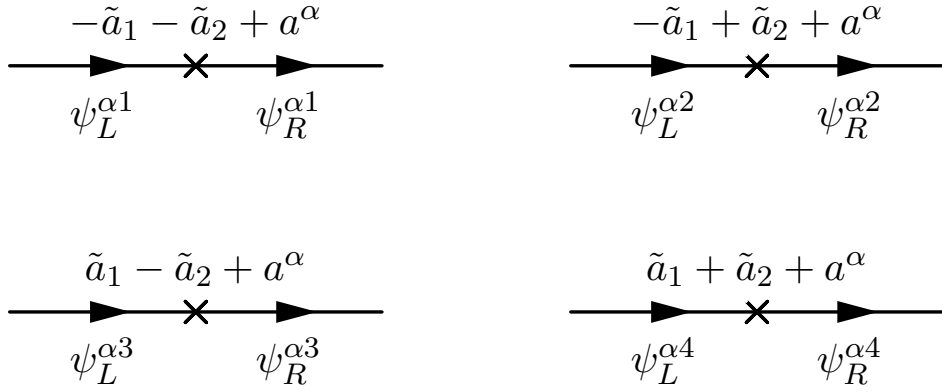


Fig. 6.2. The tree level contributions to the diagonal matrix elements of the operator $\hat{O}_{\text{dia}}^\alpha$, Eq. (6.20). The eigenvalues of the operators \tilde{N}_L^3 and $\tilde{\tau}^{13}$ on a family state i can be read in Eq. (6.14).

Taking into account Eq. (6.14) one finds for the off diagonal elements on the tree level:

$$\begin{aligned} \langle \psi^1 | \dots | \psi^2 \rangle &= \langle \psi^3 | \dots | \psi^4 \rangle = \langle \psi^2 | \dots | \psi^1 \rangle^\dagger = \langle \psi^4 | \dots | \psi^3 \rangle^\dagger = \langle \tilde{\mathbf{A}}^{\tilde{N}_L \square} \rangle, \\ \langle \psi^1 | \dots | \psi^3 \rangle &= \langle \psi^2 | \dots | \psi^4 \rangle = \langle \psi^3 | \dots | \psi^1 \rangle^\dagger = \langle \psi^4 | \dots | \psi^2 \rangle^\dagger = \langle \tilde{\mathbf{A}}^{\tilde{1} \square} \rangle. \end{aligned}$$

The corresponding diagrams for $\langle \psi^1 | \dots | \psi^2 \rangle$, $\langle \psi^2 | \dots | \psi^1 \rangle$, $\langle \psi^2 | \dots | \psi^3 \rangle$ and $\langle \psi^3 | \dots | \psi^2 \rangle$ are presented in Fig. (6.3). The vacuum expectation values of this matrix elements on the tree level are presented in the mass matrix of Eq.(6.22).

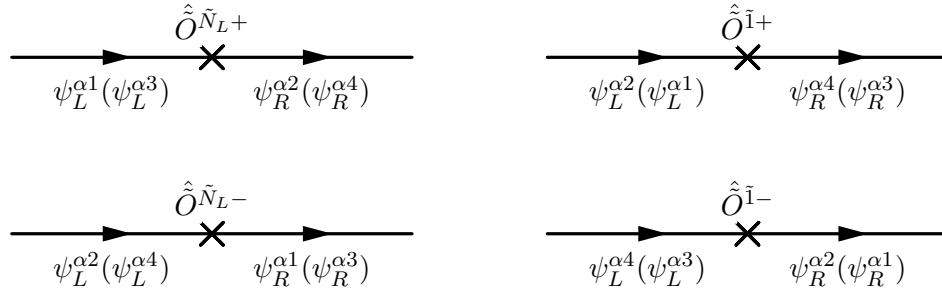


Fig. 6.3. The tree level contributions to the off diagonal matrix elements of the operators $\hat{O}^{\tilde{1} \square}$ and $\hat{O}^{\tilde{N}_L \square}$, Eq. (6.20) are presented. The application of the operators \tilde{N}_L^{\square} and $\tilde{\tau}^{\tilde{1} \square}$ on a family state i can be read in Eq. (6.14).

The contributions to the off diagonal matrix elements $\langle \psi^1 | \dots | \psi^4 \rangle$, $\langle \psi^2 | \dots | \psi^3 \rangle$, $\langle \psi^3 | \dots | \psi^2 \rangle$ and $\langle \psi^4 | \dots | \psi^1 \rangle$ are nonzero only, if one makes three steps (not two, due to the left right jumps in each step), that is indeed in the third order of correction. For $\langle \psi^1 | \dots | \psi^4 \rangle$ we have (in the basis $\frac{1}{\sqrt{2}} (|\psi_L^i\rangle + |\psi_R^i\rangle)$) and with the notation $\langle \tilde{\mathbf{A}}^{\tilde{N}_L \square} \rangle = \frac{1}{\sqrt{2}} (\langle \tilde{\mathbf{A}}_{(+)}^{\tilde{N}_L \square} \rangle + \langle \tilde{\mathbf{A}}_{(-)}^{\tilde{N}_L \square} \rangle)$ after we take into account that γ^0 (\pm) transform the right handed family members into the left handed ones and

opposite): $\langle \psi^1 | \sum_{+,-} \tilde{\tau}^{\tilde{\Box}} \langle \tilde{\mathbf{A}}^{\tilde{\Box}} \rangle \sum_k |\psi^k \rangle \langle \psi^k | \sum_{+,-} \tilde{\mathbf{N}}_{\tilde{\mathbf{L}}}^{\tilde{\Box}} \langle \tilde{\mathbf{A}}^{\tilde{\mathbf{N}}_{\tilde{\mathbf{L}}}\tilde{\Box}} \rangle |\psi^4 \rangle$
 $\langle \psi^4 | (\tilde{\mathbf{a}}_1 + \tilde{\mathbf{a}}_2 + \mathbf{a}^\alpha) |\psi^4 \rangle$. There are all together six such terms, presented in Fig. (6.4), since the diagonal term appears also at the beginning as $(-\tilde{\mathbf{a}}_1 - \tilde{\mathbf{a}}_2 + \mathbf{a}^\alpha)$ and in the middle as $(\tilde{\mathbf{a}}_1 - \tilde{\mathbf{a}}_2 + \mathbf{a}^\alpha)$, and since the operators $\sum_{+,-} \tilde{\tau}^{\tilde{\Box}} \langle \tilde{\mathbf{A}}^{\tilde{\Box}} \rangle$ and $\sum_{+,-} \tilde{\mathbf{N}}_{\tilde{\mathbf{L}}}^{\tilde{\Box}} \langle \tilde{\mathbf{A}}^{\tilde{\mathbf{N}}_{\tilde{\mathbf{L}}}\tilde{\Box}} \rangle$ appear in the opposite order as well. We simplify the notation from $|\psi^k \rangle$ to $|k \rangle$. Summing all these six terms for each of four matrix elements ($\langle 1|..|4 \rangle$, $\langle 2|..|3 \rangle$, $\langle 3|..|2 \rangle$, $\langle 4|..|1 \rangle$) one gets (taking into account Eqs. (6.19, 6.14)):

$$\begin{aligned} \langle 1|..|4 \rangle &= \mathbf{a}^\alpha \langle \tilde{\mathbf{A}}^{\tilde{\Box}} \rangle \langle \tilde{\mathbf{A}}^{\tilde{\mathbf{N}}_{\tilde{\mathbf{L}}}\tilde{\Box}} \rangle, \\ \langle 2|..|3 \rangle &= \mathbf{a}^\alpha \langle \tilde{\mathbf{A}}^{\tilde{\Box}} \rangle \langle \tilde{\mathbf{A}}^{\tilde{\mathbf{N}}_{\tilde{\mathbf{L}}}\tilde{\Box}} \rangle, \\ \langle 3|..|2 \rangle &= \mathbf{a}^\alpha \langle \tilde{\mathbf{A}}^{\tilde{\Box}} \rangle \langle \tilde{\mathbf{A}}^{\tilde{\mathbf{N}}_{\tilde{\mathbf{L}}}\tilde{\Box}} \rangle, \\ \langle 4|..|1 \rangle &= \mathbf{a}^\alpha \langle \tilde{\mathbf{A}}^{\tilde{\Box}} \rangle \langle \tilde{\mathbf{A}}^{\tilde{\mathbf{N}}_{\tilde{\mathbf{L}}}\tilde{\Box}} \rangle. \end{aligned} \quad (6.21)$$

Each matrix element is in Eq. (6.21) divided by $3!$, since it is the contribution in the third order! One notices that $\langle 4|..|1 \rangle^\dagger = \langle 1|..|4 \rangle$ and $\langle 3|..|2 \rangle^\dagger = \langle 2|..|3 \rangle$. These matrix elements are included into the mass matrix, Eq. (6.22).

To show up the symmetry of the mass matrix on the lowest level we put all the matrix elements in Eq. (6.22).

$$\begin{aligned} {}^\alpha \mathcal{M}_{(o)} = & \begin{pmatrix} -\tilde{\mathbf{a}}_1 - \tilde{\mathbf{a}}_2 + \mathbf{a}^\alpha & \langle \tilde{\mathbf{A}}^{\tilde{\mathbf{N}}_{\tilde{\mathbf{L}}}\tilde{\Box}} \rangle & \langle \tilde{\mathbf{A}}^{\tilde{\Box}} \rangle & \mathbf{a}^\alpha \langle \tilde{\mathbf{A}}^{\tilde{\Box}} \rangle \langle \tilde{\mathbf{A}}^{\tilde{\mathbf{N}}_{\tilde{\mathbf{L}}}\tilde{\Box}} \rangle \\ \langle \tilde{\mathbf{A}}^{\tilde{\mathbf{N}}_{\tilde{\mathbf{L}}}\tilde{\Box}} \rangle & -\tilde{\mathbf{a}}_1 + \tilde{\mathbf{a}}_2 + \mathbf{a}^\alpha & \mathbf{a}^\alpha \langle \tilde{\mathbf{A}}^{\tilde{\Box}} \rangle \langle \tilde{\mathbf{A}}^{\tilde{\mathbf{N}}_{\tilde{\mathbf{L}}}\tilde{\Box}} \rangle & \langle \tilde{\mathbf{A}}^{\tilde{\Box}} \rangle \\ \langle \tilde{\mathbf{A}}^{\tilde{\Box}} \rangle & \mathbf{a}^\alpha \langle \tilde{\mathbf{A}}^{\tilde{\Box}} \rangle \langle \tilde{\mathbf{A}}^{\tilde{\mathbf{N}}_{\tilde{\mathbf{L}}}\tilde{\Box}} \rangle & \tilde{\mathbf{a}}_1 - \tilde{\mathbf{a}}_2 + \mathbf{a}^\alpha & \langle \tilde{\mathbf{A}}^{\tilde{\mathbf{N}}_{\tilde{\mathbf{L}}}\tilde{\Box}} \rangle \\ \mathbf{a}^\alpha \langle \tilde{\mathbf{A}}^{\tilde{\Box}} \rangle \langle \tilde{\mathbf{A}}^{\tilde{\mathbf{N}}_{\tilde{\mathbf{L}}}\tilde{\Box}} \rangle & \langle \tilde{\mathbf{A}}^{\tilde{\Box}} \rangle & \langle \tilde{\mathbf{A}}^{\tilde{\mathbf{N}}_{\tilde{\mathbf{L}}}\tilde{\Box}} \rangle & \tilde{\mathbf{a}}_1 + \tilde{\mathbf{a}}_2 + \mathbf{a}^\alpha \end{pmatrix} \end{aligned} \quad (6.22)$$

Mass matrix is dimensionless. One notices that the diagonal terms have on the tree level the symmetry $\langle \psi^1 |..| \psi^1 \rangle + \langle \psi^4 |..| \psi^4 \rangle = 2\mathbf{a}^\alpha = \langle \psi^2 |..| \psi^2 \rangle + \langle \psi^3 |..| \psi^3 \rangle$, and that in the off diagonal elements with "three steps needed" the contribution of the fields, which depend on particular family member $\alpha = (u, d, \nu, e)$, enters.

We also notice that $\langle \psi^i |..| \psi^j \rangle^\dagger = \langle \psi^j |..| \psi^i \rangle$. We see that $\langle 1|..|3 \rangle = \langle 2|..|4 \rangle = \langle 3|..|1 \rangle^\dagger = \langle 4|..|2 \rangle^\dagger$, that $\langle 1|..|2 \rangle = \langle 3|..|4 \rangle = \langle 2|..|1 \rangle^\dagger = \langle 4|..|3 \rangle^\dagger$ and that $\langle 4|..|1 \rangle^\dagger = \langle 1|..|4 \rangle$ and $\langle 3|..|2 \rangle^\dagger = \langle 2|..|3 \rangle$, what is already written below Eq. (6.21), $\langle i|..|j \rangle$ denotes $\langle \psi^i |..| \psi^j \rangle$.

In the case that $\mathbf{a} = \langle \tilde{\mathbf{A}}^{\tilde{\Box}} \rangle = \langle \tilde{\mathbf{A}}^{\tilde{\Box}} \rangle = e$ and $\langle \tilde{\mathbf{A}}^{\tilde{\mathbf{N}}_{\tilde{\mathbf{L}}}\tilde{\Box}} \rangle = \langle \tilde{\mathbf{A}}^{\tilde{\mathbf{N}}_{\tilde{\mathbf{L}}}\tilde{\Box}} \rangle = d$, which would mean that all the matrix elements are real, the mass matrix simplifies to

$$\mathcal{M}_{(o)}^\alpha = \begin{pmatrix} -\tilde{\mathbf{a}}_1 - \tilde{\mathbf{a}}_2 + \mathbf{a}^\alpha & d & e & b \\ d & -\tilde{\mathbf{a}}_1 + \tilde{\mathbf{a}}_2 + \mathbf{a}^\alpha & b & e \\ e & b & \tilde{\mathbf{a}}_1 - \tilde{\mathbf{a}}_2 + \mathbf{a}^\alpha & d \\ b & e & d & \tilde{\mathbf{a}}_1 + \tilde{\mathbf{a}}_2 + \mathbf{a}^\alpha \end{pmatrix}, \quad (6.23)$$

with $b = \mathbf{a}^\alpha e d$.

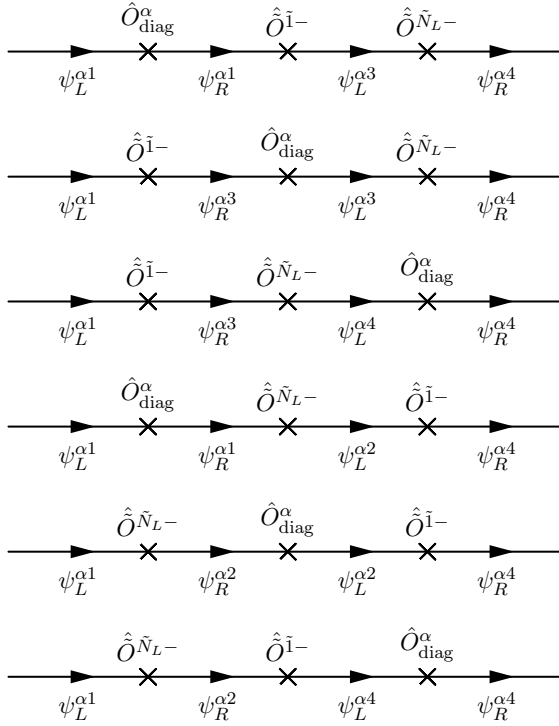


Fig. 6.4. The tree level contribution to the matrix element $\langle \psi^1 | b | \psi^4 \rangle$ is presented. One comes from $\langle \psi^1 |$ to $|\psi^4 \rangle$ in three steps: $\langle \psi^1 | \sum_{+,-} \tilde{\tau}^{\tilde{1}\tilde{1}}_{\tilde{L}} < \tilde{\mathbf{A}}^{\tilde{1}\tilde{1}}_{\tilde{L}} > \sum_k |\psi^k \rangle < \psi^k | \sum_{+,-} \tilde{\mathbf{N}}^{\tilde{1}\tilde{1}}_{\tilde{L}} < \tilde{\mathbf{A}}^{\tilde{N}_L\tilde{1}}_{\tilde{L}} > |\psi^4 \rangle < \psi^4 | (\tilde{\mathbf{a}}_1 + \tilde{\mathbf{a}}_2 + \mathbf{a}^\alpha) |\psi^4 \rangle$. There are all together six such terms, since the diagonal term appears also at the beginning as $(-\tilde{\mathbf{a}}_1 - \tilde{\mathbf{a}}_2 + \mathbf{a}^\alpha)$ and in the middle as $(\tilde{\mathbf{a}}_1 - \tilde{\mathbf{a}}_2 + \mathbf{a}^\alpha)$, and since the operators $\sum_{+,-} \tilde{\tau}^{\tilde{1}\tilde{1}}_{\tilde{L}} < \tilde{\mathbf{A}}^{\tilde{1}\tilde{1}}_{\tilde{L}} >$ and $\sum_{+,-} \tilde{\mathbf{N}}^{\tilde{1}\tilde{1}}_{\tilde{L}} < \tilde{\mathbf{A}}^{\tilde{N}_L\tilde{1}}_{\tilde{L}} >$ appear in the opposite order as well.

6.2.2 Mass matrices beyond the tree level

We discuss in this subsection the matrix elements of the mass matrix in all orders of corrections, Eq. (6.19), the tree level, $n = 0$, of which is presented in Eq. (6.22). The tree level mass matrix manifests the $\widetilde{\text{SU}}(2) \times \widetilde{\text{SU}}(2) \times \text{U}(1)$ symmetry as seen in Eq. (6.22), with $(\langle 1|x|1 \rangle + \langle 4|x|4 \rangle) - (\langle 2|x|2 \rangle + \langle 3|x|3 \rangle) = 0$ and $\langle 1|x|3 \rangle = \langle 2|x|4 \rangle = \langle 3|x|1 \rangle^\dagger = \langle 4|x|1 \rangle^\dagger$ and with $(\langle 1|xxx|4 \rangle, \langle 2|xxx|3 \rangle, \langle 3|xxx|2 \rangle, \langle 4|xxx|1 \rangle)$ related so that all are equal if $\langle \tilde{\mathbf{A}}^{\tilde{1}\tilde{1}}_{\tilde{L}} \rangle$ and $\langle \tilde{\mathbf{A}}^{\tilde{N}_L\tilde{1}}_{\tilde{L}} \rangle$ are real.

Let us repeat that the generators of the two groups which operate among families commute: $\{\tilde{\tau}^{\tilde{1}\tilde{1}}, \tilde{\mathbf{N}}^{\tilde{1}\tilde{1}}_{\tilde{L}}\}_- = 0$, and that these generators commute also with generators which distinguish among family members: $\{\tilde{\tau}^{\tilde{1}\tilde{1}}, \tau^\alpha\}_- = 0, \{\tau^\alpha, \tilde{\mathbf{N}}^{\tilde{1}\tilde{1}}_{\tilde{L}}\}_- = 0$, where τ^α represents (Q, Q', Y') (or $\tau^4, \tau^{23}, \tau^{13}$).

To study the symmetry $\widetilde{\text{SU}}(2) \times \widetilde{\text{SU}}(2) \times \text{U}(1)$ of the mass matrix, Eq. (6.22), in all orders of loop corrections, of repetition of nonzero vacuum expectation values

and of both together — loop corrections and nonzero vacuum expectation values — we just have to calculate at each order of corrections the difference between each pair of the matrix elements which are equal on the three level, as well as the Hermitian conjugated difference of such a pair.

Since the dependence of all the scalar fields on ordinary coordinates are in all cases the same, we only have to evaluate the application of the operators to the internal space of basic state, that is on the space of family and family members degrees of freedom. Correspondingly we pay attention only on this internal part — on the interaction of scalar fields with the space index (7, 8) with any family member of any of four families separately with respect to their internal space. The dependence of the mass matrix elements on the family member quantum numbers appears through the nonzero vacuum expectation value \mathbf{a}^α , Eq. (6.22), as well as through the dynamical part of $\hat{\mathbf{O}}^\alpha$, Eq. (6.20).

We demonstrate in this subsection how does the repetition of the nonzero vacuum expectation values of the scalar fields and loop corrections in all orders influence matrix elements, presented on the tree level in Eq. (6.22).

In the case that $\mathbf{a}^\alpha = 0$ (that is for $\langle \mathbf{A}^Q \rangle = 0$, $\langle \mathbf{A}^{Q'} \rangle = 0$ and $\langle \mathbf{A}^{Y'} \rangle = 0$) the symmetry in all corrections, that is in all loop corrections and all the repetition of nonzero vacuum expectation values of the scalar fields, and of both — the loop corrections and the repetitions of nonzero vacuum expectation values nonzero of all the scalar fields except \mathbf{a}^α — keep the symmetry of the tree level, presented in Eq. (6.22).

We prove in this subsection that in the case that $\langle \mathbf{A}^Q \rangle = 0$, $\langle \mathbf{A}^{Q'} \rangle = 0$ and $\langle \mathbf{A}^{Y'} \rangle = 0$, that is for $\mathbf{a}^\alpha = 0$, the symmetry of mass matrices remains unchanged in all orders of corrections: the loop ones of dynamical fields — \mathbf{A}^Q , $\mathbf{A}^{Q'}$, $\mathbf{A}^{Y'}$, $\vec{\mathbf{A}}^{\tilde{N}_L}$, $\vec{\mathbf{A}}^{\tilde{I}}$ — in the repetition of nonzero vacuum expectation values of the scalar fields carrying the family quantum numbers — $\langle \vec{\mathbf{A}}^{\tilde{N}_L} \rangle$ and $\langle \vec{\mathbf{A}}^{\tilde{I}} \rangle$ — and of all together. The symmetry of mass matrices remains in all orders of corrections the one of the tree level also if $\mathbf{a}^\alpha \neq 0$ while $\tilde{\mathbf{a}}_1 = 0$ and $\tilde{\mathbf{a}}_2 = 0$. The symmetry changes if the nonzero vacuum expectation values of all the scalar fields are nonzero.

In the case, however, that $\mathbf{a}^\alpha = 0$, the matrix elements, which are in the lowest order proportional to \mathbf{a}^α in Eq. (6.22), remain zero in all orders of corrections, while the nonzero matrix elements become dependent on family members quantum numbers due to the participations in loop corrections in all orders of the dynamical fields \mathbf{A}^Q , $\mathbf{A}^{Q'}$ and $\mathbf{A}^{Y'}$.

We study in what follows first the symmetry of mass matrices in all orders of corrections in the case that $\mathbf{a}^\alpha = 0$, and then the symmetry of the mass matrices, again in all orders of corrections, when $\mathbf{a}^\alpha \neq 0$. We also comment that the symmetry of the tree level remain the same in all orders of corrections, if $\mathbf{a}^\alpha \neq 0$, while $\tilde{\mathbf{a}}_1 = 0 = \tilde{\mathbf{a}}_2$.

Mass matrices beyond the tree level, if $\mathbf{a}^\alpha = 0$ We study corrections to which the scalar fields which distinguish among families, contribute — with their nonzero vacuum expectation values $\langle \vec{\mathbf{A}}^{\tilde{N}_L} \rangle$ and $\langle \vec{\mathbf{A}}^{\tilde{I}} \rangle$ and their dynamical parts $\vec{\mathbf{A}}^{\tilde{N}_L}$ and $\vec{\mathbf{A}}^{\tilde{I}}$ — while we assume $\mathbf{a}^\alpha = 0$ (\mathbf{a}^α denotes the vacuum expectation values to

which the tree singlet fields, distinguishing among family members, contribute, that is ($\langle \mathbf{A}^Q \rangle$, $\langle \mathbf{A}^{Q'} \rangle$, $\langle \mathbf{A}^{Y'} \rangle$), taking into account the loop corrections of the corresponding dynamical parts (\mathbf{A}^Q , $\mathbf{A}^{Q'}$, $\mathbf{A}^{Y'}$) in all orders.

We show that in such a case — that is in the case that $\mathbf{a}^\alpha = 0$ while all the other scalar fields determining mass matrices have nonzero vacuum expectation values ($\tilde{\mathbf{a}}_1 \neq 0$, $\tilde{\mathbf{a}}_2 \neq 0$, $\langle \tilde{\mathbf{A}}^{\tilde{\mathbf{N}}_L \boxplus} \rangle \neq 0$, $\langle \tilde{\mathbf{A}}^{\tilde{\mathbf{I}} \boxplus} \rangle \neq 0$) — the matrix elements, evaluated in all orders of corrections, keep the symmetry of the tree level.

We also show, that in this case the off diagonal matrix elements, represented in Eq. (6.22) as ($\mathbf{a}^\alpha \langle \tilde{\mathbf{A}}^{\tilde{\mathbf{I}} \boxplus} \rangle \langle \tilde{\mathbf{A}}^{\tilde{\mathbf{N}}_L \boxplus} \rangle$, $\mathbf{a}^\alpha \langle \tilde{\mathbf{A}}^{\tilde{\mathbf{I}} \boxplus} \rangle \langle \tilde{\mathbf{A}}^{\tilde{\mathbf{N}}_L \boxminus} \rangle$, $\mathbf{a}^\alpha \langle \tilde{\mathbf{A}}^{\tilde{\mathbf{I}} \boxminus} \rangle \langle \tilde{\mathbf{A}}^{\tilde{\mathbf{N}}_L \boxplus} \rangle$, $\mathbf{a}^\alpha \langle \tilde{\mathbf{A}}^{\tilde{\mathbf{I}} \boxminus} \rangle \langle \tilde{\mathbf{A}}^{\tilde{\mathbf{N}}_L \boxminus} \rangle$), remain zero in all orders of corrections.

Let us look how the corrections in all orders manifest for each matrix element separately.

i. We start with diagonal terms: $\langle \psi^i | \dots | \psi^i \rangle$, $i = (1, 2, 3, 4)$.

On the tree level the symmetry is:

$$\{ \langle \psi^1 | \langle \hat{\mathbf{O}}_{\text{dia}}^\alpha \rangle | \psi^1 \rangle + \langle \psi^4 | \langle \hat{\mathbf{O}}_{\text{dia}}^\alpha \rangle | \psi^4 \rangle \} - \{ \langle \psi^2 | \langle \hat{\mathbf{O}}_{\text{dia}}^\alpha \rangle | \psi^2 \rangle + \langle \psi^3 | \langle \hat{\mathbf{O}}_{\text{dia}}^\alpha \rangle | \psi^3 \rangle \} = 0.$$

i.a. It is easy to see that the tree level symmetry, $\{ \langle \psi^1 | \langle \hat{\mathbf{O}}_{\text{dia}}^\alpha \rangle | \psi^1 \rangle + \langle \psi^4 | \langle \hat{\mathbf{O}}_{\text{dia}}^\alpha \rangle | \psi^4 \rangle \} - \{ \langle \psi^2 | \langle \hat{\mathbf{O}}_{\text{dia}}^\alpha \rangle | \psi^2 \rangle + \langle \psi^3 | \langle \hat{\mathbf{O}}_{\text{dia}}^\alpha \rangle | \psi^3 \rangle \} = 0$, remains in all orders of corrections, if only the nonzero vacuum expectation values of $\langle \tilde{\mathbf{A}}^{\tilde{\mathbf{I}}^3} \rangle = \tilde{\mathbf{a}}_1$ and $\langle \tilde{\mathbf{A}}^{\tilde{\mathbf{N}}_L^3} \rangle = \tilde{\mathbf{a}}_2$ contribute in operators $\gamma^0 (\pm) \tau^{\tilde{\mathbf{I}}^3} \langle \tilde{\mathbf{A}}^{\tilde{\mathbf{I}}^3} \rangle$ and $\gamma^0 (\pm) \tilde{\mathbf{N}}_L^3 \langle \tilde{\mathbf{A}}^{\tilde{\mathbf{N}}_L^3} \rangle$. At, let say, $(2k+1)^{\text{st}}$ order of corrections we namely have $\{ (-\tilde{\mathbf{a}}_1 + \tilde{\mathbf{a}}_2)^{(2k+1)} + (\tilde{\mathbf{a}}_1 + \tilde{\mathbf{a}}_2)^{(2k+1)} \} - \{ (-\tilde{\mathbf{a}}_1 - \tilde{\mathbf{a}}_2)^{(2k+1)} + (\tilde{\mathbf{a}}_1 - \tilde{\mathbf{a}}_2)^{(2k+1)} \} = 0$.

i.b. The contributions of the dynamical terms, either (\mathbf{A}^Q , $\mathbf{A}^{Q'}$, $\mathbf{A}^{Y'}$) or ($\tilde{\mathbf{A}}^{\tilde{\mathbf{I}}^3}$, $\tilde{\mathbf{A}}^{\tilde{\mathbf{N}}_L^3}$) do not break the three level symmetry. Each of them namely always appears in an even power, Fig. (6.1), changing the order of corrections by a factor of two or $2n$ ($|\mathbf{A}^\alpha|^{2(n-k-l)}$, $|\tilde{\mathbf{A}}^{\tilde{\mathbf{I}}^3}|^{2k}$, $|\tilde{\mathbf{A}}^{\tilde{\mathbf{N}}_L^3}|^{2l}$), where $(n-k-l, k, l)$ are nonnegative integers, while $\tau^{\mathbf{A}^\alpha}$ represents $(Q^\alpha, Q'^\alpha, Y'^\alpha)$. The contribution to $|\mathbf{A}^\alpha|^{2m}$, $m = (n-k-l)$, origins in the product of $|\mathbf{A}^Q|^{2(m-p-r)} \cdot |\mathbf{A}^{Q'}|^{2p} \cdot |\mathbf{A}^{Y'}|^{2r}$. Again $(m-p-r, p, r)$ are nonnegative integers.

i.c. There are also other contributions, either those with only nonzero vacuum expectation values or with dynamical fields in addition to nonzero vacuum expectation values of scalars, in which $\hat{\mathbf{O}}^{\tilde{\mathbf{I}} \boxplus}$ and $\hat{\mathbf{O}}^{\tilde{\mathbf{N}}_L \boxplus}$ together with all kinds of diagonal terms contribute. Let us repeat again what do the operators $\hat{\mathbf{O}}^{\tilde{\mathbf{I}} \boxplus}$ and $\hat{\mathbf{O}}^{\tilde{\mathbf{N}}_L \boxplus}$, Eq. (6.20), do when they apply on ψ^i . The operators $\hat{\mathbf{O}}^{\tilde{\mathbf{I}} \boxplus}$ transforms ψ^1 into ψ^3 and ψ^2 into ψ^4 . Correspondingly the states ψ^1 and ψ^4 take under the application of $\hat{\mathbf{O}}^{\tilde{\mathbf{I}} \boxplus}$ the role of ψ^2 and ψ^3 , while ψ^2 and ψ^3 take the role of ψ^1 and ψ^4 , all carrying the correspondingly changed eigenvalues of $\tau^{\tilde{\mathbf{I}}^3}$. The operator $\hat{\mathbf{O}}^{\tilde{\mathbf{N}}_L \boxplus}$ transforms ψ^1 into ψ^2 and ψ^3 into ψ^4 . Correspondingly the states ψ^1 and ψ^2 take under the application of $\hat{\mathbf{O}}^{\tilde{\mathbf{N}}_L \boxplus}$ the role of ψ^3 and ψ^4 , while ψ^3 and ψ^4 take the role of ψ^1 and ψ^2 , carrying the correspondingly changed eigenvalues of $\tilde{\mathbf{N}}_L^3$. Either the dynamical fields or the nonzero vacuum expectation values of these scalar fields, $\hat{\mathbf{O}}^{\tilde{\mathbf{I}} \boxplus}$ and $\hat{\mathbf{O}}^{\tilde{\mathbf{N}}_L \boxplus}$, must in diagonal terms appear in the second

power or in $n \times$ the second power. We easily see that also in such cases the tree level symmetry remains in all orders.

i.c.1. To better understand the contributions in all orders to the diagonal terms, discussing here, let us calculate the contribution of the third order corrections either from the loop or from the nonzero vacuum expectation values to the diagonal matrix elements $\langle \psi^i | \dots | \psi^i \rangle$ under the assumption that $\mathbf{a}^\alpha = 0$. Let us evaluate the contributions of the operators $\langle \hat{\mathbf{O}}^{\tilde{1}3} \rangle$, $\langle \hat{\mathbf{O}}^{\tilde{N}_L 3} \rangle$, $\langle \hat{\mathbf{O}}^{\tilde{1}\Box} \rangle$ and $\langle \hat{\mathbf{O}}^{\tilde{N}_L \Box} \rangle$ in the third order. We see that $\tilde{\tau}^{\tilde{1}\Box}$ transforms ψ^3 into ψ^1 and ψ^4 into ψ^2 , while $\tilde{\tau}^{\tilde{1}\Box}$ transforms ψ^2 into ψ^4 and ψ^1 into ψ^3 . We see that \tilde{N}_L^{\Box} transforms ψ^2 into ψ^1 and ψ^4 into ψ^3 , while \tilde{N}_L^{\Box} transforms ψ^1 into ψ^2 and ψ^3 into ψ^4 . It then follows that $\{\langle \psi^1 | \text{xxx} | \psi^1 \rangle + \langle \psi^4 | \text{xxx} | \psi^4 \rangle\} - \{\langle \psi^2 | \text{xxx} | \psi^2 \rangle + \langle \psi^3 | \text{xxx} | \psi^3 \rangle\} = 0$, where xxx represent all possible acceptable combination of $\langle \hat{\mathbf{O}}^{\tilde{1}\Box} \rangle$, $\langle \hat{\mathbf{O}}^{\tilde{N}_L \Box} \rangle$ and the diagonal terms $\langle \hat{\mathbf{O}}^{\tilde{1}3} \rangle$ and $\langle \hat{\mathbf{O}}^{\tilde{N}_L 3} \rangle$. One namely obtains that the contribution of $\{\langle \psi^1 | \text{xxx} | \psi^1 \rangle + \langle \psi^4 | \text{xxx} | \psi^4 \rangle\} = \{|\langle \tilde{\mathbf{A}}^{\tilde{1}\Box} \rangle|^2 [-2(\tilde{\mathbf{a}}_1 + \tilde{\mathbf{a}}_2) + (\tilde{\mathbf{a}}_1 - \tilde{\mathbf{a}}_2)] + |\langle \tilde{\mathbf{A}}^{\tilde{N}_L \Box} \rangle|^2 [-2(\tilde{\mathbf{a}}_1 + \tilde{\mathbf{a}}_2) - (\tilde{\mathbf{a}}_1 - \tilde{\mathbf{a}}_2)] + (-\tilde{\mathbf{a}}_1 + \tilde{\mathbf{a}}_2)^3\} + |\langle \tilde{\mathbf{A}}^{\tilde{1}\Box} \rangle|^2 [2(\tilde{\mathbf{a}}_1 + \tilde{\mathbf{a}}_2) - (\tilde{\mathbf{a}}_1 - \tilde{\mathbf{a}}_2)] + |\langle \tilde{\mathbf{A}}^{\tilde{N}_L \Box} \rangle|^2 [2(\tilde{\mathbf{a}}_1 + \tilde{\mathbf{a}}_2) + (\tilde{\mathbf{a}}_1 - \tilde{\mathbf{a}}_2)] + (\tilde{\mathbf{a}}_1 + \tilde{\mathbf{a}}_2)^3\} = 0$, and for $\{\langle \psi^2 | \text{xxx} | \psi^2 \rangle + \langle \psi^3 | \text{xxx} | \psi^3 \rangle\}$ one obtains $\{|\langle \tilde{\mathbf{A}}^{\tilde{1}\Box} \rangle|^2 [-2(\tilde{\mathbf{a}}_1 - \tilde{\mathbf{a}}_2) + (\tilde{\mathbf{a}}_1 + \tilde{\mathbf{a}}_2)] + |\langle \tilde{\mathbf{A}}^{\tilde{N}_L \Box} \rangle|^2 [-2(\tilde{\mathbf{a}}_1 - \tilde{\mathbf{a}}_2) - (\tilde{\mathbf{a}}_1 + \tilde{\mathbf{a}}_2)] + (-\tilde{\mathbf{a}}_1 - \tilde{\mathbf{a}}_2)^3\} + |\langle \tilde{\mathbf{A}}^{\tilde{1}\Box} \rangle|^2 [2(\tilde{\mathbf{a}}_1 - \tilde{\mathbf{a}}_2) - (\tilde{\mathbf{a}}_1 + \tilde{\mathbf{a}}_2)] + |\langle \tilde{\mathbf{A}}^{\tilde{N}_L \Box} \rangle|^2 [2(\tilde{\mathbf{a}}_1 - \tilde{\mathbf{a}}_2) + (\tilde{\mathbf{a}}_1 + \tilde{\mathbf{a}}_2)] + (\tilde{\mathbf{a}}_1 - \tilde{\mathbf{a}}_2)^3\} = 0$. Also the dynamical fields keep the tree level symmetry of mass matrices. To prove one only must replace in the above calculation $|\langle \tilde{\mathbf{A}}^{\tilde{1}\Box} \rangle|^2$ by $|\tilde{\mathbf{A}}^{\tilde{1}\Box}|^2$ and $|\langle \tilde{\mathbf{A}}^{\tilde{N}_L \Box} \rangle|^2$ by $|\tilde{\mathbf{A}}^{\tilde{N}_L \Box}|^2$.

To the diagonal terms the three singlets contribute in absolute squared values $(|\mathbf{A}^Q|^2, |\mathbf{A}^{Q'}|^2, |\mathbf{A}^{Y'}|^2)$, each on a power, which depend on the order of corrections. This makes all the diagonal matrix elements, $\langle \psi^1 | \dots | \psi^1 \rangle$, $\langle \psi^2 | \dots | \psi^2 \rangle$, $\langle \psi^3 | \dots | \psi^3 \rangle$ and $\langle \psi^4 | \dots | \psi^4 \rangle$, dependent on the family member quantum numbers.

Such behaviour of matrix elements remains unchanged in all orders of corrections, either due to loops of dynamical fields or due to repetitions of nonzero vacuum expectation values. The reason is in the fact that the operators $\langle \hat{\mathbf{O}}^{\tilde{1}\Box} \rangle$ and $\langle \hat{\mathbf{O}}^{\tilde{N}_L \Box} \rangle$ exchange the role of the states in the way that the odd power of diagonal contributions to the diagonal matrix elements always keep the symmetry $\{\langle \psi^1 | \hat{\mathbf{U}} | \psi^1 \rangle + \langle \psi^4 | \hat{\mathbf{U}} | \psi^4 \rangle\} - \{\langle \psi^2 | \hat{\mathbf{U}} | \psi^2 \rangle + \langle \psi^3 | \hat{\mathbf{U}} | \psi^3 \rangle\} = 0$.

These proves the statement that *corrections in all orders keep the symmetry of the tree level diagonal terms in the case that $\mathbf{a}^\alpha = 0$.*

ii. Let us look at matrix element $\langle \psi^1 | \dots | \psi^3 \rangle$ and $\langle \psi^2 | \dots | \psi^4 \rangle$ in Eq. (6.22), where we have on the tree level $\langle 1|x|3 \rangle = \langle 2|x|4 \rangle$ and $\langle 3|x|1 \rangle = \langle 4|x|2 \rangle = \langle 1|x|3 \rangle^\dagger$. We again simplify the notation $\langle \psi^i | \dots | \psi^j \rangle$ into $\langle i | \dots | j \rangle$. The two matrix elements — $\langle 1|x|3 \rangle$, $\langle 2|x|4 \rangle$ — are on the tree level denoted by $\langle \tilde{\mathbf{A}}^{\tilde{1}\Box} \rangle$, while $\langle 3|x|1 \rangle$ and $\langle 4|x|2 \rangle$ are denoted by $\langle \tilde{\mathbf{A}}^{\tilde{1}\Box} \rangle$.

We have to prove that corrections, either of the loops kind or of the repetitions of the nonzero vacuum expectation values or of both kinds in any order keeps the symmetry of the tree level.

ii.a. Let us start with the corrections in which besides $\langle \tilde{\mathbf{A}}^{\dagger\Box} \rangle$ in the first power only $\langle \tilde{\mathbf{A}}^{\dagger 3} \rangle = \tilde{\mathbf{a}}_1$ and $\langle \tilde{\mathbf{A}}^{\dagger 1,3} \rangle = \tilde{\mathbf{a}}_2$ contribute, the last two together appear in an even power so that all three together contribute in an odd power.

The contribution of $\langle 1|x|1 \rangle^{2k+1} = (-\tilde{\mathbf{a}}_1 + \tilde{\mathbf{a}}_2)^{2k+1}$ in the $(2k+1)^{\text{th}}$ order is up to a sign equal to $\langle 4|x|4 \rangle^{2k+1} = (\tilde{\mathbf{a}}_1 + \tilde{\mathbf{a}}_2)^{2k+1}$, where k is a nonnegative integer, while the contribution of $\langle 2|x|2 \rangle^{2k+1} = (-\tilde{\mathbf{a}}_1 - \tilde{\mathbf{a}}_2)^{2k+1}$ is up to a sign equal to $\langle 3|x|3 \rangle^{2k+1} = (\tilde{\mathbf{a}}_1 - \tilde{\mathbf{a}}_2)^{2k+1}$. In each of the matrix elements, either $\langle 1|\dots|3 \rangle$ or $\langle 2|\dots|4 \rangle$, both factors together, $(-\tilde{\mathbf{a}}_1 + \tilde{\mathbf{a}}_2)^m (\tilde{\mathbf{a}}_1 - \tilde{\mathbf{a}}_2)^n$ in the case $\langle 1|\dots|3 \rangle$ and $(-\tilde{\mathbf{a}}_1 - \tilde{\mathbf{a}}_2)^m (\tilde{\mathbf{a}}_1 + \tilde{\mathbf{a}}_2)^n$ in the case $\langle 2|\dots|4 \rangle$, with $(m+n)$ an even nonnegative integer (since together with $\langle \tilde{\mathbf{A}}^{\dagger\Box} \rangle$ must be of an odd integer corrections to take care of the left/right nature of matrix elements) one must make the sum over all the terms contributing to corrections of the order $(m+n+1)$. It is not difficult to see that the contribution to $\langle 1|\dots|3 \rangle$ is in any order of corrections equal to the contributions to the same order of corrections to $\langle 2|\dots|4 \rangle$.

ii.a.1. To illustrate the same contribution in each order of corrections to $\langle 1|\dots|3 \rangle$ and to $\langle 2|\dots|4 \rangle$ let us calculate, let say, the third order corrections. The contribution of the third order to $\langle 1|xxx|3 \rangle$ is $-\frac{1}{3!} \langle \tilde{\mathbf{A}}^{\dagger\Box} \rangle \{(\tilde{\mathbf{a}}_1 + \tilde{\mathbf{a}}_2)^2 + (\tilde{\mathbf{a}}_1 - \tilde{\mathbf{a}}_2)^2 - (\tilde{\mathbf{a}}_1 - \tilde{\mathbf{a}}_2)(\tilde{\mathbf{a}}_1 + \tilde{\mathbf{a}}_2)\}$ and the contribution of the third order to $\langle 2|xxx|4 \rangle$ is $-\frac{1}{3!} \langle \tilde{\mathbf{A}}^{\dagger\Box} \rangle \{(\tilde{\mathbf{a}}_1 - \tilde{\mathbf{a}}_2)^2 + (\tilde{\mathbf{a}}_1 + \tilde{\mathbf{a}}_2)^2 - (\tilde{\mathbf{a}}_1 + \tilde{\mathbf{a}}_2)(\tilde{\mathbf{a}}_1 - \tilde{\mathbf{a}}_2)\}$, that is the contributions in the third order of $\langle 1|xxx|3 \rangle$ and $\langle 2|xxx|4 \rangle$ are the same.

ii.b. One can repeat the calculations with $\langle \tilde{\mathbf{A}}^{\dagger\Box} \rangle$ and the dynamical fields $\tilde{\mathbf{A}}^{\dagger\Box}$ and $\tilde{\mathbf{A}}^{\dagger\Box}$, with or without the diagonal nonzero vacuum expectation values. In all cases all the contributions keep the symmetry on the tree level due to the above discussed properties of the diagonal terms. All the dynamical terms must namely appear in absolute values squared in order to contribute to the mass matrices, as shown in Fig. 6.1. To the diagonal terms the three singlets contribute in absolute squared values $(|\mathbf{A}^Q|^2, |\mathbf{A}^{Q'}|^2, |\mathbf{A}^{Y'}|^2)$, each on some power, depending on the order of corrections. This makes the matrix element $\langle 1|\dots|3 \rangle$ and $\langle 2|\dots|4 \rangle$, $\langle 3|\dots|1 \rangle$ and $\langle 4|\dots|2 \rangle$, dependent on the family members quantum numbers.

In all cases all the contributions keep the symmetry on the tree level.

ii.c. The Hermitian conjugate values $\langle 1|\dots|3 \rangle^\dagger = \langle 2|\dots|4 \rangle^\dagger$ have the transformed value of $\langle \tilde{\mathbf{A}}^{\dagger\Box} \rangle$, that means that the value is $\langle \tilde{\mathbf{A}}^{\dagger\Box} \rangle$, provided that the diagonal matrix elements of the mass matrix are real, keeping the symmetry of the matrix elements $\langle 1|\dots|3 \rangle^\dagger = \langle 2|\dots|4 \rangle^\dagger$ in all orders of corrections.

These proves the statement that *corrections in all orders keep the symmetry of the tree level of the off-diagonal terms $\langle 1|\dots|3 \rangle$ and $\langle 2|\dots|4 \rangle$ and of their Hermitian conjugated matrix elements in the case that $\mathbf{a}^\alpha = 0$.*

iii. Let us look at matrix element $\langle 1|\dots|2 \rangle$ and $\langle 3|\dots|4 \rangle$ in Eq. (6.22), where we have on the tree level $\langle 1|x|2 \rangle = \langle 3|x|4 \rangle$. These two matrix elements are on the tree level denoted by $\langle \tilde{\mathbf{A}}^{\dagger 1\Box} \rangle$. We have to prove that corrections, either the loop corrections or the repetitions of the nonzero vacuum expectation values or both kinds of corrections, in any order, keep the $\tilde{\text{SU}}(2) \times \tilde{\text{SU}}(2) \times \text{U}(1)$ symmetry of the tree level.

The proof for the symmetry of these matrix elements is carried out in equivalent way to the proof under **ii.**

iii.a. Let us start with the corrections in which besides $\langle \tilde{\mathbf{A}}^{\tilde{\mathbf{N}}_{\perp\Box}} \rangle$ in the first power also only $\langle \tilde{\mathbf{A}}^{\tilde{\mathbf{I}}^3} \rangle = \tilde{\mathbf{a}}_1$ and $\langle \tilde{\mathbf{A}}^{\tilde{\mathbf{N}}_{\perp 3}} \rangle = \tilde{\mathbf{a}}_2$ contribute. The sum of powers of the last two \mathbf{a} must be even, so that a correction would be of an odd power due to the left/right transitions.

Again the contributions of both diagonal terms, $\langle 1|x|1 \rangle$ and $\langle 4|x|4 \rangle$, in any power — $\langle 1|x|1 \rangle^{2k+1} = (-\tilde{\mathbf{a}}_1 + \tilde{\mathbf{a}}_2)^{2k+1}$ and $\langle 4|x|4 \rangle^{2k+1} = (\tilde{\mathbf{a}}_1 + \tilde{\mathbf{a}}_2)^{2k+1}$, where k is a nonnegative integer — differ only up to a sign when they appear in an odd power and are equal when they appear in an even power. These is true also for the contributions of $\langle 2|x|2 \rangle$ and $\langle 3|x|3 \rangle$ since $\langle 2|x|2 \rangle^{2k+1} = (-\tilde{\mathbf{a}}_1 - \tilde{\mathbf{a}}_2)^{2k+1}$ is up to a sign equal to $\langle 3|x|3 \rangle^{2k+1} = (\tilde{\mathbf{a}}_1 - \tilde{\mathbf{a}}_2)^{2k+1}$. If they appear with an even power, they are equal. In each of the $(m+n+1)^{\text{th}}$ order corrections to the matrix elements, either $\langle 1|.....|2 \rangle$ or $\langle 3|.....|4 \rangle$, where $(-\tilde{\mathbf{a}}_1 + \tilde{\mathbf{a}}_2)^m (-\tilde{\mathbf{a}}_1 - \tilde{\mathbf{a}}_2)^n$ contribute to $\langle 1|.....|2 \rangle$ and $(\tilde{\mathbf{a}}_1 - \tilde{\mathbf{a}}_2)^m (\tilde{\mathbf{a}}_1 + \tilde{\mathbf{a}}_2)^n$ contribute to $\langle 3|.....|4 \rangle$, the two contributions are again equal, since both m and n are even nonnegative integers.

iii.a.1. Let us, as an example, calculate the fifth order corrections to the tree level contributions of $\langle 1|x|2 \rangle = \langle \tilde{\mathbf{A}}^{\tilde{\mathbf{N}}_{\perp\Box}} \rangle$. The contribution of the fifth order $\langle 1|xxxxx|2 \rangle$ to $\langle 1|x|2 \rangle$ is $\frac{1}{5!} \langle \tilde{\mathbf{A}}^{\tilde{\mathbf{N}}_{\perp\Box}} \rangle \{(-\tilde{\mathbf{a}}_1 - \tilde{\mathbf{a}}_2)^4 + (-\tilde{\mathbf{a}}_1 + \tilde{\mathbf{a}}_2)^4 + 3(-\tilde{\mathbf{a}}_1 + \tilde{\mathbf{a}}_2)(-\tilde{\mathbf{a}}_1 - \tilde{\mathbf{a}}_2)^3 + 6(-\tilde{\mathbf{a}}_1 + \tilde{\mathbf{a}}_2)^2(-\tilde{\mathbf{a}}_1 - \tilde{\mathbf{a}}_2)^2 + 3(-\tilde{\mathbf{a}}_1 + \tilde{\mathbf{a}}_2)^3(-\tilde{\mathbf{a}}_1 - \tilde{\mathbf{a}}_2)\}$, and the contribution of the fifth order $\langle 3|xxxxx|4 \rangle$ to $\langle 3|x|4 \rangle$ is $\frac{1}{5!} \langle \tilde{\mathbf{A}}^{\tilde{\mathbf{N}}_{\perp\Box}} \rangle \{(\tilde{\mathbf{a}}_1 + \tilde{\mathbf{a}}_2)^4 + (\tilde{\mathbf{a}}_1 - \tilde{\mathbf{a}}_2)^4 + 3(\tilde{\mathbf{a}}_1 - \tilde{\mathbf{a}}_2)(\tilde{\mathbf{a}}_1 + \tilde{\mathbf{a}}_2)^3 + 6(\tilde{\mathbf{a}}_1 - \tilde{\mathbf{a}}_2)^2(\tilde{\mathbf{a}}_1 + \tilde{\mathbf{a}}_2)^2 + 3(\tilde{\mathbf{a}}_1 - \tilde{\mathbf{a}}_2)^3(\tilde{\mathbf{a}}_1 + \tilde{\mathbf{a}}_2)\}$, which is equal to the contribution of the fifth order in the case of $\langle 1|xxxxx|2 \rangle$.

iii.b. One can repeat the calculations with dynamical fields $(\tilde{\mathbf{A}}^{\tilde{\mathbf{N}}_{\perp\Box}}, \tilde{\mathbf{A}}^{\tilde{\mathbf{N}}_{\perp\Box}})$ in all orders and with $\langle \tilde{\mathbf{A}}^{\tilde{\mathbf{I}}^3} \rangle$ and with the diagonal nonzero vacuum expectation values and with the diagonal dynamical terms, paying attention that the dynamical fields contribute to masses of any of the family members only if they appear in pairs.

To the diagonal terms the three singlets $(\mathbf{A}^Q, \mathbf{A}^{Q'}, \mathbf{A}^{Y'})$ contribute in the absolute squared values $(|\mathbf{A}^Q|^2, |\mathbf{A}^{Q'}|^2, |\mathbf{A}^{Y'}|^2)$, each on a power, which depends on the order of corrections.

In all cases all the contributions keep the symmetry on the tree level.

iii.c. The proof is valid also for $\langle 2|.....|1 \rangle = (\langle 1|.....|2 \rangle)^\dagger$ and $\langle 4|.....|3 \rangle = (\langle 3|.....|4 \rangle)^\dagger$ in any order of corrections. Namely, if diagonal mass matrix elements are real then in the matrix elements $\langle 2|.....|1 \rangle$ only $\langle \tilde{\mathbf{A}}^{\tilde{\mathbf{N}}_{\perp\Box}} \rangle$ of the matrix element $\langle 1|.....|2 \rangle$ must be replaced by $\langle \tilde{\mathbf{A}}^{\tilde{\mathbf{N}}_{\perp\Box}} \rangle$.

These proves the statement that *corrections in all orders keep the symmetry of the tree level off-diagonal terms $\langle 1|.....|2 \rangle$ and $\langle 3|.....|4 \rangle$ in the case that $\mathbf{a}^\alpha = 0$.*

iv. It remains to check the matrix elements $\langle 1|.....|4 \rangle$, $\langle 2|.....|3 \rangle$, $\langle 3|.....|2 \rangle$ and $\langle 4|.....|1 \rangle$ in all orders of corrections. The matrix elements on the third power, $\langle 1|xxx|4 \rangle$, $\langle 2|xxx|3 \rangle$, $\langle 3|xxx|2 \rangle$, $\langle 4|xxx|1 \rangle$, appearing in Eqs. (6.21, 6.22), are for $\mathbf{a}^\alpha = 0$ all equal to zero. It is not difficult to prove that these four matrix elements remain zero in all order of loop corrections. The reason is the same as in the above three cases, **i.**, **ii.**, **iii.**

The proof that the symmetry $\tilde{\mathbf{S}}\tilde{\mathbf{U}}(2) \times \tilde{\mathbf{S}}\tilde{\mathbf{U}}(2) \times \mathbf{U}(1)$ of the tree level remains unchanged in all orders of corrections, provided that $\mathbf{a}^\alpha = 0$, is completed.

There are in all these cases the dynamical singlets contributing in the absolute squared values ($|\mathbf{A}^Q|^2$, $|\mathbf{A}^{Q'}|^2$, $|\mathbf{A}^{V'}|^2$ — each on a power, which depend on the order of corrections — which make that all the matrix elements of a mass matrix, except the ($\langle 1|....|4 \rangle$, $\langle 2|....|3 \rangle$, $\langle 3|....|2 \rangle$, $\langle 4|....|1 \rangle$) which remain zero in all orders of corrections, depend on a particular family member.

Mass matrices beyond the tree level if $\mathbf{a}^\alpha \neq 0$ We demonstrated that for $\mathbf{a}^\alpha = 0$ the symmetry of the tree level remains in all orders of corrections, the loops corrections and the repetitions of nonzero vacuum expectation values of all the scalar fields contributing to mass terms, the same as on the tree level, that is $\widetilde{\text{SU}}(2) \times \widetilde{\text{SU}}(2) \times \text{U}(1)$.

Let us denote all corrections to the diagonal terms in all orders, in which the nonzero vacuum expectation values in all orders as well as their dynamical fields in all orders contribute when $\mathbf{a}^\alpha = 0$ as:

$$-(\tilde{\mathbf{a}}_1 + \tilde{\mathbf{a}}_2) := \langle \psi_L^{\alpha 1} | \dots | \psi_R^{\alpha 1} \rangle, -(\tilde{\mathbf{a}}_1 - \tilde{\mathbf{a}}_2) := \langle \psi_L^{\alpha 2} | \dots | \psi_R^{\alpha 2} \rangle, \\ (\tilde{\mathbf{a}}_1 - \tilde{\mathbf{a}}_2) := \langle \psi_L^{\alpha 3} | \dots | \psi_R^{\alpha 3} \rangle, (\tilde{\mathbf{a}}_1 + \tilde{\mathbf{a}}_2) := \langle \psi_L^{\alpha 4} | \dots | \psi_R^{\alpha 4} \rangle.$$

We study for $\mathbf{a}^\alpha \neq 0$ how does the symmetry of the diagonal and the off diagonal matrix elements of the family members mass matrices change with respect to the symmetry on the tree level, presented in Eq. (6.22), in particular for small values of $|\mathbf{a}^\alpha|$ in comparison with the contributions of all the rest of nonzero vacuum expectation values or of dynamical fields.

We discuss diagonal and off diagonal matrix elements separately. The symmetry of all depends on \mathbf{a}^α .

i. Let us start with diagonal terms: $\langle \psi^i | \dots | \psi^i \rangle$.

On the tree level the symmetry is for $\mathbf{a}^\alpha \neq 0$: $\{ \langle \psi^1 | \langle \hat{\mathbf{O}}_{\text{dia}}^\alpha \rangle | \psi^1 \rangle + \langle \psi^4 | \langle \hat{\mathbf{O}}_{\text{dia}}^\alpha \rangle | \psi^4 \rangle \} - \{ \langle \psi^2 | \langle \hat{\mathbf{O}}_{\text{dia}}^\alpha \rangle | \psi^2 \rangle + \{ \langle \psi^3 | \langle \hat{\mathbf{O}}_{\text{dia}}^\alpha \rangle | \psi^3 \rangle \} = 0$.

i.a. Let us evaluate the matrix elements $\langle \psi_L^{\alpha i} | \dots | \psi_R^{\alpha i} \rangle$. Let us denote for a while, just to simplify the derivations, $n_1 = \mathbf{a}^\alpha - (\tilde{\mathbf{a}}_1 + \tilde{\mathbf{a}}_2)$, $n_2 = \mathbf{a}^\alpha - (\tilde{\mathbf{a}}_1 - \tilde{\mathbf{a}}_2)$, $n_3 = \mathbf{a}^\alpha + (\tilde{\mathbf{a}}_1 - \tilde{\mathbf{a}}_2)$, $n_4 = \mathbf{a}^\alpha + (\tilde{\mathbf{a}}_1 + \tilde{\mathbf{a}}_2)$. One finds

$$\begin{aligned} \langle \psi_L^{\alpha 1} | \dots | \psi_R^{\alpha 1} \rangle &= [\mathbf{a}^\alpha - (\tilde{\mathbf{a}}_1 + \tilde{\mathbf{a}}_2)] \\ &- \frac{1}{3!} [(\mathbf{a}^\alpha)^3 - 3(\mathbf{a}^\alpha)^2(\tilde{\mathbf{a}}_1 + \tilde{\mathbf{a}}_2) + 3(\mathbf{a}^\alpha)(\tilde{\mathbf{a}}_1 + \tilde{\mathbf{a}}_2)^2] \\ &+ \frac{1}{5!} [(\mathbf{a}^\alpha)^5 - 5(\mathbf{a}^\alpha)^4(\tilde{\mathbf{a}}_1 + \tilde{\mathbf{a}}_2) + 10(\mathbf{a}^\alpha)^3(\tilde{\mathbf{a}}_1 + \tilde{\mathbf{a}}_2)^2 - 10(\mathbf{a}^\alpha)^2(\tilde{\mathbf{a}}_1 + \tilde{\mathbf{a}}_2)^3 \\ &+ 5(\mathbf{a}^\alpha)(\tilde{\mathbf{a}}_1 + \tilde{\mathbf{a}}_2)^4] - \dots \end{aligned} \quad (6.24)$$

Assuming that $|\mathbf{a}^\alpha| \ll (|\tilde{\mathbf{a}}_1|, |\tilde{\mathbf{a}}_2|)$ it follows

$$\begin{aligned} \langle \psi_L^{\alpha 1} | \dots | \psi_R^{\alpha 1} \rangle &= -(\tilde{\mathbf{a}}_1 + \tilde{\mathbf{a}}_2) + \mathbf{a}^\alpha \left\{ 1 - \frac{3}{3!}(\tilde{\mathbf{a}}_1 + \tilde{\mathbf{a}}_2)^2 + \frac{5}{5!}(\tilde{\mathbf{a}}_1 + \tilde{\mathbf{a}}_2)^4 \right. \\ &\left. - \frac{7}{7!}(\tilde{\mathbf{a}}_1 + \tilde{\mathbf{a}}_2)^6 + \dots \right\}. \end{aligned} \quad (6.25)$$

Correspondingly we obtain for $\langle \psi_L^{\alpha 4} | \dots | \psi_R^{\alpha 4} \rangle$ in the limit that $|\mathbf{a}^\alpha| \ll (|\tilde{\mathbf{a}}_1|, |\tilde{\mathbf{a}}_2|)$

$$\begin{aligned} \langle \psi_L^{\alpha 4} | \dots | \psi_R^{\alpha 4} \rangle &= +(\tilde{\mathbf{a}}_1 + \tilde{\mathbf{a}}_2) + \mathbf{a}^\alpha \left\{ 1 - \frac{3}{3!}(\tilde{\mathbf{a}}_1 + \tilde{\mathbf{a}}_2)^2 + \frac{5}{5!}(\tilde{\mathbf{a}}_1 + \tilde{\mathbf{a}}_2)^4 \right. \\ &\left. - \frac{7}{7!}(\tilde{\mathbf{a}}_1 + \tilde{\mathbf{a}}_2)^6 + \dots \right\}. \end{aligned} \quad (6.26)$$

For $\langle \psi_L^{\alpha 2} | \dots | \psi_R^{\alpha 2} \rangle$ one obtains in the limit that $|\mathbf{a}^\alpha| \ll (|\tilde{\mathbf{a}}_1|, |\tilde{\mathbf{a}}_2|)$

$$\begin{aligned} \langle \psi_L^{\alpha 2} | \dots | \psi_R^{\alpha 2} \rangle = & -(\tilde{\mathbf{a}}_1 - \tilde{\mathbf{a}}_2) + \mathbf{a}^\alpha \left\{ 1 - \frac{3}{3!}(\tilde{\mathbf{a}}_1 - \tilde{\mathbf{a}}_2)^2 + \frac{5}{5!}(\tilde{\mathbf{a}}_1 - \tilde{\mathbf{a}}_2)^4 \right. \\ & \left. - \frac{7}{7!}(\tilde{\mathbf{a}}_1 - \tilde{\mathbf{a}}_2)^6 + \dots \right\} \end{aligned} \quad (6.27)$$

And for $\langle \psi_L^{\alpha 2} | \dots | \psi_R^{\alpha 2} \rangle$ one obtains in the limit that $|\mathbf{a}^\alpha| \ll (|\tilde{\mathbf{a}}_1|, |\tilde{\mathbf{a}}_2|)$ the expression

$$\begin{aligned} \langle \psi_L^{\alpha 3} | \dots | \psi_R^{\alpha 3} \rangle = & -(\tilde{\mathbf{a}}_1 - \tilde{\mathbf{a}}_2) + \mathbf{a}^\alpha \left\{ 1 - \frac{3}{3!}(\tilde{\mathbf{a}}_1 - \tilde{\mathbf{a}}_2)^2 + \frac{5}{5!}(\tilde{\mathbf{a}}_1 - \tilde{\mathbf{a}}_2)^4 \right. \\ & \left. - \frac{7}{7!}(\tilde{\mathbf{a}}_1 - \tilde{\mathbf{a}}_2)^6 + \dots \right\}. \end{aligned} \quad (6.28)$$

Finally we obtain

$$\begin{aligned} (\langle \psi_L^{\alpha 1} | \dots | \psi_R^{\alpha 1} \rangle + \langle \psi_L^{\alpha 4} | \dots | \psi_R^{\alpha 4} \rangle) - \\ (\langle \psi_L^{\alpha 2} | \dots | \psi_R^{\alpha 2} \rangle + \langle \psi_L^{\alpha 3} | \dots | \psi_R^{\alpha 3} \rangle) = \\ 4 \mathbf{a}^\alpha \tilde{\mathbf{a}}_1 \tilde{\mathbf{a}}_2 \left\{ 1 - \frac{1}{12}[(\tilde{\mathbf{a}}_1)^2 + (\tilde{\mathbf{a}}_2)^2] \right\} + \dots \end{aligned} \quad (6.29)$$

The term with $(\mathbf{a}^\alpha)^2$ drops away. For small $|\mathbf{a}^\alpha|$ the term $(\mathbf{a}^\alpha)^3$ might be negligible.

It is obvious that for $\mathbf{a}^\alpha \neq 0$ the diagonal matrix elements do not keep the tree level symmetry of mass matrices (which is $(\langle \psi_L^{\alpha 1} | \dots | \psi_R^{\alpha 1} \rangle + \langle \psi_L^{\alpha 4} | \dots | \psi_R^{\alpha 4} \rangle) - (\langle \psi_L^{\alpha 2} | \dots | \psi_R^{\alpha 2} \rangle + \langle \psi_L^{\alpha 3} | \dots | \psi_R^{\alpha 3} \rangle) = 0$). But one sees as well that the contributions of higher terms to asymmetry are getting smaller and smaller and for $|\mathbf{a}^\alpha| \ll (|\tilde{\mathbf{a}}_1|, |\tilde{\mathbf{a}}_2|)$ and for $(|\tilde{\mathbf{a}}_1|, |\tilde{\mathbf{a}}_2|) < 1$, the first term is dominant and the non symmetry can be evaluated.

ii. Let us look at the matrix element $\langle 1 | \dots | 3 \rangle$ and $\langle 2 | \dots | 4 \rangle$ in all orders of corrections in the case that $\mathbf{a}^\alpha = 0$ (on the tree level, Eq. (6.22), $\langle 1 | \chi | 3 \rangle = \langle 2 | \chi | 4 \rangle = \langle 3 | \chi | 1 \rangle^\dagger = \langle 4 | \chi | 2 \rangle^\dagger$) and let in this case $\langle \tilde{\mathbf{A}}^{\dagger \square} \rangle$ represent the matrix elements $i \langle 1 | \dots | 3 \rangle$ and $\langle 2 | \dots | 4 \rangle$ in both cases in all orders of corrections. We namely showed that in this case the matrix element $\langle 1 | \dots | 3 \rangle$ is equal to $\langle 2 | \dots | 4 \rangle = \langle \tilde{\mathbf{A}}^{\dagger \square} \rangle$.

We now allow $\mathbf{a}^\alpha \neq 0$.

Taking into account that in the case that \mathbf{a}^α is zero $\langle \tilde{\mathbf{A}}^{\dagger \square} \rangle$ includes all the corrections in all orders and that also $\tilde{\mathbf{a}}_2$ includes the corrections in all orders, we find

$$\begin{aligned} (\langle \psi_L^{\alpha 1} | \dots | \psi_R^{\alpha 3} \rangle - \langle \psi_L^{\alpha 2} | \dots | \psi_R^{\alpha 4} \rangle) = \\ \langle \tilde{\mathbf{A}}^{\dagger \square} \rangle \left(1 + \frac{8}{3} \mathbf{a}^\alpha \tilde{\mathbf{a}}_2 \left\{ 1 - \frac{2}{5}(\tilde{\mathbf{a}}_2)^2 + \dots \right\} \right). \end{aligned} \quad (6.30)$$

It is obvious that for $\mathbf{a}^\alpha \neq 0$ also the non diagonal matrix elements do not keep the tree level symmetry of mass matrices ($\langle \psi_L^{\alpha 1} | \dots | \psi_R^{\alpha 3} \rangle - \langle \psi_L^{\alpha 2} | \dots | \psi_R^{\alpha 4} \rangle = 0$, which is not zero any longer). But one sees as well that the contributions of higher terms to asymmetry are getting smaller and smaller and for $|\mathbf{a}^\alpha| \ll |\tilde{\mathbf{a}}_2|$,

for $|\tilde{\mathbf{a}}_2| < 1$, the first term in corrections is dominant. One can correspondingly evaluate the amount of non symmetry.

iii. Let us look also at the matrix element $\langle 1|....|2 \rangle$ and $\langle 3|....|4 \rangle$, first in all orders of corrections in the case that $\mathbf{a}^\alpha = 0$ (on the tree level, Eq. (6.22), $\langle 1|x|2 \rangle = \langle 3|x|4 \rangle = \langle 2|x|1 \rangle^\dagger = \langle 4|x|3 \rangle^\dagger$) and let in this case $\langle \tilde{\mathbf{A}}^{\tilde{\mathbf{N}}_L \boxplus} \rangle$ represent the matrix elements $\langle 1|....|2 \rangle$ and $\langle 3|....|4 \rangle$ in all orders of corrections. We namely showed that in the case that $\mathbf{a}^\alpha = 0$ the matrix element $\langle 1|....|2 \rangle$ is equal to $\langle 3|....|4 \rangle = \langle \tilde{\mathbf{A}}^{\tilde{\mathbf{I}} \boxplus} \rangle$.

We now allow $\mathbf{a}^\alpha \neq 0$.

Taking into account that for $\mathbf{a}^\alpha = 0$ the matrix element $\langle \tilde{\mathbf{A}}^{\tilde{\mathbf{N}}_L \boxplus} \rangle$ includes corrections in all orders and that also $\tilde{\mathbf{a}}_2$ includes in this case corrections in all orders, one finds

$$\begin{aligned} & (\langle \psi_L^{\alpha 1} | \dots | \psi_R^{\alpha 2} \rangle - \langle \psi_L^{\alpha 3} | \dots | \psi_R^{\alpha 4} \rangle) = \\ & \langle \tilde{\mathbf{A}}^{\tilde{\mathbf{N}}_L \boxplus} \rangle (1 + \frac{8}{3} \mathbf{a}^\alpha \tilde{\mathbf{a}}_1 \{1 - \frac{2}{5} (\tilde{\mathbf{a}}_1)^2 + \dots\}) . \end{aligned} \quad (6.31)$$

It is obvious that for $\mathbf{a}^\alpha \neq 0$ also these non diagonal matrix elements do not keep the tree level symmetry of mass matrices ($\langle \psi_L^{\alpha 1} | \dots | \psi_R^{\alpha 3} \rangle - \langle \psi_L^{\alpha 2} | \dots | \psi_R^{\alpha 4} \rangle = 0$ is no longer the case). But one sees as well that the contributions of higher terms to asymmetry are getting smaller and smaller and for $|\mathbf{a}^\alpha| \ll |\tilde{\mathbf{a}}_1|$ and for $|\tilde{\mathbf{a}}_1| < 1$, the first term in corrections is dominant and the non symmetry, the difference $\langle \psi_L^{\alpha 1} | \dots | \psi_R^{\alpha 3} \rangle - \langle \psi_L^{\alpha 2} | \dots | \psi_R^{\alpha 4} \rangle$ can be evaluated.

iv. It remains to check the matrix elements $\langle 1|....|4 \rangle$, $\langle 2|....|3 \rangle$, $\langle 3|....|2 \rangle$ and $\langle 4|....|1 \rangle$. The matrix elements which are nonzero only in the third order of corrections, ($\langle 1|x|4 \rangle = 0 = \langle 2|x|3 \rangle = 0 = \langle 3|x|2 \rangle = \langle 4|x|1 \rangle$, the first nonzero terms are $\langle 1|xxx|4 \rangle$, $\langle 2|xxx|3 \rangle$, $\langle 3|xxx|2 \rangle$, $\langle 4|xxx|1 \rangle$, appearing in Eqs. (6.21, 6.22), which are for $\mathbf{a}^\alpha = 0$ all equal to zero in all orders of corrections.

We again take into account that for $\mathbf{a}^\alpha = 0$ the matrix element $\langle \tilde{\mathbf{A}}^{\tilde{\mathbf{I}} \boxplus} \rangle$ and $\langle \tilde{\mathbf{A}}^{\tilde{\mathbf{N}}_L \boxplus} \rangle$ include the corrections in all orders and that also $\tilde{\mathbf{a}}_1$ and $\tilde{\mathbf{a}}_2$ include the corrections in all orders. We find when $\mathbf{a}^\alpha \neq 0$

$$\begin{aligned} & \frac{\langle \psi_L^{\alpha 1} | \dots | \psi_R^{\alpha 4} \rangle}{\langle \tilde{\mathbf{A}}^{\tilde{\mathbf{I}} \boxplus} \rangle \langle \tilde{\mathbf{A}}^{\tilde{\mathbf{N}}_L \boxplus} \rangle} = \frac{\langle \psi_L^{\alpha 2} | \dots | \psi_R^{\alpha 3} \rangle}{\langle \tilde{\mathbf{A}}^{\tilde{\mathbf{I}} \boxplus} \rangle \langle \tilde{\mathbf{A}}^{\tilde{\mathbf{N}}_L \boxplus} \rangle} = \\ & \frac{\langle \psi_L^{\alpha 4} | \dots | \psi_R^{\alpha 1} \rangle}{\langle \tilde{\mathbf{A}}^{\tilde{\mathbf{I}} \boxplus} \rangle \langle \tilde{\mathbf{A}}^{\tilde{\mathbf{N}}_L \boxplus} \rangle} = \frac{\langle \psi_L^{\alpha 3} | \dots | \psi_R^{\alpha 2} \rangle}{\langle \tilde{\mathbf{A}}^{\tilde{\mathbf{I}} \boxplus} \rangle \langle \tilde{\mathbf{A}}^{\tilde{\mathbf{N}}_L \boxplus} \rangle} = \\ & -\mathbf{a}^\alpha \{1 - \frac{3}{10} [(\tilde{\mathbf{a}}_1)^2 + (\tilde{\mathbf{a}}_2)^2] + \dots\} . \end{aligned} \quad (6.32)$$

One sees that these off diagonal matrix elements keep the relations from Eq. (6.22) at least in the lowest corrections.

We demonstrated that the matrix elements of the mass matrix of Eq. (6.22) do not keep the symmetry of the tree level in all orders of corrections if $\mathbf{a}^\alpha \neq 0$, but the changes can in the case that $(|\mathbf{a}^\alpha|, |\tilde{\mathbf{a}}_1|, |\tilde{\mathbf{a}}_2|)$ are small in comparison with unity be estimated.

Mass matrices beyond the tree level if $\mathbf{a}^\alpha \neq 0$, while $\tilde{\mathbf{a}}_1 = 0 = \tilde{\mathbf{a}}_2$ One can easily see that the mass matrix of Eq. (6.22) keeps the symmetry in all orders of corrections also if $\mathbf{a}^\alpha \neq 0$ and $\tilde{\mathbf{a}}_1 = 0 = \tilde{\mathbf{a}}_2$.

One obtains in this case for the diagonal terms $\langle \psi_L^{\alpha i} | \hat{U} | \psi_R^{\alpha i} \rangle$, for each of four families ($i = (1, 2, 3, 4)$) the expression

$$\begin{aligned}
 & \langle \psi_L^{\alpha i} | \hat{U} | \psi_R^{\alpha i} \rangle = \mathbf{a}^\alpha - \\
 & \frac{1}{3!} \{ (\mathbf{a}^\alpha)^3 + \mathbf{a}^\alpha (| \langle \tilde{\mathbf{A}}^{\tilde{1}\Box} \rangle |^2 + | \langle \tilde{\mathbf{A}}^{\tilde{N}_L\Box} \rangle |^2 + |\mathbf{A}^\alpha|^2 + |\tilde{\mathbf{A}}^{\tilde{1}3}|^2 + |\tilde{\mathbf{A}}^{\tilde{1}\Box}|^2 + \\
 & |\tilde{\mathbf{A}}^{\tilde{N}_L3}|^2 + |\tilde{\mathbf{A}}^{\tilde{N}_L\Box}|^2) \} + \\
 & \frac{1}{5!} \{ (\mathbf{a}^\alpha)^5 + (\mathbf{a}^\alpha)^3 (| \langle \tilde{\mathbf{A}}^{\tilde{1}\Box} \rangle |^2 + | \langle \tilde{\mathbf{A}}^{\tilde{N}_L\Box} \rangle |^2 + |\mathbf{A}^\alpha|^2 + |\tilde{\mathbf{A}}^{\tilde{1}3}|^2 + |\tilde{\mathbf{A}}^{\tilde{1}\Box}|^2 + \\
 & |\tilde{\mathbf{A}}^{\tilde{N}_L3}|^2 + |\tilde{\mathbf{A}}^{\tilde{N}_L\Box}|^2) + \\
 & \mathbf{a}^\alpha (| \langle \tilde{\mathbf{A}}^{\tilde{1}\Box} \rangle |^4 + | \langle \tilde{\mathbf{A}}^{\tilde{N}_L\Box} \rangle |^4 + |\mathbf{A}^\alpha|^4 + \\
 & |\tilde{\mathbf{A}}^{\tilde{1}3}|^4 + |\tilde{\mathbf{A}}^{\tilde{1}\Box}|^4 + |\tilde{\mathbf{A}}^{\tilde{N}_L3}|^4 + |\tilde{\mathbf{A}}^{\tilde{N}_L\Box}|^4 + \dots + \\
 & | \langle \tilde{\mathbf{A}}^{\tilde{1}\Box} \rangle |^2 | \langle \tilde{\mathbf{A}}^{\tilde{N}_L\Box} \rangle |^2 + \dots) + \dots \} - \\
 & \frac{1}{7!} \{ (\mathbf{a}^\alpha)^7 + (\mathbf{a}^\alpha)^5 (| \langle \tilde{\mathbf{A}}^{\tilde{1}\Box} \rangle |^2 + \dots) + \dots \} + \dots .
 \end{aligned} \tag{6.33}$$

Let us denote the above expression for the diagonal terms $\langle \psi_L^{\alpha i} | \hat{U} | \psi_R^{\alpha i} \rangle$, which takes into account corrections in all orders while assuming $\tilde{\mathbf{a}}_1 = 0 = \tilde{\mathbf{a}}_2$, with $\underline{\mathbf{a}}^\alpha$. (The definition of the scalar fields is presented in Eq. (6.20)).

Let us add that the choice that the third components of the scalar fields $\tilde{\mathbf{A}}^{\tilde{1}}$ and $\tilde{\mathbf{A}}^{\tilde{N}_L}$ have no vacuum expectation values — $\langle \tilde{\mathbf{A}}^{\tilde{1}3} \rangle = \tilde{\mathbf{a}}_1 = 0$, $\langle \tilde{\mathbf{A}}^{\tilde{N}_L3} \rangle = \tilde{\mathbf{a}}_2 = 0$ — does not seem a meaningful choice. Namely, if all the components of the two triplets, $\tilde{\mathbf{A}}^{\tilde{1}}$ and $\tilde{\mathbf{A}}^{\tilde{N}_L}$, influencing the family quantum numbers of the four families, would have no vacuum expectation values, all the families would have the same mass, determined by \mathbf{a}^α and the contributions in all orders of corrections of the dynamical scalar fields, $\tilde{\mathbf{A}}^{\tilde{1}}$, $\tilde{\mathbf{A}}^{\tilde{N}_L}$ and $\mathbf{a}^\alpha = \langle \mathbf{A}^\alpha \rangle$ and the dynamical part of \mathbf{A}^α . Let be added, however, that the choice $\langle \tilde{\mathbf{A}}^{\tilde{1}\Box} \rangle \neq 0$, $\langle \tilde{\mathbf{A}}^{\tilde{N}_L\Box} \rangle \neq 0$ and $\mathbf{a}^\alpha \neq 0$, while $\tilde{\mathbf{a}}_1 = 0 = \tilde{\mathbf{a}}_2$, makes all the matrix elements of the mass matrix, Eq. (6.22), different from zero.

6.3 Conclusions

In the *spin-charge-family* theory to the 4×4 mass matrix of any family member (that is of quarks and leptons — the observed three families namely form in the *spin-charge-family* theory the 3×3 submatrices of these predicted 4×4 mass matrices) the two scalar triplets ($\tilde{\mathbf{A}}_s^{\tilde{1}}$, $\tilde{\mathbf{A}}_s^{\tilde{N}_L}$) and the three scalar singlets (\mathbf{A}_s^Q , $\mathbf{A}_s^{Q'}$, $\mathbf{A}_s^{Y'}$), $s = (7, 8)$, contribute, all with the weak and the hyper charge of the *standard model* higgs ($\pm \frac{1}{2}$, $\mp \frac{1}{2}$, respectively). The first two triplets influence the family quantum numbers, while the last three singlets influence the family members quantum numbers.

The only dependence of the mass matrix on the family member ($\alpha = (u, d, v, e)$) quantum numbers is due to the operators $\gamma^0 \begin{smallmatrix} 78 \\ (\pm) \end{smallmatrix} Q A_{\pm}^Q$, $\gamma^0 \begin{smallmatrix} 78 \\ (\pm) \end{smallmatrix} Q' A_{\pm}^{Q'}$ and $\gamma^0 \begin{smallmatrix} 78 \\ (\pm) \end{smallmatrix} Y' A_{\pm}^{Y'}$. The operator $\gamma^0 \begin{smallmatrix} 78 \\ (\pm) \end{smallmatrix}$, appearing at the contribution of the two triplet scalar fields as well as at the three singlet scalar fields, transforms the right handed members into the left handed ones, or opposite, while the family operators transform a family member of one family into the same family member of another family.

We demonstrate in this paper that the matrix elements of mass matrices 4×4 , predicted by the *spin-charge-family* theory for each family member $\alpha = (u, d, v, e)$, keep the symmetry $\widetilde{SU}(2)_{\widetilde{SO}(4)_{1+3}} \times \widetilde{SU}(2)_{\widetilde{SO}(4)_{\text{weak}}} \times U(1)$ in all orders of corrections under the assumption that either the vacuum expectation values of three singlets $\langle A^\alpha \rangle = a^\alpha$ are equal to zero, Subsect. 6.2.2, $a^\alpha = 0$, while all the other scalar fields — $\vec{\tilde{A}}^{\bar{1}}, \vec{\tilde{A}}^{\bar{N}_L}$ — can have for all the components nonzero vacuum expectation values, or that a^α does not need to be zero, $a^\alpha \neq 0$, but then the two third components of the two scalar triplets, $\langle \vec{\tilde{A}}^{\bar{1}3} \rangle = \tilde{a}_1$, $\langle \vec{\tilde{A}}^{\bar{N}_L 3} \rangle = \tilde{a}_2$, Subsect. 6.2.2, must be zero, $\tilde{a}_1 = 0$, $\tilde{a}_2 = 0$.

For the case that the two triplets and the three singlets have for all components nonzero vacuum expectation values we represent the symmetries of the mass matrices in dependence of the order of corrections, Subsect. 6.2.2.

In the first case, when $a^\alpha = 0$, to any order of corrections all the components of the two triplet scalar fields contribute, either with the nonzero vacuum expectation values or as dynamical fields or as both in all orders of corrections, while the three singlet scalar fields contribute only as dynamical fields. In this case the corrections keep the symmetry of the three level in all orders of corrections.

The contributions of the dynamical fields of the three singlets in all orders of loop corrections — together with the contributions of the two triplets which interact with spinors through the family quantum numbers either with the nonzero vacuum expectation values or as dynamical fields — make all the matrix elements dependent on the particular family member quantum numbers. Correspondingly all the mass matrices bring different masses to any of the family members and correspondingly also different mixing matrices to quarks and leptons. However, the choice $a^\alpha = 0$ keeps the four off diagonal terms, which are proportional to a^α in Eq.(6.22), equal to zero in all orders of correction.

In the second case, when $\tilde{a}_1 = 0$, $\tilde{a}_2 = 0$, in any order of corrections the three singlet scalar fields contribute either with nonzero vacuum expectation values or as dynamical fields, while the two triplets scalar fields contribute with the nonzero vacuum expectation values and the dynamical fields, except the two of the triplet components — $\vec{\tilde{A}}^{\bar{1}3}$ and $\vec{\tilde{A}}^{\bar{N}_L 3}$ — which contribute only as dynamical fields. The symmetry of the tree level is kept in all order of corrections, this choice makes, however, all the diagonal terms to remain equal in all orders of corrections.

When all the singlets and the triplets have for all the components nonzero vacuum expectation values ($a^\alpha \neq 0$, $\tilde{a}_1 \neq 0$, $\tilde{a}_2 \neq 0$, $\langle \vec{\tilde{A}}^{\bar{N}_L \bar{1}} \rangle \neq 0$, $\langle \vec{\tilde{A}}^{\bar{1} \bar{1}} \rangle \neq 0$) the symmetry of the tree level changes, but we are still able to determine the symmetry of mass in all orders of corrections, that is of the loop ones and

the repetition of the nonzero vacuum expectation values, expressing the matrix elements of mass matrices with a few parameters only, due to the fact that the symmetry of the mass matrices limit the number of free parameters. In the case that $|a^\alpha|$ is small (in comparison with $|\tilde{a}_1|$ and $|\tilde{a}_2|$), the higher order corrections drop away very quickly. When fitting the free parameters of mass matrices to the observed masses of quarks and leptons and their 3×3 submatrices of the predicted 4×4 mixing matrices, we are able to predict the masses of the fourth family members as well as the matrix elements of the fourth components to the observed free families, provided that the mixing 3×3 submatrices of the predicted 4×4 mass matrices of quarks and leptons are measured accurately enough — since the (accurate) 3×3 submatrix of a 4×4 matrix determines 4×4 matrix uniquely [21,22].

This means that although we are so far only in principle able to calculate directly the mass matrix elements of the 4×4 mass matrices, predicted by the *spin-charge-family*, yet the symmetry of mass matrices, discussed in this paper, enables us — due to the limited number of free parameters — to predict properties of the four family of quarks and lepton to the observed three families, that is the masses of the fourth families and the corresponding mixing matrices [21,22]. *We only have to wait for accurate enough data for the 3×3 mixing (sub)matrices of quarks and leptons.*

Let us add that the right handed neutrino, which is a regular member of the four families, Table 6.3, has the nonzero value of the operator $Y'A_s^{Y'}$ only.

6.4 Appendix: Short presentation of the *spin-charge-family* theory

This section follows similar sections in Refs. [1,4–7].

The *spin-charge-family* theory [1–7,9–12,15–17,19–24] assumes:

a. A simple action (Eq. (6.35)) in an even dimensional space ($d = 2n$, $d > 5$), d is chosen to be $(13 + 1)$. This choice makes that the action manifests in $d = (3 + 1)$ in the low energy regime all the observed degrees of freedom, explaining all the assumptions of the *standard model*, as well as other observed phenomena.

There are two kinds of the Clifford algebra objects, γ^a 's and $\tilde{\gamma}^a$'s in this theory with the properties.

$$\{\gamma^a, \gamma^b\}_+ = 2\eta^{ab}, \quad \{\tilde{\gamma}^a, \tilde{\gamma}^b\}_+ = 2\eta^{ab}, \quad \{\gamma^a, \tilde{\gamma}^b\}_+ = 0. \quad (6.34)$$

Fermions interact with the vielbeins f^α_a and the two kinds of the spin-connection fields — $\omega_{ab\alpha}$ and $\tilde{\omega}_{ab\alpha}$ — the gauge fields of $S^{ab} = \frac{i}{4}(\gamma^a \gamma^b - \gamma^b \gamma^a)$ and $\tilde{S}^{ab} = \frac{i}{4}(\tilde{\gamma}^a \tilde{\gamma}^b - \tilde{\gamma}^b \tilde{\gamma}^a)$, respectively.

The action

$$\begin{aligned} \mathcal{A} = \int d^d x \, E \, \frac{1}{2} (\bar{\psi} \gamma^a p_{0a} \psi) + \text{h.c.} + \\ \int d^d x \, E \, (\alpha R + \tilde{\alpha} \tilde{R}), \end{aligned} \quad (6.35)$$

in which $p_{0a} = f^\alpha_a p_{0\alpha} + \frac{1}{2E} \{p_\alpha, E f^\alpha_a\}_-, p_{0\alpha} = p_\alpha - \frac{1}{2} S^{ab} \omega_{ab\alpha} - \frac{1}{2} \tilde{S}^{ab} \tilde{\omega}_{ab\alpha}$, and

$$R = \frac{1}{2} \{f^{\alpha[a} f^{\beta b]} (\omega_{ab\alpha, \beta} - \omega_{c a \alpha} \omega^c_{b \beta})\} + \text{h.c.},$$

$$\tilde{R} = \frac{1}{2} \{f^{\alpha[a} f^{\beta b]} (\tilde{\omega}_{ab\alpha, \beta} - \tilde{\omega}_{c a \alpha} \tilde{\omega}^c_{b \beta})\} + \text{h.c.}$$

¹⁵, introduces two kinds of the Clifford algebra objects, γ^a and $\tilde{\gamma}^a$, $\{\gamma^a, \gamma^b\}_+ = 2\eta^{ab} = \{\tilde{\gamma}^a, \tilde{\gamma}^b\}_+$. f^α_a are vielbeins inverted to e^a_α , Latin letters (a, b, ..) denote flat indices, Greek letters (α, β, \dots) are Einstein indices, (m, n, ..) and (μ, ν, \dots) denote the corresponding indices in (0, 1, 2, 3), while (s, t, ..) and (σ, τ, \dots) denote the corresponding indices in $d \geq 5$:

$$e^a_\alpha f^\beta_a = \delta^\beta_\alpha, \quad e^a_\alpha f^\alpha_b = \delta^a_b, \quad (6.36)$$

$E = \det(e^a_\alpha)$.

b. The *spin-charge-family* theory assumes in addition that the manifold $M^{(13+1)}$ breaks first into $M^{(7+1)} \times M^{(6)}$ (which manifests as $SO(7, 1) \times SU(3) \times U(1)$), affecting both internal degrees of freedom — the one represented by γ^a and the one represented by $\tilde{\gamma}^a$. Since the left handed (with respect to $M^{(7+1)}$) spinors couple differently to scalar (with respect to $M^{(7+1)}$) fields than the right handed ones, the break can leave massless and mass protected $2^{((7+1)/2-1)}$ families [36]. The rest of families get heavy masses ¹⁶.

c. There is additional breaking of symmetry: The manifold $M^{(7+1)}$ breaks further into $M^{(3+1)} \times M^{(4)}$.

d. There is a scalar condensate (Table 6.5) of two right handed neutrinos with the family quantum numbers of the upper four families, bringing masses of the scale $\propto 10^{16}$ GeV or higher to all the vector and scalar gauge fields, which interact with the condensate [5].

e. There are the scalar fields with the space index (7, 8) carrying the weak (τ^{1i}) and the hyper charges ($Y = \tau^{23} + \tau^4$, τ^{1i} and τ^{2i} are generators of the subgroups of $SO(4)$, τ^4 and τ^{3i} are the generators of $U(1)_{II}$ and $SU(3)$, respectively, which are subgroups of $SO(6)$), which with their nonzero vacuum expectation values change the properties of the vacuum and break the weak charge and the hyper charge. Interacting with fermions and with the weak and hyper bosons, they bring masses to heavy bosons and to twice four groups of families. Carrying no electromagnetic ($Q = \tau^{13} + Y$) and colour (τ^{3i}) charges and no $SO(3, 1)$ spin, the scalar fields leave the electromagnetic, colour and gravity fields in $d = (3 + 1)$ massless.

The assumed action \mathcal{A} and the assumptions offer:

o. the explanation for the origin and all the properties of the observed fermions:

¹⁵ Whenever two indexes are equal the summation over these two is meant.

¹⁶ A toy model [36,37] was studied in $d = (5 + 1)$ with the same action as in Eq. (6.35). The break from $d = (5 + 1)$ to $d = (3 + 1) \times$ an almost S^2 was studied. For a particular choice of vielbeins and for a class of spin connection fields the manifold $M^{(5+1)}$ breaks into $M^{(3+1)}$ times an almost S^2 , while $2^{((3+1)/2-1)}$ families remain massless and mass protected. Equivalent assumption, although not yet proved how does it really work, is made in the $d = (13 + 1)$ case. This study is in progress.

o.i. of the family members, on Table 6.3 the family members belonging to one Weyl (fundamental) representation of massless spinors of the group $SO(13, 1)$ are presented in the "technique" [10–12,15–17,13,14] and analyzed with respect to the subgroups $SO(3, 1)$, $SU(2)_I$, $SU(2)_{II}$, $SU(3)$, $U(1)_{II}$, Eqs. (6.37, 6.38, 6.2) with the generators $\tau^{Ai} = \sum_{s,t} c^{Ai}_{st} S^{st}$,

o.ii. of the families analyzed with respect to the subgroups $(\widetilde{SO}(3, 1), \widetilde{SU}(2)_I, \widetilde{SU}(2)_{II}, \widetilde{U}(1)_{II})$ with the generators $\tilde{\tau}^{Ai} = \sum_{a,b} c^{Ai}_{ab} \tilde{S}^{st}$, Eqs. (6.40, 6.41, 6.42) — they are presented on Table 6.4 — all the families are singlets with respect to $\widetilde{SU}(3)$,

oo.i. of the observed vector gauge fields of the charges $(SU(2)_I, SU(2)_{II}, SU(3), U(1)_{II})$ discussed in Refs. ([1,4,2], and the references therein), all the vector gauge fields are the superposition of ω_{stm} , $A_m^{Ai} = \sum_{s,t} c^{Ai}_{st} \omega_{stm}$, Eq. (6.44),

oo.ii. of the Higgs's scalar and of the Yukawa couplings, explainable with the scalar fields with the space index (7, 8), there are two groups of two triplets, which are scalar gauge fields of the charges $\tilde{\tau}^{Ai}$, expressible with the superposition of $\tilde{\omega}_{abs}$, $A_s^{Ai} = \sum_{a,b} c^{Ai}_{ab} \omega_{abs}$, Eq. (6.45), and three singlets, the gauge fields of Q, Q', Y' , Eqs. (6.43, 6.45), all with the weak and the hyper charges as assumed by the *standard model* for the Higgs's scalars,

oo.iii. of the scalar fields explaining the origin of the matter-antimatter asymmetry, Ref. [5],

oo.iv. of the appearance of the dark matter, there are two decoupled groups of four families, carrying family charges $(\vec{N}_L, \vec{\tau}^1)$ and $(\vec{N}_R, \vec{\tau}^2)$, Eqs. (6.40, 6.41), both groups carry also the family members charges (Q, Q', Y') , Eq. (6.43).

The *standard model* groups of spins and charges are the subgroups of the $SO(13, 1)$ group with the generator of the infinitesimal transformations expressible with $S^{ab} (= \frac{i}{2}(\gamma^a \gamma^b - \gamma^b \gamma^a))$, $\{S^{ab}, S^{cd}\}_- = -i(\eta^{ad} S^{bc} + \eta^{bc} S^{ad} - \eta^{ac} S^{bd} - \eta^{bd} S^{ac})$ for the spin

$$\vec{N}_{\pm} (= \vec{N}_{(L,R)}) := \frac{1}{2}(S^{23} \pm iS^{01}, S^{31} \pm iS^{02}, S^{12} \pm iS^{03}), \quad (6.37)$$

for the weak charge, $SU(2)_I$, and the second $SU(2)_{II}$, these two groups are the invariant subgroups of $SO(4)$,

$$\begin{aligned} \vec{\tau}^1 &:= \frac{1}{2}(S^{58} - S^{67}, S^{57} + S^{68}, S^{56} - S^{78}), \\ \vec{\tau}^2 &:= \frac{1}{2}(S^{58} + S^{67}, S^{57} - S^{68}, S^{56} + S^{78}), \end{aligned} \quad (6.38)$$

for the colour charge $SU(3)$ and for the "fermion charge" $U(1)_{II}$, these two groups are subgroups of $SO(6)$,

$$\begin{aligned} \vec{\tau}^3 &:= \frac{1}{2}\{S^{9\ 12} - S^{10\ 11}, S^{9\ 11} + S^{10\ 12}, S^{9\ 10} - S^{11\ 12}, \\ &\quad S^{9\ 14} - S^{10\ 13}, S^{9\ 13} + S^{10\ 14}, S^{11\ 14} - S^{12\ 13}, \\ &\quad S^{11\ 13} + S^{12\ 14}, \frac{1}{\sqrt{3}}(S^{9\ 10} + S^{11\ 12} - 2S^{13\ 14})\}, \\ \tau^4 &:= -\frac{1}{3}(S^{9\ 10} + S^{11\ 12} + S^{13\ 14}), \end{aligned} \quad (6.39)$$

τ^4 is the "fermion charge", while the hyper charge $Y = \tau^{23} + \tau^4$.

The generators of the family quantum numbers are the superposition of the generators \tilde{S}^{ab} ($\tilde{S}^{ab} = \frac{i}{4} \{\tilde{Y}^a, \tilde{Y}^b\}_-$, $\{\tilde{S}^{ab}, \tilde{S}^{cd}\}_- = -i(\eta^{ad}\tilde{S}^{bc} + \eta^{bc}\tilde{S}^{ad} - \eta^{ac}\tilde{S}^{bd} - \eta^{bd}\tilde{S}^{ac})$, $\{\tilde{S}^{ab}, S^{cd}\}_- = 0$). One correspondingly finds the generators of the subgroups of $\widetilde{SO}(7, 1)$,

$$\vec{N}_{L,R} := \frac{1}{2}(\tilde{S}^{23} \pm i\tilde{S}^{01}, \tilde{S}^{31} \pm i\tilde{S}^{02}, \tilde{S}^{12} \pm i\tilde{S}^{03}), \quad (6.40)$$

which determine representations of the two $\widetilde{SU}(2)$ invariant subgroups of $\widetilde{SO}(3, 1)$, while

$$\begin{aligned} \vec{\tau}^1 &:= \frac{1}{2}(\tilde{S}^{58} - \tilde{S}^{67}, \tilde{S}^{57} + \tilde{S}^{68}, \tilde{S}^{56} - \tilde{S}^{78}), \\ \vec{\tau}^2 &:= \frac{1}{2}(\tilde{S}^{58} + \tilde{S}^{67}, \tilde{S}^{57} - \tilde{S}^{68}, \tilde{S}^{56} + \tilde{S}^{78}), \end{aligned} \quad (6.41)$$

determine representations of $\widetilde{SU}(2)_I \times \widetilde{SU}(2)_{II}$ of $\widetilde{SO}(4)$. Both, $\widetilde{SO}(3, 1)$ and $\widetilde{SO}(4)$, are the subgroups of $\widetilde{SO}(7, 1)$. One finds for the infinitesimal generator $\vec{\tau}^4$ of $\widetilde{U}(1)$, originating in $\widetilde{SO}(6)$, the expression

$$\vec{\tau}^4 := -\frac{1}{3}(\tilde{S}^{9\ 10} + \tilde{S}^{11\ 12} + \tilde{S}^{13\ 14}). \quad (6.42)$$

The operators for the charges Y and Q of the *standard model*, together with Q' and Y' , and the corresponding operators of the family charges \tilde{Y} , \tilde{Y}' , \tilde{Q} , \tilde{Q}' , are defined as follows:

$$\begin{aligned} Y &= \tau^4 + \tau^{23}, \quad Y' = -\tau^4 \tan^2 \vartheta_2 + \tau^{23}, \quad Q = \tau^{13} + Y, \quad Q' = -Y \tan^2 \vartheta_1 + \tau^{13}, \\ \tilde{Y} &= \vec{\tau}^4 + \vec{\tau}^{23}, \quad \tilde{Y}' = -\vec{\tau}^4 \tan^2 \vartheta_2 + \vec{\tau}^{23}, \quad \tilde{Q} = \tilde{Y} + \vec{\tau}^{13}, \quad \tilde{Q}' = -\tilde{Y} \tan^2 \vartheta_1 + \vec{\tau}^{13} \end{aligned} \quad (6.43)$$

Families split into two groups of four families, each manifesting the $\widetilde{SU}(2) \times \widetilde{SU}(2) \times U(1)$, with the generators of the infinitesimal transformations ($\vec{N}_L, \vec{\tau}^1, Q, Q', Y'$) and ($\vec{N}_R, \vec{\tau}^2, Q, Q', Y'$), respectively. The generators of $U(1)$ group (Q, Q', Y'), Eq. 6.43, distinguish among family members and are the same for both groups of four families, presented on Table 6.4, taken from Ref. [4].

The vector gauge fields of the charges $\vec{\tau}^1$, $\vec{\tau}^2$, $\vec{\tau}^3$ and τ^4 follow from the requirement $\sum_{A,i} \tau^{Ai} A_m^{Ai} = \sum_{s,t} \frac{1}{2} S^{st} \omega_{stm}$ and the requirement that $\tau^{Ai} = \sum_{a,b} c^{Ai}_{ab} S^{ab}$, Eq. (6.4), fulfilling the commutation relations $\{\tau^{Ai}, \tau^{Bj}\}_- = i\delta^{AB} f^{Aijk} \tau^{Ak}$, Eq. (6.5). Correspondingly we find $A_m^{Ai} = \sum_{s,t} c^{Ai}_{st} \omega_{stm}^{st}$, Eq. (6.6), with (s, t) either in $(5, 6, 7, 8)$ or in $(9, \dots, 14)$.

The explicit expressions for these vector gauge fields in terms of ω_{stm} [[4], Eq. (22)], [5]] are presented in the case that the electroweak $\vartheta_1 = \vartheta_W$ is zero and

so is ϑ_2 and in the case that the two angles, $(\vartheta_1, \vartheta_2)$, are not zero.

$$\begin{aligned}
\vec{A}_m^1 &= (\omega_{58m} - \omega_{67m}, \omega_{57m} + \omega_{68m}, \omega_{56m} - \omega_{78m}), \\
\vec{A}_m^2 &= (\omega_{58m} + \omega_{67m}, \omega_{57m} - \omega_{68m}, \omega_{56m} + \omega_{78m}), \\
A_m^Q &= \omega_{56m} - (\omega_{910m} + \omega_{1112m} + \omega_{1314m}), \\
A_m^Y &= (\omega_{56m} + \omega_{78m}) - (\omega_{910m} + \omega_{1112m} + \omega_{1314m}), \\
\vec{A}_m^3 &= (\omega_{912m} - \omega_{1011m}, \omega_{911m} + \omega_{1012m}, \omega_{910m} - \omega_{1112m}, \\
&\quad \omega_{914m} - \omega_{1013m}, \omega_{913m} + \omega_{1014m}, \omega_{1114m} - \omega_{1213m}, \\
&\quad \omega_{1113m} + \omega_{1214m}, \frac{1}{\sqrt{3}} (\omega_{910m} + \omega_{1112m} - 2\omega_{1314m})), \\
A_m^4 &= (\omega_{910m} + \omega_{1112m} + \omega_{1314m}), \\
A_m^Q &= \sin \vartheta_1 A_m^{13} + \cos \vartheta_1 A_m^Y, \\
A_m^{Q'} &= \cos \vartheta_1 A_m^{13} - \sin \vartheta_1 A_m^Y, \\
A_m^{Y'} &= \cos \vartheta_2 A_m^{23} - \sin \vartheta_2 A_m^4, \\
&\quad (m \in (0, 1, 2, 3)).
\end{aligned} \tag{6.44}$$

All ω_{stm} vector gauge fields are real fields. Here the fields contain in general the coupling constants which are not necessarily the same for all of them. The angle ϑ_1 is the angle of the electroweak break, while ϑ_2 is the angle of breaking the $SU(2)_{II}$ and $U(1)_{II}$ at much higher scale [[5,4] and references therein].

One obtains in a similar way the scalar gauge fields, which determine mass matrices of family members. They carry the space index $s = (7, 8)$. The scalar fields contain in general the coupling constants. Before the electroweak break the electroweak angle $\vartheta_1 = \vartheta_W$ is zero, while ϑ_2 is the angle determined by the break of symmetry at much higher scale.

$$\begin{aligned}
\vec{A}_s^1 &= (\tilde{\omega}_{58s} - \tilde{\omega}_{67s}, \tilde{\omega}_{57s} + \tilde{\omega}_{68s}, \tilde{\omega}_{56s} - \tilde{\omega}_{78s}), \\
\vec{A}_s^2 &= (\tilde{\omega}_{58s} + \tilde{\omega}_{67s}, \tilde{\omega}_{57s} - \tilde{\omega}_{68s}, \tilde{\omega}_{56s} + \tilde{\omega}_{78s}), \\
\vec{A}_s^{N_L} &= (\tilde{\omega}_{23s} + i\tilde{\omega}_{01s}, \tilde{\omega}_{31s} + i\tilde{\omega}_{02s}, \tilde{\omega}_{12s} + i\tilde{\omega}_{03s}), \\
\vec{A}_s^{N_R} &= (\tilde{\omega}_{23s} - i\tilde{\omega}_{01s}, \tilde{\omega}_{31s} - i\tilde{\omega}_{02s}, \tilde{\omega}_{12s} - i\tilde{\omega}_{03s}), \\
A_s^Q &= \omega_{56s} - (\omega_{910s} + \omega_{1112s} + \omega_{1314s}), \\
A_s^Y &= (\omega_{56s} + \omega_{78s}) - (\omega_{910s} + \omega_{1112s} + \omega_{1314s}), \\
A_s^4 &= -(\omega_{910s} + \omega_{1112s} + \omega_{1314s}), \\
A_s^Q &= \sin \vartheta_1 A_s^{13} + \cos \vartheta_1 A_s^Y, \quad A_s^{Q'} = \cos \vartheta_1 A_s^{13} - \sin \vartheta_1 A_s^Y, \\
A_s^{Y'} &= \cos \vartheta_2 A_s^{23} - \sin \vartheta_2 A_s^4, \\
&\quad (s \in (7, 8)).
\end{aligned} \tag{6.45}$$

All $\omega_{sts'}$, $\tilde{\omega}_{sts'}$, $(s, t, s') = (5, \dots, 14)$, $\tilde{\omega}_{i,j,s'}$ and $i\tilde{\omega}_{0,s'}$, $(i, j) = (1, 2, 3)$ scalar gauge fields are real fields.

The theory predicts, due to commutation relations of generators of the infinitesimal transformations of the family groups, $\widetilde{SU}(2)_I \times \widetilde{SU}(2)_I$ and $\widetilde{SU}(2)_{II} \times \widetilde{SU}(2)_{II}$, the first one with the generators \vec{N}_L and $\vec{\tau}^1$, and the second one with the generators \vec{N}_R and $\vec{\tau}^2$, Eqs. (6.40,6.41), two groups of four families.

The theory offers (so far) several predictions:

- i. several new scalars, those coupled to the lower group of four families — two triplets and three singlets, the superposition of ($\tilde{A}_s^1, \tilde{A}_{Ls}^N$ and A_s^Q, A_s^Y, A_s^4 , Eq. (6.45)) — some of them to be observed at the LHC ([1,5,4]),
- ii. the fourth family to the observed three to be observed at the LHC ([1,5,4] and the references therein),
- iii. new nuclear force among nucleons among quarks of the upper four families.

The theory offers also the explanation for several phenomena, like it is the “miraculous” cancellation of the *standard model* triangle anomalies [3].

The breaks of the symmetries, manifesting in Eqs. (6.37, 6.40, 6.38, 6.41, 6.2, 6.42), are in the *spin-charge-family* theory caused by the scalar condensate of the two right handed neutrinos belonging to one group of four families, Table 6.5, and by the nonzero vacuum expectation values of the scalar fields carrying the space index (7, 8) (Refs. [4,1] and the references therein). The space breaks first to $SO(7, 1) \times SU(3) \times U(1)_{II}$ and then further to $SO(3, 1) \times SU(2)_I \times U(1)_I \times SU(3) \times U(1)_{II}$, what explains the connections between the weak and the hyper charges and the handedness of spinors [3].

state	S^{03}	S^{12}	τ^{13}	τ^{23}	τ^4	Y	Q	$\tilde{\tau}^{13}$	$\tilde{\tau}^{23}$	$\tilde{\tau}^4$	\tilde{Y}	\tilde{Q}	\tilde{N}_L^3	\tilde{N}_R^3
$(v_{1R}^{VIII} \rangle_1 v_{2R}^{VIII} \rangle_2)$	0	0	0	1	-1	0	0	0	1	-1	0	0	0	1
$(v_{1R}^{VIII} \rangle_1 e_{2R}^{VIII} \rangle_2)$	0	0	0	0	-1	-1	-1	0	1	-1	0	0	0	1
$(e_{1R}^{VIII} \rangle_1 e_{2R}^{VIII} \rangle_2)$	0	0	0	-1	-1	-2	-2	0	1	-1	0	0	0	1

Table 6.5. This table is taken from [5]. The condensate of the two right handed neutrinos v_R , with the VIIIth family quantum numbers, coupled to spin zero and belonging to a triplet with respect to the generators τ^{21} , is presented together with its two partners. The right handed neutrino has $Q = 0 = Y$. The triplet carries $\tau^4 = -1$, $\tilde{\tau}^{23} = 1$, $\tilde{\tau}^4 = -1$, $\tilde{N}_R^3 = 1$, $\tilde{N}_L^3 = 0$, $\tilde{Y} = 0$, $\tilde{Q} = 0$, $\tilde{\tau}^{31} = 0$. The family quantum numbers are presented in Table 6.4.

The stable of the upper four families is the candidate for the dark matter, the fourth of the lower four families is predicted to be measured at the LHC.

6.5 Appendix: Short presentation of spinor technique [1,4,11,13,14]

This appendix is a short review (taken from [4]) of the technique [11,42,13,14], initiated and developed in Ref. [11] by one of the authors (N.S.M.B.), while proposing the *spin-charge-family* theory [2,4,5,7,9,1,15,16,10–12,17,19–24]. All the internal degrees of freedom of spinors, with family quantum numbers included, are describable with two kinds of the Clifford algebra objects, besides with γ^a 's, used in this theory to describe spins and all the charges of fermions, also with $\tilde{\gamma}^a$'s, used in this theory to describe families of spinors:

$$\{\gamma^a, \gamma^b\}_+ = 2\eta^{ab}, \quad \{\tilde{\gamma}^a, \tilde{\gamma}^b\}_+ = 2\eta^{ab}, \quad \{\gamma^a, \tilde{\gamma}^b\}_+ = 0. \quad (6.46)$$

We assume the “Hermiticity” property for γ^a ’s (and $\tilde{\gamma}^a$ ’s) $\gamma^{a\dagger} = \eta^{aa}\gamma^a$ (and $\tilde{\gamma}^{a\dagger} = \eta^{aa}\tilde{\gamma}^a$), in order that γ^a (and $\tilde{\gamma}^a$) are compatible with (6.34) and formally unitary, i.e. $\gamma^{a\dagger}\gamma^a = I$ (and $\tilde{\gamma}^{a\dagger}\tilde{\gamma}^a = I$). One correspondingly finds that $(S^{ab})^\dagger = \eta^{aa}\eta^{bb}S^{ab}$ (and $(\tilde{S}^{ab})^\dagger = \eta^{aa}\eta^{bb}\tilde{S}^{ab}$).

Spinor states are represented as products of nilpotents and projectors, formed as odd and even objects of γ^a ’s, respectively, chosen to be the eigenstates of a Cartan subalgebra of the Lorentz groups defined by γ^a ’s

$${}^{ab}_{(k)} := \frac{1}{2}(\gamma^a + \frac{\eta^{aa}}{ik}\gamma^b), \quad {}^{ab}_{[k]} := \frac{1}{2}(1 + \frac{i}{k}\gamma^a\gamma^b), \quad (6.47)$$

where $k^2 = \eta^{aa}\eta^{bb}$. We further have [4]

$$\begin{aligned} \gamma^a {}^{ab}_{(k)} &:= \frac{1}{2}(\gamma^a\gamma^a + \frac{\eta^{aa}}{ik}\gamma^a\gamma^b) = \eta^{aa} {}^{ab}_{[-k]}, & \gamma^a {}^{ab}_{[k]} &:= \frac{1}{2}(\gamma^a + \frac{i}{k}\gamma^a\gamma^a\gamma^b) = {}^{ab}_{(-k)}, \\ \tilde{\gamma}^a {}^{ab}_{(k)} &:= -i\frac{1}{2}(\gamma^a + \frac{\eta^{aa}}{ik}\gamma^b)\gamma^a = -i\eta^{aa} {}^{ab}_{[k]}, & \tilde{\gamma}^a {}^{ab}_{[k]} &:= i\frac{1}{2}(1 + \frac{i}{k}\gamma^a\gamma^b)\gamma^a = -i {}^{ab}_{(k)}, \end{aligned} \quad (6.48)$$

where we assume that all the operators apply on the vacuum state $|\psi_0\rangle$. We define a vacuum state $|\psi_0\rangle$ so that one finds $\langle {}^{ab}_{(k)} | {}^{ab}_{(k)} \rangle = 1$, $\langle {}^{ab}_{[k]} | {}^{ab}_{[k]} \rangle = 1$.

We recognize that γ^a transform ${}^{ab}_{(k)}$ into ${}^{ab}_{[-k]}$, never to ${}^{ab}_{[k]}$, while $\tilde{\gamma}^a$ transform ${}^{ab}_{(k)}$ into ${}^{ab}_{[k]}$, never to ${}^{ab}_{[-k]}$

$$\begin{aligned} \gamma^a {}^{ab}_{(k)} &= \eta^{aa} {}^{ab}_{[-k]}, \quad \gamma^b {}^{ab}_{(k)} = -ik {}^{ab}_{[-k]}, \quad \gamma^a {}^{ab}_{[k]} = {}^{ab}_{(-k)}, \quad \gamma^b {}^{ab}_{[k]} = -ik\eta^{aa} {}^{ab}_{(-k)}, \\ \tilde{\gamma}^a {}^{ab}_{(k)} &= -i\eta^{aa} {}^{ab}_{[k]}, \quad \tilde{\gamma}^b {}^{ab}_{(k)} = -k {}^{ab}_{[k]}, \quad \tilde{\gamma}^a {}^{ab}_{[k]} = i {}^{ab}_{(k)}, \quad \tilde{\gamma}^b {}^{ab}_{[k]} = -k\eta^{aa} {}^{ab}_{(k)} \end{aligned} \quad (6.49)$$

The Clifford algebra objects S^{ab} and \tilde{S}^{ab} close the algebra of the Lorentz group

$$\begin{aligned} S^{ab} &:= (i/4)(\gamma^a\gamma^b - \gamma^b\gamma^a), \\ \tilde{S}^{ab} &:= (i/4)(\tilde{\gamma}^a\tilde{\gamma}^b - \tilde{\gamma}^b\tilde{\gamma}^a), \end{aligned} \quad (6.50)$$

$$\{S^{ab}, \tilde{S}^{cd}\}_- = 0, \{S^{ab}, S^{cd}\}_- = i(\eta^{ad}S^{bc} + \eta^{bc}S^{ad} - \eta^{ac}S^{bd} - \eta^{bd}S^{ac}), \{\tilde{S}^{ab}, \tilde{S}^{cd}\}_- = i(\eta^{ad}\tilde{S}^{bc} + \eta^{bc}\tilde{S}^{ad} - \eta^{ac}\tilde{S}^{bd} - \eta^{bd}\tilde{S}^{ac}).$$

One can easily check that the nilpotent ${}^{ab}_{(k)}$ and the projector ${}^{ab}_{[k]}$ are “eigenstates” of S^{ab} and \tilde{S}^{ab}

$$\begin{aligned} S^{ab} {}^{ab}_{(k)} &= \frac{1}{2}k {}^{ab}_{(k)}, & S^{ab} {}^{ab}_{[k]} &= \frac{1}{2}k {}^{ab}_{[k]}, \\ \tilde{S}^{ab} {}^{ab}_{(k)} &= \frac{1}{2}k {}^{ab}_{(k)}, & \tilde{S}^{ab} {}^{ab}_{[k]} &= -\frac{1}{2}k {}^{ab}_{[k]}, \end{aligned} \quad (6.51)$$

where the vacuum state $|\psi_0\rangle$ is meant to stay on the right hand sides of projectors and nilpotents. This means that multiplication of nilpotents ${}^{ab}_{(k)}$ and projectors

${}^{ab}[\mathbf{k}]$ by S^{ab} get the same objects back multiplied by the constant $\frac{1}{2}k$, while \tilde{S}^{ab} multiply ${}^{ab}(\mathbf{k})$ by $\frac{k}{2}$ and ${}^{ab}[\mathbf{k}]$ by $(-\frac{k}{2})$ (rather than by $\frac{k}{2}$). This also means that when ${}^{ab}(\mathbf{k})$ and ${}^{ab}[\mathbf{k}]$ act from the left hand side on a vacuum state $|\psi_0\rangle$ the obtained states are the eigenvectors of S^{ab} .

The technique can be used to construct a spinor basis for any dimension d and any signature in an easy and transparent way. Equipped with nilpotents and projectors of Eq. (6.47), the technique offers an elegant way to see all the quantum numbers of states with respect to the two Lorentz groups, as well as transformation properties of the states under the application of any Clifford algebra object.

Recognizing from Eq.(6.50) that the two Clifford algebra objects (S^{ab}, S^{cd}) with all indexes different commute (and equivalently for $(\tilde{S}^{ab}, \tilde{S}^{cd})$), we select the Cartan subalgebra of the algebra of the two groups, which form equivalent representations with respect to one another

$$\begin{aligned} S^{03}, S^{12}, S^{56}, \dots, S^{d-1 \ d}, & \quad \text{if } d = 2n \geq 4, \\ \tilde{S}^{03}, \tilde{S}^{12}, \tilde{S}^{56}, \dots, \tilde{S}^{d-1 \ d}, & \quad \text{if } d = 2n \geq 4. \end{aligned} \quad (6.52)$$

The choice of the Cartan subalgebra in $d < 4$ is straightforward. It is useful to define one of the Casimirs of the Lorentz group — the handedness $\Gamma (\{\Gamma, S^{ab}\}_- = 0)$ (as well as $\tilde{\Gamma}$) in any $d = 2n$

$$\begin{aligned} \Gamma^{(d)} &:= (i)^{d/2} \prod_a (\sqrt{\eta^{aa}} \gamma^a), \quad \text{if } d = 2n, \\ \tilde{\Gamma}^{(d)} &:= (i)^{(d-1)/2} \prod_a (\sqrt{\eta^{aa}} \tilde{\gamma}^a), \quad \text{if } d = 2n. \end{aligned} \quad (6.53)$$

We understand the product of γ^a 's in the ascending order with respect to the index a : $\gamma^0 \gamma^1 \dots \gamma^d$. It follows from the Hermiticity properties of γ^a for any choice of the signature η^{aa} that $\Gamma^\dagger = \Gamma$, $\Gamma^2 = I$. (Equivalent relations are valid for $\tilde{\Gamma}$.) We also find that for d even the handedness anticommutes with the Clifford algebra objects γ^a ($\{\gamma^a, \Gamma\}_+ = 0$) (while for d odd it commutes with γ^a ($\{\gamma^a, \Gamma\}_- = 0$)).

Taking into account the above equations it is easy to find a Weyl spinor irreducible representation for d -dimensional space, with d even or odd ¹⁷. For d even we simply make a starting state as a product of $d/2$, let us say, only nilpotents ${}^{ab}(\mathbf{k})$, one for each S^{ab} of the Cartan subalgebra elements (Eqs.(6.52, 6.50)), applying it on an (unimportant) vacuum state. Then the generators S^{ab} , which do not belong to the Cartan subalgebra, being applied on the starting state from the left

¹⁷ For d odd the basic states are products of $(d-1)/2$ nilpotents and a factor $(1 \pm \Gamma)$.

hand side, generate all the members of one Weyl spinor.

$$\begin{aligned}
 & \begin{matrix} 0d & 12 & 35 & & d-1 & d-2 \\ (k_{0d})(k_{12})(k_{35}) \cdots (k_{d-1} \ d-2) \end{matrix} |\psi_0 \rangle \\
 & \begin{matrix} 0d & 12 & 35 & & d-1 & d-2 \\ [-k_{0d}][-k_{12}](k_{35}) \cdots (k_{d-1} \ d-2) \end{matrix} |\psi_0 \rangle \\
 & \begin{matrix} 0d & 12 & 35 & & d-1 & d-2 \\ [-k_{0d}](k_{12})[-k_{35}] \cdots (k_{d-1} \ d-2) \end{matrix} |\psi_0 \rangle \\
 & \vdots \\
 & \begin{matrix} 0d & 12 & 35 & & d-1 & d-2 \\ [-k_{0d}](k_{12})(k_{35}) \cdots [-k_{d-1} \ d-2] \end{matrix} |\psi_0 \rangle \\
 & \begin{matrix} 0d & 12 & 35 & & d-1 & d-2 \\ (k_{0d})[-k_{12}][-k_{35}] \cdots (k_{d-1} \ d-2) \end{matrix} |\psi_0 \rangle \\
 & \vdots
 \end{aligned} \tag{6.54}$$

All the states have the same handedness Γ , since $\{\Gamma, S^{ab}\}_- = 0$. States, belonging to one multiplet with respect to the group $SO(q, d - q)$, that is to one irreducible representation of spinors (one Weyl spinor), can have any phase. We could make a choice of the simplest one, taking all phases equal to one. (In order to have the usual transformation properties for spinors under the rotation of spin and under $\mathcal{C}_N \mathcal{P}_N$, some of the states must be multiplied by (-1) .)

The above representation demonstrates that for d even all the states of one irreducible Weyl representation of a definite handedness follow from a starting state, which is, for example, a product of nilpotents $(k_{ab})^{ab}$, by transforming all possible pairs of $(k_{ab})^{ab} (k_{mn})^{mn}$ into $[-k_{ab}]^{ab} [-k_{mn}]^{mn}$. There are $S^{am}, S^{an}, S^{bm}, S^{bn}$, which do this. The procedure gives $2^{(d/2-1)}$ states. A Clifford algebra object γ^a being applied from the left hand side, transforms a Weyl spinor of one handedness into a Weyl spinor of the opposite handedness.

We shall speak about left handedness when $\Gamma = -1$ and about right handedness when $\Gamma = 1$.

While S^{ab} , which do not belong to the Cartan subalgebra (Eq. (6.52)), generate all the states of one representation, \tilde{S}^{ab} , which do not belong to the Cartan subalgebra (Eq. (6.52)), generate the states of $2^{d/2-1}$ equivalent representations.

Making a choice of the Cartan subalgebra set (Eq. (6.52)) of the algebra S^{ab} and \tilde{S}^{ab} : $(S^{03}, S^{12}, S^{56}, S^{78}, S^{9 \ 10}, S^{11 \ 12}, S^{13 \ 14}), (\tilde{S}^{03}, \tilde{S}^{12}, \tilde{S}^{56}, \tilde{S}^{78}, \tilde{S}^{9 \ 10}, \tilde{S}^{11 \ 12}, \tilde{S}^{13 \ 14})$, a left handed ($\Gamma^{(13,1)} = -1$) eigenstate of all the members of the Cartan subalgebra, representing a weak chargeless u_R -quark with spin up, hyper charge $(2/3)$ and colour $(1/2, 1/(2\sqrt{3}))$, for example, can be written as

$$\begin{aligned}
 & \begin{matrix} 03 & 12 & 56 & 78 & 9 & 10 & 11 & 12 & 13 & 14 \\ (+i)(+) \mid (+)(+) \parallel (+) \mid - \mid - \end{matrix} |\psi_0 \rangle = \\
 & \frac{1}{2^7} (\gamma^0 - \gamma^3)(\gamma^1 + i\gamma^2)(\gamma^5 + i\gamma^6)(\gamma^7 + i\gamma^8) \\
 & (\gamma^9 + i\gamma^{10})(1 - i\gamma^{11}\gamma^{12})(1 - i\gamma^{13}\gamma^{14})|\psi_0 \rangle.
 \end{aligned} \tag{6.55}$$

This state is an eigenstate of all S^{ab} and \tilde{S}^{ab} which are members of the Cartan subalgebra (Eq. (6.52)).

The operators \tilde{S}^{ab} , which do not belong to the Cartan subalgebra (Eq. (6.52)), generate families from the starting u_R quark, transforming the u_R quark from Eq. (6.55) to the u_R of another family, keeping all of the properties with respect to S^{ab} unchanged. In particular, \tilde{S}^{01} applied on a right handed u_R -quark from Eq. (6.55) generates a state which is again a right handed u_R -quark, weak chargeless, with spin up, hyper charge (2/3) and the colour charge (1/2, $1/(2\sqrt{3})$)

$$\tilde{S}^{01} \begin{smallmatrix} 03 & 12 & 56 & 78 & 91011121314 \\ (+i)(+) & | & (+)(+) & || & (+) [-] [-] \end{smallmatrix} = -\frac{i}{2} \begin{smallmatrix} 03 & 12 & 56 & 78 & 91011121314 \\ [+i][+] & | & (+)(+) & || & (+) [-] [-] \end{smallmatrix} \quad (6.56)$$

One can find both states in Table 6.4, the first u_R as u_{R8} in the eighth line of this table, the second one as u_{R7} in the seventh line of this table.

Below some useful relations follow. From Eq.(6.49) one has

$$\begin{aligned} S^{ac} \begin{smallmatrix} ab & cd \\ (k)(k) \end{smallmatrix} &= -\frac{i}{2} \eta^{aa} \eta^{cc} \begin{smallmatrix} ab & cd \\ [-k][-k] \end{smallmatrix}, & \tilde{S}^{ac} \begin{smallmatrix} ab & cd \\ (k)(k) \end{smallmatrix} &= \frac{i}{2} \eta^{aa} \eta^{cc} \begin{smallmatrix} ab & cd \\ [k][k] \end{smallmatrix}, \\ S^{ac} \begin{smallmatrix} ab & cd \\ [k][k] \end{smallmatrix} &= \frac{i}{2} \begin{smallmatrix} ab & cd \\ (-k)(-k) \end{smallmatrix}, & \tilde{S}^{ac} \begin{smallmatrix} ab & cd \\ [k][k] \end{smallmatrix} &= -\frac{i}{2} \begin{smallmatrix} ab & cd \\ (k)(k) \end{smallmatrix}, \\ S^{ac} \begin{smallmatrix} ab & cd \\ (k)[k] \end{smallmatrix} &= -\frac{i}{2} \eta^{aa} \begin{smallmatrix} ab & cd \\ -k \end{smallmatrix}, & \tilde{S}^{ac} \begin{smallmatrix} ab & cd \\ (k)[k] \end{smallmatrix} &= -\frac{i}{2} \eta^{aa} \begin{smallmatrix} ab & cd \\ k \end{smallmatrix}, \\ S^{ac} \begin{smallmatrix} ab & cd \\ k \end{smallmatrix} &= \frac{i}{2} \eta^{cc} \begin{smallmatrix} ab & cd \\ (-k)[-k] \end{smallmatrix}, & \tilde{S}^{ac} \begin{smallmatrix} ab & cd \\ k \end{smallmatrix} &= \frac{i}{2} \eta^{cc} \begin{smallmatrix} ab & cd \\ (k)[k] \end{smallmatrix}. \end{aligned} \quad (6.57)$$

We conclude from the above equation that \tilde{S}^{ab} generate the equivalent representations with respect to S^{ab} and opposite.

We recognize in Eq. (6.58) the demonstration of the nilpotent and the projector character of the Clifford algebra objects $\begin{smallmatrix} ab \\ (k) \end{smallmatrix}$ and $\begin{smallmatrix} ab \\ [k] \end{smallmatrix}$, respectively.

$$\begin{aligned} \begin{smallmatrix} ab & ab \\ (k)(k) \end{smallmatrix} &= 0, & \begin{smallmatrix} ab & ab \\ (k)(-k) \end{smallmatrix} &= \eta^{aa} \begin{smallmatrix} ab \\ [k] \end{smallmatrix}, & \begin{smallmatrix} ab & ab \\ (-k)(k) \end{smallmatrix} &= \eta^{aa} \begin{smallmatrix} ab \\ [-k] \end{smallmatrix}, & \begin{smallmatrix} ab & ab \\ (-k)(-k) \end{smallmatrix} &= 0, \\ \begin{smallmatrix} ab & ab \\ [k][k] \end{smallmatrix} &= \begin{smallmatrix} ab \\ [k] \end{smallmatrix}, & \begin{smallmatrix} ab & ab \\ [k][-k] \end{smallmatrix} &= 0, & \begin{smallmatrix} ab & ab \\ [-k][k] \end{smallmatrix} &= 0, & \begin{smallmatrix} ab & ab \\ [-k][-k] \end{smallmatrix} &= \begin{smallmatrix} ab \\ [-k] \end{smallmatrix}, \\ \begin{smallmatrix} ab & ab \\ (k)[k] \end{smallmatrix} &= 0, & \begin{smallmatrix} ab & ab \\ k \end{smallmatrix} &= \begin{smallmatrix} ab \\ (k) \end{smallmatrix}, & \begin{smallmatrix} ab & ab \\ (-k)[k] \end{smallmatrix} &= \begin{smallmatrix} ab \\ (-k) \end{smallmatrix}, & \begin{smallmatrix} ab & ab \\ (-k)[-k] \end{smallmatrix} &= 0, \\ \begin{smallmatrix} ab & ab \\ -k \end{smallmatrix} &= \begin{smallmatrix} ab \\ (k) \end{smallmatrix}, & \begin{smallmatrix} ab & ab \\ [k](-k) \end{smallmatrix} &= 0, & \begin{smallmatrix} ab & ab \\ [-k](k) \end{smallmatrix} &= 0, & \begin{smallmatrix} ab & ab \\ -k \end{smallmatrix} &= \begin{smallmatrix} ab \\ (-k) \end{smallmatrix}. \end{aligned} \quad (6.58)$$

Defining

$$(\tilde{\pm}i) = \frac{1}{2}(\tilde{\gamma}^a \mp \tilde{\gamma}^b), \quad (\tilde{\pm}1) = \frac{1}{2}(\tilde{\gamma}^a \pm i\tilde{\gamma}^b), \quad [\tilde{\pm}i] = \frac{1}{2}(1 \pm \tilde{\gamma}^a \tilde{\gamma}^b), \quad [\tilde{\pm}1] = \frac{1}{2}(1 \pm i\tilde{\gamma}^a \tilde{\gamma}^b).$$

one recognizes that

$$\begin{smallmatrix} ab & ab \\ (\tilde{k})(k) \end{smallmatrix} = 0, \quad \begin{smallmatrix} ab & ab \\ (-\tilde{k})(k) \end{smallmatrix} = -i\eta^{aa} \begin{smallmatrix} ab \\ [k] \end{smallmatrix}, \quad \begin{smallmatrix} ab & ab \\ (\tilde{k})[k] \end{smallmatrix} = i \begin{smallmatrix} ab \\ (k) \end{smallmatrix}, \quad \begin{smallmatrix} ab & ab \\ (\tilde{k})[-k] \end{smallmatrix} = 0. \quad (6.59)$$

Below some more useful relations [15] are presented:

$$\begin{aligned}
 N_{+}^{\pm} &= N_{+}^1 \pm i N_{+}^2 = - \begin{pmatrix} 03 & 12 \\ \mp i & (\pm) \end{pmatrix}, & N_{-}^{\pm} &= N_{-}^1 \pm i N_{-}^2 = (\pm i) \begin{pmatrix} 03 & 12 \\ (\pm) & \end{pmatrix}, \\
 \tilde{N}_{+}^{\pm} &= - \begin{pmatrix} 03 & 12 \\ \mp i & (\pm) \end{pmatrix}, & \tilde{N}_{-}^{\pm} &= (\pm i) \begin{pmatrix} 03 & 12 \\ (\pm) & \end{pmatrix}, \\
 \tau^{1\pm} &= (\mp) \begin{pmatrix} 56 & 78 \\ (\pm) & (\mp) \end{pmatrix}, & \tau^{2\mp} &= (\mp) \begin{pmatrix} 56 & 78 \\ (\mp) & (\mp) \end{pmatrix}, \\
 \tilde{\tau}^{1\pm} &= (\mp) \begin{pmatrix} 56 & 78 \\ (\pm) & (\mp) \end{pmatrix}, & \tilde{\tau}^{2\mp} &= (\mp) \begin{pmatrix} 56 & 78 \\ (\mp) & (\mp) \end{pmatrix}.
 \end{aligned} \tag{6.60}$$

In Table 6.4 [4] the eight families of the first member in Table 6.3 (member number 1) of the eight-plet of quarks and the 25th member in Table 6.3 of the eight-plet of leptons are presented as an example. The eight families of the right handed u_{1R} quark are presented in the left column of Table 6.4 [4]. In the right column of the same table the equivalent eight-plet of the right handed neutrinos ν_{1R} are presented. All the other members of any of the eight families of quarks or leptons follow from any member of a particular family by the application of the operators $N_{R,L}^{\pm}$ and $\tau^{(2,1)\pm}$, Eq. (6.60), on this particular member.

The eight-plets separate into two group of four families: One group contains doublets with respect to \vec{N}_R and $\vec{\tau}^2$, these families are singlets with respect to \vec{N}_L and $\vec{\tau}^1$. Another group of families contains doublets with respect to \vec{N}_L and $\vec{\tau}^1$, these families are singlets with respect to \vec{N}_R and $\vec{\tau}^2$.

The scalar fields which are the gauge scalars of \vec{N}_R and $\vec{\tau}^2$ couple only to the four families which are doublets with respect to these two groups. The scalar fields which are the gauge scalars of \vec{N}_L and $\vec{\tau}^1$ couple only to the four families which are doublets with respect to these last two groups.

After the electroweak phase transition, caused by the scalar fields with the space index (7,8), the two groups of four families become massive. The lowest of the two groups of four families contains the observed three, while the fourth remains to be measured. The lowest of the upper four families is the candidate for the dark matter [1].

References

1. N.S. Mankoč Borštnik, "Spin-charge-family theory is offering next step in understanding elementary particles and fields and correspondingly universe", Proceedings to the Conference on Cosmology, Gravitational Waves and Particles, IARD conferences, Ljubljana, 6-9 June 2016, The 10th Biennial Conference on Classical and Quantum Relativistic Dynamics of articles and Fields, J. Phys.: Conf. Ser. 845 012017 [arXiv:1607.01618v2].
2. D. Lukman, N.S. Mankoč Borštnik, "Vector and scalar gauge fields with respect to $d = (3 + 1)$ in Kaluza-Klein theories and in the *spin-charge-family theory*", *Eur. Phys. J. C*, **77** (2017) 231[arXiv:1604.00675]
3. N.S. Mankoč Borštnik, H.B.F. Nielsen, "The spin-charge-family theory offers understanding of the triangle anomalies cancellation in the standard model", *Fortschritte Der Physik -Progress of Physics* (2017) 1700046, [arXiv:1607.01618]
4. N.S. Mankoč Borštnik, "The explanation for the origin of the higgs scalar and for the Yukawa couplings by the *spin-charge-family theory*", *J. of Mod. Phys.* **6** (2015) 2244-2274.

5. N.S. Mankoč Borštnik, "Can spin-charge-family theory explain baryon number non conservation?", *Phys. Rev. D* **91** (2015) 6, 065004 ID: 0703013. doi:10.1103/[arxiv:1409.7791, arXiv:1502.06786v1].
6. N.S. Mankoč Borštnik, The spin-charge-family theory is explaining the origin of families, of the Higgs and the Yukawa Couplings" *J. of Modern Phys.* **4**, 823-847 (2013) [arxiv:1312.1542].
7. N.S. Mankoč Borštnik, "Spin-charge-family theory is explaining appearance of families of quarks and leptons, of Higgs and Yukawa couplings", in *Proceedings to the 16th Workshop "What comes beyond the standard models"*, Bled, 14-21 of July, 2013, eds. N.S. Mankoč Borštnik, H.B. Nielsen and D. Lukman (DMFA Založništvo, Ljubljana, December 2013) p.113 -142, [arxiv:1312.1542].
8. N.S. Mankoč Borštnik, H.B.F. Nielsen, "Why nature made a choice of Clifford and not Grassmann coordinates", *Proceedings to the 20th Workshop "What comes beyond the standard models"*, Bled, 9-17 of July, 2017, Ed. N.S. Mankoč Borštnik, H.B. Nielsen, D. Lukman, DMFA Založništvo, Ljubljana, December 2017, p. 89-120 [arXiv:1802.05554v1v2].
9. N.S. Mankoč Borštnik, "Do we have the explanation for the Higgs and Yukawa couplings of the *standard model*", <http://arxiv.org/abs/1212.3184v2>, (<http://arxiv.org/abs/1207.6233>), in *Proceedings to the 15th Workshop "What comes beyond the standard models"*, Bled, 9-19 of July, 2012, Ed. N.S. Mankoč Borštnik, H.B. Nielsen, D. Lukman, DMFA Založništvo, Ljubljana, December 2012, p.56-71, [arxiv:1302.4305].
10. N.S. Mankoč Borštnik, "Spin connection as a superpartner of a vielbein", *Phys. Lett. B* **292**, 25-29 (1992).
11. N.S. Mankoč Borštnik, "Spinor and vector representations in four dimensional Grassmann space", *J. Math. Phys.* **34**, 3731-3745 (1993).
12. N.S. Mankoč Borštnik, "Unification of spins and charges", *Int. J. Theor. Phys.* **40**, 315-338 (2001).
13. N.S. Mankoč Borštnik, H.B.F. Nielsen, "How to generate spinor representations in any dimension in terms of projection operators", *J. of Math. Phys.* **43** (2002) 5782, [hep-th/0111257].
14. N.S. Mankoč Borštnik, H.B.F. Nielsen, "How to generate families of spinors", *J. of Math. Phys.* **44** 4817 (2003) [hep-th/0303224].
15. A. Borštnik Bračič and N.S. Mankoč Borštnik, "Origin of families of fermions and their mass matrices", *Phys. Rev. D* **74**, 073013 (2006) [hep-ph/0301029; hep-ph/9905357, p. 52-57; hep-ph/0512062, p.17-31; hep-ph/0401043 ,p. 31-57].
16. A. Borštnik Bračič, N.S. Mankoč Borštnik, "The approach Unifying Spins and Charges and Its Predictions", *Proceedings to the Euroconference on Symmetries Beyond the Standard Model*, Portorož, July 12 - 17, 2003, Ed. by N.S. Mankoč Borštnik, H.B. Nielsen, C. Froggatt, D. Lukman, DMFA Založništvo, Ljubljana December 2003, p. 31-57, hep-ph/0401043, hep-ph/0401055.
17. N.S. Mankoč Borštnik, "Unification of spins and charges in Grassmann space?", *Modern Phys. Lett. A* **10**, 587 -595 (1995).
18. D. Lukman, N.S. Mankoč Borštnik and H.B. Nielsen, "Families of spinors in $d = (1 + 5)$ with a zweibein and two kinds of spin connection fields on an almost S^2 ", *Proceedings to the 15th Workshop "What comes beyond the standard models"*, Bled, 9-19 of July, 2012, Ed. N.S. Mankoč Borštnik, H.B. Nielsen, D. Lukman, DMFA Založništvo, Ljubljana December 2012, 157-166, arxiv.1302.4305.
19. G. Bregar, M. Breskvar, D. Lukman and N.S. Mankoč Borštnik, "On the origin of families of quarks and leptons - predictions for four families", *New J. of Phys.* **10**, 093002 (2008), arXiv:hep-ph/0606159, arXiv:0708.2846, arXiv:hep-ph/0612250, p.25-50].

20. G. Bregar and N.S. Mankoč Borštnik, "Does dark matter consist of baryons of new stable family quarks?", *Phys. Rev. D* **80**, 083534 (2009) 1-16.
21. G. Bregar, N.S. Mankoč Borštnik, "Can we predict the fourth family masses for quarks and leptons?", Proceedings to the 16th Workshop "What comes beyond the standard models", Bled, 14-21 of July, 2013, Ed. N.S. Mankoč Borštnik, H.B. Nielsen, D. Lukman, DMFA Založništvo, Ljubljana December 2013, p. 31-51, [arxiv:1403.4441].
22. G. Bregar, N.S. Mankoč Borštnik, "The new experimental data for the quarks mixing matrix are in better agreement with the *spin-charge-family* theory predictions", Proceedings to the 17th Workshop "What comes beyond the standard models", Bled, 20-28 of July, 2014, Ed. N.S. Mankoč Borštnik, H.B. Nielsen, D. Lukman, DMFA Založništvo, Ljubljana December 2014, p.20-45 [arXiv:1502.06786v1] [arxiv:1412.5866]
23. N.S. Mankoč Borštnik, "Do we have the explanation for the Higgs and Yukawa couplings of the *standard model*", [arxiv:1212.3184, arxiv:1011.5765].
24. N.S. Mankoč Borštnik, "The *spin-charge-family* theory explains why the scalar Higgs carries the weak charge $\pm \frac{1}{2}$ and the hyper charge $\mp \frac{1}{2}$ ", Proceedings to the 17th Workshop "What Comes Beyond the Standard Models", Bled, July 20 - 28, 2014, p.163-182, [arxiv:1409.7791, arxiv:1212.4055].
25. A. Ali in discussions and in private communication at the Singapore Conference on New Physics at the Large Hadron Collider, 29 February - 4 March 2016.
26. M. Neubert, in discussions at the Singapore Conference on New Physics at the Large Hadron Collider, 29 February - 4 March 2016.
27. A. Lenz, "Constraints on a fourth generation of fermions from higgs boson searches", *Advances in High Energy Physics* **2013**, ID 910275.
28. N.S. Mankoč Borštnik, H.B.F. Nielsen, "Do the present experiments exclude the existence of the fourth family members?", Proceedings to the 19th Workshop "What comes beyond the standard models", Bled, 11-19 of July, 2016, Ed. N.S. Mankoč Borštnik, H.B. Nielsen, D. Lukman, DMFA Založništvo, Ljubljana December 2016, p.128-146 [arXiv:1703.09699].
29. T. P. Cheng and Marc Sher, "Mass-matrix ansatz and flavor nonconservation in models with multiple Higgs doublets", *Phys. Rev. D* **35** (1987), 3484.
30. F. Mahmoudi and O. Stål, "Flavor constraints on two-Higgs-doublet models with general diagonal Yukawa couplings", *Phys. Rev. D* **81** (2010) 035016.
31. C. Anastasiou, R. Boughezal and F. Petriello, "Mixed QCD-electroweak corrections to Higgs boson production in gluon fusion", *J. of High Energy Phys.* **04** (2009) 003.
32. C. Patrignani et al. (Particle Data Group), *Chin. Phys. C* **40** (2016) 100001.
33. A. Hoecker, "Physics at the LHC Run-2 and beyond", [arXiv:1611v1[hep-ex]].
34. N.S. Mankoč Borštnik, "The Spin-Charge-Family theory offers the explanation for all the assumptions of the Standard model, for the Dark matter, for the Matter-antimatter asymmetry, making several predictions", Proceedings to the Conference on New Physics at the Large Hadron Collider, 29 Februar - 4 March, 2016, Nanyang Executive Centre, NTU, Singapore, to be published, [arXiv: 1607.01618v1].
35. N.S. Mankoč Borštnik, D. Lukman, "Vector and scalar gauge fields with respect to $d = (3 + 1)$ in Kaluza-Klein theories and in the *spin-charge-family theory*", Proceedings to the 18th Workshop "What comes beyond the standard models", Bled, 11-19 of July, 2015, Ed. N.S. Mankoč Borštnik, H.B. Nielsen, D. Lukman, DMFA Založništvo, Ljubljana December 2015, p. 158-164 [arXiv:1604.00675].
36. D. Lukman, N.S. Mankoč Borštnik, H.B. Nielsen, "An effective two dimensionality cases bring a new hope to the Kaluza-Klein-like theories", *New J. Phys.* **13** (2011) 103027, hep-th/1001.4679v5.
37. D. Lukman and N.S. Mankoč Borštnik, "Spinor states on a curved infinite disc with non-zero spin-connection fields", *J. Phys. A: Math. Theor.* **45**, 465401 (2012) 19 pages [arxiv:1205.1714, arxiv:1312.541, hep-ph/0412208 p.64-84].

38. R. Franceshini, G.F. Giudice, J.F. Kamenik, M. McCullough, A. Pomarol, R. Rattazzi, M. Redi, F. Riva, A. Strumia, R. Torre, ArXiv:1512.04933.
39. CMS Collaboration, CMS-PAS-EXO-12-045.
40. CMS Collaboration, *Phys. Rev. D* **92** (2015) 032004.
41. N.S. Mankoč Borštnik, D. Lukman, "Vector and scalar gauge fields with respect to $d = (3 + 1)$ in Kaluza-Klein theories and in the *spin-charge-family theory*", Proceedings to the 18th Workshop "What comes beyond the standard models", Bled, 11-19 of July, 2015, Ed. N.S. Mankoč Borštnik, H.B. Nielsen, D. Lukman, DMFA Založništvo, Ljubljana December 2015, p. 158-164 [arXiv:1604.00675].
42. N.S. Mankoč Borštnik, H. B. Nielsen, "Dirac-Kähler approach connected to quantum mechanics in Grassmann space", *Phys. Rev. D* **62**, 044010, (2000)1-14, hep-th/9911032.
43. N.S. Mankoč Borštnik, H.B. Nielsen, "Discrete symmetries in the Kaluza-Klein-like theories", doi:10.1007/ *Jour. of High Energy Phys.* **04** (2014)165-174 <http://arxiv.org/abs/1212.2362v3>.
44. T. Troha, D. Lukman and N.S. Mankoč Borštnik, "Massless and massive representations in the *spinor technique*" *Int. J. of Mod. Phys. A* **29** 1450124 (2014), 21 pages. [arXiv:1312.1541].
45. N.S. Mankoč Borštnik, H.B.F. Nielsen, "Fermionization in an arbitrary number of dimensions", Proceedings to the 18th Workshop "What comes beyond the standard models", Bled, 11-19 of July, 2015, Ed. N.S. Mankoč Borštnik, H.B. Nielsen, D. Lukman, DMFA Založništvo, Ljubljana December 2015, p. 111-128 [<http://arxiv.org/abs/1602.03175>].
46. T. Kaluza, *Sitzungsber. Preuss. Akad. Wiss. Berlin, Math. Phys.* **96** (1921) 69, O. Klein, *Z. Phys.* **37** (1926) 895.
47. The authors of the works presented in *An introduction to Kaluza-Klein theories*, Ed. by H. C. Lee, World Scientific, Singapore 1983, T. Appelquist, A. Chodos, P.G.O. Freund (Eds.), *Modern Kaluza-Klein Theories*, Reading, USA: Addison Wesley, 1987.
48. D. Lukman, N. S. Mankoč Borštnik, H. B. Nielsen, *New J. Phys.* **13** (2011) 10302 [arXiv:1001.4679v4].



7 Extending Starobinsky Inflationary Model in Gravity and Supergravity

S.V. Ketov^{1,2,3} * and M.Yu. Khlopov⁴ **

¹ Physics Department, Tokyo Metropolitan University, Minami-ohsawa 1-1, Hachioji-shi, Tokyo 192-0397, Japan

² Kavli Institute for the Physics and Mathematics of the Universe (IPMU), The University of Tokyo, Chiba 277-8568, Japan

³ Research School of High Energy Physics, Tomsk Polytechnic University, Lenin ave. 30, Tomsk 634050, Russia

⁴ Institute of Physics, Southern Federal University Stachki 194, Rostov on Don 344090, Russia

Abstract. We review some recent trends in the inflationary model building, the supersymmetry (SUSY) breaking, the gravitino Dark Matter (DM) and the Primordial Black Holes (PBHs) production in supergravity. The Starobinsky inflation can be embedded into supergravity when the inflaton belongs to the massive vector multiplet associated with a (spontaneously broken) $U(1)$ gauge symmetry. The SUSY and R-symmetry can be also spontaneously broken after inflation by the (standard) Polonyi mechanism. Polonyi particles and gravitinos are super heavy and can be copiously produced during inflation via the Schwinger mechanism sourced by the Universe expansion. The overproduction and instability problems can be avoided, and the positive cosmological constant (dark energy) can also be introduced. The observed abundance of the Cold Dark Matter (CDM) composed of gravitinos can be achieved in our supergravity model too, thus providing the unifying framework for inflation, supersymmetry breaking, dark energy and dark matter genesis. Our supergravity approach may also lead to a formation of primordial non-linear structures like stellar-mass-type black holes, and may include the SUSY GUTs inspired by heterotic string compactifications, unifying particle physics with quantum gravity.

Povzetek. Avtorja obravnavata nekaj novejših modelov inflacije, zlomitve supersimetrije, temne snovi, ki jo sestavljajo gravitini in nastajanja prvotnih črnih lukenj v supergravitaciji. Inflacija Starobinskega se pojavi v supergravitaciji, če je inflaton del masivnega vektorskega multipleta, ki spontano zlomi umeritveno simetrijo $U(1)$. Supersimetrijo in simetrijo R lahko po inflaciji spontano zlomi tudi mehanizem Polonyija. Izredno masivni delci Polonyija in gravitini, lahko nastanejev dovolj velikih koločinah med inflacijo z mehanizmom Schwingerja. S tem se avtorja izogneta problemu prevelike produkcije težkih delcev in nestabilnosti ter pojasnita tudi pozitivno kozmološko konstanto (temno energijo). Njun model s supergravitacijo razloži opaženo pogostost hladne temne snovi (CDM), če jo sestavljajo gravitini in ponudi razlago za nastanek in potek inflacije, zlomitev supersimetrije, temno energijo in temno snov. Njun model lahko pojasni tudi nastanek prvotnih nelinearnih struktur, kot so črne luknje, ki imajo maso enake masi običajnih zvezd, in morda

* E-mail: ketov@tmu.ac.jp

** E-mail: khlopov@apc.in2p3.fr

vključuje supersimetrične teorije velikega poenotenja (GUT), izvirajoče iz kompaktifikacije heterotskih strun, kar bi poenotilo fiziko delcev in kvantno gravitacijo.

Keywords: inflation, modified gravity, supergravity, cold dark matter, dark energy, supersymmetry breaking, primordial black holes

7.1 Introduction

The Cosmic Microwave Background (CMB) data collected by the Planck collaboration [1–3] favours the slow-roll single-field inflationary scenarios, with an approximately flat scalar potential. The celebrated Starobinsky model [4] does provide such scenario, and relates its inflaton (called scalaron in this context) to the particular extension of Einstein-Hilbert gravity with the extra higher derivative term given by the scalar curvature squared, R^2 . However, a theoretical explanation of fundamental origin of the Starobinsky model is still missing. The viable inflationary dynamics is driven by the R^2 term dominating over the (Einstein-Hilbert) R term. This is related to a missing UV completion of the non-renormalizable $(R + R^2)$ gravity. The interesting and ambitious project for string phenomenology would be to provide a derivation of the Starobinsky model from the first principles. A first step towards this is an embedding of the Starobinsky model into four-dimensional $\mathcal{N} = 1$ supergravity. In the supergravity framework, the inflaton (scalaron) can mix with other scalars, and this mixing may ruin any initially successful inflationary mechanism.

The inflationary model building based on supergravity in the literature usually assumes that inflaton belongs to a chiral (scalar) supermultiplet [5–7]. However, there is the alternative to this assumption: inflaton can also belong to a massive $\mathcal{N} = 1$ vector multiplet. The vector multiplet-based approach avoids stabilization problems related to the inflaton (scalar) superpartner, as the way-out of the standard η -problem. The scalar potential of a vector multiplet is given by the D-term instead of the F-term. The minimal supergravity models, with inflaton belonging to a massive vector multiplet, were proposed in Refs. [8,9]. Then any desired values of the CMB observables (the scalar perturbations tilt n_s and the tensor-to-scalar perturbations ratio r) can be recast from the single-field (inflaton) scalar potential proportional to the derivative squared of arbitrary real function J . However, in these models, the vacuum energy is vanishing after inflation, thus restoring supersymmetry, and only a Minkowski vacuum is allowed. The way-out of this problem was proposed in [10,11] by adding a Polonyi (chiral) superfield with a linear superpotential [12], leading to a spontaneous SUSY breaking and allowing a de-Sitter vacuum after inflation.

A successful model of inflation in supergravity should also be consistent with the Cold Dark Matter (CDM) constraints and the Big Bang Nucleosynthesis (BBN). For example, many supergravity scenarios are plagued by the so-called gravitino problem. Gravitinos can decay, injecting hadrons and photons during the BBN epoch, which may jeopardize the good Standard Model prediction of nuclei ratios [13–16]. In very much the same way, the Polonyi (overproduction) problem and

its relation to the BBN results were extensively discussed in the literature [17–22]. In addressing these issues, the mass spectrum and the soft SUSY parameters are important. The leading (WIMP-like) dark matter production mechanisms and decay channels are selected from the mass pattern, and have either thermal or non-thermal origin.

In this paper, we review a class of the minimalistic Polonyi-Starobinsky (PS) $\mathcal{N} = 1$ supergravity models for inflation, with the inflaton belonging to a (massive) vector multiplet. These models can avoid the overproduction and BBN problems, while accounting for the right amount of CDM composed of gravitinos. In our analysis, we assume that the Polonyi field, inducing a spontaneous SUSY breaking at a high energy scale, and the gravitino, as the Dark Matter (DM) particle, are both super-heavy. The main mechanism producing DM is given by the Schwinger-type production sourced by inflationary expansion. After inflation, Polonyi particles rapidly decay into gravitinos. We find that gravitinos produced directly from Schwinger’s production and from Polonyi particles decays, can account for the correct abundance of Cold Dark Matter.

Another aspect is an inclusion of the (mini) Primordial Black Holes (PBHs) that may have been copiously produced in the early Universe, and later may have evaporated into gravitinos and other Standard Model particles [23–27]. A large amount of mini PBHs cannot be produced in our model when the other scalar and pseudo-scalar partners of inflaton are not participating in the inflationary dynamics. The Starobinsky inflaton entails a scalar potential shape that cannot lead to a large number of PBHs, because it does not allow for amplifying instabilities and has no exit out of inflation with a first order phase transition. It is still possible that dynamics of other scalar fields changes this picture. In this case, the extra moduli can exit from inflation via ending in false minima. The tunneling process from a false minimum to the true one sources the production of bubbles related to the first order phase transition.

As regards the (solar mass type) PBHs, their production in the early Universe is possible in our supergravity approach after a certain deformation of the Starobinsky scalar potential. We envisage a unification of the inflaton in a vector multiplet and the Supersymmetric Grand Unified Theories (SUSY GUTs), whose gauge group has at least one abelian factor, such as the flipped $SU(5) \times U(1)$ model arising from the compactified heterotic superstrings or the intersecting D-branes.

7.2 Starobinsky model of $(R + R^2)$ gravity

Starobinsky model of inflation is defined by the action [4]

$$S_{\text{Star.}} = \frac{M_{\text{Pl}}^2}{2} \int d^4x \sqrt{-g} \left(R + \frac{1}{6m^2} R^2 \right), \quad (7.1)$$

where we have introduced the reduced Planck mass $M_{\text{Pl}} = 1/\sqrt{8\pi G_N} \approx 2.4 \times 10^{18}$ GeV, and the scalaron (inflaton) mass m as the only parameter. We use the spacetime signature $(-, +, +, +)$. The $(R + R^2)$ gravity model (7.1) can be considered as the simplest extension of the standard Einstein-Hilbert action in the

context of (modified) $F(R)$ gravity theories with an action

$$S_F = \frac{M_{\text{Pl}}^2}{2} \int d^4x \sqrt{-g} F(R) , \quad (7.2)$$

in terms of the function $F(R)$ of the scalar curvature R .

The $F(R)$ gravity action (7.2) is classically equivalent to

$$S[g_{\mu\nu}, \chi] = \frac{M_{\text{Pl}}^2}{2} \int d^4x \sqrt{-g} [F'(\chi)(R - \chi) + F(\chi)] \quad (7.3)$$

with the real scalar field χ , provided that $F'' \neq 0$ that we always assume. Here the primes denote the derivatives with respect to the argument. The equivalence is easy to verify because the χ -field equation implies $\chi = R$. In turn, the factor F' in front of the R in (7.3) can be (generically) eliminated by a Weyl transformation of metric $g_{\mu\nu}$, that transforms the action (7.3) into the action of the scalar field χ minimally coupled to Einstein gravity and having the scalar potential

$$V = \left(\frac{M_{\text{Pl}}^2}{2} \right) \frac{\chi F'(\chi) - F(\chi)}{F'(\chi)^2} . \quad (7.4)$$

Differentiating this scalar potential yields

$$\frac{dV}{d\chi} = \left(\frac{M_{\text{Pl}}^2}{2} \right) \frac{F''(\chi) [2F(\chi) - \chi F'(\chi)]}{(F'(\chi))^3} . \quad (7.5)$$

The kinetic term of χ becomes canonically normalized after the field redefinition $\chi(\varphi)$ as

$$F'(\chi) = \exp \left(\sqrt{\frac{2}{3}} \varphi / M_{\text{Pl}} \right) , \quad \varphi = \frac{\sqrt{3} M_{\text{Pl}}}{\sqrt{2}} \ln F'(\chi) , \quad (7.6)$$

in terms of the canonical inflaton field φ , with the total action

$$S_{\text{quintessence}}[g_{\mu\nu}, \varphi] = \frac{M_{\text{Pl}}^2}{2} \int d^4x \sqrt{-g} R - \int d^4x \sqrt{-g} \left[\frac{1}{2} g^{\mu\nu} \partial_\mu \varphi \partial_\nu \varphi + V(\varphi) \right] . \quad (7.7)$$

The classical and quantum stability conditions of $F(R)$ gravity theory are given by [5]

$$F'(R) > 0 \quad \text{and} \quad F''(R) > 0 , \quad (7.8)$$

and they are obviously satisfied for Starobinsky model (7.1) for $R > 0$.

Differentiating the scalar potential V in Eq. (7.4) with respect to φ yields

$$\frac{dV}{d\varphi} = \frac{dV}{d\chi} \frac{d\chi}{d\varphi} = \frac{M_{\text{Pl}}^2}{2} \left[\frac{\chi F'' + F' - F'}{F'^2} - 2 \frac{\chi F' - F}{F'^3} F'' \right] \frac{d\chi}{d\varphi} , \quad (7.9)$$

where we have

$$\frac{d\chi}{d\varphi} = \frac{d\chi}{dF'} \frac{dF'}{d\varphi} = \frac{dF'}{d\varphi} \bigg/ \frac{dF'}{d\chi} = \frac{\sqrt{2}}{\sqrt{3} M_{\text{Pl}}} \frac{F'}{F''} . \quad (7.10)$$

This implies

$$\frac{dV}{d\varphi} = M_{\text{Pl}} \frac{2F - \chi F'}{\sqrt{6}F'^2} . \quad (7.11)$$

Combining Eqs. (7.4) and (7.11) yields R and F in terms of the scalar potential V ,

$$R = \left[\frac{\sqrt{6}}{M_{\text{Pl}}} \frac{dV}{d\varphi} + \frac{4V}{M_{\text{Pl}}^2} \right] \exp \left(\sqrt{\frac{2}{3}} \varphi / M_{\text{Pl}} \right) , \quad (7.12)$$

$$F = \left[\frac{\sqrt{6}}{M_{\text{Pl}}} \frac{dV}{d\varphi} + \frac{2V}{M_{\text{Pl}}^2} \right] \exp \left(2\sqrt{\frac{2}{3}} \varphi / M_{\text{Pl}} \right) . \quad (7.13)$$

These equations define the function $F(R)$ in the parametric form, in terms of a scalar potential $V(\varphi)$, i.e. the *inverse* transformation to (7.4). This is known [28] as the classical equivalence (duality) between the $F(R)$ gravity theories (7.2) and the scalar-tensor (quintessence) theories of gravity (7.7).

In the case of Starobinsky model (7.1), one gets the famous potential

$$V(\varphi) = \frac{3}{4} M_{\text{Pl}}^2 m^2 \left[1 - \exp \left(-\sqrt{\frac{2}{3}} \varphi / M_{\text{Pl}} \right) \right]^2 . \quad (7.14)$$

This scalar potential is bounded from below (non-negative and stable), and it has the absolute minimum at $\varphi = 0$ corresponding to a Minkowski vacuum. The scalar potential (7.14) also has a *plateau* of positive height (related to inflationary energy density), that gives rise to slow roll of inflaton in the inflationary era. The Starobinsky model (7.1) is the particular case of the so-called α -attractor inflationary models [29], and is also a member of the close family of viable inflationary models of $F(R)$ gravity, originating from higher dimensions [30].

A duration of inflation is measured in the slow roll approximation by the e-foldings number

$$N_e \approx \frac{1}{M_{\text{Pl}}^2} \int_{\varphi_{\text{end}}}^{\varphi_*} \frac{V}{V'} d\varphi , \quad (7.15)$$

where φ_* is the inflaton value at the reference scale (horizon crossing), and φ_{end} is the inflaton value at the end of inflation when one of the slow roll parameters

$$\varepsilon_V(\varphi) = \frac{M_{\text{Pl}}^2}{2} \left(\frac{V'}{V} \right)^2 \quad \text{and} \quad \eta_V(\varphi) = M_{\text{Pl}}^2 \left(\frac{V''}{V} \right) , \quad (7.16)$$

is no longer small (close to 1).

The amplitude of scalar perturbations at horizon crossing is given by [31]

$$A = \frac{V_*^3}{12\pi^2 M_{\text{Pl}}^6 (V'_*)^2} = \frac{3m^2}{8\pi^2 M_{\text{Pl}}^2} \sinh^4 \left(\frac{\varphi_*}{\sqrt{6} M_{\text{Pl}}} \right) . \quad (7.17)$$

The Starobinsky model (7.1) is the excellent model of cosmological inflation, in very good agreement with the Planck data [1–3]. The Planck satellite mission measurements of the Cosmic Microwave Background (CMB) radiation [1–3] give the scalar perturbations tilt as $n_s \approx 1 + 2\eta_V - 6\varepsilon_V \approx 0.968 \pm 0.006$ and restrict

the tensor-to-scalar ratio as $r \approx 16\epsilon_V < 0.08$. The Starobinsky inflation yields $r \approx 12/N_e^2 \approx 0.004$ and $n_s \approx 1 - 2/N_e$, where N_e is the e-foldings number between 50 and 60, with the best fit at $N_e \approx 55$ [32,33].

The Starobinsky model (7.1) is geometrical (based on gravity only), while its (mass) parameter m is fixed by the observed CMB amplitude (COBE, WMAP) as

$$m \approx 3 \cdot 10^{13} \text{ GeV} \quad \text{or} \quad \frac{m}{M_{\text{Pl}}} \approx 1.3 \cdot 10^{-5}. \quad (7.18)$$

A numerical analysis of (7.15) with the potential (7.14) yields [31]

$$\sqrt{\frac{2}{3}}\varphi_*/M_{\text{Pl}} \approx \ln\left(\frac{4}{3}N_e\right) \approx 5.5, \quad \sqrt{\frac{2}{3}}\varphi_{\text{end}}/M_{\text{Pl}} \approx \ln\left[\frac{2}{11}(4 + 3\sqrt{3})\right] \approx 0.5, \quad (7.19)$$

where $N_e \approx 55$ has been used.

7.3 Starobinsky inflation in supergravity

Let us introduce a set of two chiral superfields (Φ, H) and a real vector superfield V coupled to the supergravity sector, with the following Lagrangian:¹

$$\mathcal{L} = \int d^2\theta d^2\bar{\theta} \left\{ \frac{3}{8}(\bar{D}\bar{D} - 8\mathcal{R})e^{-\frac{1}{3}(K+2J)} + \frac{1}{4}W^\alpha W_\alpha + \mathcal{W}(\Phi) \right\} + \text{h.c.}, \quad (7.20)$$

where \mathcal{R} is the chiral scalar curvature superfield, \mathcal{E} is the chiral density superfield, $(\mathcal{D}_\alpha, \bar{\mathcal{D}}^{\dot{\alpha}})$ are the superspace covariant spinor derivatives, $K = K(\Phi, \bar{\Phi})$ is the Kähler potential, $\mathcal{W}(\Phi)$ is the superpotential, $W_\alpha \equiv -\frac{1}{4}(\bar{D}\bar{D} - 8\mathcal{R})\mathcal{D}_\alpha V$ is the abelian (chiral) superfield strength, and $J = J(\text{He}^{2gV}\bar{H})$ is a real function with the coupling constant g .

The Lagrangian (7.20) is invariant under the supersymmetric $U(1)$ gauge transformations

$$H \rightarrow H' = e^{-igZ}H, \quad \bar{H} \rightarrow \bar{H}' = e^{ig\bar{Z}}\bar{H}, \quad (7.21)$$

$$V \rightarrow V' = V + \frac{i}{2}(Z - \bar{Z}), \quad (7.22)$$

the gauge parameter of which, Z , is itself a chiral superfield. The chiral superfield H can be gauged away via the gauge fixing of these transformations by imposing the gauge condition $H = 1$. Then the Lagrangian (7.20) gets simplified to

$$\mathcal{L} = \int d^2\theta d^2\bar{\theta} \left\{ \frac{3}{8}(\bar{D}\bar{D} - 8\mathcal{R})e^{-\frac{1}{3}(K+2J)} + \frac{1}{4}W^\alpha W_\alpha + \mathcal{W} \right\} + \text{h.c.} \quad (7.23)$$

After eliminating the auxiliary fields and moving from the initial (Jordan) frame to the Einstein frame, the *bosonic* part of the Lagrangian (7.23) reads [10]²

$$e^{-1}\mathcal{L} = -\frac{1}{2}R - K_{A\bar{A}}\partial_m A\partial^m \bar{A} - \frac{1}{4}F_{mn}F^{mn} - \frac{1}{2}J''\partial_m C\partial^m C - \frac{1}{2}J''B_m B^m - \mathcal{V}, \quad (7.24)$$

¹ We use the standard notation [34] for supergravity in superspace.

² The primes and capital latin subscripts denote the derivatives with respect to the corresponding fields.

with the scalar potential

$$\mathcal{V} = \frac{g^2}{2} J'^2 + e^{K+2J} \left\{ K_{A\bar{A}}^{-1} (\mathcal{W}_A + K_A \mathcal{W}) (\bar{\mathcal{W}}_{\bar{A}} + K_{\bar{A}} \bar{\mathcal{W}}) - \left(3 - 2 \frac{J'^2}{J''} \right) \mathcal{W} \bar{\mathcal{W}} \right\} \quad (7.25)$$

in terms of the physical fields (A, C, B_m), the auxiliary fields (F, X, D) and the vector field strength $F_{mn} = \mathcal{D}_m B_n - \mathcal{D}_n B_m$.

As is clear from Eq. (7.24), the absence of ghosts requires $J''(C) > 0$, where the primes denote the differentiations with respect to the given argument. We restrict ourselves to the Kähler potential and the superpotential of the *Polonyi model* [12]:

$$K = \Phi \bar{\Phi}, \quad \mathcal{W} = \mu(\Phi + \beta), \quad (7.26)$$

with the parameters μ and β . Our model includes the single-field (C) inflationary model, whose D-type scalar potential is given by

$$V(C) = \frac{g^2}{2} (J')^2 \quad (7.27)$$

in terms of *arbitrary* function $J(C)$, with the real inflaton field C belonging to a massive vector supermultiplet. The Minkowski vacuum conditions (after inflation) can be easily satisfied when $J' = 0$, which implies [12]

$$\langle A \rangle = \sqrt{3} - 1 \quad \text{and} \quad \beta = 2 - \sqrt{3}. \quad (7.28)$$

This solution describes a *stable* Minkowski vacuum with spontaneous SUSY breaking at *arbitrary* scale $\langle F \rangle = \mu$. The related gravitino mass is given by

$$m_{3/2} = \mu e^{2-\sqrt{3}+\langle J \rangle}. \quad (7.29)$$

There is also a complex (Polonyi) scalar of mass

$$M_A = 2\mu e^{2-\sqrt{3}} \geq 2m_{3/2} \quad (7.30)$$

and a massless fermion in the physical spectrum. The inequality in Eq. (7.30) is saturated in the original Polonyi model [12] but it is not the case in our model when $\langle J \rangle < 0$.

As regards the early Universe phenomenology, our model has the following theoretically appealing features:

- there is no need to “stabilize” the single-field inflationary trajectory against scalar superpartners of inflaton, because our inflaton is the only real scalar in a massive vector multiplet,
- any values of CMB observables n_s and r are possible by choosing the J -function,
- a spontaneous SUSY breaking after inflation occurs at arbitrary scale μ ,
- there are only *a few* parameters relevant for inflation and SUSY breaking: the coupling constant g defining the inflaton mass, $g \sim m_{\text{inf.}}$, the coupling constant μ defining the scale of SUSY breaking, $\mu \sim m_{3/2}$, and the parameter β in the

constant term of the superpotential. Actually, the inflaton mass is constrained by CMB observations as $m_{inf.} \sim \mathcal{O}(10^{-6})$, while β is fixed by the vacuum solution, so that we have only *one* free parameter μ defining the scale of SUSY breaking in our model (before studying reheating and phenomenology).

The D-type scalar potential associated with the Starobinsky inflationary model of $(R + R^2)$ gravity arises when [9]

$$J(C) = \frac{3}{2} (C - \ln C) \quad (7.31)$$

that implies

$$J'(C) = \frac{3}{2} (1 - C^{-1}) \quad \text{and} \quad J''(C) = \frac{3}{2} (C^{-2}) > 0. \quad (7.32)$$

According to (7.24), a canonical inflaton field ϕ (with the canonical kinetic term) is related to the field C by the field redefinition

$$C = \exp \left(\sqrt{2/3} \phi \right). \quad (7.33)$$

Therefore, we arrive at the (Starobinsky) scalar potential

$$V_{\text{Star.}}(\phi) = \frac{9g^2}{8} \left(1 - e^{-\sqrt{2/3}\phi} \right)^2 \quad \text{with} \quad m_{inf.}^2 = 9g^2/2. \quad (7.34)$$

The full action (7.20) of this PS supergravity in curved superspace can be transformed into a supergravity extension of the $(R + R^2)$ gravity action by using the (inverse) duality procedure described in Ref. [9]. However, the dual supergravity model is described by a complicated *higher-derivative* field theory that is inconvenient for studying particle production.

Another nice feature of our model is that it can be rewritten as a supersymmetric (abelian and non-minimal) gauge theory coupled to supergravity in the presence of a *Higgs* superfield H , resulting in the super-Higgs effect with simultaneous spontaneous breaking of the gauge symmetry and SUSY. Indeed, the $U(1)$ gauge symmetry of the original Lagrangian (7.20) allows us to choose a different (*Wess-Zumino*) supersymmetric gauge by "gauging away" the chiral and anti-chiral parts of the general superfield V via the appropriate choice of the superfield parameters Z and \bar{Z} . Then the bosonic part of the Lagrangian in terms of the superfield components in the Einstein frame, after elimination of the auxiliary fields and Weyl rescaling, reads [11]

$$e^{-1} \mathcal{L} = -\frac{1}{2} R - K_{AA^*} \partial^m A \partial_m \bar{A} - \frac{1}{4} F_{mn} F^{mn} - 2J_{h\bar{h}} \partial_m h \partial^m \bar{h} - \frac{1}{2} J_{V^2} B_m B^m \\ + iB_m (J_{Vh} \partial^m h - J_{V\bar{h}} \partial^m \bar{h}) - \mathcal{V}, \quad (7.35)$$

where h, \bar{h} are the Higgs field and its conjugate.

The standard $U(1)$ Higgs mechanism arises with the canonical function $J = \frac{1}{2} h e^{2V} \bar{h}$, where we have chosen $g = 1$ for simplicity. As regards the Higgs sector, it leads to

$$e^{-1} \mathcal{L}_{\text{Higgs}} = -\partial_m h \partial^m \bar{h} + iB_m (\bar{h} \partial^m h - h \partial^m \bar{h}) - h \bar{h} B_m B^m - \mathcal{V}. \quad (7.36)$$

After changing the variables h and \bar{h} as

$$h = \frac{1}{\sqrt{2}}(\rho + \nu)e^{i\zeta}, \quad \bar{h} = \frac{1}{\sqrt{2}}(\rho + \nu)e^{-i\zeta}, \quad (7.37)$$

where ρ is the (real) Higgs boson, $\nu \equiv \langle h \rangle = \langle \bar{h} \rangle$ is the Higgs VEV, and ζ is the Goldstone boson, the unitary gauge fixing of $h \rightarrow h' = e^{-i\zeta}h$ and $B_m \rightarrow B'_m = B_m + \partial_m \zeta$, leads to the standard result

$$e^{-1}\mathcal{L}_{\text{Higgs}} = -\frac{1}{2}\partial_m \rho \partial^m \rho - \frac{1}{2}(\rho + \nu)^2 B_m B^m - \mathcal{V}. \quad (7.38)$$

The Minkowski vacuum after inflation can be easily lifted to a *de Sitter* vacuum (Dark Energy) in our model by the simple modification of the Polonyi sector and its parameters as [11]

$$\langle A \rangle = (\sqrt{3}-1) + \frac{3-2\sqrt{3}}{3(\sqrt{3}-1)}\delta + \mathcal{O}(\delta^2), \quad \beta = (2-\sqrt{3}) + \frac{\sqrt{3}-3}{6(\sqrt{3}-1)}\delta + \mathcal{O}(\delta^2), \quad (7.39)$$

where δ is a very small deformation parameter, $0 < \delta \ll 1$. It leads to a positive cosmological constant

$$V_0 = \mu^2 e^{\alpha^2} \delta = m_{3/2}^2 \delta \quad (7.40)$$

and the superpotential VEV

$$\langle \mathcal{W} \rangle = \mu(\langle A \rangle + \beta) = \mu(a + b - \frac{1}{2}\delta), \quad (7.41)$$

where $a \equiv (\sqrt{3}-1)$ and $b \equiv (2-\sqrt{3})$ provide the SUSY breaking vacuum solution to the Polonyi parameters in the absence of a cosmological constant.

The full scalar potential (7.25) is a sum of the D- and F-type terms, while there is a mix of the inflaton - and Polonyi-dependent terms in the F-type contribution. This mixing leads to instability of the (Starobinsky) inflationary trajectory that is supposed to be driven by the D-term only. This issue was resolved in Ref. [35] where a modification of the original PS supergravity action (7.20) was proposed via adding the generalized Fayet-Iliopoulos term and modifying the J-function (7.31).

7.4 Super heavy gravitino dark matter

The complete set of equations of motion in our supergravity model (Sec. 3) is very complicated. In this section, we consider only the leading order with respect to the inverse Planck mass. In addition, we neglect the coupling of Polonyi and gravitino particles to the inflaton, and introduce the effective action of the Polonyi field in the Friedmann-Lemaître-Robertson-Walker (FLRW) background (in comoving coordinates) as

$$I[A] = \int dt \int d^3x \frac{a^3}{2} \left(\dot{A}^2 - \frac{1}{a^2} (\nabla A)^2 - M_A^2 A^2 - \zeta R A^2 \right), \quad (7.42)$$

where the non-minimal coupling constant of the Polonyi field to gravity is equal to $\zeta = 1$, A is the Polonyi field, M_A stands for its mass, R is the Ricci scalar, and a is the FLRW scale factor.

The mode decomposition of the Polonyi field reads

$$A(\mathbf{x}) = \int d^3k (2\pi)^{-3/2} a^{-1}(\eta) \left[b_k h_k(\eta) e^{i\mathbf{k}\cdot\mathbf{x}} + b_k^\dagger h_k^*(\eta) e^{-i\mathbf{k}\cdot\mathbf{x}} \right], \quad (7.43)$$

where the conformal time coordinate η is introduced, b, b^\dagger are the (standard) creation/annihilation operators, and the coefficient functions h, h^+ are normalized as follows:

$$h_k h_k'^* - h_k' h_k^* = i. \quad (7.44)$$

Because of Eqs. (7.42) and (7.43), the equation of motion of the modes is

$$h_k''(\eta) + \omega_k^2(\eta) h_k(\eta) = 0, \quad \text{where} \quad \omega_k^2 = 5 \frac{a''}{a} + k^2 + M_A^2 a^2, \quad (7.45)$$

and $h'' = d^2 h / d\eta^2$. Equation (7.45) can be conveniently rescaled by using some reference scales $a(\eta_*) \equiv a_*$ and $H(\eta_*) = H_*$ as follows:

$$h_{\tilde{k}}''(\tilde{\eta}) + (\tilde{k}^2 + \tilde{b}^2 \tilde{a}^2) h_{\tilde{k}}(\tilde{\eta}) = 0, \quad (7.46)$$

in terms of the rescaled quantities

$$\tilde{\eta} = \eta a_* H_*, \quad \tilde{a} = a/a_*, \quad \tilde{k} = k/(H_* a_*).$$

The leading order of the gravitino action coincides with the massive Rarita-Schwinger action,

$$I[\psi] = \int d^4x \, e \, \bar{\psi}_\sigma \mathcal{R}^\sigma \{\psi\}, \quad (7.47)$$

where the gravitino kinetic operator has been introduced as

$$\mathcal{R}^\sigma \{\psi\} = m_{3/2} \gamma^{\sigma\nu} \psi_\nu + i \gamma^{\sigma\nu\rho} \mathcal{D}_\nu \psi_\rho, \quad (7.48)$$

and the supercovariant derivative is

$$\mathcal{D}_\mu \psi_\nu = -\Gamma_{\mu\nu}^\rho \psi_\rho + \partial_\mu \psi_\nu + \frac{1}{4} \omega_{\mu\alpha\beta} \gamma^{\alpha\beta} \psi_\nu, \quad (7.49)$$

in the γ -notation $\gamma^{\mu_1 \dots \mu_n} = \gamma^{[\mu_1} \dots \gamma^{\mu_n]}$.

Since the supergravity torsion is of the second order with respect to the inverse Planck mass, we ignore it in the leading order approximation. The $\Gamma_{\mu\nu}^\rho$ can be represented by the standard symmetric Christoffel symbols that are actually cancelled from the Rarita-Schwinger action (7.47). The Rarita-Schwinger action leads to the gravitino equation of motion,

$$(i\not{D} - m_{3/2})\psi_\mu - \left(i\mathcal{D}_\mu + \frac{m_{3/2}}{2} \gamma_\mu \right) \gamma \cdot \psi = 0. \quad (7.50)$$

In the flat FLRW background, Eq. (7.50) reduces to

$$i\gamma^{mn} \partial_m \psi_n = - \left(m_{3/2} + i \frac{a'}{a} \gamma^0 \right) \gamma^m \partial_m \psi, \quad (7.51)$$

where

$$\omega_{\mu\alpha b} = 2\dot{a}a^{-1}e_{\mu[\alpha}e_{b]}^0, \quad e_\mu^a = a(\eta)\delta_\mu^a, \quad m_{3/2} = m_{3/2}(\eta). \quad (7.52)$$

A solution to Eq. (7.51) is

$$\psi_\mu(x) = \int d^3\mathbf{p} (2\pi)^{-3} (2p_0)^{-1} \sum_\lambda \{e^{i\mathbf{k}\cdot\mathbf{x}} b_\mu(\eta, \lambda) a_{k\lambda}(\eta) + e^{-i\mathbf{k}\cdot\mathbf{x}} b_\mu^C(\eta, \lambda) a_{k\lambda}^\dagger(\eta)\}. \quad (7.53)$$

We find that the equations of motion for the 3/2-helicity gravitino modes have the same form as that of Eq. (7.45), namely,

$$b_\mu''(\eta, \lambda) + \hat{C}(k, a) b_\mu'(\eta, \lambda) + \omega^2(k, a) b_\mu(\eta, \lambda) = 0, \quad (7.54)$$

where we have introduced the notation

$$\hat{C}(k, a) b_\mu'(\eta, \lambda) = -2i\gamma^{\nu i} k_i \gamma_{\nu\eta} \partial_\eta b_\mu - 2\gamma_\nu (m_{3/2} + i\frac{a'}{a}\gamma^0) i\gamma^{\nu\eta} \partial_\eta b_\mu, \quad (7.55)$$

$$\omega^2(k, a)/2 = k^2 + m_{3/2}^2 + 2i\frac{a'}{a}\gamma^0 m_{3/2} - \left(\frac{a'}{a}\right)^2. \quad (7.56)$$

Following a procedure similar to the standard one in the case of Dirac and Klein-Gordon equations, we can reformulate the mode equations of motion in our case as

$$P_\nu P^\nu b_\mu(\eta, \lambda) = 0, \quad (7.57)$$

where we have introduced the projector operator

$$P^\nu = i\gamma^{\nu\eta} \partial_\eta - \gamma^{\nu i} k_i - \left(m_{3/2} + i\frac{a'}{a}\gamma^0\right) \gamma^\nu = 0. \quad (7.58)$$

The dynamics of the gravitino and Polonyi fields during inflation necessary lead to their quantum production. The number density of produced particles can be calculated by using a Bogoliubov transformation,

$$h_k^{\eta_1}(\eta) = \alpha_k h_k^{\eta_0}(\eta) + \beta_k h_k^{*\eta_0}(\eta). \quad (7.59)$$

This transformation is performed from the vacuum solution selected by the boundary conditions at $\eta = \eta_{in}$, corresponding to the initial time of inflation, to the final time $\eta = \eta_f$, when the particles creations process from inflation stops. In the inflationary epoch, the dynamical regime is $a'/a^2 \ll M_{Pl}$ and $M_{Pl} b a/k \ll 1$. This implies that we can consider the extremes as $\eta_{in} = -\infty$ and $\eta_f = +\infty$, performing a WKB semiclassical approximation. By assuming these boundary conditions, the energy density of the Polonyi particles produced during inflation reads

$$\rho_A(\eta) = M_A n_A(\eta) = M_A H_{inf}^3 \left(\frac{1}{\tilde{a}(\eta)}\right)^3 \mathcal{P}_A, \quad (7.60)$$

where

$$\mathcal{P}_A = \frac{1}{2\pi^2} \int_0^\infty d\tilde{k} \tilde{k}^2 |\beta_{\tilde{k}}|^2. \quad (7.61)$$

The inflaton mass sets the characteristic energy scale for the Hubble constant, calculated at fixed cosmological time $t \equiv t_f$:

$$H^2(t_f) \simeq m_\phi^2, \quad \rho(t_f) \simeq m_\phi^2 M_{\text{Pl}}^2.$$

We propose the following formula for Polonyi particles (energy-density and Polonyi mass) produced during inflation [36]:

$$(\Omega_A h^2 / \Omega_R h^2) \simeq \frac{8\pi}{3} \left(\frac{M_A}{M_{\text{Pl}}} \right) \left(\frac{T_{\text{reh}}}{T_0} \right) \frac{n_A(t_f)}{M_{\text{Pl}} H^2(t_f)}, \quad (7.62)$$

where M_A is the Polonyi mass, $\Omega_R h^2 \simeq 4.31 \times 10^{-5}$ is the radiation energy density at today's temperature T_0 , $\Omega_A h^2$ is the energy density of the produced Polonyi fields, all in the units of the critical energy density. There is about 8th-orders-of-magnitude suppression of the energy density. The normalized power spectrum \mathcal{P}_A cannot provide such suppression with our values for M_A and H_{inf} . However, it comes from the dilution factor $(\tilde{a})^{-3} = (a_f/a_i)^{-3}$ in Eq. (7.60).

To get the gravitino and Polonyi masses, we have to add a few cosmological assumptions about the relevant parameters of the reheating process and, in particular, about the reheating temperature T_{reh} . The cosmological parameters can be fixed by specifying the e-foldings number N_e in the range between 50 and 60. For a more precise estimate of the CDM abundance, we choose $N_e = 55$, as in Sec. 2. This implies $n_s = 0.964$, $r = 0.004$, $m_{\text{inf}} = 3.2 \cdot 10^{13}$ GeV and $H_{\text{inf}} = \pi M_{\text{P}} \sqrt{p_g/2} = 1.4 \cdot 10^{14}$ GeV. In our scenario, well below the inflaton mass scale the low-energy effective field theory is given by the Standard Model (SM) that has the effective number of d.o.f. as $g_* = 106.75$. It is reasonable to assume that all the SM particles originated from perturbative inflaton decay via the (Starobinsky) universal reheating mechanism, whose reheating temperature is known [37,38]:

$$T_{\text{reh}} = \left(\frac{90}{\pi^2 g_*} \right)^{1/4} \sqrt{\Gamma_{\text{tot}} M_{\text{P}}} = 3 \cdot 10^9 \text{ GeV}. \quad (7.63)$$

On the other hand, the reheating temperature for heavy gravitino is given by [39]

$$T_{\text{reh}} = 1.5 \cdot 10^8 \text{ GeV} \left(\frac{80}{g_*} \right)^{1/4} \left(\frac{m_{3/2}}{10^{12} \text{ GeV}} \right)^{3/2}. \quad (7.64)$$

Combining Eqs. (7.63) and (7.64) we get the gravitino and Polonyi masses as follows:

$$m_{3/2} = (7.7 \pm 0.8) \cdot 10^{12} \text{ GeV} \quad \text{and} \quad M_A = 2e^{-\langle J \rangle} m_{3/2} > 2m_{3/2}. \quad (7.65)$$

7.5 Primordial Black Holes in supergravity

PBHs may be formed in the early Universe by collapse of primordial density perturbations resulting from inflation, when these perturbations re-enter the horizon and are *large* enough, i.e. when gravity forces are larger than pressure, in general.

Apart from being considered as another (non-particle) source for DM, some PBHs (of stellar mass type) are also considered as the candidates for the gravitational wave effects caused by the binary black hole mergers observed by LIGO/Virgo collaboration [40,41].

The PBH *mass* M_{PBH} is related to the perturbations scale k by Carr's formula [42]

$$M_{\text{PBH}} = \gamma \rho \frac{4\pi H^{-3}}{3} \approx M_{\odot} \left(\frac{\gamma}{0.2} \right) \left(\frac{g_*}{3.36} \right)^{-\frac{1}{6}} \left(\frac{k/(2\pi)}{3 \cdot 10^{-9} \text{ Hz}} \right)^{-2}, \quad (7.66)$$

whose coefficient $\gamma = 3^{-3/2} \approx 0.2$, the (normalized) energy density is almost equal to the (normalized) entropy density $g_* \approx 3.36$, and M_{\odot} stands for the Solar mass, $M_{\odot} \approx 2 \times 10^{33} \text{ g}$.

The PBHs *abundance* $f = \Omega_{\text{PBH}}/\Omega_c$ is proportional to the *amplitude* of the scalar perturbations P_{ζ} , while for the LIGO events one finds $k/(2\pi) \sim 10^{-9} \text{ Hz}$, $P_{\zeta} \sim 10^{-2}$ and $f \sim 10^{-2}$, as the regards the orders of their magnitudes [40,41]. The value of 10^{-9} Hz corresponds to 10^6 Mpc^{-1} .

In a single-field inflation, relevant perturbations are controlled by inflaton scalar potential, so that large fluctuations $P_{\mathcal{R}} \approx \frac{\kappa^2}{2\epsilon} \left(\frac{H}{2\pi} \right)^2$ are produced when the slow roll parameter $\epsilon = r/16$ goes to zero, i.e. when the potential has a *near-inflexion point* where

$$V' \approx V'' \approx 0. \quad (7.67)$$

Since we want a copious PBH production along with observationally consistent CMB observables, we should "decouple" these events, and demand the existence of another ("short") plateau in the scalar potential after the inflationary plateau towards the end of inflation. This is not the case for the Starobinsky inflation with the scalar potential (7.14), however, it can be easily achieved in a more general framework. Our supergravity framework in Sect. 3 is an example of such framework, because it leads to a single-field inflation governed by arbitrary function J , so that the associated inflaton scalar potential is given by $V = \frac{g^2}{2} (J')^2$.

As an example, let us consider the inflaton scalar potential

$$\frac{V}{V_0} = \left(1 + \xi - e^{-\alpha\phi} - \xi e^{-\beta\phi^2} \right)^2, \quad (7.68)$$

which is a deformation of the Starobinsky potential (7.14) with $\alpha = \sqrt{2/3}$ and the new real parameters $\beta \geq 0$ and $\xi \geq 0$. The Starobinsky potential (7.14) is recovered when $\xi = 0$. The scalar potential (7.68) falls into our supergravity framework, has Minkowski minimum at $\phi = 0$ and the inflationary plateau for large positive ϕ . But, in addition, it also has an inflection point in the "waterfall" region between the inflationary plateau and the Minkowski vacuum. Indeed, the conditions (7.67) result in two equations,

$$\alpha e^{-\alpha\phi} + 2\xi\beta\phi e^{-\beta\phi^2} = 0 \quad (7.69)$$

and

$$\alpha^2 e^{-\alpha\phi} - 2\xi\beta e^{-\beta\phi^2} + 4\xi\beta^2\phi^2 e^{-\phi\phi^2} = 0, \quad (7.70)$$

respectively. They imply a quadratic equation on ϕ ,

$$\alpha\phi + 1 - 2\beta\phi^2 = 0 , \quad (7.71)$$

whose solution is given by

$$\phi_* = \frac{\alpha + \sqrt{\alpha^2 + 4\beta}}{4\beta} > 0 . \quad (7.72)$$

Then the remaining condition above is solved by

$$\xi = \frac{\alpha e^{-\alpha\phi_* + \beta\phi_*^2}}{2\beta\phi_*} . \quad (7.73)$$

Of course, there are many other possibilities to choose the scalar potential having the form of a real function squared. We just showed that it is possible to combine a viable (Starobinsky-like) inflation with a viable (stellar mass type) PBHs production in the context of supergravity.

7.6 Conclusion

Our results lead to the intriguing unifying picture of CDM, dark energy (positive cosmological constant) and cosmological inflation, in which their parameter spaces are linked to each other. This scenario also suggests the interesting phenomenology in the ultra high energy cosmic rays: super heavy Polonyi particles may decay into the SM particles, as the secondaries, in top-bottom decays. Cosmological high energy neutrinos from the primary and secondary decay channels can be tested by IceCube and ANTARES experiments.

Another interesting outcome is that some (stellar mass type) PBHs remnants produced from the supergravity fields can compose part of the CDM halo co-existing with gravitinos. In this scenario, gravitational wave signals from the PBHs mergers can be envisaged, with intriguing implications for LIGO/VIRGO experiments. In short, gravitational wave experiments may provide us with precious indirect information about the scalar sector of the inflationary supergravity.

Finally, the intriguing possibility exists for a unification of the inflaton in the vector multiplet, and the SUSY GUTs such as the flipped $SU(5) \times U(1)$ model arising from (Calabi-Yau) compactified heterotic superstrings or the intersecting D-branes.

Acknowledgements

The work by SVK on gravity and supergravity is supported by the Competitiveness Enhancement Program of Tomsk Polytechnic University in Russia. This work is also supported by a Grant-in-Aid of the Japanese Society for Promotion of Science (JSPS) under No. 26400252, and the World Premier International Research Center Initiative (WPI Initiative), MEXT, Japan. SVK is grateful to the Institute for Theoretical Physics of Hannover University in Germany for kind hospitality extended to him during part of this investigation. The work by MK on physics of dark matter was supported by grant of Russian Science Foundation (project N-18-12-00213).

References

1. P. A. R. Ade *et al.* [Planck Collaboration], "Planck 2015 results. XIII. Cosmological parameters," *Astron. Astrophys.* **594**, A13 (2016).
2. P. A. R. Ade *et al.* [Planck Collaboration], "Planck 2015 results. XX. Constraints on inflation," *Astron. Astrophys.* **594**, A20 (2016).
3. P. A. R. Ade *et al.* [BICEP2 and Keck Array Collaborations], "Improved Constraints on Cosmology and Foregrounds from BICEP2 and Keck Array Cosmic Microwave Background Data with Inclusion of 95 GHz Band," *Phys. Rev. Lett.* **116**, 031302 (2016).
4. A. A. Starobinsky, "A new type of isotropic cosmological models without singularity," *Phys. Lett.* **91B**, 99 (1980).
5. S. V. Ketov, "Supergravity and Early Universe: the Meeting Point of Cosmology and High-Energy Physics," *Int. J. Mod. Phys.* **A28**, 1330021 (2013).
6. S.V. Ketov and T. Terada, "Inflation in supergravity with a single chiral superfield," *Phys. Lett.* **B736**, 272 (2014).
7. S.V. Ketov and T. Terada, "Generic Scalar Potentials for Inflation in Supergravity with a Single Chiral Superfield" *JHEP* **12**, 062 (2014).
8. A. Farakos, A. Kehagias, and A. Riotto, "On the Starobinsky Model of Inflation from Supergravity," *Nucl. Phys.* **B876**, 187 (2013).
9. S. Ferrara, R. Kallosh, A. Linde and M. Porrati, "Minimal Supergravity Models of Inflation," *Phys. Rev.* **D88**, 085038 (2013).
10. Y. Aldabergenov and S. V. Ketov, "SUSY breaking after inflation in supergravity with inflaton in a massive vector supermultiplet," *Phys. Lett.* **B761**, 115 (2016).
11. Y. Aldabergenov and S. V. Ketov, "Higgs mechanism and cosmological constant in $N = 1$ supergravity with inflaton in a vector multiplet," *Eur. Phys. J.* **C77**, 233 (2017).
12. J. Polonyi, "Generalization of the Massive Scalar Multiplet Coupling to the Supergravity", Hungary Central Inst. Res. KFKI-77-93 preprint (1977, rec. July 1978), 5 pages, unpublished.
13. M. Y. Khlopov and A. D. Linde, "Is it easy to save the gravitino?," *Phys. Lett.* **138B**, 265 (1984).
14. M. Y. Khlopov, Y. L. Levitan, E. V. Sedelnikov and I. M. Sobol, "Nonequilibrium cosmological nucleosynthesis of light elements: calculations by the Monte Carlo method," *Phys. Atom. Nucl.* **57**, 1393 (1994) [*Yad. Fiz.* **57**, 1466 (1994)].
15. M. Kawasaki, K. Kohri and T. Moroi, "Big-Bang nucleosynthesis and hadronic decay of long-lived massive particles," *Phys. Rev.* **D71**, 083502 (2005).
16. M. Khlopov, "Cosmological Probes for Supersymmetry," *Symmetry* **7**, 815 (2015).
17. T. Banks, D. B. Kaplan and A. E. Nelson, "Cosmological implications of dynamical supersymmetry breaking," *Phys. Rev.* **D49**, 779 (1994).
18. B. de Carlos, J. A. Casas, F. Quevedo and E. Roulet, "Model independent properties and cosmological implications of the dilaton and moduli sectors of 4-d strings," *Phys. Lett.* **B318**, 447 (1993).
19. G. D. Coughlan, W. Fischler, E. W. Kolb, S. Raby and G. G. Ross, "Cosmological problems for the Polonyi potential," *Phys. Lett.* **131B**, 59 (1983).
20. T. Moroi, M. Yamaguchi and T. Yanagida, "On the solution to the Polonyi problem with $\mathcal{O}(10 \text{ TeV})$ gravitino mass in supergravity," *Phys. Lett.* **B342**, 105 (1995).
21. M. Kawasaki, T. Moroi and T. Yanagida, "Constraint on the reheating temperature from the decay of the Polonyi field," *Phys. Lett.* **B370**, 52 (1996).
22. T. Moroi and L. Randall, "Wino cold dark matter from anomaly mediated SUSY breaking," *Nucl. Phys.* **B570**, 455 (2000).
23. M. Khlopov, B. A. Malomed and I. B. Zeldovich, "Gravitational instability of scalar fields and formation of primordial black holes," *Mon. Not. Roy. Astron. Soc.* **215**, 575 (1985).

24. M. Y. Khlopov, A. Barrau and J. Grain, "Gravitino production by primordial black hole evaporation and constraints on the inhomogeneity of the early universe," *Class. Quant. Grav.* **23**, 1875 (2006).
25. M. Y. Khlopov, "Primordial black holes," *Res. Astron. Astrophys.* **10**, 495 (2010).
26. R. V. Konoplich, S. G. Rubin, A. S. Sakharov, M. Yu. Khlopov, "Formation of black holes in first-order phase transitions as a cosmological test of symmetry breaking mechanisms", *Phys. Atom. Nucl.* **62**, 1593 (1999).
27. M. Yu. Khlopov, R. V. Konoplich, S. G. Rubin, A. S. Sakharov, "First-order phase transitions as a source of black holes in the early universe", *Grav. Cosmol.* **6**, 153 (2000).
28. Y. Fujii and K-I. Maeda, "The scalar-tensor theory of gravitation", Cambridge Univ. Press, Cambridge, 2007.
29. M. Galante, R. Kallosh, A. Linde and D. Roest, "Unity of Cosmological Inflation Attractors", *Phys. Rev. Lett.* **114**, 141302 (2015).
30. H. Nakada and S. V. Ketov, "Inflation from higher dimensions", *Phys. Rev.* **D96**, 123530 (2017).
31. J. Ellis, M. A. G. Garcia, D. V. Nanopoulos and K. A. Olive, "Calculations of inflaton decays and reheating: with applications to no-scale inflation models", *JCAP* **1507**, 050 (2015).
32. V. F. Mukhanov and G. V. Chibisov, "Quantum Fluctuations and a Nonsingular Universe", *JETP Lett.* **33**, 532 (1981) [*Pisma Zh. Eksp. Teor. Fiz.* **33**, 549 (1981)].
33. S. Kaneda, S.V. Ketov and N. Watanabe, "Fourth-order gravity as the inflationary model revisited", *Mod. Phys. Lett.* **A25**, 2753 (2010).
34. J. Wess and J. Bagger, "Supersymmetry and supergravity", Princeton Univ. Press, Princeton, 1992.
35. Y. Aldabergenov and S.V. Ketov, "Removing instability of Polonyi-Starobinsky supergravity by adding FI term", *Mod. Phys. Lett.* **A33**, 1850032 (2018).
36. A. Addazi, S. V. Ketov and M. Yu. Khlopov, "Gravitino and Polonyi production in supergravity," *Eur. Phys. J.* **C78**, 642 (2017).
37. A. A. Starobinsky, "Nonsingular model of the Universe with the quantum gravitational de Sitter stage and its observational consequences", in the Proceedings of the 2nd International Seminar "Quantum Theory of Gravity" (Moscow, 13-15 October, 1981); INR Press, Moscow 1982, p. 58 (reprinted in "Quantum Gravity", M. A. Markov and P. C. West Eds., Plenum Publ. Co., New York, 1984, p. 103).
38. A. Vilenkin, "Classical and Quantum Cosmology of the Starobinsky Inflationary Model", *Phys. Rev.* **D32**, 2511 (1985).
39. K. S. Jeong and F. Takahashi, "A Gravitino-rich Universe", *JHEP* **01**, 173 (2013).
40. B.P. Abbott *et al.*, [LIGO Scientific and Virgo Collaborations], "Observation of Gravitational Waves from a Binary Black Hole Merger", *Phys. Rev. Lett.* **116**, 061102 (2016).
41. B.P. Abbott *et al.*, [LIGO Scientific and Virgo Collaborations], "The Rate of Binary Black Hole Mergers Inferred from Advanced LIGO Observations Surrounding GW150914", arXiv:1602.03842 [astro-ph.HE].
42. B.J. Carr, "The Primordial black hole mass spectrum", *Astrophys. J.* **201**, 1(1975).



8 Phenomenological Mass Matrices With a Democratic Origin

A. Kleppe *

SACT, Oslo

Abstract. Taking into account the available data on the mass sector, and without any preconceptions about a specific matrix texture, we obtain quark mass matrices with a kind of democratic underpinning. Our starting point is a factorization of the “standard” parametrization of the Cabibbo-Kobayashi-Maskawa mixing matrix, from which we derive this specific type of quark mass matrices.

Povzetek. Avtorica uporabi razpoložljive podatke o masah delcev in običajno parametrizacijo mešalne matrike Cabibba, Kobayashija in Maskawe ter poišče, ne da bi vnaprej privzela kakršnokoli zahtevo za simetrijo, masne matrike za kvarke. Izkaže se, da so zelo zblizu demokratičnim matrikam.

Keywords: Mass matrices, flavour symmetry, democratic texture

8.1 Mass states and flavour states

In this project, we take a rather phenomenological approach to the quark mass sector, by assuming that the quark mass matrices can be derived from a simple factorization of the Cabibbo-Kobayashi-Maskawa (CKM) mixing matrix [1],

$$V = \begin{pmatrix} V_{ud} & V_{us} & V_{ub} \\ V_{ud} & V_{us} & V_{ub} \\ V_{ud} & V_{us} & V_{ub} \end{pmatrix}$$

which appears in the charged current Lagrangian

$$\mathcal{L}_{cc} = -\frac{g}{2\sqrt{2}} \bar{\psi}_L \gamma^\mu V \psi'_L W_\mu + \text{h.c.} \quad (8.1)$$

where ψ and ψ' are fermion fields with charges Q and $Q - 1$, correspondingly.

\mathcal{L}_{cc} is usually interpreted as an interaction between left-handed physical particles with charge Q and superpositions of left-handed physical particles of charge $Q - 1$, e.g. between a (left-handed) up-sector quark and a superposition

* E-mail: kleppe@nbi.dk

of (left-handed) down-sector quarks. But it can just as well be interpreted as interactions between flavour states f, f' ,

$$\mathcal{L}_{cc} = -\frac{g}{2\sqrt{2}} \bar{f}_L \gamma^\mu f'_L W_\mu + \text{h.c.} \quad (8.2)$$

where

$$f = U^\dagger \psi, f' = U'^\dagger \psi', \quad \text{and} \quad UU'^\dagger = V$$

The reason we emphasize this is that f, f' appear in the mass Lagrangian

$$\mathcal{L}_{\text{mass}} = \bar{f} M f + \bar{f}' M' f' = \bar{\psi} D \psi + \bar{\psi}' D' \psi', \quad (8.3)$$

where f, f' are quark flavour states with charge $2/3$ and $-1/3$, respectively, and ψ, ψ' are the corresponding mass states. The mass matrices in the weak basis are denoted by $M = M(2/3)$ and $M' = M'(-1/3)$, which in the mass bases correspond to the diagonal matrices $D = \text{diag}(m_u, m_c, m_t)$ and $D' = \text{diag}(m_d, m_s, m_b)$. It is the form of the mass matrices M and M' in the weak basis that we are looking for, in the hope that they can shed light on the mechanism behind the hierarchical fermion mass spectra.

In the context of weak interactions it is thus crucial to distinguish between mass states and flavour states, the flavour states being the eigenstates of the weak interactions, and the mass eigenstates correspond to the “physical particles” that take part in strong and electromagnetic interactions.

The picture is that the flavour states all live in the same weak basis in flavour space, while the mass states of different charge sectors live in their separate mass bases. We go from the weak basis to the mass bases of the charge $2/3$ - and charge $-1/3$ -sector, respectively, by rotating the mass matrices $M(2/3)$ and $M'(-1/3)$ by the unitary matrices U and U' , which are factors of the CKM-matrix, $V = UU'^\dagger$.

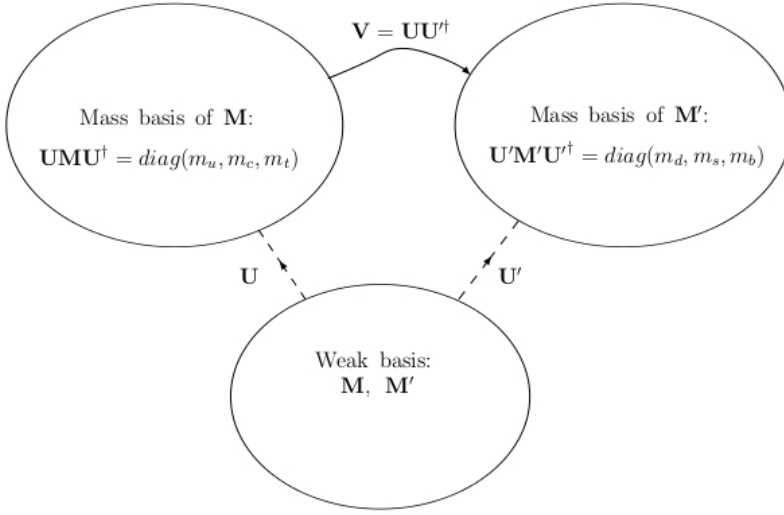
$$M \rightarrow U M U^\dagger = D = \text{diag}(m_u, m_c, m_t) \quad (8.4)$$

$$M' \rightarrow U' M' U'^\dagger = D' = \text{diag}(m_d, m_s, m_b)$$

We can always assume that the mass matrices are Hermitian [3], and diagonalized by hermitian unitary matrices. Since $V = UU'^\dagger \neq \mathbf{1}$, the up-sector mass basis is different from the down-sector mass basis, and the CKM matrix bridges the two mass bases.

It can be argued that flavour states merely exist in our fantasy, since they are not directly measurable. This line of thought is however defied by the neutrinos. Whereas in the quark sector there is a distinction between flavour states, where mass states are perceived as “physical” and the weakly interacting flavour states are defined as mixings of these physical particles, in the lepton sector the situation is quite different. This is due to the fact that as far as we know, neutrino mass states never appear on the scene - in the sense that they never take part in interactions, but merely propagate in free space. The neutrinos ν_e, ν_μ, ν_τ are flavour states, but we nonetheless perceive them as “physical”, because they are the only neutrinos that ever appear in interactions, i.e. they are the only neutrinos that we “see”.

A neutrino is defined by the charged lepton with which it interacts: what we call the electron-neutrino ν_e is the superposition of neutrino mass states which



appears together with the electron, and likewise for μ and τ ; in that sense the conservation of the lepton number is a tautology. The only mixing matrix that occurs in the lepton sector is the Pontecorvo-Maki-Nakagawa-Sakata mixing matrix U which exclusively operates on neutrino states,

$$\begin{pmatrix} \nu_e \\ \nu_\mu \\ \nu_\tau \end{pmatrix} = U_{(PMNS)} \begin{pmatrix} \nu_1 \\ \nu_2 \\ \nu_3 \end{pmatrix}$$

where (ν_1, ν_2, ν_3) are mass eigenstates, and $(\nu_e, \nu_\mu, \nu_\tau)$ are the weakly interacting flavour states. In the lepton sector, the charged currents are thus interpreted as (e, μ, τ) interacting with the neutrino flavour states $(\nu_e, \nu_\mu, \nu_\tau)$ - and the charged leptons are consequently defined as being both flavour states and mass states.

8.2 Factorizing the weak mixing matrix

The usual procedure in establishing an ansatz for the quark mass matrices is to hypothesize a mass matrix of a specific form. Here we instead look for a “natural” factorization of the Cabbibo-Kobayashi-Maskawa mixing matrix, hoping to find the “correct” rotation matrices U and U' that diagonalize the mass matrices M and M' .

The CKM matrix can of course be parametrized and factorized in many different ways, and different factorizations correspond to different rotation matrices U and U' , and correspondingly to different mass matrices M and M' . We choose what we perceive as the most obvious and “symmetric” factorization of the CKM mixing matrix, following the well-known standard parametrization [2] with three

Euler angles $\alpha, \beta, 2\theta$,

$$V = \begin{pmatrix} c_\beta c_{2\theta} & s_\beta c_{2\theta} & s_{2\theta} e^{-i\delta} \\ -c_\beta s_\alpha s_{2\theta} e^{i\delta} - s_\beta c_\alpha & -s_\beta s_\alpha s_{2\theta} e^{i\delta} + c_\beta c_\alpha & s_\alpha c_{2\theta} \\ -c_\beta c_\alpha s_{2\theta} e^{i\delta} + s_\beta s_\alpha & -s_\beta c_\alpha s_{2\theta} e^{i\delta} - c_\beta s_\alpha & c_\alpha c_{2\theta} \end{pmatrix} = U U'^\dagger \quad (8.5)$$

This corresponds to the diagonalizing rotation matrices for the up- and down-sectors

$$\begin{aligned} U &= W \begin{pmatrix} 1 & 0 & 0 \\ 0 & \cos \alpha & \sin \alpha \\ 0 & -\sin \alpha & \cos \alpha \end{pmatrix} \begin{pmatrix} e^{-i\gamma} & & \\ & 1 & \\ & & e^{i\gamma} \end{pmatrix} \begin{pmatrix} \cos \theta & 0 & \sin \theta \\ 0 & 1 & 0 \\ -\sin \theta & 0 & \cos \theta \end{pmatrix} W^\dagger \\ &= W \begin{pmatrix} c_\theta e^{-i\gamma} & 0 & s_\theta e^{-i\gamma} \\ -s_\alpha s_\theta e^{i\gamma} & c_\alpha & s_\alpha c_\theta e^{i\gamma} \\ -c_\alpha s_\theta e^{i\gamma} & -s_\alpha & c_\alpha c_\theta e^{i\gamma} \end{pmatrix} W^\dagger \end{aligned} \quad (8.6)$$

and

$$\begin{aligned} U' &= W \begin{pmatrix} \cos \beta & -\sin \beta & 0 \\ \sin \beta & \cos \beta & 0 \\ 0 & 0 & 1 \end{pmatrix} \begin{pmatrix} e^{-i\gamma} & & \\ & 1 & \\ & & e^{i\gamma} \end{pmatrix} \begin{pmatrix} \cos \theta & 0 & -\sin \theta \\ 0 & 1 & 0 \\ \sin \theta & 0 & \cos \theta \end{pmatrix} W^\dagger \\ &= W \begin{pmatrix} c_\beta c_\theta e^{-i\gamma} & -s_\beta & -c_\beta s_\theta e^{-i\gamma} \\ s_\beta c_\theta e^{-i\gamma} & c_\beta & -s_\beta s_\theta e^{-i\gamma} \\ s_\theta e^{i\gamma} & 0 & c_\theta e^{i\gamma} \end{pmatrix} W^\dagger \end{aligned} \quad (8.7)$$

respectively, where $W = W(\rho)$ is a unitary matrix which is chosen in such a way that the same phase γ appears in the mass matrices of both charge sectors, i.e. a matrix of the form

$$W(\rho) \sim \begin{pmatrix} 0 & \cos \rho & \pm \sin \rho \\ 1 & 0 & 0 \\ 0 & \mp \sin \rho & \cos \rho \end{pmatrix}, \quad \begin{pmatrix} \cos \rho & 0 & \pm \sin \rho \\ 0 & 1 & 0 \\ \mp \sin \rho & 0 & \cos \rho \end{pmatrix}, \quad \begin{pmatrix} \cos \rho & \pm \sin \rho & 0 \\ 0 & 0 & 1 \\ \mp \sin \rho & \cos \rho & 0 \end{pmatrix}$$

Here the value of the parameter ρ is unknown, whereas α, β, θ and γ correspond to the parameters in the standard parametrization, with $\gamma = \delta/2$, $\delta = 1.2 \pm 0.08$ rad, and $2\theta = 0.201 \pm 0.011^\circ$, while $\alpha = 2.38 \pm 0.06^\circ$ and $\beta = 13.04 \pm 0.05^\circ$. In our factorization scheme, α and β are the rotation angles operating in the up-sector and the down-sector, respectively. With the rotation matrices $U(\alpha, \theta, \gamma, \rho)$ and $U'(\beta, \theta, \gamma, \rho)$, we obtain the mass matrices for the up- and down-sectors, respectively,

$$M = U^\dagger \text{diag}(m_u, m_c, m_t) U \quad \text{and} \quad M' = U'^\dagger \text{diag}(m_d, m_s, m_b) U'$$

For the up-sector this gives

$$M = \begin{pmatrix} M_{11} & M_{12} & M_{13} \\ M_{21} & M_{22} & M_{23} \\ M_{31} & M_{32} & M_{33} \end{pmatrix} = W^\dagger(\rho) \begin{pmatrix} X c_\theta^2 + Y s_\theta^2 & Z s_\theta e^{-i\gamma} & (X - Y) c_\theta s_\theta \\ Z s_\theta e^{i\gamma} & Y - 2Z \cot 2\alpha & -Z c_\theta e^{i\gamma} \\ (X - Y) c_\theta s_\theta & -Z c_\theta e^{-i\gamma} & X s_\theta^2 + Y c_\theta^2 \end{pmatrix} W(\rho) \quad (8.8)$$

where

$$X = m_u, Y = m_c \sin^2 \alpha + m_t \cos^2 \alpha, \\ Z = (m_t - m_c) \sin \alpha \cos \alpha = \sqrt{(m_t - Y)(Y - m_c)},$$

and m_u, m_c, m_t are the masses of the up-, charm- and top-quark; and $W(\rho)$ is a unitary one-parameter matrix. Analogously for the down-sector mass matrix,

$$M' = \begin{pmatrix} M'_{11} & M'_{12} & M'_{13} \\ M'_{21} & M'_{22} & M'_{23} \\ M'_{31} & M'_{32} & M'_{33} \end{pmatrix} \\ = W^\dagger(\rho) \begin{pmatrix} X' s_\theta^2 + Y' c_\theta^2 & Z' c_\theta e^{i\gamma} & (X' - Y') c_\theta s_\theta \\ Z' c_\theta e^{-i\gamma} & Y' + 2Z' \cot 2\beta & -Z' s_\theta e^{-i\gamma} \\ (X' - Y') c_\theta s_\theta & -Z' s_\theta e^{i\gamma} & X' c_\theta^2 + Y' s_\theta^2 \end{pmatrix} W(\rho) \quad (8.9)$$

where $X' = m_b, Y' = m_d \cos^2 \beta + m_s \sin^2 \beta, Z' = (m_s - m_d) \sin \beta \cos \beta = \sqrt{(m_s - Y')(Y' - m_d)}$, and m_d, m_s, m_b are the masses of the down-, strange- and bottom-quark, respectively. The two mass matrices thus display similar textures.

With $Y = m_c \sin^2 \alpha + m_t \cos^2 \alpha, Z = (m_t - m_c) \sin \alpha \cos \alpha, Y' = m_d \cos^2 \beta + m_s \sin^2 \beta$, and $Z' = (m_s - m_d) \sin \beta \cos \beta$, we can moreover write

$$m_u = X, \quad m_c = Y - Z \cot \alpha, \quad m_t = Y + Z \tan \alpha, \\ m_d = Y' - Z' \tan \beta, \quad m_s = Y' + Z' \cot \beta, \quad m_b = X', \quad (8.10)$$

8.3 The matrix W

There are of course many ways to chose a one-parameter unitary matrix, but we choose a matrix $W(\rho)$ which conveniently gives mass matrices with the same phase γ for both charge sectors,

$$W(\rho) = \begin{pmatrix} \cos \rho & -\sin \rho & 0 \\ 0 & 0 & 1 \\ \sin \rho & \cos \rho & 0 \end{pmatrix} \quad (8.11)$$

This gives the up-sector mass matrix

$$M = W^\dagger \begin{pmatrix} X c_\theta^2 + Y s_\theta^2 & Z s_\theta e^{-i\gamma} & (X - Y) c_\theta s_\theta \\ Z s_\theta e^{i\gamma} & Y - 2Z \cot 2\alpha & -Z c_\theta e^{i\gamma} \\ (X - Y) c_\theta s_\theta & -Z c_\theta e^{-i\gamma} & X s_\theta^2 + Y c_\theta^2 \end{pmatrix} W = \quad (8.12) \\ = \begin{pmatrix} X \cos^2 \mu + Y \sin^2 \mu & (Y - X) \sin \mu \cos \mu & -Z \sin \mu e^{-i\gamma} \\ (Y - X) \sin \mu \cos \mu & X \sin^2 \mu + Y \cos^2 \mu & -Z \cos \mu e^{-i\gamma} \\ -Z \sin \mu e^{i\gamma} & -Z \cos \mu e^{i\gamma} & F \end{pmatrix}$$

where $\mu = \rho - \theta, X = m_u, Y = m_c \sin^2 \alpha + m_t \cos^2 \alpha, Z = \sqrt{(m_t - Y)(Y - m_c)}$ and $F = Y - 2Z \cot 2\alpha = m_c c_\alpha^2 + m_t s_\alpha^2$.

Now, depending on the value of $\mu = \rho - \theta$, we get different matrix textures, e.g. for $\rho - \theta = 0$ or π , we get the simple form

$$M(0, \pi) = \begin{pmatrix} X & 0 & 0 \\ 0 & Y & -Ze^{-i\gamma} \\ 0 & -Ze^{i\gamma} & F \end{pmatrix}, \quad (8.13)$$

and for $\rho - \theta = \pi/2$, equally simple

$$M(\pi/2) = \begin{pmatrix} Y & 0 & -Ze^{-i\gamma} \\ 0 & X & 0 \\ -Ze^{i\gamma} & 0 & F \end{pmatrix} \quad (8.14)$$

Applying the same procedure to the down-sector, we get the down-sector mass matrix

$$\begin{aligned} M' &= W(\rho)^\dagger \begin{pmatrix} X's_\theta^2 + Y'c_\theta^2 & Z'c_\theta e^{i\gamma} & (X' - Y')c_\theta s_\theta \\ Z'c_\theta e^{-i\gamma} & Y' + 2Z'\cot 2\beta & -Z's_\theta e^{-i\gamma} \\ (X' - Y')c_\theta s_\theta & -Z's_\theta e^{i\gamma} & X'c_\theta^2 + Y's_\theta^2 \end{pmatrix} W(\rho) = \\ &= \begin{pmatrix} X'\sin^2 \mu' + Y'\cos^2 \mu' & (X' - Y')\sin \mu' \cos \mu' & Z'\cos \mu' e^{i\gamma} \\ (X' - Y')\sin \mu' \cos \mu' & X'\cos^2 \mu' + Y'\sin^2 \mu' & -Z'\sin \mu' e^{i\gamma} \\ Z'\cos \mu' e^{-i\gamma} & -Z'\sin \mu' e^{-i\gamma} & F' \end{pmatrix} \end{aligned} \quad (8.15)$$

where $\mu' = \rho + \theta$, $X' = m_b$, $Y' = m_d \cos^2 \beta + m_s \sin^2 \beta$, $Z' = \sqrt{(m_s - Y')(Y' - m_d)}$ and $F' = Y' + 2Z'\cot 2\beta = m_d s_\beta^2 + m_s c_\beta^2$. Again, different μ' -values correspond to different matrices, e.g. for $\mu' = \rho + \theta = 0$ or π , we get

$$M'(0, \pi) = \begin{pmatrix} Y' & 0 & Z'e^{i\gamma} \\ 0 & X' & 0 \\ Z'e^{-i\gamma} & 0 & F' \end{pmatrix} \quad (8.16)$$

and for $\mu' = \rho + \theta = \pi/2$, we get

$$M'(\pi/2) = \begin{pmatrix} X' & 0 & 0 \\ 0 & Y' & -Z'e^{i\gamma} \\ 0 & -Z'e^{-i\gamma} & F' \end{pmatrix} \quad (8.17)$$

8.4 Texture Zero Mass Matrices

The matrices (8.13) and (8.14), as well as (8.16) and (8.17), make us wonder if our scheme is compatible with quark mass matrices of texture zero.

The study of texture zero matrices is driven by the need to reduce the number of free parameters, since the fermion mass matrices are 3×3 complex matrices, which without any constraints contain 36 real free parameters. It is however always possible to perform a unitary transformation that renders an arbitrary mass matrix Hermitian [3], so there is no loss of generality in assuming that the mass matrices are Hermitian, reducing the number of free parameters to 18. This is still a very large number, which in the end of the 1970-ies prompted Fritzsch [6],

[7] to introduce “texture zero matrices”, i.e. mass matrices where a certain number of the entries are zero.

Since then, a huge amount of articles have appeared, with analyses of the very large number of (different types of) texture zero matrices and their phenomenology. In the course of this work, a number of texture zero matrices have been ruled out. A handful of matrices have however been singled out as viable [8], which among the texture 4 zero matrices are:

$$\begin{pmatrix} A & B & 0 \\ B^* & D & C \\ 0 & C^* & 0 \end{pmatrix}, \begin{pmatrix} A & B & C \\ B^* & D & 0 \\ C^* & 0 & 0 \end{pmatrix}, \begin{pmatrix} A & 0 & B \\ 0 & 0 & C \\ B^* & C^* & D \end{pmatrix}, \begin{pmatrix} 0 & C & 0 \\ C^* & A & B \\ 0 & B^* & D \end{pmatrix}, \begin{pmatrix} 0 & 0 & C \\ 0 & A & B \\ C^* & B^* & D \end{pmatrix}, \begin{pmatrix} D & C & B \\ C^* & 0 & 0 \\ B^* & 0 & A \end{pmatrix}$$

while

$$\begin{pmatrix} A & 0 & 0 \\ 0 & C & B \\ 0 & B^* & D \end{pmatrix} \quad \text{and} \quad \begin{pmatrix} A & 0 & B \\ 0 & C & 0 \\ B^* & 0 & D \end{pmatrix}$$

are among the matrices that are ruled out. In our scheme this precisely corresponds to the matrices (8.13), (8.14), (8.16) and (8.17), which gives a constraint on the angle ρ ,

$$\rho \neq \frac{1}{2}N\pi \pm \theta \quad (8.18)$$

where $N \in \mathbb{Z}$, ruling out the matrices $M(\frac{1}{2}N\pi - \theta)$ and $M'(\frac{1}{2}N\pi + \theta)$. This implies that our mass matrices M and M' are not of texture zero. Instead, they display a kind of democratic texture [4], a feature that has merely been outlined in our earlier project [5].

8.5 Democratic mass matrices

In the Standard Model, fermions get their masses from the Yukawa couplings by the Higgs mechanism. We know that the fermion masses within one charge sector are very different, but there is no apparent reason why there should be a different Yukawa coupling for each fermion of a given charge. Taking the difference between the weak basis and the mass bases into account, the democratic philosophy proclaims that in the weak basis, the fermions of a given charge should have identical Yukawa couplings, just like they have identical couplings to the gauge bosons of the strong, weak and electromagnetic interactions.

The democratic hypothesis thus implies that in the weak basis the quark mass matrices for both charge sectors have an initial, “democratic” form

$$M_0 = k \begin{pmatrix} 1 & 1 & 1 \\ 1 & 1 & 1 \\ 1 & 1 & 1 \end{pmatrix} \equiv k\mathbf{N} \quad (8.19)$$

where k has dimension mass; and the mass spectrum $(0, 0, 3k)$ reflects the phenomenology of the fermion mass spectra with one very big and two much smaller mass values - in the mass basis. In the weak basis the matrix $M_0 = k\mathbf{N}$ is however

totally flavour symmetric, in the sense that the flavour states f_i of a given charge are indistinguishable and the initial mass Lagrangian reads

$$\mathcal{L}_{\text{mass}} = k \bar{f} \mathbf{N} f = \sum_{i,j=1}^3 k \bar{f}_i f_j$$

which is a totally flavour symmetric situation, with a discrete flavour symmetry under the cyclic permutation group Z_3 operating on the mass matrix. That the Yukawa couplings are identical for all the flavours, while the mass eigenvalues are so completely different is a reminder of the difference between flavour states and mass states.

The democratic symmetry is unchanged if we add a diagonal matrix

$$\text{diag}(X, X, X)$$

to $k\mathbf{N}$, since the new democratic mass matrix $M_0 = k\mathbf{N} + \text{diag}(X, X, X)$ still corresponds to a completely flavour symmetric mass Lagrangian,

$$\mathcal{L}_{\text{mass}} = \bar{f} M_0 f = k \sum_{i,j=1}^3 \bar{f}_i f_j + X \sum_{i=1}^3 \bar{f}_i f_i = (k + X) \sum_{i=1}^3 \bar{f}_i f_i \quad (8.20)$$

Moreover, since the up-sector mass matrix and the down sector mass matrix in this assumed democratic initial stage are structurally identical, the mixing matrix is equal to unity, so there is no CP-violation. In order to obtain the final mass spectra with the three hierarchical non-zero values, the initial democratic symmetry must be broken in such a way that we get a mixing matrix and masses that all agree with data. In the democratic scenario an ansatz thus consists of a specific choice for the flavour symmetry breaking scheme. In our approach, it however comes out of the formalism, without any presupposition of a democratic texture or a specific breaking scheme.

8.5.1 Reparametrizing the mass matrices

By reformulating the matrix elements M_{11} , M_{22} , M'_{11} , and M'_{22} in the quark mass matrices (8.12) and (8.15), using the relations

$$Xc_\mu^2 + Ys_\mu^2 = (Y - X)s_\mu^2 + X, \quad Xs_\mu^2 + Yc_\mu^2 = (Y - X)c_\mu^2 + X, \text{ and} \\ X's_\mu^2 + Y'c_\mu^2 = (Y' - X')c_\mu^2 + X', \text{ and } X'c_\mu^2 + Y's_\mu^2 = (Y' - X')s_\mu^2 + X',$$

the mass matrices can be rewritten in a way that reveals a kind of “democratic substructure”,

$$M = \begin{pmatrix} Xc_\mu^2 + Ys_\mu^2 & (Y - X)s_\mu c_\mu & -Zs_\mu e^{-i\gamma} \\ (Y - X)s_\mu c_\mu & Xs_\mu^2 + Yc_\mu^2 & -Zc_\mu e^{-i\gamma} \\ -Zs_\mu e^{i\gamma} & -Zc_\mu e^{i\gamma} & F \end{pmatrix} = \quad (8.21) \\ = B \begin{pmatrix} \sin \mu & & \\ & \cos \mu & \\ & & Ge^{i\gamma} \end{pmatrix} \begin{pmatrix} 1 & 1 & 1 \\ 1 & 1 & 1 \\ 1 & 1 & 1 \end{pmatrix} \begin{pmatrix} \sin \mu & & \\ & \cos \mu & \\ & & Ge^{-i\gamma} \end{pmatrix} + \begin{pmatrix} X & & \\ & X & \\ & & X + A \end{pmatrix}$$

and

$$M' = \begin{pmatrix} X's_{\mu'}^2 + Y'c_{\mu'}^2 & (X' - Y')s_{\mu'}c_{\mu'} & Z'c_{\mu'}e^{i\gamma} \\ (X' - Y')s_{\mu'}c_{\mu'} & X'c_{\mu'}^2 + Y's_{\mu'}^2 & -Z's_{\mu'}e^{i\gamma} \\ Z'c_{\mu'}e^{-i\gamma} & -Z's_{\mu'}e^{-i\gamma} & F' \end{pmatrix} = \quad (8.22)$$

$$= B' \begin{pmatrix} \cos \mu' & & \\ & -\sin \mu' & \\ & & G'e^{-i\gamma} \end{pmatrix} \begin{pmatrix} 1 & 1 & 1 \\ 1 & 1 & 1 \\ 1 & 1 & 1 \end{pmatrix} \begin{pmatrix} \cos \mu' & & \\ & -\sin \mu' & \\ & & G'e^{i\gamma} \end{pmatrix} + \begin{pmatrix} X' & & \\ & X' & \\ & & X' + A' \end{pmatrix}$$

where

$$X = m_u, \quad \mu = \rho - \theta, \quad B = Y - X = m_c s_\alpha^2 + m_t c_\alpha^2 - m_u,$$

$$G = -\frac{(m_t - m_c)s_\alpha c_\alpha}{(m_c s_\alpha^2 + m_t c_\alpha^2 - m_u)}, \quad A = \frac{(m_c - m_u)(m_t - m_u)}{(m_c s_\alpha^2 + m_t c_\alpha^2 - m_u)},$$

and

$$X' = m_b, \quad \mu' = \rho + \theta, \quad B' = Y' - X' = m_s s_\beta^2 + m_d c_\beta^2 - m_b,$$

$$G' = \frac{(m_s - m_d)s_\beta c_\beta}{(m_d c_\beta^2 + m_s s_\beta^2 - m_b)}, \quad A' = \frac{(m_d - m_b)(m_s - m_b)}{(m_d c_\beta^2 + m_s s_\beta^2 - m_b)},$$

$$\alpha = \arctan \left(\sqrt{\frac{m_t - Y}{Y - m_c}} \right) = 2.38 \pm 0.06^\circ, \quad \beta = \arctan \left(\sqrt{\frac{Y' - m_d}{m_s - Y'}} \right) = 13.04 \pm 0.05^\circ.$$

The matrices of the two charge sectors thus display great similarities. That $A \neq 0$ and $A' \neq 0$ moreover means that $m_c \neq m_u$, $m_t \neq m_u$, $m_d \neq m_b$ and $m_s \neq m_b$, and with the additional condition $m_c \neq m_t$ and $m_d \neq m_b$, we almost have the prerequisite for CP-violation - which basically says that CP-violation occurs once there is a third family (and a complex phase).

8.6 Discussion

We interpret the structure displayed by (8.21) and (8.22) as the result of an initial democratic matrix, where the flavour symmetry undergoes a stepwise breaking, each step corresponding to one term. If we consider the up-sector, the first term comes from

$$M_0 = k \begin{pmatrix} 1 & 1 & 1 \\ 1 & 1 & 1 \\ 1 & 1 & 1 \end{pmatrix} \Rightarrow M_1 = B \begin{pmatrix} \sin \mu & & \\ & \cos \mu & \\ & & Ge^{i\gamma} \end{pmatrix} \begin{pmatrix} 1 & 1 & 1 \\ 1 & 1 & 1 \\ 1 & 1 & 1 \end{pmatrix} \begin{pmatrix} \sin \mu & & \\ & \cos \mu & \\ & & Ge^{-i\gamma} \end{pmatrix}, \quad (8.23)$$

where k and B both have the dimension mass. This first symmetry breaking step really corresponds to shifting the flavours in such a way that $f_1 \rightarrow s_\mu f_1$, $f_2 \rightarrow c_\mu f_2$, $f_3 \rightarrow Ge^{-i\gamma} f_3$. The mass spectrum still consists of two massless and one massive state, but the flavour symmetry is partially broken, with the mass Lagrangian

$$\mathcal{L}_{\text{mass}} = \bar{f} M_1 f = \bar{\chi}_1 \chi_1 + \bar{\chi}_1 \chi_2 + \bar{\chi}_2 \chi_1 + \bar{\chi}_2 \chi_2 = (\bar{\chi}_1 + \bar{\chi}_2)(\chi_1 + \chi_2),$$

where $\chi_1 = B(s_\mu f_1 + c_\mu f_2)$, $\chi_2 = BGe^{-i\gamma} f_3$. The original total flavour symmetry is thus broken down to the partial flavour symmetry $f_1 \Leftrightarrow f_2$, but there is still only one non-vanishing eigenvalue.

In the next step, by shifting the origin from $\text{diag}(0, 0, 0)$ to $\text{diag}(X, X, X)$, we obtain a mass spectrum with one very heavy, massive state, and two lighter states with mass X , i.e.

$$M_1 \Rightarrow M_2 = B \begin{pmatrix} \sin \mu & & \\ & \cos \mu & \\ & & Ge^{i\gamma} \end{pmatrix} \begin{pmatrix} 1 & 1 & 1 \\ 1 & 1 & 1 \\ 1 & 1 & 1 \end{pmatrix} \begin{pmatrix} \sin \mu & & \\ & \cos \mu & \\ & & Ge^{-i\gamma} \end{pmatrix} + \begin{pmatrix} X & & \\ & X & \\ & & X \end{pmatrix} \quad (8.24)$$

where X has dimension mass.

In the last step, the remaining degeneracy in the mass spectrum $(X, X, X + B(G^2 + 1))$ is subsequently broken, by adding the term $\text{diag}(0, 0, A)$, where A has dimension mass. We argue that this last breaking is necessitated by the principle of minimal energy, in analogy with the Jahn-Teller effect.

$$M_2 \Rightarrow M_3 = B \begin{pmatrix} \sin \mu & & \\ & \cos \mu & \\ & & Ge^{i\gamma} \end{pmatrix} \begin{pmatrix} 1 & 1 & 1 \\ 1 & 1 & 1 \\ 1 & 1 & 1 \end{pmatrix} \begin{pmatrix} \sin \mu & & \\ & \cos \mu & \\ & & Ge^{-i\gamma} \end{pmatrix} + \begin{pmatrix} X & & \\ & X & \\ & & X \end{pmatrix} + \begin{pmatrix} 0 & & \\ & 0 & \\ & & A \end{pmatrix} \quad (8.25)$$

We identify our scheme as a democratic scenario, where the flavour symmetry is broken in the specific way described above.

8.7 Numerical values

In order to get a notion of the sizes of the parameters B, G, X, A , we calculate their values for quark masses at different μ . Using quark masses at M_Z , [9], [10], [11]

$$\begin{aligned} m_u(M_Z) &= 1.24\text{MeV}, \quad m_c(M_Z) = 624\text{MeV}, \quad m_t(M_Z) = 171550\text{MeV} \\ m_d(M_Z) &= 2.69\text{MeV}, \quad m_s(M_Z) = 53.8\text{MeV}, \quad m_b(M_Z) = 2850\text{MeV} \end{aligned} \quad (8.26)$$

we get the numerical values for the parameters:

up-sector	d-sector
$B = 171254\text{MeV} \approx m_t \cos^2 \alpha$	$B' = -2844.71\text{MeV} \approx 2m_d - m_b$
$G = 0.0414$	$G' = -0.0039$
$X = 1.24\text{MeV}$	$X' = 2850\text{MeV}$
$A = 623.83\text{MeV} \approx m_c \cos \alpha$	$A' = -2798.76\text{MeV} \approx m_s - m_d - m_b$

and as before, we use the angles $\alpha = 2.38^\circ$ and $\beta = 13.04^\circ$.

We would also like to establish some numerical value, or at least a range, for the parameter ρ . Our initial assumption was that the matrices (8.6), (8.7) which diagonalize the up-sector and down-sector mass matrices, are given by the factorization of the Cabibbi-Kobayashi-Maskawa matrix (8.5). The parameters of the CKM matrix are well-known, so the only remaining “steering-parameter” is ρ . The angles μ and μ' in the mass matrices of the up- and d-sector depend on ρ , whose value is unknown. We have the constraint

$$\rho \neq \frac{1}{2} N\pi \pm \theta \quad (8.27)$$

which excludes some values of ρ , but it remains unknown what value(s) ρ actually takes.

8.8 Conclusion

By factorizing the “standard parametrization” of the CKM weak mixing matrix in a very natural and straightforward way, we obtain mass matrices with a type of democratic texture that can be derived from a democratic matrix, followed by a well-defined scheme for breaking the primary flavour symmetry. This democratic texture unexpectedly emerges from our factorization of the weak mixing matrix, there is no presupposition about what form our resulting mass matrices would have, and no assumptions other than our factorization scheme and the choice of the unitary matrix $W(\rho)$.

References

1. M. Kobayashi, T. Maskawa; Maskawa (1973), “CP-Violation in the Renormalizable Theory of Weak Interaction”, *Progress of Theoretical Physics* 49 (2): 652–657.
2. L.L. Chau and W.-Y. Keung (1984), “Comments on the Parametrization of the Kobayashi-Maskawa Matrix”, *Phys. Rev. Letters* 53 (19): 1802.
3. D. Emmanuel-Costa and C. Simoes, *Phys. Rev. D* 79, 073006 (2009).
4. H. Harari, H. Haut and J. Weyers, *Phys. Lett. B* 78, 459 (1978).
5. A. Kleppe, “A democratic suggestion”, [hep-ph/1608.08988](https://arxiv.org/abs/hep-ph/1608.08988).
6. H. Fritzsch, *Phys. Lett. B* 70, 436 (1977), *Phys. Lett. B* 73, 317 (1978).
7. H. Fritzsch, “Texture Zero Mass Matrices and Flavor Mixing of Quarks and Leptons”, [hep-ph/1503.07927](https://arxiv.org/abs/hep-ph/1503.07927)v1.
8. S. Sharma, P. Fakay, G. Ahuja, M. Gupta, *Phys. Rev. D* 91, 053004 (2015).
9. Matthias Jamin, private communication.
10. M. Jamin, J. Antonio Oller and A. Pich, “Light quark masses from scalar sum rules”, [arXiv:hep-ph/0110194](https://arxiv.org/abs/hep-ph/0110194)v2.
11. FLAG Working Group, “Review of lattice results concerning low energy particle physics” (2014), [hep-lat/1310.8555](https://arxiv.org/abs/hep-lat/1310.8555)v2.
12. <http://pdg.lbl.gov/2017/tables/rpp2017-sum-quarks.pdf>



9 Why Nature Made a Choice of Clifford and not Grassmann Coordinates? *

N.S. Mankoč Borštnik¹ and H.B.F. Nielsen²

¹Department of Physics, University of Ljubljana,
SI-1000 Ljubljana, Slovenia

²Niels Bohr Institute, University of Copenhagen, Blegdamsvej 17,
Copenhagen Ø, Denmark

Abstract. This is a discussion on fermion fields, the internal degrees of freedom of which are described by either the Grassmann or the Clifford anticommuting “coordinates”. We prove that both fields can be second quantized so that their creation and annihilation operators fulfill the requirements of the commutation relations for fermion fields. However, while the internal spins determined by the generators of the Lorentz group of the Clifford objects S^{ab} and \tilde{S}^{ab} (in the *spin-charge-family* theory S^{ab} determine the spin degrees of freedom and \tilde{S}^{ab} the family degrees of freedom) are half integer, the internal spin determined by S^{ab} (expressible with $S^{ab} + \tilde{S}^{ab}$) is integer. Nature “made” obviously the choice of the Clifford algebra, at least in the so far observed part of our universe. We discuss here the quantization — first and second — of the fields, the internal degrees of freedom of which are functions of the Grassmann coordinates θ^a and their conjugate momenta, as well as of the fields, the internal degrees of freedom of which are functions of the Clifford γ^a . Inspiration comes from the *spin-charge-family* theory ([1,2,9,3], and the references therein), in which the action for fermions in d -dimensional space is equal to $\int d^d x \mathcal{L} = \frac{1}{2} (\bar{\psi} \gamma^a p_{0a} \psi) + \text{h.c.}$, with $p_{0a} = f^\alpha_a p_{0\alpha} + \frac{1}{2E} \{p_\alpha, E f^\alpha_a\}$, $p_{0\alpha} = p_\alpha - \frac{1}{2} S^{ab} \omega_{ab\alpha} - \frac{1}{2} \tilde{S}^{ab} \tilde{\omega}_{ab\alpha}$. We write the basic states as products of those either Grassmann or Clifford objects, which allow second quantization for fermion fields, and look for the action and solutions for free fields also in the Grassmann case in order to understand why the Clifford algebra “wins in the competition” for the physical (observable) degrees of freedom.

Povzetek. Avtorja obravnavata razliko med fermionskimi polji, katerih interne prostostne stopnje opišemo bodisi z Grassmannovimi bodisi s Cliffordovimi antikomutirajočimi “koordinatami”. Dokažeta, da lahko v obeh primerih poiščemo kreacijske in anihilacijske operatorje, ki zadoščajo komutacijskim relacijam za fermionska polja v drugi kvantizaciji. Obe vrsti opisa fermionskih polj se vseeno bistveno razlikujeta: notranji spini, določeni z generatorji Lorentzove grupe Cliffordovih objektov S^{ab} in \tilde{S}^{ab} (v teoriji *spinov-nabojev-družin* določajo S^{ab} spinsko kvantno število ter s tem spine in naboje kvarkov in leptonov, \tilde{S}^{ab} pa določajo družinska kvantna števila), imajo polštevilčen spin, medtem ko je notanji spin, ki ga določajo S^{ab} (izrazljivi z $S^{ab} + \tilde{S}^{ab}$), celoštevilčen. Narava je očitno “izbrala” Cliffordovo algebro (vsaj v opazljivem delu vesolja). Avtorja obravnavata prvo in drugo kvantizacijo polj, katerih notranje prostostne stopnje opišeta s funkcijami Grassmannovih

* This article is the expanded part of the talk presented by N.S. Mankoč Borštnik at the 21st Workshop “What Comes Beyond the Standard Models”, Bled, 23 of June to 1 of July, 2018.

koordinat θ^a in ustreznih konjugiranih momentov, pa tudi polja, katerih notranje prostostne stopnje so opisane s funkcijami Cliffordovih koordinat γ^a . Uporabo za opis fermionov v Grassmannovem prostoru je navdihnila teorija *spinov-nabojev-družin* ([1,2,9,3], in reference v njih), v kateri akcijo v d-razsežnem prostoru opiše eden od avtorjev (N.S.M.B.) z $\int d^d x \mathcal{L} = \frac{1}{2} (\bar{\psi} \gamma^a p_{0a} \psi) + \text{h.c.}$, s kovariantnim odvodom $p_{0a} = f^\alpha_a p_{0\alpha} + \frac{1}{2E} \{p_\alpha, E f^\alpha_a\}$, $p_{0\alpha} = p_\alpha - \frac{1}{2} S^{ab} \omega_{ab\alpha} - \frac{1}{2} \tilde{S}^{ab} \tilde{\omega}_{ab\alpha}$. Bazna stanja iščeta kot produkt bodisi Grassmannovih bodisi Cliffordovih "koordinat", ki dopuščajo drugo kvantizacijo, ponudita akcijo za prosta polja tudi v primeru Grassmannovih koordinat, da bi bolje razumela, zakaj je v tekmi za fizikalne prostostne stopnje "zmagala" Cliffordova algebra.

Keywords: Second quantization of fermion fields, Spinor representations, Kaluza-Klein theories, Discrete symmetries, Higher dimensional spaces, Beyond the standard model

PACS:11.30.Er,11.10.Kk,12.60.-i, 04.50.-h

9.1 Introduction

This paper is to look for the answers to the questions: Why our universe "uses" the Clifford rather than the Grassmann coordinates, although both lead in the second quantization procedure to the anti-commutation relations required for fermion degrees of freedom? Is the answer that the Clifford degrees of freedom offer the appearance of families, the half integer spin and the charges as observed so far for fermions, while the Grassmann coordinates offer the groups of (isolated) integer spin states with the charges in the adjoint representations and no families? Can the choice of the Clifford degrees of freedom explain why the simple starting action of the *spin-charge-family* theory of one of us (N.S.M.B.) [9,3,5,8,4,6,7] is doing so far extremely well in manifesting the observed properties of the fermion and boson fields in the observed low energy regime?

The questions are too demanding that this paper could offer the answers. We are trying only to make first steps towards understanding them.

Our working hypothesis is that "*nature knows all the mathematics*", accordingly therefore also both — the Grassmann and the Clifford "coordinates". In a trial to understand why Grassmann space "*was not the choice of nature*" to describe the internal degrees of freedom of fermions, we see that γ^a 's and $\tilde{\gamma}^a$'s of the *spin-charge-family* theory enable to describe not only the spin and charges of fermions, but also the existence of families of fermions (in the first and second quantized theory of fields).

This work is a part of the project of both authors, which includes the *fermionization* procedure of boson fields or the *bosonization* procedure of fermion fields, discussed in Refs. [11,12,14] for any dimension d (by the authors of this contribution, while one of them, H.B.F.N. [13], has succeeded with another author to do the *fermionization* for $d = (1 + 1)$), and which would hopefully help to better understand the content and dynamics of our universe.

In the *spin-charge-family* theory [9,3,5,8,4,6,7] — which offers explanations for all the assumptions of the *standard model*, with the appearance of families, the scalar higgs and the Yukawa couplings included, offering also the explanation for

the matter-antimatter asymmetry in our universe and for the appearance of the dark matter — a very simple starting action for massless fermions and bosons in $d = (1 + 13)$ is assumed, in which massless fermions interact with only gravity, the vielbeins f^α_a (the gauge fields of moments p_a) and the two kinds of the spin connections ($\omega_{ab\alpha}$ and $\tilde{\omega}_{ab\alpha}$, the gauge fields of the two kinds of the Clifford algebra objects γ^a and $\tilde{\gamma}^a$, respectively).

$$\mathcal{A} = \int d^d x \, E \, \frac{1}{2} (\bar{\psi} \gamma^a p_{0a} \psi) + \text{h.c.} + \int d^d x \, E \, (\alpha R + \tilde{\alpha} \tilde{R}), \quad (9.1)$$

with $p_{0a} = f^\alpha_a p_{0\alpha} + \frac{1}{2E} \{p_\alpha, E f^\alpha_a\}_-$, $p_{0\alpha} = p_\alpha - \frac{1}{2} S^{ab} \omega_{ab\alpha} - \frac{1}{2} \tilde{S}^{ab} \tilde{\omega}_{ab\alpha}$ and $R = \frac{1}{2} \{f^\alpha_{[a} f^{\beta b]} (\omega_{ab\alpha, \beta} - \omega_{ca\alpha} \omega^c_{b\beta})\} + \text{h.c.}$, $\tilde{R} = \frac{1}{2} \{f^\alpha_{[a} \tilde{f}^{\beta b]} (\tilde{\omega}_{ab\alpha, \beta} - \tilde{\omega}_{ca\alpha} \tilde{\omega}^c_{b\beta})\} + \text{h.c.}$. The two kinds of the Clifford algebra objects, γ^a and $\tilde{\gamma}^a$,

$$\begin{aligned} \{\gamma^a, \gamma^b\}_+ &= 2\eta^{ab} = \{\tilde{\gamma}^a, \tilde{\gamma}^b\}_+, \\ \{\gamma^a, \tilde{\gamma}^b\}_+ &= 0. \end{aligned} \quad (9.2)$$

anticommute (γ^a and $\tilde{\gamma}^b$ are connected with the left and the right multiplication of the Clifford objects, there is no third kind of the Clifford operators). One kind of the objects, the generators $S^{ab} = \frac{i}{4} (\gamma^a \gamma^b - \gamma^b \gamma^a)$, determines spins and charges of spinors of any family, another kind, $\tilde{S}^{ab} = \frac{i}{4} (\tilde{\gamma}^a \tilde{\gamma}^b - \tilde{\gamma}^b \tilde{\gamma}^a)$, determines the family quantum numbers. Here ${}^1 f^\alpha_{[a} f^{\beta b]} = f^\alpha_a f^{\beta b} - f^\alpha_b f^{\beta a}$. There are correspondingly two kinds of infinitesimal generators of the Lorentz transformations in the internal degrees of freedom — S^{ab} for $SO(13, 1)$ and \tilde{S}^{ab} for $\tilde{SO}(13, 1)$ — arranging states into representations.

The scalar curvatures R and \tilde{R} determine dynamics of the gauge fields — the spin connections and the vielbeins, which manifest in $d = (3 + 1)$ all the known vector gauge fields as well as the scalar fields [5] which explain the appearance of higgs and the Yukawa couplings, provided that the symmetry breaks from the starting one $SO(13, 1)$ to $SO(3, 1) \times SU(3) \times U(1)$.

The infinitesimal generators of the Lorentz transformations for the gauge fields — the two kinds of the Clifford operators and the Grassmann operators — operate as follows, Eq. (9.25)

$$\begin{aligned} \{S^{ab}, \gamma^e\}_- &= -i (\eta^{ae} \gamma^b - \eta^{be} \gamma^a), \\ \{\tilde{S}^{ab}, \tilde{\gamma}^e\}_- &= -i (\eta^{ae} \tilde{\gamma}^b - \eta^{be} \tilde{\gamma}^a), \\ \{S^{ab}, \theta^e\}_- &= -i (\eta^{ae} \theta^b - \eta^{be} \theta^a), \\ \{\mathbf{M}^{ab}, A^{d\dots e\dots g}\}_- &= -i (\eta^{ae} A^{d\dots b\dots g} - \eta^{be} A^{d\dots a\dots g}), \end{aligned} \quad (9.3)$$

¹ f^α_a are inverted vielbeins to e^a_α with the properties $e^a_\alpha f^\alpha_b = \delta^a_b$, $e^a_\alpha f^\beta_a = \delta^\beta_\alpha$, $E = \det(e^a_\alpha)$. Latin indices $a, b, \dots, m, n, \dots, s, t, \dots$ denote a tangent space (a flat index), while Greek indices $\alpha, \beta, \dots, \mu, \nu, \dots, \sigma, \tau, \dots$ denote an Einstein index (a curved index). Letters from the beginning of both the alphabets indicate a general index (a, b, c, \dots and $\alpha, \beta, \gamma, \dots$), from the middle of both the alphabets the observed dimensions $0, 1, 2, 3$ (m, n, \dots and μ, ν, \dots), indexes from the bottom of the alphabets indicate the compactified dimensions (s, t, \dots and σ, τ, \dots). We assume the signature $\eta^{ab} = \text{diag}\{1, -1, -1, \dots, -1\}$.

where \mathbf{M}^{ab} are defined by a sum of L^{ab} plus either S^{ab} or \tilde{S}^{ab} , in the Grassmann case \mathbf{M}^{ab} is $L^{ab} + S^{ab}$, which appear to be $\mathbf{M}^{ab} = L^{ab} + S^{ab} + \tilde{S}^{ab}$, as presented later in Eq. (9.26).

We discuss in what follows the first and the second quantization of the fields, the internal degrees of freedom of which are determined by the Grassmann coordinates θ^a , as well as of the fields, the internal degrees of freedom of which are determined by the Clifford coordinates γ^a (or $\tilde{\gamma}^a$) in order to understand why "*nature has made a choice*" of fermions of spins and charges (describable in the *spin-charge-family* theory by subgroups of the Lorentz group expressible with the generators S^{ab}) in the fundamental representations of the groups (which interact in the *spin-charge-family* theory through the boson gauge fields — the vielbeins and the spin connections of two kinds), rather than of fermions with the integer spins and charges. We choose correspondingly either $\theta^{a'}$ s or $\gamma^{a'}$ s (or $\tilde{\gamma}^{a'}$ s, either $\gamma^{a'}$ s or $\tilde{\gamma}^{a'}$ s [6,7,9]) to describe the internal degrees of freedom of fields.

In all these cases we treat free massless fields; masses of the fields in $d = (3 + 1)$ are in the *spin-charge-family* theory due to their interactions with the gravitational fields in $d > 4$, described by the scalar vielbeins or spin connection fields [[1,2,9,3,5,8,4,6,7], and the references therein].

9.2 Observations helping to understand why Clifford algebra manifests in the observable $d = (3 + 1)$

We present in this section properties of fields with the integer spin in d -dimensional space, expressed in terms of the Grassmann algebra objects, and the spinor fields with the half integer spin, expressed in terms of the Clifford algebra objects. Since the Clifford algebra objects are expressible with the Grassmann algebra objects (Eqs. (9.17, 9.18)), the norms of both are determined by the integral in Grassmann space, Eqs. (9.28, 9.31)².

a. Fields with the integer spin in Grassmann space

A point in d -dimensional Grassmann space of real anticommuting coordinates θ^a , ($a = 0, 1, 2, 3, 5, \dots, d$), is determined by a vector

$$\{\theta^a\} = (\theta^0, \theta^1, \theta^2, \theta^3, \theta^5, \dots, \theta^d).$$

A linear vector space over the coordinate Grassmann space has correspondingly the dimension 2^d , due to the fact that $(\theta^{a_i})^2 = 0$ for any $a_i \in (0, 1, 2, 3, 5, \dots, d)$.

Correspondingly are fields in Grassmann space expressed in terms of the Grassmann algebra objects

$$\mathbf{B} = \sum_{k=0}^d a_{a_1 a_2 \dots a_k} \theta^{a_1} \theta^{a_2} \dots \theta^{a_k} |\phi_{og} \rangle, \quad a_i \leq a_{i+1}, \quad (9.4)$$

² These observations might help also when fermionizing boson fields or bosonizing fermion fields.

where $|\phi_{og} \rangle$ is the vacuum state, here assumed to be $|\phi_{og} \rangle = |1 \rangle$, so that $\frac{\partial}{\partial \theta^a} |\phi_{og} \rangle = 0$ for any θ^a . The *Kalb-Ramond* boson fields $a_{a_1 a_2 \dots a_k}$ are antisymmetric with respect to the permutation of indexes, since the Grassmann coordinates anticommute

$$\{\theta^a, \theta^b\}_+ = 0. \quad (9.5)$$

The left derivative $\frac{\partial}{\partial \theta^a}$ on vectors of the space of monomials $\mathbf{B}(\theta)$ is defined as follows

$$\begin{aligned} \frac{\partial}{\partial \theta^a} \mathbf{B}(\theta) &= \frac{\partial \mathbf{B}(\theta)}{\partial \theta^a}, \\ \left\{ \frac{\partial}{\partial \theta^a}, \frac{\partial}{\partial \theta^b} \right\}_+ \mathbf{B} &= 0, \text{ for all } \mathbf{B}. \end{aligned} \quad (9.6)$$

Defining $p^{\theta^a} = i \frac{\partial}{\partial \theta^a}$ it correspondingly follows

$$\{p^{\theta^a}, p^{\theta^b}\}_+ = 0, \quad \{p^{\theta^a}, \theta^b\}_+ = i \eta^{ab}, \quad (9.7)$$

The metric tensor η^{ab} ($= \text{diag}(1, -1, -1, \dots, -1)$) lowers the indexes of a vector $\{\theta^a\}$: $\theta_a = \eta_{ab} \theta^b$, the same metric tensor lowers the indexes of the ordinary vector x^a of commuting coordinates.

Defining³

$$(\theta^a)^\dagger = \frac{\partial}{\partial \theta^a} \eta^{aa} = -i p^{\theta^a} \eta^{aa}, \quad (9.8)$$

it follows

$$\left(\frac{\partial}{\partial \theta^a}\right)^\dagger = \eta^{aa} \theta^a, \quad (p^{\theta^a})^\dagger = -i \eta^{aa} \theta^a. \quad (9.9)$$

Making a choice for the complex properties of θ^a , and correspondingly of $\frac{\partial}{\partial \theta^a}$, as follows

$$\begin{aligned} \{\theta^a\}^* &= (\theta^0, \theta^1, -\theta^2, \theta^3, -\theta^5, \theta^6, \dots, -\theta^{d-1}, \theta^d), \\ \left\{\frac{\partial}{\partial \theta^a}\right\}^* &= \left(\frac{\partial}{\partial \theta^0}, \frac{\partial}{\partial \theta^1}, -\frac{\partial}{\partial \theta^2}, \frac{\partial}{\partial \theta^3}, -\frac{\partial}{\partial \theta^5}, \frac{\partial}{\partial \theta^6}, \dots, -\frac{\partial}{\partial \theta^{d-1}}, \frac{\partial}{\partial \theta^d}\right), \end{aligned} \quad (9.10)$$

it follows for the two Clifford algebra objects $\gamma^a = (\theta^a + \frac{\partial}{\partial \theta^a})$, and $\tilde{\gamma}^a = i(\theta^a - \frac{\partial}{\partial \theta^a})$, Eqs. (9.17, 9.18), that γ^a is real if θ^a is real, and imaginary if θ^a is imaginary, while $\tilde{\gamma}^a$ is imaginary when θ^a is real and real if θ^a is imaginary, just as it is required in Eq. (9.23).

We define here the commuting object γ_G^a , which will be useful to find the action for Grassmann fermions, Eq. (9.37), and the appropriate discrete symmetry operators for this purpose — $(\mathcal{C}_G, \mathcal{T}_G, \mathcal{P}_G)$ in $((d-1)+1)$ -dimensional space-time

³ In Ref. [2] the definition of $\theta^{a\dagger}$ was differently chosen. Correspondingly also the scalar product needed a (slightly) different weight function in Eq. (9.28).

and $(\mathcal{C}_N, \mathcal{T}_N, \mathcal{P}_N)$ in $(3+1)$ space-time — while following the definitions of the discrete symmetry operators in the Clifford algebra case [21]

$$\begin{aligned}\gamma_G^a &= (1 - 2\theta^a \eta^{aa} \frac{\partial}{\partial \theta_a}) \\ &= -i\eta^{aa} \gamma^a \tilde{\gamma}^a, \\ \{\gamma_G^a, \gamma_G^b\}_- &= 0.\end{aligned}\tag{9.11}$$

Index a is not the Lorentz index in the usual sense. γ_G^a are commuting operators — $\{\gamma_G^a, \gamma_G^b\}_- = 0$ for all (a, b) — as expected. They are real and Hermitian.

$$\gamma_G^{a\dagger} = \gamma_G^a, \quad (\gamma_G^a)^* = \gamma_G^a.\tag{9.12}$$

Correspondingly it follows: $\gamma_G^{a\dagger} \gamma_G^a = I$, $\gamma_G^a \gamma_G^a = I$. I represents the unit operator.

By introducing [2] the generators of the infinitesimal Lorentz transformations in Grassmann space as

$$\mathbf{S}^{ab} = (\theta^a p^{\theta b} - \theta^b p^{\theta a}),\tag{9.13}$$

one finds

$$\begin{aligned}\{\mathbf{S}^{ab}, \mathbf{S}^{cd}\}_- &= i\{\mathbf{S}^{ad}\eta^{bc} + \mathbf{S}^{bc}\eta^{ad} - \mathbf{S}^{ac}\eta^{bd} - \mathbf{S}^{bd}\eta^{ac}\}, \\ \mathbf{S}^{ab\dagger} &= \eta^{aa}\eta^{bb}\mathbf{S}^{ab}.\end{aligned}\tag{9.14}$$

The basic states in Grassmann space can be arranged into representations with respect to the Cartan subalgebra of the Lorentz algebra as presented in Ref. [2,15]. The state in d -dimensional space, for example, with all the eigenvalues of the Cartan subalgebra of the Lorentz group of Eq. (9.84) equal to either i or 1 is: $(\theta^0 - \theta^3)(\theta^1 + i\theta^2)(\theta^5 + i\theta^6) \dots (\theta^{d-1} + i\theta^d)|\phi_{og} \rangle$, with $|\phi_{og} \rangle = |1 \rangle$. All the states of the representation, which start with this state, follow by the application of those \mathbf{S}^{ab} , which do not belong to the Cartan subalgebra of the Lorentz algebra. \mathbf{S}^{01} , for example, transforms $(\theta^0 - \theta^3)(\theta^1 + i\theta^2)(\theta^5 + i\theta^6) \dots (\theta^{d-1} + i\theta^d)|\phi_{og} \rangle$ into $(\theta^0\theta^3 + i\theta^1i\theta^2)(\theta^5 + i\theta^6) \dots (\theta^{d-1} + i\theta^d)|\phi_{og} \rangle$, while $\mathbf{S}^{01} - i\mathbf{S}^{02}$ transforms this state into $(\theta^0 + \theta^3)(\theta^1 - i\theta^2)(\theta^5 + i\theta^6) \dots (\theta^{d-1} + i\theta^d)|\phi_{og} \rangle$.

b. Fermion fields with the half integer spin and the Clifford objects

Let us present as well the properties of the fermion fields with the half integer spin, expressed by the Clifford algebra objects

$$\mathbf{F} = \sum_{k=0}^d a_{a_1 a_2 \dots a_k} \gamma^{a_1} \gamma^{a_2} \dots \gamma^{a_k} |\psi_{oc} \rangle, \quad a_i \leq a_{i+1},\tag{9.15}$$

where $|\psi_{oc} \rangle$ is the vacuum state. The *Kalb-Ramond* fields $a_{a_1 a_2 \dots a_k}$ are again in general boson fields, which are antisymmetric with respect to the permutation of indexes, since the Clifford objects have the anticommutation relations, Eq. (9.2),

$$\{\gamma^a, \gamma^b\}_+ = 2\eta^{ab}.\tag{9.16}$$

A linear vector space over the Clifford coordinate space has again the dimension 2^d , due to the fact that $(\gamma^{a_i})^2 = \eta^{a_i a_i}$ for any $a_i \in (0, 1, 2, 3, 5, \dots, d)$.

One can see that γ^a are expressible in terms of the Grassmann coordinates and their conjugate momenta as

$$\gamma^a = (\theta^a - i p^{\theta a}). \quad (9.17)$$

We also find $\tilde{\gamma}^a$

$$\tilde{\gamma}^a = i(\theta^a + i p^{\theta a}), \quad (9.18)$$

with the anticommutation relation of Eq. (9.16) for either γ^a and $\tilde{\gamma}^a$

$$\{\tilde{\gamma}^a, \tilde{\gamma}^b\}_+ = 2\eta^{ab}, \quad \{\gamma^a, \tilde{\gamma}^b\}_+ = 0. \quad (9.19)$$

Taking into account Eqs. (9.8, 9.17, 9.18) one finds

$$\begin{aligned} (\gamma^a)^\dagger &= \gamma^a \eta^{aa}, \quad (\tilde{\gamma}^a)^\dagger = \tilde{\gamma}^a \eta^{aa}, \\ \gamma^a \gamma^a &= \eta^{aa}, \quad \gamma^a (\gamma^a)^\dagger = I, \quad \tilde{\gamma}^a \tilde{\gamma}^a = \eta^{aa}, \quad \tilde{\gamma}^a (\tilde{\gamma}^a)^\dagger = I, \end{aligned} \quad (9.20)$$

where I represents the unit operator. Making a choice for the θ^a properties as presented in Eq. (9.10), it follows for the Clifford objects

$$\begin{aligned} \{\gamma^a\}^* &= (\gamma^0, \gamma^1, -\gamma^2, \gamma^3, -\gamma^5, \gamma^6, \dots, -\gamma^{d-1}, \gamma^d), \\ \{\tilde{\gamma}^a\}^* &= (-\tilde{\gamma}^0, -\tilde{\gamma}^1, \tilde{\gamma}^2, -\tilde{\gamma}^3, \tilde{\gamma}^5, -\tilde{\gamma}^6, \dots, \tilde{\gamma}^{d-1}, -\tilde{\gamma}^d), \end{aligned} \quad (9.21)$$

All three choices for the linear vector space — spanned over either the coordinate Grassmann space, or over the vector space of γ^a , as well as over the vector space of $\tilde{\gamma}^a$ — have the dimension 2^d .

We can express Grassmann coordinates θ^a and momenta $p^{\theta a}$ in terms of γ^a and $\tilde{\gamma}^a$ as well ⁴

$$\begin{aligned} \theta^a &= \frac{1}{2}(\gamma^a - i\tilde{\gamma}^a), \\ \frac{\partial}{\partial \theta^a} &= \frac{1}{2}(\gamma^a + i\tilde{\gamma}^a). \end{aligned} \quad (9.22)$$

It then follows $\frac{\partial}{\partial \theta^a} \theta^a |1\rangle = \eta^{aa} |1\rangle$.

Correspondingly we can use either γ^a or $\tilde{\gamma}^a$ instead of θ^a to span the vector space. In this case we change the vacuum from the one with the property $\frac{\partial}{\partial \theta^a} |\phi_{og}\rangle = 0$ to $|\psi_{oc}\rangle$ with the property [2,7,9]

$$\begin{aligned} \langle \psi_{oc} | \gamma^a | \psi_{oc} \rangle &= 0, \quad \tilde{\gamma}^a | \psi_{oc} \rangle = i\gamma^a | \psi_{oc} \rangle, \quad \tilde{\gamma}^a \gamma^b | \psi_{oc} \rangle = -i\gamma^b \gamma^a | \psi_{oc} \rangle, \\ \tilde{\gamma}^a \tilde{\gamma}^b | \psi_{oc} \rangle &|_{a \neq b} = -\gamma^a \gamma^b | \psi_{oc} \rangle, \quad \tilde{\gamma}^a \tilde{\gamma}^b | \psi_{oc} \rangle |_{a=b} = \eta^{ab} | \psi_{oc} \rangle. \end{aligned} \quad (9.23)$$

⁴ In Ref. [28] the author suggested in Eq. (47) a choice of superposition of γ^a and $\tilde{\gamma}^a$, which resembles the choice of one of the authors (N.S.M.B.) in Ref. [2] and both authors in Ref. [16,17] and in present article.

This is in agreement with the requirement

$$\begin{aligned} \gamma^a \mathbf{F}(\gamma) |\psi_{oc} > &:= \\ (a_0 \gamma^a + a_{a_1} \gamma^a \gamma^{a_1} + a_{a_1 a_2} \gamma^a \gamma^{a_1} \gamma^{a_2} + \dots + a_{a_1 \dots a_d} \gamma^a \gamma^{a_1} \dots \gamma^{a_d}) |\psi_{oc} >, \\ \tilde{\gamma}^a \mathbf{F}(\gamma) |\psi_{oc} > &:= (i a_0 \gamma^a - i a_{a_1} \gamma^{a_1} \gamma^a + i a_{a_1 a_2} \gamma^{a_1} \gamma^{a_2} \gamma^a + \dots + \\ i(-1)^d a_{a_1 \dots a_d} \gamma^{a_1} \dots \gamma^{a_d} \gamma^a) |\psi_{oc} >. \end{aligned} \quad (9.24)$$

We find the infinitesimal generators of the Lorentz transformations in Clifford space

$$\begin{aligned} S^{ab} &= \frac{i}{4} (\gamma^a \gamma^b - \gamma^b \gamma^a), \quad S^{ab\dagger} = \eta^{aa} \eta^{bb} S^{ab}, \\ \tilde{S}^{ab} &= \frac{i}{4} (\tilde{\gamma}^a \tilde{\gamma}^b - \tilde{\gamma}^b \tilde{\gamma}^a), \quad \tilde{S}^{ab\dagger} = \eta^{aa} \eta^{bb} \tilde{S}^{ab}, \end{aligned} \quad (9.25)$$

with the commutation relations for either S^{ab} or \tilde{S}^{ab} of Eq. (9.14), if S^{ab} is replaced by either S^{ab} or \tilde{S}^{ab} , respectively, while

$$\begin{aligned} \mathbf{S}^{ab} &= S^{ab} + \tilde{S}^{ab}, \\ \{S^{ab}, \tilde{S}^{cd}\}_- &= 0. \end{aligned} \quad (9.26)$$

The basic states in Clifford space can be arranged in representations, in which any state is the eigenstate of the Cartan subalgebra operators of Eq. (9.84). The state, for example, in d -dimensional space with the eigenvalues of either $S^{03}, S^{12}, S^{56}, \dots, S^{d-1 d}$ or $\tilde{S}^{03}, \tilde{S}^{12}, \tilde{S}^{56}, \dots, \tilde{S}^{d-1 d}$ equal to $\frac{1}{2}(i, 1, 1, \dots, 1)$ is $(\gamma^0 - \gamma^3)(\gamma^1 + i\gamma^2)(\gamma^5 + i\gamma^6) \dots (\gamma^{d-1} + i\gamma^d)$, where the states are expressed in terms of γ^a . The states of one representation follow from the starting state by the application of S^{ab} , which do not belong to the Cartan subalgebra operators, while \tilde{S}^{ab} , which operate on family quantum numbers, cause jumps from the starting family to the new one.

9.2.1 Norms of vectors in Grassmann and Clifford space

Let us look for the norm of vectors in Grassmann space

$$\mathbf{B} = \sum_{k=0}^d a_{a_1 a_2 \dots a_k} \theta^{a_1} \theta^{a_2} \dots \theta^{a_k} |\phi_{og} >$$

and in Clifford space

$$\mathbf{F} = \sum_{k=0}^d a_{a_1 a_2 \dots a_k} \gamma^{a_1} \gamma^{a_2} \dots \gamma^{a_k} |\psi_{oc} >,$$

where $|\phi_{og} >$ and $|\psi_{oc} >$ are the vacuum states in the Grassmann and Clifford case, respectively. In what follows we refer to Ref. [2].

a. Norms of the Grassmann vectors

Let us define the integral over the Grassmann space [2] of two functions of the Grassmann coordinates $\langle \mathbf{B}|\mathbf{C} \rangle$, $\langle \mathbf{B}|\theta \rangle = \langle \theta|\mathbf{B} \rangle^\dagger$, by requiring

$$\begin{aligned} \{d\theta^a, \theta^b\}_+ &= 0, \quad \int d\theta^a = 0, \quad \int d\theta^a \theta^a = 1, \\ \int d^d \theta \theta^0 \theta^1 \dots \theta^d &= 1, \\ d^d \theta &= d\theta^d \dots d\theta^0, \\ \omega &= \prod_{k=0}^d \left(\frac{\partial}{\partial \theta_k} + \theta^k \right), \end{aligned} \quad (9.27)$$

with $\frac{\partial}{\partial \theta_a} \theta^c = \eta^{ac}$. We shall use the weight function $\omega = \prod_{k=0}^d \left(\frac{\partial}{\partial \theta_k} + \theta^k \right)$ to define the scalar product $\langle \mathbf{B}|\mathbf{C} \rangle$

$$\langle \mathbf{B}|\mathbf{C} \rangle = \int d^{d-1} x d^d \theta^a \omega \langle \mathbf{B}|\theta \rangle \langle \theta|\mathbf{C} \rangle = \sum_{k=0}^d \int d^{d-1} x b_{b_1 \dots b_k}^* c_{b_1 \dots b_k}, \quad (9.28)$$

where, according to Eq. (9.8), follows:

$$\langle \mathbf{B}|\theta \rangle = \langle \phi_{og} | \sum_{p=0}^d (-i)^p a_{a_1 \dots a_p}^* p^{\theta_{a_p}} \eta^{a_p a_p} \dots p^{\theta_{a_1}} \eta^{a_1 a_1}.$$

The vacuum state is chosen to be $|\phi_{og}\rangle = |1\rangle$, as taken in Eq. (9.4).

The norm $\langle \mathbf{B}|\mathbf{B} \rangle$ is correspondingly always nonnegative.

b. Norms of the Clifford vectors

Let us look for the norm of vectors, expressed with the Clifford objects $\mathbf{F} = \sum_k^d a_{a_1 a_2 \dots a_k} \gamma^{a_1} \gamma^{a_2} \dots \gamma^{a_k} |\psi_{oc}\rangle$, where $|\phi_{og}\rangle$ and $|\psi_{oc}\rangle$ are the two vacuum states when the Grassmann and the Clifford objects are concerned, respectively. By taking into account Eq. (9.20) it follows that

$$(\gamma^{a_1} \gamma^{a_2} \dots \gamma^{a_k})^\dagger = \gamma^{a_k} \eta^{a_k a_k} \dots \gamma^{a_2} \eta^{a_2 a_2} \gamma^{a_1} \eta^{a_1 a_1}, \quad (9.29)$$

since $\gamma^a \gamma^a = \eta^{aa}$.

We can use Eqs. (9.27, 9.28) to evaluate the scalar product of two Clifford algebra objects $\langle \gamma|\mathbf{F} \rangle = \langle (\theta^a - i p^{\theta a})|\mathbf{F} \rangle$ and equivalently for $\langle (\theta^a - i p^{\theta a})|\mathbf{G} \rangle$. These expressions follow from Eqs. (9.17, 9.18, 9.20)). We must then choose for the vacuum state the one from the Grassmann case — $|\psi_{oc}\rangle = |\phi_{og}\rangle = |1\rangle$. It follows

$$\langle \mathbf{F}|\mathbf{G} \rangle = \int d^{d-1} x d^d \theta^a \omega \langle \mathbf{F}|\gamma \rangle \langle \gamma|\mathbf{G} \rangle = \sum_{k=0}^d \int d^{d-1} x a_{a_1 \dots a_k}^* b_{b_1 \dots b_k}. \quad (9.30)$$

{Similarly we obtain, if we express $\tilde{\mathbf{F}} = \sum_{k=0}^d a_{a_1 a_2 \dots a_k} \tilde{\gamma}^{a_1} \tilde{\gamma}^{a_2} \dots \tilde{\gamma}^{a_k} |\phi_{oc}\rangle$ and $\tilde{\mathbf{G}} = \sum_{k=0}^d b_{b_1 b_2 \dots b_k} \tilde{\gamma}^{b_1} \tilde{\gamma}^{b_2} \dots \tilde{\gamma}^{b_k} |\phi_{oc}\rangle$ and take $|\psi_{oc}\rangle = |\phi_{og}\rangle = |1\rangle$,

the scalar product

$$\langle \tilde{\mathbf{F}} | \tilde{\mathbf{G}} \rangle = \int d^{d-1}x d^d\theta^a \omega \langle \tilde{\mathbf{F}} | \tilde{\gamma} \rangle \langle \tilde{\gamma} | \tilde{\mathbf{G}} \rangle = \sum_{k=0}^d \int d^{d-1}x a_{a_1 \dots a_k}^* a_{b_1 \dots b_k} \cdot \} \quad (9.31)$$

Correspondingly we can write

$$\int d^d\theta^a \omega(a_{a_1 a_2 \dots a_k} \gamma^{a_1} \gamma^{a_2} \dots \gamma^{a_k})^\dagger (a_{a_1 a_2 \dots a_k} \gamma^{a_1} \gamma^{a_2} \dots \gamma^{a_k}) = a_{a_1 a_2 \dots a_k}^* a_{a_1 a_2 \dots a_k} \cdot \quad (9.32)$$

The norm of each scalar term in the sum of \mathbf{F} is nonnegative.

c. We have learned that in both spaces — Grassmann and Clifford — norms of basic states can be defined so that the states, which are eigenvectors of the Cartan subalgebra, are orthogonal and normalized using the same integral.

Studying the second quantization procedure in Subsect. 9.2.3 we learn that not all 2^d states can be represented as creation and annihilation operators, either in the Grassmann or in the Clifford case, since they must — in both cases — fulfill the requirements for the second quantized operators, either for states with integer spins in Grassmann space or for states with half integer spin in Clifford space.

9.2.2 Actions in Grassmann and Clifford space

Let us construct an action for free massless particles in which the internal degrees of freedom will be described: **i.** by states in Grassmann space, **ii.** by states in Clifford space. In the first case the internal degrees of freedom manifest the integer spin, in the second case the internal degrees of freedom manifest the half integer spin.

While the action in Clifford space is well known since long [22], the action in Grassmann space must be found. We shall represent it here. In both cases we look for actions for free massless states in $((d-1)+1)$ space⁵. States in Grassmann space as well as states in Clifford space will be organized to be — within each of the two spaces — orthogonal and normalized with respect to Eq. (9.27). We choose the states in each of two spaces to be the eigenstates of the Cartan subalgebra — with respect to \mathbf{S}^{ab} in Grassmann space and with respect to S^{ab} and \tilde{S}^{ab} in Clifford space, Eq. (9.84).

In both spaces the requirement that states are obtained by the application of creation operators on the vacuum states — \hat{b}_i^0 obeying the commutation relations of Eq. (9.48) on the vacuum state $|\phi_{og}\rangle = |1\rangle$ in Grassmann space, and \hat{b}_i^α obeying the commutation relation of Eq. (9.60) on the vacuum states $|\psi_{oc}\rangle$, Eq. (9.67), in Clifford space — reduces the number of states, in Clifford space more than in Grassmann space. But while in Clifford space all physically applicable states are reachable by either S^{ab} (defining family members quantum numbers)

⁵ In $(3+1)$ space the mass is due to the interaction of particles with the scalar fields, with which the particles interact in $((d-1)+1)$ space.

or by \tilde{S}^{ab} (defining family quantum numbers), the states in Grassmann space, belonging to different representations with respect to the Lorentz generators, seem not to be connected.

a. Action in Clifford space

In Clifford space the action for a free massless object must be Lorentz invariant

$$\mathcal{A} = \int d^d x \frac{1}{2} (\psi^\dagger \gamma^0 \gamma^a p_a \psi) + \text{h.c.}, \quad (9.33)$$

$p_a = i \frac{\partial}{\partial x^a}$, leading to the equations of motion

$$\gamma^a p_a |\psi^\alpha\rangle = 0, \quad (9.34)$$

which fulfill also the Klein-Gordon equation

$$\gamma^a p_a \gamma^b p_b |\psi_i^\alpha\rangle = p^a p_a |\psi_i^\alpha\rangle = 0, \quad (9.35)$$

for each of the basic states $|\psi_i^\alpha\rangle$. Correspondingly γ^0 appears in the action since we pay attention that

$$\begin{aligned} S^{ab\dagger} \gamma^0 &= \gamma^0 S^{ab}, \\ S^\dagger \gamma^0 &= \gamma^0 S^{-1}, \\ S &= e^{-\frac{i}{2} \omega_{ab} (S^{ab} + L^{ab})}. \end{aligned} \quad (9.36)$$

We choose the basic states to be the eigenstates of all the members of the Cartan subalgebra, Eq. (9.84). Correspondingly all the states, belonging to different values of the Cartan subalgebra — they differ at least in one value of either the set of S^{ab} or the set of \tilde{S}^{ab} , Eq. (9.84) — are orthogonal with respect to the scalar product defined as the integral over the Grassmann coordinates, Eq. (9.27), for a chosen vacuum state. Correspondingly the states generated by the creation operators, Eq. (9.65), on the vacuum state, Eq. (9.67), are orthogonal as well (both last equations will appear later).

b. Action in Grassmann space

We define here the action in Grassmann space, for which we require — similarly as in the Clifford case — that the action for a free massless object

$$\mathcal{A} = \frac{1}{2} \left\{ \int d^d x d^d \theta \omega \left(\phi^\dagger (1 - 2\theta^0 \frac{\partial}{\partial \theta^0}) \frac{1}{2} (\theta^a p_a + \eta^{aa} \theta^{a\dagger} p_a) \phi \right) \right\}, \quad (9.37)$$

is Lorentz invariant. We use the integral also over θ^a coordinates, with the weight function ω from Eq. (9.27). Requiring the Lorentz invariance we add after ϕ^\dagger the operator γ_G^0 ($\gamma_G^a = (1 - 2\theta^a \frac{\partial}{\partial \theta^a})$), which takes care of the Lorentz invariance. Namely

$$\begin{aligned} S^{ab\dagger} (1 - 2\theta^0 \frac{\partial}{\partial \theta^0}) &= (1 - 2\theta^0 \frac{\partial}{\partial \theta^0}) S^{ab}, \\ S^\dagger (1 - 2\theta^0 \frac{\partial}{\partial \theta^0}) &= (1 - 2\theta^0 \frac{\partial}{\partial \theta^0}) S^{-1}, \\ S &= e^{-\frac{i}{2} \omega_{ab} (L^{ab} + S^{ab})}, \end{aligned} \quad (9.38)$$

while θ^a , $\frac{\partial}{\partial \theta_a}$ and p^a transform as Lorentz vectors. The equation of motion follow from the action, Eq. (9.37),

$$\frac{1}{2}[(1 - 2\theta^0 \frac{\partial}{\partial \theta^0}) \theta^a + ((1 - 2\theta^0 \frac{\partial}{\partial \theta^0}) \theta^a)^\dagger] p_a |\phi_i^\theta\rangle = 0, \quad (9.39)$$

as well as the Klein-Gordon equation

$$\{(1 - 2\theta^0 \frac{\partial}{\partial \theta^0}) \theta^a p_a\}^\dagger \theta^b p_b |\phi_i^\theta\rangle = p^a p_a |\phi_i^\theta\rangle = 0, \quad (9.40)$$

for each of the basic states $|\psi_i^\alpha\rangle$.

c. *We learned:*

In both spaces — in Clifford and in Grassmann space — there exists the action, which leads to the equations of motion and to the corresponding Klein-Gordon equation for free massless particles. In both cases we use the operator, which does not change the Clifford or Grassmann character of states.

We shall see that, if one identifies the creation operators in both spaces with the products of odd numbers of either θ^a (in the Grassmann case) or γ^a (in the Clifford case) and the annihilation operators with their Hermitian conjugate operators, the creation and annihilation operators fulfill the anticommutation relations, required for fermions. The internal parts of states are then defined by the application of the creation operators on the vacuum state. But while the Clifford algebra defines spinors with the half integer eigenvalues of the Cartan subalgebra operators of the Lorentz algebra, the Grassmann algebra defines states with the integer eigenvalues of the Cartan subalgebra.

9.2.3 Second quantization of Grassmann vectors and Clifford vectors

States in Grassmann space as well as states in Clifford space are organized to be — within each of the two spaces — orthogonal and normalized with respect to Eq. (9.27). All the states in each of spaces are chosen to be eigenstates of the Cartan subalgebra — with respect to S^{ab} in Grassmann space, and with respect to S^{ab} and \tilde{S}^{ab} in Clifford space, Eq. (9.84).

In both spaces the requirement that states are obtained by the application of creation operators on vacuum states — \hat{b}_i^θ obeying the commutation relations of Eqs. (9.42, 9.48) on the vacuum state $|\phi_{og}\rangle = |1\rangle$ for Grassmann space, and \hat{b}_i^α obeying the commutation relation of Eq. (9.60) on the vacuum states $|\psi_{oc}\rangle$, Eq. (9.67), for Clifford space — reduces the number of states arranged into the representations of the Lorentz group. The reduction of degrees of freedom depends on whether $d = 2(2n+1)$ or $d = 4n$, n is a positive integer. The second quantization procedure with creation operators expressed by the product of Grassmann or Clifford objects requires that the product has an odd number of objects.

We shall pay attention in this paper almost only to spaces with $d = 2(2n+1)$ ⁶.

⁶ The main reason that we treat here mostly $d = 2(2n+1)$ spaces is that one Weyl representation, expressed by the product of the Clifford algebra objects, manifests in $d = (1+3)$ all the observed properties of quarks and leptons, if $d \geq 2(2n+1)$, $n = 3$.

We define in Grassmann space creation operators by an odd number of factors of superposition of θ^a 's and annihilation operators by Hermitian conjugation of the corresponding creation operators. In Clifford space we define creation operators by an odd number of factors of superposition of γ^a 's and the annihilation operators by Hermitian conjugate creation operators. Each basic state is a product of factors chosen to be eigenstates of the Cartan subalgebra of the Lorentz algebra.

But while in Clifford space all physically applicable states are reachable either by S^{ab} or by \tilde{S}^{ab} , the states, belonging to different groups with respect to the Lorentz generators, in Grassmann space two different representations of the Lorentz group are not connected by the Lorentz operators.

Let us construct creation and annihilation operators for the cases that we use **a.** Grassmann vector space, **b.** Clifford vector space. We shall see that from 2^d states in either of these two spaces there are reduced number of states generated by the creation operators, which fulfill the requirements for the creation and their Hermitian conjugate annihilation operators.

a. Quantization in Grassmann space

There are 2^d states in Grassmann space, orthogonal to each other with respect to Eq. (9.27). To any coordinate there exists the conjugate momentum. We pay attention in what follows mostly to spaces with $d = 2(2n+1)$, although also spaces with $d = 4n$ will be treated. In $d = 2(2n+1)$ spaces there are $\frac{d!}{2!2!}$ states, Eq. (9.51), divided into two separated groups of states, all states of one group reachable from a starting state by S^{ab} . These states are Grassmann odd products of eigenstates of the Cartan subalgebra. We use these products to define the creation operators and their Hermitian conjugate operators as the annihilation operators, fulfilling requirements of Eq. (9.41, 9.42). Let us see how it goes.

If $\hat{b}_i^{\theta\dagger}$ is a creation operator, which creates a state in the Grassmann space when operating on a vacuum state $|\psi_{og} \rangle$ and $\hat{b}_i^\theta = (\hat{b}_i^{\theta\dagger})^\dagger$ is the corresponding annihilation operator, then for a set of creation operators $\hat{b}_i^{\theta\dagger}$ and the corresponding annihilation operators \hat{b}_i^θ it must be

$$\begin{aligned}\hat{b}_i^\theta |\phi_{og} \rangle &= 0, \\ \hat{b}_i^{\theta\dagger} |\phi_{og} \rangle &\neq 0.\end{aligned}\tag{9.41}$$

We first pay attention on only the internal degrees of freedom — the spin.

Choosing $\hat{b}_a^\theta = \frac{\partial}{\partial \theta^a}$ it follows

$$\begin{aligned}\hat{b}_a^{\theta\dagger} &= \theta^a, \\ \hat{b}_a^\theta &= \frac{\partial}{\partial \theta^a}, \\ \{\hat{b}_a^\theta, \hat{b}_b^{\theta\dagger}\}_+ |\phi_{og} \rangle &= \delta_{ab} |\phi_{og} \rangle, \\ \{\hat{b}_a^\theta, \hat{b}_b^\theta\}_+ |\phi_{og} \rangle &= 0, \\ \{\hat{b}_a^{\theta\dagger}, \hat{b}_b^{\theta\dagger}\}_+ |\phi_{og} \rangle &= 0, \\ \hat{b}_a^{\theta\dagger} |\phi_{og} \rangle &= \theta^a |\phi_{og} \rangle, \\ \hat{b}_a^\theta |\phi_{og} \rangle &= 0.\end{aligned}\tag{9.42}$$

The vacuum state $|\phi_{og} \rangle$ is in this case $|1 \rangle$.

The identity $I (I^\dagger = I)$ can not be taken as a creation operator, since its annihilation partner does not fulfill Eq. (9.41).

We can use the products of superposition of θ^a 's as creation and products of superposition of $\frac{\partial}{\partial \theta^a}$'s as annihilation operators provided that they fulfill the requirements for the creation and annihilation operators, Eq. (9.48), with the vacuum state $|\phi_{og} \rangle = |1 \rangle$. In general they would not. Only an odd number of θ^a in any product would have the required anticommutation properties.

It is convenient to take products of superposition of vectors θ^a and θ^b to construct creation operators so that each factor is the eigenstate of one of the Cartan subalgebra member of the Lorentz algebra (9.84). We can start with the creation operators as products of $\frac{d}{2}$ states $\hat{b}_{a_i b_i}^{\theta 1} = \frac{1}{\sqrt{2}}(\theta^{a_i} \pm \epsilon \theta^{b_i})$. Then the corresponding annihilation operators have $\frac{d}{2}$ factors of $\hat{b}_{a_i b_i}^\theta = \frac{1}{\sqrt{2}}(\frac{\partial}{\partial \theta^{a_i}} \pm \epsilon^* \frac{\partial}{\partial \theta^{b_i}})$, $\epsilon = i$, if $\eta^{a_i a_i} = \eta^{b_i b_i}$ and $\epsilon = -1$, if $\eta^{a_i a_i} \neq \eta^{b_i b_i}$.

In $d = 2(2n + 1)$, n is a positive integer, we can start with the state

$$|\phi_1^{\theta 1} \rangle = (\frac{1}{\sqrt{2}})^{\frac{d}{2}} (\theta^0 - \theta^3)(\theta^1 + i\theta^2)(\theta^5 + i\theta^6) \dots (\theta^{d-1} + i\theta^d) |1 \rangle. \quad (9.43)$$

The rest of states, belonging to the same Lorentz representation, follows from the starting state by the application of the operators S^{cf} , which do not belong to the Cartan subalgebra operators.

Let us add that in $d = 4n$ we should start with the state

$$|\phi_1^{\theta 1} \rangle_{4n} = (\frac{1}{\sqrt{2}})^{\frac{d}{2}-1} (\theta^0 - \theta^3)(\theta^1 + i\theta^2)(\theta^5 + i\theta^6) \dots (\theta^{d-3} + i\theta^{d-2}) \theta^{d-1} \theta^d |1 \rangle. \quad (9.44)$$

Again the rest of states, belonging to the same Lorentz representation, follow from the starting state by the application of the operators S^{cf} , which do not belong to the Cartan subalgebra operators.

i. Taking into account Eqs. (9.8, 9.9, 9.43) one can propose the following starting creation operator and the corresponding annihilation operator

$$\begin{aligned} \hat{b}_i^{\theta 1 \dagger} &= (\frac{1}{\sqrt{2}})^{\frac{d}{2}} (\theta^0 - \theta^3)(\theta^1 + i\theta^2)(\theta^5 + i\theta^6) \dots (\theta^{d-1} + i\theta^d), \\ \hat{b}_i^{\theta 1} &= (\frac{1}{\sqrt{2}})^{\frac{d}{2}} (\frac{\partial}{\partial \theta^{d-1}} - i \frac{\partial}{\partial \theta^d}) \dots (\frac{\partial}{\partial \theta^0} - \frac{\partial}{\partial \theta^3}), \\ &\text{for } d = 2(2n + 1), \\ \hat{b}_i^{\theta 1 \dagger} &= (\frac{1}{\sqrt{2}})^{\frac{d}{2}-1} (\theta^0 - \theta^3)(\theta^1 + i\theta^2)(\theta^5 + i\theta^6) \dots (\theta^{d-3} + i\theta^{d-2}) \theta^{d-1} \theta^d, \\ \hat{b}_i^{\theta 1} &= (\frac{1}{\sqrt{2}})^{\frac{d}{2}-1} \frac{\partial}{\partial \theta^d} \frac{\partial}{\partial \theta^{d-1}} (\frac{\partial}{\partial \theta^{d-3}} - i \frac{\partial}{\partial \theta^{d-2}}) \dots (\frac{\partial}{\partial \theta^0} - \frac{\partial}{\partial \theta^3}), \\ &\text{for } d = 4n. \end{aligned} \quad (9.45)$$

The rest of the creation operators belonging to this group in either $d = 2(2n + 1)$ or in $d = 4n$ follows by the application of all the operators S^{ef} , which do not belong

to the Cartan subalgebra operators. The corresponding annihilation operators follow by the Hermitian conjugation of a particular creation operator. One finds, for example for $d = 2(2n + 1)$,

$$\begin{aligned}\hat{b}_j^{\theta^{01\dagger}} &= \left(\frac{1}{\sqrt{2}}\right)^{\frac{d}{2}-1} (\theta^0\theta^3 + i\theta^1\theta^2)(\theta^5 + i\theta^6) \dots (\theta^{d-1} + i\theta^d), \\ \hat{b}_j^{\theta^1} &= \left(\frac{1}{\sqrt{2}}\right)^{\frac{d}{2}-1} \left(\frac{\partial}{\partial\theta^{d-1}} - i\frac{\partial}{\partial\theta^d}\right) \dots \left(\frac{\partial}{\partial\theta^3} \frac{\partial}{\partial\theta^0} - i\frac{\partial}{\partial\theta^2} \frac{\partial}{\partial\theta^1}\right). \\ &\dots\end{aligned}\tag{9.46}$$

For $d = 4n$ one finds equivalently

$$\begin{aligned}\hat{b}_j^{\theta^{01\dagger}} &= \left(\frac{1}{\sqrt{2}}\right)^{\frac{d}{2}-2} (\theta^0\theta^3 + i\theta^1\theta^2)(\theta^5 + i\theta^6) \dots (\theta^{d-3} + i\theta^{d-2}) \theta^{d-1}\theta^d, \\ \hat{b}_j^{\theta^1} &= \left(\frac{1}{\sqrt{2}}\right)^{\frac{d}{2}-2} \frac{\partial}{\partial\theta^d} \frac{\partial}{\partial\theta^{d-1}} \left(\frac{\partial}{\partial\theta^{d-3}} - i\frac{\partial}{\partial\theta^{d-2}}\right) \dots \left(\frac{\partial}{\partial\theta^3} \frac{\partial}{\partial\theta^0} - i\frac{\partial}{\partial\theta^2} \frac{\partial}{\partial\theta^1}\right). \\ &\dots\end{aligned}\tag{9.47}$$

It was taken into account in the above two equations that \mathbf{S}^{01} transforms $(\frac{1}{\sqrt{2}})^2(\theta^0 - \theta^3)(\theta^1 + i\theta^2)$ into $\frac{1}{\sqrt{2}}(\theta^0\theta^3 + i\theta^1\theta^2)$ and that any \mathbf{S}^{ac} ($a \neq c$), which does not belong to Cartan subalgebra, Eq.(9.82), transforms $(\frac{1}{\sqrt{2}})^2(\theta^a + i\theta^b)(\theta^c + i\theta^d)$ ($a \neq c$ and $a \neq d$, $b \neq c$ and $b \neq d$, $\eta^{aa} = \eta^{bb}$) into $\frac{1}{\sqrt{2}}(\theta^a\theta^b + \theta^c\theta^d)$. The states are normalized and the simplest phases are chosen.

One finds that $\mathbf{S}^{ab}(\theta^a \pm \epsilon\theta^b) = \mp i \frac{\eta^{aa}}{\epsilon}(\theta^a \pm \epsilon\theta^b)$, $\epsilon = 1$ for $\eta^{aa} = 1$ and $\epsilon = i$ for $\eta^{aa} = -1$, while either \mathbf{S}^{ab} or \mathbf{S}^{cd} , applied on $(\theta^a\theta^b \pm \epsilon\theta^c\theta^d)$, gives zero.

Although all the states, generated by creation operators, which include one $(I \pm \epsilon\theta^a\theta^b)$ or several $(I \pm \epsilon\theta^{a_1}\theta^{b_1}) \dots (I \pm \epsilon\theta^{a_k}\theta^{b_k})$, are orthogonal with respect to the scalar product, Eq.(9.28), their Hermitian conjugate values include I^\dagger , which, when applying on the vacuum state $|\phi_{og}\rangle = |1\rangle$, does not give zero. Correspondingly such creation operators do not have appropriate annihilation partners, which would fulfill Eqs. (9.41, 9.42).

However, creation operators which are products of several θ 's, let say n with $n = 2, 4 \dots \frac{d}{2} - 1$ — always of an even number of θ 's, since \mathbf{S}^{ab} is a Grassmann even operator, $\theta^{a_1} \dots \theta^{a_n}$ (factors $\theta^a\theta^b$ can be "eigenstates" of the Cartan subalgebra operators provided that \mathbf{S}^{ab} belong to the Cartan subalgebra: $\mathbf{S}^{ab}\theta^a\theta^b|1\rangle = 0$) — can appear in the expression for a creation operator, provided that the rest of expression has an odd number of factors $(\frac{d}{2} - n)$ (with "eigenvalues" either $(+1$ or $-1)$ or $(+i$ or $-i)$, as can be seen in the states of Eqs. (9.45, 9.46, 9.47)). Then such creation and annihilation operators fulfill the relations, we skip the index 1 in $\hat{b}_i^{\theta^1}$

and in $\hat{b}_i^{\theta 1 \dagger}$

$$\begin{aligned}
 \{\hat{b}_i^\theta, \hat{b}_j^{\theta \dagger}\}_+ |\phi_{og}\rangle &= \delta_{ij} |\phi_{og}\rangle, \\
 \{\hat{b}_i^\theta, \hat{b}_j^\theta\}_+ |\phi_{og}\rangle &= 0 |\phi_{og}\rangle, \\
 \{\hat{b}_i^{\theta \dagger}, \hat{b}_j^{\theta \dagger}\}_+ |\phi_{og}\rangle &= 0 |\phi_{og}\rangle, \\
 \hat{b}_j^{\theta \dagger} |\phi_{og}\rangle &= |\phi_j\rangle \\
 \hat{b}_j^\theta |\phi_{og}\rangle &= 0 |\phi_{og}\rangle.
 \end{aligned} \tag{9.48}$$

It is not difficult to see that states included into a representation, which started with $\hat{b}_i^{\theta \dagger}$ as presented in Eq. (9.45) for $d = (2n + 1)2$ and $4n$ spaces, *have the properties, required by* Eq. (9.48):

i.a. In any d -dimensional space the product $\frac{\partial}{\partial \theta^{\alpha_1}} \cdots \frac{\partial}{\partial \theta^{\alpha_k}}$, with all different α_i (also if all or some of them are equal, since $(\frac{\partial}{\partial \theta^\alpha})^2 = 0$), if applied on the vacuum $|1\rangle$, is equal to zero. Correspondingly the second equation and the last equation of Eq. (9.48) are fulfilled.

i.b. In any d space the product of different θ^α s — $\theta^{\alpha_1} \theta^{\alpha_2} \cdots \theta^{\alpha_k}$ with all different θ^α 's ($\alpha_i \neq \alpha_j$) for all α_i and α_j — applied on the vacuum $|1\rangle$ is different from zero. Since all the θ 's, appearing in Eqs. (9.45, 9.46, 9.47) are different, forming normalized states, the fourth equation of Eq. (9.48) is fulfilled.

i.c. The third equation of Eq. (9.48) is fulfilled provided that there is an odd number of θ^s in the expression for a creation operator. Then, when in the anticommutation relation different θ^α 's appear (like in the case of $d = 6$ $\{\theta^0 \theta^3 \theta^5, \theta^1 \theta^2 \theta^6\}_+$), such a contribution gives zero. When two or several equal θ 's appear in the anticommutation relation, the contribution is zero (since $(\theta^\alpha)^2 = 0$).

i.d. Also for the first equation in Eq. (9.48) it is not difficult to show that it is fulfilled only for a particular creation operator and its Hermitian conjugate: Let us show this for $d = 1+3$ and the creation operator $\frac{1}{\sqrt{2}}(\theta^0 - \theta^3) \theta^1 \theta^2$ and its Hermitian conjugate (annihilation) operator: $\frac{1}{\sqrt{2}}\{\frac{\partial}{\partial \theta^2} \frac{\partial}{\partial \theta^1} (\frac{\partial}{\partial \theta^0} - \frac{\partial}{\partial \theta^3}), \frac{1}{\sqrt{2}}(\theta^0 - \theta^3) \theta^1 \theta^2\}_+$. Applying $(\frac{\partial}{\partial \theta^0} - \frac{\partial}{\partial \theta^3})$ on $(\theta^0 - \theta^3)$ gives two, while $\frac{\partial}{\partial \theta^2} \frac{\partial}{\partial \theta^1}$ applied on $\theta^1 \theta^2$ gives one.

ii. There is additional group of creation and annihilation operators which follows from the starting state

$$\begin{aligned}
 |\phi_1^{\theta 2}\rangle &> |_{2(2n+1)} = \\
 &(\frac{1}{\sqrt{2}})^{\frac{1}{2}} (\theta^0 + \theta^3)(\theta^1 + i\theta^2)(\theta^5 + i\theta^6) \cdots (\theta^{d-3} + i\theta^{d-2})(\theta^{d-1} + i\theta^d), \\
 &\text{for } d = 2(2n + 1), \\
 |\phi_1^{\theta 2}\rangle &> |_{4n} = \\
 &(\frac{1}{\sqrt{2}})^{\frac{d}{2}-1} (\theta^0 + \theta^3)(\theta^1 + i\theta^2)(\theta^5 + i\theta^6) \cdots (\theta^{d-3} + i\theta^{d-2}) \theta^{d-1} \theta^d, \\
 &\text{for } d = 4n.
 \end{aligned} \tag{9.49}$$

These two states can not be obtained from the previous group of states, presented in Eqs. (9.43, 9.44) by the application of S^{ef} , since each S^{ef} changes an even number

of factors, never an odd one. Correspondingly both starting states form a new group of states, the first in $d = 2(2n + 1)$, the second in $d = 4n$. All the rest states of this new group of states in either $d = 2(2n + 1)$ or in $d = 4n$ follow from the starting one by the application of S^{ef} . The corresponding creation and annihilation operators are

$$\begin{aligned}
 \hat{b}_{01}^{\theta 2\dagger} &= \left(\frac{1}{\sqrt{2}}\right)^{\frac{d}{2}} (\theta^0 + \theta^3)(\theta^1 + i\theta^2)(\theta^5 + i\theta^6) \dots (\theta^{d-1} + i\theta^d), \\
 \hat{b}_{01}^{\theta 2} &= \left(\frac{1}{\sqrt{2}}\right)^{\frac{d}{2}} \left(\frac{\partial}{\partial \theta^{d-1}} - i\frac{\partial}{\partial \theta^d}\right) \dots \left(\frac{\partial}{\partial \theta^0} + \frac{\partial}{\partial \theta^3}\right), \\
 &\text{for } d = 2(2n + 1), \\
 \hat{b}_{01}^{\theta 2\dagger} &= \left(\frac{1}{\sqrt{2}}\right)^{\frac{d}{2}-1} (\theta^0 + \theta^3)(\theta^1 + i\theta^2)(\theta^5 + i\theta^6) \dots (\theta^{d-3} + i\theta^{d-2})\theta^{d-1}\theta^d, \\
 \hat{b}_{01}^{\theta 2} &= \left(\frac{1}{\sqrt{2}}\right)^{\frac{d}{2}-1} \frac{\partial}{\partial \theta^d} \frac{\partial}{\partial \theta^{d-1}} \left(\frac{\partial}{\partial \theta^{d-3}} - i\frac{\partial}{\partial \theta^{d-2}}\right) \dots \left(\frac{\partial}{\partial \theta^0} + \frac{\partial}{\partial \theta^3}\right), \\
 &\text{for } d = 4n.
 \end{aligned} \tag{9.50}$$

As in the first case all the rest of creation operators can be obtained from the starting one, in each of the two kinds of spaces, by the application of S^{ac} , and the annihilation operators by the Hermitian conjugation of the creation operators. Also all these creation and annihilation operators fulfill the requirements for the creation and annihilation operators, presented in Eq. (9.48).

One can choose as the starting creation operator of the second group of operators by changing sign instead of in the factor $(\theta^0 - \theta^3)$ in the starting creation operator of the first group in any of the rest of factors in the product. In each case the same group will follow.

Let us count the number of states with the odd Grassmann character in $d = 2(2n + 1)$.

There are in $(d = 2)$ two creation $((\theta^0 \mp \theta^1, \text{ for } \eta^{ab} = \text{diag}(1, -1))$ and correspondingly two annihilation operators $(\frac{\partial}{\partial \theta^0} \mp \frac{\partial}{\partial \theta^1})$, each belonging to its own group with respect to the Lorentz transformation operators, both fulfill Eq. (9.48).

It is not difficult to see that the number of all creation operators of an odd Grassmann character in $d = 2(2n + 1)$ -dimensional space is equal to $\frac{d!}{\frac{d}{2}!\frac{d}{2}!}$.

We namely ask: In how many ways can one put on $\frac{d}{2}$ places d different θ^a 's. And the answer is — the central binomial coefficient for $x^{\frac{d}{2}} 1^{\frac{d}{2}}$ — with all x different. This is just $\frac{d!}{\frac{d}{2}!\frac{d}{2}!}$. But we have counted all the states with an odd Grassmann character, while we know that these states belong to two different groups of representations with respect to the Lorentz group.

Correspondingly one concludes: *There are two groups of states in $d = 2(2n + 1)$ with an odd Grassmann character, each of these two groups has*

$$\frac{1}{2} \frac{d!}{\frac{d}{2}!\frac{d}{2}!} \tag{9.51}$$

members.

In $d = 2$ we have two groups with one state, which have an odd Grassmann character, in $d = 6$ we have two groups of 10 states, in $d = 10$ we have two groups of 126 states with an odd Grassmann characters. And so on.

Correspondingly we have in $d = 2(2n + 1)$ -dimensional spaces two groups of creation operators with $\frac{1}{2} \frac{d!}{\frac{d}{2}! \frac{d}{2}!}$ members each, creating states with an odd Grassmann character and the same number of annihilation operators. Creation and annihilation operators fulfill anticommutation relations presented in Eq. (9.48).

The rest of creation operators [and the corresponding annihilation operators] have rather opposite Grassmann character than the ones studied so far — like $\theta^0 \theta^1 [\frac{\partial}{\partial \theta^1} \frac{\partial}{\partial \theta^0}]$ in $d = (1 + 1) (\theta^0 \mp \theta^3)(\theta^1 \pm i\theta^2) [(\frac{\partial}{\partial \theta^1} \mp i \frac{\partial}{\partial \theta^2})(\frac{\partial}{\partial \theta^0} \mp \frac{\partial}{\partial \theta^3})]$, $\theta^0 \theta^3 \theta^1 \theta^2 [\frac{\partial}{\partial \theta^2} \frac{\partial}{\partial \theta^1} \frac{\partial}{\partial \theta^3} \frac{\partial}{\partial \theta^0}]$ in $d = (3 + 1)$.

All the states $|\phi_i^\theta\rangle$, generated by the creation operators, Eq. (9.48), on the vacuum state $|\phi_{og}\rangle (= |1\rangle)$ are the eigenstates of the Cartan subalgebra operators and are orthogonal and normalized with respect to the norm of Eq. (9.27)

$$\langle \phi_i^\theta | \phi_j^\theta \rangle = \delta_{ij}. \quad (9.52)$$

If we now extend the creation and annihilation operators to the ordinary coordinate space, the relations among creation and annihilation operators at one time read

$$\begin{aligned} \{\hat{b}_i^\theta(\vec{x}), \hat{b}_j^{\theta\dagger}(\vec{x}')\}_+ |\phi_{og}\rangle &= \delta_j^i \delta(\vec{x} - \vec{x}') |\phi_{og}\rangle, \\ \{\hat{b}_i^\theta(\vec{x}), \hat{b}_j^\theta(\vec{x}')\}_+ |\phi_{og}\rangle &= 0 |\phi_{og}\rangle, \\ \{\hat{b}_i^{\theta\dagger}(\vec{x}), \hat{b}_j^{\theta\dagger}(\vec{x}')\}_+ |\phi_{og}\rangle &= 0 |\phi_{og}\rangle, \\ \hat{b}_j^\theta(\vec{x}) |\phi_{og}\rangle &= 0 |\phi_{og}\rangle \\ |\phi_{og}\rangle &= |1\rangle. \end{aligned} \quad (9.53)$$

Again the index 1 or 2 in $(\hat{b}_i^{\theta 1}, \hat{b}_i^{\theta 1\dagger})$ or in $(\hat{b}_i^{\theta 2}, \hat{b}_i^{\theta 2\dagger})$ is kept.

b. Quantization in Clifford space

In Grassmann space the requirement that products of eigenstates of the Cartan subalgebra operators represent the creation and annihilation operators, obeying the relations of Eq. (9.48), reduces the number of states from 2^d (allowed in the first quantization procedure) to two isolated groups of $\frac{1}{2} \frac{d!}{\frac{d}{2}! \frac{d}{2}!}$ (There is no operator that determines the family quantum number and would connect both isolated groups of states.)

Let us study what happens, when, let say, γ^a 's are used to create the basis and correspondingly also to create the creation and annihilation operators.

Let us point out that γ^a is expressible with θ^a and its derivative ($\gamma^a = (\theta^a + \frac{\partial}{\partial \theta_a})$), Eq. (9.17), and that we again require that creation (annihilation) operators create (annihilate) states, which are eigenstates of the Cartan subalgebra, Eq. (9.84). We could as well make a choice of $\tilde{\gamma}^a = i(\theta^a - \frac{\partial}{\partial \theta_a})$ instead of γ^a 's to create the basic states⁷. We shall follow here to some extent Ref. [19].

⁷ In the case that we would choose $\tilde{\gamma}^a$'s instead of γ^a 's, Eq.(9.17), the role of $\tilde{\gamma}^a$ and γ^a should be then correspondingly exchanged in Eq. (9.92).

Making a choice of the Cartan subalgebra eigenstates of S^{ab} , Eq. (9.84),

$$({}^{ab}k) := \frac{1}{2}(\gamma^a + \frac{\eta^{aa}}{ik}\gamma^b), \quad {}^{ab}[k] := \frac{1}{2}(1 + \frac{i}{k}\gamma^a\gamma^b), \quad (9.54)$$

where $k^2 = \eta^{aa}\eta^{bb}$, recognizing that the Hermitian conjugate values of $({}^{ab}k)$ and ${}^{ab}[k]$ are

$$({}^{ab}k)^\dagger = \eta^{aa}({}^{ab}(-k)), \quad {}^{ab}[k]^\dagger = {}^{ab}[k], \quad (9.55)$$

while the corresponding eigenvalues of S^{ab} , Eq. (9.56), and \tilde{S}^{ab} , Eq. (9.101), are

$$\begin{aligned} S^{ab}({}^{ab}k) &= \frac{1}{2}k({}^{ab}k), & S^{ab}({}^{ab}[k]) &= \frac{1}{2}k({}^{ab}[k]) \\ \tilde{S}^{ab}({}^{ab}k) &= \frac{k}{2}({}^{ab}k), & \tilde{S}^{ab}({}^{ab}[k]) &= -\frac{k}{2}({}^{ab}[k]), \end{aligned} \quad (9.56)$$

we find in $d = 2(2n + 1)$ that from the starting state with products of odd number of only nilpotents

$$|\psi_1^1\rangle > |_{2(2n+1)} = (+i)(+)(+) \cdots (+)^{d-3} (+)^{d-2} (+)^{d-1} |_{\psi_{oc}}\rangle, \quad (9.57)$$

having correspondingly an odd Clifford character⁸, all the other states of the same Lorentz representation, there are $2^{\frac{d}{2}-1}$ members, follow by the application of S^{cd} (which do not belong to the Cartan subalgebra) on the starting state⁹, Eq. (9.84): $S^{cd}|\psi_1^1\rangle > |_{2(2n+1)} = |\psi_1^1\rangle > |_{2(2n+1)}$.

The operators \tilde{S}^{cd} , which do not belong to the Cartan subalgebra of Eq. (9.84), generate states with different eigenstates of the Cartan subalgebra ($\tilde{S}^{03}, \tilde{S}^{12}, \tilde{S}^{56}, \dots, \tilde{S}^{d-1 d}$), we call the eigenvalues of their eigenstates the "family" quantum numbers. There are $2^{\frac{d}{2}-1}$ families. From the starting new member with a different "family" quantum number the whole Lorentz representation with this "family" quantum number follows by the application of S^{ef} : $S^{ef}\tilde{S}^{cd}|\psi_1^1\rangle > |_{2(2n+1)} = |\psi_i^j\rangle > |_{2(2n+1)}$. All the states of one Lorentz representation of any particular "family" quantum number have an odd Clifford character, since neither S^{cd} nor \tilde{S}^{cd} , both with an even Clifford character, can change this character.

We are interested only in states with an odd Clifford character, in order that the corresponding creation operators defining these states when being applied on an appropriate vacuum state, and their annihilation operators, will fulfill anticommutation relations required for spinors with half integer spin. We shall discuss the number of states with an odd Clifford character after defining the creation and annihilation operators.

⁸ We call the starting state in $d = 2(2n + 1)$ $|\psi_1^1\rangle > |_{2(2n+1)}$, and the starting state in $d = 4n$ $|\psi_1^1\rangle > |_{4n}$.

⁹ The smallest number of all the generators S^{ac} , which do not belong to the Cartan subalgebra, needed to create from the starting state all the other members, is $2^{\frac{d}{2}-1} - 1$. This is true for both even dimensional spaces $-2(2n + 1)$ and $4n$.

For $d = 4n$ the starting state must be the product of one projector and $4n - 1$ nilpotents applied on an appropriate vacuum state, since we again require that the corresponding creation and annihilation operators fulfill the anticommutation relations.

Let us start with the state

$$|\psi_1^1\rangle > |_{4n} = \begin{smallmatrix} 03 & 12 & 35 \\ (+) & (+) & (+) \end{smallmatrix} \cdots \begin{smallmatrix} d-3 & d-2 & d-1 & d \\ (+) & & & \end{smallmatrix} |\psi_{oc}\rangle, \quad (9.58)$$

All the other states belonging to the same Lorentz representation follow again by the application of S^{cd} on this state $|\psi_1^1\rangle > |_{4n}$, while a new family starts by the application of $\tilde{S}^{cd}|\psi_1^1\rangle > |_{4n}$ and from this state all the other members with the same "family" quantum number can be generated by $S^{ef}\tilde{S}^{cd}$ on $|\psi_1^1\rangle > |_{4n}$: $S^{ef}\tilde{S}^{cd}|\psi_1^1\rangle > |_{4n} = |\psi_i^j\rangle > |_{4n}$.

All these states in either $d = 2(2n + 1)$ space or $d = 4n$ space are orthogonal with respect to Eq. (9.27).

However, let us point out that $(\gamma^a)^\dagger = \gamma^a \eta^{aa}$. Correspondingly it follows, Eq. (9.55), that $\begin{smallmatrix} ab \\ (k) \end{smallmatrix}^\dagger = \eta^{aa} \begin{smallmatrix} ab \\ (-k) \end{smallmatrix}$, and $\begin{smallmatrix} ab \\ [k] \end{smallmatrix}^\dagger = \begin{smallmatrix} ab \\ [k] \end{smallmatrix}$.

Since any projector is Hermitian conjugate to itself, while to any nilpotent $\begin{smallmatrix} ab \\ (k) \end{smallmatrix}$ the Hermitian conjugated one has an opposite k , it is obvious that Hermitian conjugated product to a product of nilpotents and projectors can not be accepted as a new state¹⁰.

The vacuum state $|\psi_{oc}\rangle$ ought to be chosen so that $\langle \psi_{oc} | \psi_{oc} \rangle = 1$, while all the states belonging to the physically acceptable states, like $\begin{smallmatrix} 03 & 12 & 56 & 78 \\ (+) & (+) & (-) & (-) \end{smallmatrix} \cdots \begin{smallmatrix} d-3 & d-2 & d-1 & d \\ (+) & & & \end{smallmatrix} |\psi_{oc}\rangle$ in $d = 2(2n + 1)$, must not give zero for either $d = 2(2n + 1)$ or for $d = 4n$. We also want that the states, obtained by the application of either S^{cd} or \tilde{S}^{cd} or both, are orthogonal. To make a choice of the vacuum it is needed to know the relations of Eq. (9.88). It must be

$$\begin{aligned} \langle \psi_{oc} | \cdots \begin{smallmatrix} ab \\ (k) \end{smallmatrix}^\dagger \cdots | \cdots \begin{smallmatrix} ab \\ (k') \end{smallmatrix} \cdots | \psi_{oc} \rangle &= \delta_{kk'}, \\ \langle \psi_{oc} | \cdots \begin{smallmatrix} ab \\ [k] \end{smallmatrix}^\dagger \cdots | \cdots \begin{smallmatrix} ab \\ [k'] \end{smallmatrix} \cdots | \psi_{oc} \rangle &= \delta_{kk'}, \\ \langle \psi_{oc} | \cdots \begin{smallmatrix} ab \\ [k] \end{smallmatrix}^\dagger \cdots | \cdots \begin{smallmatrix} ab \\ (k') \end{smallmatrix} \cdots | \psi_{oc} \rangle &= 0. \end{aligned} \quad (9.59)$$

Our experiences in the case, when states with the integer values of the Cartan subalgebra operators were expressed by Grassmann coordinates, teach us that the requirements, that creation and annihilation operators must fulfill, influence the choice of the number of states, as well as of the vacuum state.

¹⁰ We could as well start with the state $|\psi_1^1\rangle > |_{2(2n+1)} = \begin{smallmatrix} 03 & 12 & 35 \\ (-) & (-) & (-) \end{smallmatrix} \cdots \begin{smallmatrix} d-3 & d-2 & d-1 & d \\ (-) & & & \end{smallmatrix} |\psi_{oc}\rangle$ for $d = 2(2n + 1)$ and with $|\psi_1^1\rangle > |_{4n} = \begin{smallmatrix} 03 & 12 & 35 \\ (-) & (-) & (-) \end{smallmatrix} \cdots \begin{smallmatrix} d-3 & d-2 & d-1 & d \\ (-) & & & \end{smallmatrix} |\psi_{oc}\rangle$ in the case of $d = 4n$. Then creation and annihilation operators will exchange their roles and also the vacuum state will be correspondingly changed.

Let us first repeat therefore the requirements which the creation and annihilation operators must fulfill

$$\begin{aligned}
 \{\hat{b}_i^{\alpha\gamma}, \hat{b}_k^{\beta\gamma\dagger}\}_+ |\psi_{oc} \rangle &= \delta_\beta^\alpha \delta_k^i |\psi_{oc} \rangle, \\
 \{\hat{b}_i^{\alpha\gamma}, \hat{b}_k^{\beta\gamma}\}_+ |\psi_{oc} \rangle &= 0 |\psi_{oc} \rangle, \\
 \{\hat{b}_i^{\alpha\gamma\dagger}, \hat{b}_k^{\beta\gamma\dagger}\}_+ |\psi_{oc} \rangle &= 0 |\psi_{oc} \rangle, \\
 \hat{b}_i^{\alpha\gamma} |\psi_{oc} \rangle &= 0 |\psi_{oc} \rangle, \\
 \hat{b}_i^{\alpha\gamma\dagger} |\psi_{oc} \rangle &= |\psi_i^{\alpha\gamma} \rangle,
 \end{aligned} \tag{9.60}$$

paying attention at this stage only at the internal degrees of freedom of the states, that is on their spins. Here (α, β, \dots) represent the family quantum number determined by \tilde{S}^{ac} and (i, j, \dots) the quantum number of one representation, determined by S^{ac} and index γ is to point out that these creation operators represent Clifford rather than Grassmann objects. In what follows we shall skip the index γ , since either states or creation and annihilation operators carry two indexes, while in Grassmann case there is no family quantum number.

From Eqs. (9.57, 9.58) is not difficult to extract the creation operator which, when applied on the vacuum state for either $d = 2(2n + 1)$ or $d = 4n$, generates the starting state .

i. One Weyl representation

We define the creation $\hat{b}_1^{1\dagger}$ — and the corresponding annihilation operator $\hat{b}_1^1 = (\hat{b}_1^{1\dagger})^\dagger$ — which when applied on the vacuum state $|\psi_{oc} \rangle$ create a vector of one of the two equations (9.57, 9.58), as follows

$$\begin{aligned}
 \hat{b}_1^{1\dagger} &: = \begin{matrix} 03 & 12 & 56 & \dots & d-1 & d \\ (+i) & (+) & (+) & \dots & (+) & \end{matrix}, \\
 \hat{b}_1^1 &: = \begin{matrix} d-1 & d & 56 & 12 & 03 \\ (-) & \dots & (-) & (-) & (-i) \end{matrix}, \\
 &\text{for } d = 2(2n + 1), \\
 \\
 \hat{b}_1^{1\dagger} &: = \begin{matrix} 03 & 12 & 56 & \dots & d-3 & d-2 & d-1 & d \\ (+i) & (+) & (+) & \dots & (+) & & [+] & \end{matrix}, \\
 \hat{b}_1^1 &: = \begin{matrix} d-1, d-2 & d-3 & 56 & 12 & 03 \\ [+] & (-) & \dots & (-) & (-) & (-i) \end{matrix}, \\
 &\text{for } d = 4n.
 \end{aligned} \tag{9.61}$$

We shall call the $\hat{b}_1^{1\dagger} |\psi_{oc} \rangle$, when operating on the vacuum state, the starting vector of the starting "family".

Now we can make a choice of the vacuum state for this particular "family" taking into account Eq. (9.88)

$$\begin{aligned}
 |\psi_{oc} \rangle &= \begin{matrix} 03 & 12 & 56 & \dots & d-1 & d \\ [-i] & [-] & [-] & \dots & [-] & \end{matrix} |0 \rangle, \\
 &\text{for } d = 2(2n + 1), \\
 |\psi_{oc} \rangle &= \begin{matrix} 03 & 12 & 56 & \dots & d-3 & d-2 & d-1 & d \\ [-i] & [-] & [-] & \dots & [-] & & [+] & \end{matrix} |0 \rangle, \\
 &\text{for } d = 4n,
 \end{aligned} \tag{9.62}$$

n is a positive integer, so that the requirements of Eq. (9.60) are fulfilled. We see: The creation and annihilation operators of Eq. (9.61) (both are nilpotents, $(\hat{b}_1^{1\dagger})^2 = 0$ and $(\hat{b}_1^1)^2 = 0$), $\hat{b}_1^{1\dagger}$ (generating the vector $|\psi_1^1\rangle$ when operating on the vacuum state) gives $\hat{b}_1^{1\dagger}|\psi_{oc}\rangle \neq 0$, while the annihilation operator annihilates the vacuum state $\hat{b}_1^1|\psi_0\rangle = 0$, giving $\{\hat{b}_1^1, \hat{b}_1^{1\dagger}\}|\psi_{oc}\rangle = |\psi_{oc}\rangle$, since we choose the appropriate normalization, Eq. (9.54).

All the other creation and annihilation operators, belonging to the same Lorentz representation with the same family quantum number, follow from the starting ones by the application of particular S^{ac} , which do not belong to the Cartan subalgebra (9.82).

We call $\hat{b}_2^{1\dagger}$ the one obtained from $\hat{b}_1^{1\dagger}$ by the application of one of the four generators ($S^{01}, S^{02}, S^{31}, S^{32}$). This creation operator is for $d = 2(2n + 1)$ equal to $\hat{b}_2^{1\dagger} = [-i]^{03} [-]^{12} (+)^{35} \cdots (+)^{d-1 d}$, while it is for $d = 4n$ equal to $\hat{b}_2^{1\dagger} = [-i]^{03} [-]^{12} (+)^{56} \cdots [+]$. All the other family members follow from the starting one by the application of different S^{ef} , or by the product of several S^{gh} .

We accordingly have

$$\begin{aligned}\hat{b}_i^{1\dagger} &\propto S^{ab} \dots S^{ef} \hat{b}_1^{1\dagger}, \\ \hat{b}_i^1 &\propto \hat{b}_1^1 S^{ef} \dots S^{ab},\end{aligned}\tag{9.63}$$

with $S^{ab\dagger} = \eta^{aa}\eta^{bb}S^{ab}$. We shall make a choice of the proportionality factors so that the corresponding states $|\psi_1^1\rangle = \hat{b}_1^{1\dagger}|\psi_{oc}\rangle$ will be normalized.

We recognize that [19]:

i.a. $(\hat{b}_i^{1\dagger})^2 = 0$ and $(\hat{b}_i^1)^2 = 0$, for all i .

To see this one must recognize that S^{ac} (or S^{bc}, S^{ad}, S^{bd}) transforms $(+)^{ab} (+)^{cd}$ to $[-]^{ab} [-]^{cd}$, that is an even number of nilpotents $(+)$ in the starting state is transformed into projectors $[-]$ in the case of $d = 2(2n + 1)$. For $d = 4n$, S^{ac} (or S^{bc}, S^{ad}, S^{bd}) transforms $(+)^{ab} (+)^{cd}$ into $[-]^{ab} (-)^{cd}$. Therefore for either $d = 2(2n + 1)$ or $d = 4n$ at least one of factors, defining a particular creation operator, will be a nilpotent. For $d = 2(2n + 1)$ there is an odd number of nilpotents, at least one, leading from the starting factor $(+)^{dg}$ in the creator. For $d = 4n$ a nilpotent factor can also be $(-)^{d-1 d}$ (since $(+)^{d-1 d}$ can be transformed by $S^{e d-1}$, for example into $(-)^{d-1 d}$). A square of at least one nilpotent factor (we started with an odd number of nilpotents, and oddness can not be changed by S^{ab}), is enough to guarantee that the square of the corresponding $(\hat{b}_i^{1\dagger})^2$ is zero. Since $\hat{b}_i^1 = (\hat{b}_i^{1\dagger})^\dagger$, the proof is valid also for annihilation operators.

i.b. $\hat{b}_i^{1\dagger}|\psi_{oc}\rangle \neq 0$ and $\hat{b}_i^1|\psi_{oc}\rangle = 0$, for all i .

To see this in the case $d = 2(2n + 1)$ one must recognize that $\hat{b}_i^{1\dagger}$ distinguishes from $\hat{b}_1^{1\dagger}$ in (an even number of) those nilpotents $(+)$, which have been transformed into $[-]$. When $[-]^{ab}$ from $\hat{b}_i^{1\dagger}$ meets $[-]^{ab}$ from $|\psi_{oc}\rangle$, the product gives $[-]^{ab}$ back, and correspondingly a nonzero contribution. For $d = 4n$ also the factor $(+)^{d-1 d}$ can

be transformed. It is transformed into $\begin{smallmatrix} d-1 & d \\ (-) & \end{smallmatrix}$ which, when applied to a vacuum state, gives again a nonzero contribution ($\begin{smallmatrix} d-1 & d & d-1 & d & d-1 & d \\ (-) & [+]=(-) \end{smallmatrix}$, Eq. (9.88)).

In the case of \hat{b}_i^1 we recognize that in $\hat{b}_i^{1\dagger}$ at least one factor is nilpotent; that of the same type as in the starting \hat{b}_i^1 — (+) — or in the case of $d = 4n$ it can be also $\begin{smallmatrix} d-1 & d \\ (-) & \end{smallmatrix}$. Performing the Hermitian conjugation $(\hat{b}_i^{1\dagger})^\dagger$, (+) transforms into (−), while $\begin{smallmatrix} d-1 & d \\ (-) & \end{smallmatrix}$ transforms into $\begin{smallmatrix} d-1 & d \\ (+) & \end{smallmatrix}$ in \hat{b}_i^1 . Since (−)[−] gives zero and $\begin{smallmatrix} d-1 & dd-1 & d \\ (+) & [+]= \end{smallmatrix}$ also gives zero, $\hat{b}_i^{1\dagger}|\psi_{oc} \rangle = 0$.

i.c. $\{\hat{b}_i^{1\dagger}, \hat{b}_j^{1\dagger}\}_+ = 0$, for each pair (i, j).

There are several possibilities to be discussed. A trivial one is, if both $\hat{b}_i^{1\dagger}$ and $\hat{b}_j^{1\dagger}$ have a nilpotent factor (or more than one) for the same pair of indexes, say $\begin{smallmatrix} kl \\ (+) \end{smallmatrix}$. Then the product of such two $\begin{smallmatrix} kl \\ (+) \end{smallmatrix}$ gives zero. It also happens, that $\hat{b}_i^{1\dagger}$ has a nilpotent at the place (kl) ($\begin{smallmatrix} 03 & kl & mn \\ (-) \cdots (+) \cdots (-) \cdots \end{smallmatrix}$) while $\hat{b}_j^{1\dagger}$ has a nilpotent at the place (mn) ($\begin{smallmatrix} 03 & kl & mn \\ (-) \cdots (-) \cdots (+) \cdots \end{smallmatrix}$). Then in the term $\hat{b}_i^{1\dagger}\hat{b}_j^{1\dagger}$ the product $\begin{smallmatrix} mn & mn \\ (-)(+) \end{smallmatrix}$ makes the term equal to zero, while in the term $\hat{b}_j^{1\dagger}\hat{b}_i^{1\dagger}$ the product $\begin{smallmatrix} kl & kl \\ (-)(+) \end{smallmatrix}$ makes the term equal to zero. There is no other possibility in $d = 2(2n + 1)$. In the case that $d = 4n$, it might appear also that $\hat{b}_i^{1\dagger} = \begin{smallmatrix} 03 & ij & d-1 & d \\ (-) \cdots (+) \cdots (+) \end{smallmatrix}$ and $\hat{b}_j^{1\dagger} = \begin{smallmatrix} 03 & ij & d-1 & d \\ (-) \cdots (-) \cdots (-) \end{smallmatrix}$. Then in the term $\hat{b}_i^{1\dagger}\hat{b}_j^{1\dagger}$ the factor $\begin{smallmatrix} d-1 & dd-1 & d \\ (+) & (-) \end{smallmatrix}$ makes it zero, while in $\hat{b}_j^{1\dagger}\hat{b}_i^{1\dagger}$ the factor $\begin{smallmatrix} ij & ij \\ (-)(+) \end{smallmatrix}$ makes it zero. Since there are no further possibilities, the proof is complete.

i.d. $\{\hat{b}_i^1, \hat{b}_j^1\}_+ = 0$, for each pair (i, j).

The proof goes similarly as in the case with creation operators. Again we treat several possibilities. \hat{b}_i^1 and \hat{b}_j^1 have a nilpotent factor (or more than one) with the same indexes, say $\begin{smallmatrix} kl \\ (-) \end{smallmatrix}$. Then the product of such two $\begin{smallmatrix} kl & kl \\ (-)(-) \end{smallmatrix}$ gives zero. It also happens, that \hat{b}_i^1 has a nilpotent at the place (kl) ($\begin{smallmatrix} mn & kl & 03 \\ \cdots (-) \cdots (-) \cdots (-) \end{smallmatrix}$) while \hat{b}_j^1 has a nilpotent at the place (mn) ($\begin{smallmatrix} mn & kl & 03 \\ \cdots (-) \cdots (-) \cdots (-) \end{smallmatrix}$). Then in the term $\hat{b}_i^1\hat{b}_j^1$ the product $\begin{smallmatrix} kl & kl \\ (-)(-) \end{smallmatrix}$ makes the term equal to zero, while in the term $\hat{b}_j^1\hat{b}_i^1$ the product $\begin{smallmatrix} mn & mn \\ (-)(-) \end{smallmatrix}$ makes the term equal to zero. In the case that $d = 4n$, it appears also that $\hat{b}_i^1 = \begin{smallmatrix} d-1 & d & ij & 03 \\ (+) \cdots (-) \cdots (-) \end{smallmatrix}$ and $\hat{b}_j^1 = \begin{smallmatrix} d-1 & d & ij & 03 \\ (+) \cdots (-) \cdots (-) \end{smallmatrix}$. Then in the term $\hat{b}_i^1\hat{b}_j^1$ the factor $\begin{smallmatrix} ij & ij \\ (-)(-) \end{smallmatrix}$ makes it zero, while in $\hat{b}_j^1\hat{b}_i^1$ the factor $\begin{smallmatrix} d-1 & d & d-1 & d \\ (+) & (+) \end{smallmatrix}$ makes it zero.

i.e. $\{\hat{b}_i^1, \hat{b}_j^{1\dagger}\}_+|\psi_{oc} \rangle = \delta_{ij}|\psi_{oc} \rangle$.

To prove this we must recognize that $\hat{b}_i^1 = \hat{b}_1 S^{ef} \dots S^{ab}$ and $\hat{b}_i^{1\dagger} = S^{ab} \dots S^{ef} \hat{b}_1$. Since any $\hat{b}_i^1|\psi_{oc} \rangle = 0$, we only have to treat the term $\hat{b}_i^1\hat{b}_j^{1\dagger}$. We find $\hat{b}_i^1\hat{b}_j^{1\dagger} \propto \dots \begin{smallmatrix} lm \\ (-) \end{smallmatrix} \dots \begin{smallmatrix} 03 \\ (-) \end{smallmatrix} S^{ef} \dots S^{ab} S^{lm} \dots S^{pr} \begin{smallmatrix} 03 \\ (+) \end{smallmatrix} \dots \begin{smallmatrix} lm \\ (+) \end{smallmatrix} \dots$. If we treat the term $\hat{b}_i^1\hat{b}_i^{1\dagger}$, generators $S^{ef} \dots S^{ab} S^{lm} \dots S^{pr}$ are proportional to a number and we normalize

$\langle \psi_{oc} | \hat{b}_i^1 \hat{b}_i^{1\dagger} | \psi_{oc} \rangle$ to one. When $S^{ef} \dots S^{ab} S^{lm} \dots S^{pr}$ are proportional to several products of S^{cd} , these generators change $\hat{b}_1^{1\dagger}$ into $(+)^{03} \dots [-]^{kl} \dots [-]^{np} \dots$, making the product $\hat{b}_i^1 \hat{b}_j^{1\dagger}$ equal to zero, due to factors of the type $(-)^{kl} [-]$. In the case of $d = 4n$ also a factor $(+)^{d-1} (-)^{d-1}$ might occur, which also gives zero.

We saw and proved that for the definition of the creation and annihilation operators, Eq. (9.61), for states in Eqs. (9.57, 9.58) and further for all the rest of creation and annihilation operators, Eq. (9.63), and for the choice of the vacuum states, Eq. (9.62), all the requirements of Eq. (9.60) are fulfilled, provided that creation and correspondingly also the annihilation operators have an odd Clifford character, that is that the number of nilpotents in the product is odd.

For an even number of factors of the nilpotent type in the starting state and accordingly in the starting $\hat{b}_1^{1\dagger}$, an annihilation operator \hat{b}_i^1 would appear with all factors of the type $[-]$, which on the vacuum state (Eq.(9.62)) would not give zero.

ii. Families of Weyl representations

Let $\hat{b}_i^{\alpha\dagger}$ be a creation operator, fulfilling Eq. (9.60), which creates one of the $(2^{d/2-1})$ Weyl basic states of an α -th "family", when operating on a vacuum state $|\psi_{oc} \rangle$ and let $\hat{b}_i^\alpha = (\hat{b}_i^{\alpha\dagger})^\dagger$ be the corresponding annihilation operator. We shall now proceed to define $\hat{b}_i^{\alpha\dagger}$ and \hat{b}_i^α from a chosen starting state (9.57, 9.58), which $\hat{b}_1^{1\dagger}$ creates on the vacuum state $|\psi_{oc} \rangle$.

When treating more than one Weyl representation, that is, more than one "family", we must take into account that: i. The vacuum state chosen to fulfill requirements for second quantization of the starting family might not and it will not be the correct one when all the families are taken into account. ii. The products of \tilde{S}^{ab} , which do not belong to the Cartan subalgebra set of the generators \tilde{S}^{ab} , when being applied on the starting family ψ_1^1 , generate the starting member ψ_1^α of each of the remaining families. There is correspondingly the same number of "families" as the number of vectors of one Weyl representation, namely $2^{d/2-1}$. Then the whole Weyl representation of a particular family ψ_1^α follows again with the application of S^{ef} , which do not belong to the Cartan subalgebra of S^{ab} on this starting α family state.

Any vector $|\psi_1^\alpha \rangle$ follows from the starting vector, Eqs. (9.57, 9.58), by the application of either \tilde{S}^{ef} , which change the family quantum number, or S^{gh} , which change the member of a particular family (as it can be seen from Eqs. (9.90, 9.102)) or with the corresponding product of S^{ef} and \tilde{S}^{ef}

$$|\psi_1^\alpha \rangle \propto \tilde{S}^{ab} \dots \tilde{S}^{ef} |\psi_1^1 \rangle \propto \tilde{S}^{ab} \dots \tilde{S}^{ef} S^{mn} \dots S^{pr} |\psi_1^1 \rangle . \quad (9.64)$$

Correspondingly we define $\hat{b}_i^{\alpha\dagger}$ (up to a constant) to be

$$\begin{aligned} \hat{b}_i^{\alpha\dagger} &\propto \tilde{S}^{ab} \dots \tilde{S}^{ef} S^{mn} \dots S^{pr} \hat{b}_1^{1\dagger} \\ &\propto S^{mn} \dots S^{pr} \hat{b}_1^{1\dagger} S^{ab} \dots S^{ef} . \end{aligned} \quad (9.65)$$

This last expression follows due to the property of the Clifford object $\tilde{\gamma}^a$ and correspondingly of \tilde{S}^{ab} , presented in Eqs. (9.92, 9.93).

For $\hat{b}_i^\alpha = (\hat{b}_i^{\alpha\dagger})^\dagger$ we accordingly have

$$\hat{b}_i^\alpha = (\hat{b}_i^{\alpha\dagger})^\dagger \propto S^{ef} \dots S^{ab} \hat{b}_1^1 S^{pr} \dots S^{mn}. \quad (9.66)$$

The proportionality factor will be chosen so that the corresponding states $|\psi_i^\alpha\rangle = \hat{b}_i^{\alpha\dagger} |\psi_{oc}\rangle$ will be normalized.

We ought to generalize the vacuum state from Eq. (9.62) so that $\hat{b}_i^{\alpha\dagger} |\psi_{oc}\rangle \neq 0$ and $\hat{b}_i^\alpha |\psi_{oc}\rangle = 0$ for all the members i of any family α . Since any \tilde{S}^{eg} changes $(+)(+)$ into $[+][+]$ and $[+]\dagger = [+]$, while $(+)\dagger(+) = [-]$, the vacuum state $|\psi_{oc}\rangle$ from Eq. (9.62) must be replaced by

$$\begin{aligned} |\psi_{oc}\rangle &= \\ & \quad \overset{03}{[-i]} \overset{12}{[-]} \overset{56}{[-]} \dots \overset{d-1}{[-]} \overset{d}{[-]} + \overset{03}{[+i]} \overset{12}{[+]} \overset{56}{[-]} \dots \overset{d-1}{[-]} \overset{d}{[-]} + \overset{03}{[+i]} \overset{12}{[-]} \overset{56}{[+]} \dots \overset{d-1}{[-]} \overset{d}{[-]} + \dots |0\rangle, \\ & \text{for } d = 2(2n+1), \\ |\psi_{oc}\rangle &= \\ & \quad \overset{03}{[-i]} \overset{12}{[-]} \overset{35}{[-]} \dots \overset{d-3}{[-]} \overset{d-2d-1}{[-]} \overset{d}{[+]} + \overset{03}{[+i]} \overset{12}{[+]} \overset{56}{[-]} \dots \overset{d-3}{[-]} \overset{d-2}{[+]} \overset{d-1}{[+]} \overset{d}{[+]} + \dots |0\rangle, \\ & \text{for } d = 4n, \end{aligned} \quad (9.67)$$

n is a positive integer. There are $2^{\frac{d}{2}-1}$ summands, since we step by step replace all possible pairs of $\overset{ab}{[-]} \dots \overset{ef}{[-]}$ in the starting part $\overset{03}{[-i]} \overset{12}{[-]} \overset{35}{[-]} \dots \overset{d-1}{[-]} \overset{d}{[-]}$ (or $\overset{03}{[-i]} \overset{12}{[-]} \overset{35}{[-]} \dots \overset{d-3}{[-]} \overset{d-2d-1}{[-]} \overset{d}{[+]}$) into $\overset{ab}{[+]} \dots \overset{ef}{[+]}$ and include new terms into the vacuum state so that the last $2n+1$ summands have for $d = 2(2n+1)$ case, n is a positive integer, only one factor $[-]$ and all the rest $[+]$, each $[-]$ at different position. For $d = 4n$ also the factor $\overset{d-1}{[+]} \overset{d}{[+]}$ in the starting term $\overset{03}{[-i]} \overset{12}{[-]} \overset{35}{[-]} \dots \overset{d-3}{[-]} \overset{d-2d-1}{[+]} \overset{d}{[+]}$ changes to $\overset{d-1}{[-]} \overset{d}{[-]}$. The vacuum state has then the normalization factor $1/\sqrt{2^{d/2-1}}$.

There is therefore

$$2^{\frac{d}{2}-1} 2^{\frac{d}{2}-1} \quad (9.68)$$

number of creation operators, defining the orthonormalized states when applying on the vacuum state of Eqs. (9.67) and the same number of annihilation operators, which are defined by the creation operators on the vacuum state of Eqs. (9.67). \tilde{S}^{ab} connect members of different families, S^{ab} generates all the members of one family.

We recognize that:

ii.a. The above creation and annihilation operators are nilpotent — $(\hat{b}_i^{\alpha\dagger})^2 = 0 = (\hat{b}_i^\alpha)^2$ — since the “starting” creation operator $\hat{b}_1^{1\dagger}$ and annihilation operator \hat{b}_1^1 are both made of the product of an odd number of nilpotents, while products of either S^{ab} or \tilde{S}^{ab} can change an even number of nilpotents into projectors. Any $\hat{b}_i^{\alpha\dagger}$ is correspondingly a factor of an odd number of nilpotents (at least one) (and an even number of projectors) and its square is zero. The same is true for \hat{b}_i^α .

ii.b. All the creation operators operating on the vacuum state of Eq. (9.67) give a non zero vector — $\hat{b}_i^{\alpha\dagger} |\psi_{oc}\rangle \neq 0$ — while all the annihilation operators annihilate this vacuum state — $\hat{b}_i^\alpha |\psi_0\rangle = 0$ for any α and any i .

in this right \hat{b}_1^{\dagger} after the application of all the S^{ab} in the product in front of it, or $\overset{d-1}{[+]} \overset{d}{d}$ transforms into $\overset{d-1}{(-)} \overset{d}{d}$, and since the left \hat{b}_1^{\dagger} is a product of only nilpotents $(+)$ in $d = 2(2n + 1)$, or an odd number of nilpotents and $[+]$ for $d = 4n$, while $\overset{d-1}{[+]} \overset{d}{d} \overset{d-1}{d} = 0$, the anticommutator for any two creation operators is zero.

ii.d. Any two annihilation operators anticommute: $\{\hat{b}_i^\alpha, \hat{b}_j^\beta\}_+ = 0$. According to Eq. (9.66) we can rewrite $\{\hat{b}_i^\alpha, \hat{b}_j^\beta\}_+$, up to a factor, as $\{S^{ab} \dots S^{ef} \hat{b}_1^{mn} \dots S^{pr}, S^{a'b'} \dots S^{e'f'} \hat{b}_1^{m'n'} \dots S^{p'r'}\}_+$. Whatever the product $S^{mn} \dots S^{pr} S^{a'b'} \dots S^{e'f'}$ (or $S^{m'n'} \dots S^{p'r'} S^{ab} \dots S^{ef}$) is, it always transforms an even number of $(-)$ in \hat{b}_1^1 into $[+]$. Since an odd number of nilpotents $(-)$ (at least one) remains unchanged in this \hat{b}_1^1 after the application of all the S^{ab} in the product in front of it or $\overset{d-1}{[+]} \overset{d}{d}$ is transformed into $\overset{d-1}{(-)} \overset{d}{d}$, and since \hat{b}_1^1 on the left hand side is a product of only nilpotents $(-)$ for $d = 2(2n + 1)$ (or an odd number of nilpotents and $[+]$ for $d = 4n$), while $\overset{ab}{(-)} \overset{ab}{(-)} = 0$ and $\overset{ab}{[+]} \overset{ab}{[-]} = 0$, the anticommutator of any two annihilation operators is zero.

ii.e. For any creation and any annihilation operator it follows: $\{\hat{b}_i^\alpha, \hat{b}_j^{\beta\dagger}\}_+ |\psi_{oc}\rangle = \delta^{\alpha\beta} \delta_{ij} |\psi_{oc}\rangle$. Let us prove this. According to Eqs. (9.65, 9.66) we may rewrite $\{\hat{b}_i^\alpha, \hat{b}_j^{\beta\dagger}\}_+$ up to a factor as

$$\{S^{ab} \dots S^{ef} \hat{b}_1^{mn} \dots S^{pr}, S^{m'n'} \dots S^{p'r'} \hat{b}_1^{\dagger} S^{a'b'} \dots S^{e'f'}\}_+.$$

We distinguish between two cases. It can be that both $S^{mn} \dots S^{pr} S^{m'n'} \dots S^{p'r'}$ and $S^{a'b'} \dots S^{e'f'} S^{ab} \dots S^{ef}$ are numbers. This happens when $\alpha = \beta$ and $i = j$. Then we follow **i.b.**. We normalize the states so that $\langle \psi_i^\alpha | \psi_i^\alpha \rangle = 1$.

The second case is that at least one of products $S^{mn} \dots S^{pr} S^{m'n'} \dots S^{p'r'}$ and $S^{a'b'} \dots S^{e'f'} S^{ab} \dots S^{ef}$ is not a number. Then the factors like $\overset{ab}{(-)} \overset{ab}{[-]}$ or $\overset{ab}{[+]} \overset{ab}{(-)}$ make the anticommutator equal to zero. And the proof is completed.

Let us extend the creation and annihilation operators to the ordinary coordinate space

$$\begin{aligned} \{\hat{b}_i^\alpha(\vec{x}), \hat{b}_j^{\beta\dagger}(\vec{x}')\}_+ |\phi_{oc}\rangle &= \delta_\beta^\alpha \delta_j^i \delta(\vec{x} - \vec{x}') |\phi_{oc}\rangle, \\ \{\hat{b}_i^\alpha(\vec{x}), \hat{b}_j^\beta(\vec{x}')\}_+ |\phi_{oc}\rangle &= 0 |\phi_{oc}\rangle, \\ \{\hat{b}_i^{\alpha\dagger}(\vec{x}), \hat{b}_j^{\beta\dagger}(\vec{x}')\}_+ |\phi_{oc}\rangle &= 0 |\phi_{oc}\rangle, \\ \hat{b}_j^\alpha(\vec{x}) |\phi_{oc}\rangle &= 0 |\phi_{oc}\rangle, \\ \hat{b}_j^{\alpha\dagger}(\vec{x}) |\phi_{oc}\rangle &= |\psi_i^\alpha(\vec{x})\rangle, \end{aligned} \quad (9.69)$$

with the vacuum state $|\phi_{oc}\rangle$ defined in Eq. (9.67).

c. Discrete symmetries in Grassmann space and in Clifford space in d and in $d = (3 + 1)$ space

Let $\underline{\Psi}_p^\dagger |\Psi_p\rangle$ be the creation operator creating a fermion in the state Ψ_p (which is a function of \vec{x}) and let $\Psi_p(\vec{x})$ be the second quantized field creating a fermion

at position \vec{x} either in the Grassmann or in the Clifford case. Then

$$\underline{\Psi}_p^\dagger[\Psi_p] = \int \Psi_p^\dagger(\vec{x}) \Psi_p(\vec{x}) d^{(d-1)}x, \quad (9.70)$$

describes on a vacuum state a single particle in the state Ψ

$$\{\underline{\Psi}_p^\dagger[\Psi_p] = \int \Psi_p^\dagger(\vec{x}) \Psi_p(\vec{x}) d^{(d-1)}x\} |vac >$$

so that the anti-particle state becomes

$$\{\underline{\mathbb{C}}\Psi_p^\dagger[\Psi_p^{pos}] = \int \Psi_p(\vec{x}) (\mathcal{C} \Psi_p^{pos}(\vec{x})) d^{(d-1)}x\} |vac > .$$

We distinguish in d -dimensional space two kinds of discrete operators \mathcal{C}, \mathcal{P} and \mathcal{T} operators with respect to the internal space which we use.

In the Clifford case we have [21]

$$\begin{aligned} \mathcal{C}_H &= \prod_{\gamma^a \in \mathfrak{I}} \gamma^a K, \\ \mathcal{T}_H &= \gamma^0 \prod_{\gamma^a \in \mathfrak{R}} \gamma^a K I_{x^0}, \\ \mathcal{P}_H^{(d-1)} &= \gamma^0 I_{\vec{x}}, \\ I_x x^a &= -x^a, \quad I_{x^0} x^a = (-x^0, \vec{x}), \quad I_{\vec{x}} \vec{x} = -\vec{x}, \\ I_{\vec{x}_3} x^a &= (x^0, -x^1, -x^2, -x^3, x^5, x^6, \dots, x^d). \end{aligned} \quad (9.71)$$

The product $\prod \gamma^a$ is meant in the ascending order in γ^a .

In the Grassmann case we correspondingly define

$$\begin{aligned} \mathcal{C}_G &= \prod_{\gamma_G^a \in \mathfrak{I}\gamma^a} \gamma_G^a K, \\ \mathcal{T}_G &= \gamma_G^0 \prod_{\gamma_G^a \in \mathfrak{R}\gamma^a} \gamma_G^a K I_{x^0}, \\ \mathcal{P}_G^{(d-1)} &= \gamma_G^0 I_{\vec{x}}, \end{aligned} \quad (9.72)$$

γ_G^a is defined in Eq. (9.11) as

$$\gamma_G^a = (1 - 2\theta^a \eta^{aa} \frac{\partial}{\partial \theta^a}), \quad (9.73)$$

while $I_x x^a = -x^a$, $I_{x^0} x^a = (-x^0, \vec{x})$, $I_{\vec{x}} \vec{x} = -\vec{x}$,

$$I_{\vec{x}_3} x^a = (x^0, -x^1, -x^2, -x^3, x^5, x^6, \dots, x^d).$$

Let be noticed, that since $\gamma_G^a (= -i\eta^{aa} \gamma^a \tilde{\gamma}^a)$ is always real as there is $\gamma^a i\tilde{\gamma}^a$, while γ^a is either real or imaginary, we use in Eq. (9.72) γ^a to make a choice of appropriate γ_G^a . In what follows we shall use the notation as in Eq. (9.72).

Let us define in the Clifford case and in the Grassmann case the operator "emptying" [7,9] (arxiv:1312.1541) the Dirac sea, so that operation of "emptying_N" after the charge conjugation \mathcal{C}_H in the Clifford case and "emptying_G" after the charge conjugation \mathcal{C}_G in the Grassmann case (both transform the state put on the top of either the Clifford or the Grassmann Dirac sea into the corresponding negative energy state) creates the anti-particle state to the starting particle state, both put on the top of the Dirac sea and both solving the Weyl equation, either in the Clifford case, Eq. (9.34), or in the Grassmann case, Eq. (9.39), for free massless fermions

$$\begin{aligned} \text{"emptying}_N &= \prod_{\Re \gamma^a} \gamma^a K \quad \text{in Clifford space,} \\ \text{"emptying}_G &= \prod_{\Re \gamma^a} \gamma_G^a K \quad \text{in Grassmann space,} \end{aligned} \quad (9.74)$$

although we must keep in mind that indeed the anti-particle state is a hole in the Dirac sea from the Fock space point of view. The operator "emptying" is bringing the single particle operator \mathcal{C}_H in the Clifford case and \mathcal{C}_G in the Grassmann case into the operator on the Fock space in each of the two cases. Then the anti-particle state creation operator — $\underline{\Psi}_a^\dagger[\Psi_p]$ — to the corresponding particle state creation operator — can be obtained also as follows

$$\begin{aligned} \underline{\Psi}_a^\dagger[\Psi_p] |\text{vac}\rangle &= \mathbb{C}_H \underline{\Psi}_p^\dagger[\Psi_p] |\text{vac}\rangle = \int \Psi_a^\dagger(\vec{x}) (\mathbb{C}_H \Psi_p(\vec{x})) d^{(d-1)}x |\text{vac}\rangle, \\ \mathbb{C}_H &= \text{"emptying}_N" \cdot \mathcal{C}_H \end{aligned} \quad (9.75)$$

in both cases.

The operators \mathbb{C}_H and \mathbb{C}_G

$$\mathbb{C}_H = \text{"emptying}_N" \cdot \mathcal{C}_H, \quad \mathbb{C}_G = \text{"emptying}_{NG}" \cdot \mathcal{C}_G, \quad (9.76)$$

operating on $\Psi_p(\vec{x})$ transforms the positive energy spinor state (which solves the corresponding Weyl equation for a massless free fermion) put on the top of the Dirac sea into the positive energy anti-fermion state, which again solves the corresponding Weyl equation for a massless free anti-fermion put on the top of the Dirac sea. Let us point out that either the operator "emptying_N" or the operator "emptying_{NG}" transforms the single particle operator either \mathcal{C}_H or \mathcal{C}_G into the operator operating in the Fock space.

We use the Grassmann even, Hermitian and real operators γ_G^a , Eq. (9.11), to define discrete symmetry in Grassmann space, first in $((d+1)-1)$ space and then in $(3+1)$ space, as we did in [21] in the Clifford case. In the Grassmann case we

do this in analogy with the operators in the Clifford case [21]

$$\begin{aligned}
 \mathcal{C}_{\text{NG}} &= \prod_{\gamma_G^m \in \mathfrak{R}\gamma^m} \gamma_G^m K I_{x^6 x^8 \dots x^d}, \\
 \mathcal{T}_{\text{NG}} &= \gamma_G^0 \prod_{\gamma_G^m \in \mathfrak{I}\gamma^m} K I_{x^0} I_{x^5 x^7 \dots x^{d-1}}, \\
 \mathcal{P}_{\text{NG}}^{(d-1)} &= \gamma_G^0 \prod_{s=5}^d \gamma_G^s I_{\vec{x}}, \\
 \mathbb{C}_{\text{NG}} &= \prod_{\gamma_G^s \in \mathfrak{R}\gamma^s} \gamma_G^s, I_{x^6 x^8 \dots x^d}, \\
 \mathbb{C}_{\text{NG}} \mathcal{P}_{\text{NG}}^{(d-1)} &= \gamma_G^0 \prod_{\gamma_G^s \in \mathfrak{I}\gamma^s, s=5}^d \gamma_G^s I_{\vec{x}_3} I_{x^6 x^8 \dots x^d}, \\
 \mathbb{C}_{\text{NG}} \mathcal{T}_{\text{NG}} \mathcal{P}_{\text{NG}}^{(d-1)} &= \prod_{\gamma_G^s \in \mathfrak{I}\gamma^a} \gamma_G^a I_x K. \tag{9.77}
 \end{aligned}$$

Let us try to understand the Grassmann fermions in the case $d = 5 + 1$, before the break, as well as after the break of $d = 5 + 1$ into $d = 3 + 1$, when the fifth and the sixth dimension determine the charge in $d = 3 + 1$. There are two decuplets in this case [15], both of an odd Grassmann character, which can be second quantized. The two triplets in the first decuplet— $(\psi_1^I, \psi_2^I, \psi_3^I)$ and $(\psi_4^I, \psi_5^I, \psi_6^I)$ —both solving the Eq. (9.39) for massless free fermions in Grassmann space with the space function $e^{-ip_a x^a}$. The Grassmann even operator $\mathbb{C}_{\text{NG}} \mathcal{P}_{\text{NG}}^{(d-1)}$ transforms ψ_1^I with $p^a = (|p^0|, 0, 0, |p^3|, 0, 0)$ into the antiparticle state ψ_6^I , with the positive energy $|p^0|$ and with $-|p^3|$, for example. Correspondingly transforms $\mathbb{C}_{\text{NG}} \mathcal{P}_{\text{NG}}^{(d-1)}$ the particle state ψ_3^I with the positive energy and into the antiparticle state ψ_4^I with the positive energy, and the particle ψ_3^I into the positive energy antiparticle state ψ_4^I . All belong to the same representation.

Applying the Grassmann even operators on one of the states of one the decuplets— $\mathcal{C}_G (= \gamma_G^2 \gamma_G^5, \text{Eq. (9.72)})$, $\mathcal{C}_{\text{NG}} \mathcal{P}_{\text{NG}}^{(d-1)} (= \gamma_G^1 \gamma_G^3 \gamma_G^5 \gamma_G^6 I_{x^6} I_{\vec{x}_3} K, \text{Eq. (9.72)})$ —one remains within the same decuplet. To get the positive energy antiparticle states the operator empty_{NG} in $(d-1) + 1$ and empty_{NG} in $d = (3+1)$ are needed, Eqs. (9.74, 9.76). The reader can find more discussions in Refs. [15,21].

d. What do we learn in the second quantization procedure in Grassmann and in Clifford space

We proved that basic states in both spaces can be written by creation operators operating on an appropriate vacuum state. The creation and annihilation operators fulfill in both spaces anticommutation relations as required for fermions, Eqs (9.48, 9.60).

In both spaces the creation operators are chosen to create states that are eigenstates of the corresponding Cartan subalgebra of the Lorentz algebra, the generators of which are S^{ab} , Eq. (9.13), for the Grassmann case and (S^{ab}, \tilde{S}^{ab}) , first generating spins and the second families, Eq. (9.25), for the Clifford case.

I		decuplet	\mathbf{S}^{03}	\mathbf{S}^{12}	\mathbf{S}^{56}
	1	$(\theta^0 - \theta^3)(\theta^1 + i\theta^2)(\theta^5 + i\theta^6)$	i	1	1
	2	$(\theta^0\theta^3 + i\theta^1\theta^2)(\theta^5 + i\theta^6)$	0	0	1
	3	$(\theta^0 + \theta^3)(\theta^1 - i\theta^2)(\theta^5 + i\theta^6)$	-i	-1	1
	4	$(\theta^0 - \theta^3)(\theta^1 - i\theta^2)(\theta^5 - i\theta^6)$	i	-1	-1
	5	$(\theta^0\theta^3 - i\theta^1\theta^2)(\theta^5 - i\theta^6)$	0	0	-1
	6	$(\theta^0 + \theta^3)(\theta^1 + i\theta^2)(\theta^5 - i\theta^6)$	-i	1	-1
	7	$(\theta^0 - \theta^3)(\theta^1\theta^2 + \theta^5\theta^6)$	i	0	0
	8	$(\theta^0 + \theta^3)(\theta^1\theta^2 - \theta^5\theta^6)$	-i	0	0
	9	$(\theta^0\theta^3 + i\theta^5\theta^6)(\theta^1 + i\theta^2)$	0	1	0
	10	$(\theta^0\theta^3 - i\theta^5\theta^6)(\theta^1 - i\theta^2)$	0	-1	0
II		decuplet	\mathbf{S}^{03}	\mathbf{S}^{12}	\mathbf{S}^{56}
	1	$(\theta^0 + \theta^3)(\theta^1 + i\theta^2)(\theta^5 + i\theta^6)$	-i	1	1
	2	$(\theta^0\theta^3 - i\theta^1\theta^2)(\theta^5 + i\theta^6)$	0	0	1
	3	$(\theta^0 - \theta^3)(\theta^1 - i\theta^2)(\theta^5 + i\theta^6)$	i	-1	1
	4	$(\theta^0 + \theta^3)(\theta^1 - i\theta^2)(\theta^5 - i\theta^6)$	-i	-1	-1
	5	$(\theta^0\theta^3 + i\theta^1\theta^2)(\theta^5 - i\theta^6)$	0	0	-1
	6	$(\theta^0 - \theta^3)(\theta^1 + i\theta^2)(\theta^5 - i\theta^6)$	i	1	-1
	7	$(\theta^0 + \theta^3)(\theta^1\theta^2 + \theta^5\theta^6)$	-i	0	0
	8	$(\theta^0 - \theta^3)(\theta^1\theta^2 - \theta^5\theta^6)$	i	0	0
	9	$(\theta^0\theta^3 - i\theta^5\theta^6)(\theta^1 + i\theta^2)$	0	1	0
	10	$(\theta^0\theta^3 + i\theta^5\theta^6)(\theta^1 - i\theta^2)$	0	-1	0

Table 9.1. The creation operators of the decuplet and the antidecuplet of the orthogonal group $SO(5, 1)$ in Grassmann space are presented. Applying on the vacuum state $|\phi_0\rangle = |1\rangle$ the creation operators form eigenstates of the Cartan subalgebra, Eq. (9.84), $(\mathbf{S}^{03}, \mathbf{S}^{12}, \mathbf{S}^{56})$. The states within each decuplet are reachable from any member by \mathbf{S}^{ab} . The product of the discrete operators $\mathbb{C}_{NG} (= \prod_{\mathfrak{R}\gamma^s} \gamma_G^s I_{x^6 x^8 \dots x^d}) \mathcal{P}_{NG}^{(d-1)} (= \gamma_G^0 \prod_{s=5}^d \gamma_G^s I_{\vec{x}_3})$ transforms, for example, ψ_1^1 into ψ_6^1 , ψ_2^1 into ψ_5^1 and ψ_3^1 into ψ_4^1 . Solutions of the Weyl equation, Eq. (9.39), with the negative energies belong to the "Grassmann sea", with the positive energy to the particles and antiparticles.

While in the Grassmann case the vacuum state is simple, $|\phi_{og}\rangle = |1\rangle$, in the Clifford case the vacuum state is a sum of products of $2^{\frac{d}{2}-1}$ projectors, Eq. (9.67).

In $2(2n+1)$ -dimensional spaces there are in the Clifford case $2^{\frac{d}{2}-1}$ states in one representation reachable from (any) starting state by \mathbf{S}^{ab} , while $\tilde{\mathbf{S}}^{ab}$ transform each of these states changing its family quantum number. There are correspondingly $2^{\frac{d}{2}-1} \times 2^{\frac{d}{2}-1}$ states reachable with either \mathbf{S}^{ab} or $\tilde{\mathbf{S}}^{ab}$. Each state is obtained by the corresponding creation operator on the vacuum state and is annihilated by its Hermitian conjugate operator.

In $2(2n+1)$ -dimensional spaces there are in the Grassmann case two decoupled groups with $\frac{1}{2} \frac{d!}{\frac{d}{2}! \frac{d}{2}!}$ states in each representation. Each of states can be obtained by the corresponding creation operator and is annihilated by its Hermitian conjugated operator. While all of $2^{\frac{d}{2}-1} \times 2^{\frac{d}{2}-1}$ states in Clifford space are reachable by even Clifford objects, either \mathbf{S}^{ab} or $\tilde{\mathbf{S}}^{ab}$, in Grassmann space the two

groups of representations can not be reached by an even number of Grassmann objects.

9.3 Conclusions

We have learned in the present study that one can use either Grassmann or Clifford space to express the internal degrees of freedom of fermions in any even dimensional space, either for $d = 2(2n + 1)$ or $d = 4n$. In both spaces the creation operators and their Hermitian conjugated annihilation operators fulfill the anticommutation relation requirements, needed for fermions, provided that they are expressed as odd products of either Grassmann (θ^a , $(\theta^a)^\dagger = \frac{\partial}{\partial \theta_a} \eta^{aa}$, Eq. (9.8)) or Clifford objects (either $\gamma^a = (\theta^a + \frac{\partial}{\partial \theta_a})$, Eq. (9.17) and correspondingly $\gamma^{a\dagger} = \gamma^a \eta^{aa}$, or $\tilde{\gamma}^a = i(\theta^a - \frac{\partial}{\partial \theta_a})$, Eq. (9.18), and correspondingly $\tilde{\gamma}^{a\dagger} = \tilde{\gamma}^a \eta^{aa}$). But while in the Clifford case states appear in the fundamental representations of the Lorentz group, carrying half integer spins, the states in the Grassmann case are in adjoint representations of the Lorentz group. The Clifford case, offering two kinds of the Clifford objects (γ^a and $\tilde{\gamma}^a$), enables to describe besides the spin degrees of freedom of fermion fields also their family degrees of freedom. The Grassmann case offers only one kind of objects. Assuming that "nature has both choices" for describing the internal degrees of freedom of fermion fields, the question arises why Grassmann choice is not chosen, or better, why the Clifford choice is chosen.

In the case that spin degrees in $d \geq 5$ manifest as charges in $d = (3 + 1)$, fermions in the Grassmann case manifest charges in the adjoint representations. On the other hand in the Clifford case — this is used in the *spin-charge-family* theory, which takes the Lorentz group $SO(13, 1)$ — the spin and charges appear in the fundamental representations of the corresponding groups, offering also the family degrees of freedom.

We present in this paper the action describing free massless particles with the internal degrees of freedom describable in Grassmann space, Eqs. (9.37, 9.38). The action leads to the equation of motion analogous to the Weyl equation in Clifford space, fulfilling the Klein-Gordon equation.

Since the Clifford objects γ^a and $\tilde{\gamma}^a$ are expressible with the Grassmann coordinates θ^a and their conjugate moments $\frac{\partial}{\partial \theta_a}$, either basic states in Grassmann space, Eq. (9.4), or basic states in Clifford space, Eq. (9.15), can be normalized with the same integral, Eq. (9.27, 9.28, 9.30).

To understand better the difference in the description of the fermion internal degrees of freedom with either Clifford or Grassmann space, let us replace in the starting action of the *spin-charge-family* theory, Eq. (9.1), using the Clifford algebra to describe fermion degrees of freedom, the covariant momentum $p_{0a} = f^\alpha_a p_{0\alpha}$, $p_{0\alpha} = p_\alpha - \frac{1}{2} S^{ab} \omega_{ab\alpha} - \frac{1}{2} \tilde{S}^{ab} \tilde{\omega}_{ab\alpha}$, with $p_{0\alpha} = p_\alpha - \frac{1}{2} S^{ab} \Omega_{ab\alpha}$, where $S^{ab} = S^{ab} + \tilde{S}^{ab}$, Eq. (9.26), and $\Omega_{ab\alpha}$ are the spin connection gauge fields of S^{ab} (which are the generators of the Lorentz transformations in Grassmann space!), while $f^\alpha_a p_{0\alpha}$ replaces the ordinary momentum when massless objects start to interact with the gravitational field through the vielbeins and the spin connections. Let us add that varying the action with respect to either $\omega_{ab\alpha}$ or $\tilde{\omega}_{ab\alpha}$ when no fermions are present, one learns that both spin connections are uniquely

determined by the vielbeins ([9,3,5] and references therein) and correspondingly in this particular case $\omega_{ab\alpha} = \bar{\omega}_{ab\alpha}$.

Let us use instead of p_a in the action for free massless fields using Grassmann space to describe the internal degrees of freedom, Eq. (9.37), the above covariant momentum $p_{0a} = f^\alpha_a (p_\alpha - \frac{1}{2} S^{ab} \Omega_{ab\alpha})$. One finds in this case that the representations of the Lorentz group in $d = 2(2n + 1) = 13 + 1$ and their subgroups $SO(7, 1)$, $SU(3)$ and $U(1)$ are all in the adjoint representations of the groups.

The *spin-charge-family* theory (using Clifford objects) offers the explanation for all the assumptions of the *standard model* of elementary fields, fermions and bosons, vector and scalar gauge fields, with the appearance of families included, explaining also the phenomena like the existence of the dark matter [10], of the matter-antimatter asymmetry [4], offering correspondingly the next step beyond both standard models — cosmological one and the one of the elementary fields.

We do notice, however, that the *Grassmann degrees of freedom do not offer the appearance of families at all*.

We also notice that the second quantization procedure allows in $d = 2(2n + 1)$ -dimensional space for each member of a Weyl representation in Clifford space (for each of $2^{\frac{d}{2}-1}$ "family member") $2^{\frac{d}{2}-1}$ "families", all together therefore $2^{\frac{d}{2}-1} \times 2^{\frac{d}{2}-1}$ basic states which can be second quantized, according to this paper. From 2^d Clifford objects, only those of an odd Clifford character contribute to the second quantization — half of them as creation and half of them as annihilation operators, $2^{\frac{d}{2}-1}$ projectors from the rest of objects form the vacuum state.

We notice that in case of Grassmann space and $d = 2(2n + 1)$ only twice two isolated groups of $\frac{1}{2} \frac{d!}{\frac{d}{2}! \frac{d}{2}!}$ states of an odd Grassmann character can be second quantized.

To come to the low energy regime the symmetry must break, first from $SO(13, 1)$ to $SO(7, 1) \times SU(3) \times U(1)$ and then further to $SO(3, 1) \times SU(3) \times U(1)$, in both spaces, in Grassmann and in Clifford. In Clifford case there are two kinds of generators and correspondingly two kinds of symmetries. We learned in Refs. [23–25] that when breaking symmetries only some of families stay massless and correspondingly observable in $d = (3 + 1)$.

This study is indeed to learn more about possibilities that "nature has". One of the authors (N.S.M.B.) wants to learn: **a.** Why is the simple starting action of the *spin-charge-family* theory doing so well in manifesting the observed properties of the fermion and boson fields? **b.** Under which condition can more general action lead to the starting action of Eq. (9.1)? **c.** What would more general action, if leading to the same low energy physics, mean for the history of our Universe? **d.** Could the fermionization procedure of boson fields or the bosonization procedure of fermion fields, discussed in Ref. [12] for any even dimension d (by the authors of this contribution, while one of them (H.B.F.N. [13]) has succeeded with another author to do the fermionization for $d = (1 + 1)$) tell more about the "decisions" of the universe in the history?

Although we have not yet learned enough to be able to answer these questions, yet we have learned at least that the description of the fermion internal degrees of freedom in Grassmann space would not offer families, and would not be in agreement with the spin and charges and other observations so far. We also learned

that if there are no fermion present only one kind of dynamical fields manifests, since either $\omega_{ab\alpha}$ or $\tilde{\omega}_{ab\alpha}$ are uniquely expressed by vielbeins ([9] Eq. (C9) and references therein), which could mean that the appearance of the two kinds of the spin connection fields might be due to the break of symmetries.

9.4 Appendix: Lorentz algebra and representations in Grassmann and Clifford space

The Lorentz transformations of vector components θ^a , γ^a , or $\tilde{\gamma}^a$, which all could be used to describe internal degrees of freedom of fields with the anticommutation relations of fermions, and of vector components x^a , which are real (ordinary) commuting coordinates:

$\theta'^a = \Lambda^a_b \theta^b$, $\gamma'^a = \Lambda^a_b \gamma^b$, $\tilde{\gamma}'^a = \Lambda^a_b \tilde{\gamma}^b$ and $x^a = \Lambda^a_b x^b$, leave forms $a_{a_1 a_2 \dots a_i} \theta^{a_1} \theta^{a_2} \dots \theta^{a_i}$, $a_{a_1 a_2 \dots a_i} \gamma^{a_1} \gamma^{a_2} \dots \gamma^{a_i}$, $a_{a_1 a_2 \dots a_i} \tilde{\gamma}^{a_1} \tilde{\gamma}^{a_2} \dots \tilde{\gamma}^{a_i}$ and $b_{a_1 a_2 \dots a_i} x^{a_1} x^{a_2} \dots x^{a_i}$, $i = (1, \dots, d)$, invariant.

While $b_{a_1 a_2 \dots a_i} (= \eta_{a_1 b_1} \eta_{a_2 b_2} \dots \eta_{a_i b_i} b^{b_1 b_2 \dots b_i})$ is a symmetric tensor field, $a_{a_1 a_2 \dots a_i} (= \eta_{a_1 b_1} \eta_{a_2 b_2} \dots \eta_{a_i b_i} a^{b_1 b_2 \dots b_i})$ are antisymmetric tensor *Kalb-Ramond* fields.

The requirements: $x'^a x'^b \eta_{ab} = x^c x^d \eta_{cd}$, $\theta'^a \theta'^b \varepsilon_{ab} = \theta^c \theta^d \varepsilon_{cd}$, $\gamma'^a \gamma'^b \varepsilon_{ab} = \gamma^c \gamma^d \varepsilon_{cd}$ and $\tilde{\gamma}'^a \tilde{\gamma}'^b \varepsilon_{ab} = \tilde{\gamma}^c \tilde{\gamma}^d \varepsilon_{cd}$ lead to $\Lambda^a_b \Lambda^c_d \eta_{ac} = \eta_{bd}$. Here η^{ab} (in our case $\eta^{ab} = \text{diag}(1, -1, -1, \dots, -1)$) is the metric tensor lowering the indexes of vectors ($\{x^a\} = \eta^{ab} x_b$, $\{\theta^a\} = \eta^{ab} \theta_b$, $\{\gamma^a\} = \eta^{ab} \gamma_b$ and $\{\tilde{\gamma}^a\} = \eta^{ab} \tilde{\gamma}_b$) and ε_{ab} is the antisymmetric tensor. An infinitesimal Lorentz transformation for the case with $\det \Lambda = 1$, $\Lambda^0_0 \geq 0$ can be written as $\Lambda^a_b = \delta^a_b + \omega^a_b$, where $\omega^a_b + \omega_b^a = 0$.

According to Eqs. (9.17, 9.18, 9.25) one finds, Eq. (9.3),

$$\begin{aligned} \{\gamma^a, \tilde{S}^{cd}\}_- &= 0 = \{\tilde{\gamma}^a, S^{cd}\}_-, \\ \{\gamma^a, S^{cd}\}_- &= \{\gamma^a, S^{cd}\}_- = i(\eta^{ac} \gamma^d - \eta^{ad} \gamma^c), \\ \{\tilde{\gamma}^a, S^{cd}\}_- &= \{\tilde{\gamma}^a, \tilde{S}^{cd}\}_- = i(\eta^{ac} \tilde{\gamma}^d - \eta^{ad} \tilde{\gamma}^c). \end{aligned} \quad (9.78)$$

Comments: In cases with either the basis θ^a or with the basis of γ^a or $\tilde{\gamma}^a$ the scalar products — the norms $\langle \mathbf{B} | \mathbf{B} \rangle$ and $\langle \mathbf{F} | \mathbf{F} \rangle$ (where $\langle \theta | \theta \rangle$, Eq. (9.4), and $\langle \gamma | \gamma \rangle$, Eq. (9.15), are vectors in Grassmann and Clifford space, respectively) — are non negative and equal to $\sum_{k=0}^d \int d^{d-1} x b_{b_1 \dots b_k}^* b_{b_1 \dots b_k}$.

9.4.1 Lorentz properties of basic vectors

What follows is taken from Ref. [2] and Ref. [9], Appendix B.

Let us first repeat some properties of the anticommuting Grassmann coordinates.

An infinitesimal Lorentz transformation of the proper orthochronous Lorentz group is then

$$\begin{aligned}\delta\theta^c &= -\frac{i}{2}\omega_{ab}\mathbf{S}^{ab}\theta^c = \omega^c{}_a\theta^a, \\ \delta\gamma^c &= -\frac{i}{2}\omega_{ab}S^{ab}\gamma^c = \omega^c{}_a\gamma^a, \\ \delta\tilde{\gamma}^c &= -\frac{i}{2}\omega_{ab}\tilde{S}^{ab}\tilde{\gamma}^c = \omega^c{}_a\tilde{\gamma}^a, \\ \delta\chi^c &= -\frac{i}{2}\omega_{ab}L^{ab}\chi^c = \omega^c{}_a\chi^a,\end{aligned}\tag{9.79}$$

where ω_{ab} are parameters of a transformation and γ^a and $\tilde{\gamma}^a$ are expressed by θ^a and $\frac{\partial}{\partial\theta^a}$ in Eqs. (9.17, 9.18).

Let us write the operator of finite Lorentz transformations as follows

$$\mathbf{S} = e^{-\frac{i}{2}\omega_{ab}(\mathbf{S}^{ab} + L^{ab})}.\tag{9.80}$$

We see that the Grassmann θ^a and the ordinary χ^a coordinates and the Clifford objects γ^a and $\tilde{\gamma}^a$ transform as vectors Eq. (9.80)

$$\begin{aligned}\theta'^c &= e^{-\frac{i}{2}\omega_{ab}(\mathbf{S}^{ab} + L^{ab})}\theta^c e^{\frac{i}{2}\omega_{ab}(\mathbf{S}^{ab} + L^{ab})} \\ &= \theta^c - \frac{i}{2}\omega_{ab}\{\mathbf{S}^{ab}, \theta^c\} + \dots = \theta^c + \omega^c{}_a\theta^a + \dots = \Lambda^c{}_a\theta^a, \\ \chi'^c &= \Lambda^c{}_a\chi^a, \quad \gamma'^c = \Lambda^c{}_a\gamma^a, \quad \tilde{\gamma}'^c = \Lambda^c{}_a\tilde{\gamma}^a.\end{aligned}\tag{9.81}$$

Correspondingly one finds that compositions like γ^ap_a and $\tilde{\gamma}^ap_a$, here p_a are $p_a^x (= i\frac{\partial}{\partial x^a})$, transform as scalars (remaining invariants), while $S^{ab}\omega_{abc}$ and $\tilde{S}^{ab}\tilde{\omega}_{abc}$ transform as vectors.

Also objects like

$$R = \frac{1}{2}f^{\alpha[a}f^{\beta b]}(\omega_{ab\alpha,\beta} - \omega_{ca\alpha}\omega^c{}_{b\beta})$$

and

$$\tilde{R} = \frac{1}{2}f^{\alpha[a}f^{\beta b]}(\tilde{\omega}_{ab\alpha,\beta} - \tilde{\omega}_{ca\alpha}\tilde{\omega}^c{}_{b\beta})$$

from Eq. (9.1) transform with respect to the Lorentz transformations as scalars.

Making a choice of the Cartan subalgebra set of the algebra \mathbf{S}^{ab} , S^{ab} and \tilde{S}^{ab} , Eqs. (9.13, 9.17, 9.18),

$$\begin{aligned}\mathbf{S}^{03}, \mathbf{S}^{12}, \mathbf{S}^{56}, \dots, \mathbf{S}^{d-1\ d}, \\ S^{03}, S^{12}, S^{56}, \dots, S^{d-1\ d}, \\ \tilde{S}^{03}, \tilde{S}^{12}, \tilde{S}^{56}, \dots, \tilde{S}^{d-1\ d},\end{aligned}\tag{9.82}$$

one can arrange the basic vectors so that they are eigenstates of the Cartan subalgebra, belonging to representations of \mathbf{S}^{ab} , or of S^{ab} and \tilde{S}^{ab} , with ab from Eq (9.82).

9.5 Appendix: Technique to generate spinor representations in terms of Clifford algebra objects

We shall briefly repeat the main points of the technique for generating spinor representations from Clifford algebra objects, following Ref. [16]. We advise the reader to look for details and proofs in this reference.

We assume the objects γ^a , Eq. (9.17), which fulfill the Clifford algebra, Eq (9.16).

$$\{\gamma^a, \gamma^b\}_+ = I \, 2\eta^{ab}, \quad \text{for } a, b \in \{0, 1, 2, 3, 5, \dots, d\}, \quad (9.83)$$

for any d , even or odd. I is the unit element in the Clifford algebra, while $\{\gamma^a, \gamma^b\}_\pm = \gamma^a \gamma^b \pm \gamma^b \gamma^a$.

We accept the “Hermiticity” property for γ^a ’s, Eq. (9.20), $\gamma^{a\dagger} = \eta^{aa} \gamma^a$, leading to $\gamma^{a\dagger} \gamma^a = I$. Assuming the relation of Eq. (9.17) this last relations follow.

The Clifford algebra objects S^{ab} close the Lie algebra of the Lorentz group $\{S^{ab}, S^{cd}\}_- = i(\eta^{ad} S^{bc} + \eta^{bc} S^{ad} - \eta^{ac} S^{bd} - \eta^{bd} S^{ac})$. One finds from Eq.(9.20) that $(S^{ab})^\dagger = \eta^{aa} \eta^{bb} S^{ab}$ and that $\{S^{ab}, S^{ac}\}_+ = \frac{1}{2} \eta^{aa} \eta^{bc}$.

Recognizing that two Clifford algebra objects S^{ab}, S^{cd} with all indexes different commute, we select (out of many possibilities) the Cartan sub algebra set of the algebra of the Lorentz group as follows

$$\begin{aligned} S^{0d}, S^{12}, S^{35}, \dots, S^{d-2 \, d-1}, & \quad \text{if } d = 2n, \\ S^{12}, S^{35}, \dots, S^{d-1 \, d}, & \quad \text{if } d = 2n + 1. \end{aligned} \quad (9.84)$$

To make the technique simple, we introduce the graphic representation [16] as follows

$$\begin{aligned} {}^{ab}(\mathbf{k}) &:= \frac{1}{2}(\gamma^a + \frac{\eta^{aa}}{ik} \gamma^b), \\ {}^{ab}[\mathbf{k}] &:= \frac{1}{2}(1 + \frac{i}{k} \gamma^a \gamma^b), \end{aligned} \quad (9.85)$$

where $k^2 = \eta^{aa} \eta^{bb}$. One can easily check by taking into account the Clifford algebra relation (Eq. (9.83)) and the definition of S^{ab} (Eq. (9.25)) that if one multiplies from the left hand side by S^{ab} the Clifford algebra objects ${}^{ab}(\mathbf{k})$ and ${}^{ab}[\mathbf{k}]$, it follows that

$$\begin{aligned} S^{ab} {}^{ab}(\mathbf{k}) &= \frac{1}{2} k {}^{ab}(\mathbf{k}), \\ S^{ab} {}^{ab}[\mathbf{k}] &= \frac{1}{2} k {}^{ab}[\mathbf{k}]. \end{aligned} \quad (9.86)$$

This means that ${}^{ab}(\mathbf{k})$ and ${}^{ab}[\mathbf{k}]$ acting from the left hand side on anything (on a vacuum state $|\psi_0\rangle$, for example) are eigenvectors of S^{ab} .

We further find

$$\begin{aligned} \gamma^a {}^{ab}(\mathbf{k}) &= \eta^{aa} {}^{ab}[-\mathbf{k}], & \gamma^b {}^{ab}(\mathbf{k}) &= -ik {}^{ab}[-\mathbf{k}], \\ \gamma^a {}^{ab}[\mathbf{k}] &= {}^{ab}(-\mathbf{k}), & \gamma^b {}^{ab}[\mathbf{k}] &= -ik \eta^{aa} {}^{ab}(-\mathbf{k}). \end{aligned} \quad (9.87)$$

It follows that $S^{ac} \begin{smallmatrix} ab & cd \\ (k) & (k) \end{smallmatrix} = -\frac{i}{2} \eta^{aa} \eta^{cc} \begin{smallmatrix} ab & cd \\ [-k] & [-k] \end{smallmatrix}$, $S^{ac} \begin{smallmatrix} ab & cd \\ [k] & [k] \end{smallmatrix} = \frac{i}{2} \begin{smallmatrix} ab & cd \\ (-k) & (-k) \end{smallmatrix}$, $S^{ac} \begin{smallmatrix} ab & cd \\ (k) & [-k] \end{smallmatrix} = -\frac{i}{2} \eta^{aa} \begin{smallmatrix} ab & cd \\ [-k] & (-k) \end{smallmatrix}$, $S^{ac} \begin{smallmatrix} ab & cd \\ [k] & (k) \end{smallmatrix} = \frac{i}{2} \eta^{cc} \begin{smallmatrix} ab & cd \\ (-k) & [-k] \end{smallmatrix}$. It is useful to deduce the following relations

$$\begin{aligned} \begin{smallmatrix} ab & ab \\ (k) & (k) \end{smallmatrix} &= 0, & \begin{smallmatrix} ab & ab \\ (k) & (-k) \end{smallmatrix} &= \eta^{aa} \begin{smallmatrix} ab \\ [k] \end{smallmatrix}, & \begin{smallmatrix} ab & ab \\ (-k) & (k) \end{smallmatrix} &= \eta^{aa} \begin{smallmatrix} ab \\ [-k] \end{smallmatrix}, & \begin{smallmatrix} ab & ab \\ (-k) & (-k) \end{smallmatrix} &= 0, \\ \begin{smallmatrix} ab & ab \\ [k] & [k] \end{smallmatrix} &= \begin{smallmatrix} ab \\ [k] \end{smallmatrix}, & \begin{smallmatrix} ab & ab \\ [k] & [-k] \end{smallmatrix} &= 0, & \begin{smallmatrix} ab & ab \\ [-k] & [k] \end{smallmatrix} &= 0, & \begin{smallmatrix} ab & ab \\ [-k] & [-k] \end{smallmatrix} &= \begin{smallmatrix} ab \\ [-k] \end{smallmatrix}, \\ \begin{smallmatrix} ab & ab \\ (k) & [k] \end{smallmatrix} &= 0, & \begin{smallmatrix} ab & ab \\ [k] & (k) \end{smallmatrix} &= \begin{smallmatrix} ab \\ (k) \end{smallmatrix}, & \begin{smallmatrix} ab & ab \\ (-k) & [k] \end{smallmatrix} &= \begin{smallmatrix} ab \\ (-k) \end{smallmatrix}, & \begin{smallmatrix} ab & ab \\ (-k) & [-k] \end{smallmatrix} &= 0, \\ \begin{smallmatrix} ab & ab \\ (k) & [-k] \end{smallmatrix} &= \begin{smallmatrix} ab \\ (k) \end{smallmatrix}, & \begin{smallmatrix} ab & ab \\ [k] & (-k) \end{smallmatrix} &= 0, & \begin{smallmatrix} ab & ab \\ [-k] & (k) \end{smallmatrix} &= 0, & \begin{smallmatrix} ab & ab \\ [-k] & (-k) \end{smallmatrix} &= \begin{smallmatrix} ab \\ (-k) \end{smallmatrix}. \end{aligned} \quad (9.88)$$

We recognize in the first equation of the first row and the first equation of the second row the demonstration of the nilpotent and the projector character of the Clifford algebra objects $\begin{smallmatrix} ab \\ (k) \end{smallmatrix}$ and $\begin{smallmatrix} ab \\ [k] \end{smallmatrix}$, respectively.

Whenever the Clifford algebra objects apply from the left hand side, they always transform $\begin{smallmatrix} ab \\ (k) \end{smallmatrix}$ to $\begin{smallmatrix} ab \\ [-k] \end{smallmatrix}$, never to $\begin{smallmatrix} ab \\ [k] \end{smallmatrix}$, and similarly $\begin{smallmatrix} ab \\ [k] \end{smallmatrix}$ to $\begin{smallmatrix} ab \\ (-k) \end{smallmatrix}$, never to $\begin{smallmatrix} ab \\ (k) \end{smallmatrix}$.

We define in Eq. (9.62) a vacuum state $|\psi_{oc} >$ so that one finds

$$< \begin{smallmatrix} ab \\ (k) \end{smallmatrix} \begin{smallmatrix} ab \\ (k) \end{smallmatrix} > = 1, \quad < \begin{smallmatrix} ab \\ [k] \end{smallmatrix} \begin{smallmatrix} ab \\ [k] \end{smallmatrix} > = 1. \quad (9.89)$$

Taking the above equations into account it is easy to find a Weyl spinor irreducible representation for d-dimensional space, with d even or odd. (We advise the reader to see Ref. [16].)

For d even, we simply set the starting state as a product of d/2, let us say, only nilpotents $\begin{smallmatrix} ab \\ (k) \end{smallmatrix}$ for $d = 2(2n+1)$, Eq. (9.57), or nilpotents and one projector, Eq. (9.58), for $d = 4n$, one for each S^{ab} of the Cartan subalgebra elements (Eq. (9.84)), applying it on the vacuum state, Eq. (9.62). Then the generators S^{ab} , which do not belong to the Cartan subalgebra, applied to the starting state from the left hand side, generate all the members of one Weyl spinor.

$$\begin{aligned} & \begin{smallmatrix} 0d & 12 & 35 & d-1 & d-2 \\ (k_{0d}) & (k_{12}) & (k_{35}) & \cdots & (k_{d-1} & d-2) \end{smallmatrix} |\psi_{oc} >, \\ & \begin{smallmatrix} 0d & 12 & 35 & d-1 & d-2 \\ [-k_{0d}] & [-k_{12}] & (k_{35}) & \cdots & (k_{d-1} & d-2) \end{smallmatrix} |\psi_{oc} >, \\ & \begin{smallmatrix} 0d & 12 & 35 & d-1 & d-2 \\ [-k_{0d}] & (k_{12}) & [-k_{35}] & \cdots & (k_{d-1} & d-2) \end{smallmatrix} |\psi_{oc} >, \\ & \vdots \\ & \begin{smallmatrix} 0d & 12 & 35 & d-1 & d-2 \\ (k_{0d}) & [-k_{12}] & [-k_{35}] & \cdots & [-k_{d-1} & d-2] \end{smallmatrix} |\psi_{oc} >, \\ & \text{for } d = 2(2n+1), \quad n = \text{positive integer}. \end{aligned} \quad (9.90)$$

$$\begin{aligned}
& \begin{matrix} 0d & 12 & 35 & & d-1 & d-2 \\ (k_{0d})(k_{12})(k_{35}) \cdots [k_{d-1} & d-2] \end{matrix} |\psi_{oc} >, \\
& \begin{matrix} 0d & 12 & 35 & & d-1 & d-2 \\ [-k_{0d}][-k_{12}](k_{35}) \cdots [k_{d-1} & d-2] \end{matrix} |\psi_{oc} >, \\
& \begin{matrix} 0d & 12 & 35 & & d-1 & d-2 \\ [-k_{0d}](k_{12})[-k_{35}] \cdots [k_{d-1} & d-2] \end{matrix} |\psi_{oc} >, \\
& \vdots \\
& \begin{matrix} 0d & 12 & 35 & & d-1 & d-2 \\ (k_{0d})[-k_{12}][-k_{35}] \cdots [k_{d-1} & d-2] \end{matrix} |\psi_{oc} >, \\
& \text{for } d = 4n, \quad n = \text{positive integer}.
\end{aligned} \tag{9.91}$$

9.5.1 Technique to generate "families" of spinor representations in terms of Clifford algebra objects

When all 2^d states are considered as a Hilbert space, we found in this paper that for d even there are $2^{d/2-1}$ "families members" and $2^{d/2-1}$ "families" of spinors, which can be second quantized. (The reader is advised to see also Ref. [2,26,16,17,27,9].) We shall pay attention on only even d .

One Weyl representation form a left ideal with respect to the multiplication with the Clifford algebra objects. We proved in Ref. [9], and the references therein that there is the application of the Clifford algebra object from the right hand side, which generates "families" of spinors.

Right multiplication with the Clifford algebra objects namely transforms the state with the quantum numbers of one "family member" belonging to one "family" into the state of the same "family member" (into the same state with respect to the generators S^{ab} when the multiplication from the left hand side is performed) of another "family".

We defined in Ref.[17] the Clifford algebra objects $\tilde{\gamma}^a$'s as operations which operate formally from the left hand side (as γ^a 's do) on any Clifford algebra object A as follows

$$\tilde{\gamma}^a A = i(-)^{(A)} A \gamma^a, \tag{9.92}$$

with $(-)^{(A)} = -1$, if A is an odd Clifford algebra object and $(-)^{(A)} = 1$, if A is an even Clifford algebra object.

Then it follows, in accordance with Eqs. (9.17, 9.18, 9.19), that $\tilde{\gamma}^a$ obey the same Clifford algebra relation as γ^a .

$$(\tilde{\gamma}^a \tilde{\gamma}^b + \tilde{\gamma}^b \tilde{\gamma}^a) A = -ii((-)^{(A)})^2 A (\gamma^a \gamma^b + \gamma^b \gamma^a) = I \cdot 2\eta^{ab} A \tag{9.93}$$

and that $\tilde{\gamma}^a$ and γ^a anticommute

$$(\tilde{\gamma}^a \gamma^b + \gamma^b \tilde{\gamma}^a) A = i(-)^{(A)} (-\gamma^b A \gamma^a + \gamma^b A \gamma^a) = 0. \tag{9.94}$$

We may write

$$\{\tilde{\gamma}^a, \gamma^b\}_+ = 0, \quad \text{while} \quad \{\tilde{\gamma}^a, \tilde{\gamma}^b\}_+ = I \cdot 2\eta^{ab}. \tag{9.95}$$

One accordingly finds

$$\begin{aligned}\tilde{\gamma}^a{}^{ab}(k) &:= -i(k) \gamma^a = -i\eta^{aa}{}^{ab}(k), & \tilde{\gamma}^b{}^{ab}(k) &:= -i(k) \gamma^b = -k(k), \\ \tilde{\gamma}^a{}^{ab}(k) &:= i(k) \gamma^a = i(k), & \tilde{\gamma}^b{}^{ab}(k) &:= i(k) \gamma^b = -k\eta^{aa}{}^{ab}(k).\end{aligned}\quad (9.96)$$

If we define

$$\tilde{S}^{ab} = \frac{i}{4} [\tilde{\gamma}^a, \tilde{\gamma}^b] = \frac{1}{4} (\tilde{\gamma}^a \tilde{\gamma}^b - \tilde{\gamma}^b \tilde{\gamma}^a), \quad (9.97)$$

it follows

$$\tilde{S}^{ab} A = A \frac{1}{4} (\gamma^b \gamma^a - \gamma^a \gamma^b), \quad (9.98)$$

manifesting accordingly that \tilde{S}^{ab} fulfil the Lorentz algebra relation as S^{ab} do. Taking into account Eq. (9.92), we further find

$$\{\tilde{S}^{ab}, S^{ab}\}_- = 0, \quad \{\tilde{S}^{ab}, \gamma^c\}_- = 0, \quad \{S^{ab}, \tilde{\gamma}^c\}_- = 0. \quad (9.99)$$

One also finds

$$\begin{aligned}\{\tilde{S}^{ab}, \Gamma\}_- &= 0, \quad \{\tilde{\gamma}^a, \Gamma\}_- = 0, \quad \text{for } d \text{ even,} \\ \Gamma^{(d)} &:= (i)^{d/2} \prod_a (\sqrt{\eta^{aa}} \gamma^a), \quad \text{if } d = 2n,\end{aligned}\quad (9.100)$$

where handedness Γ ($\{\Gamma, S^{ab}\}_- = 0$) is a Casimir of the Lorentz group, which means that in d even transformation of one "family" into another with either \tilde{S}^{ab} or $\tilde{\gamma}^a$ leaves handedness Γ unchanged.

We advise the reader also to read [2] where the two kinds of Clifford algebra objects follow as two different superpositions of a Grassmann coordinate and its conjugate momentum.

We present for \tilde{S}^{ab} some useful relations

$$\begin{aligned}\tilde{S}^{ab}{}^{ab}(k) &= \frac{k}{2}{}^{ab}(k), & \tilde{S}^{ab}{}^{ab}(k) &= -\frac{k}{2}{}^{ab}(k), & \tilde{S}^{ac}{}^{ab\,cd}(k)(k) &= \frac{i}{2}\eta^{aa}\eta^{cc}{}^{ab\,cd}(k)[k], \\ \tilde{S}^{ac}{}^{ab\,cd}(k)[k] &= -\frac{i}{2}{}^{ab\,cd}(k)(k), & \tilde{S}^{ac}{}^{ab\,cd}(k)[k] &= -\frac{i}{2}\eta^{aa}{}^{ab\,cd}(k)(k), & \tilde{S}^{ac}{}^{ab\,cd}(k)(k) &= \frac{i}{2}\eta^{cc}{}^{ab\,cd}(k)[k].\end{aligned}\quad (9.101)$$

We transform the state of one "family" to the state of another "family" by the application of \tilde{S}^{ac} (formally from the left hand side) on a state of the first "family" for a chosen a, c . To transform all the states of one "family" into states of another "family", we apply \tilde{S}^{ac} to each state of the starting "family". It is, of course, sufficient to apply \tilde{S}^{ac} to only one state of a "family" and then use generators of the Lorentz group (S^{ab}) to generate all the states of one Dirac spinor d -dimensional space.

One must notice that nilpotents ${}^{ab}(k)$ and projectors ${}^{ab}[k]$ are eigenvectors not only of the Cartan subalgebra S^{ab} but also of \tilde{S}^{ab} . Accordingly only \tilde{S}^{ac} , which

do not carry the Cartan subalgebra indices, cause the transition from one "family" to another "family".

The starting state of Eq. (9.90) can change, for example, to

$$[k_{0d}]^{0d} [k_{12}]^{12} [k_{35}]^{35} \cdots [k_{d-1, d-2}]^{d-1, d-2}, \quad (9.102)$$

if \tilde{S}^{01} was chosen to transform the Weyl spinor of Eq. (9.90) to the Weyl spinor of another "family".

References

1. N. Mankoč Borštnik, "Spin connection as a superpartner of a vielbein", *Phys. Lett. B* **292** (1992) 25-29.
2. N. Mankoč Borštnik, "Spinor and vector representations in four dimensional Grassmann space", *J. of Math. Phys.* **34** (1993), 3731-3745.
3. N.S. Mankoč Borštnik, "Spin-charge-family theory is offering next step in understanding elementary particles and fields and correspondingly universe", Proceedings to the Conference on Cosmology, Gravitational Waves and Particles, IARD conferences, Ljubljana, 6-9 June 2016, The 10th Biennial Conference on Classical and Quantum Relativistic Dynamics of Particles and Fields, *J. Phys.: Conf. Ser.* **845** 012017 [arXiv:1409.4981, arXiv:1607.01618v2].
4. N.S. Mankoč Borštnik, "Matter-antimatter asymmetry in the *spin-charge-family* theory", *Phys. Rev. D* **91** 065004 (2015) [arxiv:1409.7791].
5. N.S. Mankoč Borštnik, D. Lukman, "Vector and scalar gauge fields with respect to $d = (3 + 1)$ in Kaluza-Klein theories and in the *spin-charge-family* theory", *Eur. Phys. J. C* **77** (2017) 231.
6. N.S. Mankoč Borštnik, "The *spin-charge-family* theory explains why the scalar Higgs carries the weak charge $\pm \frac{1}{2}$ and the hyper charge $\mp \frac{1}{2}$ ", Proceedings to the 17th Workshop "What comes beyond the standard models", Bled, 20-28 of July, 2014, Ed. N.S. Mankoč Borštnik, H.B. Nielsen, D. Lukman, DMFA Založništvo, Ljubljana December 2014, p.163-82 [arXiv:1502.06786v1] [http://arxiv.org/abs/1409.4981].
7. N.S. Mankoč Borštnik N S, "The spin-charge-family theory is explaining the origin of families, of the Higgs and the Yukawa couplings", *J. of Modern Phys.* **4** (2013) 823 [arxiv:1312.1542].
8. N.S. Mankoč Borštnik, H.B.F. Nielsen, "The spin-charge-family theory offers understanding of the triangle anomalies cancellation in the standard model", *Fortschritte der Physik, Progress of Physics* (2017) 1700046.
9. N.S. Mankoč Borštnik, "The explanation for the origin of the Higgs scalar and for the Yukawa couplings by the *spin-charge-family* theory", *J. of Mod. Physics* **6** (2015) 2244-2274, http://dx.org./10.4236/jmp.2015.615230 [http://arxiv.org/abs/1409.4981].
10. G. Bregar and N.S. Mankoč Borštnik, "Does dark matter consist of baryons of new stable family quarks?", *Phys. Rev. D* **80**, 083534 (2009) 1-16.
11. N.S. Mankoč Borštnik, H.B.F. Nielsen, "Fermionization in an Arbitrary Number of Dimensions", Proceedings to the 18th Workshop "What comes beyond the standard models", Bled, 11-19 of July, 2015, Ed. N.S. Mankoč Borštnik, H.B. Nielsen, D. Lukman, DMFA Založništvo, Ljubljana December 2015, p. 111-128 [http://arxiv.org/abs/1602.03175].
12. N. S. Mankoč Borštnik, H.B. Nielsen, "Fermionization, Number of Families", Proceedings to the 20th Workshop "What comes beyond the standard models", Bled, 9-17 of July, 2017, Ed. N.S. Mankoč Borštnik, H.B. Nielsen, D. Lukman, DMFA Založništvo, Ljubljana, December 2017, p.232-257.

13. H. Aratyn, H.B. Nielsen, "Constraints On Bosonization In Higher Dimensions", NBI-HE-83-36, Conference: C83-10-10.2 (Ahrenshoop Sympos.1983:0260), p.0260 Proceedings.
14. H.B. Nielsen, M. Ninomya, "Dirac sea for bosons, I,II", Progress of the theoretical Physics, **113**, 606 [hep-th/0410218].
15. D. Lukman, N.S. Mankoč Borštnik, "Representations in Grassmann space", to appear in arxiv.
16. N.S. Mankoč Borštnik, H.B.F. Nielsen, *J. of Math. Phys.* **43**, 5782 (2002) [hep-th/0111257].
17. N.S. Mankoč Borštnik, H.B.F. Nielsen, *J. of Math. Phys.* **44** 4817 (2003) [hep-th/0303224].
18. N.S. Mankoč Borštnik and H.B. Nielsen, *Phys. Rev. D* **62**, 044010 (2000) [hep-th/9911032].
19. N.S. Mankoč Borštnik and H.B. Nielsen, "Second quantization of spinors and Clifford algebra objects", Proceedings to the 8th Workshop "What Comes Beyond the Standard Models", Bled, July 19 - 29, 2005, Ed. by Norma Mankoč Borštnik, Holger Bech Nielsen, Colin Froggatt, Dragan Lukman, DMFA Založništvo, Ljubljana December 2005, p.63-71, hep-ph/0512061.
20. "Why nature made a choice of Clifford and not Grassmann coordinates", Proceedings to the 20th Workshop "What comes beyond the standard models", Bled, 9-17 of July, 2017, Ed. N.S. Mankoč Borštnik, H.B. Nielsen, D. Lukman, DMFA Založništvo, Ljubljana, December 2017, p. 89-120 [arXiv:1802.05554v1v2].
21. N.S. Mankoč Borštnik and H.B.F. Nielsen, "Discrete symmetries in the Kaluza-Klein theories", *JHEP* 04:165, 2014 [arXiv:1212.2362].
22. P.A.M. Dirac *Proc. Roy. Soc. (London)*, **A 117** (1928) 610.
23. D. Lukman, N.S. Mankoč Borštnik and H.B. Nielsen, "An effective two dimensionality cases bring a new hope to the Kaluza-Klein-like theories", *New J. Phys.* 13:103027, 2011.
24. D. Lukman and N.S. Mankoč Borštnik, "Spinor states on a curved infinite disc with non-zero spin-connection fields", *J. Phys. A: Math. Theor.* 45:465401, 2012 [arxiv:1205.1714, arxiv:1312.541, hep-ph/0412208 p.64-84].
25. D. Lukman, N.S. Mankoč Borštnik and H.B. Nielsen, "Families of spinors in $d = (1 + 5)$ with a zweibein and two kinds of spin connection fields on an almost S^2 ", Proceedings to the 15th Workshop "What comes beyond the standard models", Bled, 9-19 of July, 2012, Ed. N.S. Mankoč Borštnik, H.B. Nielsen, D. Lukman, DMFA Založništvo, Ljubljana December 2012, 157-166, arxiv.1302.4305.
26. A. Borštnik Bračič, N. Mankoč Borštnik, "The approach Unifying Spins and Charges and Its Predictions", Proceedings to the Euroconference on Symmetries Beyond the Standard Model", Portorož, July 12 - 17, 2003, Ed. by Norma Mankoč Borštnik, Holger Bech Nielsen, Colin Froggatt, Dragan Lukman, DMFA Založništvo, Ljubljana December 2003, p. 31-57, hep-ph/0401043, hep-ph/0401055.
27. A. Borštnik Bračič, N. S. Mankoč Borštnik, "On the origin of families of fermions and their mass matrices", hep-ph/0512062, *Phys. Rev. D* **74** 073013-28 (2006).
28. M. Pavšič, "Quantized fields á la Clifford and unification" [arXiv:1707.05695].



10 Do We Find High Energy Physics Inside (Almost) Every Solid or Fluid at Low Temperature?

H.B. Nielsen^a and M. Ninomiya^b

^aNiels Bohr Institute, University of Copenhagen,
17 Blegdamsvej, DK 2100 Copenhagen ϕ , Denmark

^bAdvanced Mathematical Institute Osaka-city University, Sugimoto 3-3-138, Sumiyoshi-ku
Osaka, 1558-8585, Japan
and Yukawa Institute for Theoretical Physics, Kyoto University Kyoto. 606-8502, Japan

Abstract. It is an old idea of ours (H. B. Nielsen “Dual Models”, section 6 “Catastrophe Theory Program”, Scottish University Summer School, 1976) that a most general material with only translation symmetry, but otherwise no symmetries should generically (in general) have some small regions in quasi momentum space, where you “see” an approximate Weyl equation behavior. The Weyl equation is the relativistic equation for a (left handed) neutrino. This remark means that one could imagine, that there were behind the Standard Model of High energy physics, a very general crystal model with very little symmetry. Even for the Yang Mills or electrodynamics types fields a similar philosophy is possible. There are though some problems with this solid-state type of model beyond the Standard model, for which we thought have some remedy by means of homolumo gap effects.

By making use of relativistic quantum field theory on the lattice we predicted theoretically very high magneto-conduction due to Adler-Bell-Jackiw chiral anomaly effect – so called Nielsen-Ninomiya effect (or mechanism) in gapless parity violating material. Nowadays this kind of material such as chiral or Weyl semimetal and the effect are detected by experiments.

Povzetek. Avtorja obravnavata idejo HBN (H. B. Nielsen “Dual Models”, razdelek 6 “Catastrophe Theory Program”, Scottish University Summer School, 1976), da obstajajo v najbolj splošnem modelu za snov, ki ima le translacijsko simetrijo, majhna območja v prostoru kvazi gibalne količine, v katerih približno velja Weylova enačba. Ker velja Weylova enačba za relativistično gibanje (levoročnih) nevtrinov, predlagata, da razširjeni standardni model gledamo kot zelo splošen model za kristal z zelo malo simetrijami. Podoben pristop uporabita za primer elektromagnetnega polja in vsa Yang-Millsova polja. Težave, ki se pri tem pojavijo, omilita s “homo-lumo” vrzeli.

Uporaba relativistične kvantne teorije polja na rešetki napove visoko magnetno prevodnost, ki jo sproži kiralna anomalija Adler-Bell-Jackiwa, ter s tem pojav Nielsen-Ninomiye: visoko magnetno prevodnost v snoveh, ki kršijo parnost, med obema pasovoma pa ni vrzeli. Te lastnosti materialov merijo v Weylovih (kiralnih) polkovinah.

Keywords: Weyl equation, homo-lumo gap

Introduction

The authors, in particular H. B. N. have through many years the dream, that it is not important what the (most) fundamental laws of Nature might be, because almost certainly the same effective laws would come out anyway: This philosophy is called “Random Dynamics”.

Inside a piece of matter - crystal, glass, ... - one should then at very low temperature according to this dream find the Standard Model.

Recently one is about to find Cases of Relativity-behaving Quasi-particles: A material, e.g. graphene, with such simulations of relativistic particles as we talk about.

Materials with relativistic particles simulated as quasiparticles may be very applicable to say high conductivity purposes,...

Some of our publications:

- H. B. Nielsen and M. Ninomiya, “No Go Theorem for Regularizing Chiral Fermions,” Phys. Lett. **105B**, 219 (1981).
- H. B. Nielsen and M. Ninomiya, “Absence of Neutrinos on a Lattice, 1. Proof by homotopy theory” Nucl. Phys. B **185**, 20 (1981).
- H. B. Nielsen and M. Ninomiya, “Absence of Neutrinos on a Lattice. 2. Intuitive Topological Proof,” Nucl. Phys. B **193**, 173 (1981).
- As for the initiation of Random Dynamics, See “Fundamentals of Quark Models”. Proceedings: 17th Scottish Universities Summer School in Physics, St. Andrews, Aug 1976, I.M. Barbour, A.T. Davies (Glasgow U.); 1977 - 588 pages; Edinburgh: SUSSP Publ. (1977); Conference: C76-08-01; Contributions: Dual Strings, Holger Bech Nielsen (Bohr Inst.). Aug 1974, 71 pp.; NBI-HE-74-15 In the last section the idea of “Random Dynamics ” is introduced based on finding Weyl equation in “whatever”.

The present paper consists as part I and part II.

The part I: Relativity Theory found in solid state.

and

The part II “What comes beyond Topological Insulator – Nielsen-Ninomiya Effect (or Mechanism) due to ABJ Anomaly –”

Part I: Relativity-Theory found in Solid State Physics

I-1 Introduction

I-2 **Automatic:** a pet-thought: Natural laws come by themselves! (“Random Dynamics”)

I-3 **General:** A very general world with (only) momentum conservation.

I-4 **Graphene:** Example Graphene.

I-5 **Heusler:** Half-metals, Heusler compounds.

I-6 **Wang:** Thoughts about making materials having models of relativistic particles inside.

I-7 **Doubling:** Nielsen - Ninomiya theorem about doubling of such relativistic particles unavoidably on the lattice. great future; hope of seeing high energy physics in low temperature materials not out, but not quite finished. material simulates relativistic quantum field theory.

I-8 Further: Further Developments of our “Random Dynamics”

I-9 Conclusion for part I

The part II: What comes beyond Topological Insulator –Nielsen-Ninomiya Effect (or Mechanism) due to ABJ Anomaly

II-1 : Introduction

II-2 : 1+1 dimensional Example

II-3 : 3+1 dimensional case Weyl (or chiral) Fermion Adler-Bell-Jackiw Anomaly

II-4 : Parity non-invariant, Zero-gap material

II-5 : Transfer from Left- to Right- comes by Adler-Bell-Jackiw anomaly

II-6 : Further arguments

II-7 : Conclusions

Appendix A : Necessary properties of quantum field theory in this paper

Appendix B : Adler-Bell-Jackiw anomaly in continuum spacetime

I-2 Automatic

Our Old Work in 1976: Dreams Laws of Nature Automatic

“Dual Strings. Fundamentals of Quark Models.” by H. B. Nielsen, in *Scottish University Summer School in Physics, St. Andrews, 1976* (There H.B.N. still mainly is talked on String theory, but at the end a general (fermion) Hamiltonian is studied.)

Assumed was **translational invariance**, at least with respect to a lattice say, and thus a (quasi) momentum conservation, but with respect to the “**internal degrees of freedom**” there is a **very general** theory, though assuming there being essentially a finite (discrete). system of states (representing possibly spin and band degrees of freedom.).

(Trivial) Generic Considerations on Fermion Dispersion relations (1976).
We ignore all conservation laws except for

- Energy conservation and Hamiltonian development.
- Momentum Conservation.
- Particle (number) conservation.
- Free approximation (first).
- Smoothness, (so that e.g. $\mathbf{H}(\vec{p})$ is differentiable and continuous as function of \vec{p} .)
- Generic: i.e. no fine-tuned values of parameters,

and consider a single particle equation:

$$i \frac{\partial}{\partial t} \psi(\vec{p}, t) = \mathbf{H}(\vec{p}) \psi(\vec{p}), \quad (10.1)$$

where for each value of the momentum \vec{p} the $\mathbf{H}(\vec{p})$ is a Hermitian matrix.

Relativity and Dimensionality of Space time being 3+1 come out Automatically!

A priori - with no fine-tuning (=generically) - the Fermi surface would put itself at separate eigenvalues; but if for some reason (e.g. “homlumo-gap effect”)

the Fermi-level were just where $n = 2$ levels meet, then in a small neighborhood the shape of the dispersion relations would be given by taking $\mathbf{H}(\vec{\mathbf{p}})$ to be $n \times n = 2 \times 2$. We then Taylor expand

$$\mathbf{H}(\vec{\mathbf{p}}) \approx \mathbf{H}(\vec{\mathbf{p}}_0) + \sum_{\alpha, \mu} \sigma^\alpha V_\alpha^\mu p_\mu + \dots \quad (10.2)$$

where σ^α are the Pauli-matrices and the unit matrix $\sigma^0 = \mathbf{1}$. The “vierbein” V_α^μ is a set of expansion coefficients for $\mathbf{H}(\vec{\mathbf{p}})$ as function of the components p_μ (strictly speaking $\mu = 1, 2, 3$; here).

Hermitian matrix, Provided Fermi-level at Degeneracy $n = 2$ leads to Weyl Equation in 3+1 Dimensions.

In the old days we argued that in a general physics universe the **Hubble expansion** would finally lead to the Fermi-level approaching an $n = 2$ degenerate levels energy; but now H. B. N.’s Zagreb group - I. Andric, L. Jonke, D. Jurman, and HBN - have studied in general, what is called “**Homolumo-gap Effect**” meaning the by Jahn and Teller[1] first proposed effect, that the electrons filling the Fermi-sea would back react such as to increase the homolumo gap between the lowest unoccupied (LUMO) and the highest occupied (HOMO) state. This effect goes in the direction to make metals not occur, and make every materials become an insulator, but the gapless semiconductor may be too hard for the homolumo-gap effect to dispense with.

Note that this hope for getting automatically a Weyl-equation like theory had, when using just Hermitean Hamiltonian matrices and looking at the $n = 2$ degeneracy possibility, the consequence that there came only *three* spatial dimensions functioning the relativistic way, because there were only 3 Pauli matrices. Somehow arguing that the dimensions for which there are no Pauli matrices will lead to essentially zero velocity for the fermion/quasi-electron in these directions and that such dimensions will not be observed, we have come to 3+1 dimensions as an additional prediction from the very general starting theory!

With time-reversal symmetry imposed dimension prediction gets modified.

Symmetry	Square	Pauli M.	Dimension	Field
TP	$(\text{TP})^2 = 1$	σ_x, σ_z	2+1	Real
-	-	$\sigma_x, \sigma_y, \sigma_z$	3+1	Complex
TP	$(\text{TP})^2 = -1$	5 of them	5+1	Quaternions

Table 10.1. The symmetry assumed in line 1 and 3 is the combination of time reversal T and parity P to TP, which leaves the momentum $\vec{\mathbf{p}}$ invariant but is an antilinear operator effectively conjugating the complex numbers in the matrix. If then Fermi-level falls at $n = 2$ degenerate levels in addition to the Kramers-Kronig doubling in the 3rd case, one gets by Taylor expanding the 2×2 resolved into Pauli-matrices, and a generalized Weyl equation results corresponding to the in fourth column denote *space + time* dimensions. Actually the effective theory is naturally written in terms of the in column 5 mentioned division-algebra(= field).

Fundamentally in many Dimensions, but in Most dimensions the Fermion Run with Zero Velocity, we Ignore them.

In the for fundamental physics ideal situation of **no extra T or TP symmetry** the Hamiltonian matrix $\mathbf{H}(\vec{p})$ is just a generic (~ random) Hermitian matrix (with complex matrix elements), and it predicts at the two levels degenerate point - hoped to be favored at the Fermi-surface by either Hubble expansion or homolumo-gap-effect - that the Fermion only moves with appreciable velocity in as many spatial dimensions as there are Pauli-matrices. We hope that the dimensions in which the velocity gets zero, can/shall be ignored. If the zero-velocity dimensions are ignored, then we have remarkable agreement:

The number of dimensions in which the generic double degeneracy neighborhood has the fermions move just corresponds to experimental number of dimensions 3+1 and to having relativity and rotational invariance!

If TP (or T) is good symmetry and $(TS)^2 = 1$ then $\mathbf{H}(\vec{p})$ must have real matrix elements.

This is the case in which we in a crystal - with PT symmetry say - **completely ignore** the usual spin as being decoupled so as to be totally ignored.

In this case we get the effective dimensionality, if we ignore the zero-velocity directions:

$$2 + 1$$

This means that the relativistic effective fermion should appear “generically” (automatically) even in only 2 spatial dimensions.

With Genuine Spin= $\frac{1}{2}$ Electrons and Unbroken Time reversal, the “Quaternion Case” If T or TP good symmetries, and spin $\frac{1}{2}$ included, then $T^2 = (TP)^2 = -1$ we have generally doubling of all levels according to Kramers-Kronig rule.[2]

So double degeneracy is already there generally and nothing special. In this case we shall therefore instead consider that we can get 4 times degenerate levels sporadically. If we go to such a 4-times degenerate point in momentum space, we could elegantly go to a quaternion 2×2 matrices (quaternions are writable as 2×2 complex matrices, so that 2×2 quaternion matrices can be equivalent to 4×4 complex matrices with some restriction. Dimension of non-zero velocity directions:

$$5 + 1$$

I-3 Graphene

Graphene denotes the layer of carbon like the ones in graphite taken as separate, i.e. it is 2(space)dimensional material. The quasi electrons running in the graphene layers actually do show dispersion relations behaving how we above argued for the case with time reversal but ignoring the spin leading to the effective space time dimension 2+1.

On the following picture 10.1 one sees the lattice structure of graphene:

The next figure 10.2 is supposed to generally illustrate a metal, an insulator and a material with a Dirac-like quasi particle (on the figure 10.1).

Even just making a two-layer of graphene complicates the situation and the work by Gammelgaard on the next figure 10.3 illustrates a gap appearing:

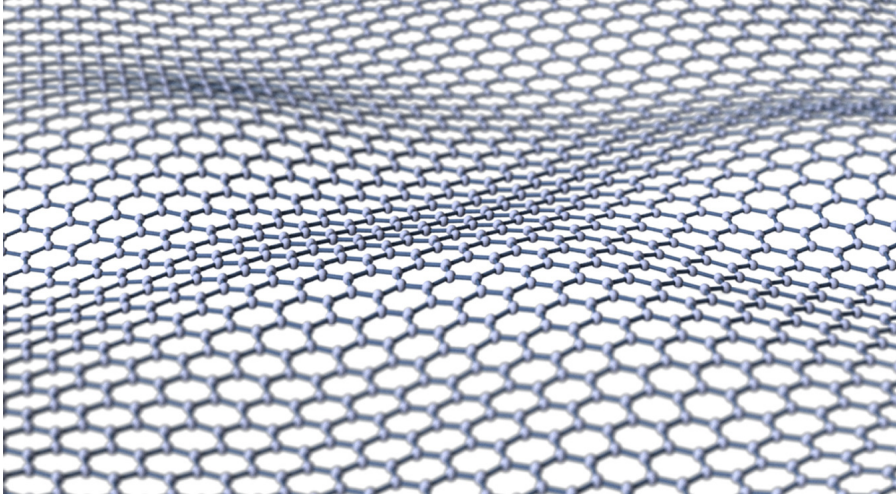


Fig. 10.1. (2+1)-dimensional Example is Graphene.

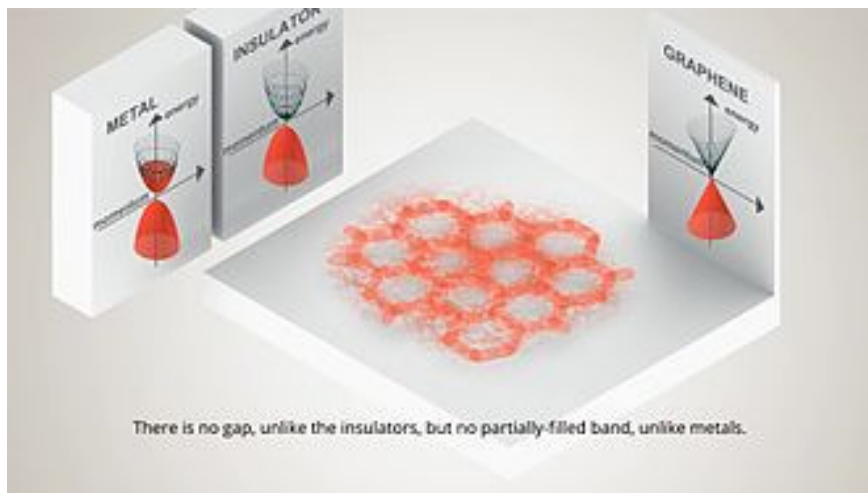


Fig. 10.2.

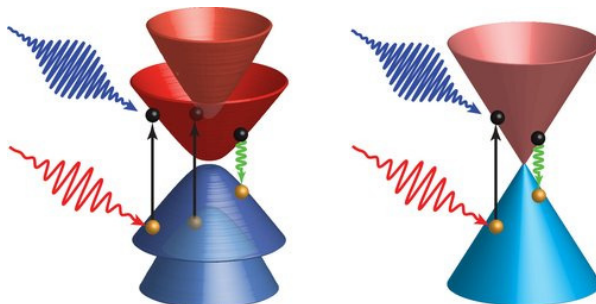


Fig. 10.3. Putting Double Layer Produces Gap.

The left dispersion law is for a double layer of graphene; the right for single layer. (Gammelgaard).

The next figures 10.4 illustrate calculation of the dispersion relations for quasi-electrons in graphene by the model described just below. Since we have a 2 space dimension material the energy can be the orbital direction up in the perspective while the two spatial momentum components form the basis plane of the three-dimensional perspective figure:

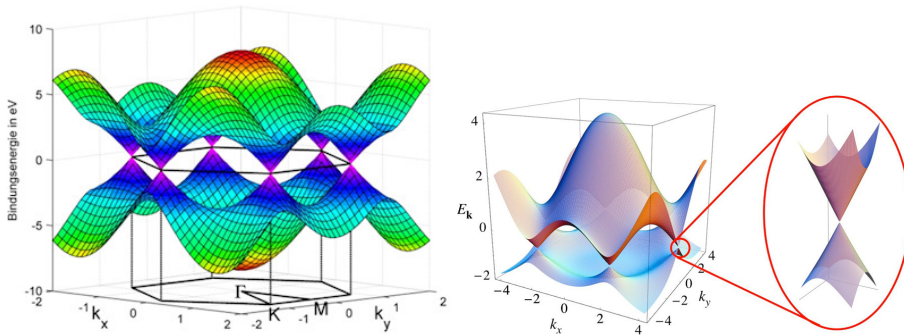


Fig. 10.4. .

The Dirac points are of course the points where two branches of the dispersion relation meet *with a cone shape*. (Fig. 10.5):

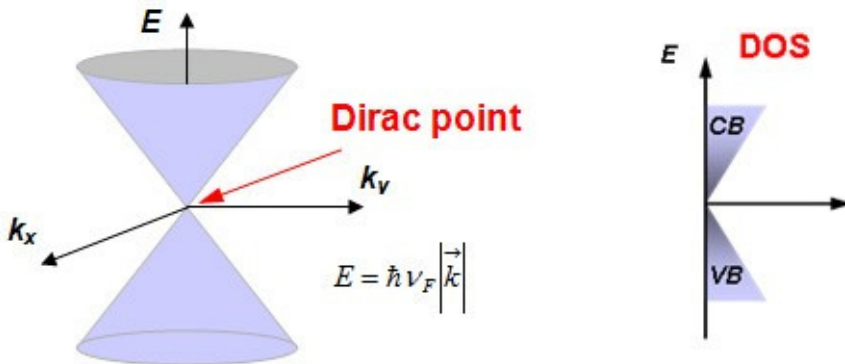


Fig. 10.5.

Dispersion Relation of Graphene The electronic properties of graphene can be described using a simple tight binding model. The electrons in the covalent bonds form deep fully filled valence bands, and thus their effects on the conductivity can be safely disregarded. The unhybridized p orbital is only slightly perturbed by the neighboring atoms. Therefore, the wave function of an electron in the system can be written as a Linear Combination of Atomic Orbitals (LCAO). Using

these orbitals as the basis set to represent the wave function, the Hamiltonian that governs the dynamics of the electron is given by:

$$H = \sum_i \epsilon_i |\psi_i\rangle\langle\psi_i| + \sum_l \sum_{\langle i|j\rangle_l} t_l (|\psi_i\rangle\langle\psi_j| + |\psi_j\rangle\langle\psi_i|) \quad (10.3)$$

where ϵ_i represents the onsite energy at the atom, $|\psi_i\rangle$ the i 'th atomic orbital, $\{\langle i|j\rangle_l\}$ the set of couples of l th-nearest neighbors, and t_l the hopping parameter between them.

In Graphene the Fermi- surface just Lies at the Double degenerate Point

So in graphene by symmetry one really get a simulation of a 2+1 dimensional massless Weyl/Dirac fermion, also w.r.t. the placing of the fermi surface.

If we think of just the generic case of a very general theory there will typically be no reason why the fermi surface should be just at the Weyl point (with the double degeneracy).

We have, however, speculated on two mechanisms, which might make the fermi-surface be driven towards the degeneracy point:

- If the world in question has a strong Hubble expansion, then filled states above the degeneracy point would be gradually emptied and holes below the degeneracy point would be also gradually be expanded away/attenuated.
- "Homolumo-gap-effect" - meaning that the fermions act back onto the various degrees of freedom that can be adjusted in the lattice in which the fermions run. This back action will be so as to in the ground state arrange to lower the energies of filled fermi states. Thereby arise the so called Homolumo-gap, or rather it gets expanded by this back action "homolumo-gap-effect". In the case that we have degeneracy point that is somehow topologically stabilized, as one might say of the Weyl points discussed here, it may not be possible for the homolumo-gap-effect to really produce a gap. In stead we expect that it will only bring the fermi surface to coincide with the degeneracy point; that would namely lower the filled states as much as possible with the "topological ensurance" of the degeneracy point.

I-4 Heusler

Heusler Compound Mn_2CoAl is a Spin Gapless Semiconductor:

Siham Oardi, G.H. Fecher, C. Felser and J. Kübler (arXiv:1210.0148v1 [cond-mat.mtrl-sci], 29 Sep. 2012.) investigated the **Heusler compound Mn_2CoAl** . They gave the article the name **Realization of spin gapless semiconductors: the Heusler compound Mn_2CoAl** .

In halfmetallic ferromagnets you have so to speak metal as far as the electrons with one direction of the spin is concerned, but insulator w.r.t. to the electrons with the opposite spin direction. Now it may further happen that we instead of the metallic we get a gapless semiconductor, namely if we have a degeneracy point as we discussed above. Once there is effectively only one spin of the electron one escapes the time reversal symmetry. Thus in such halfmettals there is a better chance to find Weyl points.

The following figure 10.6 illustrates dispersion relation along a piecewise straight curve in momentum space for the two different spin directions along the magnetization axis for the compound Mn_2CoAl . The dispersion relation for the two different spin orientations are printed respectively red and blue:

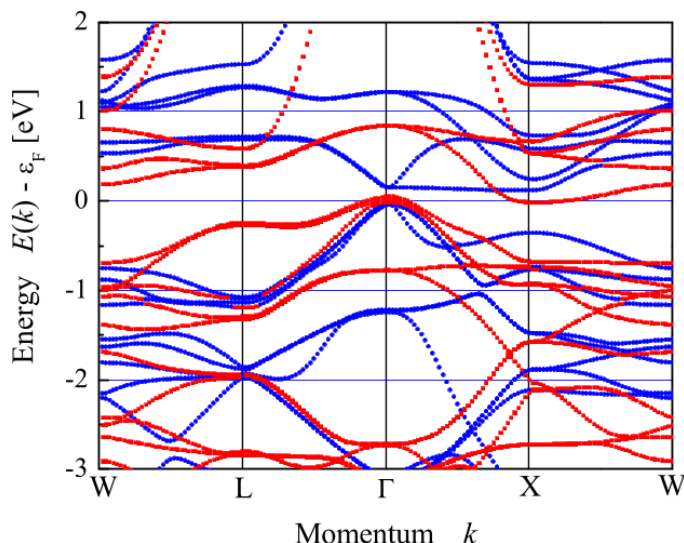


Fig. 10.6. Band structure of Mn_2CoAl , Majority spin red.

In the following figure 10.7 are then as function of temperature given some carrier properties of this material Mn_2CoAl :

On the following page from Lakhani Baisly et al. as figure 7 in their article we see the density of electron levels (DOS) for the two spin orientations separately. In the red shown DOS there can be seen crudely a gap, so for this spin orientation we have the insulator. For the other spin orientation - shown with the positive ordinate pointing upwards there is also a dip at the Fermi level, but now the DOS is going non-zero immediately by going away from the Fermi level. So for this spin we rather have the gapless semiconductor behavior.

The strong dependence of the conductivity as function of the magnetic field is just what one expects due to the Adler-Bell-Jackiw-anomaly-effect described more in part II of the present article below.

These figures are from:

Siham Ouadi et al. "Realization of Spin Gapless Semiconductors: The Heusler Compound Mn_2CoAl " DOI: 10.1103/PhysRevLett.110.100401.

Zero Gap Material with Quadratic Energy Dispersion (this is by fine tuning) HgTe is one of the few materials wherein this **quadratic dispersion law zero gap has been found, since 1950's.**

$\text{Pb}_{1-x}\text{Sn}_x\text{Te}$, $\text{Pb}_{1-x}\text{Sn}_x\text{Se}$ and $\text{Bi}_x\text{Sb}_{1-x}$ are zero-gap materials (with quadratic disp.).

But really one - Wang, Dou, and Zhang - expects that all narrow gap semiconductors by some doping or pressure could be tuned to have zero gap (with

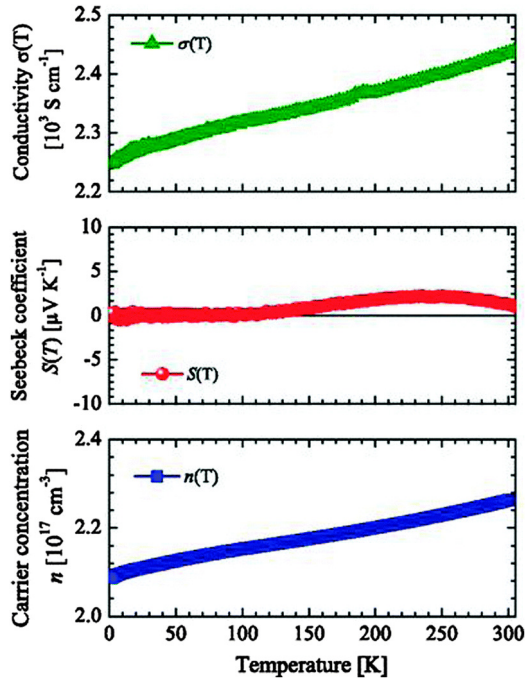


Fig. 10.7. Majority spin and Minority spin. Calculated with spin orbit coupling.

quadratic dispersion law). Then they call for finding a non-toxic material of this kind.

I-5 Wang

Physical Chemistry; Chemical Physics

Controllable electronic and magnetic properties in a two-dimensional germanene heterostructure Run-wu Zhang, Wei-xiao Ji, Chang-wen Zhang,* Sheng-shi Li,^b Ping Li, Pei-ji Wang, Feng Lia and Miao-juan Rena Author affiliations

Abstract

The control of spin without a magnetic field is one of the challenges in developing spintronic devices. Here, based on first-principles calculations, we predict a new kind of ferromagnetic half-metal (HM) with a Curie temperature of 244 K in a two-dimensional (2D) germanene Van der Waals heterostructure (HTS). Its electronic band structures and magnetic properties can be tuned with respect to external strain and electric field. More interestingly, a transition from HM to bipolar-magnetic-semiconductor (BMS) to spin-gapless-semiconductor (SGS) in a HTS can be realized by adjusting the interlayer spacing. These findings provide a promising platform for 2D germanene materials, which hold great potential for application in nanoelectronic and spintronic devices.

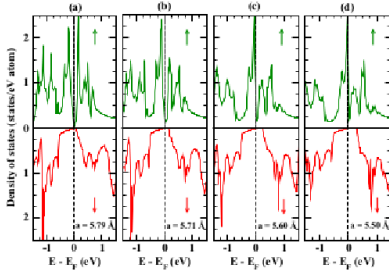


FIG. 7. (Color online) CFCG DOS versus $a(\text{\AA})$: (a) 5.79 (a_{opt}), (b) 5.71, (c) 5.60, and (d) 5.50.

of the half-metallic Co_2FeSi ($\approx 200 \text{ S/cm}$ at 300 K) [18] and Co_2MnAl ($\approx 2000 \text{ S/cm}$) [19].

IV. ELECTRONIC-STRUCTURE CALCULATIONS

To further investigate the electronic properties of CFCG, we have performed first-principles electronic-structure calculations using spin-polarized density functional theory, as employed in Vienna *ab initio* simulation package (VASP) [20] based on a projected-augmented wave basis [21]. The exchange-correlation functional was based on the generalized gradient approximation (GGA). A $16 \times 16 \times 16$ Monkhorst-Pack k -point mesh was used for the Brillouin zone integration. We have used a plane-wave cutoff of 340 eV with the convergence criteria of 0.1 meV/cell (10 kbar) for energy (stress).

The prototype of a quaternary Heusler with the composition $XX'YZ$ and space group $F\bar{4}3m$ (216) is LiMgPdSn . There are four nonequivalent configurations based on the occupation of various Wyckoff sites by different constituent elements. From the total energy calculations we found the configuration with Co at $X(0,0,0)$, Fe at $X'(1/2,1/2,1/2)$, Cr at $Y(1/4,1/4,1/4)$, and Ga at $Z(3/4,3/4,3/4)$ to be the most stable.

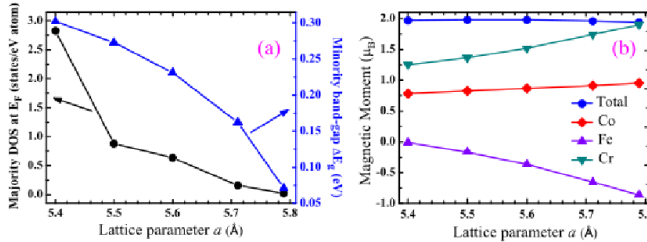


FIG. 8. (Color online) For CFCG, versus a the (a) DOS at E_F in the majority-spin state (left-hand scale) and band gap in the minority-spin state (right-hand scale) and (b) total and site magnetic moments.

045201-4

Fig. 10.8.

The spin-resolved dispersion and density of states (DOS) of CFCG in the most stable configuration with experimental lattice parameter ($a_{\text{exp}} = 5.79 \text{\AA}$) are shown in Fig. 6. A closed band-gap character in the majority-spin state and a small open band gap (near the Fermi energy, E_F) in the minority-spin state suggest CFCG to behave as a spin gapless semiconductor. The valence band maximum for the minority-spin state is slightly above E_F , yielding a negligibly small DOS at E_F (≈ 0.01 states/eV/atom), which arises from mixed contributions of d bands from Co, Fe, and Cr. Though the DOS plot apparently shows a clear gap near E_F in the minority channel, it is actually a disrupted energy gap as the values of DOS are not exactly zero (~ 0.003 states/eV/atom just above E_F) but negligibly small. With this consideration, we find a small band gap of ~ 0.07 eV in the minority-spin states. A careful analysis of various bands crossing the E_F for the minority-spin state (right panel) indicates that such small DOS at E_F arises mainly from three bands, two of which are degenerate and are composed of $\sim 54\%$ Co and $\sim 46\%$ Fe d_{xy} subband characters (i.e., $d_{x^2-y^2}$ and d_{3z^2-1}). The third band is contributed almost equally by t_{2g} subbands (i.e., d_{xy} , d_{yz} , and d_{zx}) of Co (35%), Fe (29%), and Cr (32%).

Notably, some other Ga-based Heusler alloys [7,22,23] have also been shown to have similar bands crossing the Fermi level in the minority-spin states with very small values of DOS near E_F . These materials are predicted to be half-metallic, i.e., semiconducting in the minority-spin channel as in our case (with a negligibly small DOS at E_F) and metallic in the majority-spin channel.

To study the behavior of CFCG under pressure, we have calculated DOS in the most stable configuration versus lattice parameters below a_{exp} , which are plotted in Fig. 7. Notably, the behavior of CFCG changes from SGS to half-metallic with the decrease of the lattice parameter. In the majority-spin state, the DOS at E_F increases significantly from almost zero value at a_{exp} to a finite value (under pressure); see Fig. 8(a). In addition, the band gap (ΔE_g) at E_F in the minority-spin state increases with lattice parameters decreasing below a_{exp} , indicating the collective effect of transition. The majority DOS at E_F and ΔE_g with varying lattice parameters are shown in Fig. 8(a).

Figure 8(b) shows the variation of total magnetic moment per formula unit and the individual atomic magnetic moments

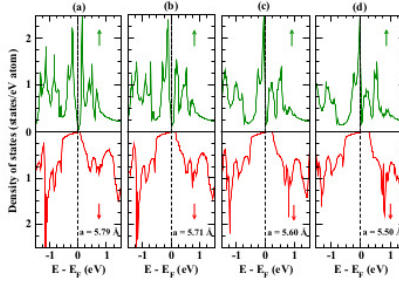


FIG. 7. (Color online) CF CG DOS versus $a(\text{\AA})$: (a) 5.79 (a_{exp}), (b) 5.71, (c) 5.60, and (d) 5.50.

of the half-metallic Co_2FeSi ($\approx 200 \text{ S/cm}$ at 300 K) [18] and Co_2MnAl ($\approx 2000 \text{ S/cm}$) [19].

IV. ELECTRONIC-STRUCTURE CALCULATIONS

To further investigate the electronic properties of CF CG, we have performed first-principles electronic-structure calculations using spin-polarized density functional theory, as employed in Vienna *ab initio* simulation package (VASP) [20] based on a projected-augmented wave basis [21]. The exchange-correlation functional was based on the generalized gradient approximation (GGA). A $16 \times 16 \times 16$ Monkhorst-Pack k -point mesh was used for the Brillouin zone integration. We have used a plane-wave cutoff of 340 eV with the convergence criteria of 0.1 meV/cell (10 kbar) for energy (stress).

The prototype of a quaternary Heusler with the composition XX'YZ and space group $F\bar{4}3m$ (216) is LiMgPdSn . There are four nonequivalent configurations based on the occupation of various Wyckoff sites by different constituent elements. From the total energy calculations we found the configuration with Co at $X(0,0,0)$, Fe at $X'(1/2,1/2,1/2)$, Cr at $Y(1/4,1/4,1/4)$, and Ga at $Z(3/4,3/4,3/4)$ to be the most stable.

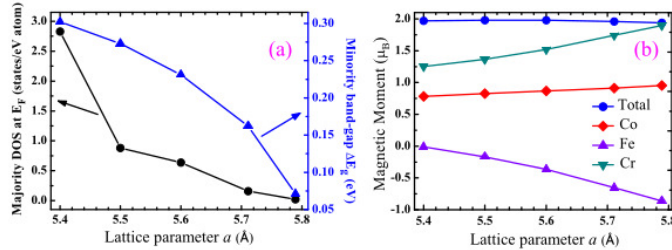


FIG. 8. (Color online) For CF CG, versus a the (a) DOS at E_F in the majority-spin state (left-hand scale) and band gap in the minority-spin state (right-hand scale) and (b) total and site magnetic moments.

The spin-resolved dispersion and density of states (DOS) of CF CG in the most stable configuration with experimental lattice parameter ($a_{\text{exp}} = 5.79 \text{\AA}$) are shown in Fig. 6. A closed band-gap character in the majority-spin state and a small open band gap (near the Fermi energy, E_F) in the minority-spin state suggest CF CG to behave as a spin gapless semiconductor. The valence band maximum for the minority-spin state is slightly above E_F , yielding a negligibly small DOS at E_F (≈ 0.011 states/eV/atom), which arises from mixed contributions of d bands from Co, Fe, and Cr. Though the DOS plot apparently shows a clear gap near E_F in the minority channel, it is actually a disrupted energy gap as the values of DOS are not exactly zero (~ 0.003 states/eV/atom just above E_F) but negligibly small. With this consideration, we find a small band gap of ~ 0.07 eV in the minority-spin states. A careful analysis of various bands crossing the E_F for the minority-spin state (right panel) indicates that such small DOS at E_F arises mainly from three bands, two of which are degenerate and are composed of $\sim 54\%$ Co and $\sim 46\%$ Fe e_g subband characters (i.e., $d_{x^2-y^2}$ and d_{3z^2-1}). The third band is contributed almost equally by t_{2g} subbands (i.e., d_{xy} , d_{yz} , and d_{zx}) of Co (35%), Fe (29%), and Cr (32%).

Notably, some other Ga-based Heusler alloys [7,22,23] have also been shown to have similar bands crossing the Fermi level in the minority-spin states with very small values of DOS near E_F . These materials are predicted to be half-metallic, i.e., semiconducting in the minority-spin channel as in our case (with a negligibly small DOS at E_F) and metallic in the majority-spin channel.

To study the behavior of CF CG under pressure, we have calculated DOS in the most stable configuration versus lattice parameters below a_{exp} , which are plotted in Fig. 7. Notably, the behavior of CF CG changes from SGS to half-metallic with the decrease of the lattice parameter. In the majority-spin state, the DOS at E_F increases significantly from almost zero value at a_{exp} to a finite value (under pressure); see Fig. 8(a). In addition, the band gap (ΔE_g) at E_F in the minority-spin state increases with lattice parameters decreasing below a_{exp} , indicating the collective effect of transition. The majority DOS at E_F and ΔE_g with varying lattice parameters are shown in Fig. 8(a).

Figure 8(b) shows the variation of total magnetic moment per formula unit and the individual atomic magnetic moments

Fig. 10.9. Hall conductivity as function of magnetic field.

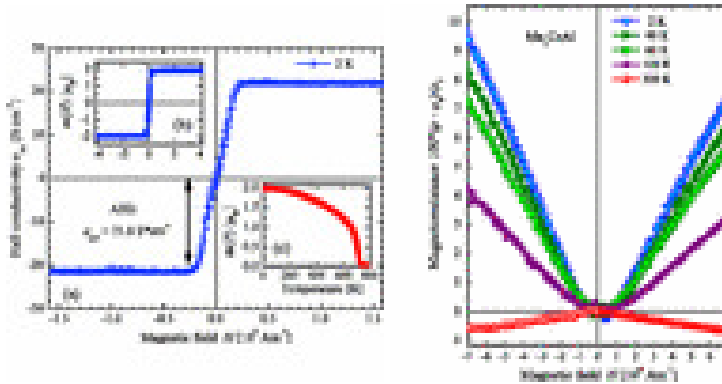


Fig. 10.10. Magnetoresistance as function of a magnetic field.

I-6 Doubling

Nielsen-Ninomiya's No-go theorem

The authors are very proud of, that we have shown a theorem saying:

When one makes the mentioned “relativistic fermions of Weyl-type” (=chirale fermion) on a lattice (so e.g. in a crystal) then you always get equally many right-spinning and left-spinning Weyl-type particle(species).

This theorem is a great challenge for those wanting to make a lattice model (with calculational purposes) for a theory with massless (or almost massless) quarks, let alone the Standard Model.

By having 3 K +3 K' Dirac-points of Compensating Handedness Our Doubling Theorem Realized in Graphene.

I-7 ABJ Anomaly

In the article

H. B. Nielsen and M. Ninomiya, “Adler-Bell-Jackiw Anomaly And Weyl Fermions In Crystal,” Phys. Lett. 130B, 389 (1983). doi:10.1016/0370-2693(83)91529-0

we have put forward how to understand intuitively the Adler-Bell-Jackiw anomaly and how it should be possible to see it in crystals. Indeed now it has -presumably- been found in Na_3Sb in its three dimensional form; at least the characteristic property that this anomaly can lead to a negative magnetoresistance seems justified for this material as should be seen from the following figure 10.12: It is clearly seen for the low temperatures that there is a dramatic peak in the resistance when the magnetic field is small, whereas the resistance becomes appreciably smaller when the magnetic field is switched on. The lower of the two figures shows the resistance in the direction of the magnetic field. It is indeed important that this increased conductivity goes in the direction of the magnetic field and thus there is a dependence of the magnetoresistance as a function also of the angle between the magnetic field and the direction of the electric field.

This subject will be explained in more detail in part II.

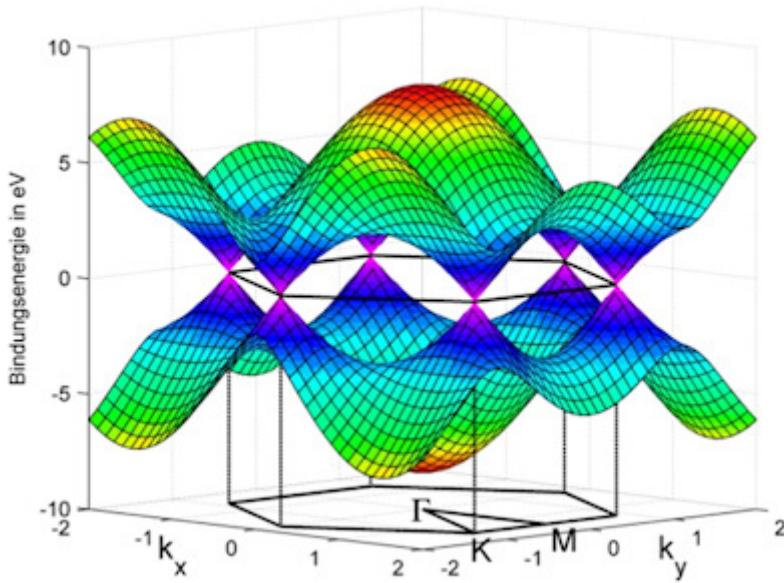


Fig.10.11. Our Doubling Theorem Realized in Graphene.

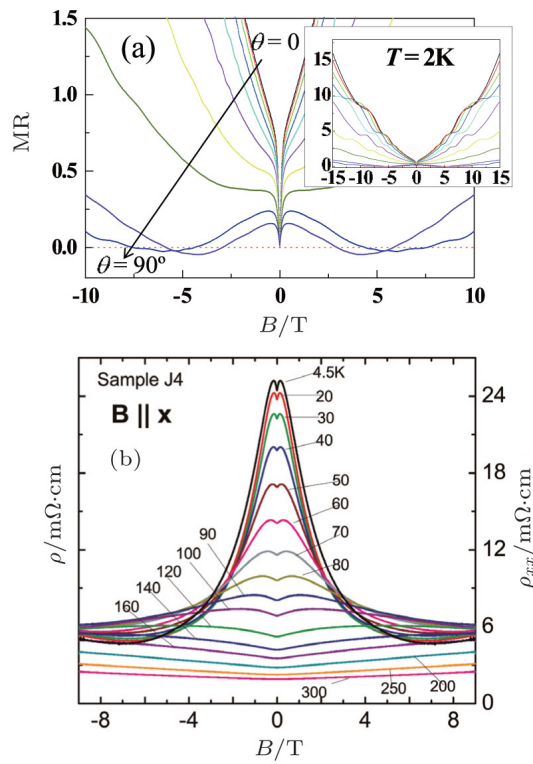


Fig.10.12.

I-8 Further

Further Developments of Our “Random Dynamics” Further speculations, calculations, supporting the idea of getting the Standard Model out as a - say low energy limit - of/from almost whatever the (most) “fundamental” physical laws (say complicated) might be:

- A low energy boson system - with only momentum conservation ... like the general fermion system considered - gives (in free approximation) free Maxwell equations.
- Remarkably: All species of particles in the Standard Model **except the Higgs boson** are either Yang-Mills particles or chiral fermions; so they would all be **massless except for effects due to the Higgs field!** This is just what one gets by asking for the low energy limit in the general theory!

I-9 Conclusion

- Hope that the type of **relativistic chiral fermions**, one finds in high energy physics Standard Model in fact **comes by itself** - and even points to the right dimensionality $3 + 1$, which just is the right one-; but there are a couple of “small” problems (different species of particles have in first go different “maximal” velocities)
- Now adays the phenomenon is about being found in real materials, graphene etc. **One can make relativity models chemically**

It should be especially stressed that **the negative magneto-resistance due to the Adler Bell Jackiw anomaly has been seen in Na_3Sb .**

II. What comes beyond Topological Insulator ?

–“Nielsen-Ninomiya Effect” due to Adler-Bell Jackiw chiral Anomaly–

II-1 Introduction

In part I we mainly argued about “Gapless Semiconductor” “Topological Insulator” and this subject has been very rapidly developing presently.

We now, in this part II, argue chiefly a new application of relativistic quantum field theory. Specifically, We investigate in condensed matter (in nano-scale $\cong 10^{-9}\text{m}$) how the Relativistic Quantum field theory Effect can appear and can be detected in material science.

Theoretically this effect was predicted already 35 years ago in 1983 by the present authors

- (H. B. N and M. N.) in a High Energy Theoretical Physics journal, Physics Letters B Vol. 130, issue 6 p 389 (1983), entitled “The Adler-Bell-Jackiw anomaly and Weyl Fermions in a Crystal”.

- Prior to the above paper one of the authors (M. N) was invited to give talks in the International Workshop on "Lattice Field Theory" in Saclay, Paris and Subsequently held XXI International Conference on High Energy Physics, Paris July 26-31, 1982 (so called "Rochester Conference series"), where he talked about Weyl fermions on lattices and the ABJ-anomaly.

In solid material there often appears crystal lattice structure. Thus we are forced to use lattice field theory which has been well developed in high energy physics. In this formulation the crucial facts for us are the following:

Suppose At each lattice site we put one Weyl fermion e.g. Ψ_L (Left-handed one).

Our Nielsen-Ninomiya Theorem states that there should appear equally many right handed and left handed Weyl fermions - looking in momentum space at different momentum values -. In the simplest construction resulting from just "naively" replacing derivatives by differences on the lattice our theorem is implemented by there appearing 2^d species (d: space dimension). Therefore in 3 space dimensions it turns out that there should be 8 species of Weyl (or chiral) fermions. Furthermore 4 of them are left-handed Ψ_L and rest 4 species are right-handed Ψ_R chiral fermions.

That is to say on the lattice there should be pairwise (left-handed and right-handed) chiral fermions. Therefore we are not able to construct chiral theory with for instance only one handed fermion on the lattice. Thus it leads to the very important consequence in high energy physics. In reality the Standard Model or, unified model of, weak and electromagnetic interactions called "Glashow-Salam-Weinberg model", or "Standard Model" of Weak and Electromagnetic Interaction cannot be constructed on the lattice! The reason is that in the Standard Model all the fermions are left-handed chiral fermions, while no right-handed fermion at all. The experimental results performed so far are all well in agreement with the standard model predictions.

If one takes serious the proposal of a new law of nature by one of us and various collaborators, "Multiple Point Principle", one can even claim an indication for, that the Standard Model contrary to the expectation of many of our colleagues, should be valid up to an energy scale of the order of 10^{18} GeV (rather close to the Planck scale):

One of the authors (H. B. N.) made together with C. D. Froggatt a theoretical calculation of m_H with recourse to the just mentioned "multiple point principle (MPP)". The value is in very good agreement with experimental value at LHC (Large Hadron Collider in CERN, Geneva) $m_H \sim 125$ GeV.

See e.g. H. B. Nielsen and M. Ninomiya "Degenerate vacua from unification of second law of thermodynamics with other laws; The derivation of Multiple point principle" Int. J. Mod. Phys. **A23** (2008) 919 DOI: 10.1142/S02177510839682, in which an argument for among other things is given MPP from a model with the action taken to be complex rather than real as it is normal.

If the Standard Model shall as from this suggestion from Multiple Point Principle etc. be valid only with tiny corrections if any almost up to the Planck scale, it would be even more mysterious that we could not put it on a lattice

because of its chiral particles. Really we could -it looks -hardly regularize it with any sensible cut off! Quite a mystery. [3]

2) ABJ anomaly on a lattice

Condensed matter researchers except for high energy physicists (including some nuclear theorists), may not have heard of the Adler-Bell-Jackiw or chiral anomaly. Therefore we briefly explained ABJ anomaly in continuum space in Appendix A.

Here we turn to our nano-scale material case. In the material there is a lattice structure Fig. 10.13.

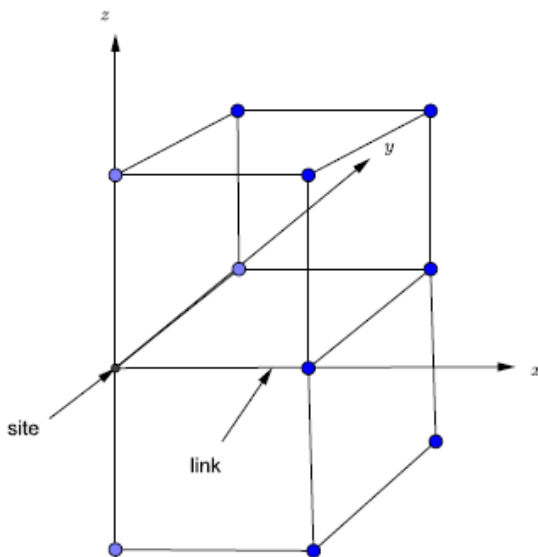


Fig. 10.13. Lattice structure.

In this 3 dimensional lattice on each sites we put one Weyl or Chiral electron e.g. e_L (Left handed electron), then according to the Nielsen-Ninomiya Theorem, there should appear somehow so many of them, that there are equally many right handed and left handed ones. In fact we get in the simplest case 4 e_L as well as 4 e_R .

To understand band structure, we go to the momentum space.

Note that due to the lattice translational invariance the momentum is conserved modulo multiple of the unit length of reciprocal lattice.

The Brillouin zone in the momentum space is topologically equivalent to the hypertorus $S^1 \times S^1 \times S^1$.

In such a topological structure of crystal lattice, the Adler-Bell-Jackiw anomaly explained for continuum spacetime in appendix B, is easily understood also, as was presented in PLB **130** n06, (1983) by the present authors.

II-2 1 + 1 dimensional example

For simplicity, as an example the 1 space 1 time dimensional case is considered. Right chiral (Weyl) fermion obeys lattice Weyl eg.

$i \frac{\partial}{\partial t} \Psi_R(na) = \frac{i}{2a} [\Psi_R((n+1)a) - \Psi_L((n-1)a)]$ where $n = 0, \pm 1, \pm 2, \dots$ denote sites and a is a lattice space. This can be easily solved and the dispersion relation is given by $w = (\frac{1}{a}) \sin pa$. Thus near $p = 0$ there is a RH (RH = right handed) species with the dispersion law $w \approx p$ and further there is a LH (LH = left handed) species near $\frac{\pi}{a}$ with the dispersion law

$$w \approx -(p - \frac{\pi}{a}).$$

These situations are illustrated in the following Fig. 10.14.

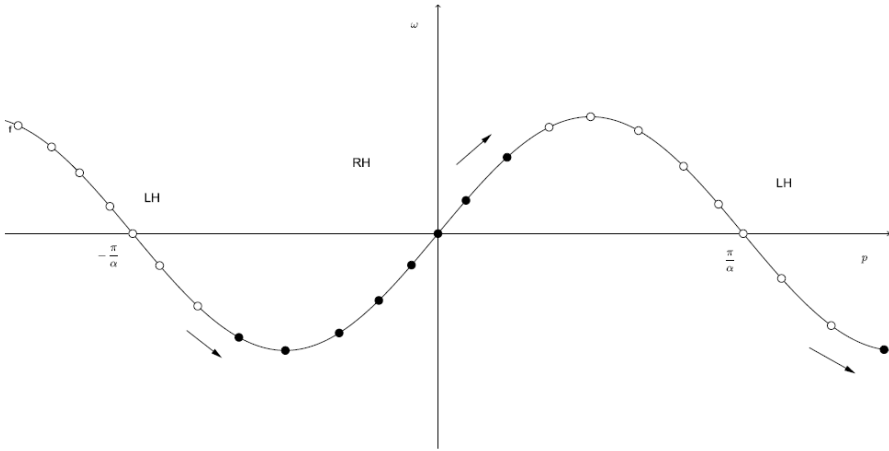


Fig. 10.14.

Note that due to topology of momentum space, there is a periodicity modulo 2π . (e.g. points $p = -\frac{\pi}{a}$ and $\frac{\pi}{a}$ are identified)

II-3 3 + 1 dimensional case

This 1 + 1 dimension example clearly tells us, that in lattice theory there appear equal number of RH and LH chiral (or Weyl) fermion species (really in 1+1 dimension one should rather talk about right mover and left mover, because there is no genuine handedness in 1+1 dimensions). It is not completely straightforward to generalize to 3 + 1 dimensions, but with use of the appropriate mathematics of homotopy (group) theory one make the analogous theorem in 3+1 or in even higher dimensions to the theorem in 1+1 that in a period real function has pass zero in positive and in negative direction equally many times per period.

II-3 (a) Weyl (or chiral) Fermion

In generic chiral (Weyl) fermion theory which obeys

$$i\dot{\Psi}(\vec{x}) = H\Psi(\vec{x}) = w\Psi(\vec{x})$$

We assume that the generic Hamiltonian satisfy the following four conditions:

- (1) Locality of interaction in the sense that $H(\vec{x} - \vec{y}) \rightarrow 0$ as $|\vec{x} - \vec{y}| \rightarrow \text{large}$ fast enough that the Fourier transform of $H(\vec{x})$ has continuous first derivative.
- (2) Translational invariance in the lattice
- (3) Hermiticity of H (reality of S)
- (4) Furthermore an assumption is that the charge (=lepton number in our case) is bilinear in the fermion field.

Under these conditions in the generic H case we gave a rigorous proof in terms of the Homotopy theory in topology in 1981 (see, II-1).

II-3 (b) Adler-Bell-Jackiw anomaly on a lattice

Let us go into the Adler-Bell-Jackiw (ABJ) anomaly on the lattice in the continuum spacetime. We reviewed this anomaly in continuum spacetime in Appendix B.

Here we argue for the lattice version of the ABJ anomaly. Firstly we as an example let us explain the $1 + 1$ dimensional lattice Weyl (chiral) fermion. In the lattice RH chiral or Weyl electron system, we put on an external uniform electric field E in x -direction denoted by $\dot{A}^1 = E$ in temporal gauge ($A^0 = 0$). Then the Weyl eq. reads

$$i\frac{\partial}{\partial t}\Psi_R(x) = (-i\frac{\partial}{\partial x} - \dot{A}^1)\Psi_R(x).$$

The dispersion law is given by $\omega(p) = p$.

In the classical eq. of the electron in the presence of the electric field is $\dot{p} = eE$ so that the RH electron in quantum theory is given by

$$\dot{\omega} = \dot{p} = eE.$$

Therefore the creation rate of the RH electrons per unit time and unit length is determined by a change of the Fermi surface that separates the filled and unfilled states as shown in Fig. 10.15.

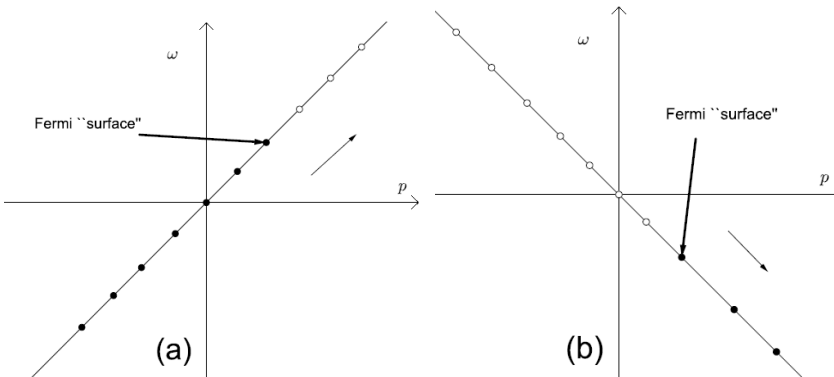


Fig. 10.15.

We denote the quantization length L , then the density of states per unit momentum is given by $\frac{L}{2\pi}$. Therefore the rate of change of the RH electron number N_R is given by $\dot{N}_R = \frac{L}{2\pi} \cdot \dot{\omega}_{fs}$

where $\dot{\omega}_{fs}$ denotes the rate of energy take up of the RH electron fermi surface per fermion, i.e. eE .

Therefore we obtain RH electron creation is given by $\dot{N}_R = \frac{e}{2\pi} E$ per unit length (namely for $L=1$). This is the ABJ anomaly.

Thus the chiral charge Q_R defined as the total number of RH particles (over the fermisea minus the number of holes) is not conserved: $\dot{Q}_R = \dot{N}_R = \frac{e}{2\pi} E$ In the same manner the annihilation rate of LH electrons with $\omega = -p$ is derived as $\dot{N}_L = -\frac{e}{2\pi} E$

This means that creation rate of the LH anti-electron is given as

$$\dot{N}_L = \frac{e}{2\pi} E$$

By adding both, the anomaly of the Dirac electrons is

$$\dot{N}_R + \dot{N}_L = \frac{e}{\pi} E, \text{ and thus}$$

$$\dot{Q}_5 = \frac{e}{\pi} E$$

To proceed to the $3 + 1$ dimension case, we should calculate the energy levels in the presence of an external uniform magnetic field, e.g. in the z -direction so that $A^2 = Hx$, and $A^\mu = 0$ otherwise. Thus we consider the equation for the two component RH electron field Ψ_R

$$\left[i \frac{\partial}{\partial t} - (\vec{p} - e\vec{A}) \cdot \vec{\sigma} \right] \Psi_R(x) = 0$$

This eq. can be solved by introducing an auxiliary field Φ as

$$\Psi_R = \left[i \frac{\partial}{\partial t} + (\vec{p} - e\vec{A}) \cdot \vec{\sigma} \right] \Phi.$$

Thus the eq. for Φ is given by

$$\left[i \frac{\partial}{\partial t} - (\vec{p} - e\vec{A}) \cdot \vec{\sigma} \right] \cdot \left[i \frac{\partial}{\partial t} + (\vec{p} - e\vec{A}) \cdot \vec{\sigma} \right] \Phi = 0$$

This eq. reduces to the harmonic oscillation type eq.

$$\left[-\left(\frac{\partial}{\partial x'}\right)^2 + (eH)^2(x' + \frac{p_2}{eH}) + (p_3)^2 + eH\sigma_3 \right] \Phi = \omega^2 \Phi \text{ with } \sigma_3 = \pm 1$$

The energy eigenvalues ω are given by the Landau levels as follows

$\omega(n, \sigma_3, p_3) = \pm \left[2eH(n + \frac{1}{2}) + (p_3)^2 + (eH\sigma_3) \right]^{\frac{1}{2}}$ with $n = 0, 1, 2, \dots$, except for the $n = 0$ and $\sigma_3 = -1$ mode. Here

$$\omega(n = 0, \sigma = -1, p_3) = \pm p_3.$$

The eigenfunction is of the form

$$\Phi_{n\sigma_3}(x) = N_{n\sigma_3}(x) \times \exp(-ip_2x^2 - ip_3x^3) \times \exp(-\frac{1}{2}eH(x' + \frac{p_2}{eH})^2) \times H_n(x' + \frac{p_2}{eH})\chi(\sigma_3)$$

where $N_{n\sigma_3}$ is normalization constant and $\chi(\sigma_3)$ denotes the eigenfunctions of Pauli spin σ_3 : $\chi(1) = \begin{pmatrix} 1 \\ 0 \end{pmatrix}$ and $\chi(-1) = \begin{pmatrix} 0 \\ 1 \end{pmatrix}$

Thus the solution of the eq. for Two-component RH electron Ψ_R becomes the relations $\Psi_R^{(n+1, \sigma_3=-1)} = \frac{N_{n+1, \sigma_3=-1}}{N_{n, \sigma_3=1}} \Psi_R^{n, \sigma_3=1}$

for $n = 0, 1, 2, \dots$

The zero mode $n = 0$ is

$$\Psi_R^{(n=0, \sigma_3=-1)} = 0 \text{ with } \omega = -p_3.$$

Therefore the ground state energy of Ψ_R is given by $\omega(n = 0, \sigma_3 = -1, p_3) = -p_3$ The energy eigenvalue for the other modes are

$\omega(n=0, \sigma_3, p_3) = \pm [2eH(n + \frac{1}{2}) + (p_3)^2 + eH\sigma_3]^{\frac{1}{2}}$
 These dispersion laws are depicted in the Fig. 10.16.

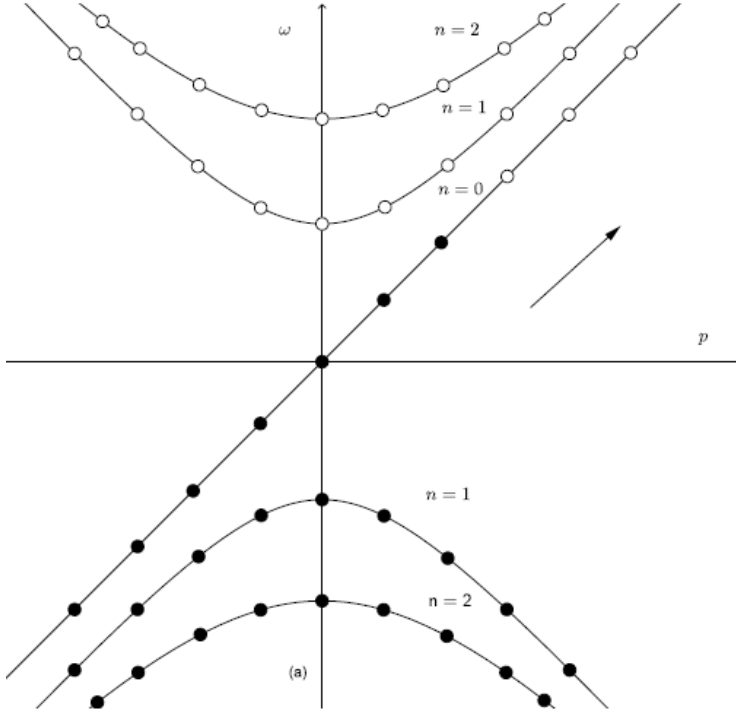


Fig. 10.16.

In the next step an external uniform electric field E is turned on along the same direction parallel to H . For the zero mode ($n=0, \sigma_3 = -1$) the dispersion law is the same as that for 1 + 1 dimensions. Thus the creation rate of the particles is calculated in a similar manner.

We should note that the electric field E is switched on adiabatically, and there is no particle creation in the $n \neq 0$ modes. The density of the state in momentum space in the magnetic field direction is for quantization length $L \propto L \frac{eH}{4\pi^2}$, and thus the creation rate (=the ABJ anomaly) is expressed as

$$\begin{aligned} \dot{N}_R &= \frac{1}{L} \frac{LeH}{4\pi^2} \omega_{fs} \quad (n=0, \sigma_3 = -1, p_3) \\ &= \frac{e^2}{4\pi^2} EH \\ &= \dot{Q}_R \end{aligned}$$

For the LH electrons annihilation rate of LH anti electron is

$$\dot{N}_L = -\frac{e^2}{4\pi} EH$$

and the creation rate of the LH anti particle is given by

$$\begin{aligned}\dot{N}_L &= \frac{e^2}{4\pi^2} EH \\ &= \dot{Q}_L\end{aligned}$$

In the case of the Dirac electron

$$\begin{aligned}\dot{N}_R + \dot{N}_L &= \frac{e^2}{2\pi^2} EH \\ &= \dot{Q}_5\end{aligned}$$

II-3 (c) Generic Case

We again look at a generic case of which Hamiltonian is given by $N \times N$ local Hermitian matrix. The N discrete energy eigenvalues are determined by the following eigenvalue eq.

$$\sum_{l=1}^N H_{kl}(\vec{p}) \Psi_l^{(i)}(\vec{p}) = \omega_i \Psi_k(\vec{p}) \quad (i = 1, \dots, N)$$

Here we assume that the i th level $\Psi_i(\vec{p})$ and $(i+1)$ th level are degenerate. The eigenvalue $\omega_i(\vec{p})$ are assumed to be degenerate with the $(i+1)$ level at several different points in momentum space, which are denoted as $(\omega_d(\vec{p}_d), \vec{p}_d)$ in the dispersion space $(\omega(\vec{p}), \vec{p})$. The i th and $(i+1)$ th levels are described by d submatrix $H^{(2)}(\vec{p})$: it has the i th and $(i+1)$ th entries of $N \times N$ matrix H .

We then expand $H^{(2)}(\vec{p})$ in powers of $(\vec{p} - \vec{p}_d)$ around are of the degenerate point $(\omega_d(\vec{p}_d), \vec{p}_d)$. In the expansion of $H^{(2)}(\vec{p})$ is given

$$H^{(2)}(\vec{p}) = H^{(2)}(\vec{p}_d) + (\vec{p} - \vec{p}_d) \frac{\partial H^{(2)}(\vec{p})}{\partial \vec{p}} \Big|_{\vec{p}=\vec{p}_d} + O((\vec{p} - \vec{p}_d)^2).$$

The derivative term is expressed by the Pauli matrices $(\mathbb{I} + \sigma_\alpha)$, $(\alpha = 1, 2, 3)$ and $\mathbb{I} = 2 \times 2$ unit matrix, as

$$\frac{\partial H^{(2)}}{\partial \vec{p}_k} \Big|_{\vec{p}=\vec{p}_d} = a_k(\vec{p}_d) \mathbb{I} + V_k^\alpha(\vec{p}_d) \sigma_\alpha$$

Here V are the constants depending on \vec{p}_d . Thus near $\vec{p} = \vec{p}_d$, $H^{(2)}(\vec{p})$ takes the form

$$H^{(2)}(\vec{p}) = \omega_d \mathbb{I} + (\vec{p} - \vec{p}_d) \vec{a} \mathbb{I} + (\vec{p} - \vec{p}_d)_k V_k^\alpha \sigma_\alpha$$

The eigenvalue eq. of the i th and $(i+1)$ th energy eigenvalues near $\vec{p} = \vec{p}_d$ $H^{(2)}(\vec{p})u = \omega u$.

This is rewritten by using a new set of variables

$$\hat{p} = \vec{p} - \vec{p}_d, \quad p^0 = \omega - \omega_d - \hat{p} \vec{a}$$

as

$$\hat{p} V \vec{\sigma} u = p^0 u$$

If we introduce

$$K^0 = p^0 \text{ and } k = \pm \hat{p} \vec{V}$$

Where \pm correspond to the sign of $\det V$. For simplicity we may take as an example $V_{k\alpha} = v\delta_{k\alpha}$ ($k, \alpha = 1, 2, 3$).

The above eigenvalue eq. becomes

$$\vec{k} \cdot \vec{\sigma} u = \pm k^0 u$$

Where the dispersion law $(k^0)^2 = v^2 k^2$. Thus, it is $\omega^2 = v^2 p^2$

In this way RH and LH Weyl eq. describes the 2 energy levels near degeneracy point in $(\omega(\vec{p}), \vec{p})$ space correspond to a species of Weyl fermions contained in the theory. Our theorem tells that RH and LH degeneracy points appear necessarily as a pair because of the Brillouin zero structure (topology). The theorem was proved by only topological arguments together with locality, as was shown our papers in 1981. The doubling of the Weyl fermions are illustrated in Fig. II-4 (page 18).

II-4 Parity non-invariant zero-gap material

We assume that we have found a parity non invariant material (i.e. a crystal should be of non-centrosymmetric symmetry; e.g. BiTeI form a non-centrosymmetric crystal. Best might be a triclinic pedial class with no point symmetry at all.) with zero-gap, which can be simulated by a Weyl, fermion theory with a dispersion law $\omega^2 = v^2 p^2$. The effect analogous to the ABJ anomaly gives rise to a peculiar behavior of the conductivity of the electric current in the presence of the magnetic field. It is enough to consider one conduction band ω_i .

The valence band ω_{i+1} (negative energy state) is assumed to be completely filled. In the absence of external field, the single electron distribution function in the thermodynamical equilibrium is of the form $f_0(\vec{p}) = [1 + \exp[(\omega(p) - u)/kT]]^{-1}$

In the presence of E and $H = 0$ there occurs a small deviation from thermodynamical equilibrium so that $f = f_0 + \delta f$, and the E field accelerates the electrons in the same direction and then

$$\left(\frac{\partial f}{\partial t}\right)_{\text{drift}} = eE \frac{\partial f}{\partial p_z}.$$

At the same time the accelerated electrons get scattered back into some states in the same cone. We assume that f fills back into f_0 exponentially with a relaxation time τ_0 so that $\delta f \propto e^{-\frac{t}{\tau_0}}$

Then

$$\left(\frac{\partial f}{\partial t}\right)_{\text{coll}} = -\frac{1}{\tau_0} (f - f_0)$$

Therefore the steady state condition is $\left(\frac{\partial f}{\partial t}\right)_{\text{drift}} = -\left(\frac{\partial f}{\partial t}\right)_{\text{coll}}$ (Boltzmann eq.).

The sol. of this is in the lowest order in E

$$f(\vec{p}) = f_0(\omega) + eE\tau_0 \frac{\partial f(\omega)}{\partial p_z}$$

Then the longitudinal current density is given by

$$J_0 = \frac{1}{L^3} \sum_{\vec{p}} (-e) v_z f(\vec{p}) (\# \text{deg. pts})$$

Where $v_z = \frac{\partial \omega}{\partial p_z}$ and (#deg. pt) denotes the number of deg. pts (= degeneracy points).

In the low temperature approximation $f_0(\omega) = \theta(\mu - \omega)$ so that

$$J_0 = \frac{1}{6\pi^2} e^2 E \left(\frac{\mu^2}{v} \right) \tau_0 (\# \text{deg. pt})$$

the relaxation time is given in terms of transition probability of electron from the state with \vec{p} into one with \vec{p}' , $W(\vec{p} \rightarrow \vec{p}')$ by

$$\frac{1}{\tau_0} = \frac{1}{L^3} \sum_{\vec{p}'} \frac{p_z - p'_z}{p_z} W(\vec{p} \rightarrow \vec{p}')$$

We assume that the interaction between the electron and the ionized impurities is given by the screened Coulomb potential (pot.) of the form

$$V(\vec{x}) = \left(\frac{4\pi e^2}{k} \right) \frac{e^{-\frac{|\vec{x}|}{\gamma_0}}}{|\vec{x}|}$$

With the screening length γ_0 and k the dielectric constant. Computing τ_0 in the first order perturbation we obtain the current as

$$J_0 = \frac{4e^2 E}{3\pi\eta_I} \left(\frac{k}{4\pi e^2} \right)^2 \left(\frac{\mu^4}{v^2} \right) \left[\ln(1 + \beta) - \frac{\beta}{1 + \beta} \right]^{-1} (\# \text{deg. pt})$$

With $\beta = \frac{2\pi k v}{e^2} (\# \text{deg. pt})$ and η_I the density of impurity.

Next compute the magneto-conductivity when H parallel to E is so strong that only the lowest states $n = 0, \sigma_3 = -1$ with dispersion law $\omega = v p_z$ or $\omega = -v p_z$ near the RH and LH degeneracy point are filled the ABJ anomaly effect will cause the movement in the momentum space of electrons from the lowest Landau level ($n = 0, \sigma_3 = -1$) at the one deg. pt. (=degeneracy point) in the LH cone to the corresponding one ($n = 0, \sigma_3 = -1$) in the RH cone (at the RH deg.pt.). Thus these moved electrons will give raise to a deviation from the thermodynamical equilibrium, that can be expressed by the different chemical potentials for the electrons at the RH degeneracy pt., μ_R and at the LH one μ_L . If one had calculated the relaxation time in the approximation where only one degeneracy point at a time was relevant -such as we did above in the $H = 0$ case- we would have found $\frac{1}{\tau} = 0$. This comes out of such a calculation due to the energy conservation factor $\delta(\omega - \omega') = \frac{1}{v} \delta(p_z - p'_z)$ contained in $W(P_Z - P'_Z)$ which makes (23) give $\frac{1}{\tau} = 0$. However we cannot neglect scattering processes involving two degeneracy point.

II-5 Transfer from LH to RH cones by Adler-Bell-Jackiw Anomaly

The mechanism for the electric current with both E can H switched on peculiarly different from the one with a negligibly weak H . In the presence of strong H the

lattice anomaly of the ABJ anomaly takes place: transfer of the particles from the LH degeneracy pt. to the RH one acts as a drift term, i.e. $\dot{N}|_{\text{drift}}$ in the Boltzmann equation. On the other hand for negligible H each degeneracy points act independently. By the ABJ anomaly the Fermi energy level μ_R in the RH cone goes up compared to that of the $H = 0$ case μ and μ_L in the LH cone is lowered. See Fig. 10.16 (a) (1 + 1 dim. case) and Fig. 10.17 (3 + 1 dim. case)

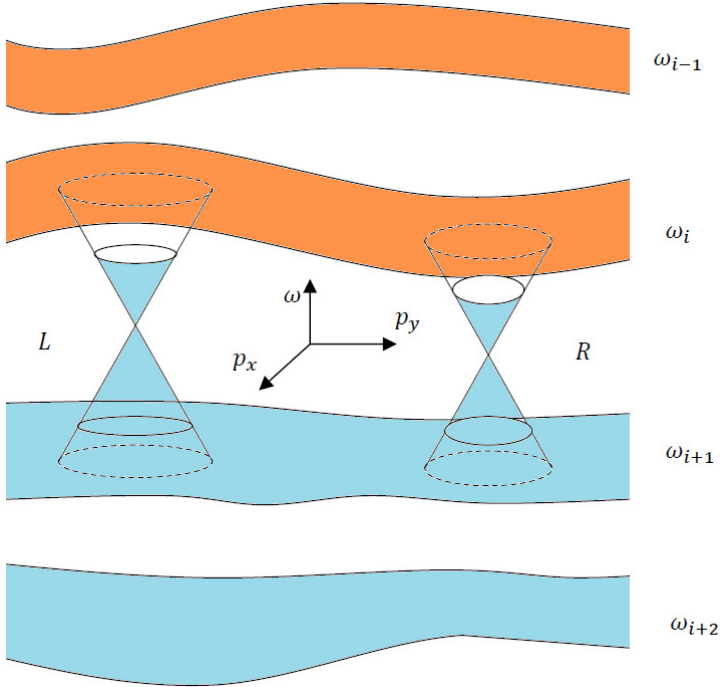


Fig. 10.17.

In order that the system is in the steady state

the excess electrons by the ABJ anomaly in the RH cone must be scattered back to the another state.

But they can not be scattered back into the state in the same cone! because, as was explained above $\tau = \infty$.

Therefore they must transfer into the states in another cone; that is from the RH cone into the LH cone.

We may call this the intercone scattering and we denote the corresponding relaxation time by τ_1 . If the intercone transition probability $W(p_z \rightarrow p'_z)$ from RH cone into the LH cone is calculated, then the collision term is given by

$$\begin{aligned} \dot{N}_R|_{\text{coll}} &= \frac{2}{L} \sum_{p_z} [f(p_z) - f_0(p_z)] \frac{1}{L} \sum_{p'_z} W(p_z \rightarrow p'_z) \\ &\equiv -\frac{p'_z}{\tau_1} (N_R - N_R^0) \end{aligned}$$

Here N_R and N_R^0 denote the total electron numbers in the RH cone above the degeneracy energy in the $H \neq 0$ and $H = 0$ cases respectively. Thus $\frac{1}{\tau_I} = \frac{2eH}{(2\pi)^2} \frac{1}{L} \sum_{p'_z} W(p_z - p'_z)$

The generation of a current associated with the ABJ anomaly can be shown by the following energy conservation argument. ABJ anomaly indicates that electrons are transferred from the LH cone into the RH cone by the rate of $\frac{e^2 EH}{(2\pi)^2}$ per unit Time, per unit volume.: Notice that the dispersion law is continuous and the RH and LH cones are connected smoothly as shown Fig. 10.17.

Since the Fermi level energies are $\mu_R > \mu_L$ the transfer costs the energy $\frac{e^2}{(2\pi)^2} EH(\mu_R - \mu_L)$. This energy must be taken from the E field by the presence of a current J_A determined by the energy balance as

$$EJ_A = \frac{e^2}{(2\pi)^2} eH(\mu_R - \mu_L)$$

At the zero temperature, in the RH cone

$$f_0(\omega) = \theta(\mu_R - \omega) \text{ and thus}$$

$$N_R = \frac{1}{L^3} \sum_{p_y p_z} f_0(\omega) \frac{eH}{(2\pi)^2} \frac{\mu_R}{v} \\ \cong N_R^0 + (\mu_R - \mu) \frac{\partial N_R}{\partial \mu}$$

Inserting this into Boltzmann eq.

$$\dot{N}_R|_{\text{drift}} = -\dot{N}_R|_{\text{col}}$$

$$\text{We obtain } \mu_R - \mu_L = evE\tau_I$$

Therefore $J_A = ev \frac{e^2}{(2\pi)^2} EH\tau_I$ (#deg.pt.) Here the subscript A stands for the anomalous current the one associated with the analogue of the ABJ anomaly. In the definition of τ_I we may approximate $W(\vec{p}_z \rightarrow p'_z) \cong W(\vec{p} - \vec{p}')$

So that $W(p_z - p'_z) \cong (\frac{4\pi^2}{k})^2 \eta_I \left[(\vec{p} - \vec{p}')^2 + \frac{1}{\gamma_H^2} \right]^{-2} 2\pi\delta(\omega - \omega')$ with $\frac{1}{\gamma_H^2} = \frac{EH}{kv}$ (#deg.pt.). According to $\hat{\vec{p}} \equiv \vec{p} - \vec{p}_d$, $p^0 = \omega - \omega_d - \hat{p} \vec{a}$, we have $\vec{p} - \vec{p}' = \vec{p}_d - \vec{p}'_d + \hat{\vec{p}} - \hat{p}'$

where $\hat{\vec{p}}$ and $\hat{\vec{p}}'$ are oscillating around \vec{p}_d and \vec{p}'_d : since they are order of $(eH)^{\frac{1}{2}}$. We may ignore the oscillatory part $(\hat{\vec{p}} - \hat{\vec{p}}')$ and $\frac{1}{\gamma_H^2}$ term in the denominator of $W(p_z - p'_z)$ when compared to the distance of the RH and LH deg. pts $\vec{p}_d - \vec{p}'_d$. In this approximation we obtain

$$J_A = \frac{e^2 v^2 E}{2\pi\eta_I} \left(\frac{k}{4\pi^2} \right)^2 (\vec{p}_d - \vec{p}'_d)^4 (\text{\#deg.pt.})$$

We then obtain the ratio of the conductivity that is defined by $f = \sigma E$ as

$$\frac{\sigma_A}{\sigma_0} = \frac{3}{16} \left(\frac{v}{\mu} \right)^4 \left[\ln(1 + \beta) - \frac{\beta}{1+\beta} \right] (\vec{p}_d - \vec{p}'_d)^4$$

By these results, for the intercom relation time τ_I the electrons must travel a “long distance” in momentum space. Thus τ_I is expected to be a large value compared to τ_0 for $H = 0$. Therefore $\frac{\sigma_A}{\sigma_0}$ given above is large.

II-6 Further arguments

So far we have presented our own theoretical predictions in 1983 although we believed sooner or later our predicted “Nielsen-Ninomiya” mechanism (or effect)

will be proved by experiment. Indeed after almost 35 year later Princeton University group led by Prof. N. Phuan Ong and R. Cava, found chiral anomaly in crystalline material. This surprising news in science community appeared in an article by Catherine Zandonella,

- office of the Dean of Research, in Science, September 3, 2015 entitled Research at Princeton: Long-sought chiral anomaly detected in crystalline material (science).

At the almost same time, scientist's article entitled.

- "Evidence for the chiral anomaly in the Dirac semimetal Na₃Bi" By J. Xiong Satya K. Kushwaha, Tian Liang, J. W. Kritzan, M. Hirsehberger, Wulin Wang, R. J. Cava, X. P. Oug, Science Express, 03 , September 2015. and
- "Signature of the chiral anomaly in a Dirac semimetal – a current plume steered by J. Xiong, S. K. Kushwaraha, T. Liang, J. W. Krizan, Wudi Wang, R. J. Cava and N. P. Ong

Since then the works on this subject is really under rapidly developing mainly in Experiments, also theories: e. g. Dirac cones, and Weyl semimetals. We believe in the rather near future we shall see some machines using "Nielsen-Ninomiya Mechanism (or Effect). See e.g. also [4].

II-7 Conclusions

In the present article we present the viewpoint at two exceptional high energy theoretical physicists new eras of condensed matter.

In the first part I we mainly considered "Topological Insulator" from random dynamics point of view. The essential point is that in generic Fermion dispersion relations i.e. in (almost) all solids or fluids at low temperature we can derive the recently found properties of Topological insulators such as graphene etc.

In the 2nd point II, we present what comes beyond topological insulator.

We believe that the Adler-Bell-Jackiw anomaly effect in the chiral non invariant gapless material, causes that

- magnetic conductance is enhanced very much (ideally permanent current)
- Chiral electron (chiral fermion in general) in lattice of the gapless material runs with a fixed speed. (This fixed speed is what in the relativity theory analogue is the speed of light.) This is so, because we by analogy can apply the relativistic quantum field theory.

To make any apparatus using the above theory will be widely opened to not only condensed matter, but chemistry, beyond artificial division such as, physics chemistry engineering etc.

Acknowledgements

One of the authors (H. B. N.) acknowledges the Niels Bohr Institute, Copenhagen University for allowance to work as emeritus and for economical support to visit

the conference in New York for which this work is the proceeding. M. N. acknowledges Advanced Mathematical Institute Osaka City University, and Yukawa Institute for Theoretical Physics, Kyoto University as emeritus.

M. N. also acknowledges the present research is supported by the JSPS Grant in Aid for Scientific Research No. ISKO 5063.

Appendix A

We consider electron in quantum field theory (Relativistic quantum mechanics.) We present only necessary properties in Appendix A

The electron in the relativistic quantum field theory it is usually described as Dirac field $\Psi = \begin{pmatrix} \Psi_L \\ \Psi_R \end{pmatrix}$ where Ψ_L and Ψ_R are 2 component fields. Now the electron has intrinsic spin \vec{S} . Thus electron has the angular momentum then \vec{J} , whose value are half integers, and the spin components is \vec{S} take values $\pm \frac{1}{2}$.

For massless fermions the right Ψ_R and the left Ψ_L componets in the (free) Dirac equation gets seperated, and we actually even find that the spin direction is the same as that of electron movement for the right components Ψ_R and the opposite for the left components Ψ_L . Let us start with the Dirac field such as an electron in the quantum field theory. The electron has intrinsic spin $\frac{1}{2}$ of fermion obeying the free Dirac eq.

$$(i\gamma^\mu \partial_\mu - m_e)\Psi_D = 0 \quad (\text{II} - 1)$$

thereafter we ignore electron mass unless described. Our notation is that of the textbook of Bjorken-Drell "Relativistic Quantum Fields". For our purpose we list up relevant notations below

- The 3 + 1 dimensional flat space metric (tensor):

$$g_{\mu\nu} = \begin{pmatrix} 1 & 0 & 0 & 0 \\ 0 & -1 & 0 & 0 \\ 0 & 0 & -1 & 0 \\ 0 & 0 & 0 & -1 \end{pmatrix}$$

- The γ matrices are

$$\gamma^0 = \begin{pmatrix} 1 & 0 \\ 0 & -1 \end{pmatrix}$$

$$\text{where } 1_- = \begin{pmatrix} 1 & 0 \\ 0 & 1 \end{pmatrix}$$

$$\text{and } \gamma^i = \begin{pmatrix} 0 & \sigma^i \\ -\sigma^i & 0 \end{pmatrix} \quad i = 1, 2, 3$$

$$\text{Here } \sigma^i \text{ denotes } 2 \times 2 \text{ Pauli matrices and } 1_- = \begin{pmatrix} 1 & 0 \\ 0 & 1 \end{pmatrix}.$$

Furthermore

$$\gamma^5 = \gamma_5 = \begin{pmatrix} 0 & 1_- \\ 1_- & 0 \end{pmatrix} \quad (\text{note } (\gamma^5)^2 = 1)$$

- The 4 component Dirac field is denoted as

$$\Psi_D(p, s)$$

and when there is no interactions obeys the free Dirac eq. as

$$(i\gamma^\mu \partial_\mu - m)\Psi = 0$$

where $\partial_\mu = \frac{\partial}{\partial x^\mu}$, in momentum representation

$$p^\mu = i \frac{\partial}{\partial x_\mu}$$

$$\Psi_D(\vec{p}, s).$$

Here s denote intrinsic spin $|s| = \frac{1}{2}$

$\Psi_D(\vec{p}, \vec{s})$ obeys

$$\not{p}\Psi_D(p, s) = 0$$

with 4 component Dirac field we may describe

$$\Psi_D(p, s) = \begin{pmatrix} \Psi_L \\ \Psi_R \end{pmatrix} (p, s)$$

Where Ψ_L and Ψ_R are 2 component spinor respectively the eigenvalue solution of free Dirac eq. $(\not{p} - m)$ is the form of

$$\Psi(p, s) = \pm \sqrt{\vec{p}^2 + m^2}$$

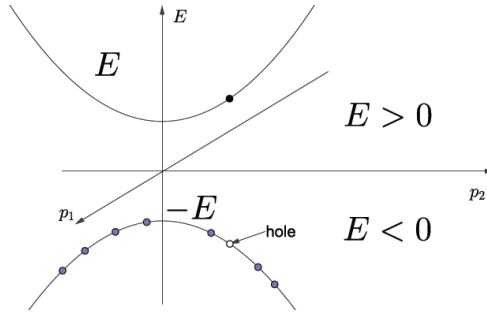


Fig. 10.18. Dirac's "hole theory".

We adopt the Dirac's "hole theory". In this theory often used in condensed matter as dispersion relation, the negative states are all filled, while the hole in the Dirac sea is antiparticle, i.e. positron e^+ .

In solid state physics where one has say a crystal lattice, which from the quantum field theory is discretized, so therefore we are interested in discretizing the quantum field theory here. The Dirac fermion wave function $\Psi_D(\vec{p}, s)$ has 4-components: 2 degree of freedom as that energy can have plus or minus. Furthermore the electron has intrinsic spin of which value is $|s| = \frac{1}{2}$. In the massless case spin/(vector) direction can be either the direction of the electron motion or the opposite. We then define for describing "chirality". It is usually distinguished by this quantity. That is to say $\gamma_5 \Psi = +1$ or -1 . Customary $+1$ is named Left moving- and -1 case is Right moving-Weyl or chiral fermion denoted Ψ_L and Ψ_R respectively. (The Lorentz or Poincare group of spacetime in $3 + 1$ dim Hermann Weyl investigated in detail and the basis is 2 component spinor called Weyl spinors Ψ_L and Ψ_R . In terms of these 4 component Dirac field Ψ such handed components can be constructed ($\Psi_D = \begin{pmatrix} \Psi_L \\ \Psi_R \end{pmatrix}$))

Appendix B

We are now ready to discuss about Adler-Bell-Jacklin anomaly. In quantum field theory there are various symmetries. One of the most interesting symmetries is chiral (or axial) symmetry. That is the interaction of Dirac field Ψ_D with electromagnetic field A_μ is given by

$$S = \int d^4x \bar{\Psi}(x) [i\gamma^\mu (\partial_\mu + ieA_\mu(x))] \Psi_D(x) \quad (*)$$

in the case of massless electron., where $\bar{\Psi}_D = \Psi^\dagger \gamma^0$. It has chiral symmetry which may be obvious, if we rewrite (*) in terms of Ψ_L and Ψ_R as the Dirac eq. can be written as

$$\begin{pmatrix} 0 & i(\partial_0 + \sigma^i(\partial_i + ieA_i)) \\ i(\partial_0 - \sigma^i(\partial_i + ieA_i)) & 0 \end{pmatrix} \begin{pmatrix} \Psi_L \\ \Psi_R \end{pmatrix} = 0.$$

In this way the equations of Ψ_L and Ψ_R are separately given by the following Weyl equations

$$\begin{aligned} i(\partial_0 - \sigma^i(\partial_i + A_i))\Psi_L &= 0 \\ \text{and} \\ i(\partial_0 + \sigma^i(\partial_i + A_i))\Psi_R &= 0. \end{aligned}$$

In these forms it is evident that the theories are invariant under the following infinitesimal Weyl transformations

$$\begin{aligned} \Psi_L &\rightarrow (1 - i\alpha^i \frac{\sigma_i}{2} - \beta^i \frac{\sigma_i}{2})\Psi_L \\ \Psi_R &\rightarrow (1 - i\alpha^i \frac{\sigma_i}{2} + \beta^i \frac{\sigma_i}{2})\Psi_R \end{aligned}$$

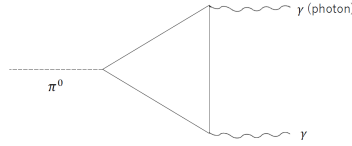
Where α^i and β^i ($i = 1, 2, 3$) are infinitesimal transformation parameters, restricted to leave the normalization of the Weyl fields invariant. This Weyl or Chiral transformation is broken due to quantum effect in quantum field theory. There were several suggestive articles, but explicit manifestation is presented by

- S. Adler, Phys. Rev. 177 (1969) 2426
- and
- J. S. Bell and R. Jackiw Nuovo Cimento 60A (1969) 4.

Furthermore the method of path integral formulation this ABJ anomaly is due to non-invariance of the path integral measure

- K. Fujikawa Phys. Rev. Lett. 42 1195 (1979)

Phenomenologically this ABJ anomaly is really important. It has been observed by experiments. Π^0 meson decays into 2 photons. When we approximate Π^0 as being massless, this decay process is expressed as the following diagram, triangle diagram of Feynman diagram



If chiral symmetry is not broken, this diagram turns out to give zero. Thus this decay is not allowed. However, experimentally this decay process certainly exists. This is the evidence that Adler-Bell-Jackiw anomaly does exist. In high energy, physics the ABJ anomaly is expressed as the non-conservation chiral current J_μ^5 such that

$$\partial^\mu J_\mu^5 = -\frac{e^2}{16\pi^2} \epsilon^{\alpha\beta\gamma\delta} F_{\alpha\beta} F_{\gamma\delta}$$

Here the chiral current J_μ^5 is defined as

$$J_\mu^5 = \lim_{\epsilon \rightarrow 0} \left\{ \bar{\Psi}\left(x + \frac{\epsilon}{2}\right) \gamma_\mu \gamma^5 \exp \left[-ie \int_{x-\frac{\epsilon}{2}}^{x+\frac{\epsilon}{2}} dz A(z) \right] \Psi\left(x + \frac{\epsilon}{2}\right) \right\}$$

We might perform the calculation to show that the above triangle diagram is non-zero due to the ABJ anomaly. But we have instead in subsection 10 alluded to a derivation of the ABJ-anomaly by using how particles are pumped up or down from or to the fermi-sea (in high energy physics the Dirac sea).

References

1. Jahn, H. A.; Teller, E. (1937). "Stability of polyatomic molecules in degenerate electronic states. I. Orbital degeneracy". *Proc. R. Soc. A*. 161 (A905): 220–235. Bibcode:1937RSPSA.161..220J. doi:10.1098/rspa.1937.0142.
2. Kramers, H. A., *Proc. Amsterdam Acad.* 33, 959 (1930) E. Wigner, Über die Operation der Zeitumkehr in der Quantenmechanik, *Nachr. Akad. Ges. Wiss. Göttingen* 31, 546–559 (1932), <http://www.digizeitschriften.de/dms/img/?PPN=GDZPPN002509032>.
3. "Weyl particles, weak interactions & origin of geometry", *Nuclear Physics B - Proceedings Supplements* Volume 29, Issues 2–3, December 1992, Pages 200–246. [https://doi.org/10.1016/0920-5632\(92\)90021-J](https://doi.org/10.1016/0920-5632(92)90021-J).
4. Qiang Li, Dmitri E.Kharzeev, "Chiral magnetic effect in condensed matter systems", *Nuclear Physics A* **956** December 2016, Pages 107–111.



11 Electric Dipole Moment and Dark Matter in a CP Violating Minimal Supersymmetric SM

T. Shindou *

Division of Liberal-Arts, Kogakuin University
Nakanomachi 2665-1, Hachioji, 192-0015, Tokyo, Japan

Abstract. We consider a dark matter scenario in the minimal supersymmetric standard model with CP violation where the Bino-like neutralino is a dark matter and its annihilation cross section is enhanced enough to reproduce the observed relic abundance of the dark matter through heavy Higgs bosons exchange. In this benchmark scenario, we examine the electric dipole moments of the electron, the mercury, and the neutron. We also consider the spin-independent cross section for the dark matter scattering with nuclei. We show that the electric dipole moments will be very powerful tool to explore the parameter space in this model, even when most of the new particles are very heavy.

Povzetek. Avtor obravnava model za temno snov v okviru minimalnega supersimetričnega standardnega modela s kršitvijo CP, v katerem temno snov tvori vrsta nevtralina z dovolj velikim sipalnim presekom za anihilacijo z izmenjavo težkih Higsovih bozonov, da da njegova gostota ustreže izmerjeni pogostosti temne snovi. V tem modelu oceni električne dipolne momente elektrona, jedra živega srebra in nevtrona. Obravnava od spina neodvisne sipalne preseke za sipanje te temne snovi na jedrih. Ugotovi, da je električni dipolni moment elektrona koristno orodje za raziskavo prostora parametrov tega modela tudi v primeru, če je večina delcev v tem supersimetričnem modelu zelo masivnih.

Keywords: dark matter, neutralino, EDM, MSSM

11.1 Introduction

Though there is no evidence of supersymmetry (SUSY) at the LHC experiments, SUSY is still an attractive candidate of physics beyond the Standard Model (SM). There are several motivations to consider the minimal SUSY Standard Model (MSSM) than it in the SM. For example, (i) the gauge coupling unification is improved in the MSSM, (ii) quadratic divergence in the scalar sector is cancelled, (iii) spin-0 scalar fields are naturally introduced, (iv) MSSM provides a well-defined ultraviolet picture of type-II two Higgs doublet model, (v) If R-parity is unbroken, the lightest SUSY particle (LSP) can be a dark matter (DM) candidate, and so on.

Among such attractive motivations, we focus on the point (v). In the SM, there are several unsolved problems and one of the most serious problems is absence of

* E-mail: shindou@cc.kogakuin.ac.jp

the DM candidate. In the MSSM, all the SM particles are R-parity even and all the SUSY partner particles are R-parity odd, so that the lightest R-parity odd particle cannot decay. Therefore, unbroken R-parity guarantees the stability of the LSP which can be a DM.

Several different candidates can be considered in the MSSM such as the neutralino, the gravitino, the axino, the saxion and the sneutrino. In this talk, we briefly review the analysis studied in Ref. [1] where a neutralino DM scenario is considered.

In the neutralino DM scenario, the relic abundance of the LSP tends to be much more than the observed value. In order to realise the observed relic abundance of the DM, a mechanism to enhance the annihilation cross section of LSP is necessary. For example, following scenarios are sometimes considered: (i) neutralinos annihilate significantly through SU(2) gauge interaction, or (ii) annihilation cross section of Bino-like neutralino is enhanced with a particular mass spectrum of other associated particles. In the former class, one possible case is the Higgsino-like neutralino DM scenario with the mass of about 1 TeV. In this scenario, phenomenology such as the direct detection of DM, contribution to the EDMs, and collider signals have been studied in Ref. [2]. There is another possibility that a neutralino DM whose main component is Bino annihilates through heavy Higgs boson resonance [3–7].

We, here, focus on the second case. In this scenario, masses of the heavy Higgs boson are about twice of the mass of the neutralino DM. This Bino-like neutralino also contains small Higgsino component so that the neutralino can directly be searched through Higgs bosons exchange by the spin-independent scattering off nucleus [8].

We consider the MSSM with CP violating phases. In this case, the CP violating phases can significantly affect the electric dipole moments (EDM). Therefore the EDMs are powerful tools to explore the CP violating phases in the model. In this talk, we examine the electron EDM, the nucleon EDM, and the mercury EDM. CP phases can also contribute to the DM-nucleon spin-independent scattering cross section. Since the pseudo scalar exchange process is strongly suppressed in the non-relativistic limit, the spin-independent cross section is suppressed with a significant size of CP phase.

11.2 The benchmark of our analysis

The superpotential and the soft SUSY breaking terms in the MSSM are given by[9]

$$\begin{aligned}
 W = & \epsilon_{ab} \left[(y_e)_{ij} H_1^a L_i^b \bar{E}_j \right. \\
 & + (y_d)_{ij} H_1^a Q_i^b \bar{D}_j \\
 & + (y_u)_{ij} H_2^a Q_i^b \bar{U}_j \\
 & \left. - \mu H_1^a H_2^b \right] ,
 \end{aligned} \tag{11.1}$$

and

$$\begin{aligned}
\mathcal{L}_{\text{soft}} = & -\frac{M_1}{2} \tilde{B} \tilde{B} - \frac{M_2}{2} \tilde{W}^\alpha \tilde{W}_\alpha - \frac{M_3}{2} \tilde{G}^A \tilde{G}_A \\
& - m_{H_1}^2 H_1^* H_1 + m_{H_2}^2 H_{2a}^* H_{2a} - \tilde{q}_{iLa}^* (M_{\tilde{q}}^2)_{ij} \tilde{q}_{jL}^a - \tilde{\ell}_{iLa}^* (M_{\tilde{\ell}}^2)_{ij} \tilde{\ell}_{jL}^a \\
& - \tilde{u}_{iR} (M_{\tilde{u}}^2)_{ij} \tilde{u}_{jR}^* - \tilde{d}_{iR} (M_{\tilde{d}}^2)_{ij} \tilde{d}_{jR}^* - \tilde{e}_{iR} (M_{\tilde{e}}^2)_{ij} \tilde{e}_{jR}^* \\
& - \epsilon_{ab} [(T_e)_{ij} H_1^a \tilde{\ell}_{iL}^b \tilde{e}_{jR} + (T_d)_{ij} H_1^a \tilde{q}_{iL}^b \tilde{d}_{jR} \\
& + (T_u)_{ij} H_2^a \tilde{q}_{iL}^b \tilde{u}_{jR} + m_3^2 H_1^a H_2^b + \text{h.c.}] , \tag{11.2}
\end{aligned}$$

respectively. In the following, we ignore the Yukawa couplings except for the third generation quarks and leptons. Then y_t , y_b , and y_τ denote the Yukawa couplings of top, bottom, and tau, respectively. We also neglecting the flavor mixing in the soft SUSY breaking terms, we take flavor diagonal soft scalar masses as $M_{\tilde{q}}^2 = (M_{\tilde{q}}^2)_{ii}$, $M_{\tilde{\ell}}^2 = (M_{\tilde{\ell}}^2)_{ii}$, $M_{\tilde{u}}^2 = (M_{\tilde{u}}^2)_{ii}$, $M_{\tilde{d}}^2 = (M_{\tilde{d}}^2)_{ii}$, and $M_{\tilde{e}}^2 = (M_{\tilde{e}}^2)_{ii}$. For the trilinear couplings, A parameters defined by $(T_u)_{33} = A_\tau y_t$, $(T_d)_{33} = A_\tau y_b$, and $(T_e)_{33} = A_\tau y_\tau$ are used. Since we consider the CP violating case, the each parameter in the above superpotential and the soft SUSY breaking Lagrangian can be a complex number.

The mass of the SM-like Higgs boson in the MSSM is calculated by the input parameters in the superpotential and the SUSY breaking Lagrangian. In order to reproduce the observed mass value $m_h = 125$ GeV, we take $\tan \beta := \langle H_2 \rangle / \langle H_1 \rangle = 30$ and we fix the stop mass parameters as $M_{\tilde{q}_3} = 7$ TeV, $M_{\tilde{t}} := M_{\tilde{u}_3} = 7$ TeV and $A_t = 10$ TeV. The other SUSY particles are irrelevant to the mass of the SM-like Higgs boson as well as the DM relic density. Therefore we can take their masses much heavier than stop. In such a case, they are decoupled from low energy observables. Here we take masses of the other sfermions as 100 TeV and $M_2 = M_3 = 10$ TeV. In our analysis, we focus on the Bino-like DM with the Higgs funnel scenario so that the heavy Higgs boson mass is close to twice the mass of the DM. In the scenario, the Bino-like neutralino rapidly annihilate through the heavy Higgs bosons resonance and the appropriate cosmic abundance for DM is reproduced. In addition, the masses of heavier neutral Higgs bosons, m_H and m_A , are close to the charged Higgs boson mass m_{H^\pm} in the MSSM. Thus we fix m_{H^\pm} to be twice of Bino mass parameter M_1 . Note that the $\tilde{\chi}\tilde{\chi}$ -Higgs boson coupling depends on non-vanishing Higgsino component in the neutralino. We choose $|\mu|$ to reproduce the correct amount of DM relic density as $\Omega_{\text{DM}} h^2 = 0.1198 \pm 0.0015$ [10]. As a consequence of these fact, both the Bino mass $|M_1|$ and the Higgsino mass $|\mu|$ should be of the order of TeV. We consider M_1 as a free parameter and solve $|\mu|$ from the measured dark matter energy density.

In the following, we summarise our benchmark parameter set:

$$|M_2| = |M_3| = 10 \text{ TeV}, \tag{11.3}$$

$$M_{\tilde{q}_{1,2}} = M_{\tilde{u}_{1,2}} = M_{\tilde{d}_{1,2,3}} = M_{\tilde{\ell}_{1,2,3}} = M_{\tilde{e}_{1,2,3}} = 100 \text{ TeV}, \tag{11.4}$$

$$M_{\tilde{q}_3} = M_{\tilde{t}} = 7 \text{ TeV}, \tag{11.5}$$

$$A_t = 10 \text{ TeV}, \tag{11.6}$$

$$m_{H^\pm} = 2M_1, \tag{11.7}$$

$$\tan \beta = 30. \tag{11.8}$$

The other A -terms are zero.

With this parameter set, CP phases in the five parameters, $(\mu, M_1, M_2, M_3, A_t)$, may be relevant to our analysis of EDMs and the spin-independent cross section. The CP phases of these parameters are described as $(\phi_\mu, \phi_{M_1}, \phi_{M_2}, \phi_{M_3}, \phi_{A_t})$, respectively, where each phases of a quantity X are defined by $X = |X|e^{i\phi_X}$.

Note that some of those CP phases are unphysical. It is known that there is a rephasing degree of freedom in the MSSM. Actually, all the physical quantities are described by the following combinations of the parameters,

$$\begin{aligned} & \arg(M_i M_j^*), \\ & \arg(M_i A_t^*), \\ & \arg(\mu M_i), \\ & \arg(\mu A_t), \\ & (i, j = 1, 2, 3). \end{aligned} \tag{11.9}$$

By using the rephasing degree of freedom, without loss of generality, we can take the basis of CP phases as $\phi_{M_3} = 0$. We also take $\phi_{A_t} = 0$ for simplicity. In general, the CP phase ϕ_{A_t} also significantly contributes to the predictions of the EDMs. However, in our benchmark parameter set given in Eqs. (11.3) – (11.8), the contribution from ϕ_{A_t} is strongly suppressed because the mass splitting between two stops is small. Therefore we scan the following four parameters,

$$(|M_1|, \phi_\mu, \phi_{M_1}, \phi_{M_2}). \tag{11.10}$$

11.3 Numerical analysis

In calculations of dark matter thermal relic density and the Higgs mass, we use `micrOMEGAs 4.3.5` [11] with `CPsuperH2.3` [12]. The Higgs mass is almost fixed to be 125 GeV in our benchmark point. When we scattered the parameters, we pick up the parameter sets which reproduce the correct DM relic abundance and the correct Higgs mass. Then we calculate the electron EDM, the neutron EDM, and the mercury EDM. We also discuss the scattering cross section for the direct detection experiments.

Since the sfermions are too heavy to contribute to the EDMs via one-loop diagrams, the two-loop Barr-Zee diagrams provide dominant contributions unless Wino, stop, and sbottom masses are heavy enough to be decoupled.

In Fig. 11.1, we show our numerical results. We can see the M_1 dependence by comparing the left panels and the right panels where $M_1 = 1$ TeV and 2 TeV, respectively. It is easily seen that larger M_1 weaken the constraint from EDM experiments. The Bino mass M_1 is approximately identified to be the mass of the dark matter neutralino. Then for larger M_1 , heavy Higgs bosons and Higgsinos become heavier, and the contributions to the EDMs become smaller. We also discuss the ϕ_μ and ϕ_{M_2} dependence of the EDMs. The left panels in Fig. 11.1 shows the electron EDM, the mercury EDM, and the neutron EDM with $\phi_{M_1} = 0$. The shaded regions are already excluded by the current upper bound on the EDMs. We find the combination of the electron EDM and the mercury EDM exclude the

large region of the parameter space. Both ϕ_μ and ϕ_{M_2} cannot be large. We also find that the electron EDM strongly depends on ϕ_{M_2} . On the other hand, ϕ_{M_2} dependence of the mercury EDM and the neutron EDM are milder.

Fig. 11.2 displays the ϕ_{M_1} dependence. Taking into account the constraint from the mercury EDM, we find that the mercury EDM and the neutron EDM are almost independent of ϕ_{M_1} . On the other hand, the dependence of the electron EDM on ϕ_{M_1} is mild but visible.

From these figures, one can see that the neutron and the mercury EDMs are sensitive to ϕ_μ , and also weakly depend on ϕ_{M_2} . On the other hand, the electron EDM is sensitive to $\phi_{M_2} + \phi_\mu$, and weakly depend on ϕ_{M_1} . Most of the parameter space in Figs. 11.1 and 11.2 are within the future prospects of the electron EDM and the neutron EDM. In Summer of 2018, the constraint on the electron EDM is updated to be $|d_e/e| < 1.1 \times 10^{-29} \text{ e-cm}$ by ACME collaboration[13]. With this new constraint, the allowed regions in Figs. 11.1 and 11.2 become very thin stripes. Thus the correlation among the EDMs in future experiments provide a strong hint to explore the CP phases in the SUSY breaking sector.

Let us discuss DM-nucleon scattering cross section. Since we consider the Higgs funnel scenario, the DM neutralino couples to neutral scalar bosons. Through these couplings, the DM neutralino and nucleon interact with each other.

Though the couplings are rather small in the scenario, the couplings lead to a significant size of the spin-independent cross section and it will be within future prospects of the DM direct detection experiments.

In Figure 11.3, the ϕ_{M_2} and ϕ_μ dependence of σ_{SI} is shown. In this figure, the parameter choice is the same as in Fig. 11.1. Figure 11.4 displays the ϕ_{M_1} and ϕ_μ dependence of σ_{SI} with the same parameter choice as in Fig. 11.2.

The spin-independent cross section is found to be smaller than the current upper bound [14–16] in all the region of the parameter space. However is within the future prospects of the DARWIN [17], the DarkSide-20k [18], and the LZ [19].

Note that the scattering cross section depends on $\phi_{M_1} + \phi_\mu$, and the ϕ_{M_2} dependence is not significant.

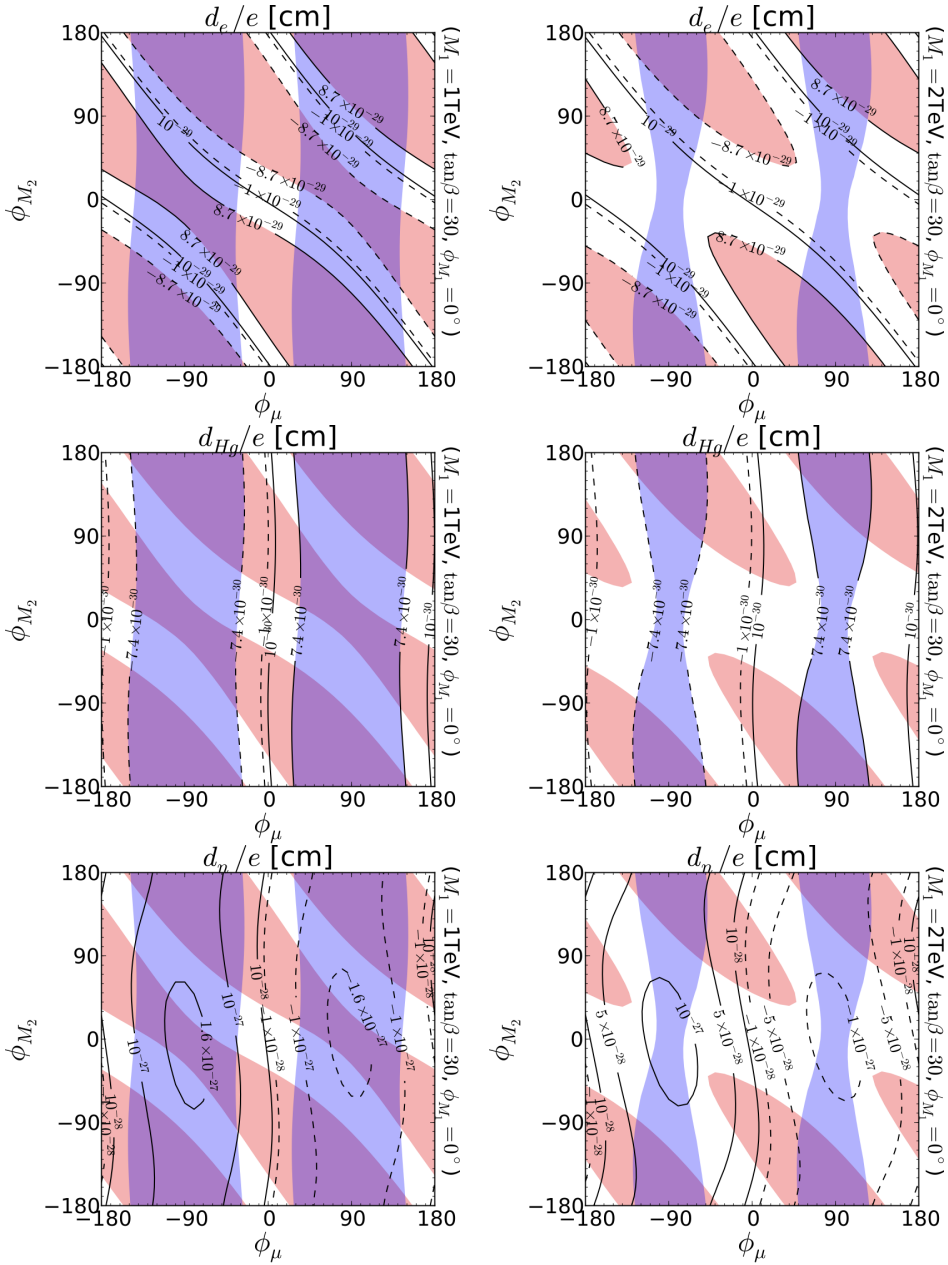


Fig. 11.1. The EDMs for $\tan \beta = 30$ and $\phi_{M_1} = 0^\circ$. The left (right) panels are for $M_1 = 1 \text{ TeV}$ ($M_1 = 2 \text{ TeV}$). The contours in the top, the center, and the bottom panels are those of the electron EDM, the mercury EDM, and the neutron EDM, respectively. The dashed lines show the negative values. The red and blue shaded regions are excluded by the electron EDM and the mercury EDM, respectively. The figures are taken from Ref. [1].

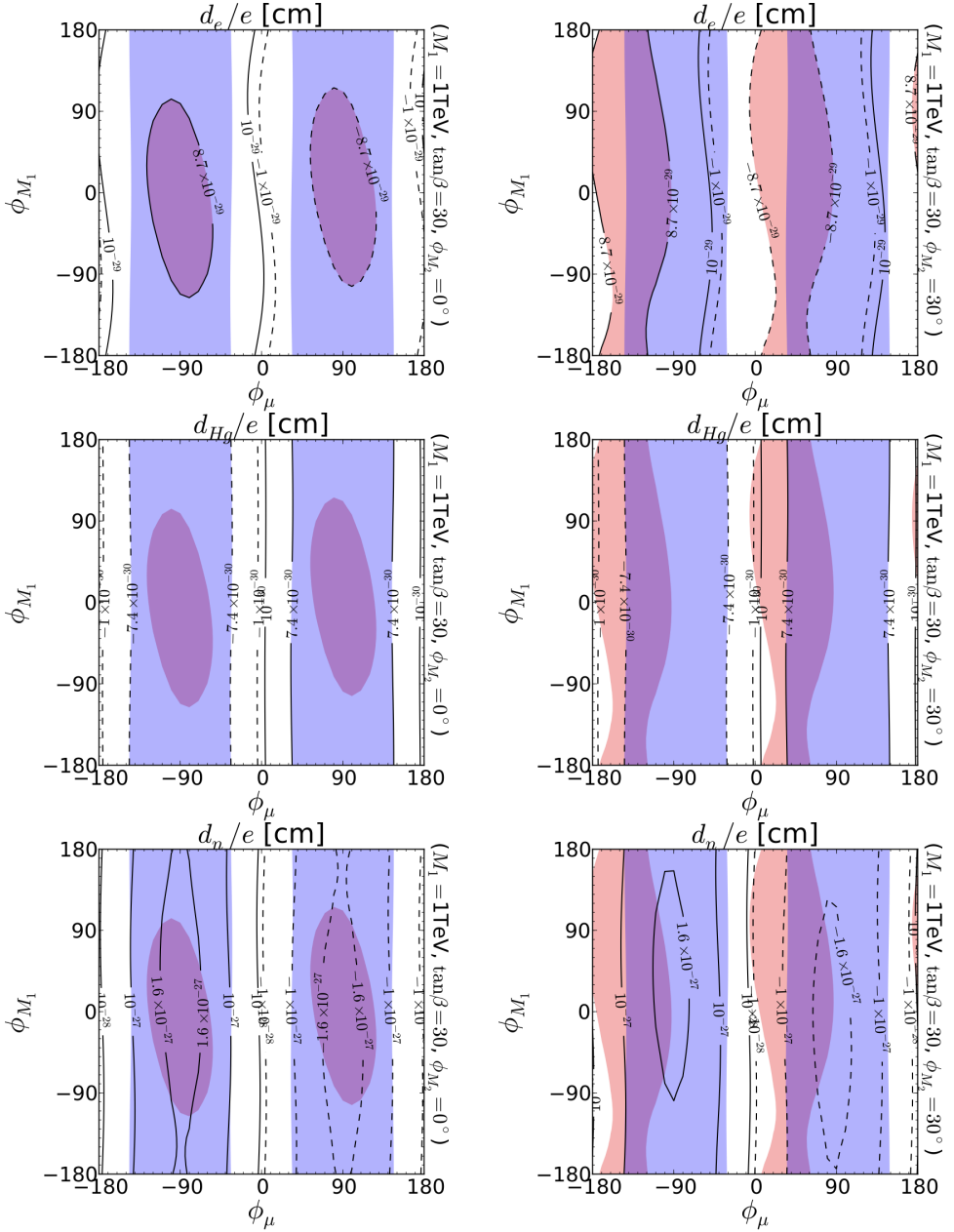


Fig. 11.2. The EDMs for $M_1 = 1 \text{ TeV}$ and $\tan \beta = 30$. In the left (right) panels, $\phi_{M_2} = 0^\circ$ (30°). The shadings and contours are the same as in Fig. 11.1. The figures are taken from Ref. [1].

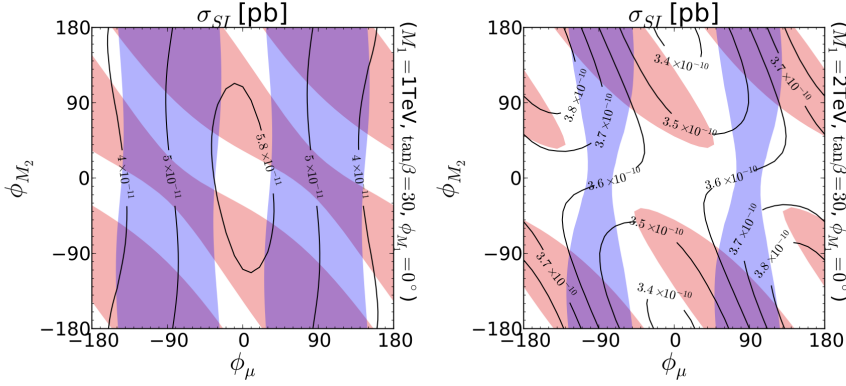


Fig. 11.3. The DM-nucleon scattering cross sections for $\tan \beta = 30$ and $\phi_{M_1} = 0^\circ$. The left (right) panel is for $|M_1| = 1$ TeV (2 TeV). The shadings are the same as in Fig. 11.1. The figures are taken from Ref. [1].

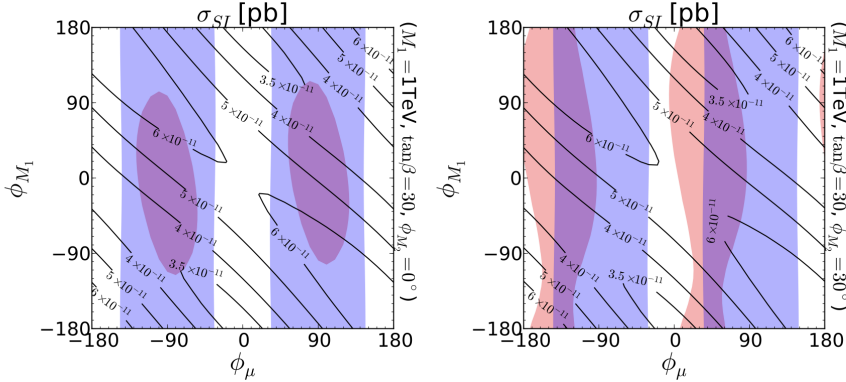


Fig. 11.4. The DM-nucleon scattering cross sections for $M_1 = 1$ TeV and $\tan \beta = 30$. The left (right) panel is for $|\phi_{M_2}| = 0^\circ$ (30°). The shadings are the same as in Fig. 11.1. The figures are taken from Ref. [1].

11.4 Summary

In this talk, we have considered the MSSM with CP phases, and we have focused on a DM scenario where the Bino-like neutralino is a DM whose annihilation cross section is enhanced enough through heavy Higgs bosons exchange so that the observed relic abundance of the DM can be explained. In this benchmark scenario, we have examined several EDMs and the spin-independent cross section for DM scattering with nuclei. We have shown that the EDMs are very powerful tool to explore the parameter space in the MSSM with CP phases even when most of the SUSY particles are very heavy.

Acknowledgements

This work was supported by JSPS KAKENHI Grant Number 17H05408 and Kogakuin University Grant for the project research.

References

1. T. Abe, N. Omoto, O. Seto and T. Shindou, Phys. Rev. D **98** (2018) no.7, 075029.
2. N. Nagata and S. Shirai, JHEP **1501**, 029 (2015) [arXiv:1410.4549 [hep-ph]].
3. M. Drees and M. M. Nojiri, Phys. Rev. D **47**, 376 (1993) [hep-ph/9207234].
4. H. Baer and M. Brhlik, Phys. Rev. D **53**, 597 (1996) [hep-ph/9508321].
5. H. Baer and M. Brhlik, Phys. Rev. D **57**, 567 (1998) [hep-ph/9706509].
6. V. D. Barger and C. Kao, Phys. Rev. D **57**, 3131 (1998) [hep-ph/9704403].
7. J. R. Ellis, T. Falk, G. Ganis, K. A. Olive and M. Srednicki, Phys. Lett. B **510**, 236 (2001) [hep-ph/0102098].
8. G. Jungman, M. Kamionkowski and K. Griest, Phys. Rept. **267**, 195 (1996) [hep-ph/9506380].
9. B. C. Allanach *et al.*, Comput. Phys. Commun. **180**, 8 (2009) [arXiv:0801.0045 [hep-ph]].
10. P. A. R. Ade *et al.* [Planck Collaboration], Astron. Astrophys. **594** (2016) A13 doi:10.1051/0004-6361/201525830 [arXiv:1502.01589 [astro-ph.CO]].
11. D. Barducci, G. Belanger, J. Bernon, F. Boudjema, J. Da Silva, S. Kraml, U. Laa and A. Pukhov, Comput. Phys. Commun. **222**, 327 (2018) [arXiv:1606.03834 [hep-ph]].
12. J. S. Lee, M. Carena, J. Ellis, A. Pilaftsis and C. E. M. Wagner, Comput. Phys. Commun. **184**, 1220 (2013) [arXiv:1208.2212 [hep-ph]].
13. V. Andreev *et al.* [ACME Collaboration], Nature **562** (2018) no.7727, 355. doi:10.1038/s41586-018-0599-8
14. D. S. Akerib *et al.* [LUX Collaboration], Phys. Rev. Lett. **118** (2017) no.2, 021303 doi:10.1103/PhysRevLett.118.021303 [arXiv:1608.07648 [astro-ph.CO]].
15. E. Aprile *et al.* [XENON Collaboration], Phys. Rev. Lett. **119** (2017) no.18, 181301 doi:10.1103/PhysRevLett.119.181301 [arXiv:1705.06655 [astro-ph.CO]].
16. X. Cui *et al.* [PandaX-II Collaboration], Phys. Rev. Lett. **119** (2017) no.18, 181302 doi:10.1103/PhysRevLett.119.181302 [arXiv:1708.06917 [astro-ph.CO]].
17. J. Aalbers *et al.* [DARWIN Collaboration], JCAP **1611**, 017 (2016) [arXiv:1606.07001 [astro-ph.IM]].
18. C. E. Aalseth *et al.*, Eur. Phys. J. Plus **133**, no. 3, 131 (2018) [arXiv:1707.08145 [physics.ins-det]].
19. D. S. Akerib *et al.* [LUX-ZEPLIN Collaboration], arXiv:1802.06039 [astro-ph.IM].

Discussion Section

The discussion section is reserved for those open problems presented and discussed during the workshop, that might start new collaboration among participants or at least stimulate participants to start to think about possible solutions of particular open problems in a different way, or to invite new collaborators on the problems, or there was not enough time for discussions and will hopefully be discussed in the next Bled workshop.

Since the time between the workshop and the deadline for contributions for the proceedings is very short and includes for most of participants also their holidays, it is not so easy to prepare there presentations or besides their presentations at the workshop also the common contributions to the discussion section.

However, the discussions, even if not presented as a contribution to this section, influenced participants' contributions, published in the main section. Contributions in this section might not be yet pedagogically enough written, although they even might be innovative and correspondingly valuable indeed.

As it is happening every year also this year quite a lot of started discussions have not succeeded to appear in this proceedings. Organizers hope that they will be developed enough to appear among the next year talks, or will just stimulate the works of the participants.

There are seven contributions in this section this year.

One contribution discusses shortly a possible influence of the "dark atom"s on the expanding universe, offering the explanations for some puzzles in the experiments trying to detect dark matter. "Dark atom" is the "atom", which contains a double electromagnetically charged "baryon" made of three stable \bar{u} quarks, decoupled from the three observed families of quarks. A bound state of an ordinary He nucleus with such a "baryon" would made the "dark atom". The elaboration of this idea looks very interesting.

There is the contribution, which is pointing out that inconsistency between the theoretical predictions and the experimental data is not necessarily a signal for new physics, since it can just be due to the higher order corrections not included in the theoretical evaluations. The authors, discussing several cases, conclude that there might not be yet any experimental data, which could be interpreted as a signal of new physics beyond the standard model.

And yet we all hope that the new data, either the cosmological ones or, hopefully, also the LHC or of other experiments ones, will confirm the theory

beyond the standard models, like it is the spin-charge-family theory, since there are (so many) assumptions in the standard model, which ought to have explanations.

The contribution presenting the Dirac operators γ^a and S^{ab} , and of the operators $\tilde{\gamma}^a$ and the corresponding \tilde{S}^{ab} , determining in the spin-charge-family theory — first the family members quantum numbers of fermions, and the second the family quantum numbers of fermions — was stimulated by participants of this year workshop. In the basic states in $(3 + 1)$ (out of $d = (13 + 1)$), the matrices have the dimension 16×16 . The contribution is to make it easier for the reader to recognize the differences between the quantum numbers describing the family members and those describing families.

The contribution discussing some representations of the second quantisable integer spin fermions is meant to recognize better the differences between the fermions with the internal degrees of freedom described in Clifford space (with the spins and charges in fundamental representations of the groups, the subgroups of the Lorentz group) and the fermions with the internal degrees of freedom described in Grassmann space (with the spins and charges in the adjoint representations of the subgroups of the Lorentz group), presented in this proceedings in the talks section. If consisting of the integer spins fermions (only), nuclei, atoms, molecules ... would in such an universe be of completely different kind. Nature has obviously "made a choice" of the Clifford space.

There is the contribution, which represents the improvement of the by the author proposed model with the broken $SU(3)$ gauged family symmetry. It reports on the parameter space region, in which all the results are in agreement with so far observed data. The mass of the $SU(2)_L$ weak singlet vector-like D quark, proposed in this theory, may be of the order of 10 TeV.

There are two contributions in which the author constructs, while recognizing the correspondence between the Clifford algebra states as represented in the *spin-charge-family* theory and the binary codes, the geometrical model with closed packed cells of two different shapes representing quarks and leptons with their observed charges. Author tries to extract out of these cells, recognizing different possible symmetries, even forces among these constituents. Although the author has almost incredible recognitions, yet it is very questionable what one can learn out of such a model, especially when one would like to look beyond the standard model to understand the origin of properties of fermion and boson fields, and in the author's case, what does determine assumptions and parameters of his model.

All discussion contributions are arranged alphabetically with respect to the authors' names.

Diskusije

Ta razdelek je namenjen odprtim vprašanjem, o katerih smo med delavnico razpravljali in bodo morda privedli do novih sodelovanj med udeleženci, ali pa so pripravili udeležence, da razmislijo o možnih rešitvah odprtih vprašanj na drugačne načine, ali pa bodo k sodelovanju pritegnili katerega od udeležencev, ali pa ni bilo dovolj časa za diskusijo na določeno temo in je upati, da bo prišla na vrsto na naslednji blejski delavnici.

Ker je čas med delavnico in rokom za oddajo prispevkov zelo kratek, vmes pa so poletne počitnice, je zelo težko pripraviti prispevek in še težje poleg prispevka, v katerem vsak udeleženec predstavi lastno delo, pripraviti še prispevek k temu razdelku.

Tako se precejšen del diskusij ne bo pojavil v letošnjem zborniku. So pa gotovo vplivale na prispevek marsikaterega udeleženca. Nekateri prispevki še morda niso dovolj pedagoško napisani, so pa vseeno lahko inovativni in zato dragoceni.

Organizatorji upamo, da bodo te diskusije do prihodnje delavnice dozorele do oblike, da jih bo mogoče na njej predstaviti.

Letos je v tem razdelku sedem prispevkov.

Eden prispevek obravnava na kratko možnost vpliva "temnih atomov" na razvoj vesolja in ponudi razlago nekaterih ugank v poskusih, ki naj bi merili temno snov. "Temni atom" je atom, ki vsebuje temno snov. "Temni atom" je atom, ki vsebuje "barion" z dvojnimi elektromagnetnim nabojem in ga tvorijo trije stabilni kvarki \bar{u} . Ti so neodvisni od treh že poznanih družin kvarkov. Vezano stanje helijevega jedra s takim "barionom" bi tvorilo "temni atom". Obravnava te ideje se zdi zanimiva.

Avtorja pokažeta, da neujemanje teoretičnih napovedi z meritvami še ne pomeni nujno, da je to signal za novo teorijo, ki preseže standardni model elektrošibke interakcije, ker so neujemanja lahko tudi posledica tega, da pri teoretičnih izračunih niso vključeni popravki dovolj visokih redov. Obravnavata več primerov in skleneta, da po njuno doslej še ni meritev, ki bi jih ne bilo mogoče pojasniti s standardnim modelom.

In vendar vsi upamo, da bodo bodisi kozmološke meritve bodisi meritve na pospeševalniku LHC ali na drugih pospeševalnikih kmalu potrdile pravilnost teorij(e), kot je denimo teorija spinov-nabojev-družin, saj standardni model s svojimi 30 privzetki nima razlage za vse te privzetke.

Prispevek, ki obravnava Diracove operatorje γ^a in ustrezne S^{ab} , ter $\tilde{\gamma}^a$ in ustrezne \tilde{S}^{ab} , ki določajo v teoriji spinov-nabojev-družin prvi spine in naboje

fermionov, drugi družinska kvantna števila fermionov, so spodbudile razprave udeležencev letošnje delavnice. Matrike imajo na baznih stanjih v prostoru $(3 + 1)$ (ki je vključen v $d = (13 + 1)$) dimenzijo 16×16 . Namen prispevka je olajšati bralcem, da prepoznajo razliko med kvantnimi števili, ki opišejo člane družin in kvantnimi števili, ki opišejo družine.

V razdelku je tudi prispevek, ki razpravlja o nekaterih upodobitvah fermionov s celoštevilčnim spinom v drugi kvantizaciji, kar naj pomaga bolje razumeti razlike med fermioni, katerih notranje prostostne stopnje opišemo v Cliffordovem prostoru (spini in naboji so v tem primeru v fundamentalnih upodobitvah grup, ki so podgrupe Lorentzove grupe), ter fermioni, katerih notranje prostostne stopnje so opisane v Grassmannovem prostoru (spini in naboji so tem primeru v adjungiranih upodobitvah podgrup Lorentzove grupe). Diskusija je povezana s prispevkom v razdelku predavanj v tem zborniku in obravnava primer, v katerem bi imeli fermioni le celoštevilčni spin. Taka izbira bi vodila do popolnoma drugačnih jeder, atomov, molekul Narava je očitno izbrala Cliffordov prostor.

Prispevek, v katerem avtor predlaga model z zlomljeno družinsko simetrijo $SU(3)$, obravnava območje parametrov, ki zagotovi ujemanje modela z izmerjenimi podatki. Maso napovedanega novega kvarka oceni na ~ 10 TeV.

Razdelek vsebuje dva prispevka, v katerih postavi avtor, upoštevajoč zveze med stanji Cliffordove algebre kot jih predstavi teorija *spinov-nabojev-družin* in binarnimi kodami, geometrijski model, v katerem so kvarki in leptoni ter njihovi naboji predstavljeni s tesno zloženimi celicami dveh oblik. Iz tega geometrijskega modela poskuša avtor izpeljati z upoštevanjem možnih simetrij, ki jih ponudi model, lastnosti in celo sile med sestavnimi delci, to je kvarki in leptoni. Avtorjev pristop je neverjetno domiselen, saj vse lastnosti osnovnih delcev in polj pripiše geometrijskim lastnostim modela. Vprašanje pa je, kaj se lahko naučimo iz takega modela, kjer parametre modela določa geometrija, zlasti, če želimo razumeti od kod lastnosti fermionskih in bozonskih polj ter v avtorjevem primeru, kaj določa parametre modela.

Prispevki v tej sekciji so, tako kot prispevki v glavnem delu, urejeni po abecednem redu priimkov avtorjev.



12 On Triple-periodic Electrical Charge Distribution as a Model of Physical Vacuum and Fundamental Particles

E.G. Dmitrieff *

Irkutsk State University, Russia

Abstract. In this study we consider triple-periodical electrical charge distributions with the pattern similar to the Weaire-Phelan structure. According to it, the space is splitted to opposite-charged cells separated with electrically neutral border.

Possible configurations obtained as results of exchanges of these cells appear to have properties that can be corresponded to the quantum numbers of known fundamental particles.

We find it promising to use models of this kind, aiming to infer the axioms and constants of the Standard Model from the emergent geometrical properties of the distribution.

Povzetek. Prispevek obravnava trojne periodične porazdelitve električnih nabojev, ki imajo vzorec podoben Weaire-Phelan strukturam. V modelu je prostor razdeljen na celice z nasprotnimi naboji, ki jih loči električno nevtralna meja.

Konfiguracije, ki sledijo z izmenjavo teh celic, imajo lastnosti, ki jih avtor poveže s kvantnimi števili kvarkov in leptonov.

Avtor meni, da ti modeli omogočijo izpeljavo privzetkov in konstant standardnega modela.

Keywords: Particle model, Weaire-Phelan tessellation

12.1 Introduction

The spin-charge-family theory presented in [1], [2], [8], [9] offers reasonable explanations for the phenomena of the Standard Model of the fundamental particles. Originating from Clifford algebra, it comes to the binary internal degrees of freedom, explaining properties of existing fundamental particles and predicting existence of extra fermion families.

In turn, we reproduce particle properties starting with *binary code* model. As we have shown in [7], Boolean models designed for fundamental particles can reproduce most of their properties, including charges (electrical, color, weak and hyper-charge), lepton- and baryon numbers, fermion flavor and family membership, and boson spin magnitude. The particles are represented as combinations or *codes* of symbols carrying one of two possible values, so these models are *binary*.

* E-mail: eliadmitrieff@gmail.com

Developing these models, we started with well-known linear codes, that consist of binary digits (*bits*) with usual values either 1 or 0. Then, in order to reduce the amount of information carried by the code, we abandoned the linear structure in favor of spatial one. Also we have symmetrized and normalized the values carried by bits, using $+\frac{1}{6}$ and $-\frac{1}{6}$ instead of 1 and 0. These values could be directly interpreted as electrical charge in units of electron charge e .

Using spatial combination of eight symbols of this kind, we managed to represent all known fundamental particles. Also, analyzing unused combinations, we proposed existence of new scalar particle forming the vacuum condensate. It could be represented by this combination that is repeated periodically, filling the space as a tessellation.

Since the tessellation can be chiral, the space filled with small alternating charged regions, comparing to simple empty space, has an advantage of offering possible explanation for difference between right- and left-handed particles in respect of the vacuum.

Different particle codes, substituting vacuum codes in the tessellation, violate the periodicity with different ways. We suppose that it may be used to infer associated rest energies (masses) instead of postulating them.

Treating vacuum expectation value as Coulomb potential between neighboring opposite-charged "bits" [11], we estimated that the distance between them should be on scale of $\approx 10^{-21}$ m.

Being inspired by idea of vacuum domains [3], we suppose that the interpretation of these "bits" as domains can explain the problem of their observations absence. As asserted originally by Zeldovich with co-authors, the vacuum domains should appear as consequence of symmetry break in the phase transition. In our models, they do exist but have the correlation radius on sub-particle scale instead of cosmological one. This should happen in case the 2-order phase transition is not yet complete but just approaches its critical point.

Having a model with some spatial distribution of charged bits, or vacuum domains, we recognize that it is necessary to find out the pattern of this distribution which is consistent with other observable properties of vacuum and particles, including their symmetry, mass spectrum, propagation, interactions and so on.

After checking simple (NaCl-like) and volume-centered (CsCl-like) cubic lattices, we found out that the A15 (Nb₃Sn-like) lattice, or Weaire-Phelan structure, has some advantages allowing it to be the possible vacuum- and particle model.

12.2 Overview of the original Weaire-Phelan tessellation

The original Weaire-Phelan structure is described in [12]. It is a foam of equal-volumed cells separated by thin walls. Among other structures, having the same cell volume, this one has the minimal (known at the present time) inter-cell wall area, so it is a candidate solution for the Kelvin problem [14]. There is evidence of self-assembling of this tessellation driven by minimization of the surface energy [13].

Cells forming the Weaire-Phelan structure have almost flat faces and just slightly curved edges, thus they can be closely approximated by irregular polyhe-

dra. It is necessary to use two *kinds* of them – dodecahedra (D) and tetrakaidecahedra (T)¹.

Unlike dodecahedra, the tetrakaidecahedra have three possible *orientations* in respect of the three Cartesian axes.

The cells of both kinds can be included in the tessellation in two ways, so they became *chiral*.

Eight cells, differing in kind, chirality, and orientation, form one translation unit. These translation units, in turn, form simple cubic grid.

Assuming the size of translation unit to be $l = 4\lambda$ in each dimension (where λ is a scale factor, and 4 is used to get most of coordinates integer), we get the unit volume $V_u = l^3 = 64\lambda^3$, and cell volume $V_c = \frac{1}{8}V_u = 8\lambda^3$ (remembering that all cells are equal-volumed).

Having the coordinate axes perpendicular to the hexagonal faces of the tetrakaidecahedra, and associating the origin with the center of one of dodecahedra, one can obtain coordinates of the centers of all other cells:

	D	T _x	T _y	T _z
R	(0,0,0)	(0,2,1)	(1,0,2)	(2,1,0)
L	(2,2,2)	(0,2,3)	(3,0,2)	(2,3,0)

These coordinates are expressed in units of λ and determined up to 4λ , meaning that one can obtain coordinates of each cell by adding of "even" vector

$$\mathbf{V}_E = (4n_x, 4n_y, 4n_z) \lambda, n_i \in \mathbb{Z}. \quad (12.1)$$

Further, we omit the scale factor λ where it shouldn't cause misunderstanding.

Here we chose the R and L mark of the chirality by the arbitrary choice.

There are four symmetry axis C_3 defined by equations $\pm x = \pm y = \pm z$.

Since the structure does not possess reflection symmetry, it is chiral, so there are two mirror-reflected structures. For instance, after reflecting in the plane $x = y$ the chirality is reversed and the coordinates are changed as the following:

	D	T _x	T _y	T _z
L	(0,0,0)	(2,0,1)	(0,1,2)	(1,2,0)
R	(2,2,2)	(2,0,3)	(0,3,2)	(3,2,0)

After performing the shift (move) of the whole infinite structure with the "odd" vector

$$\mathbf{V}_O = \mathbf{V}_E + (\pm 2, \pm 2, \pm 2)\lambda, \quad (12.2)$$

¹ The dodecahedron is a pyritohedron with twelve equal pentagonal faces, possessing tetrahedral symmetry T_h , and the tetrakaidecahedron is truncated hexagonal trapezohedron possessing rotoreflexion symmetry C_{3h} , with two hexagonal faces, four large and eight small pentagonal faces.

i.e. for the half-size of the translation unit ($2\sqrt{3}\lambda$), in direction of C_3 axis, we get the original structure again:

	D	T_x	T_y	T_z
L	(2,2,2)	(2,0,3)	(2,3,0)	(1,2,0)
R	(0,0,0)	(0,2,1)	(2,1,0)	(1,0,2)

Thus, the structure possesses global **PS** symmetry, where **P** is parity (particularly, exchange of any two coordinates) and **S** is shift along C_3 axis on the half of translation unit size (or, generally, on the odd vector).

It also means that despite of mirror asymmetry of each finite part, there is only one infinite Weaire-Phelan structure, which is either right- or left-handed depending on the choice of origin. It can be also considered as *two* overlapped chiral structures consisting of the same elements but shifted in respect of each other with the odd vector (12.2).

12.3 Dual-charged Weaire-Phelan structure

To use the Weaire-Phelan structure as a spatial version of binary-code model, we need to assume that each cell carries electrical charge with magnitude of $\frac{1}{6}$. Since the space containing no particles is electrically neutral, the counts of positive and negative cells in any volume $\gtrsim l^3$ should be the same. Any change of cell charge, that can be from $+\frac{1}{6}$ to $-\frac{1}{6}$, or back, would cause the total electric charge to change on $\pm\frac{1}{3}$. Thus, all the particles in this model will have discrete charges with step of $\frac{1}{3}$, that is according to experiments. So the existence of particles with charges, for instance, of $\pm\frac{1}{2}$, is impossible.

In general, the charge *inside* cells can be distributed being determined by physical law acting on this scale, for instance:

- all the charge can be concentrated in cell centers, in point-size sub-particles (partons or rishons);
- the charge can be distributed smoothly inside cells around their centers, falling to zero on the inter-cell borders;
- the charges of opposite sign can be concentrated on both sides of the walls between opposite-charged cells, and also can be smoothly distributed along them.

In the following subsections we consider these simplified assumptions of the charge distribution.

We assume that the basic "vacuum" alteration of charged cells in the tessellation should fulfill the following requirements:

- each translation unit should be electrically neutral, and
- cells with opposite chirality should also be opposite-charged.

So, we assume positive charge of cells of one chirality and negative for another. However, at this stage we do not recognize any natural rule that would define the absolute chirality. So, there are $2^3 = 8$ choices of T_i charges and also 2 choices of D . We make this choice as shown in the following table:

Cell type	Charge	Coordinates	Plane
D_R	—	(0, 0, 0)	$x + y + z = 4n$
T_{Ri}	+	(0, 2, 1), (1, 0, 2), (2, 1, 0)	$x + y + z = 4n + 3$
D_L	+	(2, 2, 2)	$x + y + z = 4n + 2$
T_{Li}	—	(0, 2, 3), (3, 0, 2), (2, 3, 0)	$x + y + z = 4n + 1$

In the last column of the table we show the equations of planes that contain all the cell centers of particular type.

Making the choice of charge sign for T_i , we break the symmetry between C_3 axis, so one of them becomes dedicated. Also, making this choice for D cell charge breaks symmetry between opposite handednesses. So there are two possible dual-charged Weaire-Phelan structures. That corresponds to the principal possibility of physical vacuum with reversed chirality.

12.4 Cell Centers approximation

Here we abstract from the details of spatial distribution of the electric charge, and suppose it is just concentrated somewhere in the vicinity of the cell centers. We do so to simplify the charge calculation, replacing the integration of the charge density in the volume of interest with counting the number of centers of positive and negative cells falling into it. Since the coordinates of the cell centers are integers (i.e., proportional to the scale factor λ), they can lay on the certain planes only, between which, in this approximation, there is nothing.

12.4.1 CPS symmetry

The following set of grids (Fig. 12.1) illustrates the placement of positive and negative cells' centers, as black and white circles, respectively, in the cubic translation unit of size $4 \times 4 \times 4$ starting with its left bottom front corner from the origin of reference frame. Centers of D -cells are marked with double-border.

The first grid is the cross-section for plane $z = 0$, the second one is for plane $z = 1$ and so on. The plane $z = 4$ is the same as $z = 0$ due to the periodicity.

Considering the translation unit cube that is shifted with the "even" vector $(2n + 1)(2, 2, 2)$, for instance $(-2, -2, -2)$, i.e. performing **S** operation, we get the scheme on the Fig. 12.2 (the first grid is plane $z = -2$ and so on).

After reflecting in the plane $x = y$ (**P** operation) we get the scheme on the Fig. 12.3.

One can ensure that this shift operation (**S**) followed by reflection (**P**) has the same result as the charge inversion (**C**). So these three operations being applied

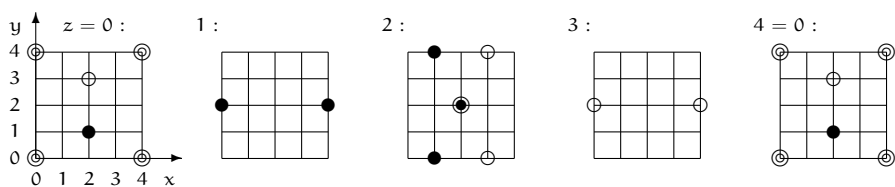


Fig. 12.1. The placement positive- and negative-charged cell centers in the translation unit

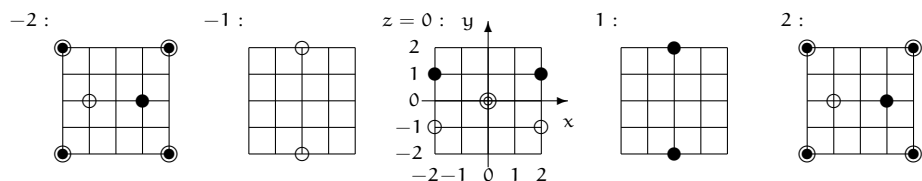


Fig. 12.2. The translation unit after S (shift) operation

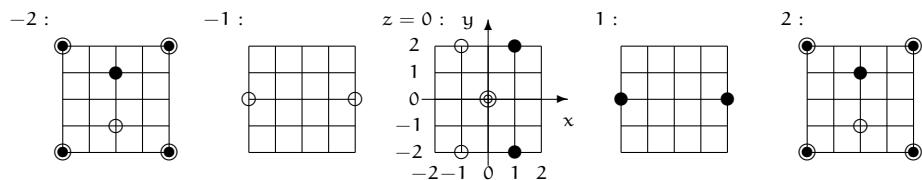


Fig. 12.3. The translation unit after sequential shift and reflection SP

consequently (in any order) turn the structure back to its original state. It means that the structure possesses the symmetry in respect of **CPS** combination, but neither in respect of **C**, **P**, **S** individually nor in respect of their pairs **CP=PC=S**, **PS=SP=C**, **CS=SC=P**.

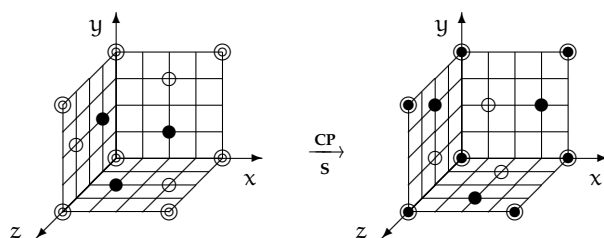


Fig. 12.4. Either CP or S operation applied to the translation unit

12.4.2 View in isometric projection

The distribution of charged cell centers also can be represented in the reference frame $\xi\zeta v$, in which ζ axis follows the diagonal of the translation unit cube. The planes containing cells of one type, that are $x + y + z = 4n + k = \zeta$, are planes ξv .

We perform the reference frame transformation $xyz \mapsto \xi\zeta\nu$ using $O(3)$ rotation matrix with Euler angles $\frac{\pi}{4}$ and $\arccos \sqrt{\frac{2}{3}}$:

$$\begin{pmatrix} \xi \\ \zeta \\ \nu \end{pmatrix} = \frac{1}{\sqrt{6}} \begin{pmatrix} \sqrt{3} & 0 & -\sqrt{3} \\ \sqrt{2} & \sqrt{2} & \sqrt{2} \\ -1 & 2 & -1 \end{pmatrix} \begin{pmatrix} x \\ y \\ z \end{pmatrix}. \quad (12.3)$$

The diagram on Fig. 12.5 illustrates six faces of the translation unit with the center in the point $(0, 0, 0)$ (the cell center in this point is not shown since it does not belong to the cube's faces). The plane $\xi\nu$ is faced to the observer while the ζ axis directs away from the observer.

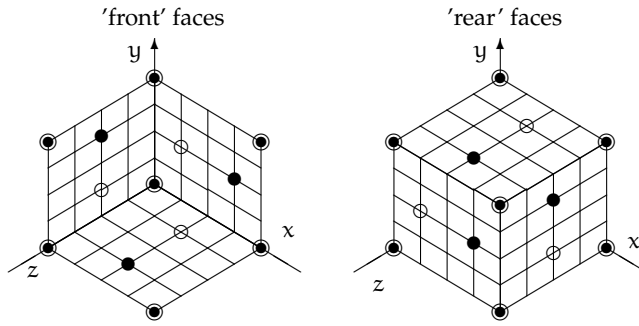


Fig. 12.5. Translation unit cube with the center in $(0, 0, 0)$ in the isometric projection on its diagonal

The projection to the $\zeta\nu$ plane (Fig. 12.6) illustrates that in each translation unit cube there are 12 planes perpendicular to its diagonal (ζ axis), that contain charged cell centers, and that these planes are different. Starting from the 0^{th} plane with $\zeta = 0$, and increasing ζ by $\frac{1}{\sqrt{3}}$, one can find that it is just the 12^{th} one at $\zeta = 12/\sqrt{3}$, where the next translation unit starts, is the same with the 0^{th} plane).

However, planes starting from the translation unit center (the 6^{th} , $\zeta = 6/\sqrt{3}$) repeat planes from 0^{th} through 5^{th} but reversed in charge. Since the translation in ζ direction on $6/\sqrt{3}$ is the **S** operation, that is equal to **CP**, they are also mirrored, i.e. parity-inversed.

So any change in this structure, that is possible in any particular place, can have its "anti-change", with opposite charge and parity, possible in places shifted on some "odd" vector \mathbf{V}_O (12.2).

The diagram on Fig. 12.7 illustrates the placement of the cell centers in the projection on the $\nu\xi$ plane:

On this diagram the cells residing on the same plane perpendicular to the ζ axis are joined together with lines and labeled with values of ζ coordinate (in units of $1/\sqrt{3}$), so one can see the *equilateral triangles* that they form².

² The visible 'constellations' of T cell centers do not form equilateral triangles in the $\nu\xi$ planes since they have different ζ .

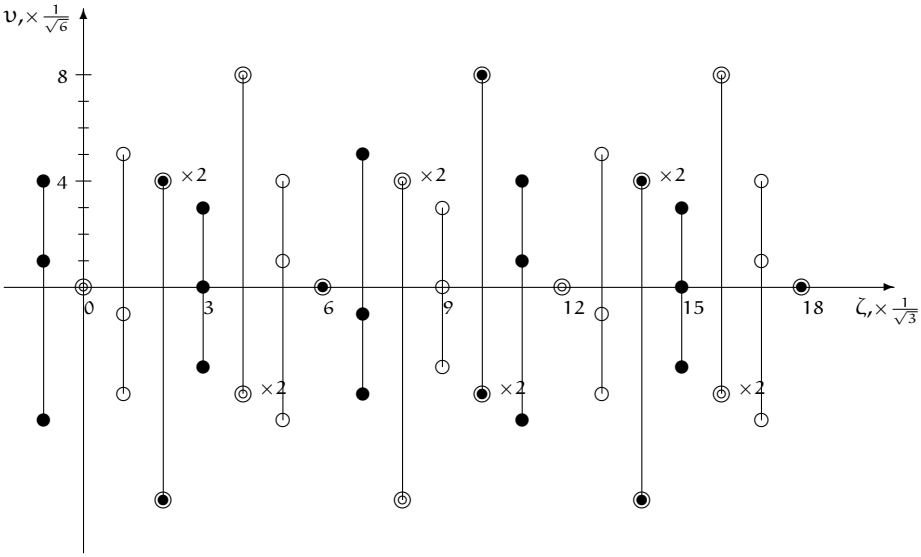


Fig. 12.6. Charged cell centers distribution in projection to the ζv plane

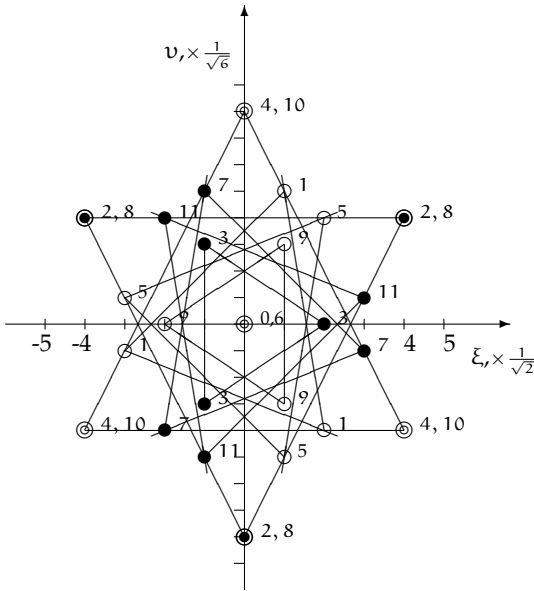


Fig. 12.7. Cell centers placement in projection on the $v\xi$ plane

The D cells of different charge overlap and hide each other along the projective direction, so behind each positive cell the negative one is assumed, and vice versa.

The planes, cell types and the shapes the cell centers form, are listed in the Table 12.1, from $\zeta = 0$ to $12/\sqrt{3}$.






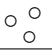


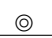

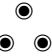


$\zeta, \times \frac{1}{\sqrt{3}}$	kind, charge	shape	size	shape description
0	D−		−	Axial D−
1	T−		$\sqrt{14}$	Large T− triangle counterclockwise
2	D+		$\sqrt{32}$	D+ triangle v-down
3	T+		$\sqrt{6}$	Small T+ triangle (ξ-right)
4	D−		$\sqrt{32}$	D− triangle v-up
5	T−		$\sqrt{14}$	Large T− triangle clockwise
6	D+		−	Axial D+
7	T+		$\sqrt{14}$	Large T+ triangle clockwise
8	D−		$\sqrt{32}$	D− triangle v-down
9	T−		$\sqrt{6}$	Small T− triangle (ξ-left)
10	D+		$\sqrt{32}$	D+ triangle v-up
11	T+		$\sqrt{14}$	Large T+ triangle counterclockwise
12	D−		−	Axial D−

Table 12.1. Shapes of cell center placements in twelve different planes

12.4.3 Small T triangle and its environment

Consider the small triangle of three T+ cells with the same charge at $\zeta = 3/\sqrt{3}$, with edge of $\sqrt{6}$. The triangle has electric charge $\Sigma q_3 = +1/2$, so its environment has the opposite charge $q_{\text{env}} = -1/2$ that ensures the total electrical neutrality.

The closest neighborhood of the small T triangle is asymmetrical: in ζ direction, there are two planes with *different* charge before it and two *negative*-charged planes after it.

Namely, at $\zeta = 1/\sqrt{3}$ there is a large (edge is $\sqrt{14}$) T− triangle carrying electric charge $q = -1/2$, and at $\zeta = 2/\sqrt{3}$ there is a D+ triangle (edge= $\sqrt{32}$) carrying $q = +1/2$, altogether $q = 0$.

On the contrary, at the two following planes ($\zeta = 4/\sqrt{3}$ and $\zeta = 5/\sqrt{3}$) there are triangles with the same structure as before, but *both* are negative-charged, carrying together $q = -1$.

The same structure, due to the **CPS** symmetry, exists around small T− triangle at $\zeta = 9/\sqrt{3}$, with all the charges (and parity) inverted: both of the triangle in this position, and of its environment.

12.4.4 Choosing the translation unit cell

In our approach, the translation unit is a substitution for concept of a point of space, as a place where a particle can reside.

Instead, a particle in the point is represented as some anti-structural defects located in the corresponding translation unit, so the presupposed concepts of a particle or material point gets unnecessary.

Since the translation unit of dual-charged Wheaire-Phelan structure consists of eight different binary elements (i.e. cells charged $\pm \frac{1}{6}e$), the translation unit has eight internal binary degrees of freedom pretending to replace the curled up dimensions in Kaluza-Klein theories [4], [5], [6], [1], [2], [8], [9].

The translation unit cell can be chosen arbitrary as long as it includes eight structure cells of different geometry³ [10].

The primitive translation unit cell is a body-centered cube (Fig. 12.5). Most of cells included in it are cross-sectioned by the imaginary borders of the unit cell. It is not quite useful for modeling purposes. Namely, the T cells are taken by halves and while one D cell is taken by eighth parts, another one, residing in the cube's center, is included as whole.

Intending to study defects in the periodical structure, we choose the non-primitive unit so the cells that would participate in the exchange are included as whole, without cross-section.

We found also possible to include additional cells, that would overlay cells with the same geometry while translating, in case these add-ons appear as mutually compensating pairs of cells having opposite parity and also opposite electrical charge.

So we choose the neutral translation unit that consist of 3 positive charged cells of small T-triangle at $\zeta = 3/\sqrt{3}$, that would participate in the exchange, and *halves* of negative charged cells of two large T-triangles both at $1/\sqrt{3}$ and at $5/\sqrt{3}$, that would remain unchanged.

We do not consider the changes that may occur in cells of *large* T triangles since each T cell belonging to any *small* triangle in one chiral sub-lattice also belongs to a large triangle in another, mirror-reflected sub-lattice.

12.4.5 Anti-structure defects

Now we consider the *inversion* of the electric charge that can occur in particular cell or cells for some reason. Namely, it should happen as result of an interaction. Since the electric charge is conserved, the inversion in any particular cell must be accompanied by reverse inversion in another cell nearby, so all the inversions are, in fact, te results of *exchanges*.

However, we focus on possible single, double and triple inversions in the cells of small T triangle supposing that the corresponding reverse inversions are migrated or propagated into some location that is enough far away.

³ See the above in this section 12.2.

Also, we can examine just one small T triangle of two, for instance, at $\zeta = 3/\sqrt{3}$; another small T triangle at $\zeta = 9/\sqrt{3}$ is located in position shifted on half-unit size, so the latter should have the same properties as the first one, but **CP**-ed, i.e. charge-inverted and mirror-reflected.

Consider the small T+triangle accompanied by several cells in its closest neighborhood, keeping total electrical charge of them to be zero (Σq_n means the electric charge of three cell with the center at n -th plane, i.e. with $\zeta = n/\sqrt{3}$):

$$\begin{aligned}
 Q &= \Sigma q_1 + \Sigma q_3 = -\frac{1}{2} + \frac{1}{2} = 0, \text{ or} \\
 Q &= \Sigma q_3 + \Sigma q_5 = \frac{1}{2} - \frac{1}{2} = 0, \text{ or} \\
 Q &= \frac{\Sigma q_1 + \Sigma q_5}{2} + \Sigma q_3 = 0, \text{ or} \\
 Q &= q_0 + \frac{\Sigma q_1}{2} + \Sigma q_3 + \frac{\Sigma q_5}{2} + q_6 = 0, \text{ or} \\
 Q &= q_0 + \Sigma q_1 + \Sigma q_3 + q_6 = -\frac{1}{6} - \frac{1}{2} + \frac{1}{2} + \frac{1}{6} = 0, \text{ or} \\
 Q &= q_0 + \frac{\Sigma q_1}{2} + \frac{\Sigma q_2}{2} + \Sigma q_3 + \frac{\Sigma q_4}{2} + \frac{\Sigma q_5}{2} + q_6 = 0.
 \end{aligned} \tag{12.4}$$

In all the cases, $Q = \Sigma q_3 + q_{env} = 0$, while $\Sigma q_3 = +\frac{1}{2}$, so the environment charge $q_{env} = -\frac{1}{2}$.

It is obvious that this q_{env} is determined by T-cells only, since it is a charge of initially neutral vacuum after "removing" three positive-charged T+cells forming the small triangle and keeping the original count of D cells. So there are three extra negative-charged T-cells while all the D-cells still compensate each other:

$$\begin{aligned}
 q_{env} &= q_{env}^T = -\frac{1}{2}; \\
 q_{env}^D &= 0.
 \end{aligned} \tag{12.5}$$

Each plane of T-cells *before* the small triangle in ζ -order has its corresponding equal-charged plane *after* it at the same distance (for instance, at $\zeta = 1/\sqrt{3}$ and $5/\sqrt{3}$). This symmetry requires a half of environment charge, that is determined by T sub-lattice, to be resided before the small triangle plane $\zeta = 3/\sqrt{3}$, and another half to be resided after it:

$$\begin{aligned}
 q_{env}^T(\zeta < \frac{3}{\sqrt{3}}) &= -\frac{1}{4}; \\
 q_{env}^T(\zeta > \frac{3}{\sqrt{3}}) &= -\frac{1}{4}.
 \end{aligned} \tag{12.6}$$

Due to the **CPS** symmetry, we also have

$$\begin{aligned}
 q_{env}^T(\zeta < \frac{9}{\sqrt{3}}) &= +\frac{1}{4}; \\
 q_{env}^T(\zeta > \frac{9}{\sqrt{3}}) &= +\frac{1}{4}
 \end{aligned} \tag{12.7}$$

for the environment of the negative-charged small T-triangle at $\zeta = 9/\sqrt{3}$.

12.4.6 Handedness change as Exchange of D triangles

Although D-sublattice has no influence on the total charge of the small T+triangle's environment q_{env} (12.5), exchanges in it can redistribute the electric charge between *rear* ($\zeta < \frac{3}{\sqrt{3}}$) and *front* ($\zeta > \frac{3}{\sqrt{3}}$) half-spaces because it is asymmetric in respect of the plane ($\zeta = 3/\sqrt{3}$).

We examine such exchanges whether they can be used to represent the particle's handedness that also does not influence on its charge.

Following the model that assumes the charge is located closely to the cell centers, we must conclude that D triangles just before and after small triangle at $\zeta = 3/\sqrt{3}$ have the charges

$$\begin{aligned}\Sigma q_2 &= q^D(\zeta = \frac{2}{\sqrt{3}}) = +\frac{1}{2}, \\ \Sigma q_4 &= q^D(\zeta = \frac{4}{\sqrt{3}}) = -\frac{1}{2},\end{aligned}\tag{12.8}$$

and in case they exchange, the charge of 1 will redistribute from rear half-space to the front one⁴.

However, considering the case when the charge of cells is *not* concentrated in their centers, being instead distributed on radii comparable to the inter-centers distance ($\approx 2 \dots \sqrt{5} \approx 2.236$), we recognize that the charge of cells in plane $\zeta = 2/\sqrt{3}$ would not reside just *before* the plane $\zeta = 3/\sqrt{3}$. It is so because the offset between these planes is significantly less than the inter-center distance: $1/\sqrt{3} \approx 0.577 < 2$ (Fig. 12.8), and is comparable with the distribution radius. That is why one should assert that some part of q_2 would reside *after* the plane $\zeta = 3/\sqrt{3}$, and some part of q_4 would, in turn, reside *before* it (see Fig. 12.8).

To be the representation of the reversed handedness, the D-exchange operation should redistribute only the half of the charge (12.8). This requirement is fulfilled in case a quarter of the charge of each D-cell in triangles is distributed on the other side of the plane $\zeta = 3/\sqrt{3}$ that is located at the $1/\sqrt{3}$ of its center. So we can use this condition to obtain more realistic rule of the charge distribution rather than simple charged point in the cell center. Now we use the *halved* values of (12.8), that are equal to q_{env}^T by the magnitude, so they can effectively compensate them:

$$\begin{aligned}q^{D*}(\zeta = \frac{2}{\sqrt{3}}) &= +\frac{1}{4}, \\ q^{D*}(\zeta = \frac{4}{\sqrt{3}}) &= -\frac{1}{4},\end{aligned}\tag{12.9}$$

In this case,

$$\begin{aligned}q_{\text{env}}(\zeta < \frac{3}{\sqrt{3}}) &= q_{\text{env}}^T(\zeta < \frac{3}{\sqrt{3}}) + q^{D*}(\zeta = \frac{2}{\sqrt{3}}) = -\frac{1}{4} + \frac{1}{4} = 0; \\ q_{\text{env}}(\zeta > \frac{3}{\sqrt{3}}) &= q_{\text{env}}^T(\zeta > \frac{3}{\sqrt{3}}) + q^{D*}(\zeta = \frac{4}{\sqrt{3}}) = -\frac{1}{4} - \frac{1}{4} = -\frac{1}{2},\end{aligned}\tag{12.10}$$

⁴ Such an exchange also can be considered as a rotation of a spatial hexagon containing all six cell centers of the both D-triangles, with the angle of 60° in any direction

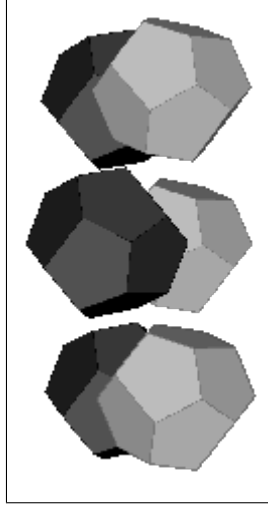


Fig. 12.8. Visually overlapping cells of two D triangles with $\zeta = 2/\sqrt{3}$ and $\zeta = 4/\sqrt{3}$ in polyhedral approximation

and after exchange between D-triangles at $\zeta = 2/\sqrt{3}$ and $4/\sqrt{3}$ they would turn into

$$\begin{aligned} q_{\text{env}}(\zeta < \frac{3}{\sqrt{3}}) &= q_{\text{env}}^T(\zeta < \frac{3}{\sqrt{3}}) + q^{D*}(\zeta = \frac{2}{\sqrt{3}}) = -\frac{1}{4} - \frac{1}{4} = -\frac{1}{2}; \\ q_{\text{env}}(\zeta > \frac{3}{\sqrt{3}}) &= q_{\text{env}}^T(\zeta > \frac{3}{\sqrt{3}}) + q^{D*}(\zeta = \frac{4}{\sqrt{3}}) = -\frac{1}{4} + \frac{1}{4} = 0. \end{aligned} \quad (12.11)$$

So we can use them to represent weak isospin and weak hypercharge for "down" particles:

$$T_3^{\text{down}} = q_{\text{env}}(\zeta < \frac{3}{\sqrt{3}}) = \frac{1}{2}(\Sigma q_1 + \Sigma q_2) \quad (12.12)$$

$$Y_W^{\text{down}}/2 = \Sigma q_3 + q_{\text{env}}(\zeta > \frac{3}{\sqrt{3}}) = \Sigma q_3 + \frac{1}{2}(\Sigma q_4 + \Sigma q_5) \quad (12.13)$$

At $\zeta = 9/\sqrt{3}$, the small T-triangle and its neighborhood are inverted in respect to $\zeta = 3/\sqrt{3}$ due to the CPS symmetry, so original

$$\begin{aligned} q_{\text{env}}(\zeta < \frac{9}{\sqrt{3}}) &= q_{\text{env}}^T(\zeta < \frac{9}{\sqrt{3}}) + q^{D*}(\zeta = \frac{8}{\sqrt{3}}) = +\frac{1}{4} - \frac{1}{4} = 0; \\ q_{\text{env}}(\zeta > \frac{9}{\sqrt{3}}) &= q_{\text{env}}^T(\zeta > \frac{9}{\sqrt{3}}) + q^{D*}(\zeta = \frac{10}{\sqrt{3}}) = +\frac{1}{4} + \frac{1}{4} = +\frac{1}{2} \end{aligned} \quad (12.14)$$

would turn after D-exchange into

$$\begin{aligned} q_{\text{env}}(\zeta < \frac{9}{\sqrt{3}}) &= q_{\text{env}}^T(\zeta < \frac{9}{\sqrt{3}}) + q^{D*}(\zeta = \frac{8}{\sqrt{3}}) = +\frac{1}{4} + \frac{1}{4} = +\frac{1}{2}; \\ q_{\text{env}}(\zeta > \frac{9}{\sqrt{3}}) &= q_{\text{env}}^T(\zeta > \frac{9}{\sqrt{3}}) + q^{D*}(\zeta = \frac{10}{\sqrt{3}}) = +\frac{1}{4} - \frac{1}{4} = 0, \end{aligned} \quad (12.15)$$

and both the values $q_{\text{env}}(\zeta < \frac{9}{\sqrt{3}})$ and $\Sigma q_9 + q_{\text{env}}(\zeta > \frac{9}{\sqrt{3}})$ would, again, coincide with weak isospin T_3 and weak hypercharge $Y_W/2$ for "up" fermions, respectively:

$$T_3^{\text{up}} = q_{\text{env}}(\zeta < \frac{9}{\sqrt{3}}) = \frac{1}{2}(\Sigma q_7 + \Sigma q_8) \quad (12.16)$$

$$Y_W^{\text{up}}/2 = \Sigma q_9 + q_{\text{env}}(\zeta > \frac{9}{\sqrt{3}}) = \Sigma q_9 + \frac{1}{2}(\Sigma q_{10} + \Sigma q_{11}) \quad (12.17)$$

So the exchange between D triangles (or, that is the same, rotation of the distorted D hexagon) can be used as a model representing switching between two handednesses.

12.4.7 Down fermions as Inversions in small T+triangle

Inverting charges of cells in the small T+triangle q_3 , namely of $q(2, 1, 0)$, $q(2, 1, 0)$ and $q(2, 1, 0)$ in (x, y, z) reference frame⁵, one can get eight possible cases (Table 12.2). The total electric charge Q , that changes with steps of $\pm \frac{1}{3}$ according to the count of inverted cells, coincides with the electric charge of eight "down"⁶ fermions.








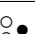


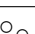
$T_3 :=$ $q_{(<3)}$	q_3^{210}	q_3^{102}	q_3^{021}	Σq_3	$q_{(>3)}$	$\frac{Y_W}{2} :=$ $q_{(\geq 3)}$	Q	symbol
 0	+	+	+	 +1/2	 -1/2	 -1/2	0	$\tilde{\nu}_L$
	-	+	+					d_R^{c1}
	+	-	+	 +1/6				d_R^{c2}
	+	+	-					d_R^{c3}
	+	-	-					\tilde{u}_L^{c1}
	-	+	-	 -1/6				\tilde{u}_L^{c2}
	-	-	+					\tilde{u}_L^{c3}
	-	-	-	 -1/2				l_R^-

Table 12.2. Eight cases of inversions in the small T-triangle at $\zeta = 3/\sqrt{3}$ with *original* (unchanged) D-triangles at $\zeta = 2/\sqrt{3}$ and $4/\sqrt{3}$, associated with weak-uncharged "down" fermions

The original unchanged state with $Q = 0$ is the vacuum state, so it takes place of the left-handed anti-neutrino, that, according to experiments, does not exist. In

⁵ In the (ξ, ζ, ν) reference frame they are $q(\sqrt{2}, \sqrt{3}, 0)$, $q(-\frac{1}{\sqrt{2}}, \sqrt{3}, -\frac{3}{\sqrt{6}})$, $q(-\frac{1}{\sqrt{2}}, \sqrt{3}, \frac{3}{\sqrt{6}})$.

⁶ We consider anti-"up" fermions as "down" ones, and vice versa. The "up" particles as well as "up" (anti-"down") anti-particles have the electric charge greater by 1 than the charge of corresponding "down" particles or anti-particles.

$T_3 :=$ $q_{(<3)}$	q_3^{210}	q_3^{102}	q_3^{021}	Σq_3	$q_{(>3)}$	$\frac{Y_W}{2} :=$ $q_{(\geq 3)}$	Q	symbol		
$\frac{1}{2} \times \begin{array}{ccc} \bigcirc & \bigcirc & \bigcirc \\ & \bigcirc & \bigcirc \end{array}$	+	+	+	$\bullet \bullet +1/2$	$\frac{1}{2} \times \begin{array}{ccc} & \bullet & \bigcirc \\ \bullet & & \bigcirc \end{array}$	+1/2	0	$\tilde{\nu}_R$		
	−	+	+	$\bullet \circ$		+1/6	−1/3	d_L^{c1}		
	+	−	+	$\circ \bullet +1/6$				d_L^{c2}		
	+	+	−	$\circ \bullet$				d_L^{c3}		
	−1/2	+	−	−		$\circ \circ \bullet$	0	−1/6	−2/3	$\tilde{u}_R^{\tilde{c}1}$
		−	+	−		$\bullet \circ -1/6$				$\tilde{u}_R^{\tilde{c}2}$
−		−	+	$\bullet \circ$	$\tilde{u}_R^{\tilde{c}3}$					
−		−	−	$\circ \circ -1/2$	−1/2	−1				l_L^-

Table 12.3. Eight cases of inversions in the small T-triangle at $\zeta = 3/\sqrt{3}$ with *exchanged* D-triangles at $\zeta = 2/\sqrt{3}$ and $4/\sqrt{3}$ associated with weak-charged "down" fermions

this model, the absence of left-handed anti-neutrino is explained by no differences between it and the vacuum state.

Also consider the same cases but combined with *exchanged* D-triangles at $\zeta = 2/\sqrt{3}$ and $4/\sqrt{3}$ (Table 12.3).

12.4.8 Up fermions as Inversions in small T-triangle

Considering the same cases but for the small T-triangle at $\zeta = 9/\sqrt{3}$, we found out that they can be as well associated with "up" fermions. It is so because the shift for half-unit (**S**) from $\zeta = 3/\sqrt{3}$ to $9/\sqrt{3}$ is equal to the **CP** operation. So this triangle and its environment have the reversed handedness and opposite-charged in respect to those considered before. The total charge Q is greater by 1 comparing to the corresponding "down" cases (Table 12.4).

Again, the original vacuum state corresponds to the non-existing particle, that is the right-handed neutrino.

12.5 Polyhedral approximation

Considering the Polyhedral approximation of the dual-charged Weaire-Phelan structure (section 12.3), one can see that walls between cells consist of flat polygonal faces. It is obvious that there are two kinds of walls, since a face can separate either *equal*-charged or *opposite*-charged cells.

Supposing the wall possesses a surface energy E that it is proportional to the face surface area S , and there is a fixed difference in surface density $\Delta\rho$ between both wall kinds, one could estimate the particle mass by the rest energy ΔE associated with a particular defect configuration:

$$m = \Delta E = \Delta\rho\Delta S. \quad (12.18)$$








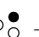

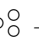







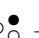

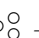
$T_3 :=$ $q_{(<9)}$	$q_9^{4\ 2\ 3}$	$q_9^{3\ 4\ 2}$	$q_9^{2\ 3\ 4}$	Σq_9	$q_{(>9)}$	$Y_W/2 :=$ $q_{(\geq 9)}$	Q	
 $\frac{1}{2} \times$ 0	+	+	+	 +1/2	 $\frac{1}{2} \times$ +1/2	+1	+1	l_L^+
	-	+	+			+2/3	+2/3	u_R^{c1}
	+	-	+	 +1/6				u_R^{c2}
	+	+	-					u_R^{c3}
	+	-	-			+1/3	+1/3	\tilde{d}_L^{c1}
	-	+	-	 -1/6				\tilde{d}_L^{c2}
	-	-	+					\tilde{d}_L^{c3}
	-	-	-	 -1/2		0	0	∇_R
 $\frac{1}{2} \times$ +1/2	+	+	+	 +1/2	 $\frac{1}{2} \times$ 0	+1/2	+1	l_R^+
	-	+	+			+1/6	+2/3	u_L^{c1}
	+	-	+	 +1/6				u_L^{c2}
	+	+	-					u_L^{c3}
	+	-	-			-1/6	+1/3	\tilde{d}_R^{c1}
	-	+	-	 -1/6				\tilde{d}_R^{c2}
	-	-	+					\tilde{d}_R^{c3}
	-	-	-	 -1/2		-1/2	0	v_L

Table 12.4. Eight cases of inversions in the small T-triangle at $\zeta = 9/\sqrt{3}$, repeated twice with original and exchanged D-triangles at $\zeta = 8/\sqrt{3}$ and $10/\sqrt{3}$, associated with “up” fermions

Since D cell has 6 equal-charged and also 6 opposite-charged neighbors, the inversion does not affect the area ($\Delta S = 0$) and

$$\Delta E_D = 0. \quad (12.19)$$

In contrast, among 14 neighbors of T cell six ones are equal-charged but there are eight opposite-charged ones. Both opposite-charged neighbors that become equal-charged ones in an inversion, are separated with the hexagonal faces with area S_6 . So

$$\Delta E_T = 2\Delta\rho S_6. \quad (12.20)$$

Assuming the energy density for wall between equal-charged cells is greater than for opposite-charged ones, $\Delta\rho > 0$ and $\Delta E > 0$.

In case of inversions of *two* neighboring cells, there is an additional effect caused by their common face.

In case two neighbor cells exchange their charge (thus, they are D and T touching each other with large pentagonal face S_{5L} or two T touching each other

with small pentagonal face S_{5s} or hexagonal one S_6) the common face remains separating opposite-charged cells, instead of being turned into separating equal-charged cells, so energy effect is negative:

$$\begin{aligned}\Delta E_{D \rightleftharpoons T} &= -2\Delta\rho S_{5L}, \\ \Delta E_{T \rightleftharpoons T_5} &= -2\Delta\rho S_{5s}, \\ \Delta E_{T \rightleftharpoons T_6} &= -2\Delta\rho S_6.\end{aligned}\tag{12.21}$$

In case of two neighbor cells inverting in the same direction, the additional effect of the common face is opposite, i.e. positive:

$$\begin{aligned}\Delta E_{D \Rightarrow T} &= 2\Delta\rho S_{5L}, \\ \Delta E_{T \Rightarrow T_5} &= 2\Delta\rho S_{5s}, \\ \Delta E_{T \Rightarrow T_6} &= 2\Delta\rho S_6.\end{aligned}\tag{12.22}$$

Note that numerical values of the faces' areas (in units of λ^2) are such that S_{5L} is *almost* equal to the arithmetic mean of S_6 and S_{5s} :

$$\begin{aligned}S_{5L} &\approx 1.77477, \\ S_{5s} &\approx 1.15338, \\ S_6 &\approx 2.41260, \text{ so} \\ S_6 + S_{5s} - 2S_{5L} &\approx 0.0164.\end{aligned}\tag{12.23}$$

Now we can build the simple hierarchical seesaw model of mass based on addition and subtraction of energy effects.

- Since D exchanges have $\Delta E = 0$, massless particles like photon and neutrino must be associated with D-only exchanges.
- Following our 8-bit model [7], associate W^+ boson with five defects combination shown on Fig. 12.9W. Note that it is colorless and has correct electric charge $Q = +1$. The affected area of these defects is

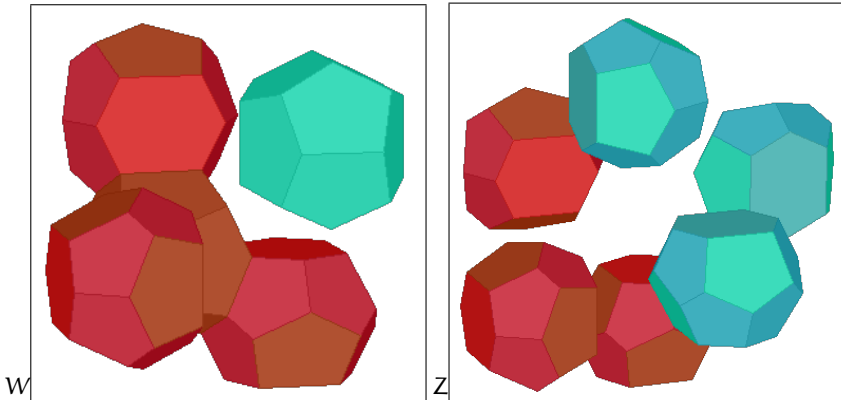


Fig. 12.9. Models of W^+ and Z^0 bosons in polyhedral approximation

$$\Delta S_W = 6 (S_6 + S_{5L}) = 25.12422. \quad (12.24)$$

Using experimental value of $m_W = 80.385 \text{ GeV}$ we get

$$\Delta\rho = \frac{m_W}{\Delta S_W} \approx 3.1995 \text{ GeV}/\lambda^2. \quad (12.25)$$

- Following the same way, we associate Z^0 boson with neutral six T defect configuration shown on Fig. 12.9Z. Using the same $\Delta\rho$ value, we get

$$m_Z = 12\Delta\rho S_6 \approx 92.629 \text{ GeV}. \quad (12.26)$$

- The Higgs boson having, accordingly to 8-bit model, the defects structure similar to Z boson but with one additional D defect pair (Fig. 12.9H), must have one of D cells isolated the same way as W has, to get the appropriate mass:

$$m_H = \Delta\rho(12S_6 + 6S_{5L}) \approx 126.699 \text{ GeV}. \quad (12.27)$$

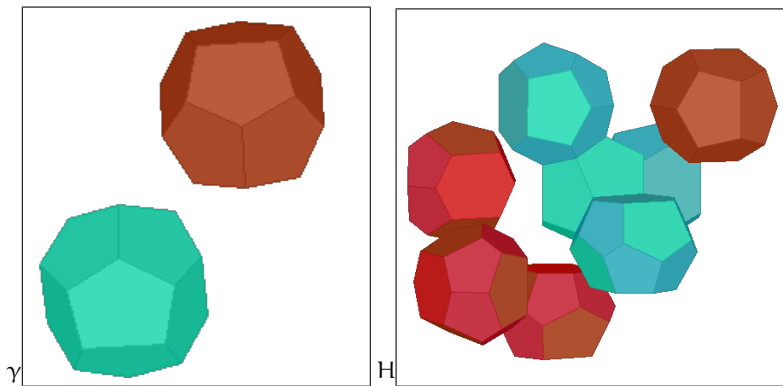


Fig. 12.10. Models of γ photon and H^0 bosons in polyhedral approximation

- For charged lepton we suppose the structure of small-T-triangle inversion combined with eight inversions of D cells providing the compensation (Fig.12.11). This mechanism does not follow the pattern used in 8-bit model for fermion families representation⁷, but it offers effective mass reduction below GeV scale.

$$m_l = \Delta\rho(6S_6 - 12S_{5s} + 6S_{5L}) \approx 0.315 \text{ GeV}. \quad (12.28)$$

- The zero-charged compensating "frame" consisting from D cells could be associated with massless neutrino (Fig.12.11ν).
- Although the exchange between two or more stacked T cells has the positive energetic effect, its magnitude does not depend on the stack length, and originates just from the non-compensated ends of the stack that has the color charge due to their asymmetry. So it can be associated with the gluon thread terminated with quarks.

⁷ the latter involves additional T-D exchange.

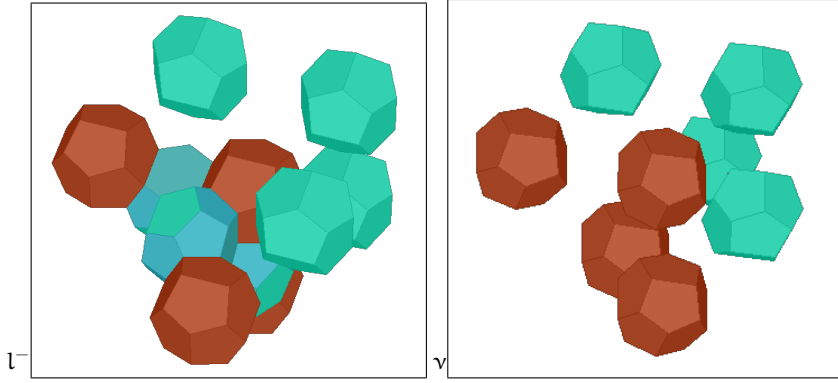


Fig. 12.11. Models of charged lepton with compensated mass, and massless neutrino in polyhedral approximation

12.6 Analytical approximation of charge distribution

In addition to the Polyhedral and Cell-Center approximations we consider an approximation of the structure by the triple-periodical analytical function of electrical charge density distribution.

The electrical charge of the cell concentrated at its center (x_0, y_0, z_0) can be expressed analytically using the δ -function:

$$q = \frac{e}{6} \int_{\mathbb{R}^3} \delta(x - x_0, y - y_0, z - z_0) dx dy dz \quad (12.29)$$

The delta function can be considered as the spherically-symmetrical Gaussian distribution with zero deviation:

$$\delta(x, y, z) = \lim_{\sigma \rightarrow 0} \delta(x, y, z, \sigma); \quad (12.30)$$

$$\delta(x, y, z, \sigma) = \frac{1}{(\sigma\sqrt{2\pi})^3} e^{-\frac{x^2+y^2+z^2}{2\sigma^2}} \quad (12.31)$$

As we have shown in section 12.4.6, the model explaining the weak isospin $T_3 = 0$ for right-handed fermions and $T_3 = \pm 1/2$ for left-handed ones by the charge exchange between D-triangles at $\zeta = 2/\sqrt{3}$ and $4/\sqrt{3}$, requires one quarter of the charge of each D cell to reside behind the section plane located at the distance of $1/\sqrt{3}$ from the cell center:

$$\int_{x=-\infty}^{-1/\sqrt{3}} \int_{y=-\infty}^{+\infty} \int_{z=-\infty}^{+\infty} \rho(x, y, z) dx dy dz = \frac{1}{4} \quad (12.32)$$

Assuming charge density $\rho(x, y, z)$ to be the Gaussian distribution (12.31), and solving the equation

$$\frac{1}{(\sigma\sqrt{2\pi})^3} \int_{x=-\infty}^{-1/\sqrt{3}} \int_{y=-\infty}^{+\infty} \int_{z=-\infty}^{+\infty} e^{-\frac{x^2+y^2+z^2}{2\sigma^2}} dx dy dz = \frac{1}{4} \quad (12.33)$$

numerically, we found $\sigma \approx 0.87377$.

Soliton model To construct the charge distribution in the analytical form, we can use, instead of each cell, some spherical-symmetrical function, which decreases quite rapidly on distance from its center, i.e. soliton.

We consider the soliton function as normalized error function

$$\rho_i = \pm \frac{e}{6\sigma\sqrt{2\pi}} \exp \left[-\frac{(x - x_i)^2 + (y - y_i)^2 + (z - z_i)^2}{2\sigma^2} \right], \quad (12.34)$$

representing positive or negative charged cell with the center at (x_i, y_i, z_i) . The charge density in the particular point is calculated as a sum of contributions of all the cells in the model:

$$\rho = \sum_i \rho_i \quad (12.35)$$

One can manage the position and charge of each individual cell, so this model should be flexible. On another hand, it requires extensive computation to calculate each point.

Triple-periodic trigonometric function Since the most interesting application of this model is to represent the only one or several defects being surrounded by the "pure" vacuum, we looked for the periodic function that has the same symmetry as the dual-charged Weaire-Phelan structure considered above. It is intended to represent the pure vacuum avoiding calculating of plenty periodically allocated solitons.

At first, we consider the real function that has zero surface close to the Schwartz P minimal surface [15].

$$\rho_0 = \cos x + \cos y + \cos z, \quad (12.36)$$

or, equivalently,

$$\rho_0 = \sum_i \cos x_i. \quad (12.37)$$

$$\rho_0 = \cos \frac{x\pi}{2\lambda} + \cos \frac{y\pi}{2\lambda} + \cos \frac{z\pi}{2\lambda}, \quad (12.38)$$

It has minimum in points $(2\pi n_x, 2\pi n_y, 2\pi n_z) = 2\pi(n_x, n_y, n_z)$ and maximum in $\pi(2n_x + 1, 2n_y + 1, 2n_z + 1)$ since

$$\frac{\partial \rho_0}{\partial x_i} = -\sin x_i = 0 \Rightarrow x_i = \pi n_i, \quad (12.39)$$

and

$$\frac{\partial^2 \rho_0}{\partial x_i^2} = -\cos x_i. \quad (12.40)$$

The last equation also means that

$$\Delta \rho_0 = -\rho_0, \quad (12.41)$$

so ρ_0 is eigenfunction of the Laplasian, with eigenvalue -1 .

The translation unit with $n_x = n_y = n_z = 0$ is a cube with $x_i \in [-\pi; \pi]$.

So, ρ_0 has one minimum in $(0, 0, 0)$ and one maximum in $\frac{\pi}{4}(2, 2, 2)$.

As the second step, we consider the surface $\rho_0 = 0$. Its saddle points are the same with the T cell center points. So we can add the function with extremals at these points, namely at centers of D cells:

$$\rho_{xz} = \frac{1}{4} \sin y (1 - \cos x) (1 + \cos z) \quad (12.42)$$

$$\rho_{yx} = \frac{1}{4} \sin z (1 - \cos y) (1 + \cos x) \quad (12.43)$$

$$\rho_{zy} = \frac{1}{4} \sin x (1 - \cos z) (1 + \cos y) \quad (12.44)$$

$$\rho_{xy} = \frac{1}{4} \sin z (1 - \cos x) (1 + \cos y) \quad (12.45)$$

$$\rho_{yz} = \frac{1}{4} \sin y (1 - \cos y) (1 + \cos z) \quad (12.46)$$

$$\rho_{zx} = \frac{1}{4} \sin y (1 - \cos z) (1 + \cos x) \quad (12.47)$$

$$\rho_R = \rho_{xy} + \rho_{yz} + \rho_{zx} \quad (12.48)$$

$$\rho_L = \rho_{yx} + \rho_{zy} + \rho_{xz} \quad (12.49)$$

We construct right and left vacuum electric charge density as

$$\rho_{0R} = \rho_0 + \rho_R \quad (12.50)$$

$$\rho_{0L} = \rho_0 + \rho_L. \quad (12.51)$$

Note that ρ_{xz} (12.42) and other ρ_{ij} can be rewritten in the following way:

$$\rho_{xz} = \frac{1}{4} (\sin y + \sin y \cos z - \sin y \cos x - \sin y \cos x \cos z), \quad (12.52)$$

so ρ_R and ρ_L can be represented as sums of four functions listed below, which accumulate summands of four particular types, that occur in (12.42).

Introducing "Schwartz P"-like distribution

$$P_\theta = \cos(x - \theta) + \cos(y - \theta) + \cos(z - \theta), \quad (12.53)$$

right and left gyroid-like distributions

$$G_R = \cos x \sin y + \cos y \sin z + \cos z \sin x, \quad (12.54)$$

$$G_L = \cos x \sin z + \cos y \sin x + \cos z \sin y, \quad (12.55)$$

and "layers-with-holes" distribution

$$H = \cos x \sin y \cos z + \cos y \sin z \cos x + \cos z \sin x \cos y, \quad (12.56)$$

we can express ρ_R through them:

$$\rho_{0R} = \frac{1}{4} [P_{\pi/2} + G_L - G_R - H] - \frac{1}{3}P_0. \quad (12.57)$$

Since G and H are also eigenfunctions of the Laplasian Δ :

$$\Delta G = -2G; \Delta H = -3H, \quad (12.58)$$

one can find the scalar electric potential:

$$\text{div grad } \varphi_{0R} = \Delta \varphi_{0R} = 4\pi\rho_{0R}, \quad (12.59)$$

$$\varphi_{0R} = +\frac{1}{12\pi}P_0 - \frac{1}{16\pi} \left[P_{\pi/2} + \frac{1}{2}G_L - \frac{1}{2}G_R - \frac{1}{3}H \right]. \quad (12.60)$$

Combining triple-periodical trigonometric equation for the vacuum state with doubled opposite-charged soliton located in particular cell centers one can obtain a model representing one or more particles surrounded by the vacuum.

12.7 Discussion

12.7.1 Two-dimension model

Consider the surface of zero potential (12.60):

$$\varphi_{0R} = +\frac{1}{12\pi}P_0 - \frac{1}{16\pi} \left[P_{\pi/2} + \frac{1}{2}G_L - \frac{1}{2}G_R - \frac{1}{3}H \right] = 0. \quad (12.61)$$

It defines the manifold with the mostly negative Gaussian curvature that can be studied using two-dimensional Einstein GRT equation.

The three-dimensional space, discrete with the grid size $l \approx 4 \cdot 10^{-21} \text{ m}$, appears in this model as a result of the foam-like structure of this two-dimensional manifold. So the continuous three-dimensional space can be considered just as an asymptotic on distances larger than the grid size. As a consequence of this approach, the three-dimensional gravity should not be considered in its usual form on distances comparable to or less than the grid size.

12.7.2 Liquid-Liquid Phase Transition model

We suppose that the structures close to one considered above can emerge in systems possessing 2-order phase transition near the critical point, for instance, in liquid-liquid mixtures like $\text{H}_2\text{O} - \text{C}_6\text{H}_5\text{OH}$.

12.7.3 Other topics

There are some topics that we'd like to mention here as directions in which the research can be continued.

Firstly, it is the dynamics. Each defect in the vacuum structure is supposed to be able to change its localization. It can be considered from several viewpoints listed above and also using other approaches, for instance, the cellular automata.

Secondly, the interactions and the virtual particles. Our approach can be also applied to bosons. Some 'bosonic' exchanges seem to have no influence on the two-dimensional manifold topology, so there is no sharp difference between particles (defects) and classical fields (distortions).

Thirdly, there can be another structures with the properties allowing to use them as a model of vacuum and particles. We have found and tested just one.

12.8 Conclusion

We presented here our approach to the particle and vacuum modeling, based on the assumption that on scale $\approx 10^{-19}$ cm there are areas with non-zero electrical charge density and they are self-assembled in the structure close to the Weaire-Phelan tessellation. This structure possesses **CPS** symmetry and allows the existence of anti-structure defects in it, that can be corresponded to known fundamental particles (at least, for one fermion family), reproducing their known properties.

References

1. N.S. Mankoč Borštnik, "Can spin-charge-family theory explain baryon number non conservation?", *Phys. Rev. D* **91** (2015) 6, 065004, [arXiv:1502.06786v1]
2. N. Mankoč Borštnik, "Spinor and vector representations in four dimensional Grassmann space", *J. of Math. Phys.* **34** (1993), 3731-3745.
3. Ya. B. Zeldovich, I. Yu. Kobzarev, and L. B. Okun': Cosmological consequences of a spontaneous breakdown of a discrete symmetry: *Zh. Eksp. Teor. Fiz.* 67, 3-11 (July 1974) [*Sov. Phys. JETP* 40, 1 (1974)].
4. Nordström, Gunnar (1914). "Über die Möglichkeit, das elektromagnetische Feld und das Gravitationsfeld zu vereinigen". *Physikalische Zeitschrift*. 15: 504–506. OCLC 1762351.
5. Kaluza, Theodor (1921). "Zum Unitätsproblem in der Physik". *Sitzungsber. Preuss. Akad. Wiss. Berlin. (Math. Phys.)*: 966–972. <https://archive.org/details/sitzungsberichte1921preussi>
6. Klein, Oskar (1926). "Quantentheorie und fünfdimensionale Relativitätstheorie". *Zeitschrift für Physik A*. 37 (12): 895–906. Bibcode:1926ZPhy...37..895K. doi:10.1007/BF01397481.
7. E.G. Dmitrieff: Experience in modeling properties of fundamental particles using binary codes, in: N.S. Mankoč Borštnik, H.B.F. Nielsen, D. Lukman: Proceedings to the 19th Workshop 'What Comes Beyond the Standard Models', Bled, 11. - 19. July 2016.
8. N.S. Mankoč Borštnik, "The explanation for the origin of the higgs scalar and for the Yukawa couplings by the *spin-charge-family* theory", *J. of Mod. Physics* **6** (2015) 2244-2274, [arXiv:1409.4981]
9. N.S. Mankoč Borštnik, "Spin-charge-family theory is offering next step in understanding elementary particles and fields and correspondingly universe", 10th IARD conference, Ljubljana 2016, *J. Phys.: Conf. Ser.* 845 (2017) 012017 and references therein [arXiv:1607.01618v2]

10. Kittel, Charles: Introduction to Solid State Physics (8th ed.). John Wiley & Sons, Inc. (2004).
11. E.G. Dmitrieff: The Hypothesis of Unity of the Higgs Field With the Coulomb Field, in: N.S. Mankoč Borštnik, H.B.F. Nielsen, D. Lukman: Proceedings to the 19th Workshop 'What Comes Beyond the Standard Models', Bled, 11. - 19. July 2016.
12. D.Weaire, R.Phelan: A counter-example to Kelvin's conjecture on minimal surfaces, *Phil. Mag. Lett.*, (1994) 69: 107–110, doi:10.1080/09500839408241577
13. Ruggero Gabbrielli, Aaron J. Meagher, Denis Weaire, Kenneth A. Brakke & Stefan Hutzler (2012) An experimental realization of the Weaire–Phelan structure in monodisperse liquid foam, *Philosophical Magazine Letters*, 92:1, 1-6, DOI: 10.1080/09500839.2011.645898
14. Lord Kelvin (Sir William Thomson) (1887), "On the Division of Space with Minimum Partitional Area" (PDF), *Philosophical Magazine*, 24 (151): 503, doi:10.1080/14786448708628135
15. Alan H. Schoen: Infinite periodic minimal surfaces without self-intersections, NASA Technical Note TN D-5541 (1970)



13 The Correspondence Between Fermion Family Members in Spin-charge-family Theory and Structure Defects in Electrically-charged Tessellations

E.G. Dmitrieff *

Irkutsk State University, Russia

Abstract. In this article we compare spinor representations in the the Spin-charge-family theory with the possible charge distributions in spatial tessellations. Particularly, we considered alternations of opposite-charged binary triangles and the Weaire-Phelan structure, and found out that the correspondence between anti-structural defects and representations of fundamental fermions can be established.

Povzetek. Prispevek primerja spinorske upodobitve v teoriji *Spinov-nabojev-družin* z možnimi porazdelitvami naboja v prostorskih teselacijah. Lastnosti alternirajočih binarnih trikotnikov z nasprotnimi naboji v Weaire-Phelanovih strukturah z antistrukturnimi defekti poveže z lastnostmi kvarkov in leptonov.

Keywords: Particle model, Weaire-Phelan tessellation, Spin-charge-family theory

13.1 Introduction

A fermion family derived in spin-charge-family theory [1] consists of 64 members, that differs from each other by their color, weak charge, hyper-charge, electric charge, handedness, and spin.

The theory starts from several assumptions, including metric, action in $13 + 1$ dimensions, and the schema of symmetry breaks. Also, the theory postulates the basic vacuum state formed by two right-handed neutrinos with opposite spins, and the set of operators, acting on this state, that are members of Clifford algebra.

Each particular fermion state is produced by applying operators

$$S^{ab} = \frac{i}{4} \{ \gamma^a, \gamma^b \}_- = \frac{i}{2} \gamma^a \gamma^b \quad (a \neq b), \quad (13.1)$$

that are infinitesimal generators of the Lorentz transformations, to the vacuum state.

One can obtain quantum numbers of each state as a combination of eigenvalues $k_{ab}/2$ of these operators,

$$(k_{ab})^2 = \eta^{aa} \eta^{bb}, \quad (13.2)$$

* E-mail: eliadmitrieff@gmail.com

that are ± 1 or $\pm i$ since the metric $\eta^{ab} = \text{diag}(-1, 1, 1 \dots 1)$:

$$S^{ab} (k_{ab}^{ab}) = \frac{k_{ab}^{ab}}{2} (k_{ab}^{ab}), S^{ab} [k_{ab}^{ab}] = \frac{k_{ab}^{ab}}{2} [k_{ab}^{ab}]. \quad (13.3)$$

Here

$$\begin{aligned} (k_{ab}^{ab}) &= \frac{1}{2} \left(\gamma^a + \frac{\eta^{aa}}{ik_{ab}} \gamma^b \right), \\ [k_{ab}^{ab}] &= \frac{1}{2} \left(I + \frac{i}{k_{ab}} \gamma^a \gamma^b \right) \end{aligned} \quad (13.4)$$

and γ^a, γ^b are the Clifford algebra objects following the defining equation

$$\{\gamma^a; \gamma^b\}_+ = 2\eta^{ab} I \quad (13.5)$$

with the metric $\eta^{ab} = \text{diag}(- + + \dots +)$ and unit matrix I .

We found out that these k_{ab} can be mapped to the structure close to the Weaire-Phelan tessellation [4], assuming its cells carrying electric charge of $\pm \frac{1}{6}e$ [5], [3].

We recognize it as a possible mechanism for manifestation of the 13+1-dimensional spin-charge-family theory in the 3-dimensional space.

13.2 Charged binary triangles

We consider the small model system containing three unordered elements having the electrical charge of either $+\frac{1}{6}e$ or $-\frac{1}{6}e$. Since the elements are unordered, one can imagine this system as an equilateral triangle with elements residing in its vertices (Fig. 13.1A). The system has three binary degrees of freedom and possesses $SU(3)$ symmetry of its possible states.

13.2.1 Charged binary triangle's state space

The state space of charged binary triangles, shown on Fig. 13.1B, contains $2^3 = 8$ states. In three-dimensional Cartesian reference frame with its axes representing states of particular elements, it looks like a cube.

One of these eight states has the total electric charge $q = 3 \times (-\frac{1}{6}) = -\frac{1}{2}$, three states have $q = -\frac{1}{6}$, another three states have $q = +\frac{1}{6}$, and, again, one has $q = +\frac{1}{2}$. These counts are binomial coefficients for $n = 3$ and the charge values coincide with eigenvalues of τ^4 , that is the $U(1)$ *fermion charge* operator in the spin-charge-family theory:

$$\tau^4 = -\frac{1}{3} (S^{9\ 10} + S^{11\ 12} + S^{13\ 14}) = -\frac{1}{6} (k_{9\ 10} + k_{11\ 12} + k_{13\ 14}). \quad (13.6)$$

One can see that among four diagonals of this cube there are three diagonals of one kind, connecting states with difference of $\frac{1}{6}$, and one of another kind,

¹ Further we omit the e unit

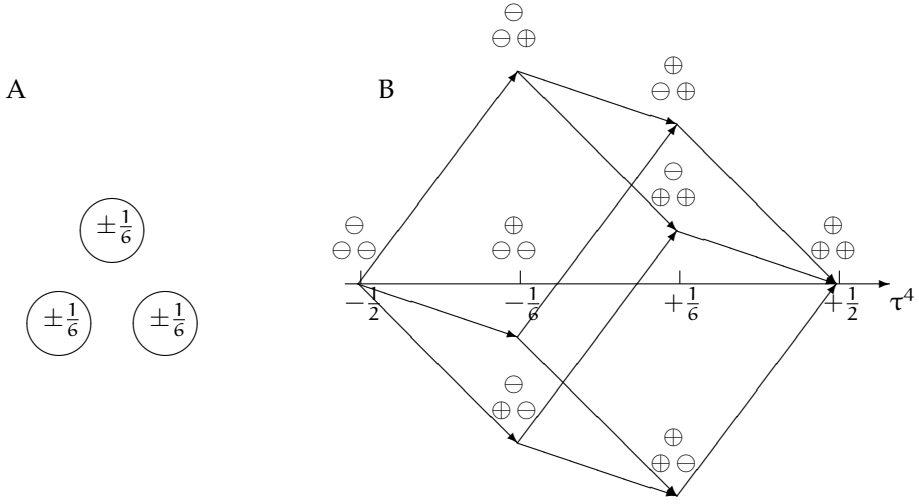


Fig. 13.1. (A) The system of three elements charged with $\pm \frac{1}{6}e$ and (B) its three-dimensional state space containing eight possible states

connecting states with the difference of 1. This dedicated "main" diagonal is the τ^4 axis since the projections of cube vertex on it coincide with τ^4 eigenvalues.

The edge of the state cube is therefore $\frac{1}{\sqrt{3}}$, and the radius from τ^4 axis to non-axial states is $r = \frac{\sqrt{2}}{3}$.

Consider the isometric projection of the state cube onto Cartesian coordinate plain that is orthogonal to the τ^4 axis (Fig. 13.2). Let the ordinate axis to be directed opposite to the edge corresponding to $k_{13\ 14}$. Then the projections of states on the abscissas and ordinate axes, divided by projection distortion of $\sqrt{\frac{2}{3}}$, coincide with *color charge* components τ^{33} and τ^{38} , respectively:

$$\begin{aligned}
 \tau^{33} &= \frac{1}{2} (S^{9\ 10} - S^{11\ 12}) = \frac{1}{4} (k^{9\ 10} - k^{11\ 12}) = \\
 &= \frac{\sqrt{2}}{3} \cos\left(\frac{\pi}{6} + \frac{\pi n}{6}\right) \times \sqrt{\frac{3}{2}} \in \left\{0; \pm \frac{1}{2}\right\}, \\
 \tau^{38} &= \frac{1}{2\sqrt{3}} (S^{9\ 10} + S^{11\ 12} - S^{13\ 14}) = \frac{1}{4\sqrt{3}} (k^{9\ 10} + k^{11\ 12} - k^{13\ 14}) = \\
 &= \frac{\sqrt{2}}{3} \sin\left(\frac{\pi}{6} + \frac{\pi n}{6}\right) \times \sqrt{\frac{3}{2}} \in \left\{\pm \frac{1}{\sqrt{3}}; \pm \frac{1}{2\sqrt{3}}\right\}.
 \end{aligned} \tag{13.7}$$

13.2.2 Model with alternation of charged binary triangles

Note that a charged binary triangle cannot be electrically neutral. Nevertheless, a pair of opposite-charged binary triangles, or, generally, any even number of them can hold zero electric charge.

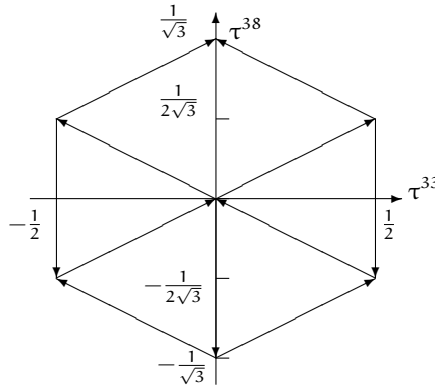


Fig. 13.2. The isometric projection of the state cube along the τ^4 axis

Consider a big system containing sufficiently large amount of opposite-charged binary triangles, half of them consisting of three positive-charged elements, and half of three negative-charged ones, arranged in alternating pattern. The whole system is electrically neutral.

Each triangle in this system, either having charge of $+\frac{1}{2}$ or $-\frac{1}{2}$, is surrounded by opposite-charged environment with the same magnitude:

$$q_{\text{env}} = -\tau^4. \quad (13.8)$$

We found out that in this system, where positive- and negative-charged triangles have different *own* places due to their alternation, the additional degree of freedom emerges for any single triangle.

For instance, the negative-charged triangle with $q = \tau^4 = -\frac{1}{2}$ in its own place must be effectively neutralized by its environment and therefore must be indistinguishable from the background. But the same triangle in the place of positive-charged one should be treated as having effective charge of -1 that emerges as a sum of the negative triangle charge and the negative charge of the environment surrounding the place where the positive triangle should be:

$$Q = \tau^4 + q_{\text{env}} = -\frac{1}{2} + \left(-\frac{1}{2}\right) = -1. \quad (13.9)$$

So the state space for the charged binary triangle that participates in the neutral alternation of such triangles, must reflect this emergent binary degree of freedom. The state space becomes four-dimensional, splitting each original state to the doublet with the triple magnitude $\frac{1}{2}$ in comparison to original $\frac{1}{6}$ (Fig. 13.3). One of the states shifts *up* in charge with $+\frac{1}{2}$ while another one shifts *down*, with $-\frac{1}{2}$.

One can ensure that among these 16 states there are neutral and integer- and fractional-charged ones with step of $\frac{1}{3}$ so the effective charges coincide with charges of known fundamental fermions and anti-fermions belonging to one family.

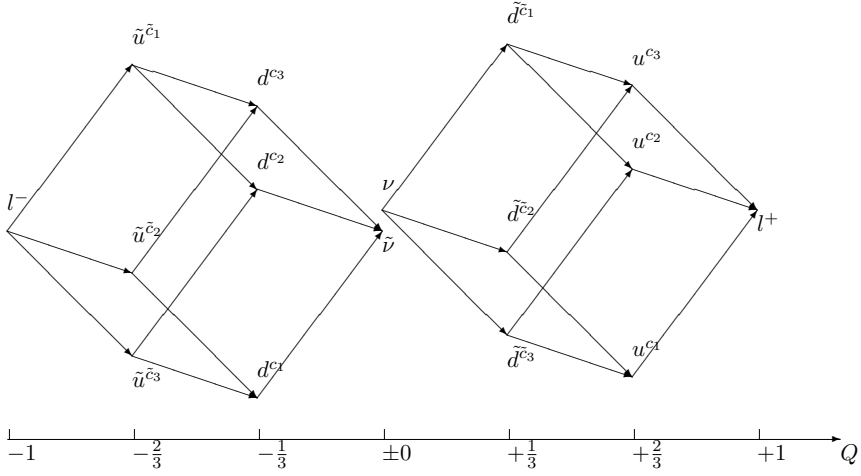


Fig. 13.3. Four-dimensional state hyper-rectangle space for the single charged binary triangle in the environment of neutral tessellation of alternating $\pm \frac{1}{2}$ -charged binary triangles, labeled with symbols of corresponding fermion family members

The degree of freedom emerging from implementing the tessellation instead of isolated triangle manifests the physical sense of the *isospin*, or the *weak charge*, connecting corresponding up and down particles.

Following the observations mentioned above, we suppose that one should search for geometrical structure containing equilateral triangles, aiming to obtain suitable model for the fundamental particles. It must be chiral to represent handedness and also must possess some additional degrees of freedom to be able to represent fermion families and fundamental bosons.

13.3 Calculation of electrical charge and Weaire-Phelan tessellation

We consider a graph for calculating the electric charge Q from values k_{ab} [1], that are the doubled eigenvalues (13.3) of Lorentz transformations infinitesimal generators S^{ab} (13.1) [1], [2]. The graph is constructed aiming to fetch all the data required for the calculation from the charges of cells in the dual-charged Weaire-Phelan tessellation [5].

In the Spin-Charge-Family theory, as well as in the Standard Model, the electric charge of a particle is calculated as a sum of the third projection of its $SU(2)_I$ weak charge τ^{13} and the hypercharge Y :

$$Q = \tau^{13} + Y. \quad (13.10)$$

Since the weak charge operator is defined as

$$\bar{\tau}^1 = \frac{1}{2} (S^{58} - S^{67}, S^{57} + S^{68}, S^{56} - S^{78}), \quad (13.11)$$

and each S^{ab} has two eigenvalues, namely $\frac{1}{2}k_{ab}$, where $k_{ab} = \pm 1$, the weak charge is expressed through k_{ab} in the following way:

$$\tau^{13} = \frac{1}{4}k_{56} - \frac{1}{4}k_{78}. \quad (13.12)$$

Therefore it can be of one of three different values:

k_{56}	k_{78}	τ^{13}
-1	-1	0
1	1	0
-1	1	-1/2
1	-1	1/2

In turn, the hypercharge is the sum of $SU(2)_{II}$ charge τ^{23} and $U(1)$ "fermion charge" τ^4 :

$$Y = \tau^{23} + \tau^4, \quad (13.13)$$

where

$$\tau^2 = \frac{1}{2} (S^{58} + S^{67}, S^{57} - S^{68}, S^{56} + S^{78}) \quad (13.14)$$

and

$$\tau^4 = -\frac{1}{3} (S^{910} + S^{1112} + S^{1314}). \quad (13.15)$$

After transition to the eigenvalues,

$$\tau^{23} = \frac{1}{4}k_{56} + \frac{1}{4}k_{78}, \quad (13.16)$$

$$\tau^4 = -\frac{1}{6}k_{910} - \frac{1}{6}k_{1112} - \frac{1}{6}k_{1314}. \quad (13.17)$$

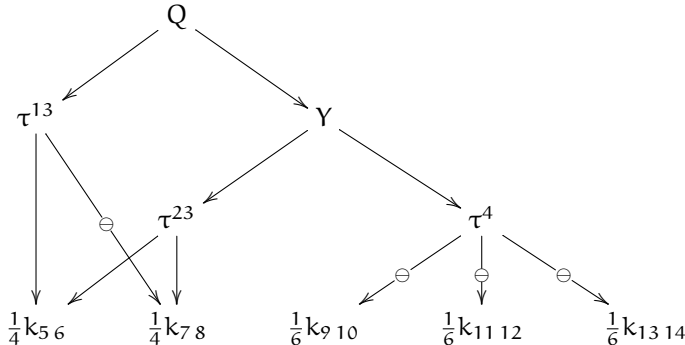
So

$$Y = \frac{1}{4}k_{56} + \frac{1}{4}k_{78} - \frac{1}{6}k_{910} - \frac{1}{6}k_{1112} - \frac{1}{6}k_{1314}, \quad (13.18)$$

and, finally,

$$Q = \frac{1}{4}k_{56} - \frac{1}{4}k_{78} + \frac{1}{4}k_{56} + \frac{1}{4}k_{78} - \frac{1}{6}k_{910} - \frac{1}{6}k_{1112} - \frac{1}{6}k_{1314}. \quad (13.19)$$

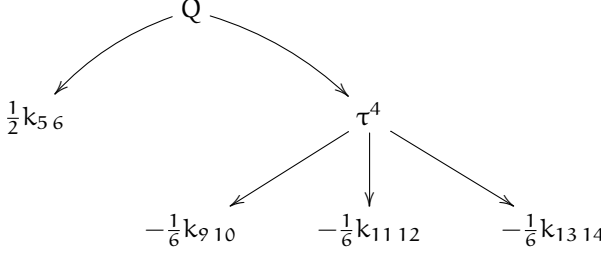
One can build the following graph illustrating how the electrical charge is calculated, where the arcs show the data dependence between nodes:



The value of k_{78} is included in equation (13.19) twice, with opposite signs, so it has no influence on the total charge Q , and the equation can be *simplified*:

$$Q = \frac{1}{2}k_{56} - \frac{1}{6}k_{910} - \frac{1}{6}k_{1112} - \frac{1}{6}k_{1314}. \quad (13.20)$$

The corresponding simplified calculation graph is the following:



In this form, the graph is equivalent to the charge calculation in our 4-bit model presented in [3]:

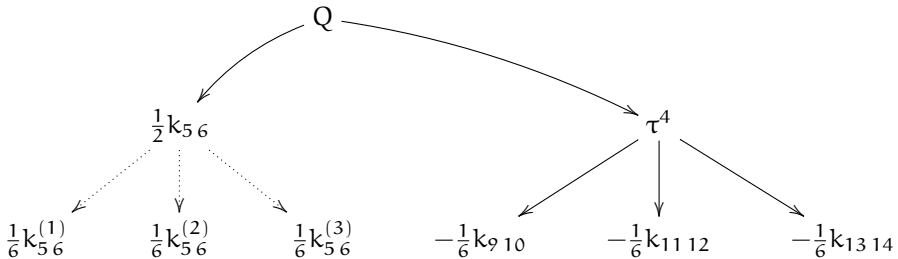
$$Q = \sum_{i=0}^2 \frac{c_i}{3} - q_2, \quad (13.21)$$

with the following correspondence:

$$\begin{aligned} \frac{1}{2}k_{56} &= -(q_2 - \frac{1}{2}) \\ \frac{1}{6}k_{910} &= -\frac{1}{3}(c_0 - \frac{1}{2}) \\ \frac{1}{6}k_{1112} &= -\frac{1}{3}(c_1 - \frac{1}{2}) \\ \frac{1}{6}k_{1314} &= -\frac{1}{3}(c_2 - \frac{1}{2}). \end{aligned} \quad (13.22)$$

The $c_i \in \{0; 1\}$ are three bits of the color code and $q_2 \in \{0; 1\}$ is the most significant bit of the electrical charge code in the *ones' complement* convention.

After splitting the node $\frac{1}{2}k_{56}$ into three nodes $\frac{1}{6}k_{56}^{(1)}$, $\frac{1}{6}k_{56}^{(2)}$, and $\frac{1}{6}k_{56}^{(3)}$, the graph becomes equivalent to our 6-bit model [3]:



$$Q = \sum_{i=0}^2 b_i^c + \sum_{i=0}^2 b_i^{T_3}, \quad (13.23)$$

where symbols b_i^c are produced from c_i by scaling and shifting down:

$$b_i^c = \frac{c_i}{3} - \frac{1}{6}, i \in \{0; 1; 2\}; b_i^c \in \left\{ -\frac{1}{6}; \frac{1}{6} \right\}. \quad (13.24)$$

The symbols $b_i^{T_3}$ are produced from q_2 by splitting it into three parts, scaling and shifting up:

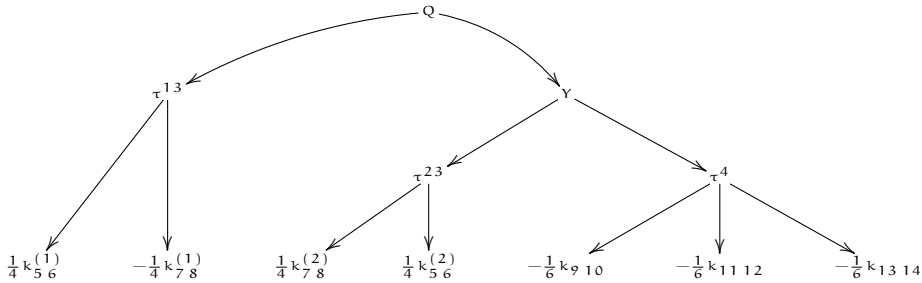
$$b_i^{T_3} = \frac{1}{6} - \frac{q_2}{3}, i \in \{0; 1; 2\}, b_i^{T_3} \in \left\{ -\frac{1}{6}; \frac{1}{6} \right\} \quad (13.25)$$

Note that we do not mean an increase in the number of degrees of freedom as a consequence of splitting nodes, at least while considering members of one fermion family, since all the three subnodes are assumed keeping the same values that are equal to value of splitted node..

Both these graphs have the following advantage in relation to the original one: they allow interpretation of particle's electrical charge as a *simple sum of values of all the nodes*² due to its tree-form and arcs meaning addition only. The last one also has an advantage of equal magnitude of nodes³.

To get these advantages in the original graph, we transform it the following way, getting rid of two loops and the subtracting arc. To do so, we assume that there are two *different* subnodes behind $\frac{1}{4}k_{56}$ and two others behind $\frac{1}{4}k_{78}$, always keeping *equal* values in the first case, and *opposite* values in the second one.

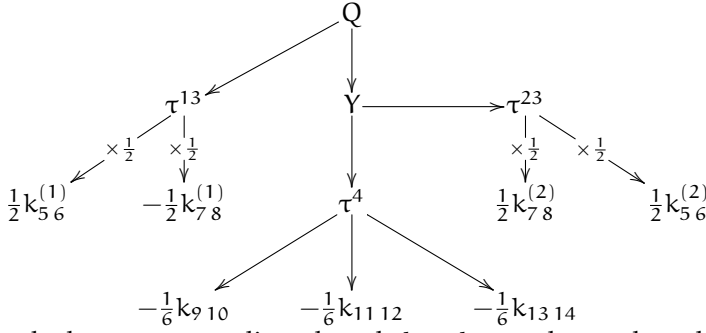
After transformation the graph becomes the following:



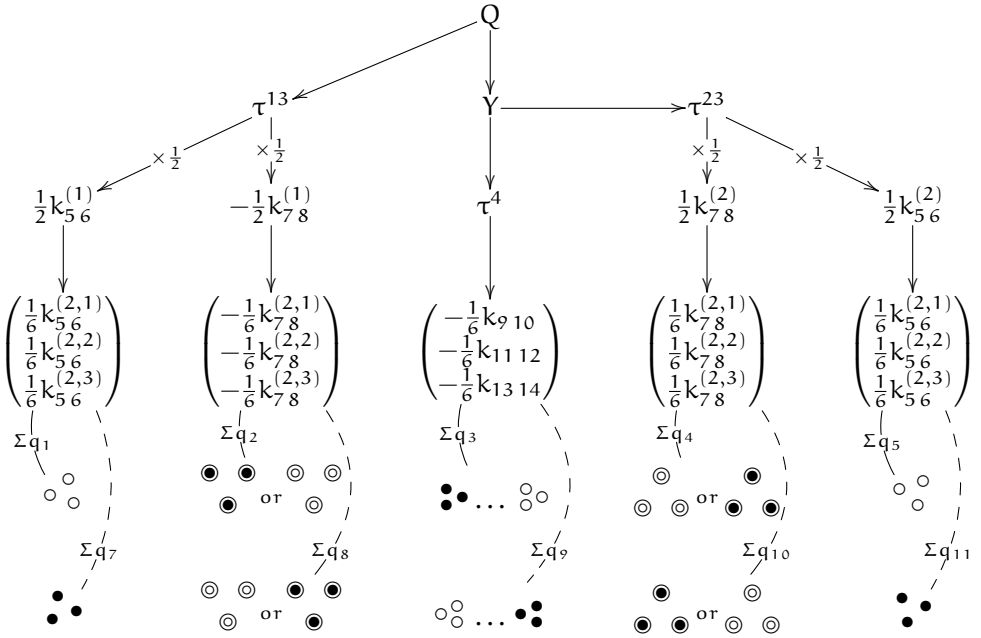
Then we double the factors in all the nodes for k_{56} and k_{78} , introducing compensating nodes that divide the corresponding values back. That makes these nodes ready to split on three sub-nodes with the factor of $\frac{1}{6}$. Arguments in favor of division in half for nodes k_{56} and k_{78} are different and given below and are discussed in detail in [5].

² or integration of charge density in continuous models

³ The choice of positive or negative eigenvalues is made while choosing the initial vacuum state corresponding to the right neutrino, and it can be changed to eliminate minus signs.



At the last step, we split each node k_{56} , k_{78} to three sub-nodes. Then we establish correspondence between these nodes and cells in the dual-charged Weaire-Phelan tessellation:



The last two rows contain the corresponding triangles of charged cells, residing in sequential ζ -planes in the tessellation. These triangles are listed in the Table 13.1 (it is borrowed from [5]). The first row contains cells triangles in planes from 1 to 5 and represents down fermions; in turn, the charge-inversed and mirror-reflected triangles in planes from 7 to 11 represent corresponding up particles.

Note that cells in planes 1 and 5, 7 and 11, that are the data sources for the k_{56} nodes, do not have any degrees of freedom and carry the negative charge for down particles and positive for up particles. Since all six cells are equal in charge and they must represent the $q_{env} = \pm \frac{1}{2}$, i.e. charge of the *environment* for cells in planes 3 or 9, their charge value is divided in half.

$\zeta_r \times \frac{1}{\sqrt{3}}$	kind, charge	shape	size	shape description
0	D–		–	Axial D–
1	T–		$\sqrt{14}$	Large T– triangle counterclockwise
2	D+		$\sqrt{32}$	D+ triangle v-down
3	T+		$\sqrt{6}$	Small T+triangle (ξ -right)
4	D–		$\sqrt{32}$	D– triangle v-up
5	T–		$\sqrt{14}$	Large T– triangle clockwise
6	D+		–	Axial D+
7	T+		$\sqrt{14}$	Large T+ triangle clockwise
8	D–		$\sqrt{32}$	D– triangle v-down
9	T–		$\sqrt{6}$	Small T– triangle (ξ -left)
10	D+		$\sqrt{32}$	D+ triangle v-up
11	T+		$\sqrt{14}$	Large T+ triangle counterclockwise
12	D–		–	Axial D–

Table 13.1. Shapes of cell center placements in twelve different planes

The cells in planes 2 and 4, 8 and 10 provide the data for the k_{78} nodes and each couple of triplets has just one degree of freedom, that represent the exchange between triangles in the coupled plane. The exchanged electrical charge of $\frac{1}{2}$ moves from one side of the plane 3 or 9 to another, representing the change of handedness and adjustment of weak charge and hyper-charge.

Since the cells in planes 2 and 4, 8 and 10 appear to have finite size, they partially overlap in projection to zeta axis, providing only *half* of charge is exchanged.

The three cells in plane 3, and three cells in plane 9 provide data for k_{910} , k_{1112} , and k_{1314} . Each of them keeps its degree of freedom, so there are eight combinations for small triangle in these planes, corresponding to eight down- and eight up particles or antiparticles. They are listed in Tables 13.2 and 13.3.

Note that in our approach the corresponding down and up particles with the same color have in this representation the *opposite* projections to the τ^{38} axis. It is so because they are mirror reflections of each other due to the **P** operation between them (C operation is not applied because we list all 8 combinations of charge for both cases, q_3 and q_9 , in the same order). The spin-charge-family theory, in contrast, provides *equal* τ^{38} values in this case [2].

13.3.1 On k numbers without influence on total electric charge

The value of k_{78} has no contribution to the total electric charge. As we have shown above, it can be considered as existing of mutually compensating cells of opposite charges. Also we note that the expression (13.19) can be *expanded* by including

$\tau^{13} =$ $q_{1,2}$	q_3^{210}	q_3^{102}	q_3^{021}	Σq_3	$\tau^4 =$ Σq_3	$\tau^{23} =$ $q_{4,5}$	$Y =$ $q_{3,4,5}$	$Q =$ $\tau^{13} + Y$	sym- bol	$\tau^{33} = \Sigma q_{3v}$ $\times \sqrt{\frac{2}{3}}$	$\tau^{38} = \Sigma q_{3\zeta}$ $\times \sqrt{\frac{2}{3}}$
$\frac{1}{2} \times \begin{matrix} \bullet & \bullet \\ \bullet & \bullet \end{matrix}$	+	+	+	+	$\bullet \bullet$		0	0	$\bar{\nu}_L$	0	0
	-	+	+	+	$\bullet \bullet$				d_R^{c1}	0	$-\frac{1}{\sqrt{3}}$
	+	-	+	+	$\bullet \bullet$		-1/3	-1/3	d_R^{c2}	+1/2	$\frac{1}{2\sqrt{3}}$
	+	+	-	-	$\bullet \bullet$	$\frac{1}{2} \times \begin{matrix} \bullet & \bullet \\ \bullet & \bullet \end{matrix}$			d_R^{c3}	-1/2	$\frac{1}{2\sqrt{3}}$
	+	-	-	-	$\bullet \bullet$				u_L^{c1}	0	$\frac{1}{\sqrt{3}}$
	-	+	-	-	$\bullet \bullet$		-2/3	-2/3	u_L^{c2}	-1/2	$-\frac{1}{2\sqrt{3}}$
	-	-	+	+	$\bullet \bullet$				u_L^{c3}	+1/2	$-\frac{1}{2\sqrt{3}}$
	-	-	-	-	$\bullet \bullet$		-1	-1	1_R^-	0	0
$\frac{1}{2} \times \begin{matrix} \bullet & \bullet \\ \bullet & \bullet \end{matrix}$	+	+	+	+	$\bullet \bullet$		+1/2	0	$\bar{\nu}_R$	0	0
	-	+	+	+	$\bullet \bullet$				d_L^{c1}	0	$-\frac{1}{\sqrt{3}}$
	+	-	+	+	$\bullet \bullet$		+1/6	-1/3	d_L^{c2}	+1/2	$\frac{1}{2\sqrt{3}}$
	+	+	-	-	$\bullet \bullet$	$\frac{1}{2} \times \begin{matrix} \bullet & \bullet \\ \bullet & \bullet \end{matrix}$			d_L^{c3}	-1/2	$\frac{1}{2\sqrt{3}}$
	+	-	-	-	$\bullet \bullet$				u_R^{c1}	0	$\frac{1}{\sqrt{3}}$
	-	+	-	-	$\bullet \bullet$		-1/6	-2/3	u_R^{c2}	-1/2	$-\frac{1}{2\sqrt{3}}$
	-	-	+	+	$\bullet \bullet$				u_R^{c3}	+1/2	$-\frac{1}{2\sqrt{3}}$
	-	-	-	-	$\bullet \bullet$		-1/2	-1	1_L^-	0	0

Table 13.2. Eight cases of inversions in the small T-triangle at $\zeta = 3/\sqrt{3}$; with original and exchanged D-triangles at $\zeta = 2/\sqrt{3}$ and $4/\sqrt{3}$, associated with "down" fermions

$\tau^{13} =$ $\Sigma q_{7,8}$	$q_7^{234} \ q_8^{123} \ q_9^{342}$	$\tau^4 =$ Σq_9	$\tau^{23} =$ $\Sigma q_{10,11}$	$Y =$ $\Sigma q_{9,10,11}$	$Q =$ $\tau^{13} + Y$	sym bol	$\tau^{33} = \Sigma q_{9,10}$ $\times \sqrt{\frac{2}{3}}$	$\tau^{33} = \Sigma q_{9,10}$ $\times \sqrt{\frac{2}{3}}$
$\frac{1}{2} \times \odot \odot \odot$	$+$	$+$	$+$	$+1$	$+1$	l_1^+	0	0
	$-$	$+$	$\odot \odot$			u_R^c	0	$\frac{1}{\sqrt{3}}$
	$+$	$-$	$\odot \odot$	$+2/3$	$+2/3$	u_R^c	$+1/2$	$-\frac{1}{2\sqrt{3}}$
	$+$	$+$	$\odot \odot$			u_R^c	$-1/2$	$-\frac{1}{2\sqrt{3}}$
0	$+$	$-$	$\odot \odot$			d_L^c	0	$-\frac{1}{\sqrt{3}}$
	$-$	$+$	$\odot \odot$	$+1/3$	$+1/3$	d_L^c	$-1/2$	$\frac{1}{2\sqrt{3}}$
	$-$	$+$	$\odot \odot$			d_L^c	$+1/2$	$\frac{1}{2\sqrt{3}}$
	$-$	$-$	$\odot \odot$	0	0	ν_R	0	0
$\frac{1}{2} \times \odot \odot \odot$	$+$	$+$	$\odot \odot$	$+1/2$	$+1$	l_1^+	0	0
	$-$	$+$	$\odot \odot$			u_L^c	0	$\frac{1}{\sqrt{3}}$
	$+$	$-$	$\odot \odot$	$+1/6$	$+2/3$	u_L^c	$+1/2$	$-\frac{1}{2\sqrt{3}}$
	$+$	$+$	$\odot \odot$			u_L^c	$-1/2$	$-\frac{1}{2\sqrt{3}}$
$+1/2$	$+$	$-$	$\odot \odot$			d_R^c	0	$-\frac{1}{\sqrt{3}}$
	$-$	$+$	$\odot \odot$	$-1/6$	$+1/3$	d_R^c	$-1/2$	$\frac{1}{2\sqrt{3}}$
	$-$	$+$	$\odot \odot$			d_R^c	$+1/2$	$\frac{1}{2\sqrt{3}}$
	$-$	$-$	$\odot \odot$	$-1/2$	0	ν_L	0	0

Table 13.3. Eight cases of inversions in the small T-triangle at $\zeta = 9/\sqrt{3}$, repeated twice with original and exchanged D-triangles at $\zeta = 8/\sqrt{3}$ and $10/\sqrt{3}$, associated with "up" fermions

additional terms, arbitrary in magnitude, that cancel each other. Since they have no influence on the electrical charge, they can't be determined from the charge analyse. We suppose that the expression of the electrical charge can also contain the last real eigenvalue, k_{12} :

$$Q = \alpha k_{12}^{(1)} - \alpha k_{12}^{(2)} + \frac{1}{4}k_{56} - \frac{1}{4}k_{78} + \frac{1}{4}k_{56} + \frac{1}{4}k_{78} - \frac{1}{6}k_{910} - \frac{1}{6}k_{1112} - \frac{1}{6}k_{1314}, \quad (13.26)$$

where α is a factor that can be equal to $1/6$. It allows to associate $k_{12}^{(1)}$, $k_{12}^{(2)}$ with the "axial" D cells at $\zeta = 0$ and $6/\sqrt{3}$ for down fermions, and $6/\sqrt{3}$ and $12/\sqrt{3}$ for up ones.

In the spin-charge theory the value of k_{03} is dependent on values of other k_{ab} since the equation

$$k_{03} = -ik_{12}k_{56}k_{78}k_{910}k_{1112}k_{1314} \quad (13.27)$$

is fulfilled for each fermion combination in [1], [2]. In our opinion, it is connected with the fact that the seven binary values of k_{ab} generate only $2^6 = 64$ combinations. For one family there are only six independent degrees of freedom represented by k_{ab} , so since there are seven of them, one (in our case, k_{03}) should be expressed through six others.

Thus, there is no degree of freedom connected with k_{03} and there is no corresponding cell in the Weaire-Phelan structure, so the value of *spin* always can be computed based on other data 13.27.

Totally, we have the following correspondence between values of k_{ab} in the Spin-Charge-Family theory and charges associated with cells of dual-charged Weaire-Phelan model:

$$\begin{aligned} k_{12} &= 3q_{-3} - 3q_{+3} \\ k_{56} &= \Sigma q_{-2} + \Sigma q_{+2} \\ k_{78} &= \Sigma q_{-1} - \Sigma q_{+1} \\ k_{910} &= 6q^{ijk} \\ k_{1112} &= 6q^{jki} \\ k_{1314} &= 6q^{kij} \\ k_{03} &= -ik_{12}k_{56}k_{78}k_{910}k_{1112}k_{1314} \end{aligned} \quad (13.28)$$

It is provided in relative form, for both up and down particles. The lower index counting the ζ -plane number relative to the plane of the small T-triangle (that is 3 for down or 9 for up fermions), and the upper index counts x,y,z coordinates of three individual cells in the triangle; the Σ sign means sum of these three cells.

13.4 Conclusion

We presented here our approach to the particle and vacuum modelling. It is, being applied to one fermion family, reproduces the same quantum numbers as those obtained in the spin-charge-family theory. The advantage of spatial tessellation model, on our opinion, is the lower dimension count, so it can fit in the usual

spacetime and be more demonstrative. Also it provides native **CPS** symmetry and emergent weak charge. We suppose that one can find out the appropriate 3- or 4-dimensional spatial model that would, keeping the shown advantages, also represent and explain fermion families and also fundamental bosons, basing on 8-bit code model [3].

References

1. N.S. Mankoč Borštnik: Can spin-charge-family theory explain baryon number non conservation? arXiv:1409.7791v3 - 24 February 2015.
2. N.S. Mankoč Borštnik: Fermions and Bosons in the Expanding Universe by the Spin-charge-family theory, in: N.S. Mankoč Borštnik, H.B.F. Nielsen, D. Lukman: Proceedings to the 20th Workshop 'What Comes Beyond the Standard Models', Bled, July 9 - 17 2017.
3. E.G. Dmitrieff: Experience in modeling properties of fundamental particles using binary codes, in: N.S. Mankoč Borštnik, H.B.F. Nielsen, D. Lukman: Proceedings to the 19th Workshop 'What Comes Beyond the Standard Models', Bled, 11. - 19. July 2016.
4. D.Weaire, R.Phelan, A counter-example to Kelvin's conjecture on minimal surfaces, *Phil. Mag. Lett.*, (1994) 69: 107–110, doi:10.1080/09500839408241577
5. E.G.Dmitrieff: On triple-periodic electrical charge distribution as a model of physical vacuum and fundamental particles, in N.S. Mankoč Borštnik, H.B.F. Nielsen, D. Lukman: Proceedings to the 21th Workshop 'What Comes Beyond the Standard Models', Bled, 23. - 29. June 2018



14 $K^0 - \bar{K}^0, D^0 - \bar{D}^0$ in a Local $SU(3)$ Family Symmetry

A. Hernandez-Galeana *

Departamento de Física, ESFM - Instituto Politécnico Nacional.
U. P. "Adolfo López Mateos". C. P. 07738, Ciudad de México, México.

Abstract. Within a broken $SU(3)$ gauged family symmetry, we report the analysis of $\Delta F = 2$ processes induced by the tree level exchange of the new massive horizontal gauge bosons, which introduce flavor-changing couplings. We provide a parameter space region where this framework can accommodate the hierarchical spectrum of quark masses and mixing and simultaneously suppress within current experimental limits the contributions to $K^0 - \bar{K}^0$ and $D^0 - \bar{D}^0$ mixing. In addition we find out that the mass of the $SU(2)_L$ weak singlet vector-like D quark introduced in this BSM, may be of the order of 10 TeV.

Povzetek. Avtor v okviru svojega predloga teorije z zlomljeno družinsko simetrijo $SU(3)$ analizira procese tipa $\Delta F = 2$, ki jih inducira izmenjava novih masivnih horizontalnih umeritvenih bozonov na drevesnem nivoju, kar privede do sklopitev, ki spremenijo okus. Najde območje v prostoru parametrov, ki dovoljuje izmerjeni masni spekter kvarkov ter njihovo mešalno matriko, pri tem pa so prispevki mešanja $K^0 - \bar{K}^0$ in $D^0 - \bar{D}^0$ pod trenutnimi eksperimentalnimi mejami. Maso napovedanega kvarka D, ki je šibki singlet vektorskega tipa $SU(2)_L$, oceni na ~ 10 TeV.

Keywords: Quark and lepton masses and mixing, Flavor symmetry,
 $\Delta F = 2$ Processes.

PACS: 14.60.Pq, 12.15.Ff, 12.60.-i

14.1 Introduction

Flavor physics and rare processes play an important role to test any Beyond Standard Model(BSM) physics proposal, and hence, it is crucial to explore the possibility to suppress properly these type of flavor violating processes.

Within the framework of a vector-like gauged $SU(3)$ family symmetry model[1,2], we study the contribution to $\Delta F = 2$ processes[3]-[6] in neutral mesons at tree level exchange diagrams mediated by the gauge bosons with masses of the order of some TeV's, corresponding to the lower scale of the $SU(3)$ family symmetry breaking.

* E-mail: albino@esfm.ipn.mx

The reported analysis is performed in a scenario where light fermions obtain masses from radiative corrections mediated by the massive bosons associated to the broken $SU(3)$ family symmetry, while the heavy fermions; top and bottom quarks and tau lepton become massive from tree level See-saw mechanisms. Previous theories addressing the problem of quark and lepton masses and mixing with spontaneously broken $SU(3)$ gauge symmetry of generations include the ones with chiral local $SU(3)_H$ family symmetry as well as other $SU(3)$ family symmetries. See for instance [7]-[14] and references therein.

14.2 $SU(3)$ family symmetry model

The model is based on the gauge symmetry

$$G \equiv SU(3)_F \otimes SU(3)_C \otimes SU(2)_L \otimes U(1)_Y \quad (14.1)$$

where $SU(3)$ is a completely vector-like and universal gauged family symmetry. That is, the corresponding gauge bosons couple equally to Left and Right Handed ordinary Quarks and Leptons, with g_H , g_s , g and g' the corresponding coupling constants. The content of fermions assumes the standard model quarks and leptons:

$$\Psi_q^o = (3, 3, 2, \frac{1}{3})_L \quad , \quad \Psi_l^o = (3, 1, 2, -1)_L \quad (14.2)$$

$$\Psi_u^o = (3, 3, 1, \frac{4}{3})_R \quad , \quad \Psi_d^o = (3, 3, 1, -\frac{2}{3})_R \quad , \quad \Psi_e^o = (3, 1, 1, -2)_R \quad (14.3)$$

where the last entry is the hypercharge Y , with the electric charge defined by $Q = T_{3L} + \frac{1}{2}Y$.

The model includes two types of extra fermions: Right Handed Neutrinos: $\Psi_{\nu_R}^o = (3, 1, 1, 0)_R$, introduced to cancel anomalies [7], and a new family of $SU(2)_L$ weak singlet vector-like fermions: Vector like quarks $U_L^o, U_R^o = (1, 3, 1, \frac{4}{3})$ and $D_L^o, D_R^o = (1, 3, 1, -\frac{2}{3})$, Vector Like electrons: $E_L^o, E_R^o = (1, 1, 1, -2)$, and New Sterile Neutrinos: $N_L^o, N_R^o = (1, 1, 1, 0)$.

The particle content and gauge symmetry assignments are summarized in Table 14.1. Notice that all $SU(3)$ non-singlet fields transform as the fundamental representation under the $SU(3)$ symmetry.

14.3 $SU(3)$ family symmetry breaking

To implement the SSB of $SU(3)$, we introduce two flavon scalar fields:

$$\eta_i = (3, 1, 1, 0) = \begin{pmatrix} \eta_{i1}^o \\ \eta_{i2}^o \\ \eta_{i3}^o \end{pmatrix} \quad , \quad i = 1, 2 \quad (14.4)$$

	SU(3)	SU(3) _C	SU(2) _L	U(1) _Y
ψ_q^o	3	3	2	$\frac{1}{3}$
ψ_{uR}^o	3	3	1	$\frac{4}{3}$
ψ_{dR}^o	3	3	1	$-\frac{2}{3}$
ψ_l^o	3	1	2	-1
ψ_{eR}^o	3	1	1	-2
$\psi_{\nu R}^o$	3	1	1	0
Φ^u	3	1	2	-1
Φ^d	3	1	2	+1
η_i	3	1	1	0
$U_{L,R}^o$	1	3	1	$\frac{4}{3}$
$D_{L,R}^o$	1	3	1	$-\frac{2}{3}$
$E_{L,R}^o$	1	1	1	-2
$N_{L,R}^o$	1	1	1	0

Table 14.1. Particle content and charges under the gauge symmetry

with the "Vacuum ExpectationValues" (VEV's):

$$\langle \eta_1 \rangle^T = (\Lambda_1, 0, 0) \quad , \quad \langle \eta_2 \rangle^T = (0, \Lambda_2, 0) . \quad (14.5)$$

It is worth to mention that these two scalars in the fundamental representation is the minimal set of scalars to break down completely the SU(3) family symmetry. The interaction Lagrangian of the SU(3) gauge bosons to the SM massless fermions is

$$i\mathcal{L}_{\text{int}, \text{SU}(3)_F} = g_H \begin{pmatrix} \bar{f}_1^o & \bar{f}_2^o & \bar{f}_3^o \end{pmatrix} \gamma_\mu \begin{pmatrix} \frac{Z_1^\mu}{2} + \frac{Z_2^\mu}{2\sqrt{3}} & \frac{Y_1^{+\mu}}{\sqrt{2}} & \frac{Y_2^{+\mu}}{\sqrt{2}} \\ \frac{Y_1^{-\mu}}{\sqrt{2}} & -\frac{Z_2^\mu}{\sqrt{3}} & \frac{Y_3^{+\mu}}{\sqrt{2}} \\ \frac{Y_2^{-\mu}}{\sqrt{2}} & \frac{Y_3^{-\mu}}{\sqrt{2}} & -\frac{Z_1^\mu}{2} + \frac{Z_2^\mu}{2\sqrt{3}} \end{pmatrix} \begin{pmatrix} f_1^o \\ f_2^o \\ f_3^o \end{pmatrix} \quad (14.6)$$

where g_H is the SU(3) coupling constant, Z_1, Z_2 and $Y_j^\pm = \frac{Y_j^1 \mp iY_j^2}{\sqrt{2}}$, $j = 1, 2, 3$ are the eight gauge bosons.

Thus, the contribution to the horizontal gauge boson masses from the VEV's in Eq.(14.5) read

- $\langle \eta_1 \rangle$: $\frac{g_H^2 \Lambda_1^2}{2} (Y_1^+ Y_1^- + Y_2^+ Y_2^-) + \frac{g_H^2 \Lambda_1^2}{4} (Z_1^2 + \frac{Z_2^2}{3} + 2Z_1 \frac{Z_2}{\sqrt{3}})$
- $\langle \eta_2 \rangle$: $\frac{g_H^2 \Lambda_2^2}{2} (Y_1^+ Y_1^- + Y_3^+ Y_3^-) + g_H^2 \Lambda_2^2 \frac{Z_2^2}{3}$

The "Spontaneous Symmetry Breaking" (SSB) of SU(3) occurs in two stages

$$\text{SU}(3) \times G_{SM} \xrightarrow{\langle \eta_2 \rangle} \text{SU}(2) \times G_{SM} \xrightarrow{\langle \eta_1 \rangle} G_{SM}$$

FCNC ?

Notice that the hierarchy of scales $\Lambda_2 > \Lambda_1$ yield an "approximate $SU(2)$ global symmetry" in the spectrum of $SU(2)$ gauge boson masses.

Therefore, neglecting tiny contributions from electroweak symmetry breaking, we obtain the gauge boson mass terms.

$$(M_1^2 + M_2^2) Y_1^+ Y_1^- + M_1^2 Y_2^+ Y_2^- + M_2^2 Y_3^+ Y_3^- + \frac{1}{2} M_1^2 Z_1^2 + \frac{1}{2} \frac{M_1^2 + 4M_2^2}{3} Z_2^2 + \frac{1}{2} (M_1^2) \frac{2}{\sqrt{3}} Z_1 Z_2 \quad (14.7)$$

$$M_1^2 = \frac{g_H^2 \Lambda_1^2}{2}, \quad M_2^2 = \frac{g_H^2 \Lambda_2^2}{2} \quad (14.8)$$

	Z_1	Z_2
Z_1	M_1^2	$\frac{M_1^2}{\sqrt{3}}$
Z_2	$-\frac{M_1^2}{\sqrt{3}}$	$\frac{M_1^2 + 4M_2^2}{3}$

Table 14.2. $Z_1 - Z_2$ mixing mass matrix

Diagonalization of the $Z_1 - Z_2$ squared mass matrix yield the eigenvalues

$$M_-^2 = \frac{2}{3} \left(M_1^2 + M_2^2 - \sqrt{(M_2^2 - M_1^2)^2 + M_1^2 M_2^2} \right) \quad (14.9)$$

$$M_+^2 = \frac{2}{3} \left(M_1^2 + M_2^2 + \sqrt{(M_2^2 - M_1^2)^2 + M_1^2 M_2^2} \right) \quad (14.10)$$

and finally

$$(M_1^2 + M_2^2) Y_1^+ Y_1^- + M_1^2 Y_2^+ Y_2^- + M_2^2 Y_3^+ Y_3^- + M_-^2 \frac{Z_-^2}{2} + M_+^2 \frac{Z_+^2}{2}, \quad (14.11)$$

where

$$\begin{pmatrix} Z_1 \\ Z_2 \end{pmatrix} = \begin{pmatrix} \cos \phi & \sin \phi \\ -\sin \phi & \cos \phi \end{pmatrix} \begin{pmatrix} Z_- \\ Z_+ \end{pmatrix} \quad (14.12)$$

$$\cos \phi \sin \phi = \frac{\sqrt{3}}{4} \frac{M_1^2}{\sqrt{M_1^4 + M_2^2(M_2^2 - M_1^2)}} \quad (14.13)$$

14.4 Electroweak symmetry breaking

For electroweak symmetry breaking we introduce two triplets of SU(2)_L Higgs doublets, namely;

$$\Phi^u = (3, 1, 2, -1) \quad , \quad \Phi^d = (3, 1, 2, +1) \quad , \quad (14.14)$$

with the VEV's

$$\langle \Phi^u \rangle = \begin{pmatrix} \langle \Phi_1^u \rangle \\ \langle \Phi_2^u \rangle \\ \langle \Phi_3^u \rangle \end{pmatrix} \quad , \quad \langle \Phi^d \rangle = \begin{pmatrix} \langle \Phi_1^d \rangle \\ \langle \Phi_2^d \rangle \\ \langle \Phi_3^d \rangle \end{pmatrix} \quad , \quad (14.15)$$

where

$$\langle \Phi_i^u \rangle = \frac{1}{\sqrt{2}} \begin{pmatrix} v_{ui} \\ 0 \end{pmatrix} \quad , \quad \langle \Phi_i^d \rangle = \frac{1}{\sqrt{2}} \begin{pmatrix} 0 \\ v_{di} \end{pmatrix} . \quad (14.16)$$

The contributions from $\langle \Phi^u \rangle$ and $\langle \Phi^d \rangle$ generate the W and Z_0 SM gauge boson masses

$$\frac{g^2}{4} (v_u^2 + v_d^2) W^+ W^- + \frac{(g^2 + g'^2)}{8} (v_u^2 + v_d^2) Z_0^2 \quad (14.17)$$

$$+ \text{tiny contribution to the SU(3) gauge boson masses and mixing} \quad (14.18)$$

$$\text{with } Z_0, \quad (14.19)$$

$v_u^2 = v_{1u}^2 + v_{2u}^2 + v_{3u}^2$, $v_d^2 = v_{1d}^2 + v_{2d}^2 + v_{3d}^2$. So, if $M_W \equiv \frac{1}{2}gv$, we may write $v = \sqrt{v_u^2 + v_d^2} \approx 246 \text{ GeV}$.

14.5 Fermion masses

14.5.1 Dirac See-saw mechanisms

The scalars and fermion content allow for quarks the gauge invariant Yukawa couplings

$$H_u \bar{\psi}_q^0 \Phi^u U_R^0 + h_{iu} \bar{\psi}_{uR}^0 \eta_i U_L^0 + M_u \bar{U}_L^0 U_R^0 + \text{h.c} \quad (14.20)$$

$$H_d \bar{\psi}_q^0 \Phi^d D_R^0 + h_{id} \bar{\psi}_{dR}^0 \eta_i D_L^0 + M_D \bar{D}_L^0 D_R^0 + \text{h.c} \quad (14.21)$$

M_u, M_D are free mass parameters and H_u, H_d, h_{iu}, h_{id} are Yukawa coupling constants. When the involved scalar fields acquire VEV's, we get in the gauge basis $\psi_{L,R}^0{}^T = (e^0, \mu^0, \tau^0, E^0)_{L,R}$, the mass terms $\bar{\psi}_L^0 \mathcal{M}^0 \psi_R^0 + \text{h.c}$, where

$$\mathcal{M}^o = \begin{pmatrix} 0 & 0 & 0 & h v_1 \\ 0 & 0 & 0 & h v_2 \\ 0 & 0 & 0 & h v_3 \\ h_1 \Lambda_1 & h_2 \Lambda_2 & 0 & M \end{pmatrix} \equiv \begin{pmatrix} 0 & 0 & 0 & a_1 \\ 0 & 0 & 0 & a_2 \\ 0 & 0 & 0 & a_3 \\ b_1 & b_2 & 0 & M \end{pmatrix}. \quad (14.22)$$

\mathcal{M}^o is diagonalized by applying a biunitary transformation $\psi_{L,R}^o = V_{L,R}^o \chi_{L,R}$.

$$V_L^{oT} \mathcal{M}^o V_R^o = \text{Diag}(0, 0, -\lambda_3, \lambda_4) \quad (14.23)$$

$$V_L^{oT} \mathcal{M}^o \mathcal{M}^{oT} V_L^o = V_R^{oT} \mathcal{M}^{oT} \mathcal{M}^o V_R^o = \text{Diag}(0, 0, \lambda_3^2, \lambda_4^2), \quad (14.24)$$

where λ_3 and λ_4 are the nonzero eigenvalues, λ_4 being the fourth heavy fermion mass, and λ_3 of the order of the top, bottom and tau mass for u, d and e fermions, respectively. We see from Eqs.(14.23,14.24) that from tree level the See-saw mechanism yields two massless eigenvalues associated to the light fermions:

14.6 One loop contribution to fermion masses

The one loop diagram of Fig. 1 gives the generic contribution to the mass term $m_{ij} \bar{e}_{iL}^o e_{jR}^o$,

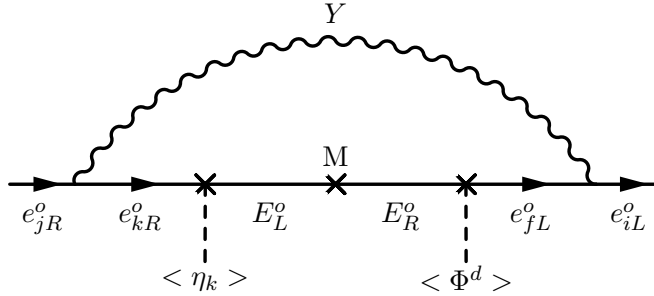


Fig. 14.1. Generic one loop diagram contribution to the mass term $m_{ij} \bar{e}_{iL}^o e_{jR}^o$

$$m_{ij} = c_Y \frac{\alpha_H}{\pi} \sum_{k=3,4} m_k^o (V_L^o)_{ik} (V_R^o)_{jk} f(M_Y, m_k^o) \quad , \quad \alpha_H \equiv \frac{g_H^2}{4\pi}, \quad (14.25)$$

M_Y being the mass of the gauge boson, c_Y is a factor coupling constant, Eq.(14.6), $m_3^o = -\lambda_3$ and $m_4^o = \lambda_4$, and $f(x, y) = \frac{x^2}{x^2 - y^2} \ln \frac{x^2}{y^2}$,

$$\sum_{k=3,4} m_k^o (V_L^o)_{ik} (V_R^o)_{jk} f(M_Y, m_k^o) = \frac{a_i b_j M}{\lambda_4^2 - \lambda_3^2} F(M_Y), \quad (14.26)$$

$i = 1, 2, 3$, $j = 1, 2$, and $F(M_Y) \equiv \frac{M_Y^2}{M_Y^2 - \lambda_4^2} \ln \frac{M_Y^2}{\lambda_4^2} - \frac{M_Y^2}{M_Y^2 - \lambda_3^2} \ln \frac{M_Y^2}{\lambda_3^2}$. Adding up all possible the one loop diagrams, we get the contribution $\bar{\psi}_L^o \mathcal{M}_1^o \psi_R^o + \text{h.c.}$,

$$\mathcal{M}_1^0 = \begin{pmatrix} D_{11} & D_{12} & 0 & 0 \\ D_{21} & D_{22} & 0 & 0 \\ D_{31} & D_{32} & D_{33} & 0 \\ 0 & 0 & 0 & 0 \end{pmatrix} \frac{\alpha_H}{\pi}, \quad (14.27)$$

$$D_{11} = \mu_{11} \left(\frac{F_{Z_1}}{4} + \frac{F_{Z_2}}{12} + F_m \right) + \frac{1}{2} \mu_{22} F_1 \quad D_{12} = \mu_{12} \left(-\frac{F_{Z_2}}{6} - F_m \right)$$

$$D_{21} = \mu_{21} \left(-\frac{F_{Z_2}}{6} - F_m \right) \quad D_{22} = \frac{1}{2} \mu_{11} F_1 + \frac{1}{3} \mu_{22} F_{Z_2}$$

$$D_{31} = \mu_{31} \left(-\frac{F_{Z_1}}{4} + \frac{F_{Z_2}}{12} \right) \quad D_{32} = \mu_{32} \left(-\frac{F_{Z_2}}{6} + F_m \right)$$

$$D_{33} = \frac{1}{2} (\mu_{11} F_2 + \mu_{22} F_3)$$

$$\alpha_H = \frac{g_H^2}{4\pi}, \quad F_1 \equiv F(M_{Y_1}), \quad F_2 \equiv F(M_{Y_2}), \quad F_3 \equiv F(M_{Y_3}) \quad (14.28)$$

$$F_{Z_1} = \cos^2 \phi F(M_-) + \sin^2 \phi F(M_+) \quad (14.29)$$

$$F_{Z_2} = \sin^2 \phi F(M_-) + \cos^2 \phi F(M_+) \quad (14.30)$$

$$F_m = \frac{\cos \phi \sin \phi}{2\sqrt{3}} [F(M_+) - F(M_-)]. \quad (14.31)$$

F_{Z_1} , F_{Z_2} are the contributions from the diagrams mediated by the Z_1 , Z_2 gauge bosons, F_m comes from the $Z_1 - Z_2$ mixing diagrams, with M_1, M_2, M_-, M_+ the horizontal boson masses, Eqs.(7-11),

$$\mu_{ij} = \frac{a_i b_j M}{\lambda_4^2 - \lambda_3^2} = \frac{a_i b_j}{a b} \lambda_3 c_\alpha c_\beta, \quad (14.32)$$

$c_\alpha = \cos \alpha$, $c_\beta = \cos \beta$, $s_\alpha = \sin \alpha$, $s_\beta = \sin \beta$ are the mixing angles from the diagonalization of \mathcal{M}^0 . Therefore, up to one loop corrections the fermion masses are

$$\bar{\psi}_L^0 \mathcal{M}^0 \psi_R^0 + \bar{\psi}_L^0 \mathcal{M}_1^0 \psi_R^0 = \bar{\chi}_L \mathcal{M} \chi_R, \quad (14.33)$$

where $\psi_{L,R}^0 = V_{L,R}^0 \chi_{L,R}$, and $\mathcal{M} \equiv [\text{Diag}(0, 0, -\lambda_3, \lambda_4) + V_L^{0T} \mathcal{M}_1^0 V_R^0]$ may be written as:

$$\mathcal{M} = \begin{pmatrix} m_{11} & m_{12} & c_\beta m_{13} & s_\beta m_{13} \\ m_{21} & m_{22} & c_\beta m_{23} & s_\beta m_{23} \\ c_\alpha m_{31} & c_\alpha m_{32} & (-\lambda_3 + c_\alpha c_\beta m_{33}) & c_\alpha s_\beta m_{33} \\ s_\alpha m_{31} & s_\alpha m_{32} & s_\alpha c_\beta m_{33} & (\lambda_4 + s_\alpha s_\beta m_{33}) \end{pmatrix}, \quad (14.34)$$

The diagonalization of \mathcal{M} , Eq.(14.34) gives the physical masses for u and d quarks, e charged leptons and ν Dirac neutrino masses.

Using a new biunitary transformation $\chi_{L,R} = V_{L,R}^{(1)} \Psi_{L,R}$; $\bar{\chi}_L \mathcal{M} \chi_R = \bar{\Psi}_L V_L^{(1)\dagger} \mathcal{M} V_R^{(1)} \Psi_R$, with $\Psi_{L,R}^T = (f_1, f_2, f_3, F)_{L,R}$ the mass eigenfields, that is

$$V_L^{(1)\dagger} \mathcal{M} \mathcal{M}^T V_L^{(1)} = V_R^{(1)\dagger} \mathcal{M}^T \mathcal{M} V_R^{(1)} = \text{Diag}(m_1^2, m_2^2, m_3^2, M_F^2), \quad (14.35)$$

$m_1^2 = m_e^2$, $m_2^2 = m_\mu^2$, $m_3^2 = m_\tau^2$ and $M_F^2 = M_E^2$ for charged leptons. So, the rotations from massless to mass fermions eigenfields in this scenario reads

$$\psi_L^o = V_L^o V_L^{(1)} \Psi_L \quad \text{and} \quad \psi_R^o = V_R^o V_R^{(1)} \Psi_R \quad (14.36)$$

14.6.1 Quark Mixing Matrix V_{CKM}

We recall that vector like quarks are $SU(2)_L$ weak singlets, and hence the interaction of L-handed up and down quarks; $f_{uL}^o{}^T = (u^o, c^o, t^o)_L$ and $f_{dL}^o{}^T = (d^o, s^o, b^o)_L$, to the W charged gauge boson is

$$\frac{g}{\sqrt{2}} \bar{f}_{uL}^o \gamma_\mu f_{dL}^o W^{+\mu} = \frac{g}{\sqrt{2}} \bar{\Psi}_{uL} (V_{CKM})_{4 \times 4} \gamma_\mu \Psi_{dL} W^{+\mu}, \quad (14.37)$$

where the non-unitary quark mixing matrix V_{CKM} of dimension 4×4 is

$$(V_{CKM})_{4 \times 4} = [(V_{uL}^o V_{uL}^{(1)})_{3 \times 4}]^T (V_{dL}^o V_{dL}^{(1)})_{3 \times 4} \quad (14.38)$$

14.7 Numerical results for quark masses and mixing

As an example of the possible spectrum of quark masses and mixing from this scenario, we show up the following fit of parameters at the M_Z scale [15]

Using the input values for the horizontal boson masses, Eq.(8), and the coupling constant of the $SU(3)$ symmetry:

$$M_1 = 3.3 \times 10^3 \text{ TeV} \quad , \quad M_2 = 3.3 \times 10^5 \text{ TeV} \quad , \quad \frac{\alpha_H}{\pi} = 0.05, \quad (14.39)$$

we write the tree level \mathcal{M}_q^o , and up to one loop corrections \mathcal{M}_q^o quark mass matrices, as well as the corresponding mass eigenvalues and mixing:

d-quarks:

Tree level see-saw mass matrix:

$$\mathcal{M}_d^o = \begin{pmatrix} 0 & 0 & 0 & 906.643 \\ 0 & 0 & 0 & 5984.81 \\ 0 & 0 & 0 & 8139.76 \\ 3.00124 \times 10^6 & -670943.0 & 9.10502 \times 10^6 & \end{pmatrix} \text{MeV}, \quad (14.40)$$

the mass matrix up to one loop corrections:

$$\mathcal{M}_d = \begin{pmatrix} -5.64571 & -11.0583 & 46.8646 & 15.829 \\ -29.9051 & -39.4588 & -11.5894 & -3.91444 \\ 40.9245 & -30.3588 & -2859.86 & 130.424 \\ 0.0409246 & -0.0303588 & 0.386143 & 9.61036 \times 10^6 \end{pmatrix} \text{MeV}, \quad (14.41)$$

the d-quark mass eigenvalues

$$(m_d, m_s, m_b, M_D) = (2.97549, 51.0, 2860.72, 9.61036 \times 10^6) \text{MeV}, \quad (14.42)$$

and the product of mixing matrices:

$$V_{dL} = V_{dL}^o V_{dL}^{(1)}:$$

$$\begin{pmatrix} 0.981831 & 0.17522 & -0.0728363 & 0.0000922 \\ -0.183881 & 0.783786 & -0.593184 & 0.0005976 \\ 0.0468496 & -0.5958 & -0.801765 & 0.0008133 \\ -0.0000187 & -6.6982 \times 10^{-10} & 0.0010134 & 0.999999 \end{pmatrix} \quad (14.43)$$

$$V_{dR} = V_{dR}^o V_{dR}^{(1)}:$$

$$\begin{pmatrix} 0.146421 & -0.175219 & -0.922135 & 0.312291. \\ 0.577678 & -0.783785 & 0.217014 & -0.0698145 \\ 0.803005 & 0.595801 & 0.0142936 & 4.3164 \times 10^{-9} \\ -0.0056951 & -9.0660 \times 10^{-8} & 0.319949 & 0.947418 \end{pmatrix} \quad (14.44)$$

u-quarks:

$$\mathcal{M}_u^o = \begin{pmatrix} 0 & 0 & 0 & 673649. \\ 0 & 0 & 0 & 5.57857 \times 10^6 \\ 0 & 0 & 0 & 7.8041 \times 10^6 \\ 4.10528 \times 10^8 & -4.1775 \times 10^7 & 0 & 1.92243 \times 10^{10} \end{pmatrix} \text{MeV}, \quad (14.45)$$

$$\mathcal{M}_u = \begin{pmatrix} -0.47816 & -0.551837 & 5.4868 & 0.117774 \\ -3.21341 & 602.954 & 4467.75 & 95.9001 \\ 4.51209 & 1368.75 & -173107. & 714.009 \\ 0.00225605 & 0.684377 & 16.632 & 1.92287 \times 10^{10} \end{pmatrix} \text{MeV}, \quad (14.46)$$

the u-quark mass eigenvalues

$$(m_u, m_c, m_t, M_u) = (1.37677, 638.055, 173170, 1.92287 \times 10^{10}) \text{MeV} \quad (14.47)$$

and the product of mixing matrices:

$$V_{uL} = V_{uL}^o V_{uL}^{(1)}:$$

$$\begin{pmatrix} 0.996356 & 0.0468431 & -0.0712817 & 0.0000350 \\ -0.0010006 & -0.829224 & -0.558915 & 0.0002900 \\ -0.0852899 & 0.556949 & -0.826155 & 0.0004057 \\ 0 & 0.0000128 & 0.0004998 & 1. \end{pmatrix} \quad (14.48)$$

$$V_{uR} = V_{uR}^o V_{uR}^{(1)}:$$

$$\begin{pmatrix} 0.0003359 & 0.0934631 & -0.995394 & 0.0213497 \\ 0.0032952 & 0.995617 & 0.0934386 & -0.0021725 \\ 0.999995 & -0.0033122 & 0.0000265 & 0 \\ -1.4066 \times 10^{-8} & 0.0001676 & 0.0214593 & 0.99977 \end{pmatrix} \quad (14.49)$$

and the quark mixing matrix V_{CKM} :

$$\begin{pmatrix} 0.974441 & 0.224613 & -0.0035948 & 0.0000219 \\ 0.224564 & -0.973557 & 0.041928 & -0.0000382 \\ -0.0059177 & 0.0416636 & 0.999114 & -0.0010126 \\ 6.3092 \times 10^{-8} & -8.2754 \times 10^{-6} & -0.0004999 & 5.0666 \times 10^{-7} \end{pmatrix} \quad (14.50)$$

14.8 $\Delta F = 2$ Processes in Neutral Mesons

Here we study the tree level FCNC interactions that contribute to $K^0 - \bar{K}^0$, $D^0 - \bar{D}^0$ mixing via Z_1 , Y_2^\pm exchange from the depicted diagram in Fig. 2.

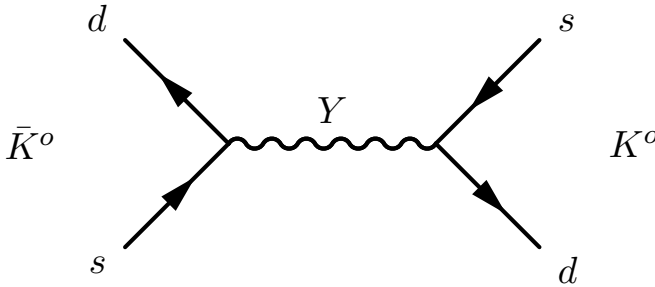


Fig. 14.2. Generic tree level exchange contribution to $K^0 - \bar{K}^0$ from the SU(3) horizontal gauge bosons.

The Z_1 , Y_2^\pm ($Y_2^\pm = \frac{Y_1 \mp iY_2}{\sqrt{2}}$) gauge bosons become massive at the second stage of the SU(3) symmetry breaking, and have flavor changing couplings in both left- and right-handed fermions, and then contribute the $\Delta S = 2$ effective operators

$$\mathcal{O}_{LL} = (\bar{d}_L \gamma_\mu s_L)(\bar{d}_L \gamma^\mu s_L) \quad , \quad \mathcal{O}_{RR} = (\bar{d}_R \gamma_\mu s_R)(\bar{d}_R \gamma^\mu s_R) \quad (14.51)$$

$$\mathcal{O}_{LR} = (\bar{d}_L \gamma_\mu s_L)(\bar{d}_R \gamma^\mu s_R) \quad (14.52)$$

The SU(3) couplings to fermions, Eq.(14.6), when written in the mass basis yield the gauge couplings

$$\mathcal{L}_{\text{int}, Z_1} = \frac{g_H}{2} (C_{L Z_1} \bar{d}_L \gamma_\mu s_L + C_{R Z_1} \bar{d}_R \gamma_\mu s_R) Z_1^\mu \quad (14.53)$$

$$\mathcal{L}_{\text{int}, Y_2^1} = \frac{g_H}{2} (C_{L Y_2^1} \bar{d}_L \gamma_\mu s_L + C_{R Y_2^1} \bar{d}_R \gamma_\mu s_R) Y_1^{1\mu} \quad (14.54)$$

$$\mathcal{L}_{\text{int}, Y_2^2} = \frac{g_H}{2} (C_{L Y_2^2} \bar{d}_L \gamma_\mu s_L + C_{R Y_2^2} \bar{d}_R \gamma_\mu s_R) Y_1^{2\mu} \quad (14.55)$$

with the coefficients

$$\begin{aligned} C_{L Z_1} &= L_{11} L_{12} - L_{31} L_{32} \quad , \quad C_{R Z_1} = R_{11} R_{12} - R_{31} R_{32} \\ C_{L Y_2^1} &= L_{12} L_{31} + L_{11} L_{32} \quad , \quad C_{R Y_2^1} = R_{12} R_{31} + R_{11} R_{32} \\ C_{L Y_2^2} &= (L_{12} L_{31} - L_{11} L_{32}) \quad , \quad C_{R Y_2^2} = (R_{12} R_{31} - R_{11} R_{32}) \end{aligned} \quad (14.56)$$

where $V_{L,R} \equiv V_{L,R}^0 V_{L,R}^{(1)}$, and $L_{ij} \equiv V_{L ij}$, $R_{ij} \equiv V_{R ij}$. For each gauge boson, the effective four-fermion hamiltonian at the scale of the gauge boson mass is

$$\mathcal{H}_{Z_1} = \frac{g_H^2}{4M_{Z_1}^2} (C_{L Z_1}^2 \mathcal{O}_{LL} + 2 C_{L Z_1} C_{R Z_1} \mathcal{O}_{LR} + C_{R Z_1}^2 \mathcal{O}_{RR}) \quad (14.57)$$

$$\mathcal{H}_{Y_2^1} = \frac{g_H^2}{4M_1^2} (C_{L Y_2^1}^2 \mathcal{O}_{LL} + 2 C_{L Y_2^1} C_{R Y_2^1} \mathcal{O}_{LR} + C_{R Y_2^1}^2 \mathcal{O}_{RR}) \quad (14.58)$$

$$\mathcal{H}_{Y_2^2} = -\frac{g_H^2}{4M_1^2} (C_{L Y_2^2}^2 \mathcal{O}_{LL} + 2 C_{L Y_2^2} C_{R Y_2^2} \mathcal{O}_{LR} + C_{R Y_2^2}^2 \mathcal{O}_{RR}) \quad (14.59)$$

with $M_{Y_2^1} = M_{Y_2^2} = M_1$. Therefore, the total four-fermion hamiltonian $\mathcal{H}_{SU(2)} = \mathcal{H}_{Z_1} + \mathcal{H}_{Y_2^1} + \mathcal{H}_{Y_2^2}$ can be written as

$$\begin{aligned}
\mathcal{H}_{\text{SU}(2)} = & \frac{g_H^2}{4M_1^2} \left[(C_{LZ_1}^2 + C_{LY_2}^2 - C_{LY_2^2}^2) \mathcal{O}_{LL} + (C_{RZ_1}^2 + C_{RY_2}^2 + C_{RY_2^2}^2) \mathcal{O}_{RR} \right. \\
& \left. + 2(C_{LZ_1} C_{RZ_1} + C_{LY_2} C_{RY_2} - C_{LY_2^2} C_{RY_2^2}) \mathcal{O}_{LR} \right] \\
& + \frac{g_H^2}{4} \left(\frac{1}{M_{Z_1}^2} - \frac{1}{M_1^2} \right) [C_{LZ_1}^2 \mathcal{O}_{LL} + C_{RZ_1}^2 \mathcal{O}_{RR} + 2C_{LZ_1} C_{RZ_1} \mathcal{O}_{LR}] \quad (14.60)
\end{aligned}$$

From the coefficients in eq.(14.56) we obtain:

$$C_{LZ_1}^2 + C_{LY_2}^2 - C_{LY_2^2}^2 = \delta_L^2, \quad C_{RZ_1}^2 + C_{RY_2}^2 - C_{RY_2^2}^2 = \delta_R^2, \quad , \quad (14.61)$$

$$\begin{aligned}
C_{L,Z_1} C_{R,Z_1} + C_{L,Y_2} C_{R,Y_2} - C_{L,Y_2^2} C_{R,Y_2^2} &= \delta_L \delta_R \\
+ 2(L_{11} R_{31} - L_{31} R_{11})(L_{32} R_{12} - L_{12} R_{32}), & \quad (14.62)
\end{aligned}$$

and we can write

$$\begin{aligned}
\mathcal{H}_{\text{SU}(2)} = & \frac{g_H^2}{4M_1^2} [\delta_L^2 \mathcal{O}_{LL} + \delta_R^2 \mathcal{O}_{RR} + \delta_{LR}^2 \mathcal{O}_{LR}] \quad (14.63) \\
& + \frac{g_H^2}{4} \left(\frac{1}{M_{Z_1}^2} - \frac{1}{M_1^2} \right) [(L_{11} L_{12} - L_{31} L_{32})^2 \mathcal{O}_{LL} + (R_{11} R_{12} - R_{31} R_{32})^2 \mathcal{O}_{RR} \\
& + 2(L_{11} L_{12} - L_{31} L_{32})(R_{11} R_{12} - R_{31} R_{32}) \mathcal{O}_{LR}]
\end{aligned}$$

with

$$\delta_L = L_{11} L_{12} + L_{31} L_{32}, \quad \delta_R = R_{11} R_{12} + R_{31} R_{32} \quad (14.64)$$

$$\delta_{LR} = 2(\delta_L \delta_R + 2(L_{11} R_{31} - L_{31} R_{11})(L_{32} R_{12} - L_{12} R_{32})) \quad (14.65)$$

The reported parameter space region in section 7 generate $M_{Z_1} \approx M_1$ with quite good approximation, and then the dominant contribution to neutral meson mixing comes from the four-fermion Hamiltonian in eq.(14.63). The suppression of the generic meson mixing couplings $\frac{\zeta_{ij}}{\Lambda^2} (\bar{q}_{iL} \gamma^\mu P_{L,R} q_j)^2$ come out as follows

14.8.1 $K^0 - \bar{K}^0$ meson mixing

$$\begin{aligned}
\delta_L &= 0.144124, \quad \frac{M_1}{\frac{g_H}{2} |\delta_L|} = 32594.5 \text{ TeV} \\
\delta_R &= 0.452775, \quad \frac{M_1}{\frac{g_H}{2} |\delta_R|} = 10375.2 \text{ TeV} \\
\sqrt{|\delta_{LR}|} &= 0.361261, \quad \frac{M_1}{\frac{g_H}{2} \sqrt{|\delta_{LR}|}} = 13003.4 \text{ TeV}
\end{aligned} \quad (14.66)$$

14.8.2 $D^0 - \bar{D}^0$ meson mixing

$$\begin{aligned}
 \delta_L &= -0.000829741 \quad , \quad \frac{M_1}{\frac{g_H}{2} |\delta_L|} = 5.66157 \times 10^6 \text{ TeV} \\
 \delta_R &= -0.00328084 \quad , \quad \frac{M_1}{\frac{g_H}{2} |\delta_R|} = 1.43184 \times 10^6 \text{ TeV} \\
 \sqrt{|\delta_{LR}|} &= 0.456165 \quad , \quad \frac{M_1}{\frac{g_H}{2} \sqrt{|\delta_{LR}|}} = 10298.1 \text{ TeV}
 \end{aligned} \tag{14.67}$$

These numerical values are within the suppression required for BSM contributions reported for instance in the review "CKM Quark - Mixing Matrix" in PDG2018[16].

14.9 Conclusions

Horizontal gauge bosons from the local SU(3) family symmetry introduce flavor changing couplings, and in particular mediate $\Delta F = 2$ processes at tree level. We reported the analytic and numerical contribution to $K^0 - \bar{K}^0$ and $D^0 - \bar{D}^0$ meson mixing from tree level exchange diagrams mediated by the SU(2) horizontal gauge bosons Z_1, Y_2^\pm . We provided in section 7 a particular parameter space region where this scenario can accommodate the hierarchy spectrum of quark masses and mixing, and simultaneously suppress properly the $\Delta S = 2$ and $\Delta C = 2$ processes.

Acknowledgements

It is my pleasure to thank the organizers N.S. Mankoc-Borstnik, H.B. Nielsen, M. Y. Khlopov, and participants for the stimulating Workshop at Bled, Slovenia. The author is grateful for the warm hospitality at the APC Laboratory, Paris, France, during sabbatical staying. This work was partially supported by the "Instituto Politécnico Nacional", (Grants from EDI and COFAA) in Mexico.

14.10 Appendix: Diagonalization of the generic Dirac See-saw mass matrix

$$\mathcal{M}^o = \begin{pmatrix} 0 & 0 & 0 & a_1 \\ 0 & 0 & 0 & a_2 \\ 0 & 0 & 0 & a_3 \\ 0 & b_2 & b_3 & c \end{pmatrix} \tag{14.68}$$

The tree level \mathcal{M}^o 4×4 See-saw mass matrix is diagonalized by a biunitary transformation $\psi_L^o = V_L^o \chi_L$ and $\psi_R^o = V_R^o \chi_R$. The diagonalization of $\mathcal{M}^o \mathcal{M}^{o\top}$ ($\mathcal{M}^{o\top} \mathcal{M}^o$) yield the nonzero eigenvalues

$$\lambda_3^2 = \frac{1}{2} \left(B - \sqrt{B^2 - 4D} \right) \quad , \quad \lambda_4^2 = \frac{1}{2} \left(B + \sqrt{B^2 - 4D} \right) \tag{14.69}$$

and rotation mixing angles

$$\cos \alpha = \sqrt{\frac{\lambda_4^2 - a^2}{\lambda_4^2 - \lambda_3^2}} \quad , \quad \sin \alpha = \sqrt{\frac{a^2 - \lambda_3^2}{\lambda_4^2 - \lambda_3^2}} \quad , \quad (14.70)$$

$$\cos \beta = \sqrt{\frac{\lambda_4^2 - b^2}{\lambda_4^2 - \lambda_3^2}} \quad , \quad \sin \beta = \sqrt{\frac{b^2 - \lambda_3^2}{\lambda_4^2 - \lambda_3^2}} \quad .$$

$$B = a^2 + b^2 + c^2 = \lambda_3^2 + \lambda_4^2 \quad , \quad D = a^2 b^2 = \lambda_3^2 \lambda_4^2 \quad , \quad (14.71)$$

$$a^2 = a_1^2 + a_2^2 + a_3^2 \quad , \quad b^2 = b_1^2 + b_2^2 + b_3^2 \quad (14.72)$$

The rotation matrices V_L^o, V_R^o admit several parametrizations related to the two zero mass eigenstates, for instance

$$V_L^o = \begin{pmatrix} c_1 & -s_1 s_2 & s_1 c_2 c_\alpha & s_1 c_2 s_\alpha \\ 0 & c_2 & s_2 c_\alpha & s_2 s_\alpha \\ -s_1 & -c_1 s_2 & c_1 c_2 c_\alpha & c_1 c_2 s_\alpha \\ 0 & 0 & -s_\alpha & c_\alpha \end{pmatrix} \quad , \quad V_R^o = \begin{pmatrix} 1 & 0 & 0 & 0 \\ 0 & c_r & s_r c_\beta & s_r s_\beta \\ 0 & -s_r & c_r c_\beta & c_r s_\beta \\ 0 & 0 & -s_\beta & c_\beta \end{pmatrix} \quad (14.73)$$

$$a_n = \sqrt{a_1^2 + a_2^2} \quad , \quad b_n = \sqrt{b_1^2 + b_2^2} \quad , \quad a = \sqrt{a_n^2 + a_3^2} \quad , \quad b = \sqrt{b_n^2 + b_3^2} \quad , \quad (14.74)$$

$$s_1 = \frac{a_1}{a_n} \quad , \quad c_1 = \frac{a_3}{a_n} \quad , \quad s_2 = \frac{a_2}{a} \quad , \quad c_2 = \frac{a_n}{a} \quad , \quad s_r = \frac{b_2}{b} \quad , \quad c_r = \frac{b_3}{b} \quad (14.75)$$

References

1. A. Hernandez-Galeana, Rev. Mex. Fis. **Vol. 50(5)**, (2004) 522. hep-ph/0406315.
2. A. Hernandez-Galeana, Bled Workshops in Physics, (ISSN:1580-4992), **Vol. 17, No. 2**, (2016) Pag. 36; arXiv:1612.07388[hep-ph]; **Vol. 16, No. 2**, (2015) Pag. 47; arXiv:1602.08212[hep-ph]; **Vol. 15, No. 2**, (2014) Pag. 93; arXiv:1412.6708[hep-ph]; **Vol. 14, No. 2**, (2013) Pag. 82; arXiv:1312.3403[hep-ph]; **Vol. 13, No. 2**, (2012) Pag. 28; arXiv:1212.4571[hep-ph]; **Vol. 12, No. 2**, (2011) Pag. 41; arXiv:1111.7286[hep-ph]; **Vol. 11, No. 2**, (2010) Pag. 60; arXiv:1012.0224[hep-ph]; Bled Workshops in Physics, **Vol. 10, No. 2**, (2009) Pag. 67; arXiv:0912.4532[hep-ph];
3. E. Golowich, J. Hewett, S. Pakvasa, and A. Petrov, Phys. Rev. D **76**, 095009 (2007).
4. E. Golowich, J. Hewett, S. Pakvasa, and A. Petrov, Phys. Rev. D **79**, 114030 (2009).
5. M. Kirk, A. Lenz, and T. Rauh, arXiv:1711.02100[hep-ph]; T. Jubb, M. Kirk, A. Lenz, and G. Tetlalmatzi-Xolocotzi, arXiv:1603.07770[hep-ph];
6. C. Bobeth, A. J. Buras, A. Celis, and M. Junk, arXiv:1703.04753[hep-ph]; A. J. Buras, arXiv:1611.06206[hep-ph]; arXiv:1609.05711[hep-ph];
7. T. Yanagida, Phys. Rev. D **20**, 2986 (1979).

8. Z. Berezhiani and M. Yu.Khlopov: Theory of broken gauge symmetry of families, Sov.J.Nucl.Phys. **51**, 739 (1990).
9. Z. Berezhiani and M. Yu.Khlopov: Physical and astrophysical consequences of family symmetry breaking, Sov.J.Nucl.Phys. **51**, 935 (1990).
10. J.L. Chkareuli, C.D. Froggatt, and H.B. Nielsen, Nucl. Phys. B **626**, 307 (2002).
11. Z.G. Berezhiani: The weak mixing angles in gauge models with horizontal symmetry: A new approach to quark and lepton masses, Phys. Lett. B **129**, 99 (1983).
12. T. Appelquist, Y. Bai and M. Piai: SU(3) Family Gauge Symmetry and the Axion, Phys. Rev. D **75**, 073005 (2007).
13. T. Appelquist, Y. Bai and M. Piai: Neutrinos and SU(3) family gauge symmetry, Phys. Rev. D **74**, 076001 (2006).
14. T. Appelquist, Y. Bai and M. Piai: Quark mass ratios and mixing angles from SU(3) family gauge symmetry, Phys. Lett. B **637**, 245 (2006).
15. Zhi-zhong Xing, He Zhang and Shun Zhou, Phys. Rev. D **86**, 013013 (2012).
16. M. Tanabashi *et al.* (Particle Data Group), Phys. Rev. D **98**, 030001 (2018).
17. See PDG review: CKM Quark-Mixing Matrix, by A. Ceccucci (CERN), Z. Ligeti (LBNL) and Y. Sakai (KEK).



15 Beyond the Standard Models of Particle Physics and Cosmology

M.Yu. Khlopov *

Institute of Physics, Southern Federal University
Stachki 194, Rostov on Don 344090, Russia

Abstract. The modern Standard cosmological model of inflationary Universe and baryosynthesis deeply involves particle theory beyond the Standard model (BSM). Inevitably, models of BSM physics lead to cosmological scenarios beyond the Standard cosmological paradigm. Scenarios of dark atom cosmology in the context of puzzles of direct and indirect dark matter searches, of clusters of massive primordial black holes as the source of gravitational wave signals and of antimatter globular cluster as the source of cosmic antihelium are discussed.

Povzetek. V standardni kozmološki model inflacijskega vesolja in tvorbe barionov vključi avtor tudi teorijo osnovnih delcev in polj, kar razširi standardni model. Avtor obravnava model "temnih atomov", to je atomov, ki vsebujejo fermione družine z veliko maso. Predstavi prispevek temnih atomov v eksperimentih, ki naj bi detektirali temno snov, vlogo temnih atomov kopic masivnih prvotnih črnih lukenj, ki sevajo gravitacijske valove ter v globularnih kopicah antisnovi, ki naj bi bil izvor antihelija v vesolju.

Keywords: cosmoparticle physics, inflation, baryosynthesis, dark matter, dark atoms, clusters of massive primordial black holes, antimatter, double charged particles, nuclear reactions, nucleosynthesis

PACS: 12.60.-i; 95.35.+d; 14.80.-j; 21.90.+f; 36.10.-k; 98.80.-k; 98.80.Cq; 98.80.Ft; 04.70.-s;

15.1 Introduction

The basis of the modern Standard cosmological paradigm, involving inflation, baryosynthesis and dark matter as its necessary basic elements, is related to new physics predicted in theory beyond the Standard model (BSM) of elementary particles (see e.g. Ref. [1] for review and reference). However, BSM models, reproducing the necessary basic elements of the modern cosmology, inevitably contain additional model dependent consequences that lead beyond the Standard cosmological scenario [2].

Methods of cosmoparticle physics, studying fundamental relationship of cosmology and particle physics in the combination of its physical, astrophysical and

* E-mail: khlopov@apc.in2p3.fr

cosmological signatures, involve such model dependent cosmological predictions to probe models of BSM physics and cosmological scenarios, based on them. [3–5].

Here we show that BSM physics leads to cosmological scenarios accomplished by nontrivial deviations from the Standard cosmological model that deserve special interest in the context of the recent experimental progress.

We address a possibility of existence of stable double charged particles O^{--} bound with primordial helium in neutral nuclear interacting O-helium dark atoms (Section 15.2) and consider advantages of this scenario to resolve puzzles of direct and indirect dark matter searches, as well as the open problems of OHe interaction with matter. We show that BSM physics of inflationary models that naturally leads to strong primordial inhomogeneities and to clusters of massive primordial black holes, in particular, is possibly reflected in the gravitational wave signal from massive black hole coalescence (Section 15.3). We discuss in Section 15.4 existence of antimatter stars in our Galaxy, originated from nonhomogeneous baryosynthesis in baryon asymmetrical Universe and reflected in cosmic antihelium fluxes, possibly detected by AMS02 [6,7].

15.2 Dark atom physics and cosmology

In the simplest case physics of dark matter is reduced to prediction by BSM model of new neutral elementary weakly interacting massive particle (WIMP). This type of prediction is beyond the standard model of elementary particles, but fits perfectly well the standard cosmological LambdaCDM paradigm. Supersymmetric (SUSY) models, predicting WIMP candidates, seemed to support this simple approach to dark matter physics. However negative results of experimental underground WIMP searches, as well as of collider searches for SUSY particles appeal to other possible BSM solutions for the dark matter problem. Possibly, SUSY physics and cosmology corresponds to superhigh energy scales as discussed in this Volume in [8].

In fact, the necessary conditions for dark matter candidates to be stable, satisfy the measured dark matter density and be decoupled from plasma and radiation at least before the beginning of matter dominated stage in no case demand these particle candidates to be weakly or superweakly interacting. Even nuclear interacting particles can play the same role due to decoupling of the gas of such particles from plasma and radiation before the end of radiation dominated stage. It gives rise to models of dark matter in the form of Strongly Interacting Massive Particles (SIMPs) [9–14].

By definition dark matter should be ‘dark’, nonluminous, what seem to favor neutral elementary particles. However ordinary atomic matter is neutral but it is composite and consists of electrically charged particles (nuclei and electrons). In the same way O-helium dark atoms represent a specific example of composite SIMPs, in which hypothetical double charged O^{--} particles are bound with primordial helium nuclei by ordinary Coulomb force [15–20].

15.2.1 OHe and O-nuclearites

The main problem for hypothetical stable charged particles is their absence in the matter. If they do exist, they should be bound with ordinary matter and form anomalous isotopes. Severe experimental constraints on such isotopes, on anomalous hydrogen especially, seem to exclude a possibility for stable charged particles. However, if there exist stable particles with charge -2 in excess over corresponding particles with charge +2, such negatively charged particles are captured by primordial helium and form neutral OHe dark atom. There are various models, in which such stable -2 charged particles O^{--} are predicted [15–20]. Moreover, if these particles possess electroweak SU(2) gauge charges, their excess can be equilibrated by electroweak sphaleron transitions with baryon excess, as it is the case in Walking Technicolor models [17].

The general analysis of the bound states of single O^{--} with nuclei was developed in a simple model [21–23]. For small nuclei the Coulomb binding energy is like in hydrogen atom and is given by

$$E_b = \frac{1}{2} Z^2 Z_O^2 \alpha^2 A m_p. \quad (15.1)$$

For large nuclei O^{--} is inside nuclear radius and the harmonic oscillator approximation is valid for the estimation of the binding energy

$$E_b = \frac{3}{2} \left(\frac{ZZ_O \alpha}{R} - \frac{1}{R} \left(\frac{ZZ_O \alpha}{A m_p R} \right)^{1/2} \right). \quad (15.2)$$

Here Z is the charge of nucleus, A is its atomic number, R is radius of nucleus, $Z_O = 2$ is the charge of O^{--} , m_p is the proton mass and $\alpha = 1/137$ is the fine structure constant. In the case of OHe $ZZ_O \alpha A m_p R \leq 1$, what proves its Bohr-atom-like structure (see [19,20] for review and references). However, the radius of Bohr orbit in these “atoms” [15,17] $r_o \sim 1/(Z_O Z_{He} \alpha m_{He}) \approx 2 \cdot 10^{-13}$ cm is of the order the size of He nucleus. Therefore the corresponding correction to the binding energy due to non-point-like charge distribution in He nucleus is significant.

O^{--} particles are either elementary lepton-like states, or clusters of heavy \bar{U} quarks with charge $-2/3 \bar{U}\bar{U}\bar{U}$, which have strongly suppressed QCD interaction. In the contrary to ordinary atoms OHe has heavy lepton-like core and nuclear interacting shell.

If multiple O^{--} are captured by a heavy nucleus, the corresponding neutral bound system can acquire the form of O-nuclearites, in which negative charge of O^{--} is compensated by positive charge of protons in the nucleus [24]. The energy of such a O-nuclearite is given by [24]

$$\mathcal{E} = -16 \text{MeV} \cdot A - \int d^3r (n_p - 2n_O) V - \int d^3r \frac{(\nabla V)^2}{8\pi e^2} + \mathcal{E}_{\text{kin}}^O. \quad (15.3)$$

Here the first term is the volume energy of the atomic nucleus with atomic number A , next two terms describe the electromagnetic energy, and

$$\mathcal{E}_{\text{kin}}^O = \int d^3r \int_0^{p_{F,O}} \frac{p^2 dp}{\pi^2} \frac{p^2}{2m_O} \quad (15.4)$$

is the kinetic energy of the O-fermions of the mass m_O ; $V = -e\phi$ is the potential well for the electron in the field of the positive charge ($e > 0$, $\phi > 0$) and on the other hand it is the potential well also for the protons in the field of the negative charge of O-particles.

The most energetically favorable O-particle distribution inside the nucleus is that follows the proton one, fully compensating the Coulomb field. Thereby O-particles, if their number were $N_O \geq A/4$, would be re-distributed to minimize the energy, and finally the density of O inside the atomic nucleus becomes $n_O = n_p/2 = (n_p^0/2) \theta(r - R)$ for O-nuclearite, that corresponds to $V = \text{const}$ for $r < R$. Excessive O-particles are pushed out.

15.2.2 Cosmoparticle physics of OHe model

After the Standard Big Bang Nucleosynthesis (SBBN) O^{--} charged particles capture ^4He nuclei in neutral OHe “atoms” [15]. For the mass of O^{--} $m_O \sim 1 \text{ TeV}$, O^{--} abundance is much smaller than helium abundance, so that He is in excess in such capture, making the abundance of frozen out free O^{--} exponentially small.

The cosmological scenario of OHe Universe involves only one parameter of new physics – the mass of O^{--} . Such a scenario is insensitive to the properties of O^{--} (except for its mass), since the main features of the OHe dark atoms are determined by their nuclear interacting helium shell.

Before the end of radiation domination stage the rate of expansion exceeds the rate of energy and momentum transfer from plasma to OHe gas and the latter decouples from plasma and radiation. Then OHe starts to dominate at the Matter Dominated stage, playing the role of Warmer than Cold Dark Matter in the process of Large Scale Structure formation [15,19]. This feature is due to conversion of small scale fluctuations in acoustic waves before OHe decoupling and to their corresponding suppression. However, the suppression of such fluctuations is not as strong as the free streaming suppression for few keV dark matter particles in Warm Dark matter models.

In terrestrial matter OHe dark atoms are slowed down and cannot cause significant nuclear recoil in the underground detectors, making them elusive for detection based on nuclear recoil. The positive results of DAMA experiments (see [25] for review and references) can find in this scenario a nontrivial explanation due to a low energy radiative capture of OHe by intermediate mass nuclei [19,1,20]. This explains the negative results of the XENON100 and LUX experiments. The rate of this capture is proportional to the temperature: this leads to a suppression of this effect in cryogenic detectors, such as CDMS.

OHe collisions in the central part of the Galaxy lead to OHe excitations, and de-excitations with pair production in E0 transitions can explain the excess of the positron-annihilation line, observed by INTEGRAL in the galactic bulge [1,20,26,27]. Due to the large uncertainty of DM distribution in the galactic bulge this interpretation of the INTEGRAL data is possible in a wide range of masses of O-helium with the minimal required central density of O-helium dark matter at $m_O = 1.25 \text{ TeV}$. For smaller or larger values of m_O one needs larger central density to provide effective excitation of O-helium in collisions. Current analysis

favors lowest values of central dark matter density, making possible O-helium explanation for this excess only for a narrow window around this minimal value.

In a two-component dark atom model, based on Walking Technicolor, a sparse WIMP-like component of atom-like state, made of positive and negative doubly charged techniparticles, is present together with the dominant OHe dark atoms. Decays of doubly positive charged techniparticles to pairs of same-sign leptons can explain [28] the excess of high-energy cosmic-ray positrons, found in PAMELA and AMS02 experiments[29–32]. Since even pure lepton decay channels are inevitably accompanied by gamma radiation the important constraint on this model follows from the measurement of cosmic gamma ray background in FERMI/LAT experiment[33]. The multi-parameter analysis of decaying dark atom constituent model determines the maximal model independent value of the mass of decaying +2 charge particle, at which this explanation is possible

$$m_O < 1\text{TeV}.$$

One should take into account that even in this range hypothesis on decaying composite dark matter, distributed in the galactic halo, can lead according to [34] to gamma ray flux exceeding the measurement by FERMI/LAT. It can make more attractive interpretation of these data by an astrophysical pulsar local source[35] or by some local source of dark matter annihilation or decay.

Experimental probes for OHe dark matter at the LHC strongly differ from the usual way of search for dark matter at accelerators, involving missed energy and momentum detection. Pending on the nature of the double charge constituents it may be search for new stable U-hadrons (heavy stable hadrons that appear in the result of production of $U\bar{U}$ pair) or search for stable double charged lepton-like particles. In the first case there are applicable constraints from the search for supersymmetric R-hadrons, having similar experimental signatures and giving the minimal mass for UUU close to 3 TeV. It excludes OHe interpretation of the cosmic positron anomalies in terms of heavy quark cluster constituents of OHe.

The possibility to interpret cosmic positron anomalies in terms of OHe constituents that appear in the experiments as stable lepton-like double charged particles is also close to complete test. The ATLAS and CMS collaborations at the LHC are searching for the double charged particles since 2011 [36–38]. The most stringent results achieved so far exclude the existence of such particles up to their mass of 680 GeV. This value was obtained by both ATLAS and CMS collaborations independently. It is expected that if these two collaborations combine their independently gathered statistics of LHC Run 2 (2015–2018), the lower mass limit of double charged particles could reach the level of about 1.3 TeV. It will make search for exotic long-living double charged particles an *experimentum crucis* for interpretation of low and high energy positron anomalies by composite dark matter [39,40].

The successful and self-consistent OHe scenario implies the existence of dipole Coulomb barrier, arising in OHe-nuclear interaction and supporting dominance of elastic OHe-nuclear scattering. This problem of nuclear physics of OHe remains the main open question of composite dark matter, which implies correct quantum mechanical solution [41]. The lack of such a barrier and essential contribution

of inelastic OHe-nucleus processes seem to lead to inevitable overproduction of anomalous isotopes [42]. The advantages of the qualitative picture of OHe scenario appeal to increase the efforts to solve this problem.

15.3 Primordial massive black hole clusters

The standard cosmological model considers homogeneous and isotropic Universe as the result of inflation. The observed celestial objects and strong inhomogeneities are evolved from small primordial density fluctuations that are also originated from small fluctuations of the inflaton field. It seems that there is no room for strong primordial inhomogeneities in this picture. Moreover, the existence of large scale inhomogeneities at the scales $\gg 100\text{Mpc}$ is excluded by the measured isotropy of CMB.

However, BSM physics, predicting new fields and mechanisms of symmetry breaking, adds new elements in this simple scenario that provide the existence of strong primordial inhomogeneities. Such predictions are compatible with the observed global homogeneity and isotropy of the Universe, if the strongly inhomogeneous component i with $(\delta\rho/\rho)_i \sim 1$ contributes into the total density ρ_{tot} within the observed level of the large scale density fluctuations $(\delta\rho/\rho) = \delta_0 \ll 1$. It implies either large scale inhomogeneities, suppressed by the small contribution of the component i into the total density $\rho_i/\rho_{\text{tot}} \leq \delta_0$, or inhomogeneities at small scales.

A simple example of an axion-like model with U(1) symmetry broken spontaneously and then explicitly illustrates these two possible forms of strong primordial inhomogeneities.

In this model spontaneous U(1) symmetry breaking is induced by the vacuum expectation value

$$\langle\psi\rangle = f \quad (15.5)$$

of a complex scalar field

$$\Psi = \psi \exp(i\theta), \quad (15.6)$$

having also explicit symmetry breaking term in its potential

$$V_{\text{eb}} = \Lambda^4(1 - \cos\theta) \quad (15.7)$$

If the first phase transition takes place after inflation at $T = f$ and $f \gg \Lambda$, the potential Eq. (15.7) doesn't influence continuous degeneracy of vacua on θ and string network is formed, which is converted in a walls-surrounded-by-strings network, separating regions with discrete vacuum degeneracy $\theta_{\text{vac}} + 0, 2\pi, \dots$ after the second phase transition at $T = \Lambda$. The vacuum structure network is unstable and decays, but the energy density distribution of θ field oscillations is strongly inhomogeneous and retains the large scale structure of this network, as it was shown in the example of axion models in [43–45]. To fit the observational constraints on the inhomogeneity at large scales the contribution into the total density of such structure, called *archioles*, should be suppressed. It causes serious

problem for CDM models, in which the dominant form of dark matter is explained by axions [43–45].

If the first phase transition takes place at the inflationary stage and $f \gg \Lambda$, as it was considered in [46], there appears a valley relative to values of phase in the field potential in this period. Fluctuations of the phase θ along this valley, being of the order of $\Delta\theta \sim H/(2\pi f)$ (here H is the Hubble parameter at inflationary stage) change in the course of inflation its initial value within the regions of smaller size. Owing to such fluctuations, for the fixed value of θ_{60} in the period of inflation with *e-folding* $N = 60$ corresponding to the part of the Universe within the modern cosmological horizon, strong deviations from this value appear at smaller scales, corresponding to later periods of inflation with $N < 60$. If $\theta_{60} < \pi$, the fluctuations can move the value of θ_N to $\theta_N > \pi$ in some regions of the Universe.

After reheating, when the Universe cools down to temperature $T = \Lambda$ the phase transition to the true vacuum states, corresponding to the minima of V_{eb} takes place. For $\theta_N < \pi$ the minimum of V_{eb} is reached at $\theta_{vac} = 0$, whereas in the regions with $\theta_N > \pi$ the true vacuum state corresponds to $\theta_{vac} = 2\pi$. For $\theta_{60} < \pi$ in the bulk of the volume within the modern cosmological horizon $\theta_{vac} = 0$. However, within this volume there appear regions with $\theta_{vac} = 2\pi$. These regions are surrounded by massive domain walls, formed at the border between the two vacua. Since regions with $\theta_{vac} = 2\pi$ are confined, the domain walls are closed. After their size equals the horizon, closed walls can collapse into black holes.

The mass range of formed BHs is constrained by fundamental parameters of the model f and Λ . The maximal BH mass is determined by the condition that the wall does not dominate locally before it enters the cosmological horizon. Otherwise, local wall dominance leads to a superluminal $a \propto t^2$ expansion for the corresponding region, separating it from the other part of the Universe. This condition corresponds to the mass [47]

$$M_{\max} = \frac{m_{pl}}{f} m_{pl} \left(\frac{m_{pl}}{\Lambda} \right)^2. \quad (15.8)$$

The minimal mass follows from the condition that the gravitational radius of BH exceeds the width of wall and it is equal to [47,48]

$$M_{\min} = f \left(\frac{m_{pl}}{\Lambda} \right)^2. \quad (15.9)$$

This mechanism can lead to formation of primordial black holes of a whatever large mass (up to the mass of active galactic nuclei (AGNs) [49,50], see [51] for the latest review). Such black holes appear in the form of primordial black hole clusters, exhibiting fractal distribution in space [47,48,52,51]. It can shed new light on the problem of galaxy formation [47,50,51].

Closed wall collapse leads to primordial GW spectrum, peaked at

$$\nu_0 = 3 \cdot 10^{11} (\Lambda/f) \text{ Hz} \quad (15.10)$$

with energy density up to

$$\Omega_{GW} \approx 10^{-4} (f/m_{pl}). \quad (15.11)$$

At $f \sim 10^{14}$ GeV this primordial gravitational wave background can reach $\Omega_{\text{GW}} \approx 10^{-9}$. For the physically reasonable values of

$$1 < \Lambda < 10^8 \text{ GeV} \quad (15.12)$$

the maximum of spectrum corresponds to

$$3 \cdot 10^{-3} < \nu_0 < 3 \cdot 10^5 \text{ Hz}. \quad (15.13)$$

In the range from tens to thousand Hz such background may be a challenge for Laser Interferometer Gravitational-Wave Observatory (LIGO) experiment.

Another profound signature of the considered scenario are gravitational wave signals from merging of BHs in PBH cluster. Being in cluster, PBHs with the masses of tens M_\odot form binaries much easier, than in the case of their random distribution. In this aspect detection of signals from binary BH coalescence in the gravitational wave experiments [53–57] may be considered as a positive evidence for this scenario. Repeatedly detected signals localized in the same place would provide successive support in its favor [51,58].

15.4 Antihelium from antimatter stars in our Galaxy

Primordial strong inhomogeneities can also appear in the baryon charge distribution. The appearance of antibaryon domains in the baryon asymmetrical Universe, reflecting the inhomogeneity of baryosynthesis, is the profound signature of such strong inhomogeneity [59]. On the example of the model of spontaneous baryosynthesis (see [60] for review) the possibility for existence of antimatter domains, surviving to the present time in inflationary Universe with inhomogeneous baryosynthesis was revealed in [61].

The mechanism of spontaneous baryogenesis [60,62,63] implies the existence of a complex scalar field

$$\chi = (f/\sqrt{2}) \exp(i\theta) \quad (15.14)$$

carrying the baryonic charge. The $U(1)$ symmetry, which corresponds to the baryon charge, is broken spontaneously and explicitly, similar to the case, considered in the previous Section 15.3. The explicit breakdown of $U(1)$ symmetry is caused by the phase-dependent term, given by Eq. (15.7).

Baryon and lepton number violating interaction of the field χ with matter fields can have the following structure [60]

$$\mathcal{L} = g\chi\bar{Q}L + \text{h.c.}, \quad (15.15)$$

where fields Q and L represent a heavy quark and lepton, coupled to the ordinary matter fields.

In the early Universe, at a time when the friction term, induced by the Hubble constant, becomes comparable with the angular mass $m_\theta = \frac{\Lambda^2}{f}$, the phase θ starts to oscillate around the minima of the PNG potential and decays into matter fields according to (15.15). The coupling (15.15) gives rise to the following [60]: as the phase starts to roll down in the clockwise direction, it preferentially creates excess

of baryons over antibaryons, while the opposite is true as it starts to roll down in the opposite direction. If fluctuations of θ on inflational stage move its value above π in some region, it starts to roll down anticlockwise and, simultaneously, there should appear a closed wall, separating this region. As we discussed in the previous Section, collapse of such wall leads to formation of black hole with the mass in the range, determined by f and Λ .

The fate of such antimatter regions depends on their size. If the physical size of some of them is larger than the critical surviving size $L_c = 8h^2$ kpc [61], they survive annihilation with surrounding matter.

The possibility of formation of dense antistars within an extension of the Affleck-Dine scenario of baryogenesis and the strategies for their search were considered in [64].

Evolution of sufficiently dense antimatter domains can lead to formation of antimatter globular clusters [65]. The existence of such cluster in the halo of our Galaxy should lead to the pollution of the galactic halo by antiprotons. Their annihilation can reproduce [66] the observed galactic gamma background in the range tens-hundreds MeV. The gamma background data put upper limit on the total mass of antimatter stars. The prediction of antihelium component of cosmic rays [67], as well as of antimatter meteorites [68] provides the direct experimental test for this hypothesis. In the mechanism of spontaneous baryosynthesis there appears an interesting possibility of PBH, associated with dense antimatter domain, and the observational constraints on presence of massive black holes in globular clusters put constraints on the parameters f and Λ .

Cosmic antihelium flux is a well motivated stable signature of antimatter stars in our Galaxy [65,67]. Antimatter nucleosynthesis produces antihelium 4 as the most abundant (after antiprotons) primordial element. Antimatter stellar nucleosynthesis increases its primordial abundance. Heavy antinuclei, released in anti-Supernova explosions, annihilate with interstellar gas (dominantly hydrogen) and give rise to multiple antihelium fragments in the result of annihilation [65,67]. Propagation of antihelium-4 in the matter gas is also accompanied by its annihilation, in which about 25% of events give fragments of antihelium-3, either directly or after antitritium decay.

The minimal mass of antimatter globular cluster is determined by the condition of the sufficient survival size of antimatter domain, corresponding to $10^3 M_{\odot}$. It leads to a minimal cosmic antihelium flux accessible to searches for cosmic ray antihelium in AMS02 experiment.

Possible evidences for positive results of these searches continuously appear in the presentations by the AMS collaboration [6,7]. To the present time there are about ten clear candidates for antihelium-3 and two events that may be interpreted as antihelium-4. These results need further analysis and confirmation. It is expected that more statistics and the 5σ result will be available to 2024. It would be interesting to check whether significant amount of matter in the aperture of AMS02 detector hinder antihelium-4, but increase antihelium-3 fraction in the result of antihelium-4 annihilation with matter. Confirmation of antihelium-3 events that cannot be explained as secondary from cosmic ray interactions [69] would favor antimatter globular cluster hypothesis appealing to its detailed analysis.

15.5 Conclusions

To conclude, the BSM physical basis leads to nontrivial features in cosmological scenario and the current experimental progress probably gives evidences favoring their existence. However these evidences need further confirmation as well more theoretical work is needed to confront these predicted features with the experimental data.

Indeed, even in the simplest case of OHe dark atoms the open problem of OHe interaction with nuclei hinders a possible OHe solution for the puzzles of direct dark matter searches. On the other hand, indirect effects of OHe dark matter can explain anomalies of low and high energy cosmic positrons only for masses of hypothetical stable double charged within the reach of the search for such particles at the LHC. It opens new line of accelerator probes for dark matter.

Prediction of primordial strong inhomogeneities in the distribution of total, dark and baryonic matter in the Universe is the new important phenomenon of cosmological models, based on BSM physics with hierarchy of symmetry breaking. The current progress in detection of gravitational waves and cosmic antimatter nuclei is probably approaching confirmation for the corresponding nonstandard cosmological scenarios.

Here we have given examples of nontrivial cosmological consequences coming from some minimal extensions of particle Standard model, involving prediction of extra stable double charged particles or additional global U(1) symmetry. One can expect much richer set of predictions in a more extensive theoretical framework of BSM physics and the platform of Bled Workshops will provide a proper place for extensive nonformal discussion of such a rich new physics and its cosmological impact.

Acknowledgements

The work was supported by grant of Russian Science Foundation (project N-18-12-00213).

References

1. M. Yu. Khlopov: Fundamental Particle Structure in the Cosmological Dark Matter, Int. J. Mod. Phys. A **28**, 1330042 (2013).
2. M.Y. Khlopov: Nonstandard cosmologies from physics beyond the Standard model, Bled Workshops in Physics **17**, 52 (2016)
3. M.Y. Khlopov: *Cosmoparticle Physics*, World Scientific, Singapore, 1999.
4. M.Y. Khlopov: *Fundamentals of Cosmoparticle Physics*, CISP-Springer, Cambridge, UK, 2012.
5. M.Y. Khlopov: Cosmoparticle physics: Cross-disciplinary study of physics beyond the standard model, Bled Workshops in Physics **7**, 51 (2006)
6. S. Ting: The First Five Years of the Alpha Magnetic Spectrometer on the ISS (2016).
7. V. A. Choutko: AMS days at la Palma, Spain (2018)
8. S.Ketov and M.Khlopov: Extending Starobinsky inflationary model in gravity and supergravity, this Volume, arXiv:1809.09975.

9. C. B. Dover *et al.*: Cosmological Constraints On New Stable Hadrons Phys. Rev. Lett. **42**, 1117 (1979).
10. S. Wolfram: Abundances Of Stable Particles Produced In The Early Universe, Phys. Lett. B **82**, 65 (1979).
11. G. D. Starkman *et al.*: Opening the window on strongly interacting dark matter, Phys. Rev. D **41**, 3594 (1990).
12. D. Javorsek *et al.*: New experimental limits on strongly interacting massive particles at the TeV scale, Phys. Rev. Lett. **87**, 231804 (2001).
13. S. Mitra: Uranus' anomalously low excess heat constrains strongly interacting dark matter, Phys. Rev. D **70**, 103517 (2004).
14. G. D. Mack *et al.*: Towards Closing the Window on Strongly Interacting Dark Matter: Far-Reaching Constraints from Earth's Heat Flow, Phys. Rev. D **76**, 043523 (2007).
15. M.Yu. Khlopov: Composite dark matter from 4th generation JETP Lett. **83**, 1 (2006).
16. D. Fargion, M. Khlopov and C. A. Stephan: Cold dark matter by heavy double charged leptons?, Class. Quantum Grav. **23**, 7305 (2006).
17. M. Y. Khlopov and C. Kouvaris: Strong Interactive Massive Particles from a Strong Coupled Theory, Phys. Rev. D **77**, 065002 (2008).
18. M.Y. Khlopov and N.S. Mankoč Borštnik: Can the Stable Fifth Family of the "Spin-charge-family-theory" Proposed by N.S. Mankoč Boštnik Fulfil the M.Y. Khlopov Requirements and Form the Fifth Antibaryon Clusters with Ordinary He Nucleus? Bled Workshops in Physics **11**, 177 (2010)
19. M. Y. Khlopov: Physics of Dark Matter in the Light of Dark Atoms, Mod. Phys. Lett. A **26**, 2823 (2011)
20. M. Yu. Khlopov: Dark Atoms and Puzzles of Dark Matter Searches, Int. J. Mod. Phys. A **29**, 1443002 (2014).
21. R. N. Cahn and S. L. Glashow: Chemical Signatures for Superheavy Elementary Particles, Science **213**, 607 (1981).
22. M. Pospelov: Particle Physics Catalysis of Thermal Big Bang Nucleosynthesis, Phys. Rev. Lett. **98**, 231301 (2007).
23. K. Kohri and F. Takayama: Big bang nucleosynthesis with long-lived charged massive particles, Phys. Rev. D **76**, 063507 (2007).
24. V.A.Gani, M.Yu.Khlopov and D.N.Voskresensky: "Double charged heavy constituents of dark atoms and superheavy nuclear objects." arXiv:1808.06816.
25. R. Bernabei, *et al.*: Dark Matter investigation by DAMA at Gran Sasso, Int. J. Mod. Phys. A **28**, 1330022 [71 pages] (2013)
26. M. Y. Khlopov and C. Kouvaris: Composite dark matter from a model with composite Higgs boson, Phys. Rev. D **78**, 065040 (2008)
27. J.-R. Cudell, M.Yu.Khlopov and Q.Wallemacq: Dark atoms and the positron-annihilation-line excess in the galactic bulge, Advances in High Energy Physics, vol. **2014**, Article ID 869425, 5 pages, (2014).
28. K. Belotsky, M. Khlopov, C. Kouvaris, M. Laletin: Decaying Dark Atom constituents and cosmic positron excess, Advances in High Energy Physics, vol. **2014**, Article ID 214258, 10 p (2014).
29. PAMELA Collaboration: Phys. Rev. Lett. **111**, 081102 (2013).
30. AMS collaboration: Phys. Rev. Lett, **110**, 141102 (2013).
31. M. Aguilar *et al.*: Phys. Rev. Lett. **113**, 121102 (2014).
32. L. Accardo *et al.*: Phys. Rev. Lett. **113**, 121101 (2014).
33. M. Ackermann *et al.* (Fermi/LAT Collaboration): Phys.Rev. D **86** (2012), arXiv:1205.2739v1
34. K. Belotsky, R. Budaev, A.Kirillov, M. Laletin: Fermi-LAT kills dark matter interpretations of AMS-02 data. Or not? JCAP **1701**, 021 (2017).

35. M. Kachelriess, A. Neronov and D. V. Semikoz: Signatures of a two million year old supernova in the spectra of cosmic ray protons, antiprotons and positrons, *Phys. Rev. Lett.* **115**, 181103 (2015) .
36. ATLAS Collaboration, G. Aad et al.: Search for long-lived, multi-charged particles in pp collisions at $\sqrt{s} = 7$ TeV using the ATLAS detector, *Phys. Lett. B* **722**, 305 (2013).
37. ATLAS Collaboration, G. Aad et al.: Search for heavy long-lived multi-charged particles in pp collisions at $\sqrt{s} = 8$ TeV using the ATLAS detector, *Eur. Phys. J. C* **75**, 362 (2015).
38. CMS Collaboration, S. Chatrchyan et al.: Searches for long-lived charged particles in pp collisions at $\sqrt{s} = 7$ and 8 TeV, *JHEP* **1307**, 122 (2013).
39. O. V. Bulekov, M.Yu.Khlopov, A. S. Romaniouk, Yu. S. Smirnov: Search for Double Charged Particles as Direct Test for Dark Atom Constituents. *Bled Workshops in Physics* **18**, 11 (2017)
40. M.Yu.Khlopov: Probes for Dark Matter Physics, *Int. J. Mod. Phys. D* **27**, 1841013 (16 pages) (2018).
41. J.-R. Cudell, M.Yu.Khlopov and Q.Wallemacq: The nuclear physics of OHe. *Bled Workshops in Physics* **13**, 10 (2012)
42. J.-R. Cudell, M.Yu.Khlopov and Q.Wallemacq: Some Potential Problems of OHe Composite Dark Matter, *Bled Workshops in Physics* **15**, 66 (2014)
43. Sakharov A. S.; Khlopov, M. Yu. The nonhomogeneity problem for the primordial axion field *Phys. Atom. Nucl.* **1994**, 57, 485-487
44. Sakharov A. S.; Khlopov, M. Yu.; Sokoloff, D. D. Large scale modulation of the distribution of coherent oscillations of a primordial axion field in the Universe *Phys. Atom. Nucl.* **1996**, 59, 1005-1010.
45. Sakharov A. S.; Khlopov, M. Yu.; Sokoloff, D. D. The nonlinear modulation of the density distribution in standard axionic CDM and its cosmological impact *Nucl. Phys. B Proc. Suppl.* **1999**, 72, 105-109.
46. S. G. Rubin, M. Yu. Khlopov,; A. S. Sakharov: Primordial black holes from non-equilibrium second order phase transitions, *Gravitation and Cosmology Suppl.* **6**, 51 (2000).
47. M. Yu. Khlopov, S. G. Rubin: *Cosmological pattern of microphysics in inflationary universe*, Kluwer, Dordrecht, 2004.
48. M. Yu. Khlopov, S. G. Rubin, A. S. Sakharov: Strong Primordial Nonhomogeneities and Galaxy Formation, *Gravitation and Cosmology Suppl.* **8**, 57 (2002).
49. S. G. Rubin, A. S. Sakharov, M. Yu. Khlopov: Formation of primordial galactic nuclei at phase transitions in the early Universe, *JETP* **92**, 921 (2001).
50. V. Dokuchaev, Y. Eroshenko, S. Rubin: Quasars formation around clusters of primordial black holes, *Grav. Cosmol.* **11**, 99 (2005).
51. K.M.Belotsky et al: Clusters of primordial black holes. e-Print: arXiv:1807.06590.
52. M. Yu. Khlopov, S. G. Rubin, A. S. Sakharov: Primordial Structure of Massive Black Hole Clusters, *Astropart. Phys.* **23**, 265 (2005).
53. B. P. Abbott et al.: Observation of Gravitational Waves from a Binary Black Hole Merger, *Phys. Rev. Lett.* **116** , 061102 (2016).
54. B. P. Abbott et al.: GW151226: Observation of Gravitational Waves from a 22-Solar-Mass Binary Black Hole Coalescence, *Phys. Rev. Lett.* **116** , 241103 (2016) .
55. B. P. Abbott et al., GW170104: Observation of a 50-Solar-Mass Binary Black Hole Coalescence at Redshift 0.2, *Phys. Rev. Lett.* **118**, 221101 (2017).
56. B. P. Abbott et al.: GW170814: A Three-Detector Observation of Gravitational Waves from a Binary Black Hole Coalescence, *Phys. Rev. Lett.* **119**,141101 (2017).
57. B. P. Abbott et al.: GW170608: Observation of a 19 Solar-mass Binary Black Hole Coalescence, *Astrophys. J. Lett.* **851**, L35 (2017).

58. T. Bringmann, P. F. Depta, V. Domcke, K. Schmidt-Hoberg: Strong constraints on clustered primordial black holes as dark matter, arXiv:1808.05910 [astro-ph.CO]
59. V.M. Chechetkin, M.Yu. Khlopov, M.G. Sapozhnikov, Ya.B. Zeldovich: Astrophysical aspects of antiproton interaction with He (Antimatter in the Universe), Phys. Lett. B **118**, 329 (1982).
60. A. D. Dolgov: Matter and antimatter in the universe, Nucl. Phys. Proc. Suppl. **113**, 40 (2002).
61. M.Yu. Khlopov, S.G. Rubin, A.S.Sakharov: Possible origin of antimatter regions in the baryon dominated universe, Phys. Rev. D **62**, 083505 (2000).
62. A. Dolgov, J. Silk: Baryon isocurvature fluctuations at small scales and baryonic dark matter, Phys.Rev. D **47**, , 4244 (1993).
63. A.D. Dolgov,M. Kawasaki,N. Kevlishvili: Inhomogeneous baryogenesis, cosmic antimatter, and dark matter, Nucl.Phys. B **807**, 229 (2009).
64. S. I. Blinnikov, A. D. Dolgov, K. A. Postnov: Antimatter and antistars in the universe and in the Galaxy, Phys. Rev. D **92**, 023516 (2015)
65. M.Yu. Khlopov: An antimatter globular cluster in our galaxy: A probe for the origin of matter, Gravitation and Cosmology **4**, 69 (1998).
66. Yu.A. Golubkov, M.Yu. Khlopov: Anti-protons annihilation in the galaxy as a source of diffuse gamma background, Phys. Atom. Nucl. **64**, 1821-1829 (2001).
67. K.M. Belotsky, Yu.A. Golubkov,; M.Yu. Khlopov, R.V. Konoplich, A.S.Sakharov: Anti-helium flux as a signature for antimatter globular clusters in our galaxy, Phys. Atom. Nucl. **63**, 233 (2000).
68. D. Fargion, M.Yu.Khlopov: Antimatter bounds by anti-asteroids annihilations on planets and sun, Astropart.Phys. **19**, 441 (2003).
69. V. Poulin, P. Salati, I. Cholis, M. Kamionkowski, J. Silk: Where do the AMS-02 anti-helium events come from? arXiv:1808.08961 [astro-ph.HE].



16 The γ^a Matrices, $\tilde{\gamma}^a$ Matrices and Generators of Lorentz Rotations in Clifford Space — Determining in the *Spin-charge-family* Theory Spins, Charges and Families of Fermions — in $(3 + 1)$ -dimensional Space *

D. Lukman and N.S. Mankoč Borštnik¹

¹Department of Physics, University of Ljubljana,
SI-1000 Ljubljana, Slovenia

Abstract. In the *spin-charge-family* theory there are in d -dimensional space 2^d Clifford vectors, describing internal degrees of freedom of fermions — their families and family members. Due to two kinds of the Clifford algebra objects, defined in this theory as γ^a and $\tilde{\gamma}^a$ [2–7], each vector carries two kinds of indices. Operators $\gamma^a \gamma^b$ determine in $d = (3 + 1)$ space the spin and all the charges of quarks and leptons, $\tilde{\gamma}^a \tilde{\gamma}^b$ determine families of quarks and leptons. In this contribution basis in $d = (3 + 1)$ Clifford space is chosen in a way that the matrix representation of the γ^a matrices and of the generators of the Lorentz transformations in internal space $S^{ab} = \frac{i}{4}(\gamma^a \gamma^b - \gamma^b \gamma^a)$ coincide for each family quantum number, determined with $\tilde{S}^{ab} = \frac{i}{4}(\tilde{\gamma}^a \tilde{\gamma}^b - \tilde{\gamma}^b \tilde{\gamma}^a)$, with Dirac matrices. We do not take here into account the second quantization requirements [?], which reduce the number of states from 2^d to $2^{\frac{d}{2}-1}$ families of $2^{\frac{d}{2}-1}$ family members each, but this is the case for $d = 2(2n + 1)$, since in the *spin-charge-family* theory $d > 4$.

Povzetek. V teoriji *spinov-nabojev-družin* je v d -razsežnem prostoru 2^d Cliffordovih vektorjev, ki opisujejo notranje prostostne stopnje fermionov, to je njihove družine in člane družin. Ker imamo dve vrsti Cliffordovih objektov, ki so v tej teoriji definirani kot γ^a in $\tilde{\gamma}^a$ [2–7], ima vsak vektor dve vrsti indeksov. Operatorji $S^{ab} = \frac{i}{4}(\gamma^a \gamma^b - \gamma^b \gamma^a)$ določajo v $d = (3 + 1)$ -razsežnem prostoru spin in vse naboje kvarkov in leptonov, $\tilde{S}^{ab} = \frac{i}{4}(\tilde{\gamma}^a \tilde{\gamma}^b - \tilde{\gamma}^b \tilde{\gamma}^a)$ pa kvantna števila njihovih družin. V tem prispevku je baza v $d = (3 + 1)$ Cliffordovem prostoru izbrana tako, da matrične upodobitve operatorjev γ^a in generatorjev Lorentzovih transformacij S^{ab} v notranjem prostoru sovpadajo z Diracovimi matrikami za vsako družinsko kvantno število, določeno s \tilde{S}^{ab} . V prispevku ne upoštevamo zahtev druge kvantizacije [8], ki zmanjšajo število stanj z 2^d na $2^{\frac{d}{2}-1}$ družin s po $2^{\frac{d}{2}-1}$ člani. Vendar velja v teoriji *spinov-nabojev-družin* to le za $d = 2(2n + 1)$, kjer je $d > 4$.

* This contribution is written to help readers of the Bled proceedings and participants at future Bled Workshops "What Comes Beyond the Standard Models" to understand the difference between the Dirac γ^a matrices and the $\tilde{\gamma}^a$ matrices, which are all defined in 2^d space and used in the *spin-charge-family* theory to describe families and family members [2–7].

Keywords: Dirac matrices, Clifford algebra, Kaluza-Klein theories, Higher dimensional spaces, Beyond the standard model, Lepton and quark families

PACS: 04.50.-h, 04.50.Cd, 11.30.Ly

16.1 Introduction

In the *spin-charge-family* theory there are in d -dimensional space two kinds of operators, γ^a and $\tilde{\gamma}^a$, which operate on 2^d Clifford vectors, describing internal degrees of freedom of fermions; $\tilde{\gamma}^a$ determine family quantum numbers, γ^a determine family members. Due to these two kinds of the Clifford algebra objects each vector carries two kinds of indexes [2–7]. Operators $\frac{1}{2}\gamma^a\gamma^b$ determine in $d = (3 + 1)$ space the spin and all the charges of quarks and leptons, $\frac{1}{2}\tilde{\gamma}^a\tilde{\gamma}^b$ determine families of quarks and leptons.

Here only basis in $d = (3 + 1)$ Clifford space is discussed, which in the *spin-charge-family* theory is only a part of $d = (13 + 1)$. The basis is chosen in a way that the matrix representation of the γ^a matrices and of the generators of the Lorentz transformations in internal space $S^{ab} = \frac{i}{4}(\gamma^a\gamma^b - \gamma^b\gamma^a)$ coincide for each family quantum number, determined with $\tilde{S}^{ab} = \frac{i}{4}(\tilde{\gamma}^a\tilde{\gamma}^b - \tilde{\gamma}^b\tilde{\gamma}^a)$, with Dirac matrices.

This contribution is written to help the reader of the proceedings of Bled workshops "What comes beyond the standard models" to realize the differences between the Dirac matrices (operators) γ^a and the operators $\tilde{\gamma}^a$ [2].

We do not take here into account the second quantization requirements [8], which reduce the number of states from 2^d to $2^{\frac{d}{2}-1}$ families of $2^{\frac{d}{2}-1}$ family members each, since these requirements concern the states in $d = 2(2n + 1)$, and not at all the particular subspace, in our case $d = (3 + 1)$.

We use in this contribution 2^d vectors in Clifford space, expressible with γ^a with the properties

$$\{\gamma^a, \gamma^b\}_+ = 2\eta^{ab}. \quad (16.1)$$

A general vector can correspondingly be written as

$$\mathbf{B} = \sum_{k=0}^d a_{a_1 a_2 \dots a_k} \gamma^{a_1} \gamma^{a_2} \dots \gamma^{a_k} |\psi_{oc} \rangle, \quad a_i \leq a_{i+1}, \quad (16.2)$$

where $|\psi_o \rangle$ is the vacuum state. We arrange these vectors as products of nilpotents and projectors

$$\begin{aligned} {}^{ab}(\mathbf{k}) &= \frac{1}{2}(\gamma^a + \frac{\eta^{aa}}{ik}\gamma^b), \\ {}^{ab}[\mathbf{k}] &= \frac{1}{2}(1 + \frac{i}{k}\gamma^a\gamma^b), \end{aligned} \quad (16.3)$$

where $k^2 = \eta^{aa}\eta^{bb}$, their Hermitian conjugate values are

$${}^{ab}(\mathbf{k})^\dagger = \eta^{aa} {}^{ab}(-\mathbf{k}), \quad {}^{ab}[\mathbf{k}]^\dagger = {}^{ab}[\mathbf{k}], \quad (16.4)$$

and that they all are eigenstates of the Cartan subalgebra of the generators of the Lorentz transformations $S^{ab} = \frac{i}{4}(\gamma^a \gamma^b - \gamma^{ab} \gamma^a)$ in this internal space

$$S^{03}, S^{12}, S^{56}, \dots, S^{d-1 \ d}, \quad (16.5)$$

with the eigenvalues

$$S^{ab} \begin{pmatrix} ab \\ k \end{pmatrix} = \frac{1}{2} k \begin{pmatrix} ab \\ k \end{pmatrix}, \quad S^{ab} \begin{pmatrix} ab \\ [k] \end{pmatrix} = \frac{1}{2} k \begin{pmatrix} ab \\ [k] \end{pmatrix}. \quad (16.6)$$

We find in this Clifford algebra space two kinds of the Clifford algebra objects, besides γ^a also $\tilde{\gamma}^a$ [2–7], which anticommute with γ^a

$$\begin{aligned} \{\gamma^a, \tilde{\gamma}^b\}_+ &= 0, \\ \{\gamma^a, \tilde{\gamma}^b\}_+ &= I \ 2\eta^{ab}, \quad \text{for } a, b \in \{0, 1, 2, 3, 5, \dots, d\}, \end{aligned} \quad (16.7)$$

for any d , even or odd. I is the unit element in the Clifford algebra. One of the authors (N.S.M.B.) recognized these two possibilities in Grassmann space [2]. But one can as well as understand the appearance of the two kinds of the Clifford algebra object by recognizing

$$\begin{aligned} \gamma^a \mathbf{B} |\psi_o\rangle &:= (a_0 \gamma^a + a_{a_1} \gamma^a \gamma^{a_1} + a_{a_1 a_2} \gamma^a \gamma^{a_1} \gamma^{a_2} + \dots + \\ &\quad a_{a_1 \dots a_d} \gamma^a \gamma^{a_1} \dots \gamma^{a_d}) |\psi_{oc}\rangle, \\ \tilde{\gamma}^a \mathbf{B} |\psi_o\rangle &:= (i a_0 \gamma^a - i a_{a_1} \gamma^{a_1} \gamma^a + i a_{a_1 a_2} \gamma^{a_1} \gamma^{a_2} \gamma^a + \dots + \\ &\quad i (-1)^d a_{a_1 \dots a_d} \gamma^{a_1} \dots \gamma^{a_d} \gamma^a) |\psi_o\rangle. \end{aligned} \quad (16.8)$$

The nilpotents and projectors of Eq. (16.3) are the eigenstates also of the generators of the Cartan subalgebra

$$\tilde{S}^{03}, \tilde{S}^{12}, \tilde{S}^{56}, \dots, \tilde{S}^{d-1 \ d}, \quad (16.9)$$

with the eigenvalues

$$\tilde{S}^{ab} \begin{pmatrix} ab \\ k \end{pmatrix} = \frac{k}{2} \begin{pmatrix} ab \\ k \end{pmatrix}, \quad \tilde{S}^{ab} \begin{pmatrix} ab \\ [k] \end{pmatrix} = -\frac{k}{2} \begin{pmatrix} ab \\ [k] \end{pmatrix}. \quad (16.10)$$

One finds the relations

$$\begin{aligned} \gamma^a \begin{pmatrix} ab \\ k \end{pmatrix} &= \eta^{aa} \begin{pmatrix} ab \\ [-k] \end{pmatrix}, \quad \gamma^b \begin{pmatrix} ab \\ k \end{pmatrix} = -ik \begin{pmatrix} ab \\ [-k] \end{pmatrix}, \quad \gamma^a \begin{pmatrix} ab \\ [k] \end{pmatrix} = \begin{pmatrix} ab \\ (-k) \end{pmatrix}, \quad \gamma^b \begin{pmatrix} ab \\ [k] \end{pmatrix} = -ik \eta^{aa} \begin{pmatrix} ab \\ (-k) \end{pmatrix}, \\ \tilde{\gamma}^a \begin{pmatrix} ab \\ k \end{pmatrix} &= -i \eta^{aa} \begin{pmatrix} ab \\ [k] \end{pmatrix}, \quad \tilde{\gamma}^b \begin{pmatrix} ab \\ k \end{pmatrix} = -k \begin{pmatrix} ab \\ [k] \end{pmatrix}, \quad \tilde{\gamma}^a \begin{pmatrix} ab \\ [k] \end{pmatrix} = i \begin{pmatrix} ab \\ (k) \end{pmatrix}, \quad \tilde{\gamma}^b \begin{pmatrix} ab \\ [k] \end{pmatrix} = -k \eta^{aa} \begin{pmatrix} ab \\ (k) \end{pmatrix}. \end{aligned} \quad (16.11)$$

We discuss in what follows the representations of the operators γ^a , $\tilde{\gamma}^a$, S^{ab} and \tilde{S}^{ab} only in $d = (3 + 1)$.

In Ref. [8], as well as in this proceedings, the second quantization in Clifford and in Grassmann space is discussed. There the restrictions on the choices of products of nilpotents and projectors, which can be recognized as independent

states in the Clifford space, and yet allow the second quantization, is analyzed. The restrictions reduce, as noticed above, the number of states from 2^d to $2^{\frac{d}{2}-1}$ families with $2^{\frac{d}{2}-1}$ family members each. All the states of this contribution appear as a part of states (included as factors) already in $d = (5 + 1)$.

In what follows we shall not pay attention on these limitations. We only present matrices of the operators γ^a , $\tilde{\gamma}^a$, S^{ab} and \tilde{S}^{ab} for all possible states.

16.2 Basis in $d = (3 + 1)$

There are $2^4 = 16$ basic states in $d = (3 + 1)$. We make a choice of products of nilpotents and projectors, which are eigenstates of the Cartan subalgebra operators as presented in Eqs. (16.6, 16.10). The family members are reachable by S^{ab} , or by γ^a representing twice two vectors of definite handedness $\Gamma^{(d)}$ in $d = (3 + 1)$

$$\Gamma^{(d)} := (i)^{d/2} \prod_a (\sqrt{\eta^{a\bar{a}}} \gamma^a), \quad \text{if } d = 2n. \quad (16.12)$$

Each vector carries also the family handedness

$$\tilde{\Gamma}^{(d)} := (i)^{d/2} \prod_a (\sqrt{\eta^{a\bar{a}}} \tilde{\gamma}^a), \quad \text{if } d = 2n. \quad (16.13)$$

In what follows we first define the basic states and then represent all the operators — γ^a , S^{ab} , $\tilde{\gamma}^a$, \tilde{S}^{ab} , $\Gamma^{(d)}$ ($= -4iS^{03}S^{12}$ in $d = 4$), $\tilde{\Gamma}^{(d)}$ ($= -4i\tilde{S}^{03}\tilde{S}^{12}$ in $d = 4$) — as 16×16 matrices in this basis. We see that the operators have a 4×4 diagonal or off diagonal or partly diagonal and partly off diagonal substructure.

Let us start with the definition of the basic states, presented in Table 16.1.

As seen in Table 16.1 γ^a change handedness. S^{ab} , which do not belong to Cartan subalgebra, generate all the states of one representation of particular handedness, Eq. (16.12), and particular family quantum number. \tilde{S}^{ab} , which do not belong to Cartan subalgebra, transform a family member of one family into the same family member of another family, $\tilde{\gamma}^a$ change the family quantum number as well as the handedness $\tilde{\Gamma}^{(3+1)}$, Eq. (16.13).

Dirac matrices γ^a and S^{ab} do not distinguish among the families, they "see" all the families in the same way and correspondingly "see" only four states — instead of 4×4 states. The operators γ^a and S^{ab} are correspondingly 4×4 matrices.

Let us define, to simplify the notation, the unit 4×4 submatrix and the submatrix with all the matrix elements equal to zero as follows

$$\mathbf{1} = \begin{pmatrix} 1 & 0 \\ 0 & 1 \end{pmatrix}, \quad \mathbf{0} = \begin{pmatrix} 0 & 0 \\ 0 & 0 \end{pmatrix}. \quad (16.14)$$

We also use (2×2) Pauli matrices:

$$\sigma^1 = \begin{pmatrix} 0 & 1 \\ 1 & 0 \end{pmatrix}, \quad \sigma^2 = \begin{pmatrix} 0 & -i \\ i & 0 \end{pmatrix}, \quad \sigma^3 = \begin{pmatrix} 1 & 0 \\ 0 & -1 \end{pmatrix}. \quad (16.15)$$

d = 4	ψ_i	$\gamma^0 \psi_i$	$\gamma^1 \psi_i$	$\gamma^2 \psi_i$	$\gamma^3 \psi_i$	$\tilde{\gamma}^0 \psi_i$	$\tilde{\gamma}^1 \psi_i$	$\tilde{\gamma}^2 \psi_i$	$\tilde{\gamma}^3 \psi_i$	S^{03}	S^{12}	\tilde{S}^{03}	\tilde{S}^{12}	Γ^{3+1}	$\tilde{\Gamma}^{3+1}$
ψ_1^1	(+i)(+)	ψ_3^1	ψ_4^1	$i\psi_4^1$	ψ_3^1	$-i\psi_1^2$	$-i\psi_1^3$	ψ_1^3	$-i\psi_1^2$	$\frac{i}{2}$	$\frac{1}{2}$	$\frac{i}{2}$	$\frac{1}{2}$	1	1
ψ_2^1	[-i][-]	ψ_4^1	ψ_3^1	$-i\psi_3^1$	$-\psi_4^1$	$i\psi_2^2$	$i\psi_2^3$	$-\psi_2^3$	$i\psi_2^2$	$-\frac{i}{2}$	$-\frac{1}{2}$	$-\frac{i}{2}$	$-\frac{1}{2}$	1	1
ψ_3^1	[-i](+)	ψ_1^1	$-\psi_2^1$	$-i\psi_2^1$	$-\psi_1^1$	$i\psi_3^2$	$i\psi_3^3$	$-\psi_3^3$	$i\psi_3^2$	$-\frac{i}{2}$	$\frac{1}{2}$	$-\frac{i}{2}$	$\frac{1}{2}$	-1	1
ψ_4^1	(+i)[-]	ψ_2^1	$-\psi_1^1$	$i\psi_1^1$	ψ_2^1	$-i\psi_4^2$	$-i\psi_4^3$	ψ_4^3	$-i\psi_4^2$	$\frac{i}{2}$	$-\frac{1}{2}$	$\frac{i}{2}$	$-\frac{1}{2}$	-1	1
ψ_1^2	[+i](+)	ψ_3^2	$-\psi_4^2$	$-i\psi_4^2$	ψ_3^2	$i\psi_1^1$	$i\psi_1^4$	$-\psi_1^4$	$-i\psi_1^1$	$\frac{i}{2}$	$\frac{1}{2}$	$-\frac{i}{2}$	$\frac{1}{2}$	1	-1
ψ_2^2	(-i)[-]	ψ_4^2	$-\psi_3^2$	$i\psi_3^2$	$-\psi_4^2$	$-i\psi_2^1$	$-i\psi_2^4$	ψ_2^4	$i\psi_2^1$	$-\frac{i}{2}$	$-\frac{1}{2}$	$-\frac{i}{2}$	$-\frac{1}{2}$	1	-1
ψ_3^2	(-i)(+)	ψ_1^2	ψ_2^2	$i\psi_2^2$	$-\psi_1^2$	$-i\psi_3^1$	$-i\psi_3^4$	ψ_3^4	$i\psi_3^1$	$-\frac{i}{2}$	$\frac{1}{2}$	$-\frac{i}{2}$	$\frac{1}{2}$	-1	-1
ψ_4^2	[+i][-]	ψ_2^2	ψ_1^2	$-i\psi_1^2$	ψ_2^2	$i\psi_4^1$	$i\psi_4^4$	$-\psi_4^4$	$-i\psi_4^1$	$\frac{i}{2}$	$-\frac{1}{2}$	$\frac{i}{2}$	$-\frac{1}{2}$	-1	-1
ψ_1^3	(+i)[+]	ψ_3^3	$-\psi_4^3$	$-i\psi_4^3$	ψ_3^3	$i\psi_1^1$	$-i\psi_1^1$	$-\psi_1^1$	$i\psi_1^1$	$\frac{i}{2}$	$\frac{1}{2}$	$\frac{i}{2}$	$-\frac{1}{2}$	1	-1
ψ_2^3	[-i](-)	ψ_4^3	$-\psi_3^3$	$i\psi_3^3$	$-\psi_4^3$	$-i\psi_2^1$	$i\psi_2^1$	ψ_2^1	$-i\psi_2^1$	$-\frac{i}{2}$	$-\frac{1}{2}$	$-\frac{i}{2}$	$\frac{1}{2}$	1	-1
ψ_3^3	[-i][+]	ψ_1^3	ψ_2^3	$i\psi_2^3$	$-\psi_1^3$	$-i\psi_3^1$	$i\psi_3^1$	ψ_3^1	$-i\psi_3^1$	$-\frac{i}{2}$	$\frac{1}{2}$	$-\frac{i}{2}$	$\frac{1}{2}$	-1	-1
ψ_4^3	(+i)(-)	ψ_2^3	ψ_1^3	$-i\psi_1^3$	ψ_2^3	$i\psi_4^1$	$-i\psi_4^1$	$-\psi_4^1$	$i\psi_4^1$	$\frac{i}{2}$	$-\frac{1}{2}$	$\frac{i}{2}$	$-\frac{1}{2}$	-1	-1
ψ_1^4	[+i][+]	ψ_3^4	ψ_4^4	$i\psi_4^4$	ψ_3^4	$-i\psi_1^1$	$i\psi_1^2$	ψ_1^2	$i\psi_1^1$	$\frac{i}{2}$	$\frac{1}{2}$	$-\frac{i}{2}$	$-\frac{1}{2}$	1	1
ψ_2^4	(-i)(-)	ψ_4^4	ψ_3^4	$-i\psi_3^4$	$-\psi_4^4$	$i\psi_2^1$	$-i\psi_2^2$	$-\psi_2^2$	$-i\psi_2^1$	$-\frac{i}{2}$	$-\frac{1}{2}$	$-\frac{i}{2}$	$-\frac{1}{2}$	1	1
ψ_3^4	(-i)[+]	ψ_1^4	$-\psi_2^4$	$-i\psi_2^4$	$-\psi_1^4$	$i\psi_3^1$	$-i\psi_3^2$	$-\psi_3^2$	$-i\psi_3^1$	$-\frac{i}{2}$	$\frac{1}{2}$	$-\frac{i}{2}$	$\frac{1}{2}$	-1	1
ψ_4^4	[+i](-)	ψ_2^4	$-\psi_1^4$	$i\psi_1^4$	ψ_2^4	$-i\psi_4^1$	$i\psi_8$	ψ_4^4	$i\psi_4^4$	$\frac{i}{2}$	$-\frac{1}{2}$	$\frac{i}{2}$	$-\frac{1}{2}$	-1	1

Table 16.1. In this table $2^d = 16$ vectors, describing internal space of fermions in $d = (3+1)$, are presented. Each vector carries the family member quantum number — determined by S^{03} and S^{12} , Eqs. (16.6) — and the family quantum number — determined by \tilde{S}^{03} and \tilde{S}^{12} , Eq. (16.10).

Looking in Table 16.1 one easily finds the matrix representations for $\gamma^0, \gamma^1, \gamma^2$ and γ^3

$$\gamma^0 = \begin{pmatrix} \begin{smallmatrix} 0 & \sigma^1 \\ \sigma^1 & 0 \end{smallmatrix} & \begin{smallmatrix} 0 & 0 \\ 0 & 0 \end{smallmatrix} \\ \begin{smallmatrix} 0 & 0 \\ 0 & 0 \end{smallmatrix} & \begin{smallmatrix} \begin{smallmatrix} 0 & \sigma^1 \\ \sigma^1 & 0 \end{smallmatrix} & \begin{smallmatrix} 0 & 0 \\ 0 & 0 \end{smallmatrix} \end{smallmatrix} \end{pmatrix}, \quad (16.16)$$

$$\gamma^1 = \begin{pmatrix} \begin{smallmatrix} 0 & \sigma^1 \\ -\sigma^1 & 0 \end{smallmatrix} & \begin{smallmatrix} 0 & 0 \\ 0 & 0 \end{smallmatrix} \\ \begin{smallmatrix} 0 & 0 \\ 0 & 0 \end{smallmatrix} & \begin{smallmatrix} \begin{smallmatrix} 0 & -\sigma^1 \\ \sigma^1 & 0 \end{smallmatrix} & \begin{smallmatrix} 0 & 0 \\ -\sigma^1 & 0 \end{smallmatrix} \end{smallmatrix} \end{pmatrix}, \quad (16.17)$$

$$\gamma^2 = \begin{pmatrix} \begin{smallmatrix} 0 & -\sigma^2 \\ \sigma^2 & 0 \end{smallmatrix} & \begin{smallmatrix} 0 & 0 \\ 0 & 0 \end{smallmatrix} \\ \begin{smallmatrix} 0 & 0 \\ 0 & 0 \end{smallmatrix} & \begin{smallmatrix} \begin{smallmatrix} 0 & \sigma^2 \\ -\sigma^2 & 0 \end{smallmatrix} & \begin{smallmatrix} 0 & 0 \\ \sigma^2 & -\sigma^2 \end{smallmatrix} \end{smallmatrix} \end{pmatrix}, \quad (16.18)$$

$$\gamma^3 = \begin{pmatrix} \begin{smallmatrix} 0 & \sigma^3 \\ -\sigma^3 & 0 \end{smallmatrix} & \begin{smallmatrix} 0 & 0 \\ 0 & 0 \end{smallmatrix} \\ \begin{smallmatrix} 0 & 0 \\ 0 & 0 \end{smallmatrix} & \begin{smallmatrix} \begin{smallmatrix} 0 & \sigma^3 \\ -\sigma^3 & 0 \end{smallmatrix} & \begin{smallmatrix} 0 & 0 \\ -\sigma^3 & \sigma^3 \end{smallmatrix} \end{smallmatrix} \end{pmatrix}. \quad (16.19)$$

One sees as well the 4×4 substructure along the diagonal of 16×16 matrices.

The representations of the $\tilde{\gamma}^a$, these do not appear in the Dirac case, manifest the off diagonal structure as follows

$$\tilde{\gamma}^0 = \begin{pmatrix} 0 & i\sigma^3 & 0 & 0 \\ -i\sigma^3 & 0 & 0 & 0 \\ 0 & i\sigma^3 & 0 & 0 \\ 0 & 0 & i\sigma^3 & 0 \\ 0 & 0 & 0 & -i\sigma^3 \\ 0 & 0 & 0 & i\sigma^3 \end{pmatrix}, \quad (16.20)$$

$$\tilde{\gamma}^1 = \begin{pmatrix} 0 & 0 & -i\sigma^3 & 0 \\ 0 & 0 & 0 & i\sigma^3 \\ -i\sigma^3 & 0 & 0 & 0 \\ 0 & i\sigma^3 & 0 & 0 \\ 0 & i\sigma^3 & 0 & 0 \\ 0 & 0 & 0 & 0 \end{pmatrix}, \quad (16.21)$$

$$\tilde{\gamma}^2 = \begin{pmatrix} 0 & 0 & -\sigma^3 & 0 \\ 0 & 0 & 0 & \sigma^3 \\ \sigma^3 & 0 & 0 & 0 \\ 0 & -\sigma^3 & 0 & 0 \\ 0 & -\sigma^3 & 0 & 0 \\ 0 & 0 & 0 & 0 \end{pmatrix}, \quad (16.22)$$

$$\tilde{\gamma}^3 = \begin{pmatrix} 0 & -i\sigma^3 & 0 & 0 \\ -i\sigma^3 & 0 & 0 & 0 \\ 0 & i\sigma^3 & 0 & 0 \\ 0 & 0 & 0 & i\sigma^3 \\ 0 & 0 & i\sigma^3 & 0 \\ 0 & 0 & 0 & -i\sigma^3 \end{pmatrix}. \quad (16.23)$$

Matrices S^{ab} have again the 4×4 substructure along the diagonal structure, as expected, manifesting the repetition of the Dirac 4×4 matrices, since the Dirac S^{ab} do not distinguish among families.

$$S^{01} = \begin{pmatrix} \frac{i}{2}\sigma^1 & 0 & 0 & 0 & 0 \\ 0 & -\frac{i}{2}\sigma^1 & 0 & 0 & 0 \\ 0 & 0 & -\frac{i}{2}\sigma^1 & 0 & 0 \\ 0 & 0 & 0 & \frac{i}{2}\sigma^1 & 0 \\ 0 & 0 & 0 & 0 & -\frac{i}{2}\sigma^1 \end{pmatrix}, \quad (16.24)$$

$$S^{02} = \begin{pmatrix} -\frac{i}{2}\sigma^2 & 0 & 0 & 0 & 0 \\ 0 & \frac{i}{2}\sigma^2 & 0 & 0 & 0 \\ 0 & \frac{i}{2}\sigma^2 & 0 & 0 & 0 \\ 0 & 0 & \frac{i}{2}\sigma^2 & 0 & 0 \\ 0 & 0 & 0 & -\frac{i}{2}\sigma^2 & 0 \end{pmatrix}, \quad (16.25)$$

$$S^{03} = \begin{pmatrix} \frac{i}{2}\sigma^3 & 0 & 0 & 0 & 0 \\ 0 & -\frac{i}{2}\sigma^3 & 0 & 0 & 0 \\ 0 & 0 & \frac{i}{2}\sigma^3 & 0 & 0 \\ 0 & 0 & 0 & -\frac{i}{2}\sigma^3 & 0 \\ 0 & 0 & 0 & 0 & \frac{i}{2}\sigma^3 \\ 0 & 0 & 0 & 0 & 0 & -\frac{i}{2}\sigma^3 \end{pmatrix}, \quad (16.26)$$

$$S^{12} = \begin{pmatrix} \frac{1}{2}\sigma^3 & 0 & 0 & 0 & 0 \\ 0 & \frac{1}{2}\sigma^3 & 0 & 0 & 0 \\ 0 & 0 & \frac{1}{2}\sigma^3 & 0 & 0 \\ 0 & 0 & 0 & \frac{1}{2}\sigma^3 & 0 \\ 0 & 0 & 0 & 0 & \frac{1}{2}\sigma^3 \\ 0 & 0 & 0 & 0 & 0 & \frac{1}{2}\sigma^3 \end{pmatrix}, \quad (16.27)$$

$$S^{13} = \begin{pmatrix} \frac{1}{2}\sigma^2 & 0 & 0 & 0 & 0 \\ 0 & \frac{1}{2}\sigma^2 & 0 & 0 & 0 \\ 0 & 0 & -\frac{1}{2}\sigma^2 & 0 & 0 \\ 0 & 0 & 0 & -\frac{1}{2}\sigma^2 & 0 \\ 0 & 0 & 0 & 0 & -\frac{1}{2}\sigma^2 \\ 0 & 0 & 0 & 0 & 0 & \frac{1}{2}\sigma^2 \end{pmatrix}, \quad (16.28)$$

$$S^{23} = \begin{pmatrix} \frac{1}{2}\sigma^1 & 0 & 0 & 0 & 0 \\ 0 & \frac{1}{2}\sigma^1 & 0 & 0 & 0 \\ 0 & 0 & -\frac{1}{2}\sigma^1 & 0 & 0 \\ 0 & 0 & 0 & -\frac{1}{2}\sigma^1 & 0 \\ 0 & 0 & 0 & 0 & -\frac{1}{2}\sigma^1 \\ 0 & 0 & 0 & 0 & 0 & \frac{1}{2}\sigma^1 \end{pmatrix}. \quad (16.29)$$

$$\Gamma^{3+1} = -4iS^{03}S^{12} = \begin{pmatrix} 1 & 0 & 0 & 0 & 0 \\ 0 & -1 & 0 & 0 & 0 \\ 0 & 0 & 1 & 0 & 0 \\ 0 & 0 & 0 & -1 & 0 \\ 0 & 0 & 0 & 0 & 1 \\ 0 & 0 & 0 & 0 & 0 & -1 \end{pmatrix}. \quad (16.30)$$

The operators \tilde{S}^{ab} have again off diagonal 4×4 substructure, except \tilde{S}^{03} and \tilde{S}^{12} , which are diagonal.

$$\tilde{S}^{01} = \begin{pmatrix} 0 & 0 & 0 & -\frac{i}{2}\mathbf{1} \\ 0 & 0 & -\frac{i}{2}\mathbf{1} & 0 \\ 0 & -\frac{i}{2}\mathbf{1} & 0 & 0 \\ -\frac{i}{2}\mathbf{1} & 0 & 0 & 0 \end{pmatrix}, \quad (16.31)$$

$$\tilde{S}^{02} = \begin{pmatrix} 0 & 0 & 0 & \frac{1}{2}\mathbf{1} \\ 0 & 0 & \frac{1}{2}\mathbf{1} & 0 \\ 0 & -\frac{1}{2}\mathbf{1} & 0 & 0 \\ -\frac{1}{2}\mathbf{1} & 0 & 0 & 0 \end{pmatrix}, \quad (16.32)$$

$$\tilde{S}^{03} = \begin{pmatrix} \frac{i}{2}\mathbf{1} & 0 & 0 & 0 \\ 0 & -\frac{i}{2}\mathbf{1} & 0 & 0 \\ 0 & 0 & \frac{i}{2}\mathbf{1} & 0 \\ 0 & 0 & 0 & -\frac{i}{2}\mathbf{1} \end{pmatrix}, \quad (16.33)$$

$$\tilde{S}^{12} = \begin{pmatrix} \frac{1}{2}\mathbf{1} & 0 & 0 & 0 \\ 0 & \frac{1}{2}\mathbf{1} & 0 & 0 \\ 0 & 0 & -\frac{1}{2}\mathbf{1} & 0 \\ 0 & 0 & 0 & -\frac{1}{2}\mathbf{1} \end{pmatrix}, \quad (16.34)$$

$$\tilde{S}^{13} = \begin{pmatrix} 0 & 0 & 0 & -\frac{i}{2}\mathbf{1} \\ 0 & 0 & \frac{i}{2}\mathbf{1} & 0 \\ 0 & -\frac{i}{2}\mathbf{1} & 0 & 0 \\ \frac{i}{2}\mathbf{1} & 0 & 0 & 0 \end{pmatrix}, \quad (16.35)$$

$$\tilde{S}^{23} = \begin{pmatrix} 0 & 0 & 0 & -\frac{1}{2}\mathbf{1} \\ 0 & 0 & \frac{1}{2}\mathbf{1} & 0 \\ 0 & \frac{1}{2}\mathbf{1} & 0 & 0 \\ -\frac{1}{2}\mathbf{1} & 0 & 0 & 0 \end{pmatrix}. \quad (16.36)$$

$$\tilde{F}^{3+1} = -4i\tilde{S}^{03}\tilde{S}^{12} = \begin{pmatrix} 1 & 0 & 0 & 0 \\ 0 & -1 & 0 & 0 \\ 0 & 0 & -1 & 0 \\ 0 & 0 & 0 & 1 \end{pmatrix}. \quad (16.37)$$

References

1. P.A.M. Dirac, "The Quantum Theory of the Electron", Proc. Roy. Soc. (London) **A117** (1928) 610.
2. N.S. Mankoč Borštnik, "Spinor and vector representations in four dimensional Grassmann space", *J. Math. Phys.* **34**, 3731-3745 (1993).
3. N.S. Mankoč Borštnik, "Can spin-charge-family theory explain baryon number non conservation?", Phys. Rev. D **91** (2015) 6, 065004 ID: 0703013. doi:10.1103; [arxiv:1409.7791, arXiv:1502.06786v1].
4. N.S. Mankoč Borštnik, "Spin-charge-family theory is offering next step in understanding elementary particles and fields and correspondingly universe", Proceedings to the Conference on Cosmology, Gravitational Waves and Particles, IARD conferences, Ljubljana, 6-9 June 2016, The 10th Biennial Conference on Classical and Quantum Relativistic Dynamics of articles and Fields, J. Phys.: Conf. Ser. **845** 012017 [arXiv:1607.01618v2].
5. N.S. Mankoč Borštnik, "The explanation for the origin of the higgs scalar and for the Yukawa couplings by the *spin-charge-family* theory", *J. of Mod. Phys.* **6** (2015) 2244-2274.
6. N.S. Mankoč Borštnik, H.B.F. Nielsen, "How to generate spinor representations in any dimension in terms of projection operators", *J. of Math. Phys.* **43** (2002) 5782, [hep-th/0111257].
7. N.S. Mankoč Borštnik, H.B.F. Nielsen, "How to generate families of spinors", *J. of Math. Phys.* **44** 4817 (2003) [hep-th/0303224].
8. "Why nature made a choice of Clifford and not Grassmann coordinates", Proceedings to the 20th Workshop "What comes beyond the standard models", Bled, 9-17 of July, 2017, Ed. N.S. Mankoč Borštnik, H.B. Nielsen, D. Lukman, DMFA Založništvo, Ljubljana, December 2017, p. 89-120 [arXiv:1802.05554v1v2].
9. D. Lukman and N.S. Mankoc Borstnik, "Representations in Grassmann space and fermion degrees of freedom", [arXiv:1805.06318].



17 Properties of Fermions With Integer Spin Described in Grassmann Space *

D. Lukman and N.S. Mankoč Borštnik¹

¹Department of Physics, University of Ljubljana,
Jadranska 19, SI-1000 Ljubljana, Slovenia

Abstract. In Ref. [1] one of the authors (N.S.M.B.) study the second quantization of fermions with integer spin while describing the internal degrees of freedom of fermions in Grassmann space. In this contribution we study the representations in Grassmann space of the groups $SO(5, 1)$, $SO(3, 1)$, $SU(3) \times U(1)$, and $SO(4)$, which are of particular interest as the subgroups of the group $SO(13, 1)$. The second quantized integer spin fermions, appearing in Grassmann space, not observed so far, could be an alternative choice to the half integer spin fermions, appearing in Clifford space. The *spin-charge-family* theory, using two kinds of Clifford operators — γ^a and $\tilde{\gamma}^a$ — for the description of spins and charges (first) and family quantum numbers (second), offers the explanation for not only the appearance of families but also for all the properties of quarks and leptons, the gauge fields, scalar fields and others [2–5]. In both cases the gauge fields in $d \geq (13 + 1)$ — the spin connections $\omega_{ab\alpha}$ (of the two kinds in Clifford case and of one kind in Grassmann case) and the vielbeins f^α_α — determine in $d = (3 + 1)$ scalars, those with the space index $\alpha = (5, 6, \dots, d)$, and gauge fields, those with the space index $\alpha = (0, 1, 2, 3)$. While states of the Lorentz group and all its subgroups (in any dimension) are in Clifford space in the fundamental representations of the groups, with the family degrees of freedom included [2,3,1], states in Grassmann space manifest with respect to the Lorentz group adjoint representations, allowing no families.

Povzetek. V članku [1], ki uporabi za opis notranjih prostostnih stopenj fermionov Grassmannov prostor, predstavi eden od avtorjev (N.S.M.B.) drugo kvantizacijo fermionov s celoštevilskimi spini. Prispevek predstavi lastnosti upodobitev grup $SO(5, 1)$, $SO(3, 1)$, $SU(3) \times U(1)$ in $SO(4)$ v Grassmannovem prostoru. Te grupe so posebej zanimive kot podgrupe grupe $SO(13, 1)$. Kreacijski in anihilacijski operatorji, ki ustrezajo komutacijskim relacijam za fermione, nosijo v Grassmannovem prostoru celoštevilčni spin. Fermioni s celoštevilčnim spinom ponudijo alternativni opis fermionom v Cliffordovem prostoru, ki nosijo polštevilčni spin. Opaženi so le fermioni s polštevilčnim spinom. Teorija *spinov-nabojev-družin*, ki uporabi dve vrsti operatorjev γ v Cliffordovem prostoru — γ^a in $\tilde{\gamma}^a$ — prvega za opis spina in vseh nabojev in drugega za opis družinskega kvantnega števila, ponuja razlago ne samo za pojav družin, ampak tudi pojasni vse lastnosti kvarkov in leptonov, umeritvenih polj, skalarnih polj in drugo [2–5]. Umeritvena polja v $d \geq (13 + 1)$ — spinske povezave $\omega_{ab\alpha}$ (dveh vrst v Cliffordovem primeru in ene vrste v Grassmannovem primeru) in “vielbeini” f^α_α — določajo v obeh primerih v $d = (3 + 1)$ skalarje, če nosijo prostorski indeks $\alpha = (5, 6, \dots, d)$, ter umeritvena polja, kadar imajo prostorski indeks

* This contribution developed during the discussions at the 20th — Bled, 09-17 of July, 2017 — and 21st — Bled, 23 of June to 1 of July — Workshops “What Comes Beyond the Standard Models”, Bled, 09-17 of July, 2017.

$\alpha = (0, 1, 2, 3)$. Stanja Lorentzove grupe in vseh njenih podgrup so za poljubno dimenzijo v Cliffordovem prostoru v fundamentalni upodobitvi in vključujejo družinske prostostne stopnje [2,3,1], v Grassmannovem prostoru pa so glede na Lorentzovo grupo v adjungirani upodobitvi in ne dopuščajo družin.

Keywords: Spinor representations in Grassmann space, Second quantization of fermion fields in Grassmann space, Higher dimensional spaces, Kaluza-Klein theories, Beyond the standard model

PACS:04.50.-Cd, 11.10.Kk, 11.25.Mj, 11.30.Hv, 12.10.-g, 12.60.-i

17.1 Introduction

In Ref. [2] the representations in Grassmann and in Clifford space were discussed. In Ref. ([1] and the references therein) the second quantization procedure in both spaces — in Clifford space and in Grassmann space — were discussed in order to try to understand “why nature made a choice of Clifford rather than Grassmann space” during the expansion of our universe, although in both spaces the creation operators \hat{b}_j^\dagger and the annihilation operators \hat{b}_j exist fulfilling the anticommutation relations required for fermions [1]

$$\begin{aligned}\{\hat{b}_i, \hat{b}_j^\dagger\}_+ |\psi_o\rangle &= \delta_{ij} |\psi_o\rangle, \\ \{\hat{b}_i, \hat{b}_j\}_+ |\psi_o\rangle &= 0 |\psi_o\rangle, \\ \{\hat{b}_i^\dagger, \hat{b}_j^\dagger\}_+ |\psi_o\rangle &= 0 |\psi_o\rangle, \\ \hat{b}_j^\dagger |\psi_o\rangle &= |\psi_j\rangle \\ \hat{b}_j |\psi_o\rangle &= 0 |\psi_o\rangle.\end{aligned}\tag{17.1}$$

$|\psi_o\rangle$ is the vacuum state. We use $|\psi_o\rangle = |1\rangle$.

The creation operators can be expressed in both spaces by products of eigenstates of the Cartan subalgebra, Eq. (17.33), of the Lorentz algebra, Eqs. (17.3, 17.11). Starting with one state (Ref. [1]) all the other states of the same representation are reachable by the generators of the Lorentz transformations (which do not belong to the Cartan subalgebra), with S^{ab} presented in Eq. (17.32) in Grassmann space and with either S^{ab} or \tilde{S}^{ab} , Eq. (17.34), in Clifford space.

But while there are in Clifford case two kinds of the generators of the Lorentz transformations — S^{ab} and \tilde{S}^{ab} , the first transforming members of one family among themselves, and the second transforming one member of a particular family into the same member of other families — there is in Grassmann space only one kind of the Lorentz generators — S^{ab} . Correspondingly are all the states in Clifford space, which can be second quantized as products of nilpotents and projectors [9,10,1], reachable with one of the two kinds of the operators S^{ab} and \tilde{S}^{ab} , while different representations are in Grassmann space disconnected.

On the other hand the vacuum state is in Grassmann case simple — $|\psi_o\rangle = |1\rangle$ — while in Clifford case is the sum of products of projectors, Eq. (17.17).

In Grassmann space states are in the adjoint representations with respect to the Lorentz group, while states in Clifford space belong to the fundamental

representations with respect to both generators, S^{ab} and \tilde{S}^{ab} , or they are singlets. Correspondingly are properties of fermions, described with the *spin-charge-family* theory [3,4,6,5,8,7], which uses the Clifford space to describe fermion degrees of freedom, in agreement with the observations, offering explanation for all the assumptions of the *standard model* (with families included) and also other observed phenomena.

In Grassmann case the spins manifest, for example, in the case of $SO(6)$ or $SO(5, 1)$ decuplets or singlets — triplets and singlets in Clifford case, Table 17.2 — while with respect to the subgroups $SU(3)$ and $U(1)$ of $SO(6)$ the states belong to either singlets, or triplets or sextets, Tables 17.3, 17.4 — triplets and singlets in the Clifford case.

In what follows we discuss representations, manifesting as charges and spins of fermions, of subgroups of $SO(13, 1)$, when internal degrees of freedom of fermions are described in Grassmann space and compare properties of these representations with the properties of the corresponding representations appearing in Clifford space. We assume, as in the *spin-charge-family* theory, that both spaces, the internal and the ordinary space, have $d = 2(2n + 1)$ -dimensions, n is positive integer, $d \geq 14$ and that all the degrees of freedom of fermions and bosons originate in $d = 2(2n + 1)$, in which fermions interact with gravity only.

After the break of the starting symmetry $SO(13, 1)$ into $SO(7, 1) \times SU(3) \times U(1)$, and further to $SO(3, 1) \times SU(2) \times SU(2) \times SU(3) \times U(1)$, fermions manifest in $d = (3 + 1)$ the spin and the corresponding charges and interact with the gauge fields, which are indeed the spin connections with the space index $m = (0, 1, 2, 3)$, originating in $d = (13, 1)$ [7]. Also scalar fields originate in gravity: Those spin connections with the space index $a = (5, 6, 7, 8)$ determine masses of fermions, those with the space index $a = (9, 10, \dots, 14)$ contribute to particle/antiparticle asymmetry in our universe [4].

We pay attention on fermion fields, the creation and annihilation operators of which fulfill the anticommutation relations of Eq. (17.1).

17.1.1 Creation and annihilation operators in Grassmann space

In Grassmann $d = 2(2n + 1)$ -dimensional space the creation and annihilation operators follow from the starting two creation and annihilation operators, both with an odd Grassmann character, since those with an even Grassmann character do not obey the anticommutation relations of Eq. (17.1) [1]

$$\begin{aligned}
 \hat{b}_1^{\theta 1 \dagger} &= \left(\frac{1}{\sqrt{2}}\right)^{\frac{d}{2}} (\theta^0 - \theta^3)(\theta^1 + i\theta^2)(\theta^5 + i\theta^6) \cdots (\theta^{d-1} + i\theta^d), \\
 \hat{b}_1^{\theta 1} &= \left(\frac{1}{\sqrt{2}}\right)^{\frac{d}{2}} \left(\frac{\partial}{\partial \theta^{d-1}} - i\frac{\partial}{\partial \theta^d}\right) \cdots \left(\frac{\partial}{\partial \theta^0} - \frac{\partial}{\partial \theta^3}\right), \\
 \hat{b}_1^{\theta 2 \dagger} &= \left(\frac{1}{\sqrt{2}}\right)^{\frac{d}{2}} (\theta^0 + \theta^3)(\theta^1 + i\theta^2)(\theta^5 + i\theta^6) \cdots (\theta^{d-1} + i\theta^d), \\
 \hat{b}_1^{\theta 2} &= \left(\frac{1}{\sqrt{2}}\right)^{\frac{d}{2}} \left(\frac{\partial}{\partial \theta^{d-1}} - i\frac{\partial}{\partial \theta^d}\right) \cdots \left(\frac{\partial}{\partial \theta^0} + \frac{\partial}{\partial \theta^3}\right).
 \end{aligned} \tag{17.2}$$

All the creation operators are products of the eigenstates of the Cartan subalgebra operators, Eq. (17.33)

$$\begin{aligned} \mathbf{S}^{ab}(\theta^a \pm \epsilon \theta^b) &= \mp i \frac{\eta^{aa}}{\epsilon} (\theta^a \pm \epsilon \theta^b), \\ \epsilon &= 1, \text{ for } \eta^{aa} = 1, \quad \epsilon = i, \text{ for } \eta^{aa} = -1, \\ \mathbf{S}^{ab}(\theta^a \theta^b \pm \epsilon \theta^c \theta^d) &= 0, \quad \mathbf{S}^{cd}(\theta^a \theta^b \pm \epsilon \theta^c \theta^d) = 0. \end{aligned} \quad (17.3)$$

The two creation operators, $\hat{b}_1^{\theta 1 \dagger}$ and $\hat{b}_1^{\theta 2 \dagger}$, if applied on the vacuum state, form the starting two states ϕ_1^1 and ϕ_1^2 of the two representations, respectively. The vacuum state is chosen to be the simplest one [1] — $|\phi_0\rangle = |1\rangle$. The rest of creation operators of each of the two groups, $\hat{b}_i^{\theta 1 \dagger}$ and $\hat{b}_i^{\theta 2 \dagger}$, follow from the starting one by the application of the generators of the Lorentz transformations in Grassmann space \mathbf{S}^{ab} , Eq. (17.32), which do not belong to the Cartan subalgebra, Eq. (17.33), of the Lorentz algebra. They generate either $|\phi_j^1\rangle$ of the first group or $|\phi_j^2\rangle$ of the second group.

Annihilation operators $\hat{b}_i^{\theta 1}$ and $\hat{b}_i^{\theta 2}$ follow from the creation ones by the Hermitian conjugation [1], when taking into account the assumption

$$(\theta^a)^\dagger = \frac{\partial}{\partial \theta_a} \eta^{aa} = -i p^{\theta a} \eta^{aa}, \quad (17.4)$$

from where it follows

$$\left(\frac{\partial}{\partial \theta_a}\right)^\dagger = \eta^{aa} \theta^a, \quad (p^{\theta a})^\dagger = -i \eta^{aa} \theta^a. \quad (17.5)$$

The annihilation operators $\hat{b}_i^{\theta 1}$ and $\hat{b}_i^{\theta 2}$ annihilate states $|\phi_i^1\rangle$ and $|\phi_i^2\rangle$, respectively.

The application of \mathbf{S}^{01} on $\hat{b}_1^{\theta 1 \dagger}$, for example, transforms this creation operator into $\hat{b}_2^{\theta 1 \dagger} = \left(\frac{1}{\sqrt{2}}\right)^{\frac{d}{2}-1} (\theta^0 \theta^3 + i \theta^1 \theta^2) (\theta^5 + i \theta^6) \dots (\theta^{d-1} - i \theta^d)$. Correspondingly its Hermitian conjugate annihilation operator is equal to $\hat{b}_2^{\theta 1} = \left(\frac{1}{\sqrt{2}}\right)^{\frac{d}{2}-1} \left(\frac{\partial}{\partial \theta^{d-1}} - i \frac{\partial}{\partial \theta^d}\right) \dots \left(\frac{\partial}{\partial \theta^3} \frac{\partial}{\partial \theta^0} - i \frac{\partial}{\partial \theta^2} \frac{\partial}{\partial \theta^1}\right)$.

All the states are normalized with respect to the integral over the Grassmann coordinate space [2]

$$\begin{aligned} \langle \phi_i^a | \phi_j^b \rangle &= \int d^{d-1} x d^d \theta^a \omega \langle \phi_i^a | \theta \rangle \langle \theta | \phi_j^b \rangle = \delta^{ab} \delta_{ij}, \\ \omega &= \Pi_{k=0}^d \left(\frac{\partial}{\partial \theta_k} + \theta^k \right), \end{aligned} \quad (17.6)$$

where ω is a weight function, defining the scalar product $\langle \phi_i^a | \phi_j^b \rangle$, and we require that [2]

$$\begin{aligned} \{d\theta^a, \theta^b\}_+ &= 0, \quad \int d\theta^a = 0, \quad \int d\theta^a \theta^a = 1, \\ \int d^d \theta \theta^0 \theta^1 \dots \theta^d &= 1, \\ d^d \theta &= d\theta^d \dots d\theta^0, \end{aligned} \quad (17.7)$$

with $\frac{\partial}{\partial \theta^a} \theta^c = \eta^{ac}$.

There are $\frac{1}{2} \frac{d!}{\frac{d!}{2} \frac{d!}{2}}$ in each of these two groups of creation operators of an odd Grassmann character in $d = 2(2n + 1)$ -dimensional space.

The rest of creation operators (and the corresponding annihilation operators) would have rather opposite Grassmann character than the ones studied so far: like **a.** $\theta^0 \theta^1$ for the creation operator and $[\frac{\partial}{\partial \theta^1}, \frac{\partial}{\partial \theta^0}]$ for the corresponding annihilation operator in $d = (1 + 1)$ (since $\{\theta^0 \theta^1, \frac{\partial}{\partial \theta^1} \frac{\partial}{\partial \theta^0}\}_+$ gives $(1 + (1 + 1)\theta^0 \theta^1 \frac{\partial}{\partial \theta^1} \frac{\partial}{\partial \theta^0})$), and like **b.** $(\theta^0 \mp \theta^3)(\theta^1 \pm i\theta^2)$ for creation operator and $[(\frac{\partial}{\partial \theta^1} \mp i \frac{\partial}{\partial \theta^2})(\frac{\partial}{\partial \theta^0} \mp \frac{\partial}{\partial \theta^3})]$ for the annihilation operator, or $\theta^0 \theta^3 \theta^1 \theta^2$ for the creation operator and $[\frac{\partial}{\partial \theta^2} \frac{\partial}{\partial \theta^1} \frac{\partial}{\partial \theta^3} \frac{\partial}{\partial \theta^0}]$ for the annihilation operator in $d = (3 + 1)$ (since, let say, $\{\frac{1}{2}(\theta^0 - \theta^3)(\theta^1 + i\theta^2), \frac{1}{2}(\frac{\partial}{\partial \theta^1} - i \frac{\partial}{\partial \theta^2})(\frac{\partial}{\partial \theta^0} - \frac{\partial}{\partial \theta^3})\}_+$ gives $(1 + \frac{1}{4}(1 + 1)(\theta^0 - \theta^3)(\theta^1 + i\theta^2)(\frac{\partial}{\partial \theta^1} - i \frac{\partial}{\partial \theta^2})(\frac{\partial}{\partial \theta^0} - \frac{\partial}{\partial \theta^3}))$ and equivalently for other cases), but applied on a vacuum states some of them still fulfill some of the relations of Eq. (17.1), but not all (like $\{\frac{1}{2}(\theta^0 - \theta^3)(\theta^1 + i\theta^2), \frac{1}{2}(\theta^0 + \theta^3)(\theta^1 - i\theta^2)\}_+ = i\theta^0 \theta^1 \theta^2 \theta^3$, while it should be zero).

Let us add that, like in Clifford case, one can simplify the scalar product in Grassmann case by recognizing that the scalar product is equal to $\delta^{ab} \delta_{ij}$

$$\langle \phi_i^a | \theta \rangle \langle \theta | \phi_j^b \rangle = \delta^{ab} \delta_{ij}, \quad (17.8)$$

without integration over the Grassmann coordinates. Let us manifest this in the case of $d = (1 + 1)$: $\langle 1 | \frac{1}{\sqrt{2}}(\frac{\partial}{\partial \theta^0} - \frac{\partial}{\partial \theta^1}) \frac{1}{\sqrt{2}}(\theta^0 - \theta^1) | 1 \rangle = 1$, $|1\rangle$ is the normalized vacuum state, $\langle 1 | 1 \rangle = 1$. It is true in all dimensions, what can easily be understood for all the states, which are defined by the creation operators \hat{b}_i^\dagger on the vacuum state $|1\rangle$, $|\phi_i^b\rangle = \hat{b}_i^\dagger |1\rangle$, fulfilling the anticommutation relations of Eq. (17.1).

17.1.2 Creation and annihilation operators in Clifford space

There are two kinds of Clifford objects [2], ([3] and Refs. therein), γ^a and $\tilde{\gamma}^a$, both fulfilling the anticommutation relations

$$\begin{aligned} \{\gamma^a, \gamma^b\}_+ &= 2\eta^{ab} = \{\tilde{\gamma}^a, \tilde{\gamma}^b\}_+, \\ \{\gamma^a, \tilde{\gamma}^b\}_+ &= 0. \end{aligned} \quad (17.9)$$

Both Clifford algebra objects are expressible with θ^a and $\frac{\partial}{\partial \theta^a}$ [2,1], ([3] and Refs. therein)

$$\begin{aligned} \gamma^a &= (\theta^a + \frac{\partial}{\partial \theta_a}), \\ \tilde{\gamma}^a &= i(\theta^a - \frac{\partial}{\partial \theta_a}), \\ \theta^a &= \frac{1}{2}(\gamma^a - i\tilde{\gamma}^a), \\ \frac{\partial}{\partial \theta_a} &= \frac{1}{2}(\gamma^a + i\tilde{\gamma}^a), \end{aligned} \quad (17.10)$$

from where it follows: $(\gamma^a)^\dagger = \gamma^a \eta^{aa}$, $(\tilde{\gamma}^a)^\dagger = \tilde{\gamma}^a \eta^{aa}$, $\gamma^a \gamma^a = \eta^{aa}$, $\gamma^a (\gamma^a)^\dagger = 1$, $\tilde{\gamma}^a \tilde{\gamma}^a = \eta^{aa}$, $\tilde{\gamma}^a (\tilde{\gamma}^a)^\dagger = 1$.

Correspondingly we can use either γ^a or $\tilde{\gamma}^a$ instead of θ^a to span the internal space of fermions. Since both, γ^a and $\tilde{\gamma}^a$, are expressible with θ^a and the derivatives with respect to θ^a , the norm of vectors in Clifford space can be defined by the same integral as in Grassmann space, Eq.(17.6), or we can simplify the scalar product (as in the Grassmann case, Eq. (17.8) by introducing the Clifford vacuum state $|\psi_{oc} \rangle$, Eq. (17.17), instead of $|1 \rangle$ in Grassmann case.

We make use of γ^a to span the vector space. As in the case of Grassmann space we require that the basic states are eigenstates of the Cartan subalgebra operators of S^{ab} and \tilde{S}^{ab} , Eq. (17.33).

$$\begin{aligned} {}^{ab}(\mathbf{k}) &:= \frac{1}{2}(\gamma^a + \frac{\eta^{aa}}{ik}\gamma^b), & {}^{ab}(\mathbf{k})^\dagger &= \eta^{aa} {}^{ab}(-\mathbf{k}), \\ {}^{ab}[\mathbf{k}] &:= \frac{1}{2}(1 + \frac{i}{k}\gamma^a\gamma^b), & {}^{ab}[\mathbf{k}]^\dagger &= {}^{ab}[\mathbf{k}], \\ S^{ab} {}^{ab}(\mathbf{k}) &= \frac{1}{2}k {}^{ab}(\mathbf{k}), & S^{ab} {}^{ab}[\mathbf{k}] &= \frac{1}{2}k {}^{ab}[\mathbf{k}], \\ \tilde{S}^{ab} {}^{ab}(\mathbf{k}) &= \frac{1}{2}k {}^{ab}(\mathbf{k}), & \tilde{S}^{ab} {}^{ab}[\mathbf{k}] &= -\frac{1}{2}k {}^{ab}[\mathbf{k}], \end{aligned} \quad (17.11)$$

with $k^2 = \eta^{aa}\eta^{bb}$. To calculate $\tilde{S}^{ab} {}^{ab}(\mathbf{k})$ and $\tilde{S}^{ab} {}^{ab}[\mathbf{k}]$ we use [10,9] the relation on any Clifford algebra object A as follows

$$(\gamma^a A = i(-)^{(A)} A \gamma^a) |\psi_{oc} \rangle, \quad (17.12)$$

where A is any Clifford algebra object and $(-)^{(A)} = -1$, if A is an odd Clifford algebra object and $(-)^{(A)} = 1$, if A is an even Clifford algebra object, $|\psi_{oc} \rangle$ is the vacuum state, replacing the vacuum state $|\psi_o \rangle = |1 \rangle$, used in Grassmann case, with the one of Eq. (17.17), in accordance with the relation of Eqs. (17.10, 17.6, 17.7), Ref. [1].

We can define now the creation and annihilation operators in Clifford space so that they fulfill the requirements of Eq. (17.1). We write the starting creation operator and its Hermitian conjugate one (in accordance with Eq. (17.11) and Eq.(17.33)) in $2(2n+1)$ -dimensional space as follows [1]

$$\begin{aligned} \hat{b}_1^{1\dagger} &= (+i)(+)(+) \cdots (+), \\ \hat{b}_1^1 &= (-) \cdots (-)(-)(-i). \end{aligned} \quad (17.13)$$

The starting creation operator $\hat{b}_1^{1\dagger}$, when applied on the vacuum state $|\psi_{oc} \rangle$, defines the starting family member of the starting "family". The corresponding starting annihilation operator is its Hermitian conjugated one, Eq. (17.11).

All the other creation operators of the same family can be obtained by the application of the generators of the Lorentz transformations S^{ab} , Eq. (17.34), which do not belong to the Cartan subalgebra of $SO(2(2n+1)-1, 1)$, Eq. (17.33).

$$\begin{aligned} \hat{b}_i^{1\dagger} &\propto S^{ab} \cdots S^{ef} \hat{b}_1^{1\dagger}, \\ \hat{b}_i^1 &\propto \hat{b}_1^1 S^{ef} \cdots S^{ab}, \end{aligned} \quad (17.14)$$

with $S^{ab\dagger} = \eta^{aa}\eta^{bb}S^{ab}$. The proportionality factors are chosen so, that the corresponding states $|\psi_1^1\rangle = \hat{b}_i^{1\dagger}|\psi_{oc}\rangle$ are normalized, where $|\psi_{oc}\rangle$ is the normalized vacuum state, $\langle\psi_{oc}|\psi_{oc}\rangle = 1$.

The creation operators creating different "families" with respect to the starting "family", Eq. (17.13), can be obtained from the starting one by the application of \tilde{S}^{ab} , Eq. (17.34), which do not belong to the Cartan subalgebra of $\widetilde{SO}(2(2n+1) - 1, 1)$, Eq. (17.33). They all keep the "family member" quantum number unchanged.

$$\hat{b}_i^{\alpha\dagger} \propto \tilde{S}^{ab} \dots \tilde{S}^{ef} \hat{b}_i^{1\dagger}. \quad (17.15)$$

Correspondingly we can define (up to the proportionality factor) any creation operator for any "family" and any "family member" with the application of S^{ab} and \tilde{S}^{ab} [1]

$$\begin{aligned} \hat{b}_i^{\alpha\dagger} &\propto \tilde{S}^{ab} \dots \tilde{S}^{ef} S^{mn} \dots S^{pr} \hat{b}_1^{1\dagger} \\ &\propto S^{mn} \dots S^{pr} \hat{b}_1^{1\dagger} S^{ab} \dots S^{ef}. \end{aligned} \quad (17.16)$$

All the corresponding annihilation operators follow from the creation ones by the Hermitian conjugation.

There are $2^{\frac{d}{2}-1} \times 2^{\frac{d}{2}-1}$ creation operators of an odd Clifford character and the same number of annihilation operators, which fulfill the anticommutation relations of Eq. (17.1) on the vacuum state $|\psi_{oc}\rangle$ with $2^{\frac{d}{2}-1}$ summands

$$\begin{aligned} |\psi_{oc}\rangle &= \\ &\propto ([-i]^{03} [-]^{12} [-]^{56} \dots [-]^{d-1} d + [+i]^{03} [+]^{12} [-]^{56} \dots [-]^{d-1} d + [+i]^{03} [-]^{12} [+]^{56} \dots [-]^{d-1} d + \dots) |0\rangle, \\ \alpha &= \frac{1}{\sqrt{2^{\frac{d}{2}-1}}}, \\ &\text{for } d = 2(2n+1), \end{aligned} \quad (17.17)$$

n is a positive integer. For a chosen $\alpha = \frac{1}{\sqrt{2^{\frac{d}{2}-1}}}$ the vacuum is normalized: $\langle\psi_{oc}|\psi_{oc}\rangle = 1$.

It is proven in Ref. [1] that the creation and annihilation operators fulfill the anticommutation relations required for fermions, Eq. (17.1).

17.2 Properties of representations of the Lorentz group $SO(2(2n+1))$ and of subgroups in Grassmann and in Clifford space

The purpose of this contribution is to compare properties of the representations of the Lorentz group $SO(2(2n+1))$, $n \geq 3$, when for the description of the internal degrees of freedom of fermions either i. Grassmann space or ii. Clifford space is used. The *spin-charge-family* theory ([6,5,3,4,8,7,11] and the references therein) namely predicts that all the properties of the observed either quarks and leptons or vector gauge fields or scalar gauge fields originate in $d \geq (13+1)$, in

which massless fermions interact with the gravitational field only — with its spin connections and vielbeins.

However, both — Clifford space and Grassmann space — allow second quantized states, the creation and annihilation operators of which fulfill the anticommutation relations for fermions of Eq. (17.1).

But while Clifford space offers the description of spins, charges and families of fermions in $d = (3 + 1)$, all in the fundamental representations of the Lorentz group $SO(13, 1)$ and the subgroups of the Lorentz group, in agreement with the observations, the representations of the Lorentz group are in Grassmann space the adjoint ones, in disagreement with what we observe.

We compare properties of the representations in Grassmann case with those in Clifford case to be able to better understand "the choice of nature in the expanding universe, making use of the Clifford degrees of freedom", rather than Grassmann degrees of freedom.

In introduction we briefly reviewed properties of creation and annihilation operators in both spaces, presented in Ref. [1] (and the references therein). We pay attention on spaces with $d = 2(2n + 1)$ of ordinary coordinates and $d = 2(2n + 1)$ internal coordinates, either of Clifford or of Grassmann character.

i. In Clifford case there are $2^{\frac{d}{2}-1}$ creation operators of an odd Clifford character, creating "family members" when applied on the vacuum state. We choose them to be eigenstates of the Cartan subalgebra operators, Eq.(17.33), of the Lorentz algebra. All the members can be reached from any of the creation operators by the application of S^{ab} , Eq. (17.34). Each "family member" appears in $2^{\frac{d}{2}-1}$ "families", again of an odd Clifford character, since the corresponding creation operators are reachable by \tilde{S}^{ab} , Eq. (17.34), which are Clifford even objects.

There are correspondingly $2^{\frac{d}{2}-1} \cdot 2^{\frac{d}{2}-1}$ creation and the same number ($2^{\frac{d}{2}-1} \cdot 2^{\frac{d}{2}-1}$) of annihilation operators. Also the annihilation operators, annihilating states of $2^{\frac{d}{2}-1}$ "family members" in $2^{\frac{d}{2}-1}$ "families", have an odd Clifford character, since they are Hermitian conjugate to the creation ones.

The rest of $2 \cdot 2^{\frac{d}{2}-1} \cdot 2^{\frac{d}{2}-1}$ members of the Lorentz representations have an even Clifford character, what means that the corresponding creation and annihilation operators can not fulfill the anticommutation relations required for fermions, Eq. (17.1). Among these $2^{\frac{d}{2}-1}$ products of projectors determine the vacuum state, Eq. (17.17).

ii. In Grassmann case there are $\frac{d!}{\frac{d}{2}! \frac{d}{2}!}$ operators of an odd Grassmann character, which form the creation operators, fulfilling with the corresponding annihilation operators the requirements of Eq. (17.1). All the creation operators are chosen to be products of the eigenstates of the Cartan subalgebra S^{ab} , Eq. (17.33). The corresponding annihilation operators are the Hermitian conjugated values of the creation operators, Eqs. (17.4, 17.5, 17.2). The creation operators form, when applied on the simple vacuum state $|\phi_0\rangle = |1\rangle$, two independent groups of states. The members of each of the two groups are reachable from any member of a group by the application of S^{ab} , Eq. (17.32). All the states of any of the two decuplets are orthonormalized.

We comment in what follows the representations in $d = (13 + 1)$ in Clifford and in Grassmann case. In *spin-charge family* theory there are breaks of the starting symmetry from $SO(13, 1)$ to $SO(3, 1) \times SU(2) \times SU(3) \times U(1)$ in steps, which lead to the so far observed quarks and leptons, gauge and scalar fields and gravity. One of the authors (N.S.M.B.), together with H.B. Nielsen, defined the discrete symmetry operators for Kaluza-Klein theories for spinors in Clifford space [19]. In Ref. [1] the same authors define the discrete symmetry operators in the case that for the description of fermion degrees of freedom Grassmann space is used. Here we comment symmetries in both spaces for some of subgroups of the $SO(13, 1)$ group, as well as the appearance of the Dirac sea.

17.2.1 Equations of motion in Grassmann and Clifford space

We define [1] the action in Grassmann space, for which we require — similarly as in Clifford case — that the action for a free massless object

$$\mathcal{A} = \frac{1}{2} \left\{ \int d^d x \, d^d \theta \, \omega \left(\phi^\dagger (1 - 2\theta^0 \frac{\partial}{\partial \theta^0}) \frac{1}{2} (\theta^a p_a + \eta^{aa} \theta^{a\dagger} p_a) \phi \right) \right\}, \quad (17.18)$$

is Lorentz invariant. The corresponding equation of motion is

$$\frac{1}{2} \left[(1 - 2\theta^0 \frac{\partial}{\partial \theta^0}) \theta^a + ((1 - 2\theta^0 \frac{\partial}{\partial \theta^0}) \theta^a)^\dagger \right] p_a |\phi_i^\theta \rangle = 0, \quad (17.19)$$

$p_a = i \frac{\partial}{\partial x^a}$, leading to the Klein-Gordon equation

$$\{ (1 - 2\theta^0 \frac{\partial}{\partial \theta^0}) \theta^a p_a \}^\dagger \theta^b p_b |\phi_i^\theta \rangle = p^a p_a |\phi_i^\theta \rangle = 0. \quad (17.20)$$

In the Clifford case the action for massless fermions is well known

$$\mathcal{A} = \int d^d x \, \frac{1}{2} (\psi^\dagger \gamma^0 \gamma^a p_a \psi) + \text{h.c.}, \quad (17.21)$$

leading to the equations of motion

$$\gamma^a p_a |\psi^\alpha \rangle = 0, \quad (17.22)$$

which fulfill also the Klein-Gordon equation

$$\gamma^a p_a \gamma^b p_b |\psi_i^\alpha \rangle = p^a p_a |\psi_i^\alpha \rangle = 0. \quad (17.23)$$

17.2.2 Discrete symmetries in Grassmann and Clifford space

We follow also here Ref. [1] and the references therein. We distinguish in d -dimensional space two kinds of discrete operators \mathcal{C} , \mathcal{P} and \mathcal{T} operators with respect to the internal space which we use.

In the Clifford case [19], when the whole d -space is treated equivalently, we have

$$\begin{aligned} \mathcal{C}_{\mathcal{H}} &= \prod_{\gamma^a \in \mathcal{I}} \gamma^a K, \quad \mathcal{T}_{\mathcal{H}} = \gamma^0 \prod_{\gamma^a \in \mathcal{R}} \gamma^a K I_{x^0}, \quad \mathcal{P}_{\mathcal{H}}^{(d-1)} = \gamma^0 I_{\vec{x}}, \\ I_x x^a &= -x^a, \quad I_{x^0} x^a = (-x^0, \vec{x}), \quad I_{\vec{x}} \vec{x} = -\vec{x}, \\ I_{\vec{x}_3} x^a &= (x^0, -x^1, -x^2, -x^3, x^5, x^6, \dots, x^d). \end{aligned} \quad (17.24)$$

The product $\prod \gamma^a$ is meant in the ascending order in γ^a .

In the Grassmann case we correspondingly define

$$\mathcal{C}_G = \prod_{\gamma_G^a \in \mathfrak{I}\gamma^a} \gamma_G^a K, \quad \mathcal{T}_G = \gamma_G^0 \prod_{\gamma_G^a \in \mathfrak{R}\gamma^a} \gamma_G^a K I_{x^0}, \quad \mathcal{P}_G^{(d-1)} = \gamma_G^0 I_{\vec{x}}, \quad (17.25)$$

with γ_G^a defined as

$$\gamma_G^a = (1 - 2\theta^a \eta^{aa} \frac{\partial}{\partial \theta_a}), \quad (17.26)$$

while $I_x, I_{\vec{x}}$ is defined in Eq. (17.24). Let be noticed, that since $\gamma_G^a (= -i\eta^{aa} \gamma^a \tilde{\gamma}^a)$ is always real as there is $\gamma^a i\tilde{\gamma}^a$, while γ^a is either real or imaginary, we use in Eq. (17.25) γ^a to make a choice of appropriate γ_G^a . In what follows we shall use the notation as in Eq. (17.25).

We define, according to Ref. [1] (and the references therein) in both cases — Clifford Grassmann case — the operator "emptying" [6,5] (arxiv:1312.1541) the Dirac sea, so that operation of "emptying_N" after the charge conjugation \mathcal{C}_H in the Clifford case and "emptying_G" after the charge conjugation \mathcal{C}_G in the Grassmann case (both transform the state put on the top of either the Clifford or the Grassmann Dirac sea into the corresponding negative energy state) creates the anti-particle state to the starting particle state, both put on the top of the Dirac sea and both solving the Weyl equation, either in the Clifford case, Eq. (17.22), or in the Grassmann case, Eq. (17.19), for free massless fermions

$$\begin{aligned} \text{"emptying}_N &= \prod_{\mathfrak{R}\gamma^a} \gamma^a K \quad \text{in Clifford space,} \\ \text{"emptying}_G &= \prod_{\mathfrak{R}\gamma^a} \gamma_G^a K \quad \text{in Grassmann space,} \end{aligned} \quad (17.27)$$

although we must keep in mind that indeed the anti-particle state is a hole in the Dirac sea from the Fock space point of view. The operator "emptying" is bringing the single particle operator \mathcal{C}_H in the Clifford case and \mathcal{C}_G in the Grassmann case into the operator on the Fock space in each of the two cases. Then the anti-particle state creation operator — $\underline{\Psi}_a^\dagger[\Psi_p]$ — to the corresponding particle state creation operator — can be obtained also as follows

$$\begin{aligned} \underline{\Psi}_a^\dagger[\Psi_p] |vac> &= \mathbb{C}_H \underline{\Psi}_p^\dagger[\Psi_p] |vac> = \int \Psi_a^\dagger(\vec{x}) (\mathbb{C}_H \Psi_p(\vec{x})) d^{(d-1)}x |vac>, \\ \mathbb{C}_H &= \text{"emptying}_N \cdot \mathcal{C}_H \end{aligned} \quad (17.28)$$

in both cases.

The operators \mathbb{C}_H and \mathbb{C}_G

$$\begin{aligned} \mathbb{C}_H &= \text{"emptying}_N \cdot \mathcal{C}_H, \\ \mathbb{C}_G &= \text{"emptying}_{NG} \cdot \mathcal{C}_G, \end{aligned} \quad (17.29)$$

operating on $\Psi_p(\vec{x})$ transforms the positive energy spinor state (which solves the corresponding Weyl equation for a massless free fermion) put on the top of

the Dirac sea into the positive energy anti-fermion state, which again solves the corresponding Weyl equation for a massless free anti-fermion put on the top of the Dirac sea. Let us point out that either the operator "emptying_N" or the operator "emptying_{NG}" transforms the single particle operator either \mathcal{C}_H or \mathcal{C}_G into the operator operating in the Fock space.

We use the Grassmann even, Hermitian and real operators γ_G^a , Eq. (17.26), to define discrete symmetry in Grassmann space, first we did in $((d+1)-1)$ space, Eq. (17.25), now we do in $(3+1)$ space, Eq. (17.30), as it is done in [19] in the Clifford case. In the Grassmann case we do this in analogy with the operators in the Clifford case [19]

$$\begin{aligned}
 \mathcal{C}_{NG} &= \prod_{\gamma_G^m \in \Re \gamma^m} \gamma_G^m K I_{x^6 x^8 \dots x^d}, \\
 \mathcal{T}_{NG} &= \gamma_G^0 \prod_{\gamma_G^m \in \Im \gamma^m} K I_{x^0} I_{x^5 x^7 \dots x^{d-1}}, \\
 \mathcal{P}_{NG}^{(d-1)} &= \gamma_G^0 \prod_{s=5}^d \gamma_G^s I_{\vec{x}}, \\
 \mathbb{C}_{NG} &= \prod_{\gamma_G^s \in \Re \gamma^s} \gamma_G^s, I_{x^6 x^8 \dots x^d}, \\
 \mathbb{C}_{NG} \mathcal{P}_{NG}^{(d-1)} &= \gamma_G^0 \prod_{\gamma_G^s \in \Im \gamma^s, s=5}^d \gamma_G^s I_{\vec{x}_3} I_{x^6 x^8 \dots x^d}, \\
 \mathbb{C}_{NG} \mathcal{T}_{NG} \mathcal{P}_{NG}^{(d-1)} &= \prod_{\gamma_G^s \in \Im \gamma^a} \gamma_G^a I_x K.
 \end{aligned} \tag{17.30}$$

17.2.3 Representations in Grassmann and in Clifford space in $d = (13+1)$

In the *spin-charge-family* theory the starting dimension of space must be $\geq (13+1)$, in order that the theory manifests in $d = (3+1)$ all the observed properties of quarks and leptons, gauge and scalar fields (explaining the appearance of higgs and the Yukawa couplings), offering as well the explanations for the observations in cosmology.

Let us therefore comment properties of representations in both spaces when $d = (13+1)$, if we analyze one group of "family members" of one of families in Clifford space, and one of the two representations of $\frac{1}{2} \frac{d!}{\frac{d}{2}! \frac{d}{2}!}$.

a. Let us start with Clifford space [3,5,4,6,13,12,2]. Each "family" representation has $2^{\frac{d}{2}-1} = 64$ "family members". If we analyze this representation with respect to the subgroups $SO(3,1)$, $(SU(2) \times SU(2))$ of $SO(4)$ and $(SU(3) \times U(1))$ of $SO(6)$ of the Lorentz group $SO(13,1)$, we find that the representations have quantum numbers of all the so far observed quarks and leptons and anti-quarks and antileptons, all with spin up and spin down, as well as of the left and right handedness, with the right handed neutrino included as the member of this representation.

Let us make a choice of the "family", which follows by the application of $\tilde{\S}^{15}$ on the "family", for which the creation operator of the right-handed neutrino

with spin $\frac{1}{2}$ would be $\overset{03}{(+i)} \overset{12}{(+)} \overset{56}{(+)} \overset{78}{(+)} \parallel \overset{9\ 10}{(+)} \overset{11\ 12}{(+)} \overset{13\ 14}{(+)}$. (The corresponding annihilation operator of this creation operator is $\overset{13\ 14}{(-)} \overset{11\ 12}{(-)} \overset{9\ 10}{(-)} \parallel \overset{78}{(-)} \overset{56}{(-)} \overset{12}{(-)} \overset{03}{(-i)}$). In Table 6.3 (see pages 112–113 in this volume) presented creation operators for all the “family members” of this family follow by the application of S^{ab} on $\tilde{S}^{15} \overset{03}{(+i)} \overset{12}{(+)} \overset{56}{(+)} \overset{78}{(+)} \parallel \overset{9\ 10}{(+)} \overset{11\ 12}{(+)} \overset{13\ 14}{(+)}$. (The annihilation operator of $\tilde{S}^{15} \overset{03}{(+i)} \overset{12}{(+)} \overset{56}{(+)} \overset{78}{(+)} \parallel \overset{9\ 10}{(+)} \overset{11\ 12}{(+)} \overset{13\ 14}{(+)}$ is $\overset{03}{[-]} \overset{12}{[-]} \overset{56}{[-]} \overset{78}{[-]} \parallel \overset{9\ 10}{(-)} \overset{11\ 12}{(-)} \overset{13\ 14}{(-)}$.)

This is the representation of Table 6.3 (see pages 112–113 in this volume), in which all the “family members” of one “family” are classified with respect to the subgroups $SO(3, 1) \times SU(2) \times SU(2) \times SU(3) \times U(1)$. The vacuum state on which the creation operators, represented in the third column, apply is defined in Eq. (17.17). All the creation operators of all the states are of an odd Clifford character, fulfilling together with the annihilation operators (which have as well the equivalent odd Clifford character, since the Hermitian conjugation do not change the Clifford character) the requirements of Eq. (17.1). Since the Clifford even operators S^{ab} and \tilde{S}^{ab} do not change the Clifford character, all the creation and annihilation operators, obtained by products of S^{ab} or \tilde{S}^{ab} or both, fulfill the requirements of Eq. (17.1).

We recognize in Table 6.3 (see pages 112–113 in this volume) that quarks distinguish from leptons only in the $SO(6)$ part of the creation operators. Quarks belong to the colour ($SU(3)$) triplet carrying the “fermion” ($U(1)$) quantum number $\tau^4 = \frac{1}{6}$, antiquarks belong to the colour antitriplet, carrying the “fermion” quantum number $\tau^4 = -\frac{1}{6}$. Leptons belong to the colour ($SU(3)$) singlet, carrying the “fermion” ($U(1)$) quantum number $\tau^4 = -\frac{1}{2}$, while antileptons belong to the colour antisinglet, carrying the “fermion” quantum number $\tau^4 = \frac{1}{2}$.

Let us also comment that the oddness and evenness of part of states in the subgroups of the $SO(13, 1)$ group change: While quarks and leptons have in the part of $SO(6)$ an odd Clifford character, have antiquarks and antileptons in this part an even odd Clifford character. Correspondingly the Clifford character changes in the rest of subgroups.

Families are generated by \tilde{S}^{ab} applying on any one of the “family members”. Again all the “family members” of this “family” follow by the application of all S^{ab} (not belonging to Cartan subalgebra).

The spontaneous break of symmetry from $SO(13, 1)$ to $SO(7, 1) \times SU(3) \times U(1)$, Refs. [3–5], makes in the *spin-charge-family* theory all the families, generated by \tilde{S}^{mt} and \tilde{S}^{st} , [$m = (0, 1, 2, 3)$, $s = (5, 6, 7, 8)$, $t = (9, 10, 11, 12, 13, 14)$], massive of the scale of $\geq 10^{16}$ GeV [14–16]. Correspondingly there are only eight families of quarks and leptons, which split into two groups of four families, both manifesting the symmetry $\widetilde{SU}(2) \times \widetilde{SU}(2) \times U(1)$. (The fourth of the lower four families is predicted to be observed at the LHC, the stable of the upper four families contributes to the dark matter [17].)

In the *spin-charge-family* theory fermions interact with only gravity, which manifests after the break of the starting symmetry in $d = (3 + 1)$ as all the known vector gauge fields, ordinary gravity and the higgs and the Yukawa couplings [7,3–

5,11]. There are scalar fields which bring masses to family members. The theory explains not only all the assumptions of the *standard model* with the appearance of families, the vector gauge fields and the scalar fields, it also explains appearance of the dark matter [17], matter/antimatter asymmetry [4] and other phenomena, like the miraculous cancellation of the triangle anomalies in the *standard model* [8].

b. We compare representations of $SO(13, 1)$ in Clifford space with those in Grassmann space. We have **no "family" quantum numbers in Grassmann space**. We only have two groups of creation operators, defining — when applied on the vacuum state $|1\rangle \sim \frac{1}{2} \frac{d!}{\frac{d}{2}! \frac{d}{2}!}$ equal in $d = (13 + 1)$ to 1716 members in each of the two groups in comparison in Clifford case with 64 "family members" in one "family" and 64 "families", which the breaks of symmetry reduce to 8 "families", making all the $(64 - 8)$ "families" massive and correspondingly not observable at low energies ([5,14] and the references therein).

Since the 1716 members are hard to be mastered, let us look therefore at each subgroup — $SU(3) \times U(1)$, $SO(3, 1)$ and $SU(2) \times SU(2)$ of $SO(13, 1)$ — separately.

Let us correspondingly analyze the subgroups: $SO(6)$ from the point of view of the two subgroups $SU(3) \times U(1)$, and $SO(7, 1)$ from the point of view of the two subgroups $SO(3, 1) \times SO(4)$, and let us also analyze $SO(4)$ as $SU(2) \times SU(2)$.

17.2.4 Examples of second quantizable states in Grassmann and in Clifford space

We compare properties of representations in Grassmann and in Clifford space for several choices of subgroups of $SO(13, 1)$ in the case that in both spaces creation and annihilation operators fulfill requirements of Eq. (17.1), that is that both kinds of states can be second quantized. Let us again point out that in Grassmann case fermions carry integer spins, while in Clifford case they carry half integer spin.

States in Grassmann and in Clifford space for $d = (5 + 1)$ We study properties of representations of the subgroup $SO(5, 1)$ (of the group $SO(13, 1)$), in Clifford and in Grassmann space, requiring that states can be in both spaces second quantized, fulfilling therefore Eq. (17.1).

a. In Clifford space there are $2^{\frac{d}{2}-1}$, each with $2^{\frac{d}{2}-1}$ family members, that is 4 families, each with 4 members. All these sixteen states are of an odd Clifford character, since all can be obtained by products of S^{ab} , \tilde{S}^{ab} or both from an Clifford odd starting states and are correspondingly second quantizable as required in Eq. (17.1). All the states are the eigenstates of the Cartan subalgebra of the Lorentz algebra in Clifford space, Eq. (17.33), solving the Weyl equation for free massless spinors in Clifford space, Eq. (17.22). The four families, with four members each, are presented in Table 17.1. All of these 16 states are reachable from the first one in each of the four families by S^{ab} , or by \tilde{S}^{ab} if applied on any family member.

Each of these four families have positive and negative energy solutions, as presented in [19], in Table I.. We present in Table 17.1 only states of a positive energy, that is states above the Dirac sea. The antiparticle states are reachable from the particle states by the application of the operator $\mathbb{C}_{\mathcal{N}} \mathcal{P}_{\mathcal{N}}^{(d-1)} = \gamma^0 \gamma^5 I_{\vec{x}_3} I_{x_6}$,

keeping the spin $\frac{1}{2}$, while changing the charge from $\frac{1}{2}$ to $-\frac{1}{2}$. All the states above the Dirac sea are indeed the hole in the Dirac sea, as explained in Ref. [19].

	ψ	S^{03}	S^{12}	S^{56}	\bar{S}^{03}	\bar{S}^{12}	\bar{S}^{56}
ψ_1^I	$\begin{smallmatrix} 03 & 12 & 56 \\ (+i)(+)(+) \end{smallmatrix}$	$\frac{i}{2}$	$\frac{1}{2}$	$\frac{1}{2}$	$\frac{i}{2}$	$\frac{1}{2}$	$\frac{1}{2}$
ψ_2^I	$\begin{smallmatrix} 03 & 12 & 56 \\ [-i][-](+) \end{smallmatrix}$	$-\frac{i}{2}$	$-\frac{1}{2}$	$\frac{1}{2}$	$\frac{i}{2}$	$\frac{1}{2}$	$\frac{1}{2}$
ψ_3^I	$\begin{smallmatrix} 03 & 12 & 56 \\ [-i](+)[-] \end{smallmatrix}$	$-\frac{i}{2}$	$\frac{1}{2}$	$-\frac{1}{2}$	$\frac{i}{2}$	$\frac{1}{2}$	$\frac{1}{2}$
ψ_4^I	$\begin{smallmatrix} 03 & 12 & 56 \\ (+i)[-][-] \end{smallmatrix}$	$\frac{i}{2}$	$-\frac{1}{2}$	$-\frac{1}{2}$	$\frac{i}{2}$	$\frac{1}{2}$	$\frac{1}{2}$
ψ_1^{II}	$\begin{smallmatrix} 03 & 12 & 56 \\ [+i]+ \end{smallmatrix}$	$\frac{i}{2}$	$\frac{1}{2}$	$\frac{1}{2}$	$-\frac{i}{2}$	$-\frac{1}{2}$	$\frac{1}{2}$
ψ_2^{II}	$\begin{smallmatrix} 03 & 12 & 56 \\ (-i)(-)(+) \end{smallmatrix}$	$-\frac{i}{2}$	$-\frac{1}{2}$	$\frac{1}{2}$	$-\frac{i}{2}$	$-\frac{1}{2}$	$\frac{1}{2}$
ψ_3^{II}	$\begin{smallmatrix} 03 & 12 & 56 \\ (-i)[+][-] \end{smallmatrix}$	$-\frac{i}{2}$	$\frac{1}{2}$	$-\frac{1}{2}$	$-\frac{i}{2}$	$-\frac{1}{2}$	$\frac{1}{2}$
ψ_4^{II}	$\begin{smallmatrix} 03 & 12 & 56 \\ [+i](-)[-] \end{smallmatrix}$	$\frac{i}{2}$	$-\frac{1}{2}$	$-\frac{1}{2}$	$-\frac{i}{2}$	$-\frac{1}{2}$	$\frac{1}{2}$
ψ_1^{III}	$\begin{smallmatrix} 03 & 12 & 56 \\ [+i](+)[+] \end{smallmatrix}$	$\frac{i}{2}$	$\frac{1}{2}$	$\frac{1}{2}$	$-\frac{i}{2}$	$\frac{1}{2}$	$-\frac{1}{2}$
ψ_2^{III}	$\begin{smallmatrix} 03 & 12 & 56 \\ (-i)[-][+] \end{smallmatrix}$	$-\frac{i}{2}$	$-\frac{1}{2}$	$\frac{1}{2}$	$-\frac{i}{2}$	$\frac{1}{2}$	$-\frac{1}{2}$
ψ_3^{III}	$\begin{smallmatrix} 03 & 12 & 56 \\ (-i)(+)(-) \end{smallmatrix}$	$-\frac{i}{2}$	$\frac{1}{2}$	$-\frac{1}{2}$	$-\frac{i}{2}$	$\frac{1}{2}$	$-\frac{1}{2}$
ψ_4^{III}	$\begin{smallmatrix} 03 & 12 & 56 \\ [+i]- \end{smallmatrix}$	$\frac{i}{2}$	$-\frac{1}{2}$	$-\frac{1}{2}$	$-\frac{i}{2}$	$\frac{1}{2}$	$-\frac{1}{2}$
ψ_1^{IV}	$\begin{smallmatrix} 03 & 12 & 56 \\ (+i)[+][+] \end{smallmatrix}$	$\frac{i}{2}$	$\frac{1}{2}$	$\frac{1}{2}$	$\frac{i}{2}$	$-\frac{1}{2}$	$-\frac{1}{2}$
ψ_2^{IV}	$\begin{smallmatrix} 03 & 12 & 56 \\ [-i](-)[+] \end{smallmatrix}$	$-\frac{i}{2}$	$-\frac{1}{2}$	$\frac{1}{2}$	$\frac{i}{2}$	$-\frac{1}{2}$	$-\frac{1}{2}$
ψ_3^{IV}	$\begin{smallmatrix} 03 & 12 & 56 \\ [-i][+](-) \end{smallmatrix}$	$-\frac{i}{2}$	$\frac{1}{2}$	$-\frac{1}{2}$	$\frac{i}{2}$	$-\frac{1}{2}$	$-\frac{1}{2}$
ψ_4^{IV}	$\begin{smallmatrix} 03 & 12 & 56 \\ (+i)(-)(-) \end{smallmatrix}$	$\frac{i}{2}$	$-\frac{1}{2}$	$-\frac{1}{2}$	$\frac{i}{2}$	$-\frac{1}{2}$	$-\frac{1}{2}$

Table 17.1. The four families, each with four members. For the choice $p^a = (p^0, 0, 0, p^3, 0, 0)$ have the first and the second member the space part equal to $e^{-i|p^0|x^0+i|p^3|x^3}$ and $e^{-i|p^0|x^0-i|p^3|x^3}$, representing the particles with spin up and down, respectively. The third and the fourth member represent the antiparticle states, with the space part equal to $e^{-i|p^0|x^0-i|p^3|x^3}$ and $e^{-i|p^0|x^0+i|p^3|x^3}$, with the spin up and down respectively. The antiparticle states follow from the particle state by the application of $\mathbb{C}_{\mathcal{N}} \mathcal{P}_{\mathcal{N}}^{(d-1)} = \gamma^0 \gamma^5 I_{\bar{x}_3} I_{x_6}$. The charge of the particle states is $\frac{1}{2}$, for antiparticle states $-\frac{1}{2}$.

b.0 In Grassmann space there are $\frac{d!}{\frac{d}{2}!\frac{d}{2}!}$ second quantizable states as required in Eq. (17.1), forming in $d = (5 + 1)$ two decuplets — each with $\frac{1}{2} \frac{d!}{\frac{d}{2}!\frac{d}{2}!}$ states — all are the eigenstates of the Cartan subalgebra of the Lorentz algebra in (internal) Grassmann space. All the states of one (anyone of the two) decuplets are reachable by the application of the operators S^{ab} on a starting state. The two decuplets are presented in Table 17.2

Let us first find the solution of the equations of motion for free massless fermions, Eq. (17.19), with the momentum $p^a = (p^0, p^1, p^2, p^3, 0, 0)$. One obtains for $\psi_I = \alpha(\theta^0 - \theta^3)(\theta^1 + i\theta^2)(\theta^5 + i\theta^6) + \beta(\theta^0\theta^3 + i\theta^1\theta^2)(\theta^5 + i\theta^6) + \gamma(\theta^0 +$

$\theta^3)(\theta^1 - i\theta^2)(\theta^5 + i\theta^6)$ the solution

$$\begin{aligned}\beta &= \frac{2\gamma(p^1 - ip^2)}{(p^0 - p^3)} = \frac{2\gamma(p^0 + p^3)}{(p^1 + ip^2)} = -\frac{2\alpha(p^0 - p^3)}{(p^1 - ip^2)} = -\frac{2\alpha(p^1 + ip^2)}{(p^0 + p^3)}, \\ (p^0)^2 &= (p^1)^2 + (p^2)^2 + (p^3)^2, \\ \frac{\beta}{-\alpha} &= \frac{2(p^0 - p^3)}{(p^1 - ip^2)}, \quad \frac{\gamma}{-\alpha} = \frac{(p^0 - p^3)^2}{(p^1 - ip^2)^2}.\end{aligned}\quad (17.31)$$

One has for $p^0 = |p^0|$ the positive energy solution, describing a fermion above the "Dirac sea", and for $p^0 = -|p^0|$ the negative energy solution, describing a fermion in the "Dirac sea". The "charge" of the "fermion" is 1. Similarly one finds the solution for the other three states with the negative "charge" -1 , again with the positive and negative energy. The space part of the "fermion" state is for "spin up" equal to $e^{-i|p^0|x^0 + i\vec{p}\vec{x}}$, for his antiparticle for the same internal spin $e^{-i|p^0|x^0 - i\vec{p}\vec{x}}$.

The discrete symmetry operator $\mathbb{C}_{NG} \mathcal{P}_{NG}^{(d-1)}$, which is in our case equal to $\gamma_G^0 \gamma_G^5 I_{\vec{x}^6}$, transforms the first state in Table 17.2 into the sixth, the second state into the fifth, the third state into the fourth, keeping the same spin while changing the "charge" of the superposition of the three states ψ_{Ip} . Both superposition of states, Eq. (17.31) represent the positive energy states put on the top of the "Dirac" sea, the first describing a particle with "charge" 1 and the second superposition of the second three states ψ_{Ia} , describing the antiparticle with the "charge" -1 . We namely apply $\mathbb{C}_{NG} \mathcal{P}_{NG}^{(d-1)}$ on $\Psi_p^\dagger[\Psi_I^{pos}]$ by applying $\mathbb{C}_{NG} \mathcal{P}_{NG}^{(d-1)}$ on Ψ_I^{pos} as follows: $\mathbb{C}_{NG} \mathcal{P}_{NG}^{(d-1)} \Psi_p^\dagger[\Psi_I^{pos}] (\mathbb{C}_{NG} \mathcal{P}_{NG}^{(d-1)})^{-1} = \Psi_{aNG}^\dagger[\mathbb{C}_{NG} \mathcal{P}_{NG}^{(d-1)} \Psi_I^{pos}]$. One recognizes that it is $\mathbb{C}_{NG} \mathcal{P}_{NG}^{(d-1)} \Psi_I^{pos} = \Psi_{II}^{pos}$ (Table 17.2), which must be put on the top of the "Dirac" sea, representing the hole in the particular state in the "Dirac" sea, which solves the corresponding equation of motion for the negative energy.

Properties of SO(6) in Grassmann and in Clifford space when SO(6) is embedded into SO(13, 1) a. Let us first repeat properties of the SO(6) part of the SO(13, 1) representation of 64 "family members" in Clifford space, presented in Table 6.3 (see pages 112–113 in this volume). As seen in Table 6.3 (see pages 112–

113 in this volume) there are one quadruplet ($2^{\frac{4}{2}-1} = 4$) — $\begin{smallmatrix} 9 & 10 & 11 & 12 & 13 & 14 \\ (+) & (-) & (-) & (-) \end{smallmatrix}$,

$\begin{smallmatrix} 9 & 10 & 11 & 12 & 13 & 14 & 9 & 10 & 11 & 12 & 13 & 14 \\ (-) & (+) & (-) & (-) & (-) & (-) & (+) & (+) & (+) & (+) \end{smallmatrix}$, representing quarks and leptons

— and one antiquadruplet — $\begin{smallmatrix} 9 & 10 & 11 & 12 & 13 & 14 & 9 & 10 & 11 & 12 & 13 & 14 \\ (-) & (+) & (+) & (+) & (-) & (+) & (+) & (+) & (-) & (-) \end{smallmatrix}$,

$\begin{smallmatrix} 9 & 10 & 11 & 12 & 13 & 14 \\ (-) & (-) & (-) & (-) \end{smallmatrix}$, representing antiquarks and antileptons, which both belong to

the 64th-plet, if SO(6) is embedded into SO(13, 1). The creation operators (and correspondingly their annihilation operators) have for 32 members (representing quarks and leptons) the SO(6) part of an odd Clifford character (and can be correspondingly second quantized (by themselves [1] or) together with the rest of space, manifesting SO(7, 1) (since it has an even Clifford character). The rest of 32 creation operators (representing antiquarks and antileptons) has in the SO(6) part an even Clifford character and correspondingly in the rest of the Clifford space in SO(7, 1) an odd Clifford character.

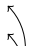


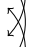


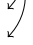





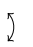





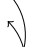








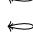





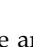
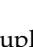
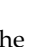
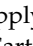
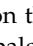
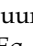
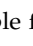
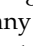
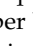
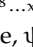
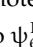
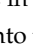
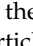
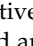
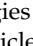
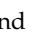
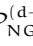
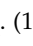



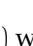

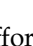
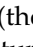
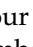
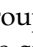
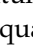
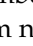
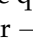
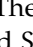
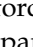
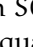
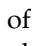
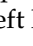
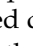

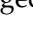

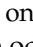
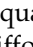

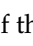
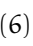

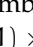
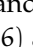
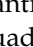
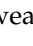

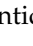






I		decuplet	\mathbf{S}^{03}	\mathbf{S}^{12}	\mathbf{S}^{56}	\mathcal{C}_{GN}	$\mathcal{C}_{GN}\mathcal{P}_{GN}^{(d-1)}$	$\mathbb{C}_{GN}\mathcal{P}_{GN}^{(d-1)}$
	1	$(\theta^0 - \theta^3)(\theta^1 + i\theta^2)(\theta^5 + i\theta^6)$	i	1	1			
	2	$(\theta^0\theta^3 + i\theta^1\theta^2)(\theta^5 + i\theta^6)$	0	0	1			
	3	$(\theta^0 - \theta^3)(\theta^1 - i\theta^2)(\theta^5 + i\theta^6)$	$-i$	-1	1			
	4	$(\theta^0 + \theta^3)(\theta^1 - i\theta^2)(\theta^5 - i\theta^6)$	i	-1	-1			
	5	$(\theta^0\theta^3 - i\theta^1\theta^2)(\theta^5 - i\theta^6)$	0	0	-1			
	6	$(\theta^0 + \theta^3)(\theta^1 + i\theta^2)(\theta^5 - i\theta^6)$	$-i$	1	-1			
	7	$(\theta^0 - \theta^3)(\theta^1\theta^2 + \theta^5\theta^6)$	i	0	0			
	8	$(\theta^0 + \theta^3)(\theta^1\theta^2 - \theta^5\theta^6)$	$-i$	0	0			
	9	$(\theta^0\theta^3 + i\theta^5\theta^6)(\theta^1 + i\theta^2)$	0	1	0			
	10	$(\theta^0\theta^3 - i\theta^5\theta^6)(\theta^1 - i\theta^2)$	0	-1	0			
								
								
								
								
								
								
								
								
								
								
								
								
								
								
								
								
								
								
								
								

Table 17.2. The creation operators of the decuplet and the antidecuplet of the orthogonal group $SO(5, 1)$ in Grassmann space are presented. Applying on the vacuum state $|\phi_0\rangle = |1\rangle$ the creation operators form eigenstates of the Cartan subalgebra, Eq. (17.33), $(\mathbf{S}^{03}, \mathbf{S}^{12}, \mathbf{S}^{56})$. The states within each decuplet are reachable from any member by \mathbf{S}^{ab} . The product of the discrete operators $\mathbb{C}_{NG} (= \prod_{\mathfrak{R}\gamma^s} \gamma_G^s I_{x^6 x^8 \dots x^d}$, denoted as \mathbb{C} in the last column) $\mathcal{P}_{NG}^{(d-1)} (= \gamma_G^0 \prod_{s=5}^d \gamma_G^s I_{\bar{x}_3})$ transforms, for example, ψ_1^I into ψ_6^I , ψ_2^I into ψ_5^I and ψ_3^I into ψ_4^I . Solutions of the Weyl equation, Eq. (17.19), with the negative energies belong to the “Grassmann sea”, with the positive energy to the particles and antiparticles. Also the application of the discrete operators \mathcal{C}_{GN} , Eq. (17.30) and $\mathcal{C}_{NG} \mathcal{P}_{NG}^{(d-1)}$, Eq. (17.30) is demonstrated.

Let us discuss the case with the quadruplet of $SO(6)$ with an odd Clifford character. From the point of view of the subgroups $SU(3)$ (the colour subgroup) and $U(1)$ (the $U(1)$ subgroup carrying the “fermion” quantum number), the quadruplet consists of one $SU(3)$ singlet with the “fermion” quantum number $-\frac{1}{2}$ and one triplet with the “fermion” quantum number $\frac{1}{6}$. The Clifford even $SO(7, 1)$ part of $SO(13, 1)$ define together with the Clifford odd $SO(6)$ part the quantum numbers of the right handed quarks and leptons and of the left handed quarks and leptons of the *standard model*, the left handed weak charged and the right handed weak chargeless.

In the same representation of $SO(13, 1)$ there is also one antiquadruplet, which has the even Clifford character of $SO(6)$ part and the odd Clifford character in the $SO(7, 1)$ part of the $SO(13, 1)$. The antiquadruplet of the $SO(6)$ part consists of one $SU(3)$ antisinglet with the “fermion” quantum number $\frac{1}{2}$ and one antitriplet with the “fermion” quantum number $-\frac{1}{6}$. The $SO(7, 1) \times SO(6)$ antiquadruplet of $SO(13, 1)$ carries quantum numbers of left handed weak chargeless antiquarks

and antileptons and of the right handed weak charged antiquarks and antileptons of the *standard model*.

Both, quarks and leptons and antiquarks and antileptons, belong to the same representation of $SO(13, 1)$, explaining the miraculous cancellation of the triangle anomalies in the *standard model* without connecting by hand the handedness and the charges of quarks and leptons [8], as it must be done in the $SO(10)$ models.

b. In Grassmann space there are one $(\frac{1}{2}, \frac{d!}{\frac{d}{2}! \frac{d}{2}!} = 10)$ decuplet representation of $SO(6)$ and one antidecuplet, both presented in Table 17.3. To be able to second quantize the theory, the whole representation must be Grassmann odd. Both decuplets in Table 17.3 have an odd Grassmann character, what means that products of eigenstates of the Cartan subalgebra in the rest of Grassmann space must be of an Grassmann even character to be second quantizable. Both decuplets would, however, appear in the same representation of $SO(13, 1)$, and one can expect also decuplets of an even Grassmann character, if $SO(6)$ is embedded into $SO(13, 1)$ ¹.

With respect to $SU(3) \times U(1)$ subgroups of the group $SO(6)$ the decuplet manifests as one singlet, one triplet and one sextet, while the antidecuplet manifests as one antisinglet, one antitriplet and one antisextet. All the corresponding quantum numbers of either the Cartan subalgebra operators or of the corresponding diagonal operators of the $SU(3)$ or $U(1)$ subgroups are presented in Table 17.3.

While in Clifford case the representations of $SO(6)$, if the group $SO(6)$ is embedded into $SO(13, 1)$, are defining a Clifford odd quadruplet and an Clifford even antiquadruplet, the representations in Grassmann case define one decuplet and one antidecuplet, both of the same Grassmann character, the odd one in our case. The two quadruplets in Clifford case manifest with respect to the subgroups $SU(3)$ and $U(1)$ as a triplet and a singlet, and as an antitriplet and an antisinglet, respectively. In Grassmann case the two decuplets manifest with respect to the subgroups $SU(3)$ and $U(1)$ as a (triplet, singlet, sextet) and as an (antitriplet, antisinglet, antisextet), respectively. The corresponding multiplets are presented in Table 17.4. The "fermion" quantum number τ^4 has for either singlets or triplets in Grassmann space, Table 17.4, twice the value of the corresponding singlets and triplets in Clifford space, Table 6.3 (see pages 112–113 in this volume): $(-1, +1)$ in

¹ This can easily be understood, if we look at the subgroups of the group $SO(6)$. **i.** Let us look at the subgroup $SO(2)$. There are two creation operators of an odd Grassmann character, in this case $(\theta^9 - i\theta^{10})$ and $(\theta^9 + i\theta^{10})$. Both appear in either decuplet or in antidecuplet — together with $\theta^9\theta^{10}$ with an even Grassmann character — multiplied by the part appearing from the rest of space $d = (11, 12, 13, 14)$. But if $SO(2)$ is not embedded in $SO(6)$, then the two states, corresponding to the creation operators, $(\theta^9 \mp i\theta^{10})$, belong to different representations, and so is $\theta^9\theta^{10}$. **ii.** Similarly we see, if we consider the subgroup $SO(4)$ of the group $SO(6)$. All six states, $(\theta^9 + i\theta^{10}) \cdot (\theta^{11} + i\theta^{12})$, $(\theta^9 - i\theta^{10}) \cdot (\theta^{11} - i\theta^{12})$, $(\theta^9\theta^{10} + \theta^{11}\theta^{12})$, $(\theta^9 + i\theta^{10}) \cdot (\theta^{11} - i\theta^{12})$, $(\theta^9 - i\theta^{10}) \cdot (\theta^{11} + i\theta^{12})$, $(\theta^9\theta^{10} - \theta^{11}\theta^{12})$, appear in the decuplet and in the antidecuplet, multiplied with the part appearing from the rest of space, in this case in $d = (13, 14)$, if $SO(4)$ is embedded in $SO(6)$. But, in $d = 4$ space there are two decoupled groups of three states [2]: $[(\theta^9 + i\theta^{10}) \cdot (\theta^{11} + i\theta^{12}), (\theta^9\theta^{10} + \theta^{11}\theta^{12}), (\theta^9 - i\theta^{10}) \cdot (\theta^{11} - i\theta^{12})]$ and $[(\theta^9 - i\theta^{10}) \cdot (\theta^{11} + i\theta^{12}), (\theta^9\theta^{10} - \theta^{11}\theta^{12}), (\theta^9 + i\theta^{10}) \cdot (\theta^{11} - i\theta^{12})]$. Neither of these six members could be second quantized in $d = 4$ alone.

I	decuplet	$\mathbf{S}^{9\,10}$	$\mathbf{S}^{11\,12}$	$\mathbf{S}^{13\,14}$	τ^4	τ^{33}	τ^{38}
1	$(\theta^9 + i\theta^{10})(\theta^{11} + i\theta^{12})(\theta^{13} + i\theta^{14})$	1	1	1	-1	0	0
2	$(\theta^9 + i\theta^{10})(\theta^{11}\theta^{12} + \theta^{13}\theta^{14})$	1	0	0	$-\frac{1}{3} + \frac{1}{2}$	$+\frac{1}{2\sqrt{3}}$	$+\frac{1}{2\sqrt{3}}$
3	$(\theta^9 + i\theta^{10})(\theta^{11} - i\theta^{12})(\theta^{13} - i\theta^{14})$	1	-1	-1	$+\frac{1}{3}$	+1	$+\frac{1}{\sqrt{3}}$
4	$(\theta^9\theta^{10} + \theta^{11}\theta^{12})(\theta^{13} + i\theta^{14})$	0	0	1	$-\frac{1}{3}$	0	$-\frac{1}{\sqrt{3}}$
5	$(\theta^9 - i\theta^{10})(\theta^{11} - i\theta^{12})(\theta^{13} + i\theta^{14})$	-1	-1	-1	$+\frac{1}{3}$	0	$-\frac{2}{\sqrt{3}}$
6	$(\theta^{11} + i\theta^{12})(\theta^9\theta^{10} + \theta^{13}\theta^{14})$	0	1	0	$-\frac{1}{3}$	$-\frac{1}{2}$	$+\frac{1}{2\sqrt{3}}$
7	$(\theta^9 - i\theta^{10})(\theta^{11} + i\theta^{12})(\theta^{13} - i\theta^{14})$	-1	1	-1	$+\frac{1}{3}$	-1	$+\frac{1}{\sqrt{3}}$
8	$(\theta^9\theta^{10} - \theta^{11}\theta^{12})(\theta^{13} - i\theta^{14})$	0	0	-1	$+\frac{1}{3}$	0	$+\frac{1}{\sqrt{3}}$
9	$(\theta^9\theta^{10} - \theta^{13}\theta^{14})(\theta^{11} - i\theta^{12})$	0	-1	0	$+\frac{1}{3}$	$+\frac{1}{2}$	$-\frac{1}{2\sqrt{3}}$
10	$(\theta^9 - i\theta^{10})(\theta^{11}\theta^{12} - \theta^{13}\theta^{14})$	-1	0	0	$+\frac{1}{3}$	$-\frac{1}{2}$	$-\frac{2}{2\sqrt{3}}$
II	decuplet	$\mathbf{S}^{9\,10}$	$\mathbf{S}^{11\,12}$	$\mathbf{S}^{13\,14}$	τ^4	τ^{33}	τ^{38}
1	$(\theta^9 - i\theta^{10})(\theta^{11} - i\theta^{12})(\theta^{13} - i\theta^{14})$	-1	-1	-1	+1	0	0
2	$(\theta^9 - i\theta^{10})(\theta^{11}\theta^{12} + \theta^{13}\theta^{14})$	-1	0	0	$+\frac{1}{3}$	$-\frac{1}{2}$	$-\frac{1}{2\sqrt{3}}$
3	$(\theta^9 - i\theta^{10})(\theta^{11} + i\theta^{12})(\theta^{13} + i\theta^{14})$	-1	1	1	$-\frac{1}{3}$	-1	$-\frac{1}{\sqrt{3}}$
4	$(\theta^9\theta^{10} + \theta^{11}\theta^{12})(\theta^{13} - i\theta^{14})$	0	0	-1	$+\frac{1}{3}$	0	$+\frac{1}{\sqrt{3}}$
5	$(\theta^9 + i\theta^{10})(\theta^{11} + i\theta^{12})(\theta^{13} - i\theta^{14})$	1	1	-1	$-\frac{1}{3}$	0	$+\frac{2}{\sqrt{3}}$
6	$(\theta^{11} - i\theta^{12})(\theta^9\theta^{10} + \theta^{13}\theta^{14})$	0	-1	0	$+\frac{1}{3}$	$+\frac{1}{2}$	$-\frac{1}{2\sqrt{3}}$
7	$(\theta^9 + i\theta^{10})(\theta^{11} - i\theta^{12})(\theta^{13} + i\theta^{14})$	1	-1	1	$-\frac{1}{3}$	+1	$-\frac{1}{\sqrt{3}}$
8	$(\theta^9\theta^{10} - \theta^{11}\theta^{12})(\theta^{13} + i\theta^{14})$	0	0	1	$-\frac{1}{3}$	0	$-\frac{1}{\sqrt{3}}$
9	$(\theta^9\theta^{10} - \theta^{13}\theta^{14})(\theta^{11} + i\theta^{12})$	0	1	0	$-\frac{1}{3}$	$-\frac{1}{2}$	$+\frac{1}{2\sqrt{3}}$
10	$(\theta^9 + i\theta^{10})(\theta^{11}\theta^{12} - \theta^{13}\theta^{14})$	1	0	0	$-\frac{1}{3}$	$+\frac{1}{2}$	$+\frac{1}{2\sqrt{3}}$

Table 17.3. The creation operators of the decuplet and the antidecuplet of the orthogonal group $\text{SO}(6)$ in Grassmann space are presented. Applying on the vacuum state $|\phi_0\rangle = |1\rangle$ the creation operators form eigenstates of the Cartan subalgebra, Eq. (17.33), ($\mathbf{S}^{9\,10}$, $\mathbf{S}^{11\,12}$, $\mathbf{S}^{13\,14}$). The states within each decouplet are reachable from any member by \mathbf{S}^{ab} . The quantum numbers (τ^{33} , τ^{38}) and τ^4 of the subgroups $\text{SU}(3)$ and $\text{U}(1)$ of the group $\text{SO}(6)$ are also presented, Eq. (17.38).

Grassmann case to be compared with $(-\frac{1}{2}, +\frac{1}{2})$ in Clifford case and $(+\frac{1}{3}, -\frac{1}{3})$ in Grassmann case to be compared with $(+\frac{1}{6}, -\frac{1}{6})$ in Clifford case.

When $\text{SO}(6)$ is embedded into $\text{SO}(13, 1)$, the $\text{SO}(6)$ representations of either even or odd Grassmann character contribute to both of the decuplet, 1716 states of $\text{SO}(13, 1)$ representations contribute, provided that the $\text{SO}(8)$ content has the opposite Grassmann character than the $\text{SO}(6)$ content. The product of both representations must be Grassmann odd in order that the corresponding creation and annihilation operators fulfill the required anticommutation relations for fermions, Eq. (17.1).

Properties of the subgroups $\text{SO}(3, 1)$ and $\text{SO}(4)$ of the group $\text{SO}(8)$ in Grassmann and in Clifford space, when $\text{SO}(8)$ is embedded into $\text{SO}(13, 1)$ a. Let us again repeat first properties of the $\text{SO}(3, 1)$ and $\text{SO}(4)$ parts of the $\text{SO}(13, 1)$ representation of 64 "family members" in Clifford space, presented in Table 6.3 (see pages 112–113 in this volume). As seen in Table 6.3 (see pages 112–113 in

I			τ^4	τ^{33}	τ^{38}
singlet		$(\theta^9 + i\theta^{10})(\theta^{11} + i\theta^{12})(\theta^{13} + i\theta^{14})$	-1	0	0
triplet	1	$(\theta^9 + i\theta^{10})(\theta^{11}\theta^{12} + \theta^{13}\theta^{14})$	$-\frac{1}{3}$	$+\frac{1}{2}$	$+\frac{1}{2\sqrt{3}}$
	2	$(\theta^9\theta^{10} + \theta^{11}\theta^{12})(\theta^{13} + i\theta^{14})$	$-\frac{1}{3}$	0	$-\frac{1}{\sqrt{3}}$
	3	$(\theta^{11} + i\theta^{12})(\theta^9\theta^{10} + \theta^{13}\theta^{14})$	$-\frac{1}{3}$	$-\frac{1}{2}$	$+\frac{1}{2\sqrt{3}}$
sextet	1	$(\theta^9 + i\theta^{10})(\theta^{11} - i\theta^{12})(\theta^{13} - i\theta^{14})$	$\frac{1}{3}$	+1	$+\frac{1}{\sqrt{3}}$
	2	$(\theta^9 - i\theta^{10})(\theta^{11} - i\theta^{12})(\theta^{13} + i\theta^{14})$	$\frac{1}{3}$	0	$-\frac{2}{\sqrt{3}}$
	3	$(\theta^9 - i\theta^{10})(\theta^{11} + i\theta^{12})(\theta^{13} - i\theta^{14})$	$\frac{1}{3}$	-1	$+\frac{1}{\sqrt{3}}$
	4	$(\theta^9\theta^{10} - \theta^{11}\theta^{12})(\theta^{13} - i\theta^{14})$	$\frac{1}{3}$	0	$+\frac{1}{\sqrt{3}}$
	5	$(\theta^9\theta^{10} - \theta^{13}\theta^{14})(\theta^{11} - i\theta^{12})$	$\frac{1}{3}$	$+\frac{1}{2}$	$-\frac{1}{2\sqrt{3}}$
	6	$(\theta^9 - i\theta^{10})(\theta^{11}\theta^{12} - \theta^{13}\theta^{14})$	$\frac{1}{3}$	$-\frac{1}{2}$	$-\frac{1}{2\sqrt{3}}$
II			τ^4	τ^{33}	τ^{38}
antisinglet		$(\theta^9 - i\theta^{10})(\theta^{11} - i\theta^{12})(\theta^{13} - i\theta^{14})$	+1	0	0
antitriplet	1	$(\theta^9 - i\theta^{10})(\theta^{11}\theta^{12} + \theta^{13}\theta^{14})$	$+\frac{1}{3}$	$-\frac{1}{2}$	$-\frac{1}{2\sqrt{3}}$
	2	$(\theta^9\theta^{10} + \theta^{11}\theta^{12})(\theta^{13} - i\theta^{14})$	$+\frac{1}{3}$	0	$+\frac{1}{\sqrt{3}}$
	3	$(\theta^{11} - i\theta^{12})(\theta^9\theta^{10} + \theta^{13}\theta^{14})$	$+\frac{1}{3}$	$+\frac{1}{2}$	$-\frac{1}{2\sqrt{3}}$
antisextet	1	$(\theta^9 - i\theta^{10})(\theta^{11} + i\theta^{12})(\theta^{13} + i\theta^{14})$	$-\frac{1}{3}$	-1	$-\frac{1}{\sqrt{3}}$
	2	$(\theta^9 + i\theta^{10})(\theta^{11} + i\theta^{12})(\theta^{13} - i\theta^{14})$	$-\frac{1}{3}$	0	$+\frac{2}{\sqrt{3}}$
	3	$(\theta^9 + i\theta^{10})(\theta^{11} - i\theta^{12})(\theta^{13} + i\theta^{14})$	$-\frac{1}{3}$	+1	$-\frac{1}{\sqrt{3}}$
	4	$(\theta^9\theta^{10} - \theta^{11}\theta^{12})(\theta^{13} + i\theta^{14})$	$-\frac{1}{3}$	0	$-\frac{1}{\sqrt{3}}$
	5	$(\theta^9\theta^{10} - \theta^{13}\theta^{14})(\theta^{11} + i\theta^{12})$	$-\frac{1}{3}$	$-\frac{1}{2}$	$+\frac{1}{2\sqrt{3}}$
	6	$(\theta^9 + i\theta^{10})(\theta^{11}\theta^{12} - \theta^{13}\theta^{14})$	$-\frac{1}{3}$	$+\frac{1}{2}$	$+\frac{1}{2\sqrt{3}}$

Table 17.4. The creation operators in Grassmann space of the decuplet of Table 17.3 are arranged with respect to the SU(3) and U(1) subgroups of the group SO(6) into a singlet, a triplet, a sextet. The corresponding antidecuplet manifests as an antisinglet, an antitriplet and an antisextet. $\tau^{33} = \frac{1}{2}(\mathbf{S}^9{}^{10} - \mathbf{S}^{11}{}^{12})$, $\tau^{38} = \frac{1}{2\sqrt{3}}(\mathbf{S}^9{}^{10} + \mathbf{S}^{11}{}^{12} - 2\mathbf{S}^{13}{}^{14})$, $\tau^4 = -\frac{1}{3}(\mathbf{S}^9{}^{10} + \mathbf{S}^{11}{}^{12} + \mathbf{S}^{13}{}^{14})$; $\mathbf{S}^{ab} = i(\theta^a \frac{\partial}{\partial \theta^b} - \theta^b \frac{\partial}{\partial \theta^a})$.

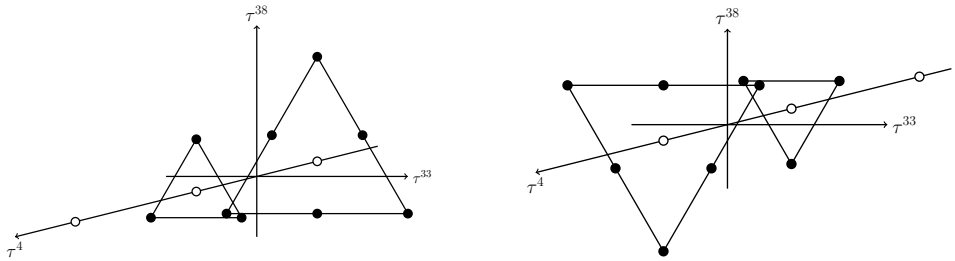


Fig. 17.1. Representations of the subgroups SU(3) and U(1) of the group SO(6) in Grassmann space for two Grassmann odd representations of Table 17.4 are presented. On the abscissa axis and on the ordinate axis the values of the two diagonal operators, τ^{33} and τ^{38} of the colour (SU(3)) subgroup are presented, respectively, with full circles. On the third axis the values of the subgroup of the "fermion number" U(1) is presented with the open circles, the same for all the representations of each multiplet. There are one singlet, one triplet and one sextet on the left hand side and one antisinglet, one antitriplet and one antisextet on the right hand side.

this volume) there are four octets and four antioctets of $SO(8)$. All four octets, having an even Clifford character and forming 32 states when embedded into $SO(13, 1)$, are the same for either quarks or for leptons, they distinguish only in the $SO(6)$ part (of an Clifford odd character) of the $SO(13, 1)$ group, that is in the colour ($SU(3)$) part and the "fermion quantum number" ($U(1)$) part. Also the four antioctets, having an odd Clifford character, are all the same for the 32 family members of antiquarks and antileptons, they again distinguish only in the Clifford even $SO(6)$ part of $SO(13, 1)$, that is in the anticolour ($SU(3)$) part and the "fermion quantum number" ($U(1)$) part.

The 64^{th} -plet of creation operators has an odd Clifford character either for quarks and leptons or for antiquarks and antileptons — correspondingly have an odd Clifford character also their annihilation operators — and can be second quantized [1].

Let us analyze first the octet ($2^{\frac{8}{2}-1} = 8$), which is the same for all 32 members of quarks and leptons. The octet has an even Clifford character. All the right handed u_R -quarks and ν_R -leptons have the $SO(4)$ part of $SO(8)$ equal to $\begin{smallmatrix} 56 & 78 \\ + & + \end{smallmatrix}$, while their left handed partners have the $SO(4)$ part of $SO(8)$ equal to $\begin{smallmatrix} 56 & 78 \\ + & - \end{smallmatrix}$. All the right handed d_R -quarks and e_R -leptons have the $SO(4)$ part of $SO(8)$ equal to $\begin{smallmatrix} 56 & 78 \\ - & - \end{smallmatrix}$, while their left handed partners have the $SO(4)$ part of $SO(8)$ equal to $\begin{smallmatrix} 56 & 78 \\ - & + \end{smallmatrix}$. The left handed quarks and leptons are doublets with respect to $\vec{\tau}^1$ and singlets with $\vec{\tau}^2$, while the right handed quarks and leptons are singlets with respect to $\vec{\tau}^1$ and doublets with $\vec{\tau}^2$. The left and right handed quarks and lepton belong with respect to the $SO(3, 1)$ group to either left handed or the right handed spinor representations, respectively.

b. In Grassmann space the $SO(8)$ group of an odd Grassmann character has $\frac{1}{2} \frac{8!}{4!4!} = 35$ creation operators in each of the two groups and the same number of annihilation operators, obtained from the creation operators by Hermitian conjugation, Eq. (17.4). The corresponding states, created by the creation operators on the vacuum state $|\phi_0\rangle$, can be therefore second quantized. But if embedded the group $SO(8)$ into the group $SO(13, 1)$ the subgroup $SO(6)$ must have an even Grassmann character in order that the states in $SO(13, 1)$ can be second quantized according to Eq. (17.1).

According to what we learned in the case of the group $SO(6)$, each of the two independent representations of the group $SO(13, 1)$ of an odd Grassmann character must include either the even $SO(7, 1)$ part and the odd $SO(6)$ part or the odd $SO(7, 1)$ part and the even $SO(6)$ part. To the even $SO(7, 1)$ representation either the odd $SO(3, 1)$ and the odd $SO(4)$ parts contribute or both must be of the Grassmann even character. In the case that the $SO(7, 1)$ part has an odd Grassmann character (in this case the $SO(6)$ has an even Grassmann character) then one of the two parts $SO(3, 1)$ and $SO(4)$ must be odd and the other even.

17.3 Concluding remarks

We learned in this contribution that although either Grassmann or Clifford space offer the second quantizable description of the internal degrees of freedom of fermions (Eq. (17.1)), the Clifford space offers more: It offers not only the description of all the "family members", explaining all the degrees of freedom of the observed quarks and leptons and antiquark and antileptons, but also the explanation for the appearance of families.

The interaction of fermions with the gravity fields — the vielbeins and the spin connections — in the $2(2n + 1)$ -dimensional space can be achieved, as suggested by the *spin-charge-family* theory ([5,4] and references therein), by replacing the momentum p_a in the Lagrange density function for a free particle by the covariant momentum, equally appropriate for both representations. In Grassmann space we have: $p_{0a} = f^\alpha_a p_{0\alpha}$, with $p_{0\alpha} = p_\alpha - \frac{1}{2} S^{ab} \Omega_{ab\alpha}$, where f^α_a is the vielbein in $d = 2(2n + 1)$ -dimensional space and $\Omega_{ab\alpha}$ is the spin connection field of the Lorentz generators S^{ab} . In Clifford space we have equivalently: $p_{0a} = f^\alpha_a p_{0\alpha}$, $p_{0\alpha} = p_\alpha - \frac{1}{2} S^{ab} \omega_{ab\alpha} - \frac{1}{2} \tilde{S}^{ab} \tilde{\omega}_{ab\alpha}$. Since $S^{ab} = S^{ab} + \tilde{S}^{ab}$ we find that when no fermions are present either $\Omega_{ab\alpha}$ or $\omega_{ab\alpha}$ or $\tilde{\omega}_{ab\alpha}$ are uniquely expressible by vielbeins f^α_a ([5,4] and references therein). It might be that "our universe made a choice between the Clifford and the Grassmann algebra" when breaking the starting symmetry by making condensates of fermions, since that for breaking symmetries Clifford space offers better opportunity".

17.4 Appendix: Useful relations in Grassmann and Clifford space

The generator of the Lorentz transformation in Grassmann space is defined as follows [2]

$$S^{ab} = (\theta^a p^{\theta b} - \theta^b p^{\theta a}) = S^{ab} + \tilde{S}^{ab}, \quad \{S^{ab}, \tilde{S}^{cd}\}_- = 0, \quad (17.32)$$

where S^{ab} and \tilde{S}^{ab} are the corresponding two generators of the Lorentz transformations in the Clifford space, forming orthogonal representations with respect to each other.

We make a choice of the Cartan subalgebra of the Lorentz algebra as follows

$$\begin{aligned} & S^{03}, S^{12}, S^{56}, \dots, S^{d-1 \ d}, \\ & S^{03}, S^{12}, S^{56}, \dots, S^{d-1 \ d}, \\ & \tilde{S}^{03}, \tilde{S}^{12}, \tilde{S}^{56}, \dots, \tilde{S}^{d-1 \ d}, \\ & \text{if } d = 2n. \end{aligned} \quad (17.33)$$

We find the infinitesimal generators of the Lorentz transformations in Clifford space

$$\begin{aligned} S^{ab} &= \frac{i}{4} (\gamma^a \gamma^b - \gamma^b \gamma^a), \quad S^{ab\dagger} = \eta^{aa} \eta^{bb} S^{ab}, \\ \tilde{S}^{ab} &= \frac{i}{4} (\tilde{\gamma}^a \tilde{\gamma}^b - \tilde{\gamma}^b \tilde{\gamma}^a), \quad \tilde{S}^{ab\dagger} = \eta^{aa} \eta^{bb} \tilde{S}^{ab}, \end{aligned} \quad (17.34)$$

where γ^a and $\tilde{\gamma}^a$ are defined in Eq. (17.10). The commutation relations for either S^{ab} or S^{ab} or \tilde{S}^{ab} , $S^{ab} = S^{ab} + \tilde{S}^{ab}$, are

$$\begin{aligned} \{S^{ab}, \tilde{S}^{cd}\}_- &= 0, \\ \{S^{ab}, S^{cd}\}_- &= i(\eta^{ad}S^{bc} + \eta^{bc}S^{ad} - \eta^{ac}S^{bd} - \eta^{bd}S^{ac}), \\ \{\tilde{S}^{ab}, \tilde{S}^{cd}\}_- &= i(\eta^{ad}\tilde{S}^{bc} + \eta^{bc}\tilde{S}^{ad} - \eta^{ac}\tilde{S}^{bd} - \eta^{bd}\tilde{S}^{ac}). \end{aligned} \quad (17.35)$$

The infinitesimal generators of the two invariant subgroups of the group $SO(3, 1)$ can be expressed as follows

$$\vec{N}_{\pm}(= \vec{N}_{(L,R)}) := \frac{1}{2}(S^{23} \pm iS^{01}, S^{31} \pm iS^{02}, S^{12} \pm iS^{03}). \quad (17.36)$$

The infinitesimal generators of the two invariant subgroups of the group $SO(4)$ are expressible with S^{ab} , $(a, b) = (5, 6, 7, 8)$ as follows

$$\begin{aligned} \vec{\tau}^1 &:= \frac{1}{2}(S^{58} - S^{67}, S^{57} + S^{68}, S^{56} - S^{78}), \\ \vec{\tau}^2 &:= \frac{1}{2}(S^{58} + S^{67}, S^{57} - S^{68}, S^{56} + S^{78}), \end{aligned} \quad (17.37)$$

while the generators of the $SU(3)$ and $U(1)$ subgroups of the group $SO(6)$ can be expressed by S^{ab} , $(a, b) = (9, 10, 11, 12, 13, 14)$

$$\begin{aligned} \vec{\tau}^3 &:= \frac{1}{2}\{S^{9\ 12} - S^{10\ 11}, S^{9\ 11} + S^{10\ 12}, S^{9\ 10} - S^{11\ 12}, \\ &\quad S^{9\ 14} - S^{10\ 13}, S^{9\ 13} + S^{10\ 14}, S^{11\ 14} - S^{12\ 13}, \\ &\quad S^{11\ 13} + S^{12\ 14}, \frac{1}{\sqrt{3}}(S^{9\ 10} + S^{11\ 12} - 2S^{13\ 14})\}, \\ \tau^4 &:= -\frac{1}{3}(S^{9\ 10} + S^{11\ 12} + S^{13\ 14}). \end{aligned} \quad (17.38)$$

The hyper charge Y can be defined as $Y = \tau^{23} + \tau^4$.

The equivalent expressions for the "family" charges, expressed by \tilde{S}^{ab} follow if in Eqs. (17.36 - 17.38) S^{ab} are replaced by \tilde{S}^{ab} .

The breaks of the symmetries, manifesting in Eqs. (17.36, 17.37, 17.38), are in the *spin-charge-family* theory caused by the condensate and the nonzero vacuum expectation values (constant values) of the scalar fields carrying the space index $(7, 8)$ (Refs. [5,3] and the references therein). The space breaks first to $SO(7, 1) \times SU(3) \times U(1)_{II}$ and then further to $SO(3, 1) \times SU(2)_I \times U(1)_I \times SU(3) \times U(1)_{II}$, what explains the connections between the weak and the hyper charges and the handedness of spinors.

Let us present some useful relations [3]

$$\begin{aligned} \overset{ab}{(k)}\overset{ab}{(k)} &= 0, & \overset{ab}{(k)}\overset{ab}{(-k)} &= \eta^{aa}\overset{ab}{[k]}, & \overset{ab}{(-k)}\overset{ab}{(k)} &= \eta^{aa}\overset{ab}{[-k]}, & \overset{ab}{(-k)}\overset{ab}{(-k)} &= 0, \\ \overset{ab}{[k]}\overset{ab}{[k]} &= \overset{ab}{[k]}, & \overset{ab}{[k]}\overset{ab}{[-k]} &= 0, & \overset{ab}{[-k]}\overset{ab}{[k]} &= 0, & \overset{ab}{[-k]}\overset{ab}{[-k]} &= \overset{ab}{[-k]}, \\ \overset{ab}{(k)}\overset{ab}{[k]} &= 0, & \overset{ab}{[k]}\overset{ab}{(k)} &= \overset{ab}{(k)}, & \overset{ab}{(-k)}\overset{ab}{[k]} &= \overset{ab}{(-k)}, & \overset{ab}{(-k)}\overset{ab}{[-k]} &= 0, \\ \overset{ab}{(k)}\overset{ab}{[-k]} &= \overset{ab}{(k)}, & \overset{ab}{[k]}\overset{ab}{(-k)} &= 0, & \overset{ab}{[-k]}\overset{ab}{(k)} &= 0, & \overset{ab}{[-k]}\overset{ab}{(-k)} &= \overset{ab}{(-k)}. \end{aligned} \quad (17.39)$$

Acknowledgment

The author N.S.M.B. thanks Department of Physics, FMF, University of Ljubljana, Society of Mathematicians, Physicists and Astronomers of Slovenia, for supporting the research on the *spin-charge-family* theory by offering the room and computer facilities and Matjaž Breskvar of Beyond Semiconductor for donations, in particular for the annual workshops entitled "What comes beyond the standard models".

References

1. N. S. Mankoč Borštnik, H.B. Nielsen, "Why nature made a choice of Clifford and not Grassmann coordinates", Proceedings to the 20th Workshop "What comes beyond the standard models", Bled, 9-17 of July, 2017, Ed. N.S. Mankoč Borštnik, H.B. Nielsen, D. Lukman, DMFA Založništvo, Ljubljana, December 2017, p. 89-120 [arXiv:1802.05554v1v2] [arXiv:1806.01629 whole proceedings].
2. N. Mankoč Borštnik, "Spinor and vector representations in four dimensional Grassmann space", *J. of Math. Phys.* **34** (1993), 3731-3745.
3. N.S. Mankoč Borštnik, "Spin-charge-family theory is offering next step in understanding elementary particles and fields and correspondingly universe", Proceedings to the Conference on Cosmology, Gravitational Waves and Particles, IARD conferences, Ljubljana, 6-9 June 2016, The 10th Biennial Conference on Classical and Quantum Relativistic Dynamics of Particles and Fields, J. Phys.: Conf. Ser. 845 012017 [arXiv:1409.4981, arXiv:1607.01618v2].
4. N.S. Mankoč Borštnik, "Matter-antimatter asymmetry in the *spin-charge-family* theory", *Phys. Rev. D* **91** 065004 (2015) [arxiv:1409.7791].
5. N.S. Mankoč Borštnik, "The explanation for the origin of the Higgs scalar and for the Yukawa couplings by the *spin-charge-family* theory", *J. of Mod. Physics* **6** (2015) 2244-2274, <http://dx.org./10.4236/jmp.2015.615230> [http://arxiv.org/abs/1409.4981].
6. N.S. Mankoč Borštnik N S, "The spin-charge-family theory is explaining the origin of families, of the Higgs and the Yukawa couplings", *J. of Modern Phys.* **4** (2013) 823 [arxiv:1312.1542].
7. N.S. Mankoč Borštnik, D. Lukman, "Vector and scalar gauge fields with respect to $d = (3 + 1)$ in Kaluza-Klein theories and in the *spin-charge-family* theory", *Eur. Phys. J. C* **77** (2017) 231.
8. N.S. Mankoč Borštnik, H.B.F. Nielsen, "The spin-charge-family theory offers understanding of the triangle anomalies cancellation in the standard model", *Fortschritte der Physik, Progress of Physics* (2017) 1700046.
9. N.S. Mankoč Borštnik, H.B.F. Nielsen, *J. of Math. Phys.* **43**, 5782 (2002) [hep-th/0111257].
10. N.S. Mankoč Borštnik, H.B.F. Nielsen, *J. of Math. Phys.* **44** 4817 (2003) [hep-th/0303224].
11. N.S. Mankoč Borštnik, "The *spin-charge-family* theory explains why the scalar Higgs carries the weak charge $\pm \frac{1}{2}$ and the hyper charge $\mp \frac{1}{2}$ ", Proceedings to the 17th Workshop "What comes beyond the standard models", Bled, 20-28 of July, 2014, Ed. N.S. Mankoč Borštnik, H.B. Nielsen, D. Lukman, DMFA Založništvo, Ljubljana December 2014, p.163-82 [arXiv:1502.06786v1] [http://arxiv.org/abs/1409.4981].
12. A. Borštnik Bračič, N.S. Mankoč Borštnik, "The approach Unifying Spins and Charges and Its Predictions", Proceedings to the Euroconference on Symmetries Beyond the Standard Model", Portorož, July 12 - 17, 2003, Ed. by N.S. Mankoč Borštnik, H.B. Nielsen, C. Froggatt, D. Lukman, DMFA Založništvo, Ljubljana December 2003, p. 31-57, hep-ph/0401043, hep-ph/0401055.

13. A. Borštnik Bračič and N.S. Mankoč Borštnik, "Origin of families of fermions and their mass matrices", *Phys. Rev. D* **74**, 073013 (2006) [hep-ph/0301029; hep-ph/9905357, p. 52-57; hep-ph/0512062, p.17-31; hep-ph/0401043, p. 31-57].
14. D. Lukman, N.S. Mankoč Borštnik and H.B. Nielsen, "An effective two dimensionality cases bring a new hope to the Kaluza-Klein-like theories", *New J. Phys.* 13:103027, 2011.
15. D. Lukman and N.S. Mankoč Borštnik, "Spinor states on a curved infinite disc with non-zero spin-connection fields", *J. Phys. A: Math. Theor.* 45:465401, 2012 [arxiv:1205.1714, arxiv:1312.541, hep-ph/0412208 p.64-84].
16. D. Lukman, N.S. Mankoč Borštnik and H.B. Nielsen, "Families of spinors in $d = (1 + 5)$ with a zweibein and two kinds of spin connection fields on an almost S^2 ", Proceedings to the 15th Workshop "What comes beyond the standard models", Bled, 9-19 of July, 2012, Ed. N.S. Mankoč Borštnik, H.B. Nielsen, D. Lukman, DMFA Založništvo, Ljubljana December 2012, 157-166, arxiv:1302.4305.
17. G.regar and N.S. Mankoč Borštnik, "Does dark matter consist of baryons of new stable family quarks?", *Phys. Rev. D* **80**, 083534 (2009) 1-16.
18. A. Borštnik Bračič, N. S. Mankoč Borštnik, "On the origin of families of fermions and their mass matrices", hep-ph/0512062, *Phys Rev. D* **74** 073013-28 (2006).
19. N.S. Mankoč Borštnik, H.B. Nielsen, "Discrete symmetries in the Kaluza-Klein-like theories", *Jour. of High Energy Phys.* **04** (2014) 165 [<http://arxiv.org/abs/1212.2362v3>].



18 Could Experimental Anomalies Reflect Non-perturbative Effects?

H.B. Nielsen¹ and C.D. Froggatt²

¹Niels Bohr Institute, University of Copenhagen, Blegdamsvej 17,
Copenhagen Ø, Denmark

²Glasgow University, Department of Physics and Astronomy
Glasgow University, Glasgow G12 8QQ, Scotland, UK

Abstract. We investigate whether some of the rather few anomalies, in the sense of deviations from the Standard Model, could be explained as due to non-perturbative effects caused by the top-Yukawa-coupling being of order unity (in a sense to be discussed briefly in this article). The main achievement of our non-perturbative rule or model is to relate the deviations of ratios between B-meson decay rates for flavour universality violation for neutral currents to the deviations for the charged current flavour universality violations. In fact the anomaly in the ratio $R(D^*)$ for a charged current with τ and its neutrino relative to the rate with the μ and its neutrino is being related in our model for non-perturbative effects to an analogous effect in a neutral current B-meson decay. It is suggested that the ratio of the anomalous amplitudes contributing to these two combinations of decay processes are to very first approximation given by the squared mass ratio of the heaviest lepton involved in the two ratios, which by their deviation from the Standard Model prediction signal lack of flavour universality.

The muon $g - 2$ anomaly also fits well in our non-perturbative model. But we have to mutilate the model somewhat in order to avoid a far too large anomaly prediction for, say $B_s - \bar{B}_s$, particle - antiparticle mixing.

Povzetek. Avtorja v prispevku raziskujeta, ali lahko odstopanja od napovedi Standardnega modela pojasnita z neperturbativnimi efekti, ki se pojavijo, ker so Yukawine sklopitve za top kvark reda ena (v smislu razloženem v prispevku). Povežeta odstopanja med dosedanjimi napovedmi razmerij razpadnih stanj B mezonov za kršitve univerzalnosti tokov za nevtralne in za nabite tokove in rezultati meritev. Odstopanje v razmerju $R(D^*)$ za nabite tokove za delec τ in njegov nevtrino in za delec μ in njegov nevtrino je povezano z analognimi odstopanji v primeru razpadov nevtralnih mezonov B. Predlagata, da je razmerje anomalnih amplitud, ki prispevajo k tem dvem kombinacijam razpadnih procesov, v prvem približku dano s kvadratom razmerij mas najtežjih leptonov v teh razpadih. Odstopanje od napovedi Standardnega modela nakazuje odvisnost od okusa (flavor).

Model je uporabljen tudi za odstopanja med poskusi in računi za vrednost $g - 2$ za mione, denimo za mešanje $B_s - \bar{B}_s$, če model popačita in se tako izogneta velikim odstopanjem.

Keywords: Decay rate anomalies, non-perturbative effects, flavor universality

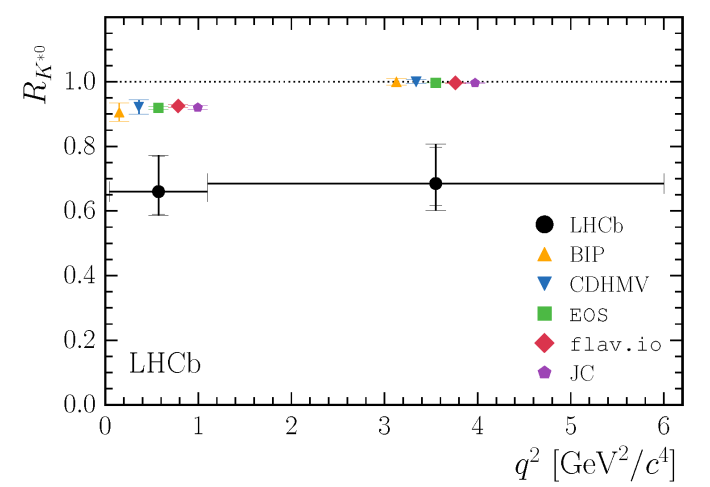
18.1
Introduction

Are the Tensions in LHCb etc data due to Non-perturbative Effects in the Pure Standard Model ?

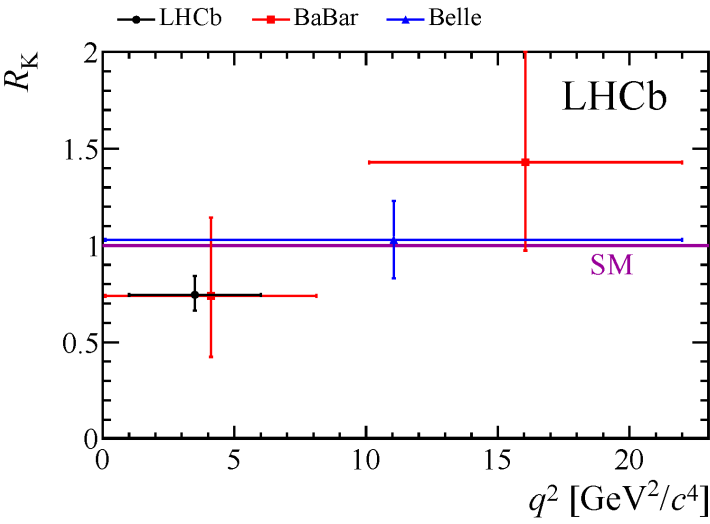
The Standard Model works surprisingly well for LHC physics: Almost no new physics, and at least nothing truly statistically significant! However there is a small number of tensions in the data with a few standard deviations significance: Small lepton universality violating deviations [1–3] , say.

The present proposal is that even these small tensions are not due to genuine new physics, but rather to effects forgotten because of the systematic use of perturbation theory except for the QCD-sector; i.e. the tensions should be non-perturbative effects.

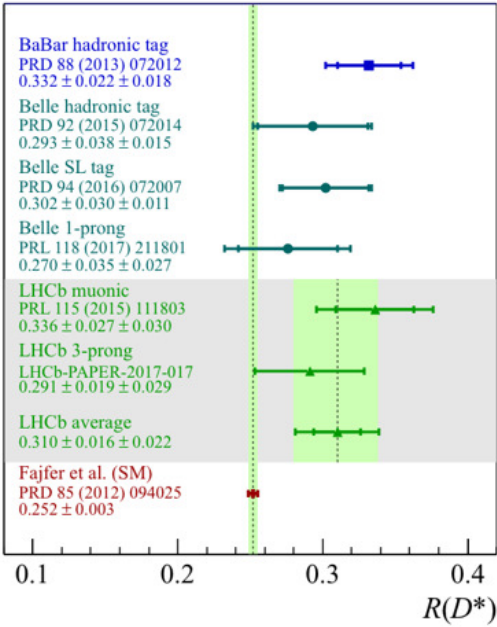
Ratio R_{K^*} of $\mu\mu$ versus ee for $B \rightarrow K^*\bar{l}l$, anomalous.



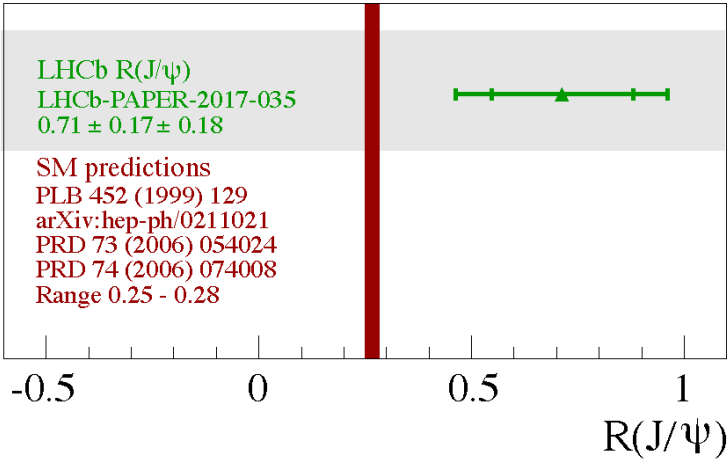
Ratio R_K of $\mu\bar{\mu}$ to $e\bar{e}$ Ratio for $B^+ \rightarrow K^+\bar{l}l$ decay, anomalous for separate q^2 ?.



Ratio $\tau\nu_\tau$ versus $\mu\nu_\mu$ for $B \rightarrow D^*\nu + \text{lepton}$, an anomaly



Ratio $R(J/\psi)$ of $\tau\nu_\tau$ versus $\mu\nu_\mu$ also in $B \rightarrow J/\psi + \nu + \text{lepton}$, an anomaly.



The two Deviations from SM at LHCb:

In the following table we summarize the two deviations from the Standard Model at LHCb and compare our prediction for the ratio of the corresponding anomaly amplitudes with the data.

Channel	Branch. fraction	"R" Ratio	Deviation relative	Anomaly- amplitude
$B \rightarrow K^* \mu^+ \mu^-$ neutral c current	10^{-6}	exp. 0.66 SM 1.00	-34 %	$-0.34\sqrt{10^{-6}}/2$ $= -1.7 * 10^{-4}$ $= -1.7 * 10^{-3} \sqrt{\%}$
$B \rightarrow D^* \tau \nu_\tau$ charged current	2%	exp. 0.31 SM 0.25	+24 %	$0.24\sqrt{0.02}/2$ $= 0.017$ $= 0.17\sqrt{\%}$
Ratio	$2 * 10^4$			-10^2
Pred. ratio				$\sim 0.4 * (\frac{m_\tau}{m_\mu})^2$ $= \sim 115$

In the table we perform a very crude estimate of the ratio of the anomalous contributions to the amplitude of the two decay processes $B \rightarrow D^* \tau \nu_\tau$ (which is a charged current process) relative to the anomalous contribution for $B \rightarrow K^* \mu^+ \mu^-$ (which is a neutral current one). It is based on a few very crude but we think reasonable assumptions in our model:

- Since our non-perturbative anomalous prediction is strongly increasing with the mass of the charged lepton involved, we of course blame practically the whole anomaly on the decay rate for the process involved in the ratio revealing the deviation from lepton universality, which has the biggest mass. In $R(D^*)$ for instance it is the τ channel that has the anomaly, while for $R(K^*)$ which is a ratio between a μ and an e channel it is the μ channel that carries the anomaly.
- We make the approximation that the channels all have the same phase space - which means ignoring the differences between the masses of the particles in the final state of the decays (compared roughly to the B-meson mass). This also implies that, in this approximation, we can simply talk about the amplitude for going into the single final state for each of the considered channels of decay. This allows us to use the normalization of simply writing the amplitude of a decay measured in square roots of %, and simply in this notation have the decay fraction to a channel be the square numerically of the added up amplitudes.

The columns of the table denote the following

- The first column represents the decay channel, corresponding to the two different ratios revealing the violation of flavour universality (for leptons), which has the heavier lepton in the decay. These decay channels are thus, according to our assumption, the ones that are (most) anomalous in our model. We shall neglect the anomaly in the other decay channels in the ratios.
- The next column gives the branching fraction of these two channels thought to be carrying an anomaly.
- The next - 3rd - column now gives both the experimental ratio and the Standard Model predictions for the ratio associated with the channels lined up in column

1. That is to say for the first row, or rather the one associated with $B \rightarrow K^* \mu^+ \mu^-$, we talk about the ratio $R(K^*)$ being the ratio of this decay rate to the corresponding one with the muons replaced by electrons. Similarly the second of the genuine rows refers to the ratio of the decay listed in first column divided by the corresponding one with the lepton replaced by the lighter lepton, in this case thus $B \rightarrow D^* \mu \nu_\mu$.
- The relative deviation between experiment and Standard Model is calculated in the next - the 4th - column. In our philosophy this also gives the relative deviation between the size of the decay in column 1 experimentally relative to the Standard Model. Thus the anomalous probability contribution is the product of this relative percentage and the rate as in column 2.
- Finally in the last column we identify the deviation corresponding to the anomaly with 2 times the amplitude - meaning the square root - of the rate (from column 2) multiplied with the “anomalous amplitude”. It is then the latter that is presented in the last column.

Finally the result of interest is that we estimate the ratio of the anomalous amplitudes for the anomalous parts of the decay amplitudes of the two “rows”. It is this ratio we have a chance to predict, because as a ratio it means that our parameter K gets divided out.

The calculation in the table, which we can at the moment hope to confront with our model, is an *order of magnitude one* meaning that neither factors 2 or π etc nor even the sign are under our control so far.

It might seem that just substituting a mu-coupling by a tau-coupling would only change the anomalous amplitude by a very well-defined real positive ratio given by the masses actually very precisely. However, in our comparison, we have it interfere with the Standard Model amplitude for two very different processes from the Standard Model point of view. So to get even the sign one would need the relative sign of these Standard Model amplitudes, something that would be quite a complicated task. We hope to come back to this exercise of calculating the relative sign of the Standard Model amplitudes, so as to make possible a sign prediction for our model about the sign of the ratio of the two anomalies which we studied.

0.4 some order of unity number in the last entry in the table.

In fact the order unity factor 0.4 in our predicted ratio is given in our non-perturbative model by

$$\frac{V_{tb} V_{ts} g_2^2}{V_{bc} g_t^2} = 0.4. \quad (18.1)$$

The numerically more significant factor is the ratio

$$\frac{g_\tau^2}{g_\mu^2} = \frac{m_\tau^2}{m_\mu^2} = \frac{1777^2}{105.7^2} = 283. \quad (18.2)$$

The numerical coincidence, that should suggest the truth of our non-perturbative effect idea, is:

$$\frac{(R(D^*)|_{\text{exp}}/R(D^*)|_{\text{SM}} - 1)\sqrt{B(B \rightarrow D^*\tau\nu_\tau)}}{(R(K^*)|_{\text{exp}}/R(K^*)|_{\text{SM}} - 1)\sqrt{B(B \rightarrow K^*\mu\bar{\mu})}} \approx \frac{m_\tau^2}{m_\mu^2}. \quad (18.3)$$

Here the “R” ratios are defined as:

$$R(K^*) = \frac{B(B \rightarrow K^*\mu\bar{\mu})}{B(B \rightarrow K^*e\bar{e})}; \quad (18.4)$$

$$R(D^*) = \frac{B(B \rightarrow D^*\tau\nu_\tau)}{B(B \rightarrow D^*\mu\nu_\mu)}. \quad (18.5)$$

Note that these “R” ratios test the lepton universality, the numerator and the denominator only deviating by the flavour of the lepton pair produced. But in $R(D^*)$ it is the ratio τ -pair over μ -pair, while $R(K^*)$ is for μ -pair over e -pair.

Decays into channels only deviating by “hadronic details” support such models as e.g. our “non-perturbative” model.

That is to say the approximate equalities

$$\frac{R(K)|_{\text{exp}}}{R(K)|_{\text{SM}}} = 0.75 \approx 0.66 = \frac{R(K^*)_{\text{exp}}}{R(K^*)_{\text{SM}}}, \quad (18.6)$$

$$\frac{R(J/\psi)|_{\text{exp}}}{R(J/\psi)|_{\text{SM}}} = 2.3 \approx 1.24 = \frac{R(D^*)_{\text{exp}}}{R(D^*)_{\text{SM}}} \quad (18.7)$$

confirm that the anomaly is approximately the same for different hadronic developments with the same underlying weak process behind, thus supporting an e.g. non-perturbative effect, or a new physics at the weak scale.

Have now to build arguments that the lepton pair needs to couple twice with its Higgs Yukawa coupling to the strongly interacting particles/sector.

We imagine there is some coupling g_t which is so strong that very complicated diagrams involving it become relevant. But somehow we hope to argue that the leptons only get interacting with the bunch of “new strong” interaction particles via two Higgs couplings in the processes we looked at with the anomalies.

Also an agreement for the anomaly in the anomalous magnetic moment for the muon, $a_\mu = (g - 2)/2|_\mu$.

We get a correction to the anomalous magnetic moment for the muon in our non-perturbative model, using an overall fitting constant K for the non-perturbative effects (to be explained later):

$$(a_\mu|_{\text{full}} - a_\mu|_{\text{perturbative}}) * \frac{e}{m_\mu} \approx K * <\Phi_{\text{Higgs}}> \left(\frac{g_\mu}{g_t}\right)^3. \quad (18.8)$$

With our fitted value $K \sim \frac{1}{5\text{GeV}^2}$, we get

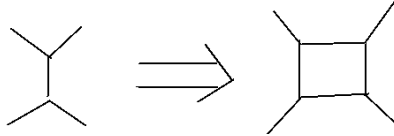
$$a_\mu|_{\text{full}} - a_\mu|_{\text{perturbative}} \approx \frac{246\text{GeV} * 0.105\text{GeV}}{5\text{GeV}^2 * 1700^3} = 1 * 10^{-9}$$

to be compared with the anomaly found experimentally $2.7 * 10^{-9}$.

18.2 Strong Coupling

Except for α_s the strongest coupling in Standard Model is the Top Yukawa Coupling g_t .

Adding one loop to a Feynman diagram:



does it increase or decrease in numerical size ?

Very crudely a factor

$$g^2 \int \frac{d^4 q}{(2\pi)^4} \frac{1}{(q^2 + m^2)^n}$$

The Coupling on the Border between Weak and Strong Interactions for Particle with Only One Component is $g \sim 4\pi$.

Taking very crudely by a “dimensional argument”

$$\int \frac{d|q|}{|q|} \sim 1 \text{ (by dimensional argument)}$$

and the borderline coupling g_{border} to

have the increase factor by adding a loop of

$$g^2 \int \frac{d^4 q}{(2\pi)^4 |q|^4} \approx 1 \text{ (ignoring the mass squares}$$

in the propagators) we get

$$g_{\text{border}} \approx \sqrt{\frac{(2\pi)^4}{\pi^2}} = 4\pi. \quad (18.9)$$

Another crude estimate of the border coupling corresponds to taking the Rydberg constant

$$R_\infty = \frac{\alpha^2 m_e c}{4\pi \hbar}$$

to be of the order of the mass-energy $m_e c^2$:

$$R_\infty = m_e c^2 \quad (18.10)$$

$$\text{implying} \quad (18.11)$$

$$\alpha^2 = 4\pi \text{ for } c = \hbar = 1. \quad (18.12)$$

meaning

$$e = \sqrt[4]{(4\pi)^3} \approx 6 \quad (18.13)$$

Size of Borderline Coupling and Number of “Components”

If there were e.g. a color quantum number taking N values for the particle type encircling the loop, then there would be N various loops for each one. According to our philosophy of the increase factor by inserting a loop

$$g_{\text{border}}^2 N \int \frac{d^4 q}{(2\pi)^4 |q|^4} \approx 1 \quad (18.14)$$

then the N -dependence of the borderline coupling between perturbative and non-perturbative regimes would be

$$g_{\text{border}} \propto \sqrt{\frac{1}{N}}. \quad (18.15)$$

For say 16 “Components” Borderline Coupling ~ 1.5 to 3

Very crudely counting particle and antiparticle also as different “components” and counting together both the Higgs with its 4 real components and the top with its $3 \times 2 \times 2 = 12$ components, we get in total for the particles interacting via the top Yukawa coupling g_t $12 + 4 = 16$ components. Thus the borderline value for g_t becomes

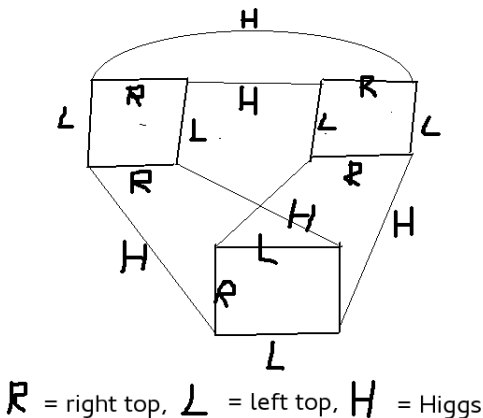
$$g_{t \text{ border}} \approx (6 \text{ to } 4\pi) / \sqrt{16} = 1.5 \text{ to } 3. \quad (18.16)$$

Experimentally

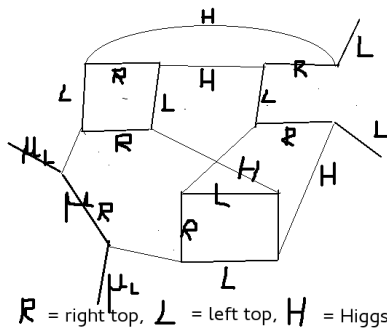
$$g_{t \text{ exp}} = 0.935 \quad (18.17)$$

18.3 Procedure

Very High Order Diagrams Likely to be Important



Diagrams with Almost Only Top-Yukawa Couplings of High Order Could be Significant and give the Anomalies about to be Statistically Significant “Tensions”.



L	can be both left top and left bottom, strange, d
R	right can be only top.
H	can be both eaten Higgs and the "radial" observed Higgs

Suggested Procedure of Model

We imagine a lot of Feynman diagrams - that shall be summed up of course - each with almost only the top-Yukawa coupling g_t in it, and only a few external lines/propagators of other types (like muon say). Then the rules/assumptions of our non-perturbative model are as follows:

- The sum over the many diagrams with only g_t (from which we modify a bit by putting external lines on) is supposed to give just one **overall factor K, which we must fit**.
- When we use an external L line as a left bottom, strange or d quark line, we include a V_{tb} , V_{ts} , or V_{td} **mixing angle factor**
- Other couplings than g_t needed must give rise to the extra factors being these couplings, compared to the g_t they replace.
- Propagators for W, Higgs, top,... are similar order of magnitudewise, and we ignore the differences in our crude rule.

From the Physics involving Rather Heavy Particles the Result of the Non-perturbative Effects should be Effective Lagrangian Terms of Unrenormalizable Dimensionality.

The rather high mass of the particles, like the top quark and Higgs particle, involved in the diagrams developing non-perturbative effects suggests these effects at the relatively low energies involved, in B-meson decay say, should be described by an effective field theory. The effective terms which have an operator dimension like in renormalizable theory are already present in the Standard Model. Thus such non-perturbative effects contributing to terms with dimension less than or equal to $[\text{GeV}^4]$ would just be absorbed into these terms already present in the Standard Model.

We can only realistically hope to measure terms not of this renormalizable type, because otherwise we would need some knowledge about the bare couplings not coming from the usual measurements:

Denoting say leptons and quark fields by ψ_q and ψ_l and the bosons as W_μ , Z_μ and ϕ , effective field theory terms that might result from non-perturbative

effects could have e.g. the forms (P_L is left handed γ_5 projector)

$$\begin{aligned} \bar{\psi}_t \phi \psi_t &: \text{of renormalizable theory dimension } [\text{GeV}^4] \\ \bar{\psi}_b \gamma_\nu P_L \psi_s \bar{\psi}_\mu \gamma^\nu P_L \psi_\mu &: \text{Dimension } [\text{GeV}^6], \text{ so not renormalizable.} \end{aligned}$$

Example of an Effective Lagrangian Density Coefficient Estimated in Our Non-perturbative Scheme:

Say we want the coefficient to the term of the form

$$\bar{\psi}_b(x) \gamma_\nu \psi_s(x) \bar{\psi}_\mu(x) \gamma^\nu \psi_\mu(x),$$

which can represent that a bottom quark b described by $\psi_b(x)$ becomes a strange quark s described by ψ_s by a “neutral current exchange” and the production of a muon antimuon pair produced by the operator

$$\bar{\psi}_\mu(x) \gamma^\nu \psi_\mu(x).$$

Then we need a non-perturbative diagram with the four external particles corresponding to $b \rightarrow s$, μ and $\bar{\mu}$. In fact it shall be a series of diagrams with an arbitrary number of g_t vertices and associated with t_L , t_R and Higgs, but as few as possible other - and therefore smaller - couplings (except we might include the strong QCD couplings).

If the b and the s are taken to be of the left handed helicity, b_L and s_L , we are really interested in the coefficient to the effective term

$$\bar{\psi}_b(x) \gamma_\nu P_L \psi_s(x) \bar{\psi}_\mu(x) \gamma^\nu \psi_\mu(x). \quad (18.18)$$

We can interpret it, that the weak $SU(2)$ partners of the left handed top-components t_L , which are also allowed in the bulk of our diagrams, are already present with amplitudes V_{tb} and V_{ts} respectively for the left handed b_L and s_L . So they do not “cost” extra coupling factors except for these CKM matrix elements, V_{tb} and V_{ts} .

Ignoring the propagators and thereby the masses, we have in the bulk diagram perfect formal conservation of weak charge $SU(2)$, and thus the two left handed quarks b and s being doublets cannot couple to only one Higgs. We must have **two** external Higgs bosons coupling to the muon-antimuon pair.

The muon cannot be interpreted as being already there in the bulk diagram and must instead be coupled, as we already argued, to two Higgs-bosons. This causes the applicable type of diagram to include a factor g_μ^2 - or if we want to consider it a replacement of g_t couplings by analogous g_μ 's, it must include a factor $\left(\frac{g_\mu}{g_t}\right)^2$. So the coefficient to the $b \rightarrow s, \bar{\mu}, \mu$ transition operator (18.18) becomes

$$\text{“coefficient to } c \rightarrow s \bar{\mu} \mu \text{”} = K * V_{tb} V_{ts} \left(\frac{g_\mu}{g_t}\right)^2. \quad (18.19)$$

Here K is an overall constant depending on the non-perturbative part of the calculation, which we cannot do. Thus we must fit via this overall factor K , while g_t , and g_μ are the Yukawa couplings to the Higgs of the top quark and the muon respectively. V_{tb} and V_{ts} are the mixing matrix elements.

Another Example: $b \rightarrow c, \bar{\tau}, \nu_{\tau}$; Charged Current Process

The coefficient to the “non-renormalizable” charged current simulating effective field theory term

$$\bar{\psi}_b \gamma_{\nu} P_L \psi_c \bar{\psi}_{\tau} \gamma^{\nu} P_L \psi_{\nu_{\tau}} \quad (18.20)$$

becomes similarly

$$K * V_{tb}(V_{tb}V_{bc} + V_{ts}V_{sc} + V_{td}V_{dc}) \left(\frac{g_2}{g_t} \frac{g_{\tau}}{g_t} \right)^2. \quad (18.21)$$

Here g_2 is the weak SU(2) gauge theory coupling, and as before: K is the overall non-perturbative constant, V_{qj} , the mixing matrix elements, and g_t, g_{τ} the respective Yukawa Higgs couplings. Order of magnitudewise we only care for the dominant one of the three mixing matrix element products.

Fitting our overall constant K :

With the notation

$$H_{\text{eff}} = -\frac{4G_F}{\sqrt{2}} V_{tb} V_{ts}^* \frac{e^2}{16\pi} \sum (C_i O_i + C_i' O_i') + \text{h.c.} \quad (18.22)$$

and

$$O_9^{(')} = (\bar{s} \gamma_{\mu} P_{L(R)} b) (\bar{l} \gamma^{\mu} l), \quad (18.23)$$

the fit of the “new physics” NP in the coefficient C_9 to the effective term O_9 , which we considered is about

$$C_9 \approx -1.3. \quad (18.24)$$

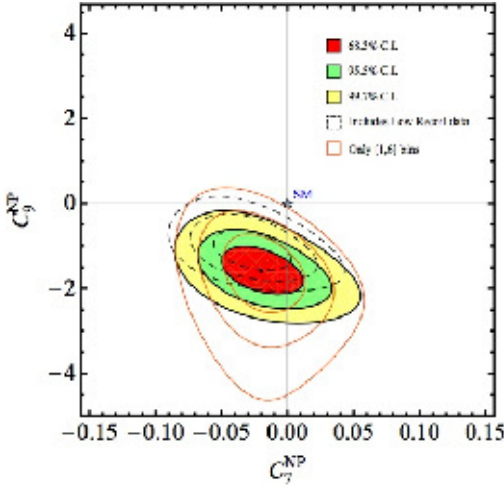


FIG. 1: Fit to (C_7^{NP}, C_9^{NP}) , using the three large-recoil bins for $B \rightarrow K^* \mu^+ \mu^-$ observables, together with $B \rightarrow X_s \gamma$, $B \rightarrow X_s \mu^+ \mu^-$, $B \rightarrow K^* \gamma$ and $B_s \rightarrow \mu^+ \mu^-$. The dashed contours include both large- and low-recoil bins, whereas the orange (solid) ones use only the 1-6 GeV² bin for $B \rightarrow K^* \mu^+ \mu^-$ observables. The origin $C_7^{NP} = (0, 0)$ corresponds to the SM values for the Wilson coefficients $C_{\text{eff},9}^{\text{SM}} = (-0.29, 1.07)$ at $\mu_b = 4.8$ GeV.

The conventional $V_{tb}V_{ts}^*$ factors in

$$H_{\text{eff}} = -\frac{4G_F}{\sqrt{2}} V_{tb} V_{ts}^* \frac{e^2}{16\pi} \sum (C_i O_i + C'_i O'_i) + \text{h.c.}$$

are just the same as in our formula for the non-perturbative effect coefficient

$$\text{“coefficient to } c \rightarrow s \bar{\mu} \mu \text{”} = K * V_{tb} V_{ts} \left(\frac{g_\mu}{g_t} \right)^2.$$

Thus we should fit to

$$\begin{aligned} K * \left(\frac{g_\mu}{g_t} \right)^2 &= -\frac{4G_F}{\sqrt{2}} \frac{e^2}{16\pi} * C_9 = -\frac{G_F}{\sqrt{2}} \alpha * C_9 \\ &= 1.1663787(6) \times 10^{-5} \text{GeV}^{-2} / (\sqrt{2} * 137.037) * (-1.3) \\ &= -6.01847886 * 10^{-8} \text{GeV}^{-2} * (-1.3). \end{aligned}$$

Since $\left(\frac{g_\mu}{g_t} \right)^2 = (0.1056583745/172.44)^2 = 3.77 * 10^{-7}$, we get from fitting the O_9 coefficient

$$K = \frac{6.018 * 10^{-8} \text{GeV}^{-2}}{3.77 * 10^{-7}} * 1.3 \quad (18.25)$$

$$= 0.21 \text{GeV}^{-2} \quad (18.26)$$

$$= \frac{1}{4 \text{ to } 5 \text{ GeV}^2} \quad (18.27)$$

Embarrassingly Huge Overall Constant $K \sim \frac{1}{4 \text{ GeV}^2}$ for the Non-perturbative Effect.

Imagine that the non-perturbative effect in reality is the effect of some loop with, or just the effect of, a bound state formed from the top-quarks and the Higgs. If consisting, as we usually speculate, of 6 top + 6 anti-top quarks its constituent mass would be $12m_t = 2.1 \text{ TeV}$. So, even if we did not count suppression from there being a loop say, an order of magnitude $K \sim \frac{1}{4 \text{ TeV}^2}$ would have been rather expected.

But now, if we have about 12 constituents in the bound state, a top-quark or a Higgs would couple to such a bound state with a total coupling of the order of $12g_t$. Very optimistically a diagram with four external lines would have four such factors and the resulting K would be enhanced by a factor $(12g_t)^4 \approx 20000$ which would bring $K \sim \frac{1}{4 \text{ TeV}^2}$ up to $K \sim \frac{1}{200 \text{ GeV}^2}$.

If the bound state mass were say 750 GeV rather than 2.1 TeV , a reduction by a factor $(2.1/.75)^2$ of the above speculated value $\frac{1}{200 \text{ GeV}^2}$ would be argued for. Then we might say that we could understand if K were of order of magnitude $\frac{1}{20 \text{ GeV}^2}$, but the fitted value $K \sim \frac{1}{4 \text{ GeV}^2}$ still seems to be a bit - a factor 5 - bigger than we would even speculate optimistically.

But of course the point is that it is too hard to compute or even speculate on the overall strength K , so that we must rather trust a fit to the data.

Our Prediction for the Ratio of the anomalous Charged Current $B \rightarrow X_c \tau \nu_\tau$ to the anomalous Neutral Current $B \rightarrow X_s \bar{\mu} \mu$ amplitudes

The ratio of the experimentally found quite separate anomalies measured in their rates/branching ratios is

$$\frac{\text{"Anomalous rate } B \rightarrow X_c \tau \nu_\tau \text{"}}{\text{"Anomalous rate } B \rightarrow X_s \mu \nu_\mu \text{"}} = (-) 1 * 10^4$$

while the ratio of the normal rates is:

$$\frac{BR(B \rightarrow X_c \tau \nu_\tau)}{BR(B \rightarrow X_s \mu \nu_\mu)} = \frac{2\%}{2 * 10^{-6}} = 1 * 10^4$$

corresponding to an amplitude ratio:

$$\frac{A(B \rightarrow X_c \tau \nu_\tau)}{A(B \rightarrow X_s \mu \nu_\mu)} = \sqrt{\frac{2\%}{2 * 10^{-6}}} = 1 * 10^2.$$

By accident it does not matter whether the anomalies come by interference - as we think they do - or by just adding to the rate. In any case it is needed experimentally that the ratio of the two anomalous parts of the amplitude must be ~ 100 :

$$\frac{A_{an}(B \rightarrow X_c \tau \nu_\tau)}{A_{an}(B \rightarrow X_s \bar{\mu} \mu)} = 100. \quad (18.28)$$

Is that then what our model predicts? Our prediction for the ratio of the anomalous parts of the amplitudes is:

$$\begin{aligned} \frac{A_{an}(B \rightarrow X_c \tau \nu_\tau)}{A_{an}(B \rightarrow X_s \bar{\mu} \mu)} &= \frac{K * V_{tb}(V_{tb} V_{bc} " + " V_{ts} V_{sc} " + " V_{td} V_{dc}) \left(\frac{g_2}{g_t} \frac{g_\tau}{g_t} \right)^2}{K * V_{tb} V_{ts} \left(\frac{g_\mu}{g_t} \right)^2} \\ &\approx \frac{V_{tb} V_{bc}}{V_{ts}} * \frac{g_2^2 g_\tau^2}{g_\mu^2 g_t^2} \\ &\approx 1 * 0.4 * \frac{m_\tau^2}{m_\mu^2} \\ &= 0.4 * \frac{1777^2}{105^2} = 115. \end{aligned} \quad (18.29)$$

Very good agreement with experiment!

Dominant Anomaly in $B^+ \rightarrow K^+ \tau^+ \tau^-$

Our prediction for the branching ratio for $B^+ \rightarrow K^+ \tau^+ \tau^-$:

The anomaly amplitude is enhanced by the factor m_τ^2/m_μ^2 compared to the $B^+ \rightarrow K^+ \mu^+ \mu^-$ anomaly amplitude and therefore **dominates the usual SM** amplitude.

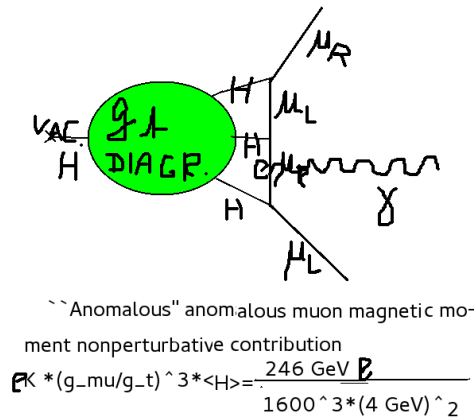
So the branching ratio value for $B^+ \rightarrow K^+ \tau^+ \tau^-$ is:

	Branching ratio
For SM	$\sim 2 \times 10^{-7}$
For our anomaly	$\sim 3 \times 10^{-4}$
Experiment.	$< 2.25 \times 10^{-3}$

18.4 g minus 2

There is a small deviation from experiment in the perturbative Standard Model prediction for the anomalous magnetic moment for the muon. The non-perturbative

contribution of our model is illustrated in the following diagram, which is followed by a list of comments on it.



- The muon anomalous magnetic moment term in the effective Lagrangian density

$$a_{\mu} \bar{\psi}_{\mu}(x) F_{\nu\rho}(x) \gamma^{\nu} \gamma^{\rho} \psi_{\mu}(x) = a_{\mu} \bar{\mu}(x) F_{\nu\rho}(x) \gamma^{\nu} \gamma^{\rho} \mu(x) \quad (18.30)$$

makes a transition between the chirality left to right or opposite. (Contrary to simple electromagnetic coupling making it left to left or right to right.)

- Thus we need to couple the muon line series an **odd** number of times to **Higgs** in our non-perturbative contribution.
- Only **one Higgs exchanged would just give a renormalization of the Higgs propagator**, and would thus already be included in the Standard Model calculation and not count as an anomalous term for the anomalous magnetic moment.
- This contribution must then, because we ignore the propagator masses in it, have a Higgs-line **couple to vacuum via the expectation value** $\langle H \rangle = 246 \text{ GeV}$, so that it **conserves weak isospin**.
- These remarks give the factor $\left(\frac{g_{\mu}}{g_t}\right)^3 \langle H \rangle$.
- When we use our speculated non-perturbative effect, we have the "overall" factor $K \sim \frac{1}{4 \text{ GeV}^2}$.
- Finally we get a non-perturbative contribution to $a_{\mu} = (g - 2)/2|_{\mu}$ for the muon.

$$a_{\mu}|_{\text{full}} - a_{\mu}|_{\text{perturbative}} \approx \frac{246 \text{ GeV} * 0.105 \text{ GeV}}{4 \text{ GeV}^2 * 1700^3} = 1.3 * 10^{-9}. \quad (18.31)$$

This is to be compared with the anomaly found experimentally $2.7 * 10^{-9}$.

18.5 Mixing

The mixing of mesons and their antiparticles such as B_s mixing with \bar{B}_s is a problem, as was pointed out by a member of the audience when HBN gave a talk

about this work in Tallinn. The problem is that at first sight it looks as though we have, according to our rule above, just a few mixing angles suppressing the transition from say B_s to \bar{B}_s . This is very analogous to the way we got the b to s transition, using that both s and b can for the left handed case be considered to be in the doublet with the left handed top and thus indeed participating significantly in the diagrams supposed to be of very high order and still important. However this is not quite true, because the quarks that have to be converted in the mixing process for pseudoscalar mesons - which are w.r.t. strong interactions stable ones, so that mixing experiments can be practically performed - are both right handed and left handed.

18.5.1 Formal

If we take completely formally our rules as set up, including the rule of neglecting propagators and thereby especially the masses of the quarks and leptons in the strong diagram, then a right handed quark of electric charge 2/3 (like the top) can, by interaction with a Higgs-doublet, only be converted into the left handed one of the same flavour or the weak isodoublet partner of this left handed one of the same flavour. This weak isodoublet partner is a superposition of all three flavours of the quark with the other electric charge than the starting right quark. This superposition carries in principle the signal of the flavour of the starting right handed quark. If we ignore the masses and only have it interact via the Higgses in the supposed to dominate diagrams, this superposition can only go back to the right handed quark of just the same flavour as from the start. In this way the "right flavour" has become formally a conserved quantum number, as long as we exclude other interactions than in our rule.

Only if there is transition into a right handed quark of the other charge, i.e. charge -1/3, will another set of Yukawa-couplings (namely the -1/3 charge ones) come into the game and more complicated flavour changes become possible.

The value of $K = \frac{1}{(4 \text{ to } 5) \text{GeV}^2}$ we found, by fitting flavour universality violations, would give us a non-renormalizable Lagrangian term for say top-quark scattering, which would not be suppressed,

$$\sim \frac{1}{5 \text{GeV}^2} \bar{t}(x) \gamma^\mu t(x) * \bar{t}(x) \gamma_\mu t(x). \quad (18.32)$$

This is quite absurd, if you think of using it up to a cut-off scale of say the order of $\Lambda \sim 0.5 \text{ TeV}$ or a "lattice scale" of the order $a \sim \frac{1}{0.5 \text{ TeV}}$.

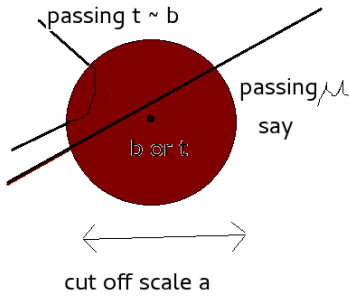
We would in fact like to argue *that you cannot use perturbation theory for such a coupling unless for*

$$K * \bar{t}(x) \gamma^\mu t(x) * \bar{t}(x) \gamma_\mu t(x) \quad (18.33)$$

one has

$$K/a^2 \leq 1. \quad (18.34)$$

Too Strong (Effective) Coupling Term gets Absurd/not Perturbatively Applicable, when $K/a^2 > 1$ for $\text{dim}=6$



This figure is supposed to make clear the absurdity in the too strong coupling regime, which does not at least crudely obey $K/a^2 < 1$. The figure is based on the assumption that inside the interacting particles (in our example top quarks) we have some structure or fields with which they interact with the other particle, and now illustrates how one particle passes into the field or matter belonging to the other one.

Then the idea is to estimate the phase rotation of the amplitude of the scattering, i.e. after the passage. For the case that the particles did indeed pass within the distance a , we can argue dimensionally that the phase rotation δ must be of the order

$$\delta \approx K/a^2 \quad (18.35)$$

or if there is some suppression factor such as e.g. "suppression" $^{-1} = \frac{g_u^2}{g_t^2}$:

$$\delta \approx \frac{K}{\text{"suppression"} a^2}. \quad (18.36)$$

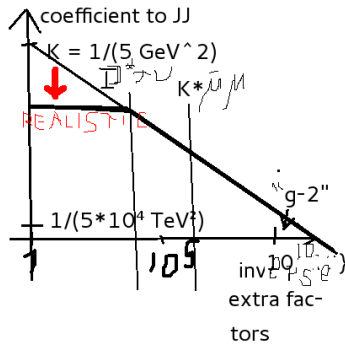
Now the important point is that such a phase rotation δ only makes sense modulo 2π . So it cannot be expected to give any sensible result when it becomes very big compared to 2π . First the point is that you simply cannot "see" the difference in various sizes once the 2π is past. Realistically, we would physically rather imagine that interference between slightly different passage ways of the one particle through the field or matter around the other one would get relative to 2π rather big phase differences, so that strong (destructive) interference would take place. Spoiled by such interference it seems unavoidable that, seen from outside, the end result would be an effective coupling looking much smaller than the a priori one $K/\text{"suppression"}$. Therefore we would like to conclude that the very strong coupling, not obeying our requirement $K/(\text{"suppression"} a^2) < 1$ is not realistic in practice.

Basically the strong interaction would cause further interactions or make different details in the interaction come out of phase. Thus the effective resulting interaction would be brought back to a size obeying the upper limit, which we suggest.

A slightly different way to think of this "strong couplings killing themselves down" to only of order unity, would be to notice that passing a region with too strong interactions would cause reflection. So the particle would never come

through but rather get reflected on the surface. In this way the interaction would be reduced to a size compatible with only the surface regions being used in the effective interaction as seen from outside. This is illustrated in the figure by the track of a particle turning around and going out again.

If there is not a correction factor reducing the K to be sensible, we cannot take it seriously, but must correct it down:



On this figure we now illustrate what we shall effectively do in our model, so as to take into account that the absurdly strong couplings cannot be taken seriously. From the rule of our non-perturbative model one starts from our fitted constant K and then has to put various factors such as g_μ/g_t to some powers etc. so that one at the end divide by a “suppression” - a suppression factor.

In the figure to give an idea of what we shall do, this suppression factor “suppression” is plotted as the abscissa. As the ordinate is plotted the effective field theory term coupling coefficient. If we did not modify our model this effective field theory coupling would of course just be $K/\text{“suppression”}$ and that is represented by the skew straight line, simply with slope -1 in the logarithmic plot. If the suppression factor is sufficiently big, perturbation theory on top of our non-perturbative effect is still o.k. and we can take the result seriously. If, however, the suppression factor for some effective field theory interaction, we look for, turns out so small that the effective coupling becomes bigger than the limit, we should cut the coupling down to agree with the limit. This is indicated by the red arrow on the figure.

So in reality we shall use the kinky curve given on this figure which for small “suppression” is flat, but for large enough “suppression” kinks into the -1 slope straight curve piece.

In order that we can claim the success of our main result on the ratio of the anomalous amplitudes for the two B-meson anomalies, it is crucial that they both fall in the region with the skew part of the curve. I.e. that suppression is enough.

18.5.2 Conservations

In order to put forward a little better the problems with making contributions to meson anti-meson mixing in our scheme, we shall think of a certain truncated Standard Model:

In the region of our new strong interaction it is only right and left top quarks and the Higgs doublet, which are present. We must though consider the left top to also include a certain superposition of bottom, strange and down left quarks, namely the one that is in a doublet with the left top.

At least for pedagogical reasons, but also really logically, we are allowed to use as a strictly speaking more accurate model a restriction of the Standard Model which also includes the three important particles for the new strong sector: the right top, the Higgs doublet and the doublet containing the left top.

Let us indeed for our study, pedagogically or logically, choose the model with all the quarks and for that matter also the leptons, both right and left, and the Higgs doublet. However, we do not let into this restricted model the gauge bosons, so there is no transverse W nor transverse Z . (Only the longitudinal components in the form of eaten Higgses are let in).

This sub-model contains all the components that are crucial for the non-perturbative effects. So it is in principle “better” than the only new strong interaction approximation.

Now let us contemplate the conserved quantities of this “better” restriction of the Standard Model, and let us in the spirit of our proposed rule of ignoring the propagators or at least their masses, take all the quarks and leptons to be massless except for vacuum expectation values for the Higgs. But the Higgs vacuum expectation is assumed to be small on the mass scale we have in mind, so we indeed ignore the masses in the propagators, even for the Higgs, which has a mass of a similar order of magnitude.

In this our “better” restricted Standard Model the weak isospin is only a **global** $SU(2)$ symmetry, as is also the electric charge. We can without problems use a different flavour basis for the $T_3 = 1/2$ and the $T_3 = -1/2$ quarks, as one in fact does in practice. In such a notation then all the flavours get totally conserved. Roughly speaking: We switched off the weak interactions and then the flavours are conserved. It should though be borne in mind that our restricted sub-model of the Standard Model only had the transverse weak gauge bosons switched off, while the longitudinal components in the form of eaten Higgs components are still included.

But this is then at first very promising for the mixing of the various pseudoscalar mesons with their antiparticles in our model. Namely in first approximation, in which we could claim that we only need the just constructed restricted Standard Model, we can say that flavour changing is totally forbidden. Without flavour changing we can have no meson anti-meson mixing and thus our non-perturbative sector cannot produce any contribution to the mixing in this first approximation.

18.5.3 Problem

However, there still seems to be a problem: The Standard Model contribution to meson anti meson mixing already has in amplitude two W -exchanges - as are needed for the flavour violation. Now the experimental method of measuring mixing is very sensitive and we cannot rely on the anomalous contribution

from our non-perturbative model being negligible even if decorated with two W -propagators.

We could therefore expect a non-negligible anomalous contribution basically simulating the Standard model term, but letting the two top quark propagators present in the Standard Model main term for the mixing interact via our non-perturbative effect. This would mean crudely some usual top-propagators, being of the order $1/m_t$ each, if counted as fermion propagators, would in our anomalous term be replaced - following dimensionality rules - by a top-quark scattering effective coupling proportional to our K parameter with associated suppression factors. However, for top quark scattering we have in our model no further suppression and thus we simply get a K replacing the factor $1/m_t^2$ from the Standard Model perturbatively. Our estimating of the correction factor to the full contribution from the Standard Model would then be of the order $m_t^2 K = \frac{173^2}{5} \approx 5000$. This prediction would of course be catastrophic for the hope that our model could be right. There is certainly no place for an extra mixing even of the same order as the Standard Model mixing, let alone 5000 times as much.

Now, however, although formally correct according to our rules, such an estimate is physically rather crazy. We must realistically expect that the effectively "new physics", due to the non-perturbative effects, has to do with say some bound state or some little clump of a new vacuum or whatever, which only truly comes into play when the interacting particles come sufficiently close to each other that the bound state or a couple of them say could be exchanged between them. Such bound state would presumably already have been observed if it were not of mass of the order of say the by now disappearing $F(750)$ digamma.

Let us say that, since no such bound state or replacement for it has been seen, a mass of the order of 1 TeV at least should be estimated.

We would then say that we have an effective field theory and may take the scale μ for it to be of the order of 1 TeV.

18.5.4 Coupling's Maximum

Now we then want to argue that when we consider an effective field theory at a scale $\mu = a^{-1}$, where a is the typical length for the scale of phenomena considered, there must be an upper bound of what the effective field theory coupling G on some vertex such as $G\bar{\psi}_1\bar{\psi}_2...\psi_3\psi_4$ can physically be. Here the ... just stands for some γ -matrices or the like. In fact we want to argue that order of magnitudewise we must have

$$\mu^2 G = G/a^2 < O(1). \quad (18.37)$$

This condition is of course the same as that given in eq. (18.34) and discussed above.

It is very natural, when we have our bound state ideas, to think of the particles for the purpose of estimating what goes on as having extensions of the order $a = \mu^{-1}$. Then one particle passing another one will get a phase rotation of its wave function as it goes by given by G , in such a way that when it has passed through it is by dimensional arguments rotated by $\mu^2 G = G/a^2$. But if this dimensionless quantity is big compared to unity (or 2π) there will not result a particle with a phase

as estimated, but rather some superposition of particles with many somewhat different phases for their amplitudes, and they may typically interfere out to much less. So we cannot really expect a coupling not obeying our suggested bound to have any chance to survive in practice.

This means that unless we have enough suppression factors, such as the g_μ/g_t to some power, to bring the $\mu^2 G$ a priori equal to $\mu^2 K$ down to under 1, we are not allowed to take our model seriously. But now with our suggested number of $\mu = 1 \text{ TeV}$ and our fit $K = 1/(5 \text{ GeV}^2)$, we have $\mu^2 K = 200000$. So unless our suppression factors for the interacting particles - the Yukawa couplings needed etc. - make a suppression of a factor 200000, we cannot take our model seriously. We must then claim that, for the physical reason of the particles being able to pass through each other, we must anyway suppress the non-perturbative effect by the rest of this needed factor 200000.

The idea now is that this suppression by the full factor 200000 is needed in the least suppressed case of top on top interaction as we use in the mixing. This should help to reduce our discrepancy w.r.t. mixing predictions.

In the cases of the anomalies, which we fitted as our main point, even in the least suppressed of the two cases we had a suppression factor $m_\tau^2/m_t^2 \approx 1/10000$. This is only barely enough suppression to avoid further suppression in order to get down by 200000. However the factor 200000 was really somewhat arbitrary, and we could fit the μ to be a bit smaller by a square root of 20. But our problem with mixing getting predicted too strong of course gets worse by such a choice.

18.6 Review

We have worked for a long time on the speculation that non-perturbative effects in the Standard Model produce a very strongly bound state of 6 top + 6 anti-top quarks [4–6], and a new vacuum with a condensate of such bound states. This idea leads to a model of dark matter[7–10] without any physics beyond the Standard Model:

- Dark matter consists of bubbles of a new phase of the vacuum filled with atoms.
- These dark matter “pearls” with mass $\sim 500000t$ made 6400 volcanoes of the Kimberlite pipe type found on earth (and probably many more not found).

Some Successful Numbers Fitted/Predicted by Our Non-perturbative Standard Model Based Model for Dark Matter:

Quantity	Predicted	“experiment”	from
Weak scale	$\sim 30\text{GeV}$	$\sim 100\text{GeV}$	“Tunguska”
3.5 keV line	4.5 keV	3.5 keV	“homolumo-gap”
“Life time, 3.5 keV”	10^{29} s?	10^{28} s	pearl collisions
Double supernova burst	14 hours	5 hours	neutron-eating

18.7 Conclusion

- We proposed, that two (small) tensions found in respectively neutral current ($c \rightarrow s$) and charged current ($b \rightarrow c$) transitions in B-decay are due to non-perturbative effects inside the Standard Model.
- The observed ratio between the anomalous amplitudes for the two processes/decays of B-mesons $B \rightarrow X_s \bar{\mu} \mu$ and $B \rightarrow X_c \tau \nu_\tau$ seems to be $\sim \frac{1}{100}$. This is in agreement with the prediction resulting from our “practical procedure” for calculating this ratio of amplitudes from our assumption that they result from non-perturbative effects, due to the top-Yukawa coupling g_t being of order unity.
- So the Standard Model could be perfectly correct even with these anomalies/tensions being true physical effects.
- In the neutral current decay $B \rightarrow K \tau^+ \tau^-$ we PREDICT the anomaly to dominate.
- We have earlier used this non-perturbative effect for a model for dark matter, thus completely inside the Standard Model.

Acknowledgement

HBN wishes to thank the Niels Bohr Institute for status as emeritus, under which this work were performed and for support to go Bled where this talk was given. Further he thanks COST for going to Tallinn, where the first version of this talk was given, and where a clever participant revealed the catastrophic situation w.r.t. overpredicting the rate of mixing in the unmodified version of our model. CDF would like to acknowledge the hospitality and support from Glasgow University and the Niels Bohr Institute.

References

1. LHCb Collaboration, Phys. Rev. Lett. **115** (2015) 111803.
2. LHCb Collaboration, JHEP **08** (2017) 055.
3. LHCb Collaboration 2014 Phys. Rev. Lett. **113** (2014) 151601.
4. C.D. Froggatt and H.B. Nielsen, Surveys High Energy Phys. **18**, (2003) 55-75; hep-ph/0308144.
5. C.D. Froggatt, H.B. Nielsen and L.V. Laperashvili, Int. J. Mod. Phys. A **20**, 1268 (2005); hep-ph/0406110.
6. C.D. Froggatt and H.B. Nielsen, Phys. Rev. D **80**, 034033 (2009); arXiv:0811.2089.
7. C. D. Froggatt and H. B. Nielsen, Phys. Rev. Lett. **95** (2005) 231301 [arXiv:astro-ph/0508513]
8. C. D. Froggatt and H. B. Nielsen, Int. J. Mod. Phys. A **30** (2015) no.13, 1550066
9. C. D. Froggatt and H. B. Nielsen, Mod. Phys. Lett. **A30**, no.36, 1550195 (2015).
10. H.B. Nielsen, C.D. Froggatt and D. Jurman PoS(CORFU2017)075.

Virtual Institute of Astroparticle Physics Presentation



19 The Platform of Virtual Institute of Astroparticle Physics in Studies of Physics Beyond the Standard Model

M.Yu. Khlopov^{1,2,3,4}

¹ Centre for Cosmoparticle Physics "Cosmion"

² National Research Nuclear University "Moscow Engineering Physics Institute",
115409 Moscow, Russia

³ APC laboratory 10, rue Alice Domon et Léonie Duquet
75205 Paris Cedex 13, France

⁴ Institute of Physics, Southern Federal University
Stachki 194, Rostov on Don 344090, Russia

Abstract. Being a unique multi-functional complex of science and education online, Virtual Institute of Astroparticle Physics (VIA) operates on website <http://viavca.in2p3.fr/site.html>. It supports presentation online for the most interesting theoretical and experimental results, participation online in conferences and meetings, various forms of collaborative scientific work as well as programs of education at distance, combining online videoconferences with extensive library of records of previous meetings and Discussions on Forum. Since 2014 VIA online lectures combined with individual work on Forum acquired the form of Open Online Courses. Aimed to individual work with students the Course is not Massive, but the account for the number of visits to VIA site converts VIA in a specific tool for MOOC activity. VIA sessions are now a traditional part of Bled Workshops' programme. At XXI Bled Workshop it provided a world-wide discussion of the open questions of physics beyond the standard model, supporting world-wide propagation of the main ideas, presented at this meeting.

Povzetek. Virtual Institute of Astroparticle Physics (VIA) je večnamensko spletišče za znanost in izobraževanje na naslovu <http://viavca.in2p3.fr/site.html>. Podpira neposredne predstavitve najbolj zanimivih teoretičnih in eksperimentalnih rezultatov, sodelovanje v neposrednih konferencah in srečanjih, podporo za različne oblike znanstvenega sodelovanja, programe za izobraževanje na daljavo, pri čemer ponuja kombinacije videokonferenc z obširno knjižnico zapisov prejšnjih srečanj in diskusije na Forumu. Po letu 2014 so predavanja VIA na daljavo, kombinirana z individualnim delom na forumu, dobila obliko odprtih tečajev na daljavo. Ker cilja na individualno delo s posameznimi študenti, ni množična, vendar je, glede na število obiskov spletišča VIA, le to postalo orodje za množične aktivnosti učenja na daljavo (MOOC). Seje VIA so postale tradicionalen del programa te blejske delavnice. Na letošni enaindvajseti delavnici so omogočile diskusije o odprtih vprašanjih fizike onkraj standardnih modelov za udeležence iz vseh koncev sveta in razširjanje idej, predstavljenih na delavnici, po vsem svetu.

Keywords: astroparticle physics, physics beyond the Standard model, e-learning, e-science, MOOC

19.1 Introduction

Studies in astroparticle physics link astrophysics, cosmology, particle and nuclear physics and involve hundreds of scientific groups linked by regional networks (like ASPERA/ApPEC [1,2]) and national centers. The exciting progress in these studies will have impact on the knowledge on the structure of microworld and Universe in their fundamental relationship and on the basic, still unknown, physical laws of Nature (see e.g. [3,4] for review). The progress of precision cosmology and experimental probes of the new physics at the LHC and in nonaccelerator experiments, as well as the extension of various indirect studies of physics beyond the Standard model involve with necessity their nontrivial links. Virtual Institute of Astroparticle Physics (VIA) [5] was organized with the aim to play the role of an unifying and coordinating platform for such studies.

Starting from the January of 2008 the activity of the Institute takes place on its website [6] in a form of regular weekly videoconferences with VIA lectures, covering all the theoretical and experimental activities in astroparticle physics and related topics. The library of records of these lectures, talks and their presentations was accomplished by multi-lingual Forum. Since 2008 there were **195 VIA online lectures**, VIA has supported distant presentations of **112 speakers at 25 Conferences** and provided transmission of talks at **64 APC Colloquiums**.

In 2008 VIA complex was effectively used for the first time for participation at distance in XI Bled Workshop [7]. Since then VIA videoconferences became a natural part of Bled Workshops' programs, opening the virtual room of discussions to the world-wide audience. Its progress was presented in [8–16]. Here the current state-of-art of VIA complex, integrated since 2009 in the structure of APC Laboratory, is presented in order to clarify the way in which discussion of open questions beyond the standard models of both particle physics and cosmology were presented at the XXI Bled Workshop with the of VIA facility to the world-wide audience.

19.2 VIA structure and activity

19.2.1 VIA activity

The structure of VIA complex is illustrated by the Fig. 19.1. The home page, presented on this figure, contains the information on the coming and records of the latest VIA events. The menu links to directories (along the upper line from left to right): with general information on VIA (About VIA), entrance to VIA virtual rooms (Rooms), the library of records and presentations (Previous) of VIA Lectures (Previous → Lectures), records of online transmissions of Conferences (Previous → Conferences), APC Colloquiums (Previous → APC Colloquiums), APC Seminars (Previous → APC Seminars) and Events (Previous → Events), Calendar of the past and future VIA events (All events) and VIA Forum (Forum). In the upper right angle there are links to Google search engine (Search in site) and to contact information (Contacts). The announcement of the next VIA lecture and VIA online transmission of APC Colloquium occupy the main part of the homepage with

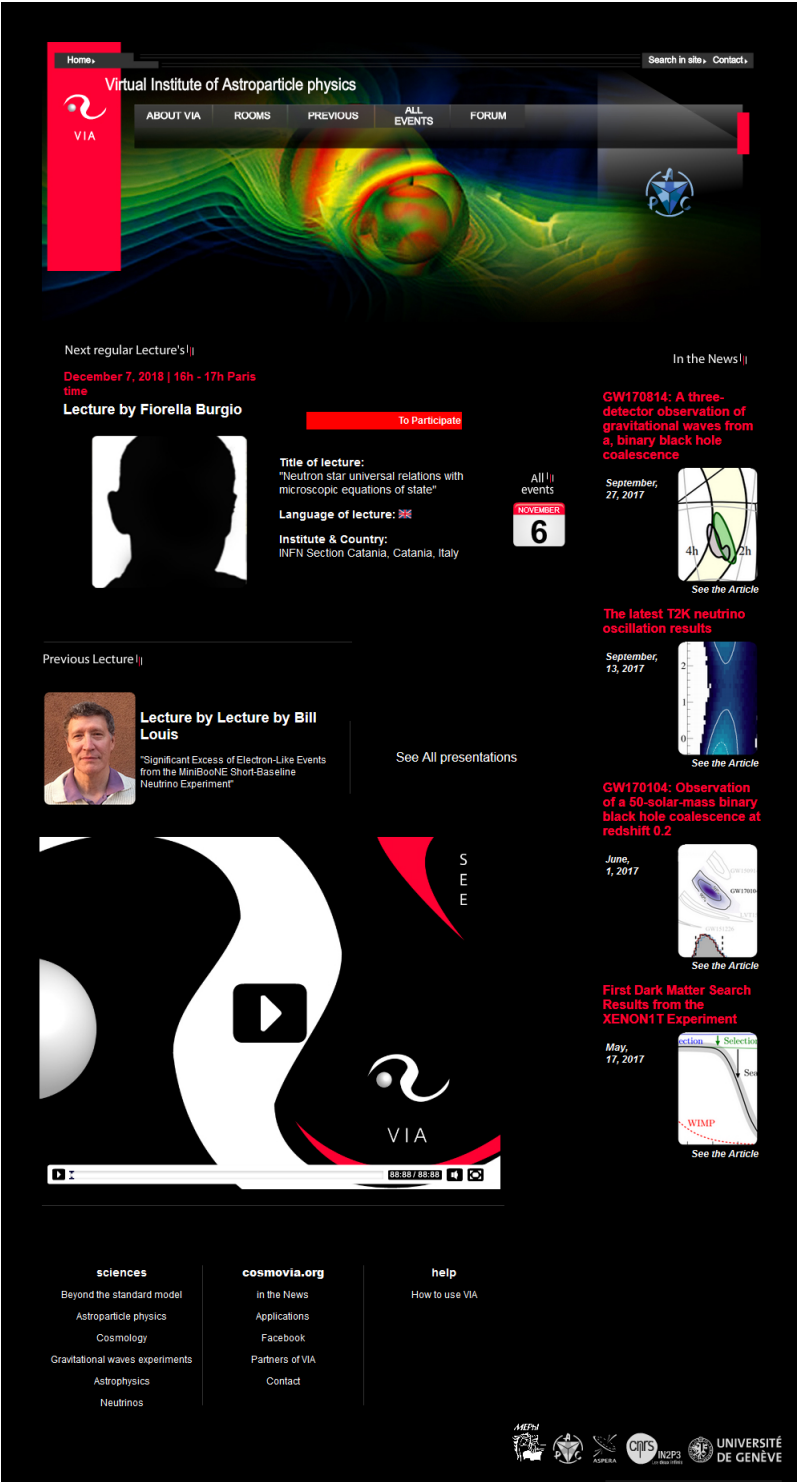


Fig. 19.1. The home page of VIA site

the record of the most recent VIA events below. In the announced time of the event (VIA lecture or transmitted APC Colloquium) it is sufficient to click on "to participate" on the announcement and to Enter as Guest (printing your name) in the corresponding Virtual room. The Calendar shows the program of future VIA lectures and events. The right column on the VIA homepage lists the announcements of the regularly up-dated hot news of Astroparticle physics and related areas.

In 2010 special COSMOVIA tours were undertaken in Switzerland (Geneva), Belgium (Brussels, Liege) and Italy (Turin, Pisa, Bari, Lecce) in order to test stability of VIA online transmissions from different parts of Europe. Positive results of these tests have proved the stability of VIA system and stimulated this practice at XIII Bled Workshop. The records of the videoconferences at the XIII Bled Workshop are available on VIA site [17].

Since 2011 VIA facility was used for the tasks of the Paris Center of Cosmological Physics (PCCP), chaired by G. Smoot, for the public programme "The two infinities" conveyed by J.L.Robert and for effective support a participation at distance at meetings of the Double Chooz collaboration. In the latter case, the experimentalists, being at shift, took part in the collaboration meeting in such a virtual way.

The simplicity of VIA facility for ordinary users was demonstrated at XIV Bled Workshop in 2011. Videoconferences at this Workshop had no special technical support except for WiFi Internet connection and ordinary laptops with their internal webcams and microphones. This test has proved the ability to use VIA facility at any place with at least decent Internet connection. Of course the quality of records is not as good in this case as with the use of special equipment, but still it is sufficient to support fruitful scientific discussion as can be illustrated by the record of VIA presentation "New physics and its experimental probes" given by John Ellis from his office in CERN (see the records in [18]).

In 2012 VIA facility, regularly used for programs of VIA lectures and transmission of APC Colloquiums, has extended its applications to support M.Khlopov's talk at distance at Astrophysics seminar in Moscow, videoconference in PCCP, participation at distance in APC-Hamburg-Oxford network meeting as well as to provide online transmissions from the lectures at Science Festival 2012 in University Paris7. VIA communication has effectively resolved the problem of referee's attendance at the defence of PhD thesis by Mariana Vargas in APC. The referees made their reports and participated in discussion in the regime of VIA videoconference. In 2012 VIA facility was first used for online transmissions from the Science Festival in the University Paris 7. This tradition was continued in 2013, when the transmissions of meetings at Journées nationales du Développement Logiciel (JDEV2013) at Ecole Polytechnique (Paris) were organized [20].

In 2013 VIA lecture by Prof. Martin Pohl was one of the first places at which the first hand information on the first results of AMS02 experiment was presented [19].

In 2014 the 100th anniversary of one of the founders of Cosmoparticle physics, Ya. B. Zeldovich, was celebrated. With the use of VIA M.Khlopov could contribute the programme of the "Subatomic particles, Nucleons, Atoms, Universe:

Processes and Structure International conference in honor of Ya. B. Zeldovich 100th Anniversary" (Minsk, Belarus) by his talk "Cosmoparticle physics: the Universe as a laboratory of elementary particles" [21] and the programme of "Conference YaB-100, dedicated to 100 Anniversary of Yakov Borisovich Zeldovich" (Moscow, Russia) by his talk "Cosmology and particle physics" [22].

In 2015 VIA facility supported the talk at distance at All Moscow Astrophysical seminar "Cosmoparticle physics of dark matter and structures in the Universe" by Maxim Yu. Khlopov and the work of the Section "Dark matter" of the International Conference on Particle Physics and Astrophysics (Moscow, 5-10 October 2015). Though the conference room was situated in Milan Hotel in Moscow all the presentations at this Section were given at distance (by Rita Bernabei from Rome, Italy; by Juan Jose Gomez-Cadenas, Paterna, University of Valencia, Spain and by Dmitri Semikoz, Martin Bucher and Maxim Khlopov from Paris) and its work was chaired by M. Khlopov from Paris [27]. In the end of 2015 M. Khlopov gave his distant talk "Dark atoms of dark matter" at the Conference "Progress of Russian Astronomy in 2015", held in Sternberg Astronomical Institute of Moscow State University.

In 2016 distant online talks at St. Petersburg Workshop "Dark Ages and White Nights (Spectroscopy of the CMB)" by Khatri Rishi (TIFR, India) "The information hidden in the CMB spectral distortions in Planck data and beyond", E. Kholupenko (Ioffe Institute, Russia) "On recombination dynamics of hydrogen and helium", Jens Chluba (Jodrell Bank Centre for Astrophysics, UK) "Primordial recombination lines of hydrogen and helium", M. Yu. Khlopov (APC and MEPHI, France and Russia) "Nonstandard cosmological scenarios" and P. de Bernardis (La Sapienza University, Italy) "Balloon techniques for CMB spectrum research" were given with the use of VIA system [28]. At the defense of PhD thesis by F. Gregis VIA facility made possible for his referee in California not only to attend at distance at the presentation of the thesis but also to take part in its successive jury evaluation.

Since 2018 VIA facility is used for collaborative work on studies of various forms of dark matter in the framework of the project of Russian Science Foundation based on Southern Federal University (Rostov on Don). In September 2018 VIA supported online transmission of **17 presentations** at the Commemoration day for Patrick Fleury, held in APC [29].

The discussion of questions that were put forward in the interactive VIA events is continued and extended on VIA Forum. Presently activated in English, French and Russian with trivial extension to other languages, the Forum represents a first step on the way to multi-lingual character of VIA complex and its activity. Discussions in English on Forum are arranged along the following directions: beyond the standard model, astroparticle physics, cosmology, gravitational wave experiments, astrophysics, neutrinos. After each VIA lecture its pdf presentation together with link to its record and information on the discussion during it are put in the corresponding post, which offers a platform to continue discussion in replies to this post.

19.2.2 VIA e-learning, OOC and MOOC

One of the interesting forms of VIA activity is the educational work at distance. For the last eleven years M.Khlopov's course "Introduction to cosmoparticle physics" is given in the form of VIA videoconferences and the records of these lectures and their ppt presentations are put in the corresponding directory of the Forum [23]. Having attended the VIA course of lectures in order to be admitted to exam students should put on Forum a post with their small thesis. In this thesis students are proposed to chose some BSM model and to study the cosmological scenario based on this chosen model. The list of possible topics for such thesis is proposed to students, but they are also invited to chose themselves any topic of their own on possible links between cosmology and particle physics. Professor's comments and proposed corrections are put in a Post reply so that students should continuously present on Forum improved versions of work until it is accepted as admission for student to pass exam. The record of videoconference with the oral exam is also put in the corresponding directory of Forum. Such procedure provides completely transparent way of evaluation of students' knowledge at distance.

In 2018 the test has started for possible application of VIA facility to remote supervision of student's scientific practice. The formulation of task and discussion of progress on work are recorded and put in the corresponding directory on Forum together with the versions of student's report on the work progress.

Since 2014 the second semester of the course on Cosmoparticle physics is given in English and converted in an Open Online Course. It was aimed to develop VIA system as a possible accomplishment for Massive Online Open Courses (MOOC) activity [24]. In 2016 not only students from Moscow, but also from France and Sri Lanka attended this course. In 2017 students from Moscow were accompanied by participants from France, Italy, Sri Lanka and India [25]. The students pretending to evaluation of their knowledge must write their small thesis, present it and, being admitted to exam, pass it in English. The restricted number of online connections to videoconferences with VIA lectures is compensated by the wide-world access to their records on VIA Forum and in the context of MOOC VIA Forum and videoconferencing system can be used for individual online work with advanced participants. Indeed Google Analytics shows that since 2008 VIA site was visited by more than **242 thousand** visitors from **153** countries, covering all the continents by its geography (Fig. 19.2). According to this statistics more than half of these visitors continued to enter VIA site after the first visit. Still the form of individual educational work makes VIA facility most appropriate for PhD courses and it is planned to be involved in the International PhD program on Fundamental Physics, which can be started on the basis of Russian-French collaborative agreement. In 2017 the test for the ability of VIA to support fully distant education and evaluation of students (as well as for work on PhD thesis and its distant defense) was undertaken. Steve Branchu from France, who attended the Open Online Course and presented on Forum his small thesis has passed exam at distance. The whole procedure, starting from a stochastic choice of number of examination ticket, answers to ticket questions, discussion by professors in the absence of student and announcement of result of exam to him was recorded and put on VIA Forum [26].

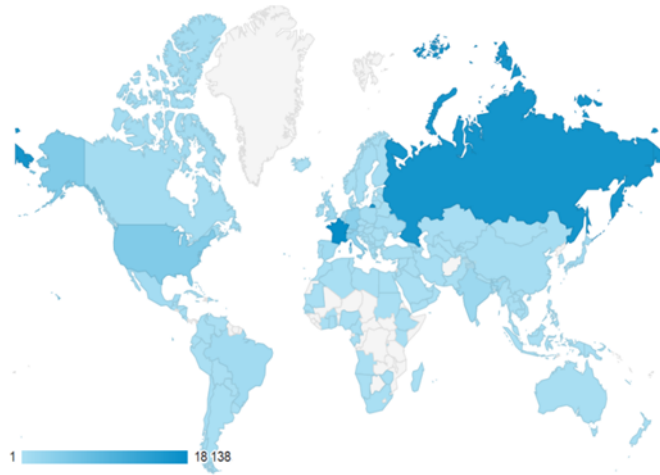


Fig. 19.2. Geography of VIA site visits according to Google Analytics

19.2.3 Organisation of VIA events and meetings

First tests of VIA system, described in [5,7–9], involved various systems of videoconferencing. They included skype, VRVS, EVO, WEBEX, marratech and adobe Connect. In the result of these tests the adobe Connect system was chosen and properly acquired. Its advantages are: relatively easy use for participants, a possibility to make presentation in a video contact between presenter and audience, a possibility to make high quality records, to use a whiteboard tools for discussions, the option to open desktop and to work online with texts in any format.

Initially the amount of connections to the virtual room at VIA lectures and discussions usually didn't exceed 20. However, the sensational character of the exciting news on superluminal propagation of neutrinos acquired the number of participants, exceeding this allowed upper limit at the talk "OPERA versus Maxwell and Einstein" given by John Ellis from CERN. The complete record of this talk and is available on VIA website [30]. For the first time the problem of necessity in extension of this limit was put forward and it was resolved by creation of a virtual "infinity room", which can host any reasonable amount of participants. Starting from 2013 this room became the only main virtual VIA room, but for specific events, like Collaboration meetings or transmissions from science festivals, special virtual rooms can be created. This solution strongly reduces the price of the licence for the use of the adobeConnect videoconferencing, retaining a possibility for creation of new rooms with the only limit to one administrating Host for all of them.

The ppt or pdf file of presentation is uploaded in the system in advance and then demonstrated in the central window. Video images of presenter and participants appear in the right window, while in the lower left window the list of all the attendees is given. To protect the quality of sound and record, the participants are required to switch out their microphones during presentation and to use the upper left Chat window for immediate comments and urgent questions.

The Chat window can be also used by participants, having no microphone, for questions and comments during Discussion. The interactive form of VIA lectures provides oral discussion, comments and questions during the lecture. Participant should use in this case a "raise hand" option, so that presenter gets signal to switch out his microphone and let the participant to speak. In the end of presentation the central window can be used for a whiteboard utility as well as the whole structure of windows can be changed, e.g. by making full screen the window with the images of participants of discussion.

Regular activity of VIA as a part of APC includes online transmissions of all the APC Colloquiums and of some topical APC Seminars, which may be of interest for a wide audience. Online transmissions are arranged in the manner, most convenient for presenters, prepared to give their talk in the conference room in a normal way, projecting slides from their laptop on the screen. Having uploaded in advance these slides in the VIA system, VIA operator, sitting in the conference room, changes them following presenter, directing simultaneously webcam on the presenter and the audience.

19.3 VIA Sessions at XXI Bled Workshop

VIA sessions of XXI Bled Workshop continued the tradition coming back to the first experience at XI Bled Workshop [7] and developed at XII, XIII, XIV, XV, XVI, XVII, XVIII, XIX and XX Bled Workshops [8–16]. They became a regular part of the Bled Workshop's program.

In the course of XXI Bled Workshop, the list of open questions was stipulated, which was proposed for wide discussion with the use of VIA facility. The list of these questions was put on VIA Forum (see [31]) and all the participants of VIA sessions were invited to address them during VIA discussions. During the XXI Bled Workshop the announcement of VIA sessions was put on VIA home page, giving an open access to the videoconferences at VIA sessions. Though the experience of previous Workshops principally confirmed a possibility to provide effective interactive online VIA videoconferences even in the absence of any special equipment and qualified personnel at place, VIA Sessions were directed at XXI Workshop by M.Khlopov at place. Only laptop with microphone and webcam together with WiFi Internet connection was proved to support not only attendance, but also VIA presentations and discussions.

In the framework of the program of XXI Bled Workshop, S. Ketov, gave his talk "Starobinsky Inflation in Gravity and Supergravity" (Fig. 19.3), from Japan, while his co-author M.Khlopov continued the talk in Bled. VIA session also included discussion of searches for new physics at the LHC with participation at distance by A.Romaniouk from CERN. It provided an additional demonstration of the ability of VIA to support the creative non-formal atmosphere of Bled Workshops (see records in [32]).

The talks "Theories for initial conditions" by Holger B. Nielsen (Fig. 19.4) "Experimental consequences of spin-charge family theory" by Norma Mankoc-Borstnik (Fig. 19.5) were given at Bled, inviting distant participants to join the discussion.

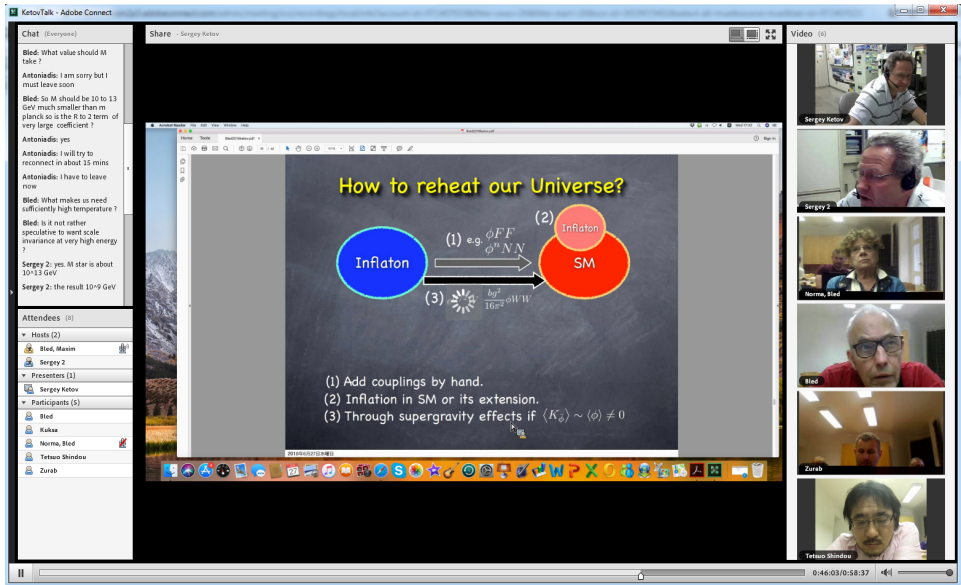


Fig. 19.3. VIA talk "Starobinsky Inflation in Gravity and Supergravity" by S. Ketov from Japan at XXI Bled Workshop

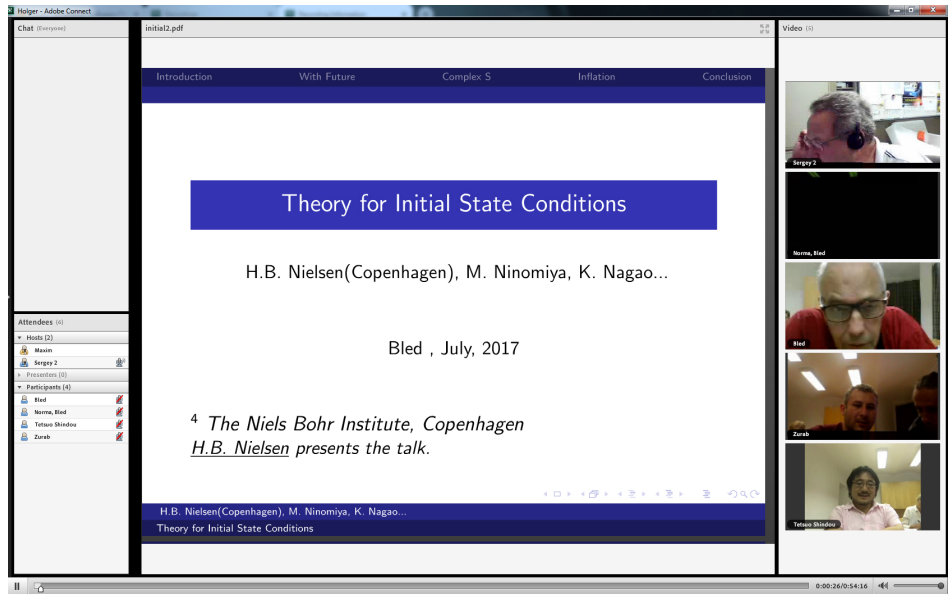


Fig. 19.4. VIA talk by Holger B. Nielsen "Theories for initial conditions" at XXI Bled Workshop

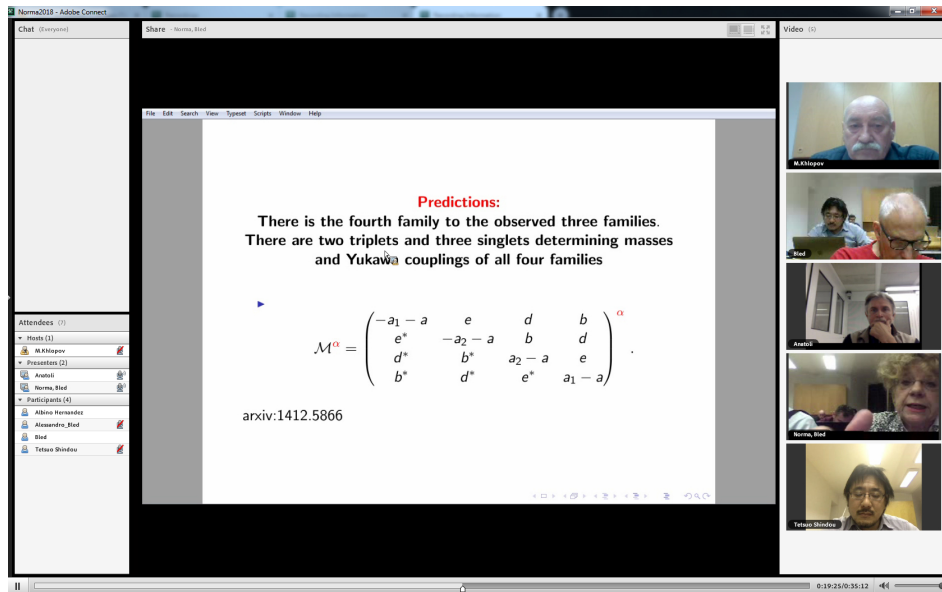


Fig. 19.5. VIA talk “Experimental consequences of spin-charge family theory” by Norma Mankoc-Borstnik at XXI Bled Workshop

The records of all these lectures and discussions can be found in VIA library [32].

19.4 Conclusions

The Scientific-Educational complex of Virtual Institute of Astroparticle physics provides regular communication between different groups and scientists, working in different scientific fields and parts of the world, the first-hand information on the newest scientific results, as well as support for various educational programs at distance. This activity would easily allow finding mutual interest and organizing task forces for different scientific topics of astroparticle physics and related topics. It can help in the elaboration of strategy of experimental particle, nuclear, astrophysical and cosmological studies as well as in proper analysis of experimental data. It can provide young talented people from all over the world to get the highest level education, come in direct interactive contact with the world known scientists and to find their place in the fundamental research. These educational aspects of VIA activity is now being evolved in a specific tool for International PhD programme for Fundamental physics. VIA applications can go far beyond the particular tasks of astroparticle physics and give rise to an interactive system of mass media communications.

VIA sessions became a natural part of a program of Bled Workshops, maintaining the platform of discussions of physics beyond the Standard Model for distant participants from all the world. This discussion can continue in posts and post replies on VIA Forum. The experience of VIA applications at Bled Workshops

plays important role in the development of VIA facility as an effective tool of e-science and e-learning.

Acknowledgements

The initial step of creation of VIA was supported by ASPERA. I am grateful to P.Binetruy, J.Ellis and S.Katsanevas for permanent stimulating support, to J.C. Hamilton for support in VIA integration in the structure of APC laboratory, to K.Belotsky, A.Kirillov, M.Laletin and K.Shibaev for assistance in educational VIA program, to A.Mayorov, A.Romaniouk and E.Soldatov for fruitful collaboration, to M.Pohl, C. Kouvaris, J.-R.Cudell, C. Giunti, G. Cella, G. Fogli and F. DePaolis for cooperation in the tests of VIA online transmissions in Switzerland, Belgium and Italy and to D.Rouable for help in technical realization and support of VIA complex. The work was supported by grant of Russian Science Foundation (project N-18-12-00213). I express my gratitude to N.S. Mankoč Borštnik, D. Lukman and all Organizers of Bled Workshop for cooperation in the organization of VIA Sessions at XXI Bled Workshop.

References

1. <http://www.aspera-eu.org/>
2. <http://www.appec.org/>
3. M.Yu. Khlopov: *Cosmoparticle physics*, World Scientific, New York -London-Hong Kong - Singapore, 1999.
4. M.Yu. Khlopov: *Fundamentals of Cosmic Particle Physics*, CISP-Springer, Cambridge, 2012.
5. M. Y. Khlopov, Project of Virtual Institute of Astroparticle Physics, arXiv:0801.0376 [astro-ph].
6. <http://viavca.in2p3.fr/site.html>
7. M. Y. Khlopov, Scientific-educational complex - virtual institute of astroparticle physics, *Bled Workshops in Physics* **9** (2008) 81–86.
8. M. Y. Khlopov, Virtual Institute of Astroparticle Physics at Bled Workshop, *Bled Workshops in Physics* **10** (2009) 177–181.
9. M. Y. Khlopov, VIA Presentation, *Bled Workshops in Physics* **11** (2010) 225–232.
10. M. Y. Khlopov, VIA Discussions at XIV Bled Workshop, *Bled Workshops in Physics* **12** (2011) 233–239.
11. M. Y. .Khlopov, Virtual Institute of astroparticle physics: Science and education online, *Bled Workshops in Physics* **13** (2012) 183–189.
12. M. Y. .Khlopov, Virtual Institute of Astroparticle physics in online discussion of physics beyond the Standard model, *Bled Workshops in Physics* **14** (2013) 223–231.
13. M. Y. .Khlopov, Virtual Institute of Astroparticle physics and "What comes beyond the Standard model?" in Bled, *Bled Workshops in Physics* **15** (2014) 285-293.
14. M. Y. .Khlopov, Virtual Institute of Astroparticle physics and discussions at XVIII Bled Workshop, *Bled Workshops in Physics* **16** (2015) 177-188.
15. M. Y. .Khlopov, Virtual Institute of Astroparticle Physics — Scientific-Educational Platform for Physics Beyond the Standard Model *Bled Workshops in Physics* **17** (2016) 221-231.

16. M. Y. Khlopov: Scientific-Educational Platform of Virtual Institute of Astroparticle Physics and Studies of Physics Beyond the Standard Model. *Bled Workshops in Physics* **18** (2017) 273-283.
17. In <http://viavca.in2p3.fr/> Previous - Conferences - XIII Bled Workshop
18. In <http://viavca.in2p3.fr/> Previous - Conferences - XIV Bled Workshop
19. In <http://viavca.in2p3.fr/> Previous - Lectures - Martin Pohl
20. In <http://viavca.in2p3.fr/> Previous - Events - JDEV 2013
21. In <http://viavca.in2p3.fr/> Previous - Conferences - Subatomic particles, Nucleons, Atoms, Universe: Processes and Structure International conference in honor of Ya. B. Zeldovich 100th Anniversary
22. In <http://viavca.in2p3.fr/> Previous - Conferences - Conference YaB-100, dedicated to 100 Anniversary of Yakov Borisovich Zeldovich
23. In <http://viavca.in2p3.fr/> Forum - Discussion in Russian - Courses on Cosmoparticle physics
24. In <http://viavca.in2p3.fr/> Forum - Education - From VIA to MOOC
25. In <http://viavca.in2p3.fr/> Forum - Education - Lectures of Open Online VIA Course 2017
26. In <http://viavca.in2p3.fr/> Forum - Education - Small thesis and exam of Steve Branchu
27. <http://viavca.in2p3.fr/> Previous - Conferences - The International Conference on Particle Physics and Astrophysics
28. <http://viavca.in2p3.fr/> Previous - Conferences - Dark Ages and White Nights (Spectroscopy of the CMB)
29. <http://viavca.in2p3.fr/> Previous - Events - Commemoration day for Patrick Fleury.
30. In <http://viavca.in2p3.fr/> Previous - Lectures - John Ellis
31. In <http://viavca.in2p3.fr/> Forum - CONFERENCES BEYOND THE STANDARD MODEL - XXI Bled Workshop "What comes beyond the Standard model?"
32. In <http://viavca.in2p3.fr/> Previous - Conferences - XXI Bled Workshop "What comes beyond the Standard model?"

Poem by Astri Kleppe



20 June

Astri Kleppe

*Tonight they all spring into blossom, Lilacs,
Bird Cherry
with strands of willow, weaving
their way to the beginning;
How it all
was meant to be.*

*Birdsong, sound of running steps,
of tea and cups;
Soon the larvae will be heading
for the bird cherry, enfolding it
in silvery cocoons;
and soon
warm nights of August will bring
darkness, for Orion
to be seen.
But in this night of early June
it's all in ecstasy, in vigil
for the blossom;
No one sleeps, the birds, the flies
are all awake.*

*Who are you then, I asked
the Lilacs
We are strangers here, the answer came,
and we belong to no one
But tell me who you are, I begged
And flower clusters sprinkled over me,
a waterfall
of petals,
We just arrived, tonight,
what more is there to say?*

II

*A loose dream from a corner of the universe
 is driving towards us, our island;
 Clouds
 awakening of granite and cadavers, blue
 and earth;
 A boomerang towards The Milky Way, its icy stars
 and howling wolves, and tightly curved
 around the little heat
 from our own speed. We are but animals
 of auguries, of hope and salt;
 and though great dreams
 of Leibniz,
 Alan Guth and Hubble led us,
 it was other tokens
 that the Universe imagined,
 of another
 kind;
 And suddenly this otherness
 sticks out: a tree
 With roots in galaxies and whispers,
 in galactic summer, leaves
 that dance in morning breeze
 and drizzle, with a scent
 of seed and clover, pregnant
 visions,
 over paths through rain-gray
 grass.*

*Beware of those
 who tread on dew and stop
 under that tree. So slowly
 night is turning, in this space
 of the improbable, a darkness
 where a tree can grow
 from nothing, rise
 with flower buds and day.*

*It was in June, an early morning
 in a sea before the blue
 of skies, before all grass and oxygen;
 but still a sea,
 a meadow, all its flowers.*

III

*They gave us this, a place
so wonderful,
our garden with its tender plants
and trees of darkest mold
with branches stretching out
to heaven, all the blue.*

*And over time we built
our house,
with kitchen windows with a view
of oaks, and in the winter nights
the dog lay by the oven.
And from stone and dust and clay
we built our roads, from sand
and metal
the first street light, zippers
and TV.
The dogs got leashes, we got
blogs, so marvelous
our garden, and so tall
the skyscrapers;
In street dust and the growing noise
we saw the progress, in the dying trees
the halved diversity
of everything.*

*Do you remember all these woods? So vast
and wild, the rugged mountains
roaring over trees and oceans.
O, the ocean! Waving waves
around the boat, like fingers
through a golden field, the time
when the first crops
were grown.
This was our Earth, with seas
and meadows, timothy,
all life born within this triangle
where ice and clouds meet seas
and rivers.
It was ours.
We had all this,
the grass, the water, sky
and clouds.
Our garden
was complete.*

IV

*The elements are four, they said, it's
Fire, Earth and Air
and Water.*

*Air is made of eyes, the Earth is
made of red
and green, and Water
shapes our dreams.*

*Only Fire, that's the Sun, is still
unstained. No smog
is registered
in solar atmospheres, no drought,
no poison or depletion of the soil.
Fire alone
is pure.
It burns, it is;
It shall not want.*

*Three things, they said to me,
are good things.
Four is still OK, and five is not
so bad, but six
is already too much, and seven
is pure waste.
But seven, I protested, is a lovely
number, seven
good things is far more
than three.
Three or seven, never mind, they said.
Our only worry
is when letters are forgotten
or when too many
are added;*

*And in the early morning
flocks of black deer
ran beneath us, dark clouds
of pure music
on the newgrown grass.*

BLEJSKE DELAVNICE IZ FIZIKE, LETNIK 19, ŠT. 2, ISSN 1580-4992

BLED WORKSHOPS IN PHYSICS, VOL. 19, NO. 2

Zbornik 21. delavnice 'What Comes Beyond the Standard Models', Bled, 23. – 29. junij 2018

Proceedings to the 21st workshop 'What Comes Beyond the Standard Models', Bled, June 23.–29., 2018

Uredili Norma Susana Mankoč Borštnik, Holger Bech Nielsen in Dragan Lukman

Izid publikacije je finančno podprla Javna agencija za raziskovalno dejavnost RS iz sredstev državnega proračuna iz naslova razpisa za sofinanciranje domačih znanstvenih periodičnih publikacij

Brezplačni izvod za udeležence

Tehnični urednik Matjaž Zaveršnik

Založilo: DMFA – založništvo, Jadranska 19, 1000 Ljubljana, Slovenija

Natisnila tiskarna Itagraf v nakladi 100 izvodov

Publikacija DMFA številka 2077
